

Materials Forming, Machining and Tribology

Golam Kibria

Muhammad P. Jahan

B. Bhattacharyya *Editors*

# Micro-electrical Discharge Machining Processes

Technologies and Applications

 Springer

# **Materials Forming, Machining and Tribology**

## **Series editor**

J. Paulo Davim, Department of Mechanical Engineering, University of Aveiro,  
Aveiro, Portugal

This series fosters information exchange and discussion on all aspects of materials forming, machining and tribology. This series focuses on materials forming and machining processes, namely, metal casting, rolling, forging, extrusion, drawing, sheet metal forming, microforming, hydroforming, thermoforming, incremental forming, joining, powder metallurgy and ceramics processing, shaping processes for plastics/composites, traditional machining (turning, drilling, milling, broaching, etc.), non-traditional machining (EDM, ECM, USM, LAM, etc.), grinding and others abrasive processes, hard part machining, high speed machining, high efficiency machining, micro and nanomachining, among others. The formability and machinability of all materials will be considered, including metals, polymers, ceramics, composites, biomaterials, nanomaterials, special materials, etc. The series covers the full range of tribological aspects such as surface integrity, friction and wear, lubrication and multiscale tribology including biomedical systems and manufacturing processes. It also covers modelling and optimization techniques applied in materials forming, machining and tribology. Contributions to this book series are welcome on all subjects of “green” materials forming, machining and tribology. To submit a proposal or request further information, please contact Dr. Mayra Castro, Publishing Editor Applied Sciences, via [mayra.castro@springer.com](mailto:mayra.castro@springer.com) or Prof. J. Paulo Davim, Book Series Editor, via [pdavim@ua.pt](mailto:pdavim@ua.pt)

More information about this series at <http://www.springer.com/series/11181>

Golam Kibria · Muhammad P. Jahan  
B. Bhattacharyya  
Editors

# Micro-electrical Discharge Machining Processes

Technologies and Applications

 Springer



*Editors*

Golam Kibria  
Department of Mechanical Engineering  
Aliah University  
Kolkata, India

B. Bhattacharyya  
Department of Production Engineering  
Jadavpur University  
Kolkata, India

Muhammad P. Jahan  
Department of Mechanical  
and Manufacturing Engineering  
Miami University  
Oxford, OH, USA

ISSN 2195-0911 ISSN 2195-092X (electronic)  
Materials Forming, Machining and Tribology  
ISBN 978-981-13-3073-5 ISBN 978-981-13-3074-2 (eBook)  
<https://doi.org/10.1007/978-981-13-3074-2>

Library of Congress Control Number: 2018960187

© Springer Nature Singapore Pte Ltd. 2019

This work is subject to copyright. All rights are reserved by the Publisher, whether the whole or part of the material is concerned, specifically the rights of translation, reprinting, reuse of illustrations, recitation, broadcasting, reproduction on microfilms or in any other physical way, and transmission or information storage and retrieval, electronic adaptation, computer software, or by similar or dissimilar methodology now known or hereafter developed.

The use of general descriptive names, registered names, trademarks, service marks, etc. in this publication does not imply, even in the absence of a specific statement, that such names are exempt from the relevant protective laws and regulations and therefore free for general use.

The publisher, the authors and the editors are safe to assume that the advice and information in this book are believed to be true and accurate at the date of publication. Neither the publisher nor the authors or the editors give a warranty, express or implied, with respect to the material contained herein or for any errors or omissions that may have been made. The publisher remains neutral with regard to jurisdictional claims in published maps and institutional affiliations.

This Springer imprint is published by the registered company Springer Nature Singapore Pte Ltd. The registered company address is: 152 Beach Road, #21-01/04 Gateway East, Singapore 189721, Singapore

# Preface

With emerging trends toward miniaturization and developments in the areas of micro- and nanotechnologies, it has become more important to machine micro- and nanoscale features in functional and difficult-to-cut materials. Micro-electrical discharge machining (micro-EDM) is an important and cost-effective manufacturing process for machining electrically conductive materials irrespective of their hardness. The applications of micro-EDM not are just limited to the machining of hard materials, but also cover the production of difficult-to-make microstructures for micromolds, fuel injection nozzles, spinneret holes for synthetic fibers, electronic and optical devices, micromechatronic actuator parts and microtools for producing these devices, etc. The application of micro-EDM has been extended to various industries including automotive, aerospace, biomedical, and semiconductor. Although the working principle of micro-EDM is fundamentally the same as the conventional macro-scale EDM process, many distinctive features have made micro-EDM an independent micromachining process. The micro-EDM process differs from the conventional macro-EDM process in terms of the size of the tool used, in situ fabrication methods of micro-sized tools, design and development of pulse generators for supplying controlled discharge energy, movement resolution of machine tools' axes, sparking and gap control phenomena, and type of dielectric flushing techniques. The micro-EDM process can be considered as a flexible manufacturing process, allowing a variation in the process mechanism and tooling based on the application needs. The most common varieties of micro-EDM are found to be die-sinking micro-EDM, micro-wire EDM (micro-WEDM), micro-EDM drilling, micro-EDM milling, block micro-EDM, micro-electrical-discharge grinding (micro-EDG), and so on. In addition, there has been a significant amount of research on the development of sequential and hybrid micromachining processes based on micro-EDM for improving the capability of micro-EDM.

This book provides a comprehensive reference for the micro-EDM process, its varieties, technologies, and applications. This book aims to include extensive state-of-the-art research on micro-EDM in a comprehensive collection, which is currently available in journal articles, conference proceedings, and in the form of chapters. The goal is to provide a complete reference to the undergraduate and

graduate students, as well as researchers, educators, and industry personnel working on the micro-EDM area. This book can be used as a reference material for MS and Ph.D. students. In addition, this book can serve as an important reference for students, researchers, engineers, educators, and industry professionals carrying out research on micro-EDM- and micro-EDM-based sequential and hybrid machining process. Altogether, this book contains 13 chapters considering all the major aspects of micro-EDM to make it a more valuable source of knowledge to all.

Chapter 1 of the book provides a concise overview of the most common variety of the micro-EDM process, named micro-EDM drilling. The chapter discusses the working principle of the micro-EDM drilling process, provides an overview of the operating and performance parameters, and discusses important applications of the micro-EDM drilling in various difficult-to-cut materials such as nickel alloys, titanium alloys, and hardened steels. Chapter 2 focuses on another variety of the micro-EDM process, named micro-EDM milling. The chapter discusses the working principle of the micro-EDM milling process, techniques of tool fabrication for using in micro-EDM milling, analysis of tool wear and wear compensation in micro-EDM milling, and the applications of micro-EDM milling. Chapter 3 introduces a novel variation of micro-EDM, named micro-electrical-discharge slotting (MEDS). In the chapter, a new microelectrode fabrication technique named foil as a tool electrode has been discussed in addition to the effect of various machining parameters on the MEDS process. Chapter 4 discusses one of the most common micro-EDM processes, named micro-WEDM. The chapter provides an overview of the micro-WEDM process including process mechanism, system components, parameters, variants, and applications of the micro-WEDM process. Chapter 5 discusses the reverse micro-EDM process, which is mainly used to fabricate high-aspect-ratio micro-electrodes for machining arrays of microholes using micro-EDM drilling. The chapter also discusses the effect of applying vibration to the tool electrode on the accuracy of the fabricated micro-electrodes and process stability during the reverse micro-EDM. Chapter 6 presents the effect of various dielectric fluids on the micro-EDM performance. The chapter discusses the state-of-the-art research works on the application of various dielectric fluids in micro-EDM, including liquid-based dielectrics such as hydrocarbon oil and deionized water and gaseous dielectrics such as oxygen, air, helium, and argon. Chapter 7 discusses a micro-EDM-based hybrid machining process, named powder-mixed micro-EDM. The chapter discusses the effect of powder-suspended dielectric on the surface roughness, material removal rate, and tool wear. Chapter 8 discusses another hybrid process, named vibration-assisted micro-EDM. The chapter includes a discussion on how the assistance of workpiece and/or tool vibration can improve the machining stability and, hence, micro-EDM performance, by effective debris removal. Chapter 9 focuses on tool wear during machining, which is one of the most important issues in micro-EDM. The chapter discusses various tool wear compensation methods developed by researchers to minimize the negative effect of tool wear by compensating the wear during machining. Chapter 10 presents a concise overview of various sequential micro-EDM processes reported in the literature along with the application of each process.

The chapter also discusses how the sequential micro-EDM can resolve the issues faced in a single process. Chapter 11 presents the application of micro-EDM and micro-WEDM in near-net-shape machining, showing the capability of micro-EDM for fabrication of complex 3D microstructures in functional materials. Chapter 12 presents an overview of another micro-EDM-based hybrid micromachining process, named micro-electrical-chemical discharge machining (micro-ECDM). The chapter discusses the process mechanism, system components, configurations, parameters, and process capabilities of the micro-ECDM process. Finally, Chap. 13 presents the state-of-the-art review on the multi-response optimization techniques used for optimizing the machining parameters for improved micro-EDM performance.

The editors acknowledge Springer Nature for this opportunity and for their professional support. The editors would also like to sincerely thank all the authors of chapters for their valuable contributions to this book.

Kolkata, India  
Oxford, USA  
Kolkata, India  
July 2018

Golam Kibria  
Muhammad P. Jahan  
B. Bhattacharyya

# Acknowledgements

This book has become a reality due to the constant inspirations and encouragement received from the senior professors and colleagues, such as Dr. B. Doloi, Dr. D. Banerjee, and Dr. S. Chakraborty of Department of Production Engineering, Jadavpur University, Kolkata, and Dr. B. B. Pradhan of Sikkim Manipal Institute of Technology, Sikkim, India. The editors would like to convey warm regards to Dr. A. Manna, Dr. S. Dhobe, Dr. V. U. Rathod, Dr. Sandip S. Anasane, Dr. Mukandar Sekh, and Dr. Shamim Haidar, for constant support and active participation in preparing the manuscripts of this book.

Financial support from the University Grants Commission (UGC), All India Council for Technical Education (AICTE), Department of Science and Technology (DST), and Council of Scientific and Industrial Research (CSIR) for carrying out research in this area has proved to be useful for utilizing research outcomes to enrich this book. The financial support from Miami University Committee on Faculty Research Award for carrying out research on the micro-EDM area is also acknowledged.

The editors acknowledge Springer for this opportunity and for their enthusiastic and professional support. The team members of Springer, Ms. Rini Christy, Project Coordinator, Books Production, and Dr. Akash Chakraborty, Associate Editor, Applied Sciences and Engineering, have put their constant effort in transforming this book into its final shape. Finally, the editors would like to thank all the contributors of chapters for their availability for this work.

Golam Kibria  
Muhammad P. Jahan  
B. Bhattacharyya

# Contents

<b>1</b>	<b>Micro-EDM Drilling</b> . . . . .	<b>1</b>
	S. N. B. Oliaei, Muhammad P. Jahan and Asma Perveen	
<b>2</b>	<b>Micro-electrical Discharge Milling Operation</b> . . . . .	<b>23</b>
	Mahavir Singh, Vijay Kumar Jain and Janakarajan Ramkumar	
<b>3</b>	<b>Micro-EDM with Translational Tool Motion: The Concept of Micro-Electro-Discharge-Slotting</b> . . . . .	<b>53</b>
	Vishal John Mathai and Harshit K. Dave	
<b>4</b>	<b>Micro-Wire-EDM</b> . . . . .	<b>67</b>
	Taylor Daniel, Chong Liu, Junyu Mou and Muhammad P. Jahan	
<b>5</b>	<b>Reverse Micro-EDM</b> . . . . .	<b>93</b>
	Sachin Adinath Mastud	
<b>6</b>	<b>Micro-EDM Performance Using Different Dielectrics</b> . . . . .	<b>125</b>
	Ved Prakash, Alok Kumar Das and Somnath Chattopadhyay	
<b>7</b>	<b>Powder-Mixed Microelectric Discharge Machining</b> . . . . .	<b>137</b>
	Basil Kuriachen	
<b>8</b>	<b>Vibration-Assisted Micro-EDM Process</b> . . . . .	<b>161</b>
	K. Mishra, B. R. Sarkar and B. Bhattacharyya	
<b>9</b>	<b>Tool Wear Compensation in Micro-EDM</b> . . . . .	<b>185</b>
	Rahul Nadda, Chandrakant Kumar Nirala and Probir Saha	
<b>10</b>	<b>Sequential Micro-EDM</b> . . . . .	<b>209</b>
	MD. Rashef Mahbub, Asma Perveen and Muhammad P. Jahan	
<b>11</b>	<b>Near Net Shape Machining by Micro-EDM and Micro-WEDM</b> . . .	<b>231</b>
	Tanveer Saleh and Rubina Bahar	
<b>12</b>	<b>Micro-electrochemical Discharge Machining</b> . . . . .	<b>265</b>
	Ravindra Nath Yadav and Ajay Suryavanshi	

**13 Multi-response Optimization of Micro-EDM Processes:  
A State-of-the-Art Review** ..... 293  
Soumava Boral, Sarabjeet Singh Sidhu, Prasenjit Chatterjee,  
Shankar Chakraborty and Agam Gugaliya

**Index** ..... 311

## About the Editors

**Dr. Golam Kibria** is Assistant Professor in the Department of Mechanical Engineering, Aliah University, Kolkata. He graduated in mechanical engineering from Kalyani Government Engineering College, West Bengal. He completed his M.Tech. in production engineering at Jadavpur University, Kolkata, in 2008, followed by his Ph.D. at the same university in 2014. After working at Sikkim Manipal University for a year, he joined Aliah University, Kolkata. His research interests include non-conventional machining processes, micromachining, and advanced manufacturing and forming technology. He is a life member of The Institution of Engineers (India) (IEI). He has published more than 24 research articles in peer-reviewed international and national journals and about 43 papers in conference proceedings. He has authored five chapters and is also an editorial board member and reviewer for a number of respected journals.

**Dr. Muhammad P. Jahan** is Assistant Professor in the Department of Mechanical and Manufacturing Engineering at Miami University. His research and teaching interests include advanced manufacturing, non-conventional manufacturing processes, and micro- and nanomachining. He received his B.S. and Ph.D. in mechanical engineering from Bangladesh University of Engineering and Technology (BUET) and National University of Singapore (NUS), respectively. He has published over 90 research articles in peer-reviewed journals and international conferences and also contributed 16 book chapters.

**Dr. B. Bhattacharyya** is Professor and former Head of the Department of Production Engineering, Jadavpur University. He is also Coordinator of the Center of Advanced Study Program at the University Grants Commission (UGC) and the AICTE Quality Improvement Programme at Jadavpur University. His major research areas include non-traditional machining, micromachining, and advanced manufacturing systems. He has published more than 138 research articles in national



and international journals and around 298 papers in conference proceedings. He has guided several doctoral students and also successfully completed a number of research projects. In addition to authoring several chapters, he has recently published a book titled *Electrochemical Micromachining for Nanofabrication, MEMS and Nanotechnology*. He is also a recipient of the Career Award of UGC, New Delhi.

# Chapter 1

## Micro-EDM Drilling



S. N. B. Oliaei, Muhammad P. Jahan and Asma Perveen

**Abstract** Micro-EDM drilling becomes an important fabrication process for several different industrial applications. Micro-EDM drilling provides comparative advantages over conventional mechanical micro-drilling process owing to its capability of machining difficult-to-cut materials. This chapter provides a concise overview of micro-EDM drilling process. It presents working principle of the micro-EDM drilling as well as both operating and performance parameters along with some important applications. This chapter also covers micro-EDM drilling for difficult-to-cut materials such as steel alloys, Ti alloys and Ni alloys.

**Keywords** Micro-EDM · Holes · Nozzle · High aspect ratio · Taper · Debris

### 1.1 Introduction

During past few decades, several important industries such as aerospace, automotive and biomedical have adapted new materials increasingly. Most of these alloys having higher toughness, less heat sensitivity, more resistance to corrosion are also difficult-to-machine materials, and conventional machining has failed to remain a feasible process for these materials. However, due to the excellent properties of these difficult-to-machine alloys, and their possible usage in different industries, machining of these alloys can open up new doors of opportunities too [1]. This gives a push to

---

S. N. B. Oliaei

Department of Mechanical Engineering, Atilim University, Ankara, Turkey

e-mail: [samad.nadimi@atilim.edu.tr](mailto:samad.nadimi@atilim.edu.tr)

M. P. Jahan

Department of Mechanical and Manufacturing Engineering,

Miami University, Oxford, OH 45056, USA

e-mail: [jahanmp@miamioh.edu](mailto:jahanmp@miamioh.edu)

A. Perveen (✉)

Department of Mechanical Engineering, Nazarbayev University, Astana, Kazakhstan

e-mail: [asma.perveen@nu.edu.kz](mailto:asma.perveen@nu.edu.kz)

© Springer Nature Singapore Pte Ltd. 2019

G. Kibria et al. (eds.), *Micro-electrical Discharge Machining Processes*, Materials

Forming, Machining and Tribology, [https://doi.org/10.1007/978-981-13-3074-2\\_1](https://doi.org/10.1007/978-981-13-3074-2_1)

the development of new non-conventional process or improvising the existing one. Electro-discharge machining (EDM) is considered one of such extensive processes which has been improvised into so many different types over the last few decades. EDM process is basically an electro-thermal process where spark generated between workpiece and tool removes materials by melting and vaporizing as the temperature goes as high as 12,000 °C. As the spark comes with high temperature, it not only removes material from workpiece but also from tool. Being electro-thermal process, it has the advantage of not sensitive towards the hardness, strength and toughness of the workpiece materials. This makes EDM an excellent process to machine materials with enhanced mechanical properties [2, 3].

As with the increased demand of miniature devices and micro-features, dimension of drilled holes also becomes smaller which is in the range of few microns of diameter. Different hole drilling processes such as mechanical and thermal satisfy the requirements of applications so far. Nevertheless, mechanical micro-drilling of few micron size hole using micro-drills becomes infeasible due to the rigidity issue of smaller tools and hard-to-machine materials. In contrast, EDM extends its capability to machine micro-scale with the help of micro-EDM process where discharge energy produced during machining, tool size as well as axis resolution are scaled down. Micro-EDM becomes successful with the development of new CNC system and advanced spark generator controller. Although tool rigidity is compromised due to downscaling of tool size, it does not impact the process much since EDM is a non-contact process. This process is free from cutting force, mechanical strains and vibration; however, materials with certain value of conductivity are required for micro-EDM process. Other advantages are low overhead cost and setting time for this EDM. Nevertheless, this process is not free of drawbacks, for instance long machine time meaning lower material removal rate but with higher tool wear.

Micro-EDM technology itself is subdivided into micro-wire EDM, die-sinking micro-EDM, micro-EDM drilling and micro-EDM milling [4]. This chapter will focus on micro-EDM drilling aspect which is mostly used for making hole in hard-to-machine materials. Researches associated with different performance parameters such as materials removal rate, tool wear and dimensional accuracy are addressed along with future direction of EDM-micro-drilling.

## 1.2 Necessity for Micro-EDM Drilling

Due to the miniaturization of product, micro-scale features like micro-holes or micro-structures have been found to have huge demand. Recently, micro-scale holes appear to be in use for several different applications such as injection nozzles, pressure sensor, probes (neural, surface), spinneret holes, gear trains, micro-droplet generators, miniature robots, inertial sensors analysers, imagers and biomedical filters [5]. Micro-holes can be either through holes or blind holes, or depending on the application it may require vertical sidewall or slant sidewall. These micro-holes not

necessarily are round, but could be other shapes too. Since the aspect ratio for the drilled hole increases, it presents much more challenges for the fabrication process.

Although micro-EDM drilling of difficult-to-cut material carries paramount importance considering their application areas, it is limited due to debris accumulation in the hole arising from insufficient flushing as well as unstable machining. Micro-EDM drilling can be widely used to make holes of different sorts for consumer products, aerospace, automotive, fluidics, chemical industries, electro-communication, biomedicine as well as mould machining industries [5].

### 1.3 Working Principle

Material removal in micro-EDM process is based on the eroding effect of consecutive electrical discharges due to melting and evaporation of the workpiece material. In this process, when the voltage difference between cathode and anode at their closest position reaches to the ignition voltage, a strong electric field develops in the gap. The movement of electrons towards the workpiece starts under the influence of this strong electric field, which results in breakdown initiation. Accelerated electrons collide to the natural species in the dielectric fluid causing the creation of an electron avalanche [6]. The distortion in the electric field and streamers development towards both electrodes results in established discharges, which are known as arc discharges based on discharge duration and current density. According to Lee [7], the emission of electron from the cathode tool is mainly because of secondary, thermionic and field emissions. Under the conditions of EDM discharges, where there exists strong temperature and electrical field, according to Thomas–Fermi theory the emission process is greatly reliant on both fields [8]. In addition to the electron emission phenomenon, since there are always some microscopic contaminants (debris) suspended in the dielectric fluid with diameter of order similar as gap size and surface irregularity of the workpiece, these suspended contaminants will also be persuaded by the electric field and will concentrate at the strongest point of the field. As a result, a high-conductive bridge known as plasma channel forms across the gap. At the initial stage, the plasma channel has a uniform growth followed by a faster growth phenomenon. As a result, much energy will be deposited in the brightly lit plasma column connecting electrode and workpiece. In this phase, not only temperature but also pressure rapidly increasing in the plasma channel generates a spark. At the point of spark contact, insignificant amount of material melts and evaporates from the electrode and the workpiece. A bubble composed of gaseous by-products of vaporization rapidly expands outwards from the spark channel. When the pressure of the expanded bubble drops lower than the atmospheric pressure, the bubble collapse occurs and liquid jets infiltrate into the bubble. This liquid jet strikes into the generated molten crater and ejects molten material [9]. At the end of pulse duration, dielectric recovers its strength because of the recombination of ions and electrons [8] and flushes away molten and ejected materials from both electrode and workpiece.

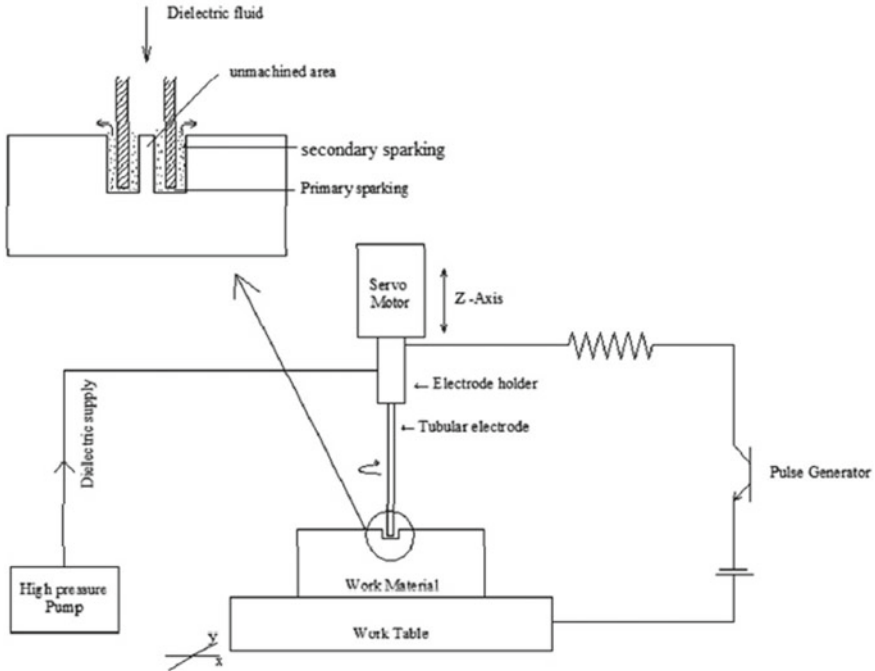


Fig. 1.1 Micro-EDM drilling set-up [10]

The working principle (Fig. 1.1) discussed above is also valid for conventional EDM processes. However, since micro-EDM is based on small discharge energies, short pulses and has a quite small gap, it is expected to observe some phenomena different than conventional EDM processes. Qian et al. [11] have conducted some experiments using RC-type generators to understand the fundamental characteristics of micro-EDM process. They reported that after normal discharges, resonance with large amplitude and frequency occurs, in the tank circuit which composed of parasitic inductance of the cable, charging capacitance, parasitic capacitor of the discharge gap and discharge cable and gap voltage. Due to high-frequency nature of the sparks, developed plasma channel does not have enough time to be fully neutralized. Consequently, due to high negative voltage and debris accumulation, gap breakdown may occur under reverse polarity and may lead to alternating current flow. On the other hand, the hypothesis of open plasma channel after regular discharges reveals the existence of flow of alternating current in micro-EDM, which causes multiple sparking and increased material removal rates with respect to the discharging without negative current flow.

In another study, to better understand the characteristics of micro-EDM, Wong et al. [12] have come up with the idea of a single spark generator to investigate the differences in material removal mechanism of conventional EDM and micro-EDM. Their findings revealed that for sufficiently low energy discharges ( $<50 \mu\text{J}$ ),

the specific material removal energy (defines as the energy essential to eradicate unit volume of material) is smaller than that of high energy discharges. Also, their observations showed that at small energies, more consistent and uniform craters are generated. Variation of material removal mechanism due to various pulse durations has been analysed by Singh and Ghosh [13]. Based on their study, removal mechanism differs for different EDM regimes based on pulse duration. At very short pulse duration ( $<5 \mu\text{s}$ ), which is considered dominant pulse duration in micro-EDM, melting cannot be considered as the dominant material removal mechanism. This is due to the fact that material has barely adequate time to be sufficiently heated to its melting/evaporation point. However, due to the presence of large electrostatic forces acting on the surface of the material yielding can cause the removal of the material from the workpiece. Therefore, based on the recent findings regarding the mechanism involved in material removal during micro-EDM process, it can be seen that micro-EDM relies on a very complex material removal mechanism when compared to conventional EDM processes. This implies that when modelling material removal in micro-EDM thermal models may be insufficient, other material removal mechanisms should also be included to accurately predict the process outputs.

## 1.4 Process Parameters and Performance Criteria

The main idea behind using the micro-EDM drilling is the production of high-precision deep micro-holes in difficult-to-machine materials, which is challenging or impossible to be manufactured using other machining methods. However, there are several factors which may result in uncertainty in the measurement of micro-hole diameters, including poor surface quality and imperfections in the micro-hole geometry [14]. These characteristics are functions of micro-EDM process variables such as discharge energy, electrode material and polarity, pulse duration and electrode rotational speed. Therefore, attempt should be made to select proper micro-EDM drilling process parameters in order to have a cost-effective, precise and efficient micro-drilling operation. Additionally, the production of high-precision microelectrodes can also be considered as an important requirement for successful EDM hole drilling. To produce high-precision microelectrodes, either wire electro-discharge grinding (WEDG) [15] or centerless grinding [16] can be used, for example centerless grinding has been used by Her and Weng [17] to obtain high-precision microelectrodes. A foremost methodological challenge for micro-EDM drilling is the production of holes with high aspect ratio and diameters smaller than  $100 \mu\text{m}$ .

In order to improve the micro-hole quality, it is necessary to use low discharge energies. One efficient way of reducing discharge energy is to decrease the stray capacitance between workpiece and electrode [18]. However, the most significant of all the aforementioned controlling parameters are micro-drilling process parameters which are selected during process planning for micro-EDM hole drilling. The awareness about the function and influence of each parameter could be of paramount importance to conduct a successful micro-EDM hole drilling task. Therefore, several

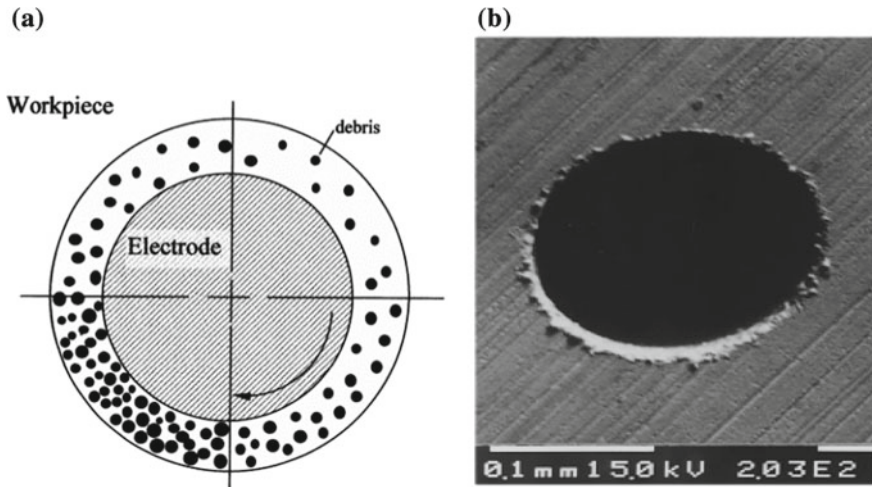
studies in the literature are devoted to explore the effect of process input parameters on the performance measures of micro-EDM hole drilling such as material removal rate (MRR), electrode wear ratio (EWR), taperness, micro-hole enlargement, surface quality, achievable aspect ratio and circularity.

In a study conducted by Her and Weng [17], the effect of electrode polarity on the process outputs of micro-EDM hole drilling of copper plates using tungsten carbide and copper electrodes has been investigated. The reason for selecting tungsten carbide as electrode material is reported as its high wear resistance, high temperature resistance and its high stiffness which makes it conceivable to produce high aspect ratio ( $L/D$ ) micro-holes. Their results revealed that positive polarity can result in smaller tool wear and micro-hole enlargement, while MRR is low. Alternatively, when using negative polarity machining speed can be increased which also results in larger tool wear. Their results also showed that the use of rotating electrode is helpful in debris evacuation and increasing material removal rate; however, it results in an increased surface roughness and electrode wear. Based on their results, electrode made of copper materials could deliver superior surface quality and lesser electrode wear with lower material removal rate compared to tungsten carbide electrode.

Micro-hole drilling of carbide using copper electrodes has been reported by Yan et al. [18]. In their study, attempts have been made to minimize hole enlargement and tool wear by selecting optimum tool rotational speed, electrode polarity and electrode shape (diameter and notch size). Their results revealed that by increasing diameter of the electrode, hole enlargement increases. This increment is attributed to the increased possibility of secondary sparks due to an increased debris concentration in the gap. Change in the tangential velocities as a result of change in the diameter of the electrode has also been reported as another factor affecting hole enlargement because of its effect on the fluid flow and turbulence in the gap along with its effect on debris evacuation. It has been observed that hole enlargement can be reduced by increased tool rotational speed. Creation of a notch is reported to affect hole enlargement, since it would help debris evacuation and reduce the chance of secondary discharges. However, the notch size should be optimized in a way that to minimize hole enlargement without increasing electrode wear.

Debris evacuation is quite problematic in micro-EDM hole drilling operation. Although horizontal set-up can be used to reduce the effect of gravity [19], it may also result in micro-holes with elliptical shapes due to concentrated debris at the bottom of the discharge gap as illustrated in Fig. 1.2 [18]. Debris can also be deposited on the electrode which results in a larger effective electrode diameter and consequently hole enlargement.

Yu et al. [19] studied the effectiveness of using planetary motion of the electrode for deep hole micro-drilling operations where aspect ratios up to 18 were achieved on stainless steel. Their results revealed that using planetary motion of the electrode can provide enough space for debris evacuation and reduce their concentration in the gap. Therefore, accuracy and material removal can be increased and electrode wear can be significantly reduced.



**Fig. 1.2** **a** Model of debris distribution in horizontal micro-EDM. **b** Elliptical micro-hole due to debris accumulation [18]

High electrode wear ratio, considerably low material removal rate and difficulty in machining holes with aspect ratios larger than 20 have been reported as the drawbacks of micro-EDM hole drilling process [20].

It has been reported by Fu et al. [20] that the type of dielectric fluid affects electrode wear. They used two different materials (tungsten and tungsten carbide) as tool material, and their results revealed that irrespective of tool materials, deionized water presents lesser electrode wear compared to dielectric oil. This has been reported as the reason to prefer deionized water in most practical applications. Their observations also revealed that the tungsten electrode wear is lesser compared to tungsten carbide regardless of the type of dielectric fluid used.

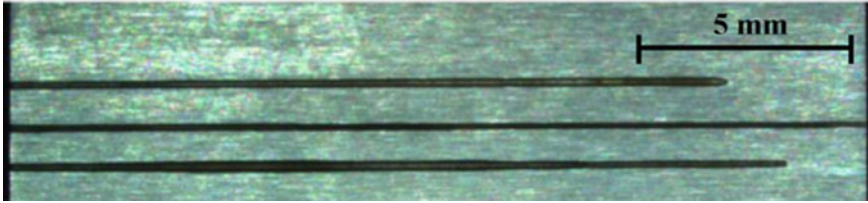
In order to select a suitable electrode material, the erosion resistance index can be used [21]. This index can be used as an indication of electro-discharge machinability of different materials and can be calculated as follows:

$$C_m = \lambda c T_m^2$$

where  $\lambda$  is the thermal conductivity,  $c$  is the specific heat and  $T_m$  is the melting point.

Ay et al. [22] have studied on Inconel 718 alloy using grey rational analysis. Hole taperness and overcut are considered as process performance parameters for micro-EDM drilling while discharge current and pulse duration are considered as process input variables at a constant rotational speed of 300 RPM. In their study, copper—tungsten electrodes (Cu–75 wt% W) of 500  $\mu\text{m}$  diameter are used. As per the research investigation, pulse current seems to have greater effect on multi-performance characteristics of micro-EDM drilling process compared to pulse duration. In addition,





**Fig. 1.3** Ultra-high aspect micro-holes abtained by Parylene C-insulated electrodes [24]

shortening pulse duration and decreasing discharge current have shown to be helpful in reducing crack and damages on the machined surfaces.

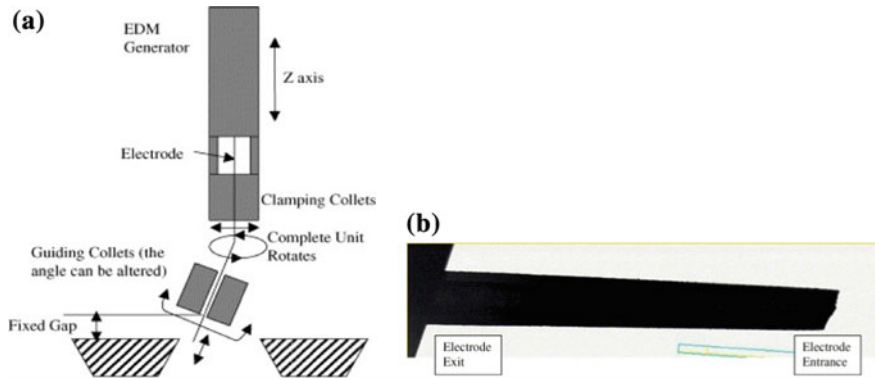
It is understood that for deep micro-hole drilling, the most important limiting factor is the accumulation of melted materials at the bottom of the electrode. It results in an unstable drilling process due to the creation of abnormal discharges such as arcing and short circuiting along with reduced accuracy and increased taperness due to excessive electrode wear [23].

By integrating an ultrasonic unit into EDM process, debris concentration in the gap can become more uniform and material removal can be improved as a result of variation of the hydrostatic pressure of the dielectric fluid [23]. The ultrasonic-induced vibrations are used because they mainly increase the wetting capability of the dielectric fluid, meaning that they provide the opportunity to drive the dielectric fluid even within a narrow gap [24]. These methods are shown to be promising for producing deep micro-holes, but are shown to be still insufficient for the production of micro-holes with ultra-high aspect ratio ( $AR > 30$ ).

Insulation of the sidewall of the electrode by applying a low electrically conductive coating has been reported by Ferraris et al. [24] as an efficient method to achieve micro-holes with ultra-high aspect ratio. The idea was to reduce the possibility of the generation of secondary sparks between the flank face of the electrode and workpiece. Their results revealed that when using Parylene C as a coating material, holes with aspect ratios up to 126 can be achieved. Figure 1.3 shows a cross section of the drilled micro-holes having ultra-high aspect ratio using Parylene C-coated tools.

## 1.5 Micro-EDM Drilling of Hard-to-Cut Materials

Micro-drilling can be realized using various manufacturing techniques such as laser beam machining (LBM), electron beam machining (EBM), electro-discharge machining (EDM), mechanical micro-drilling and micro-punching. Among these techniques, LBM, EBM and micro-punching methods are well suited for micro-holes with small aspect ratios. While mechanical micro-drilling can be used to drill micro-holes with high aspect ratio, workpiece hardness and machinability are the major problems in this process [25]. Therefore, workpiece with higher hardness requires mostly non-conventional machining such as micro-EDM drilling.



**Fig. 1.4** **a** Improved experimental design for fabricating reversed micro-holes and **b** tapered hole ( $35\ \mu\text{m}/\text{mm}$ ) using improved techniques [27]

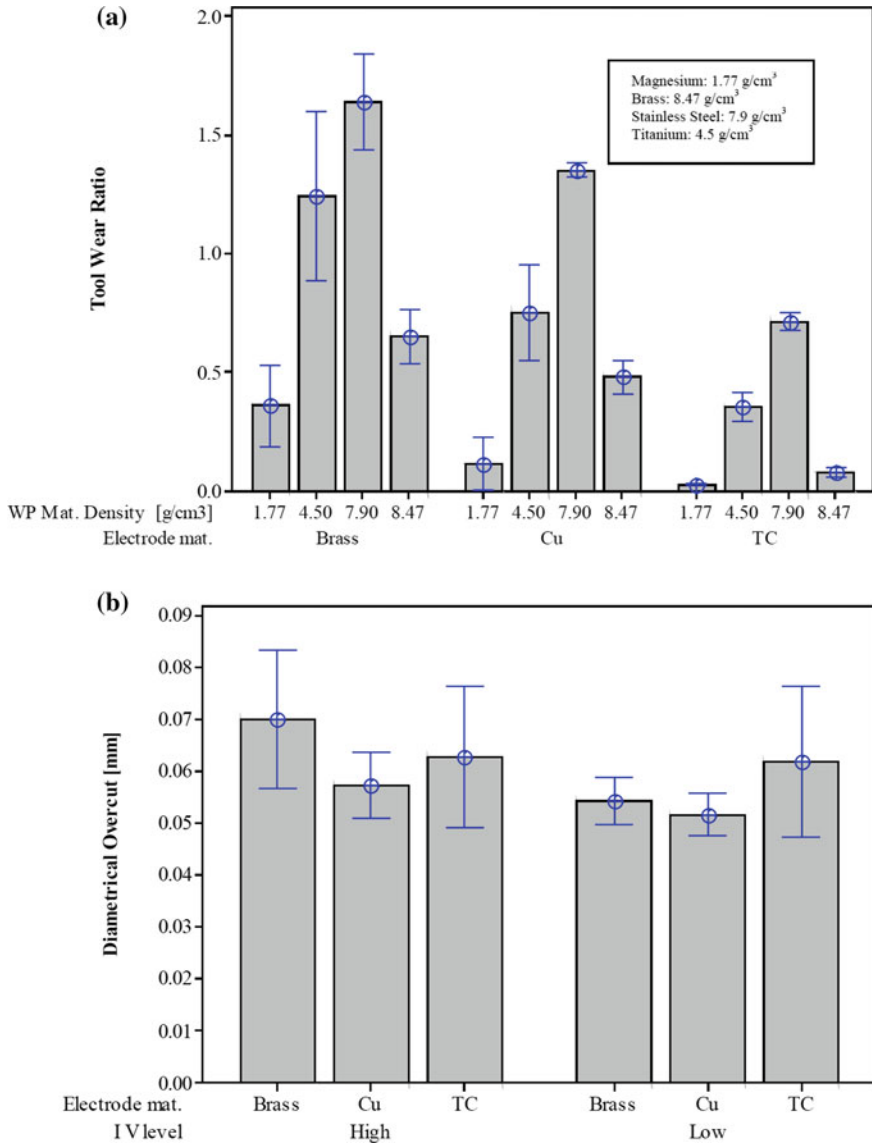
### 1.5.1 Stainless Steel

Since micro-EDM requires no mechanical contact between electrode and workpiece, it can be successfully used for deep hole micro-drilling of hard-to-machine materials. Several researchers have reported the successful employment of micro-EDM hole drilling for deep hole micro-drilling of hard-to-cut materials. Masuzawa et al. [25] have reported micro-EDM drilling of holes with aspect ratios of 10 using brass electrodes in hardened and tempered high carbon steel SK5. The results of their experiments revealed that when using an electrode having diameter of  $80\ \mu\text{m}$ , the process is quite fast at the first  $500\ \mu\text{m}$  of drilling; however, the process slows down as the depth of hole increases.

Deep hole micro-drilling of austenitic stainless steel (SUS 304) and cemented tungsten carbide (WC-Co) have been investigated by Jahan et al. [26] using an RC-type pulse generator at different discharge energies with electrodes having different electro-thermal properties. In their study, the quality and accuracy of micro-holes (hole enlargement, taperness and circularity), machining stability, MRR and EWR are considered as micro-drilling process performance characteristics.

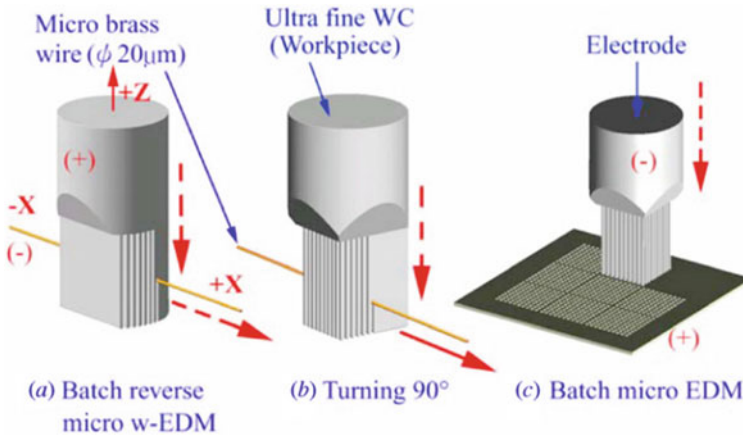
Diver et al. [27] proposed new experimental design to fabricate reversed micro-holes where taperness of holes can be controlled on case-hardened steel plate as can be seen in Fig. 1.4. With the aid of this new fixture, tapered holes with larger exit diameter ( $160\text{-}\mu\text{m}$ -diameter exit,  $100\text{-}\mu\text{m}$ -diameter entry) is possible to manufacture. This technique appears to be repeatable, stable and eliminates the necking effect that usually appears on the exit.

On another research by D'Urso et al. [28], effect of electrode materials and shape as well as electrical parameters were investigated on brass, magnesium, stainless steel and titanium (grade 2). Considering TWR, tungsten carbide electrode outperforms copper and brass electrodes, whereas brass experiences severe TWR (Fig. 1.5). Nevertheless, electrode material has no significant effect on the geometry



**Fig. 1.5** a TWR versus tool materials and b diametrical overcut versus tool materials [28]

of the micro-holes fabricated. Cylindrical electrode shows low TWR for steel and brass sample, whereas tubular electrode shows low value of TWR for titanium as well as magnesium. D’Urso et al. [29] also investigated on steel materials using ANOVA technique where effect of tubular tungsten carbide and brass tool as well as process parameters was evaluated. Their result revealed better MRR by brass



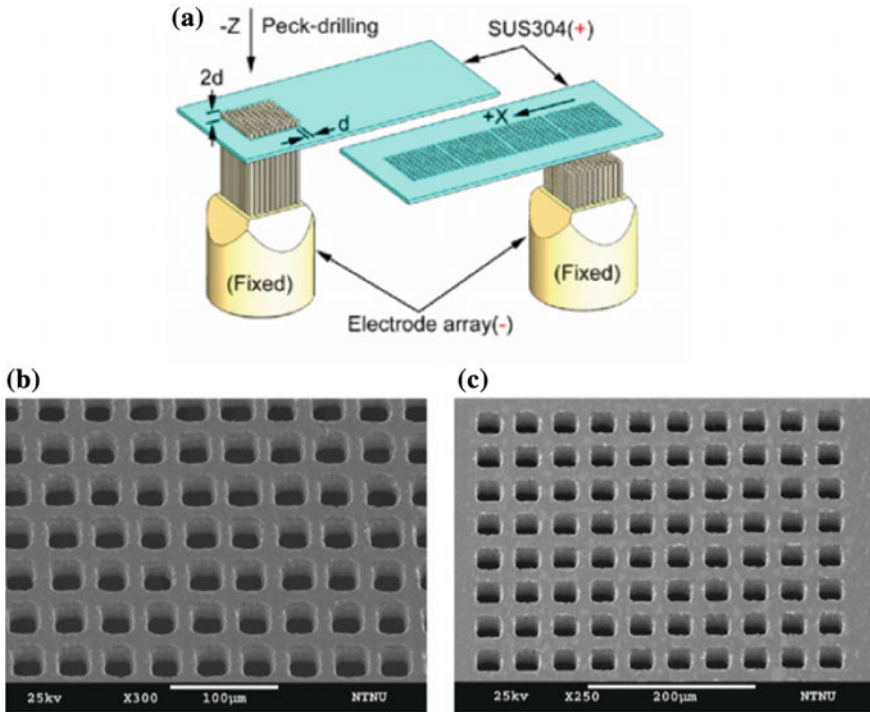
**Fig. 1.6** Batch production of arrays of micro-holes [31]

electrode despite of high TWR due to higher electrical conductivity of brass. Both the electrodes show higher MRR with the increase of discharge energy.

Apart from usual EDM drilling, dry EDM drilling on SS304 material was studied by Joshi et al. [30] where L27 orthogonal design array was used for three levels of six input parameters. As per statistical analysis, MRR is affected considerably by process current, gap voltage as well as tool rotational speed. Almost zero tool wear and deposition of work materials on the tool were observed. They also reported on larger crater size and higher MRR for dry EDM drilling compared to the one with liquid dielectric.

Manufacturing of bulk amount of micro-holes using a  $10 \times 10$  microstructure array of width of  $21 \mu\text{m}$ , height of  $700 \mu\text{m}$  and spacing of  $21 \mu\text{m}$  on stainless steel has been also investigated by Chen [31] as depicted in Fig. 1.6. It has been shown that the geometry of the tip of each micro-pillar-shaped electrode directly affects the quality and size of the machined micro-holes, where when using circular pyramid tip electrode, better edge qualities and smaller holes can be achieved compared to the square flat end electrodes. The batch micro-hole proposed by Chen [31] showed a threefold decrease in micro-hole production time compared to single-electrode micro-EDM hole drilling.

Batch production of micro-holes on SUS304 using upward batch reverse micro-EDM drilling was successfully demonstrated by Chen [32]. Applications of batch micro-holes are found in the biomedical components, inkjet nozzles and micro-droplet spraying parts. In order to fabricate the batch micro-holes, electrode with micro-arrays was fabricated using wire EDM technique and then this array of electrodes was moving upward towards the  $30 \mu\text{m}$  thickness SUS304 plate to drill arrays of holes (Fig. 1.7a). This technique facilitates efficient debris removal and reduces the abnormal discharges generation with the help of gravity and pumping effect. Eventually, improved machining time as well as burr-free holes can be achieved.

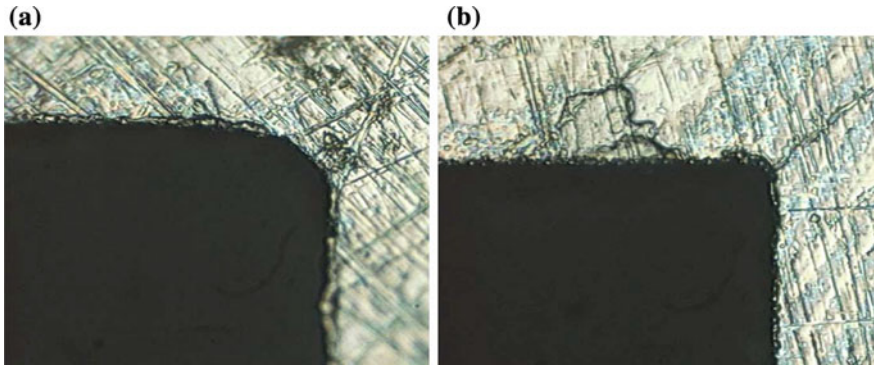


**Fig. 1.7** a Schematic of upward micro-EDM for batch production, b array of micro-holes: entrance side and c exit side [32]

Chern et al. [33] also investigated on vibration-assisted micro-EDM to fabricate circular and non-circular electrodes of below 200  $\mu\text{m}$  diameter with better surface finish. These electrodes were used to punch micro-holes successfully on brass and SUS304 stainless steel using vibration-aided micro-EDM drilling. However, in order to improve the corner geometry of non-circular micro-hole, finish micro-EDM drilling is also conducted right after the rough machining (Fig. 1.8). Yu et al. [23] also demonstrated micro-holes of 29 aspect ratio with the application of ultrasonic vibration and planetary movement due to the reduction of viscous resistance of dielectric.

### 1.5.2 Ni Alloys

The feasibility of using micro-EDM hole drilling to produce micro-holes on hard-to-machine materials like nickel alloy (Ni-79 wt%, Mo-4 wt%) has been studied by Liu et al. [34], since it is extremely challenging to drill micro-holes in this alloy by conventional machining techniques because of its high toughness and hardness. The



**Fig. 1.8** Corner in square micro-holes after, **a** rough EDM and **b** finish EDM [33]

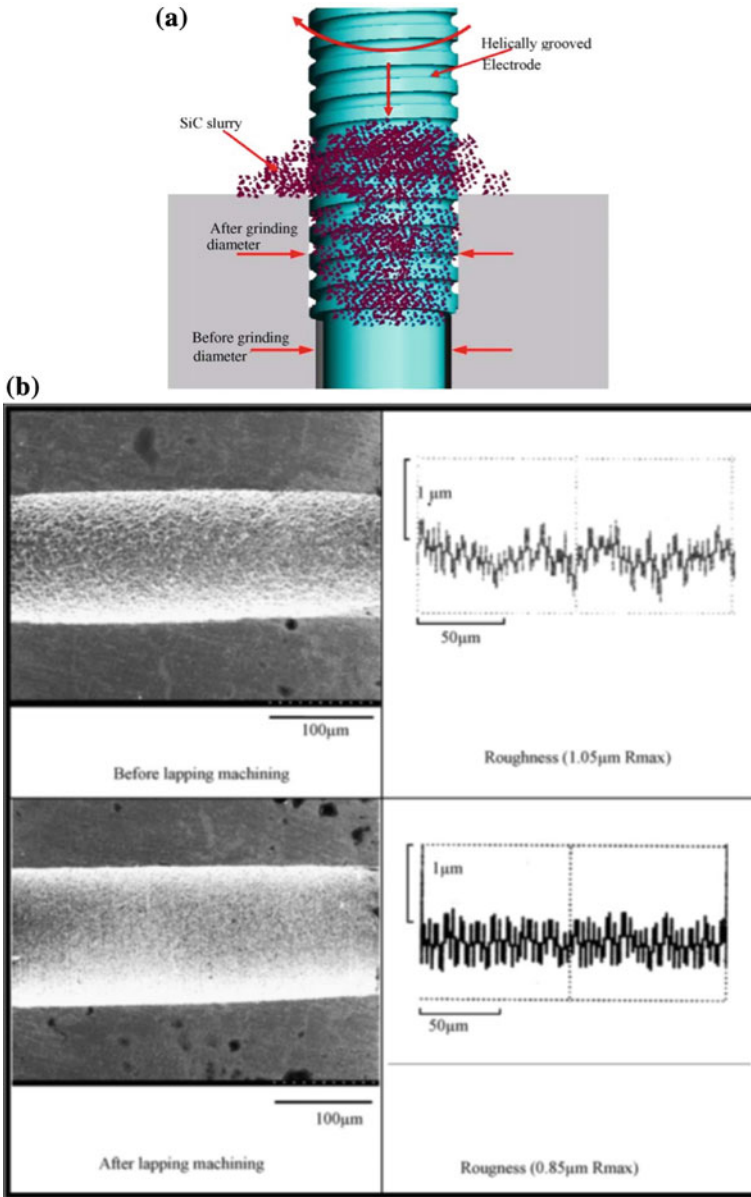
reason for studying high nickel alloy was because of its excellent magnetic shielding properties which makes it a suitable material for micro-electro-mechanical system (MEMS) applications. Liu et al. used a two-stage electrode having stepped diameter (Fig. 1.9a) to achieve a better circularity of micro-holes. This method also helps to enhance the surface condition of the micro-holes due to subsequent lapping action as seen in Fig. 1.9b.

Ay et al. [22] investigated on Inconel 718 superalloy in order to correlate the effect of pulse duration as well as pulse current with taperness and hole overcut using grey rational analysis and reported the significance of pulse current compared to pulse duration. Figure 1.10 shows the effect of both input variables on the exit and entrance of micro-hole. Pulse duration and pulse current both contribute to discharge energy. Increase of energy density and duration can affect the hole roundness as well as increased heat-affected zone as seen in Fig. 1.10. Figure 1.11 also shows the incremental hole dilation for increased discharge current as well as pulse duration.

Imran et al. [35] have compared the micro-holes fabricated by micro-EDM drilling, laser drilling and mechanical micro-drilling on Inconel 718. As per their observation, both EDM and laser are capable of producing high aspect ratio holes but it comes with taperness effect, micro-cracks as well as larger hardness on machined area. On the other hand, mechanical micro-drilling offers better surface roughness and circularity, comes with no recast layer but with high tool wear.

Hung et al. [36] effectively demonstrated micro-EDM drilling of Ni alloy with better surface roughness using on-machine fabricated stepped diameter electrode. Micro-tool is fabricated using sequential WEDG and electrodeposition of Ni-SiC is exploited to micro-EDM drilling on Ni Alloy. Additional step of micro-grinding on micro-holes using the larger diameter of electrode can reduce surface roughness from 1.47 to 0.462  $\mu\text{m}$ .

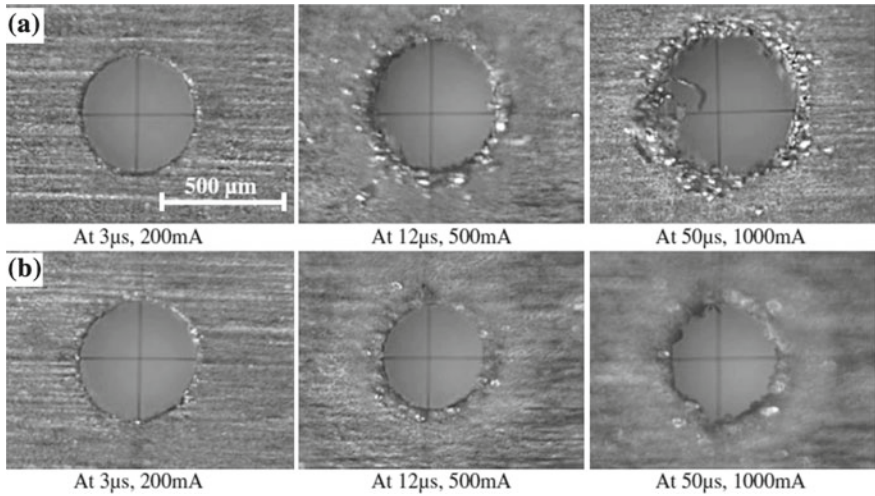
While investigating on micro-EDM drilling of Ni X Alloy, Perveen et al. [37] modelled the crater size generated on blind holes. Their study used Box-Behnken design and response surface method in order to find the combined effect of input parameters (voltage, capacitance, tool rotation) on the crater size which also indicates the surface



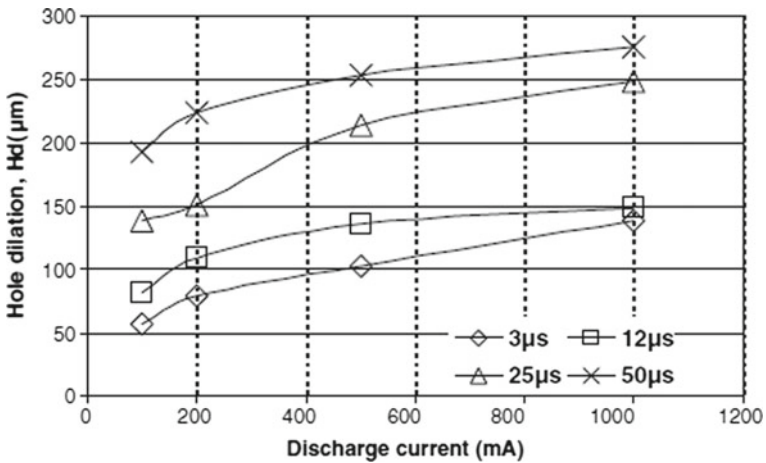
**Fig. 1.9** a Schematic of stepped micro-electrode used by Liu et al. [34], b scanning electron microscopy image of micro-hole before and after lapping machining process (current = 500 mA)

roughness on blind micro-holes. On another study, Perveen et al. [38] also conducted comparative micro-EDM drilling study on Ni X alloy, using uncoated and diamond-coated tungsten carbide tool. Their observation suggested reduced machining time





**Fig. 1.10** Entrance (a) and exit (b) photograph of micro-holes for various values of current and pulse duration using 500- $\mu\text{m}$  electrode [22]



**Fig. 1.11** Variation of hole dilation due to discharge current as well as pulse duration [22]

for increased discharge energy, and the trends remain same for both tools. Nevertheless, amount of overcut generated is less for coated tool compared to uncoated tool. Bhosle et al. [39] also investigated on Inconel 600 alloy using grey rational analysis and optimized input variables such as capacitance, voltage, feed rate for maximizing MRR and minimizing taper, diameter variation as well as overcut. Their research also revealed capacitance as most influential input parameter.



### 1.5.3 *Ti Alloys*

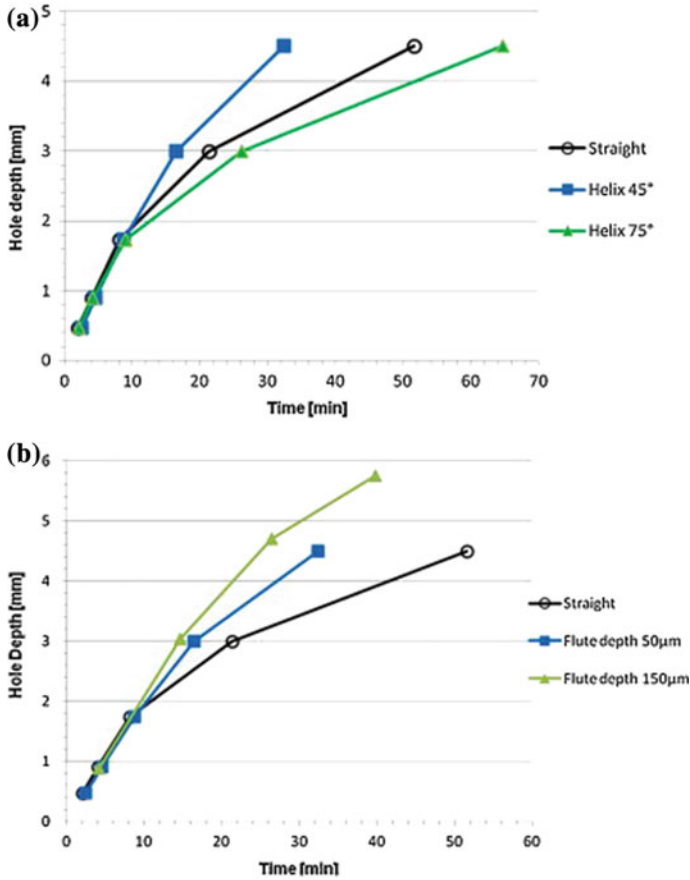
Titanium alloys which have found widespread applications in different industries including aerospace and biomedical are another important class of difficult-to-cut materials due to their relatively lower thermal conductivity, large elastic recovery as well as strong chemical reactivity for other materials. Their tendency for built-up edge (BUE) formation could be quite problematic because of changing cutting-edge geometry, which may result in an accelerated tool wear or premature tool failure during cutting and drilling operations. Therefore, the use of non-traditional machining processes for drilling these materials is gaining a significant importance as the demand for using these materials in different industries increases rapidly.

In a study conducted by Meena and Azad [40], micro-EDM drilling of Ti6Al4V alloy has been studied using grey relational analysis to examine the effect of process variables on the performance measures of the process such as MRR, EWR and overcut. Their results showed that voltage is the most contributing input parameter followed by current, pulse width and frequency. Li et al. [41] have also investigated on the feasibility of using micro-EDM hole drilling for micro-drilling of Ti6Al4V. They used a tungsten carbide electrode of 250  $\mu\text{m}$  as electrode material. The low thermal conductivity of titanium alloy has been reported to have a detrimental effect on surface quality and stability of the micro-EDM drilling process. They also compared the micro-EDM drillability of Ti6Al4V with SUS 316 stainless steel. Their results showed that SUS 316 has better drillability characteristics in terms of either achievable surface quality or deep hole drillability. It has also been reported that for same micro-EDM drilling parameters, the micro-holes in titanium alloy produce larger heat-affected zone.

In order to address inefficient debris removal during deep hole micro-drilling, Plaza et al. [42] recommended a novel approach of using helical tool for micro-EDM drilling of Ti6Al4V. As per their observation, 37% of machining time is achieved while using 45° helix angle as well as 50  $\mu\text{m}$  of flute depth (Fig. 1.12). As a result, their approach can reach aspect ratio up to 10:1 effectively.

Kibria et al. [43] also investigated on Ti alloy using pure kerosene, kerosene and deionized water mixed with boron carbide. As per their observation, deionized water enhances both MRR and TWR compared to kerosene. In addition, presence of boron carbide particles in dielectric such as deionized water aids in increased MRR; however, kerosene aids in reduced TWR [43].

Another study done by Jahan et al. [44], on tungsten workpiece, demonstrated that better surface roughness can be obtained by compromising high MRR, relative wear ratio, whereas surface roughness and electrode wear will be compromised when opted for higher MRR. Wangsheng et al. [45] demonstrated micro-EDM drilling of hole with more than 15 aspect ratio successfully with the aid of ultrasonic vibration. Their research suggested improved liquid flow in the gap and avoidance of debris due to vibration-assisted micro-EDM drilling, thus enhancing the machining efficacy and stability.



**Fig. 1.12** **a** Effect of helix angle on hole depth for 800- $\mu$ m-diameter electrode, **b** effect of flute depth on hole depth using 800- $\mu$ m-diameter electrode [42]

Perveen et al. [46] also applied full factorial design to investigate the machinability of Ti-6Al-4V alloy with the help of solid end mill made of carbide and proposed statistical model for each output parameter. In their study, main effect plot, interaction plot as well as Pareto chart were used for better comprehension of the individual and combined effect of machining parameters on the time taken for machining, electrode wear and hole dilation. Similar study was conducted by Tiwary et al. [47] for through-hole micro-EDM drilling where central composite experimental design was used for running the experiment. Multi-objective optimization using response surface method for performance parameters such as MRR, TWR, OC and taper was conducted, and it was suggested that performance parameters were influenced by input parameters such as discharge current, pulse on time, spark gap as well as flushing pressure. Jahan et al. [48] also conducted similar study using full factorial design on Ti-6Al-4V alloys. In

addition, Krishnaraj et al. [49] used Taguchi design for optimization of parameters and recommended peak current as well as pulse current as most significant input parameters to influence the output parameters.

## 1.6 Challenges and Future Trends of Micro-EDM Drilling

Although micro-EDM drilling seems to be an amazing and promising technology due to its flexibility to cater the needs coming from the miniaturization trends, it is somehow experiencing some challenges as reported by the researchers.

- Low MRR, i.e. slow machining process, is an inherent issue associated with micro-EDM drilling process. This makes it more difficult to act as a mass production process for industrial usage.
- Another important drawback arises due to debris removal during deep hole drilling, which eventually limits not only the effectiveness of the process but also the aspect ratio of the drilled holes. Deep holes also come with tapered wall and significant overcut issue. It was reported to achieve aspect ratio of 10 while micro-EDM drilling of nickel alloy. Nevertheless, vibration-assisted micro-EDM drilling can enhance the aspect ratio slightly.
- In addition, tool wear causes serious issue during micro-EDM drilling process, as it can affect the dimensional accuracy significantly. Also fabrication of small scale holes needs the fabrication of small micro-tools, which in turn requires smaller discharge energy meaning smaller capacitance and smaller voltage settings [50].

Future research direction and development in the area of micro-EDM drilling will be aiming on the underpinning principle of the process apart from widening this process application to other industries. Few points of future research directions are mentioned categorically as follows.

- Hybrid process combining two or more than two processes will be explored in future, where each process will complement the weakness of others, thus facilitating reduced drawbacks arise from single manufacturing process. Hybrid process combining micro-EDM drilling plus laser is already in the research phase and demonstrates paramount potential not only in terms of material removal rate but also dimensional accuracy.
- Future research also may focus on the micro-EDM drilling of semi-conductive/non-conductive ceramics along with assisted electrode micro-EDM drilling, or conductive coating as well as carbon nanofibres mixed dielectric [2].
- Another important aspect of future research might be the automation of micro-EDM drilling process for larger batch manufacturing. While considering this automation technique, on-machine fabrication of tool, dimensional measurement and correction during the process should also be incorporated.
- Another important research trend will be to develop multi-purpose machine tool which will facilitate the hybrid machining as well as sequential machining processes in a single set-up.

- Further size reduction in hole diameter will necessitate the pulse generator to produce nano-joule discharge energy, which will accelerate the potential nano-EDM drilling process [50].

## 1.7 Summary

This chapter has presented one of the most imperative non-conventional techniques, micro-EDM drilling process and its application to difficult-to-cut materials. Detailed description of machining as well as performance variables for micro-EDM Drilling process was narrated. Recent development in the micro-EDM drilling process has demonstrated its competency to manufacture large aspect ratio micro-holes. Because of its several unique process characteristics, micro-EDM drilling continues to find its application in several important industries from aerospace to microelectronics. Recent research trends show that micro-EDM drilling experiences some inherent process limitations such as longer machining time, inferior surface finish as well as taperness issue; therefore, combining this process with other mechanical or thermal processes appears to be effective where one process can complement other process. Since the most important aspect of micro-EDM drilling is the power generator, continued development of micro-EDM power generator can enable it to achieve further breakthroughs in the future.

## References

1. Yamane Y, Sekiya K (2004) An evaluation of difficulty in machining difficult-to-cut materials by using difficult-to-cut rating. *J JSPE* 70(3):407–411
2. Prakash V, Kumar P, Hussain M, Das AK, Chattopadhyaya S (2017) Micro-electrical discharge machining of difficult-to-machine materials: a review. *Proc Inst Mech Eng, Part B: J Eng Manuf.* <https://doi.org/10.1177/0954405417718591>
3. Ho KH, Newman ST (2003) State of the art electrical discharge machining (EDM). *Int J Mach Tools Manuf* 43(13):1287–1300
4. Pham DT, Dimov SS, Bigot S, Ivanov A, Popov K (2004) Micro-EDM—recent developments and research issues. *J Mater Process Technol* 149(1–3):50–57
5. Masuzawa T (2000) State of the art of micromachining. *CIRP Ann Manuf Technol* 49(2):473–488
6. Meek JM, Craggs JD (1978) *Electrical breakdown of gases*. Wiley, New York
7. Lee TH (1959) T-F theory of electron emission in high-current arcs. *J Appl Phys* 30(2):166–171
8. Kunieda M, Lauwers B, Rajurkar MP, Schumacher BM (2005) Advancing EDM through fundamental insight into the process. *CIRP Ann Manuf Technol* 54(2):64–87
9. Hockenberry TO, Williams EM (1967) Dynamic evolution of events accompanying the low-voltage discharges employed in EDM. *IEEE Trans Ind Gen Appl* 4:302–309
10. Kumar K, Rawal SK, Singh VP, Bala A (2018) Experimental study on diametric expansion and taper rate in EDM drilling for high aspect ratio micro holes in high strength materials. *Mater Today: Proc* 5(2, Part 2):7363–7372
11. Qian J, Yang F, Wang J, Lauwers B, Reynaerts D (2015) Material removal mechanism in low-energy micro-EDM process. *CIRP Ann* 64(1):225–228

12. Wong YS, Rahman M, Lim HS, Han H, Ravi N (2003) Investigation of micro-EDM material removal characteristics using single RC-pulse discharges. *J Mater Process Technol* 140(1–3):303–307
13. Singh A, Ghosh A (1999) A thermo-electric model of material removal during electric discharge machining. *Int J Mach Tools Manuf* 39(4):669–682
14. Muralikrishnan B, Stone J, Stoup J (2009) Diameter and form measurement of a micro-hole in a fuel injector nozzle with the NIST fiber probe. In: Proceedings of ASPE annual meeting, Monterey, Canada
15. Masuzawa T, Fujino M, Kobayashi K, Suzuki T, Kinoshita N (1985) Wire electro-discharge grinding for micro-machining. *CIRP Ann Manuf Technol* 34(1):431–434
16. Rowe W, Miyashita M, Koenig W (1989) Centreless grinding research and its application in advanced manufacturing technology. *CIRP Ann Manuf Technol* 38(2):617–625
17. Her M-G, Weng F-T (2001) Micro-hole machining of copper using the electro-discharge machining process with a tungsten carbide electrode compared with a copper electrode. *Int J Adv Manuf Technol* 17(10):715–719
18. Yan B, Huang FY, Chow HM, Tsai JY (1999) Micro-hole machining of carbide by electric discharge machining. *J Mater Process Technol* 87(1–3):139–145
19. Yu Z, Rajurkar KP, Shen H (2002) High aspect ratio and complex shaped blind micro holes by micro EDM. *CIRP Ann Manuf Technol* 51(1):359–362
20. Fu Y, Miyamoto T, Natsu W, Zhao W, Yu Z (2016) Study on influence of electrode material on hole drilling in micro-EDM. *Procedia CIRP* 42:516–520
21. Reynaerts D, Heeren PH, Brussel HV (1997) Microstructuring of silicon by electro-discharge machining (EDM)—part I: theory. *Sens Actuators A: Phys* 60(1–3):212–218
22. Ay M, Çaydaş U, Hasçalık A (2013) Optimization of micro-EDM drilling of Inconel 718 superalloy. *Int J Adv Manuf Technol* 66(5–8):1015–1023
23. Yu ZY, Zhang Y, Li J, Luan J, Zhao F, Guo D (2009) High aspect ratio micro-hole drilling aided with ultrasonic vibration and planetary movement of electrode by micro-EDM. *CIRP Ann* 58(1):213–216
24. Ferraris E, Castiglioni V, Ceyskens F, Annoni M, Lauwers B, Reynaerts D (2013) EDM drilling of ultra-high aspect ratio micro holes with insulated tools. *CIRP Ann* 62(1):191–194
25. Masuzawa T, Tsukamoto J, Fujino M (1989) Drilling of deep microholes by EDM. *CIRP Ann Manuf Technol* 38(1):195–198
26. Jahan MP, Wong YS, Rahman M (2010) A comparative experimental investigation of deep-hole micro-EDM drilling capability for cemented carbide (WC–Co) against austenitic stainless steel (SUS 304). *Int J Adv Manuf Technol* 46(9–12):1145–1160
27. Diver C, Atkinson J, Helml HJ, Li L (2004) Micro-EDM drilling of tapered holes for industrial applications. *J Mater Process Technol* 149(1):296–303
28. D’Urso G, Merla C (2014) Workpiece and electrode influence on micro-EDM drilling performance. *Precis Eng* 38(4):903–914
29. D’Urso G, Maccarini G, Ravasio C (2014) Process performance of micro-EDM drilling of stainless steel. *Int J Adv Manuf Technol* 72(9):1287–1298
30. Govindan P, Joshi SS (2010) Experimental characterization of material removal in dry electrical discharge drilling. *Int J Mach Tools Manuf* 50(5):431–443
31. Chen ST (2007) A high-efficiency approach for fabricating mass micro holes by batch micro EDM. *J Micromech Microeng* 17(10):1961
32. Chen ST (2008) Fabrication of high-density micro holes by upward batch micro EDM. *J Micromech Microeng* 18(8):085002
33. Chern GL, Chuang Y (2006) Study on vibration-EDM and mass punching of micro-holes. *J Mater Process Technol* 180(1–3):151–160
34. Liu HS, Yan BH, Huang FY, Qiu KH (2005) A study on the characterization of high nickel alloy micro-holes using micro-EDM and their applications. *J Mater Process Technol* 169(3):418–426
35. Imran M, Mativenga PT, Gholinia A, Withers PJ (2015) Assessment of surface integrity of Ni superalloy after electrical-discharge, laser and mechanical micro-drilling processes. *Int J Adv Manuf Technol* 79(5–8):1303–1311

36. Hung JC, Wu WC, Yan BH, Huang FY, Wu KL (2007) Fabrication of a micro-tool in micro-EDM combined with co-deposited Ni–SiC composites for micro-hole machining. *J Micromech Microeng* 17(4):763
37. Perveen A, Jahan MP (2018) Application of Box Behnken design to model crater size generated during micro-EDM of NI-X alloy. *Int J Mech Eng Rob Res* 7(3):229–234
38. Perveen A, Jahan MP (2018) Comparative micro-EDM studies on Ni based X-alloy using coated and uncoated tools. *Mater Sci Forum* 911:13–19
39. Bhosle RB, Sharma SB (2017) Multi-performance optimization of micro-EDM drilling process of Inconel 600 alloy. *Mater Today: Proc* 4(2, Part A):1988–1997
40. Meena VK, Azad MS (2012) Grey relational analysis of micro-EDM machining of Ti-6Al-4V alloy. *Mater Manuf Process* 27(9):973–977
41. Li Y, Yu W, Xu J, Yu H (2016) A comparative investigation of micro-EDM drilling capability for Ti-6Al-4V alloy against austenitic stainless steel SUS 316. In: *IEEE international conference on mechatronics and automation*, Harbin, China, 7–10 Aug 2016
42. Plaza S, Sanchez JA, Perez E, Gil R, Izquierdo B, Ortega N, Pombo I (2014) Experimental study on micro EDM-drilling of Ti6Al4V using helical electrode. *Precis Eng* 38(4):821–827
43. Kibria G, Sarkar BR, Pradhan BB, Bhattacharyya B (2010) Comparative study of different dielectrics for micro-EDM performance during microhole machining of Ti-6Al-4V alloy. *Int J Adv Manuf Technol* 48(5–8):557–570
44. Jahan MP, Wong YS, Rahman M (2012) Experimental investigations into the influence of major operating parameters during micro-electro discharge drilling of cemented carbide. *Mach Sci Technol* 16(1):131–156
45. Wansheng Z, Zhenlong W, Shichun D, Guanxin C, Hongyu W (2002) Ultrasonic and electric discharge machining to deep and small hole on titanium alloy. *J Mater Process Technol* 120(1):101–106
46. Perveen A, Jahan MP, Zhumagulov S (2018) Statistical modelling and optimization of micro electro discharge machining of Ti Alloy. *Mater Today: Proc* 5(2):4803–4810
47. Tiwary AP, Pradhan BB, Bhattacharyya B (2015) Study on the influence of micro-EDM process parameters during machining of Ti–6Al–4V superalloy. *Int J Adv Manuf Technol* 76(1):151–160
48. Alavi F, Jahan MP (2017) Optimization of process parameters in micro-EDM of Ti-6Al-4V based on full factorial design. *Int J Adv Manuf Technol* 92(1–4):167–187
49. Krishnaraj V (2016) Optimization of process parameters in micro-EDM of Ti-6Al-4V Alloy. *J Manuf Sci Prod* 16(1):41–49
50. Jahan MP, Rahman M, Wong YS (2011) A review on the conventional and micro-electrodischarge machining of tungsten carbide. *Int J Mach Tools Manuf* 51(12):837–858

# Chapter 2

## Micro-electrical Discharge Milling Operation



Mahavir Singh, Vijay Kumar Jain and Janakarajan Ramkumar

**Abstract** This chapter introduces a novel variant of electric discharge machining (EDM) process entitled to electrical discharge milling (ED-Milling) operation. Although the mechanism of material removal is essentially identical to that of conventional EDM process, the intricacies arise predominantly pertaining to the multiple zones involved simultaneously during the sparking phenomenon. Unlike the Ram/die-sinking EDM or ED-Drilling operations comprising merely unidirectional control of the tool electrode, the ED-Milling operation is characterized by the synchronized movement of the tool in multiple axes (generally  $x$ -,  $y$ -, and  $z$ -axis) besides the high-speed rotation about its axis. This controlled motion of the tool electrode governed by the programmed instructions similar to the computerized numerical control (CNC) of conventional milling operation makes it a prospective contender especially for fabrication of 3D micro/macro-profiles. Incorporating a comparatively simpler cylindrical or in exceptional instances rectangular/square cross-sectional tool electrode to generate a complex three-dimensional feature is the distinctive capability of this operation. The chapter comprises the basic introduction to EDM process in conjunction with ED-Milling operation, different techniques of micro-tool production as well as micro-fabrication, suitability of ED-Milling operation for a variety of sophisticated areas, analysis of tool wear and the possible applications areas of the process.

---

M. Singh · V. K. Jain · J. Ramkumar (✉)  
Department of Mechanical Engineering, Indian Institute  
of Technology Kanpur, Kanpur 208016, U.P., India  
e-mail: [jrkumar@iitk.ac.in](mailto:jrkumar@iitk.ac.in)

M. Singh  
e-mail: [mahavir@iitk.ac.in](mailto:mahavir@iitk.ac.in)

V. K. Jain  
e-mail: [vkjain@iitk.ac.in](mailto:vkjain@iitk.ac.in); [vkj.iitk@gmail.com](mailto:vkj.iitk@gmail.com)

V. K. Jain  
Department of Mechanical Engineering, Maulana Azad National Institute  
of Technology Bhopal, Bhopal 462003, M.P., India

© Springer Nature Singapore Pte Ltd. 2019  
G. Kibria et al. (eds.), *Micro-electrical Discharge Machining Processes*, Materials  
Forming, Machining and Tribology, [https://doi.org/10.1007/978-981-13-3074-2\\_2](https://doi.org/10.1007/978-981-13-3074-2_2)

**Keywords** Micro-channels · Tool wear · Computer numerical control  
Taper angle · Micro-tools · Debris

## Nomenclature

$C$	Capacitance of the capacitor ( $\mu\text{F}$ )
$V_d$	Discharge voltage (V)
$I$	Machining current (A)
$t$	Pulse on time ( $\mu\text{s}$ or ns)
$\Delta x$	Average machining depth of a single layer ( $\mu\text{m}$ or mm)
$\Delta d$	Compensated depth of the tool considering the longitudinal wear ( $\mu\text{m}$ or mm)
$A_e$	Cross-sectional area of the tool in the $x$ - $y$ plane ( $\mu\text{m}^2$ or $\text{mm}^2$ )
$A_w$	Cross-sectional area of the workpiece in the $x$ - $y$ plane ( $\mu\text{m}^2$ or $\text{mm}^2$ )
$\alpha$	Wear ratio (ratio of the volume of tool material removed to the volume of workpiece removed)
$l_e$	Compensation accuracy ( $\mu\text{m}$ or mm)
$L$	Machining length ( $\mu\text{m}$ or mm)
nJ	Nano-Joule
3D	Three-dimensional
AMPs	Advanced machining processes
IEG	Inter-electrode gap
EDG	Electric discharge grinding
AJM	Abrasive jet machining
WJM	Water jet machining
AWJM	Abrasive water jet machining
LIGA	Lithographie, Galvanoformung, Abformung
HAZ	Heat-affected zone
$\mu$	Micro

## 2.1 Introduction

Conventional milling operation incorporating a multipoint tool generally termed as “milling cutter” is a technique of removing surplus materials in the form of tiny chips to generate different three-dimensional features. Material removal occurs due to shear deformation induced in primary shear deformation zone through direct contact of the harder tool with the workpiece. Depending upon the shape of the intended geometry, the milling cutter is given the corresponding shape such as form milling cutter, slot milling cutter to machine various 3D profiles, namely channels, pockets, slots, keyways. Among the two prevalently recognized orientation of the axis



of milling cutter with respect to the job, viz. horizontal and vertical milling operations, in vertical milling operation mainly a cylindrical shape tool having cutting edges/inserts at the end face of the tool as well as on the side surface of the tool is used. Unlike in the horizontal milling cutter, the end mill or face mill is characterized by the discrete cutting points provided on the periphery as well as on the end cross-section of the tool. The trajectory of the tool is controlled precisely exploiting the capabilities of computerized numerical control (CNC) of the machine tool. Therefore, a comparatively simpler tool (end mill/face mill) can create different three-dimensional profiles dominated by the numeric control of the different axes of the machine tool. Though the conventional end milling is an extremely resourceful technique, the extent of miniaturization limits the minimum size of end milling cutter that can be fabricated successfully. Apart from the fabrication of end mill cutter, the dynamic forces involved into the operation put limitations on the stability and operational life of micro-sized milling tool owing to the nature of contact during the operation and large strain rate which material undergoes. Conventional milling operation poses some troubles while machining of fragile components and processing in inaccessible areas. Several superfluous phenomena prevalent in conventional micro-milling such as tool breakage, burr formation, and chatter are highly unpredictable and depend mostly on the cutting process [1].

Keeping in view the aforementioned inadequacies associated with conventional milling operation, it has become imperative to strive for the development of machining processes which can overcome these limitations up to a great extent if not eliminated completely. Non-traditional or unconventional or advanced machining processes are the group of material subtractive processes, machining characteristics of which are independent of the hardness, ductility, delicacy, complexity, and miniaturization of the components. This group of machining techniques has the potential to address some of the issues of the conventional micro-milling operation. The processes fulfilling the principle of being categorized as advanced machining processes (AMPs) are jet machining (AJM, WJM, and AWJM), ultrasonic machining (USM), electric discharge machining (EDM), laser beam machining (LBM), electrochemical machining (ECM), chemical machining (ChM), etc. [2]. Various energies in its direct form such as mechanical energy in the form of kinetic energy of jet, thermal energy, and light beam energy directly applied to the infinitesimally small area, electrical energy to assist anodic dissolution and chemical etching by suitable etchant are utilized to facilitate the material removal phenomenon in non-traditional machining processes [3].

Electrical discharge machining (EDM) is an electrothermal process which derives thermal energy essential for melting and even evaporation of the electrically conductive material through the conversion of input electrical power [4]. Since the inception of the process, it has gone through the numerous advancements to demonstrate its suitability for different micro-machining purposes. Initially, the EDM process used to be operated in the die-sinking mode only, wherein a profiled tool is plunged into the workpiece to replicate the negative contour on it. Fabrication of dies, molds for injection molding parts, and micro-castings are some of the typical applications areas of ED-Die sinking to name a few. Drilling of closely spaced micro-holes for filters, high-

aspect-ratio cooling passes for turbine blades, inkjet printers, diesel engine fuel spray nozzle, etc., can be successfully drilled by electrical discharge drilling operation using a cylindrical tool rotating at high speed [5]. It is worth mentioning here with regard to ED-Die sinking, and ED-Drilling operations that only unidirectional positioning of the tool is essential for functioning of the respective operations. Moreover, ED-Die sinking and ED-Drilling operations are restricted to two-dimensional geometries only. Rapid growth in the automatic functioning of machinery and machine tool had necessitated the control of different axes of the machine tool through computerized numeric control. The integration of computer-aided design (CAD) and computer-aided-manufacturing (CAM) tools has eradicated the labor-intensive operations, the error induced as a part of the human fault, complex tool fabrication, etc. Numerical control of different machine elements necessitates the information to be arranged in the form of alphabets, numbers, etc. Exploring the highly precise motion control, accuracy and ultra-fine resolution achieved with the numerically controlled machine tool, the EDM process witnessed a revolution in transforming the machining strategy from the primitive two-dimensional features to the complex three-dimensional features. Milling operation employing a simple cylindrical shape tool for the machining of micro-channels, micro-pockets, micro-stepped structures, and so on using the thermal erosion phenomenon of EDM process is considered to be one of the most appropriate techniques. CNC-controlled ED-Milling can be accessed with an extensive range of technical specifications, including changeable degree of stage precision, tool rotation speeds, and computerization. Therefore, the ED-Milling operation can be conceived as an adaptation of conventional EDM technique, which entails a simple cylindrical tool to achieve the intended shape according to the instructions programmed analogously to the conventional milling operation [6]. The advantages of the ED-Milling operation over the conventional milling process comprise the use of a simple tool regardless of the shape of the final geometry being generated in difficult-to-machine materials. Machining in inaccessible areas that are either difficult or impossible to process through conventional machining techniques can be carried out by exploiting the contactless nature of the ED-Milling operation.

Figure 2.1 depicts the schematic illustration of ED-Milling operation using a cylindrical tool. From the schematic diagram, it can be perceived that the cylindrical tool follows a straight-line path to create straight profile channels having rectangular or square cross-sections. At the end of each milling path, the tool wears out from the circumferential surface as well as at the bottom face of the tool. The detrimental consequence of the tool wear can be found in the channel taper and the reduction in channel depth at the exit cross-section as compared to the inlet cross-section. Not only straight channels can be precisely machined through ED-Milling operation but also semi-circular-, circular-, zigzag-, freeform-shaped micro-features are possible by the integration of CAD tool with CAM system to generate the required tool path plan. Tool path strategy, required number of passes, and tool-wear compensation are some of the critical issues that determine the topography and surface integrity of the produced features.

Figure 2.2a shows a typical micro-channel machined by micro-ED-Milling technique. The experiments are performed using a tungsten carbide tool of 500  $\mu\text{m}$

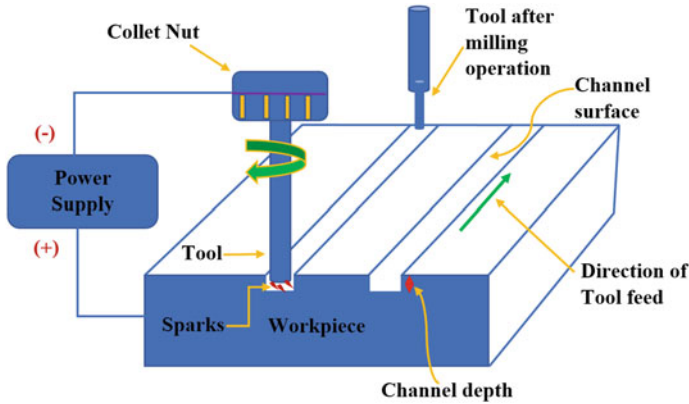


Fig. 2.1 Schematic diagram representing ED-Milling operation

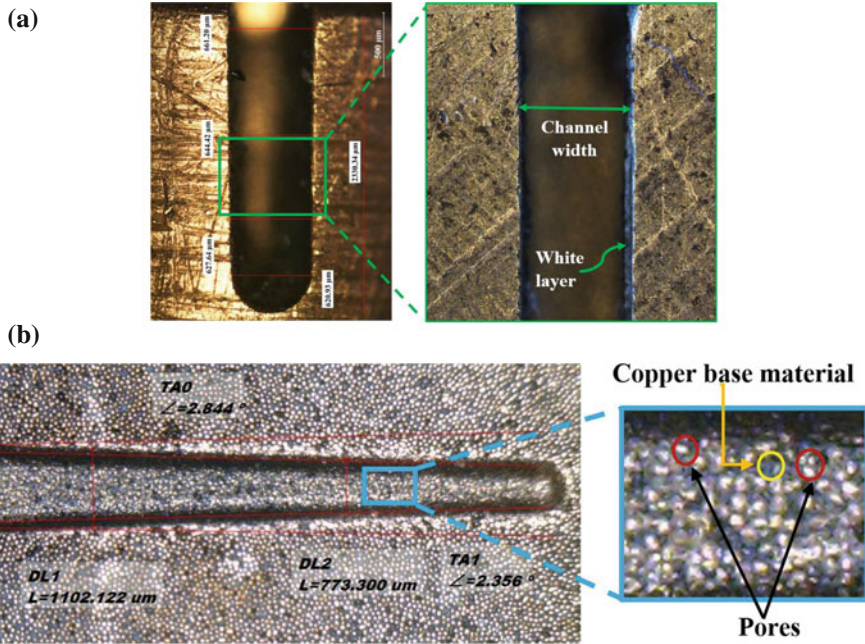
diameter on the copper workpiece. An effort has also been made to process porous copper material with 1-mm tungsten carbide tool (Fig. 2.2b). Micro-slots as small as  $10\ \mu\text{m}$  width separated by a thin wall of  $2.5\ \mu\text{m}$  on stainless steel workpiece show the capabilities of the process Fig. 2.3a [7]. The letters “NUS” machined by micro-ED-Milling operation are shown in Fig. 2.3b [8].

## 2.2 Approaches to Generate Depth in Micro-ED-Milling Operation

To machine the stipulated depth of the features (channel, slot, pocket, keyhole, etc.), ED-Milling operation faces some challenges, unlike conventional milling operation where tool wear is not so prevalent. Whereas, milling operation incorporating EDM operation accounts for severe tool wear that changes the depth and width of the feature from the theoretically predicted feature in superlative circumstances. Therefore, the prerequisite depth of the micro-features can be accomplished by dividing the depth into several layers with specified thickness, or it can be achieved by machining the full depth in one pass. These two approaches are explained in the following subsections.

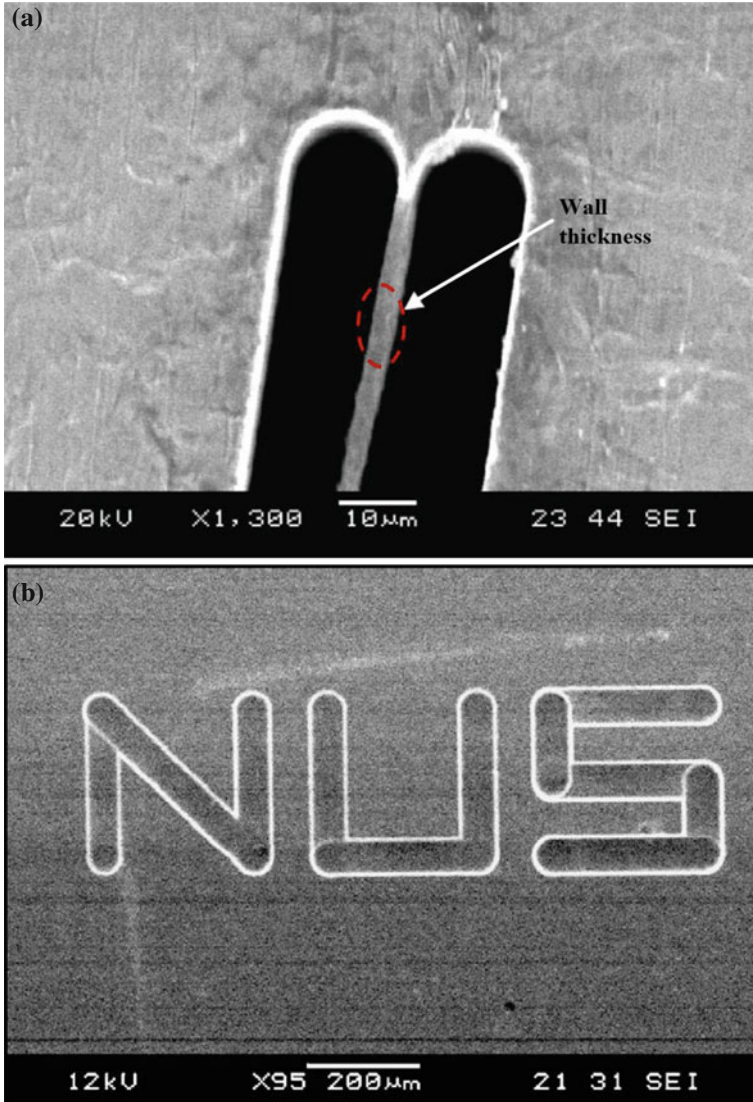
### 2.2.1 Layer-by-Layer Machining Approach

This approach is generally considered to be the converse to the additive manufacturing process where the subsequent addition of current layers on the posterior layer generates a complete 3D product. The layer-by-layer approach of machining in ED-Milling operation machines the full depth of features in multiple passes. In a single



**Fig. 2.2** **a** Straight micro-channel fabricated on Cu workpiece, **b** machining of porous copper material using the  $\mu$ ED-Milling operation (At Micro-Manufacturing Laboratory, Department of Mechanical Engineering, IIT Kanpur)

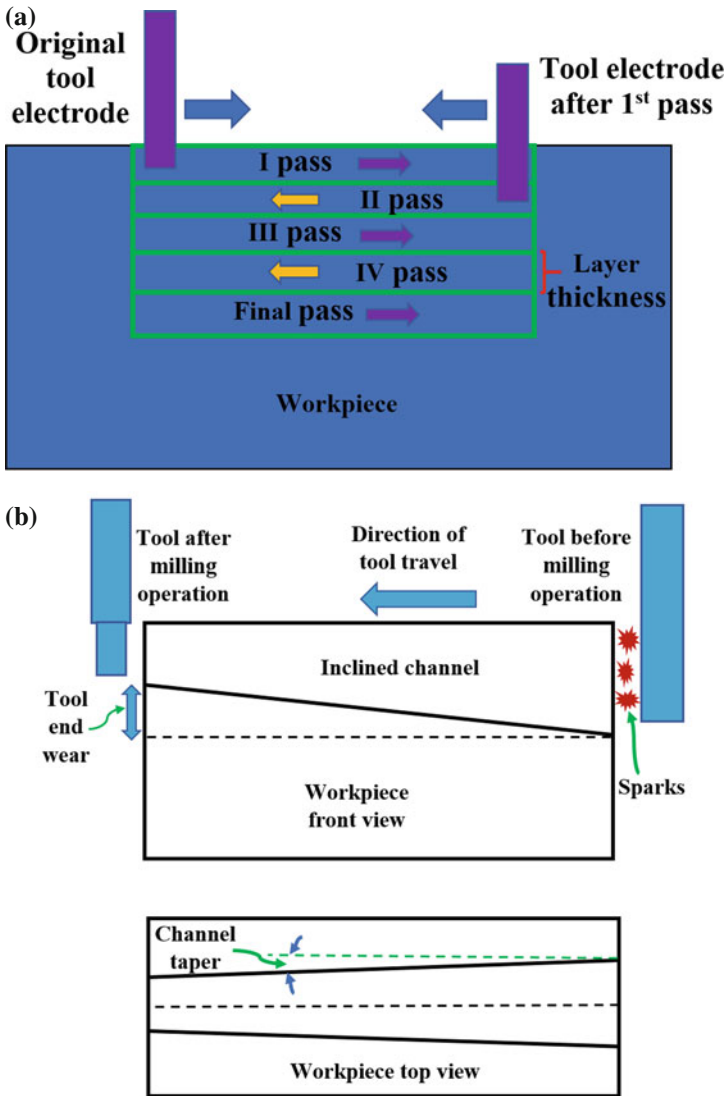
pass of machining, the tool is plunged by the single layer thickness and then moved in the  $x$ - $y$  plane according to NC code. Past every layer of machining, the tool is provided vertical motion into the workpiece equal to the single layer thickness followed by the movement in the  $x$ - $y$  plane to machine the next layer. This procedure is repeated until the full depth is machined. The cumulative depth of different layers machined confirms the predestined depth of the feature. The thermal energy of discharge in ED-Milling operation would reduce the length of the tool caused by the longitudinal wear. The longitudinal wear of the tool is generally compensated by applying uniform wear method (UWM). Therefore, in UWM method it is assumed that the tool tip remains flat after each layer of machining. Total machining time is the summation of the time required for each layer of machining. Therefore, large depth of feature and small single layer thickness would machine the feature in very high time. Figure 2.4a shows the schematic representation of layer-by-layer machining approach.



**Fig. 2.3** μED-Milling operation, **a** micro-slots of 10 μm width with ultra-thin wall of thickness 2.5 μm, **b** acronym NUS machined on stainless steel workpiece [7, 8]

### 2.2.2 Bulk Machining Approach

This method is considered to be a single-pass machining, wherein the complete depth of the channel or pocket is machined in one go. The tool is first given the pre-determined depth and then follows straight, inclined, or curved path depending upon



**Fig. 2.4** Schematic illustration of **a** layer-by-layer machining approach, **b** bulk machining approach in ED-Milling operation

the shape of the profile required. The main advantage of bulk machining approach includes low machining time compared to layer-by-layer approach. However, the bulk machining approach experiences longitudinal as well as circumferential wear of the micro-tool as both the surfaces are exposed to discharges. Therefore, the machined profile would be inclined from the channel inlet to its exit (front view) and tapered (top view) as shown in Fig. 2.4b.



## 2.3 Micro- Versus Macro-ED-Milling Operation: Possible Modifications

$\mu$ ED-Milling operation is generally specified as a micro-fabrication method for the features ranging from 1 to 999  $\mu\text{m}$  [9]. This range of dimensions categorized as micro-features is incessantly changing with the speedy evolution in miniaturization of the products. Nowadays, the micro-channels are being commonly used in various MEMS applications, and these are usually below 300  $\mu\text{m}$  and they can approach as small as 30  $\mu\text{m}$  [10]. The transformation of the machine tool as well as process physics for adaptation in micro-domain is not merely the reduced size of the tool and feature creation, but also it entails consistency in the scaling down laws applied to the process variables in micro-domain. The possible modification in the mechanical system, as well as the process physics, can be summarized as follows.

### 2.3.1 Discharge Energy Per Pulse

Knowing the fact that the dimensions of the features are getting smaller and smaller to comply the requirements of different industries, the discharge energy applied to the inter-electrode gap (IEG) in ED-Milling process must be lowered down significantly as it determines the minimum machinable dimension, volume of material removal (tool and workpiece both) and induced surface roughness [11]. The reduction in discharge energy per pulse generates a crater with smaller radius and depth. Therefore, the resultant feature dimensions, surface integrity, dimensional accuracy will accomplish the requirement of micron or sub-micron size machining. The extent of miniaturization in the machined feature is directly affected by the crater size which in turn depends upon the energy supplied per pulse. Resistance–capacitance (RC) circuits find their popularity largely for small discharge energy and nanosecond pulses. The capacitance of the capacitor can be reduced down to picofarad capacity, thus allowing the energy of single pulse to be very small. Hence, RC-based pulsed generator always has upper hand to the transistor-based pulsed generator, especially for  $\mu$ ED-Milling operation. Discharge energy as low as 3 nJ has been reported using RC-based pulse generator exploiting only the stray capacitance and extremely low open-circuit voltage [12]. Though the discharge energy is comparatively small in micro-EDM, the power density is found to be higher (30%) in micro-EDM owing to the fact that the small pulsed duration (ns) restricts the expansion of plasma channel allowing the energy to be concentrated on a minute area [13].

### **2.3.2 Tool Electrode**

EDM is the process of producing reverse replica of the tool on the workpiece that necessitates the superior tool fabrication techniques and its stability during the machining. A slight deformation and change in the shape and size of the micro-tool produce an inferior quality product.  $\mu$ ED-Milling operation demands tool to be fabricated complying the size to be smaller than the dimensions of the intended feature. The width of the channel or slot generated through single-pass  $\mu$ ED-Milling operation is inevitably equal to the diameter of the tool plus two times the side spark gap. The side spark gap is prevalently known as overcut in EDM process which is undesirable but bound to happen. The overcut produced is unwanted since it introduces the dimensional inaccuracies in the micro-features. However, a minimum side spark gap is always desirable for the effective flushing of fresh dielectric to the machining zone and expulsion of debris particle out of the small discharge gap. Therefore, to achieve the requisite dimensional accuracy the tool size must be designed using a scientific approach something similar to the “*Correction Factor Method*” used for designing the tools for EC-Drilling operations [14]. This approach develops a mathematical model for the overcut and then accounts for it while designing the tool using different machining parameters.

### **2.3.3 Inter-Electrode Gap**

Inter-electrode gap (IEG) or discharge gap is the bare minimum distance between the electrodes (tool and workpiece) indispensable to avoid short circuit and prevents the direct contact of tool and workpiece. Contrary to macro-ED-Milling in  $\mu$ ED-Milling operation, the IEG is generally kept very small (5–25  $\mu$ m) to allow the breakdown of dielectric fluid at smaller discharge voltage. Higher the IEG higher will be the ignition delay time and larger will be the required discharge voltage. Consequently, the circulation/flushing of fresh dielectric in the small discharge gap becomes imperative. An optimum setting of IEG is always a critical task in EDM operation as the flushing efficiency is dependent on the gap size. If a generalized predictive model can be developed for the IEG for different combinations of tool and workpiece materials, dielectric and machining parameters, it will be a big help in the development of a “*Correction Factor Method*” for designing a tool for macro- and micro-EDM process.

### **2.3.4 Resolution of the Machine Tool Axes**

High-dimensional stability, vibration isolation, high stiffness and fine resolution of machine tool axes are of paramount importance when it comes to  $\mu$ ED-Milling oper-



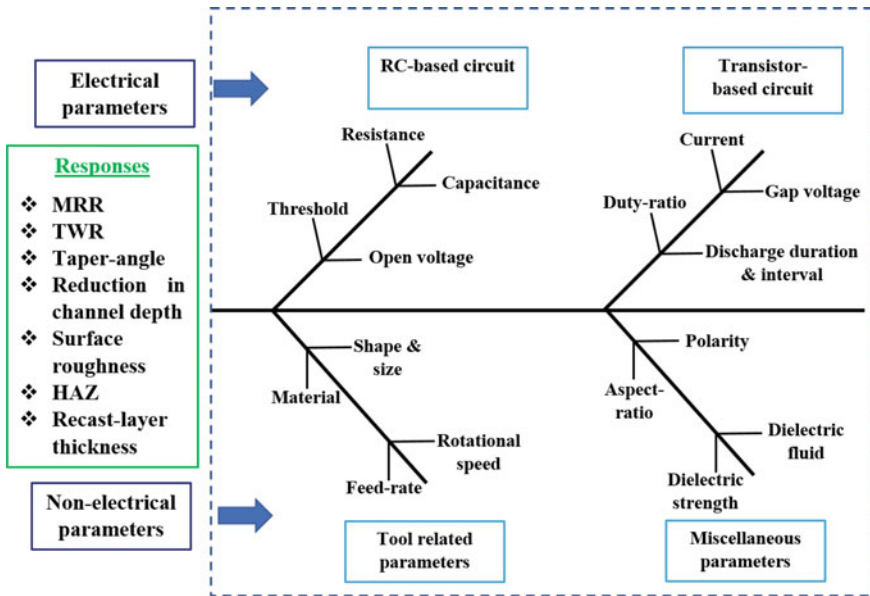
ation. A slight variation in these parameters might result in high relative inaccuracies and short circuit causing poor productivity. Generally, the EDM machine tool used in micro-machining has a resolution as fine as 100 nm and dimensional accuracy of  $\pm 1 \mu\text{m}$  for 100- $\mu\text{m}$ -axis travel. The spindle run-out error must always be below  $1 \mu\text{m}$  [15].

### **2.3.5 Short-Circuit Detection**

Servo system should have high sensitivity to detect the variation in average gap voltage with respect to reference servo voltage to prevent any short circuit during machining. Short circuits occur whenever the tool touches the workpiece or in some instances, the debris bridges the gap causing direct metallic contact. The threshold value determines the maximum duration of the short circuit above which the servo system would retract the tool and then in-feed it as soon as the gap enlarges. Therefore, the lower threshold value is recommended for  $\mu\text{ED}$ -Milling operation.

## **2.4 Process Variables and Responses Pertaining to the $\mu\text{ED}$ -Milling Operation**

The process parameters also identified as controllable variables are the factors which affect the output or responses of a certain operation. Similar to conventional ED-Die-sinking process, here the process parameters can be classified into electrical and non-electrical parameters. Electrical parameters govern the amount of discharge energy available per pulse, servomechanism functioning, control of pulse duration and interval, etc. Depending upon the use of particular pulse generator, there is a slight variation in these parameters. For a typical RC-based pulsed generator commonly employed in micro-EDM, the major electrical parameters include open-circuit voltage, the capacitance of the capacitor, gap resistance, threshold value, and short-circuit detection time, whereas in case of transistor-based pulsed generator, the number of input variables is quite high. In the transistor-based circuit, users have the flexibility of providing different parameters, viz. open voltage or gap voltage, peak current, discharge duration, discharge interval, duty factor. The discharge current, pulse interval, and discharge duration in the RC equipped circuit are solely governed by the capacitance of the capacitor used. Generally, higher the capacitance higher will be the discharging time and greater will be the current as a higher capacitor can hold high charge, and conversely, it will acquire more time for discharging. Polarity can be straight (a tool as a cathode) or reverse (a tool as an anode) depending upon the tool and workpiece material combination, pulse duration and type of dielectric fluid being used. Talking about non-electrical process parameters, the most commonly used parameters consist of spindle/tool rotational speed, tool feed speed, the aspect



**Fig. 2.5** Fishbone/cause-and-effect diagram displaying major process variables related to the  $\mu$ ED-Milling operation

ratio of the micro-features, type of dielectric fluid used, tool material, tool diameter, cross-section, etc. It has also been analyzed that larger the tool diameter, greater is the relative electrode wear ratio due to skin effect and increased area of spark [16]. The electrical and non-electrical process parameters associated with ED-Milling operation are presented in the form of a fishbone diagram as shown in Fig. 2.5.

The performance characteristics and productivity associated with any machining process are largely analyzed by means of various responses which are the direct function of input parameters. The responses of interest in  $\mu$ ED-Milling operation include material removal rate (volumetric or mass removal rate), tool wear rate, depth of the micro-features at inlet and outlet, taper produced in the micro-features, surface characteristics (surface roughness value, the thickness of recast layer, heat-affected zone, and residual stresses). Among the various output parameters briefly explained, reduction in channel depth at exit and taper in micro-channel are the prominent factors as these are the consequence of tool wear during the operation.

## 2.5 Various Micro-fabrication Techniques

In this section, the endeavor is to present the different techniques being commonly employed for micro-fabrication along with their unique capabilities, advantages over other techniques and some inherent limitations of each process. These processes con-

**Table 2.1** Some micro-fabrication techniques and their comparisons [17–19]

S. No.	Micro-fabrication techniques	Mechanism of material removal	M.R.R.	Advantages	Limitations	Materials suitability
1	Micro-milling	Mechanical fracture (shearing)	Highest among micro-fabrication techniques	High MRR, possibility of 3D microstructures using a 5-axis machine	Tool material must be harder than workpiece material It requires tool nose radius in nanometers	All grades of steel, Al, Ti, Br, Cu, polymers, ceramics, etc.
2	Micro-turning	Mechanical shear (sub-grain level of uncut chip thickness)	High (high surface finish is the primary purpose)	Ultra-precision machining	High degree of rigidity, and accuracy of machine tool required.	Steel, Cu, Al, Br etc.
3	Micro-EDM	Melting and Vaporization	Low	Machinability independent of workpiece hardness, high relative accuracy	Low machining rate, high tool wear rate	Only electrically conductive materials
4	Laser micro-machining	Vaporization	High	High resolution	Low energy efficiency, high cost, large HAZ	All kind of materials except those having high thermal conductivity and high reflectivity, e.g., Cu and Al
5	Electrochemical milling	Electrolysis	Moderate	No HAZ, No residual stresses, independent of workpiece hardness	Corrosion, intricate tool design	All electrically conductive materials
6	Focused ion beam	Striking of ions	Very low	Suitable for nano-fabrication	Low machining/deposition rate	All materials
7	Electroforming	Electrodeposition	Low	High accuracy and precision, complex geometry can be generated	Long time of deposition, non-uniform thickness of deposition, internal stresses	Ni, Cu, Ag, Fe, Au, and few alloys

sist of conventional micro-turning, micro-milling, micro-electric discharge machining, laser beam micro-machining, electrochemical micro-machining, focused ion beam machining, and electroforming. The various conventional as well as advanced techniques frequently used for micro-fabrication are briefly summarized in Table 2.1.

The comparative analysis of the various micro-fabrication techniques shows that all the processes are equally competitive. The endeavors to enhance the performance characteristics, productivity, and environmental sustainability have led to the appreciable development of the techniques. Conventional micro-fabrication techniques (micro-turning and micro-milling) have their distinctive limitations as discussed in the introduction section. Among the advanced techniques focused ion beam machining is more suitable for nano-fabrication. Also, the extremely low deposition/machining rate puts the limitations on its applicability to mass production. The

potential of machining complicated  $\mu$ -features with sub-micron-level dimensional accuracy in difficult-to-machine materials have made the  $\mu$ ED-Milling operation fairly accepted AMP. However, it can be concluded with regard to the ED-Milling operation that the machining time must be reduced in order to appreciate its competitiveness with other techniques. Therefore, for the economic viability of EDM process in micro-machining, low volumetric material removal rate and high tool wear rate problems must be resolved.

## 2.6 Tool Fabrication Techniques for Micro-ED-Milling Operation

The successful implementation of EDM process for any micro-machining purpose principally governs by the fabrication techniques of micro-tools as it determines the uniformity, dimensional stability, deformation, and requisite surface integrity of the tool electrode. The dimension of the required tool must always be smaller than the size of the feature to be machined. For instance, the machining of the straight channel of 10  $\mu\text{m}$  width essentially needs a tool of diameter less than 10  $\mu\text{m}$  taking into account the diametric overcut produced in the process. Appropriate handling, mounting, and disassembling of delicate micro-tools are a strenuous challenge. However, fabrication of the tools on-site (in situ fabrication) can overcome these challenges in a convenient way. EDM process itself has the desired capabilities for the fabrication of micro-tools with high-dimensional accuracy, surface finish, and uniformity over the desired length. Switching the polarity from straight to reverse (a tool as an anode) and adjusting the necessary feed and rotation of the tool with respect to the sacrificial electrode can reduce the diameter of the tool. In reverse polarity commonly employed for tool fabrication, the tool acts as an anode, whereas the sacrificial electrode behaves as a cathode. Therefore, the material removal rate is higher and it reduces its diameter at higher rate as compared to the straight polarity. The variants of EDM process applicable for micro-tool fabrication are also-called as Block Electric Discharge Grinding (block-EDG) and wire Electric Discharge Grinding (wire-EDG).

Block EDG has two versions including stationary sacrificial block EDG in which a stationary block is used as a tool electrode (cathode) and the tool whose diameter is to be reduced acts as a workpiece electrode (anode). The series of sparking between the rotating tool and sacrificial block would remove material from the tool as well as from the block. Continuous feed is provided to the tool either horizontally or vertically to ensure the uniform material removal from its entire periphery. Another variant of block-EDG replaces the sacrificial block with a thin rotating disk for better dimensional accuracy. The principle of material removal remains the same as block EDG, except the uniform wear of the disk due to rotation imparted to it. A continuously rotating thin wire guided over the pulley is employed in wire-EDG process. The rotation of wire ensures wear-free wire electrode and vibration-free operation contrary to block and disk EDG processes. Electrodes as small as

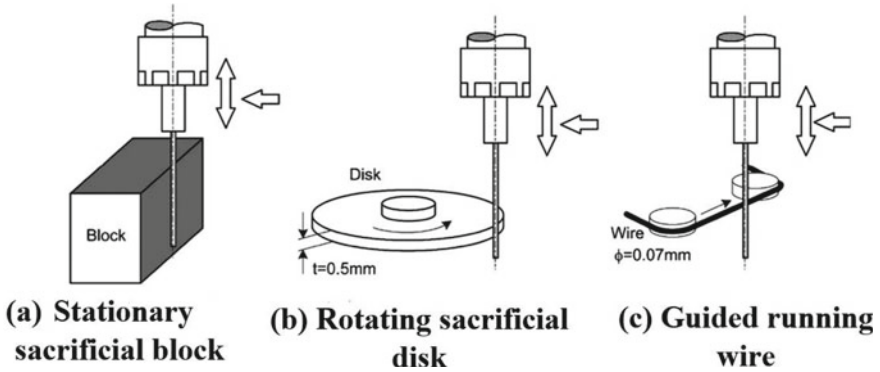


Fig. 2.6 Different micro-tool fabrication techniques using the spark erosion phenomenon [20]

1  $\mu\text{m}$  have been successfully fabricated in situ through the wire-EDG process [11]. The decisive advantages of the process embrace damage free micro-tool handling as the tools are fabricated on the machining site itself where it can be used for  $\mu\text{ED-Milling}$  or  $\text{ED-Drilling}$  operations merely by reversing the electrode polarity. Figure 2.6 schematically illustrates the variant of the EDM process suitable for micro-tool fabrication and these micro-tools are usually employed for  $\mu\text{ED-Milling}$ ,  $\mu\text{ED-Drilling}$  operations, etc.

Besides the variants of EDM process, several other techniques have equal competitiveness when it comes to the production of precise tool electrode. Conventional micro-machining operation, such as micro-turning, micro-grinding, has the requisite capabilities to excel in micro-fabrication with high-dimensional accuracy and good surface characteristics. However, the micro-cutting tool used for the processing of extremely precise components suffer from the problems such as low rigidity, loss of cutting tool sharpness, and unavailability of the tremendously small cutting tool itself.

## 2.7 Physical Behavior of the Micro-ED-Milling Operation

The microscopic investigations of the micro-channels fabricated utilizing  $\mu\text{ED-Milling}$  operation revealed a distinct physical phenomenon. The flow of molten liquid pool, its deposition on the machined surface (recast layer) as well as on the parent material and removal of debris caused by the movement of the tool electrode and its high-speed rotation make the process more complicated than a hole drilling or  $\text{ED-sinking}$  operations.

Spherical debris particles are formed due to sudden cooling of molten material known as globules. The spherical shape is governed by the low spheroidization time as compared to solidification time [21]. These globules are non-crystalline and mostly

hollow from the core. The size of the globules goes on increasing with increase in discharge energy (For RC Circuit  $= \frac{1}{2} \times C \times V_d^2$  and for transistor circuit  $= V_d \times I \times t$ ). Due to viscous force, the globules attain an angular motion around the rotating tool, whereas the centrifugal force tries to separate the globules from the tool and dissipate it toward the workpiece surface [22].

Rotation of tool electrode contributes to the flow of molten material which in turn deposits the material non-uniformly about the channel axis. The direction of tool rotation can explain the phenomenon. The molten material is pulled into the machining zone on one part and consequently pushed outside on another side. This results in the unsymmetrical redeposition on either side of the channel surface. The non-uniform taper of the channels is one of the consequences of this phenomena. Milling marks are also observed on the channel bottom surface due to the rotation of molten material [23]. The milling marks vanish partly due to next subsequent sparks. The discharge energy level also determines the extent of milling marks left on the newly developed surface.

## 2.8 Micro-ED-Milling Operation with Different Variants

### 2.8.1 *Insulating Ceramics*

Direct machining of electrically non-conductive ceramics through the conventional technique of EDM is not possible since a minimum electrical conductivity of both tool as well as workpiece material is essential for the creation, conduction, and transfer of charges (electrons, positive ions, etc.). However, with certain modification in the conventional EDM technique insulating (electrically non-conducting) ceramics have been machined by EDM process successfully. In order to complete the electrical circuit for the initiation of spark, a conductive path is required. This conductive path is generally provided by means of an assisted/dummy electrode, wherein a thin coating of some electrically conductive material is applied over the insulating ceramics [24]. The mechanism of material removal in this assisted electrode method can be understood in the following manner.

The electrically conductive coating on the insulating ceramics facilitates the generation of sparks between the tool electrode and the dummy electrode in the manner similar to any EDM technique. The sparks remove the material from this conductive layer, and at the same time, the dissociation of hydrocarbon oil (dielectric fluid) generates the carbon particle which reacts with the parent insulating ceramic material to form a layer of carbon substance [24]. This formed layer of carbon remains on the newly generated surface and assists in the formation of sparks between the tool and this carbon layer. The heat generated in the spark in the proximity of the workpiece is transferred to the workpiece, and it is enough to melt and, in some cases, even to vaporize the workpiece material. Subsequently, the material is removed from the insulating ceramics, and the desired feature is created. This dummy electrode

method has been successfully used for the  $\mu$ ED-Milling operation of  $ZrO_2$  ceramics using copper layer (60  $\mu$ m). EDX spectroscopy of micro-channels surface shows the abundance of carbon particles [25]. Silver foil (45% Ag) is also attempted as a starting conductive layer for ED-Milling operation of  $ZrO_2$ . The surface roughness obtained on  $ZrO_2$  is two to three times higher than that obtained on metals with the same machining conditions [26]. Formation of ZrC is probably the reason for the subsequent sparks as the compound is electrically conductive, though the correct composition needs to be investigated. The threshold value of electrical resistivity of the ceramics for the machining through EDM process is likely to be 100  $\Omega$ cm [27]. However, exploiting reverse polarity (a tool as an anode and dummy workpiece as a cathode) for the machining of silicon carbide ceramics with high electrical resistivity (500  $\Omega$ cm) showed high MRR, low TWR, and improved surface finish than that achieved with straight polarity [28]. Therefore, the machining of insulating ceramics employing EDM technique relies primarily on the thickness of the assisting layer and the type of dielectric fluid used.

### ***2.8.2 Modifications in the Dielectric Fluid***

The dielectric fluid is one of the essential elements of EDM process as it facilitates the formation of the plasma channel, generates the spark, and confines the plasma channel. Owing to its viscosity and inertia, the bubble growth pressure increases and hence increases the volume of material removed per pulse [29]. Therefore, the properties of the dielectric fluid play an important role in determining the ionization, confinement of plasma channel, spark gap, etc. Liquid dielectrics are most commonly used in EDM process. However, dry, near dry (mist), spray-based dielectric, and powder-mixed dielectric systems are also finding their popularity due to several reasons. These modified dielectric fluids are equally appropriate to all variants of EDM process, viz. ED-Die sinking, ED-Drilling, ED-Milling, wire-EDM, EDG. The disposal of huge quantity of liquid dielectrics and the generation of fumes due to dissociation of the dielectric liquid are some of the concerns with liquid-based dielectrics [30]. Dry EDM, in which high-pressure air or gas is supplied to the spark gap, is an alternative to the liquid-based dielectrics [31]. Extensively, high machining rate is achieved predominantly when oxygen is used as a gas dielectric possibly due to oxidation of the surface [32]. Dry EDM, particularly with non-oxidizing dielectrics, has certain shortcomings such as low MRR, thick recast layer, and high thermal damage to the machined components [33]. The low cooling capacity of gases and inability to remove the debris are the possible reasons for the high thermal damage and presence of thick recast layer. In order to overcome the limitations associated with dry EDM, a mixture of liquid and gas (mist) in near dry-EDM process and atomized droplet supplied to the machining zone to form a thin layer of liquid dielectric has also been applied effectively. Among these modified dielectrics, the atomized-based/spray dielectrics are found to be more suitable for high MRR, an acceptable level of tool wear and less accumulation of debris near the sparking zone [34].

Powder particles such as Graphite, Si, Al, Si, SiC, Ti, Cu, Cr, B<sub>4</sub>C, Mn, TiC, W are added in the liquid dielectric to evaluate the consequence of the powder-mixed dielectric on responses such as MRR, TWR, R<sub>a</sub> [35]. The electrically conductive powder-mixed dielectric modifies the machining variables and thus creates more favorable conditions for sparks to form. Addition of fine conductive powder in liquid dielectric reduces the dielectric strength of the medium. Since the minimum spark gap is inversely proportional to dielectric strength, higher spark gap can be used in powder-mixed dielectric. Therefore, discharge can occur at the higher inter-electrode gap (IEG) keeping the discharge voltage to be constant. Higher IEG removes the debris particles more easily and reduces the occurrence of short circuit. The powder particles align themselves in the regions of strongest electric field (less IEG) and bridge the gap. The dielectric strength of the liquid dielectric would be such that discharge happens immediately at this location. In the absence of these particles, the discharge would have occurred at comparatively small IEG due to high dielectric strength of the fluid. Therefore, the reduced dielectric strength results in the formation of larger discharge gap and diminishes the accumulation of the debris in the IEG.

## 2.9 Allied EDM Processes for 3D Fabrication

$\mu$ ED-Milling operation is predominantly used for the fabrication of 3D micro/macro-features of various shapes. Use of a comparatively simpler tool, independent of the shape of the intended geometry, is one of the key advantages of the process. However, for the machining of micro-features having a high aspect ratio, ED-Milling operation suffers from some of the drawbacks such as accumulation of debris in the machining zone, severe tool wear, deflection of tool having thin cross-section and high machining time required. Alternatively, researchers have attempted a few allied processes of EDM for 3D micro/macro-fabrication. Thin foil/sheet as a tool electrode has been used in EDM process [36]. The experimental investigations confirm a substantial improvement in the machining rate as well as the achieved aspect ratio (ratio of channel depth to the width). The probable reasons for the higher machining rate can be attributed to the enlarged spark area. The higher aspect ratio of the features is associated with the debris evacuation since the accumulation of the debris would result in short circuit resulting in unstable machining. Gravity assisted  $\mu$ EDM (GAME) is a novel technique proposed for the sedimentation of the debris as the orientation of the tool and workpiece (workpiece at the top and tool below that) is reversed to that of the conventional EDM process [37]. Further, a series of holes and pockets are also drilled in the plate electrode and this resulted in a much improved performance as the removal of debris is accelerated with the passes provided on the tool [38]. The position and geometry of these holes and pockets are also found to be critical though the accurate explanation of the physical phenomenon prevailing is still required.



## 2.10 Tool Wear Analysis in ED-Milling Operation

The intense heat generated due to the discharge energy diffusion from plasma channel to the tool electrode and workpiece electrode results in severe temperature generation during discharge on period. However, the fraction of heat conducted to the tool (cathode) and workpiece (anode) in straight polarity is determined by the contributions of positive ions and electrons, respectively. Generally, at low pulse duration, the fraction of heat available at the anode is always higher than the cathode. However, a reverse trend has been reported by different researchers as the pulse duration becomes high [39]. This can be attributed to the time available for the acceleration of positive ions; at low pulse duration, they have inadequate time to accelerate; hence, small fraction of heat goes to the cathode [28]. But at high pulse duration, the positive ions get sufficient time to attain the kinetic energy and therefore higher fraction of energy transferred to the cathode. Based on this analysis, it can be concluded that the electrode polarity must be decided judiciously on the basis of discharge duration. The fraction of discharge energy supplied to the tool is undesirable as it melts and even vaporizes the tool material leading to unavoidable wear of tool electrode. Tool wear is both inevitable and unpredictable owing to the stochastic nature of the EDM process [40]. Tool wear in EDM process cannot be eliminated completely though it can be reduced to some extent by the appropriate selection of tool-workpiece materials' combination, polarity, dielectric, flushing condition, etc.

The detrimental effects of tool wear in ED-Drilling operation cause a reduction in hole depth and taper along the depth of the hole. Though the reduction in hole depth can be compensated by accurately analyzing the longitudinal wear of the tool and providing higher programmed depth of the hole by the amount equal to the end wear of the tool, the hole taper cannot be eliminated as the side wear is problematic to circumvent. The wear of form tool in ED-Die sinking results in deficient dimensional accuracy and inferior replication of the profile. Analysis and compensation of tool wear in  $\mu$ ED-Milling operation are complicated due to the multiple zones that eroded simultaneously as a tool has to trace the path in three-dimensional space. However, as mentioned earlier, an attempt can be made to minimize the taper by developing a "Correction Factor Method" for EDM operation in general and ED-Milling operation in particular.

### 2.10.1 Tool Wear Compensation Techniques in Layer-by-Layer Machining

#### 2.10.1.1 Uniform Wear Method (UWM)

As discussed earlier in Sect. 2.2.1, the layer-by-layer method of ED-Milling operation assumes tool end face to be uniform after machining [41]. The reduction in tool length is compensated by plunging the tool into the workpiece by the amount equal to the

length of tool reduced in addition to the theoretical layer thickness. Therefore, the cross-section of the machined cavity will be free from inclined surface.

Taking into consideration the small thickness of individual layer/pass, the side wear of the tool is negligible and it is not considered in layer-by-layer machining. However, after the machining of the cavity of a certain length, the tool wears out in the longitudinal direction and the depth of cavity measured at the exit will be less than the theoretical depth expected without any wear of the tool. Therefore,  $\Delta x$  is assumed to be the average thickness of an individual layer machined, as the thickness reduces continuously from the entrance to the exit of the channel.

For the next reverse pass, the tool must be fed into the workpiece taking into account the length of the tool reduced. Therefore,  $\Delta d$  is the depth of the tool feed considering the longitudinal wear such that after 'n' layers of machining, the total depth of cavity would be  $d = n \times \Delta d$ , where  $d$  is the proposed depth of the cavity.

Hence, the volume of tool removed after n layer of machining is given by:

$$(n \times \Delta d - n \times \Delta x) \times A_e = \alpha \times n \times A_w \times \Delta x \quad (1)$$

$$\Delta d = \Delta x \left( 1 + \alpha \times \frac{A_w}{A_e} \right) = \Delta x + \Delta Z_t \quad (2)$$

where  $\alpha$  represents the ratio of the volume of material removed from the tool to the volume of material removed from the workpiece termed as wear ratio.  $A_e$  and  $A_w$  are the cross-sectional area of tool electrode and workpiece in the  $x$ - $y$  plane.  $\Delta Z_t$  is the compensation length added prior to the commencement of next layer of machining.

Equation 2 depicts the compensated depth of cut envisaged by the UWM which is always higher than  $\Delta x$  since  $\alpha$  is essentially positive. The applicability of the UWM of longitudinal tool wear compensation is verified by machining various complex cavities.

### 2.10.1.2 Linear Compensation Method

Uniform wear method (UWM) considers that tool is fed downward posterior the completion of a single layer of machining of certain length. In doing this, the machined feature achieved is inclined as the length of the tool has been shortened. To further eliminate the adverse effect of tool wear in terms of the non-uniform inclined cross-section, linear compensation method (LCM) was developed. LCM of tool wear in ED-Milling operation compensates the longitudinal wear by feeding the tool toward the workpiece after a small length of tool travel in the  $x$ - $y$  direction. Let travel length of the tool during ED-Milling operation is  $L$  and  $\Delta L$  is the distance traveled by the tool after which the compensation is given. Assuming the compensated length of the tool is  $\Delta y$ , then according to LCM method, the ratio of  $\Delta y$  to  $\Delta L$  remains constant. The compensation depth is merely dependent on the empirical data, which necessitates enormous experiments. This method found appropriateness in overcoming the unfavorable effects of the longitudinal axis of tool wear in the machining of

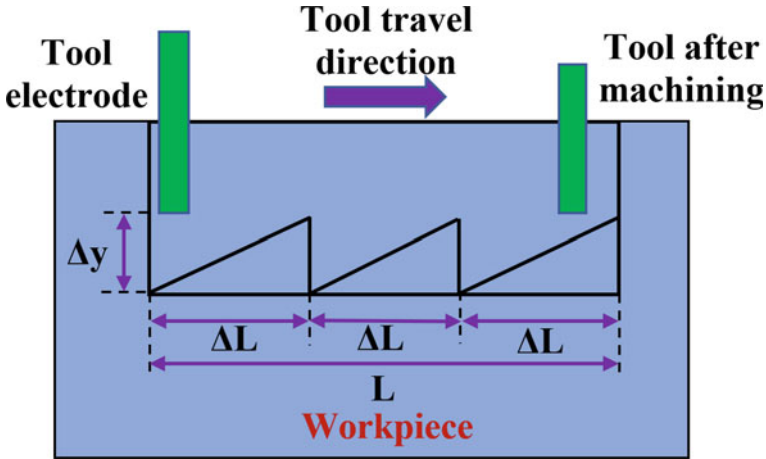


Fig. 2.7 Schematic diagram of linear compensation method (LCM)

the square cavity with a flatness within  $2 \mu\text{m}$  [42]. However, this technique is still inadequate for the machining of complex 3D cavities.

Figure 2.7 depicts a schematic illustration of LCM, wherein the triangular cross-section is shown after machining a length of  $\Delta L$  due to a reduction in tool length. The total travel length of the tool in the  $x$ - $y$  plane is divided into a number of small length segments, and after each small length segments, the tool is fed downward by the amount  $\Delta y$ .

### 2.10.1.3 Combination of UWM and LCM: Development of CLU Method

Though the linear compensation method proves to be quite accurate, versatile, and reliable in obtaining a flat surface, extensive experiments are required to determine the travel length ( $\Delta L$ ) and compensation depth ( $\Delta y$ ). No theoretical model is available to establish the relationship between travel distance and compensation length. Amalgamations of the proposed tool wear compensation methods, viz. UWM and LCM, resulted in the more consistent method, wherein the compensation depth is determined according to uniform wear method and the travel length  $\Delta L$  remains as per the LCM method. This combined technique is termed as CLU method [43].

The algorithm of CLU method is as follows:

Similar to linear compensation method, the total compensation depth of the tool  $\Delta Z_t$  is uniformly divided into small several small length  $\Delta Z$ .

The number of compensation times for single layer of machining is determined as follows:

$$N = \frac{\Delta Z_t}{\Delta Z} = \frac{\Delta d - \Delta x}{\Delta Z} \text{ [From Eq. (2)]}$$

Let the total length of the layer be  $L$ . Therefore, the distance travel can be calculated as follows:

$$1L = \frac{L}{N}$$

This represents that the distance tool must travel before the application of the tool compensation depth  $\Delta Z_t$ .

According to CLU method, higher the number of compensation times per layer of machining, greater will be the uniformity of the resultant surface.

#### 2.10.1.4 Fixed-Length Compensation Method

This approach is much similar to linear compensation method. However, the electrode end wear can be calculated based on the machining length. According to this method, the electrode is compensated whenever the electrode wear exceeds a certain value ( $l_c$ ). This value ( $l_c$ ) is termed as compensation accuracy. The machining length ( $L$ ) is termed as compensation length. As the compensation is provided after the machining of a fixed length, this technique is called as fixed-length compensation method. The increase in layer thickness would result in a conical profile of tool electrode. Therefore, cross-section of the workpiece after machining resembles a series of triangles [44]. Based on this conical electrode, a wear model is formulated to precisely evaluate the machining length ( $L$ ) [45].

Furthermore, an improved fixed-length compensation method was proposed and validated experimentally by replacing a cylindrical tool with a tubular-shaped tool [46]. The tubular tool transforms into a truncated cone-shaped after milling operation. Since the end cross-section of the tool remains flat due to tubular shape, the resultant machined surface becomes smooth and free from triangular impressions. A theoretical model is developed relating the compensation length ( $L$ ) in terms of final milling depth, volumetric wear ratio, discharge gap, tool inner and outer diameter, and compensation accuracy. Applying this compensation technique, the longitudinal wear of tool can be successfully implemented if the target depth is known.

### 2.10.2 Tool Wear in Bulk Machining Approach

Layer-by-layer machining has distinctive advantages such as less effect of electrode wear as the compensation methods are fairly reliable and pragmatic. However, the proposed wear compensation methods in layer-by-layer approach are subjected to comparatively simpler geometries and found difficulties when complex 3D micro-features are to be machined. Also, successful implementation of the algorithm demands extensive experimental data. The total machining time required for the fabrication of a cavity depends on the thickness of the single layer and the depth of the

cavity. The low productivity associated with the layer-by-layer machining approach can be circumvented by machining the full depth of the cavity in a single pass. This approach is termed as bulk machining approach or peripheral machining approach as machining takes place by the periphery of the tool in addition to the end face.

The general rules of bulk machining approach related to  $\mu$ ED-Milling can be summarized as follows:

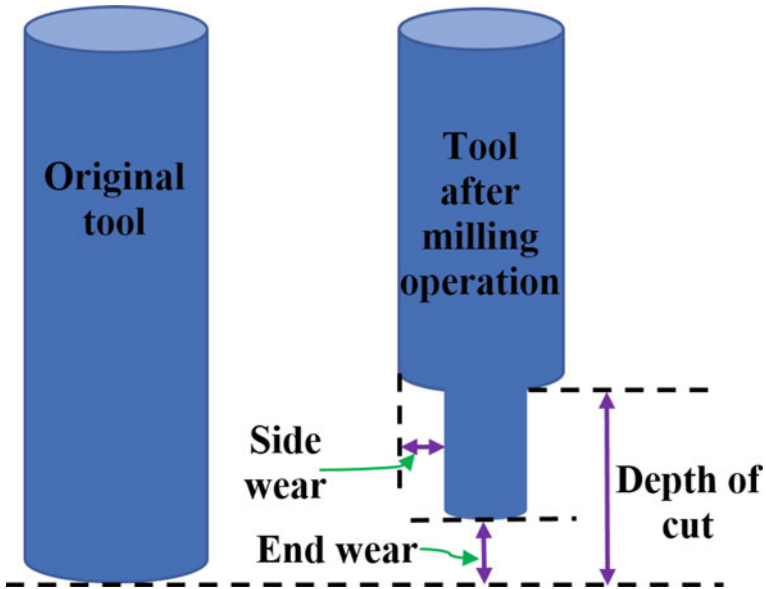
- (i) The tool electrode is first sunk into the workpiece up to the required depth of the feature.
- (ii) Generation and execution of NC codes to dictate the tool path in the  $x$ - $y$  plane, i.e., in the plane perpendicular to the depth of cut.
- (iii) Movement of the tool in the  $x$ - $y$  plane. This movement can follow any desired path depending upon the shape of the cavity intended. For the fabrication of semi-circular cavity, the tool will follow circular interpolation in the  $x$ - $y$  plane after it has plunged into the prerequisite depth.
- (iv) Retracting the tool out of the workpiece by following the motion just opposite to that in (i).

Contrary to layer-by-layer machining approach wherein merely the axial/longitudinal wear of the tool occurs due to the small depth of the layer, the bulk machining approach of  $\mu$ ED-Milling operation suffers from circumferential as well as longitudinal wear of the tool electrode. Therefore, the compensation algorithms are not so easy to develop owing to the complex tool wear phenomenon. Longitudinal wear of tool generates a cavity with inclined cross-section; i.e., the depth of cavity at the outlet will be lower than that at the entrance. Assuming the full depth to be a single layer and conducting experiments at fixed process parameters, the approximate reduction in cavity depth can be evaluated. Therefore, the final coordinate of the tool in the  $z$ -direction can be determined and preset considering the average reduction in the depth.

The portion (length) of the tool electrode plunged into the workpiece (equal to the depth of feature) erodes enormously due to the secondary discharges occurring between the tool and workpiece. This enlarges the feature dimension in the direction perpendicular to the axis of the tool also. Therefore, the side wear of tool in bulk machining approach is inevitable since the side surface also forms discharge gap and develops the craters. Eventually, the final shape of the tool after machining by this approach resembles a step-turned shaft having reduced diameter in the portion engaged in the machining and original diameter in the remaining shank portion. Figure 2.8 shows schematically different zones in the tool electrode which wear out during machining especially using single depth of cut.

Unlike machining by layer-by-layer approach in ED-Milling operation, in bulk machining approach hardly there is any compensation algorithm proposed by the researchers. This can be easily understood by the intricate wear phenomenon arising due to simultaneous machining from the end, side, and corner surface of the tool electrode.

Toward the compensation of tool electrode wear and abolish the detrimental effect of it on the geometrical accuracy of the resultant micro-features, machining employ-



**Fig. 2.8** Schematic diagram showing tool wear in bulk machining approach

ing multiple pass approach has been proposed [47]. The taper in the micro-feature machined can be reduced and with appropriate investigations can be eliminated by redressing the tool electrode after the machining of a single pass. Redressing the tool by merely reversing the polarity (generally by the wire-EDG process) would remove the material from the tool as it acts as an anode. Therefore, the portion of the tool having reduced diameter can be removed, and apparently, a wear-free tool is available for the next reverse pass. This approach of multiple pass ED-Milling operation is still at its preliminary phase and demands a lot of experimental data in order to determine the number of passes required. Total machining time to produce a feature includes the productive time (time in which EDM operation is performed) and nonproductive time (the time devoted to the redressing of the tool). Henceforth, a judicious decision must be taken while selecting the particular machining approach (layer-by-layer or bulk machining approach) in ED-Milling operation.

However, the correction factor method used in EC-Drilling operation can be adopted in ED-Milling operation. The method formulates a simple model for the tool design in EC-Drilling operation. This model computes the error between the desired and predicted shape and evaluates the resultant error. Based on this error, a factor called correction factor is calculated and applied to modify the tool shape. Repetition of the procedure brings the shape much closer to the desired one.

## 2.11 Potential Applications

Micro-EDM process in general and  $\mu$ ED-Milling operation, in particular, owing to its impeccable capabilities for the machining of ultra-hard and exotic materials has gained popularity over the last few decades. The advantages of  $\mu$ ED-Milling operation for the making of 3D micro-features include superior dimensional accuracies, exploitation of ultra-thin tool, machining of complex micro-features and machining in unapproachable zones. Micro-electromechanical system (MEMS) demands the precise micro-channels for the analysis of fluid flow, mixing of different fluids in micro-domain [48]. Micro-fluidics is the study of fluid flow through micro-devices, namely micro-heat-exchanger, miniaturized actuator, micro-combustor, micro-fuel cell. Micro-channels are the most important part of micro-fluidics devices, wherein the behavior of different fluids and their mixing are achieved through precisely fabricated channels. The flow of fluid in the channels below 1 mm is considered to be microscopic flow, whereas the flow in the channels with dimensions above 1 mm and below 1  $\mu$ m is macroscopic and nanoscopic, respectively. The high rate of heat transfer is facilitated by the enhanced surface to volume ratio in micro-heat exchanger devices. Though various fabrication techniques are available for the processing of silicon-based materials predominantly used in MEMS devices, these methods are more suitable for merely two-dimensional features. These techniques include lithography, etching, LIGA, etc. Application of these processes is limited to some specific materials only. Apart from silicon-based materials, metals are also gaining its acceptance in MEMS industries because of the varying range of physical and mechanical properties. Therefore, the  $\mu$ ED-Milling operation for the fabrication of complex micro-channels, micro-mixers, micro-printed circuit board, etc., is equally competitive and constructive.

Machining of a finished turbine impeller and micro-compressor has proved the potential of micro-ED-Milling operation as far as complex 3D cutting is concerned [49]. Micro-texturing of surfaces for inducing hydrophobicity is one of the emerging areas, wherein the micro/nano-patterns are developed in the form of pillars, dimples, diamond patterns, etc. [50].  $\mu$ ED-Milling operation is considered to be a very competent technique for large area texturing employing a simple cylindrical-, square-, or rectangular-shaped micro-tool. The depth of micro-feature achieved by EDM process is significantly high as compared to commonly used machining technique for micro-texturing of surfaces. Fabrication of micro-swiss-roll combustor used in various electronic components for the re-circulation of heat is one of the potential applications [51]. High-aspect-ratio micro-flow channels on the metallic bipolar plate have shown greater performance than the other techniques such as electroforming and electrochemical machining [52]. Manufacturing of a master mold through  $\mu$ ED-Milling operation is a promising application area. This master mold is generally used in the embossing of polymer parts. Through cut macro-features relying on conventional EDM technique consumes higher power and machining time as the complete material of the cavity is required to be removed. Exploiting the numerical control of the EDM process, a primitive micro-cylindrical tool can be actuated on the outer

periphery of the macro-cavity, thus machining the outer layer of the cavity only. Therefore, different through shapes such as square, circular, elliptical, or freeform having dimensions comparatively larger than the tool size is machined in trepanning mode by just controlling the trajectory of the tool much similar to ED-Milling operation.

## 2.12 Advantages

- (1) This technique does not necessitate the fabrication of complex tool irrespective of the shape of the anticipated features.
- (2) Execution of NC codes makes it pretty easy to manipulate the motion of the tool in different axes simultaneously.
- (3) Any desirable shape can be produced provided the tool path is generated accurately. Micro-channels with different shapes such as straight, circular/semi-circular, freeform, serpentine, T-shaped are possible to create through the  $\mu$ ED-Milling operation.
- (4) Using layer-by-layer approach, a 3D cavity with inclined surfaces is possible to machine by applying suitable tool wear compensation.
- (5) High-speed rotation of a cylindrical tool distributes the wear of tool uniformly about the axis of the tool. Therefore, channel taper can be predicted accurately.
- (6) Superior dimensional accuracy and relative tolerances of the machined features are the foremost benefits of this technique.

## 2.13 Disadvantages

- (1) Tool wear and its pessimistic impacts on the dimensional accuracy of the micro-features restrict the full applications of the process.
- (2) Comparatively low machining rate puts a restriction.
- (3) Fabrication of micro-tool itself is a tedious process, though the in situ fabrication of micro-tool overcomes these limitations up to a great extent.
- (4) Formation of recast layer particularly due to poor flushing conditions requires secondary operations for removal of this hard layer as micro-cracks propagate into the parent material through this layer.

## 2.14 Summary

Electric discharge milling operation as an effective means of micro-fabrication is still an emerging area. The incessant development in the numerical control of machine tool has made it possible to avail the capability of EDM process. The current prospects



in  $\mu$ ED-Milling operation include fabrication of micro-channels, slots, grooves, and optimization of machining process parameters, analysis of tool wear and its compensation, application of various dielectric fluids including powder-mixed dielectric, etc. Majority of the research available in ED-Milling operation is centered on the production of micro-features on flat surfaces. Fabrication of micro-channels, grooves, micro-textures on non-flat surfaces (circular, curved), and freeform surfaces using a five-axis control of EDM machine tool can be the next level of research in ED-Milling operation. Theoretical analysis of  $\mu$ ED-Milling operation to predict the profile of the final geometry and inescapable taper in terms of machining parameters and physical quantities of the feature can make the process more predictable. Insulating ceramics due to its superior mechanical and physical properties are attracting the researchers to discover the apposite machining techniques. ED-Milling technique has by now shown the feasibility to process these materials through dummy electrode method. However, detailed investigations are still required to precisely determine the thickness of the initial conducting layer, type of dielectric fluid, and the chemical compound being formed. Tool wear compensation technique to account for circumferential as well as longitudinal wear in bulk machining approach is one of the areas that demand a lot of theoretical as well as numerical investigations.

## References

1. Davoudinejad A, Tosello G, Parenti P, Annoni M (2017) 3D finite element simulation of micro end-milling by considering the effect of tool run-out. *Micromachines* 8(6):1–20
2. Jain VK (2007) *Advanced machining processes*. Allied Publishers Private Limited, New-Delhi
3. Jain VK (2008) *Advanced (non-traditional) machining processes*. In: *Machining*. Springer, London, pp 299–327
4. Ho KH, Newman ST (2003) State of the art electrical discharge machining (EDM). *Int J Mach Tools Manuf* 43(13):1287–1300
5. Ferraris E, Castiglioni V, Ceysens F, Annoni M, Lauwers B, Reynaerts D (2013) EDM drilling of ultra-high aspect ratio micro holes with insulated tools. *CIRP Ann—Manuf Technol* 62(1):191–194
6. Karthikeyan G, Ramkumar J, Dhamodaran S, Aravindan S (2010) Micro electric discharge milling process performance: an experimental investigation. *Int J Mach Tools Manuf* 50(8):718–727
7. Rahman M, Asad ABMA, Masaki T, Saleh T, Wong YS, Senthil Kumar A (2010) A multiprocess machine tool for compound micromachining. *Int J Mach Tools Manuf* 50(4):344–356
8. Asad ABMA, Masaki T, Rahman M, Lim HS, Wong YS (2007) Tool-based micro-machining. *J Mater Process Technol* 192–193:204–211
9. Jain VK (2018) *Introduction to micromachining*. Narosa Publication House, New Delhi
10. Gad-el-Hak M (2002) *The MEMS handbook*. CRC Press
11. Egashira K, Mizutani K (2005) EDM at low open-circuit voltage. *Int J Electr Mach* 10:21–25
12. Egashira K, Matsugasako A, Tsuchiya H, Miyazaki M (2006) Electrical discharge machining with ultralow discharge energy. *Precis Eng* 30:414–420
13. Zahiruddin M, Kunieda M (2012) Comparison of energy and removal efficiencies between micro and macro EDM. *CIRP Ann—Manuf Technol* 61:187–190
14. Reddy MS, Jain VK, Lal GK (1988) Tool design for ECM: correction factor method. *J Eng Ind* 110(2):111–118

15. Câmara MA, Rubio JCC, Abrão AM, Davim JP (2012) State of the art on micromilling of materials, a review. *J Mater Sci Technol* 28(8):673–685
16. Liu Q, Zhang Q, Zhu G, Wang K, Zhang J, Dong C (2016) Effect of electrode size on the performances of micro EDM. *Mater Manuf Process* 31(4):391–396
17. Hernandez P, Campos D, Socorro P, Benitez A, Ortega F, Díez N, Marrero MD (2015) Electroforming applied to manufacturing of microcomponents. *Procedia Eng* 132:655–662
18. Uriarte L, Herrero S, Ivanov A, Oosterling H, Staemmler L, Tang PT, Allen D (2006) Comparison between microfabrication technologies for metal tooling. *Proc Inst Mech Eng, Part C: J Mech Eng Sci* 220(11):1665–1676
19. Jain VK, Sidpara A, Balasubramaniam R, Lodha GS, Dhamgaye VP, Shukla R (2014) Micro-manufacturing: a review—Part I. *Proc Inst Mech Eng, Part B: J Eng Manuf* 228(9):973–994
20. Rahman M, Lim HS, Neo KS, Senthil Kumar A, Wong YS, Li XP (2007) Tool-based nanofinishing and micromachining. *J Mater Process Technol* 185(1–3):2–16
21. Khanra AK, Pathak LC, Godkhindi MM (2007) Microanalysis of debris formed during electrical discharge machining (EDM). *J Mater Sci* 42(3):872–877
22. Karthikeyan G, Garg AK, Ramkumar J, Dhamodaran S (2012) A microscopic investigation of machining behavior in Micro ED-milling process. *J Manuf Process* 14(3):297–306
23. Tao J, Shih AJ, Ni J (2008) Experimental study of the dry and near-dry electrical discharge milling processes. *J Manuf Sci Eng* 130(1):011002
24. Mohri N, Fukuzawa Y, Tani T, Saito N, Furutani K (1996) Assisting electrode method for machining insulating ceramics. *CIRP Ann* 45(1):201–204
25. Sabur A, Ali MY, Maleque MA, Moudood MA (2014) Micro-EDM for micro-channel fabrication on nonconductive ZrO<sub>2</sub> ceramics. *Int J Automot Mech Eng* 10:1841–1851
26. Schubert A, Zeidler H, Hahn M, Hackert-Oschätzchen M, Schneider J (2013) Micro-EDM milling of electrically nonconducting zirconia ceramics. *Procedia CIRP* 6:297–302
27. König W, Dauw DF, Levy G, Panten U (1988) EDM-Future Steps towards the Machining of Ceramics. *CIRP Ann—Manuf Technol* 37(2):623–631
28. Liu YH, Ji R, Li Q, Yu L, Li X (2008) Electric discharge milling of silicon carbide ceramic with high electrical resistivity. *Int J Mach Tools Manuf* 48(12–13):1504–1508
29. Liang SY, Shih AJ (2016) *Analysis of machining and machine tools*. Springer, Berlin
30. Shen Y, Liu Y, Zhang Y, Dong H, Sun W, Wang X (2015) High-speed dry electrical discharge machining. *Int J Mach Tools Manuf* 93:19–25
31. Kunieda M, Yoshida M (1996) Electrical discharge machining in gas. *CIRP Ann—Manuf Technol* 46(1):143–146
32. Kunieda M, Mlyashl Y, Takaya T (2003) High speed 3D milling by Dry EDM. *CIRP Ann—Manuf Technol* 52(1):147–150
33. Shen Y, Liu Y, Sun W, Zhang Y, Dong H, Zheng C (2016) High-speed near dry electrical discharge machining. *J Mater Process Technol* 233:9–18
34. Pattabhiraman A, Marla D, Kapoor SG (2016) Atomized dielectric spray-based electric discharge machining (spray-EDM) for sustainable manufacturing. In: *Proceedings of ASME 2015 international manufacturing science and engineering conference, vol 1: Processing, Charlotte, North Carolina, USA, 8–12 June 2015*
35. Marashi H, Jafarlou DM, Sarhan AAD, Hamdi M (2016) State of the art in powder mixed dielectric for EDM applications. *Precis Eng* 46:11–33
36. Yeo SH, Murali M (2003) A new technique using foil electrodes for the electro-discharge machining of micro grooves. *J Micromech Microeng* 16:N1
37. Murali M, Yeo SH (2004) A novel spark erosion technique for the fabrication of high aspect ratio micro-grooves. *Microsyst Technol* 10(8–9):628–632
38. Flaño O, Ayesta I, Izquierdo B, Sánchez JA, Zhao Y, Kunieda M (2018) Improvement of EDM performance in high-aspect ratio slot machining using multi-holed electrodes. *Precis Eng* 51:223–231
39. Kunieda M, Lauwers B, Rajurkar KP, Schumacher BM (2005) Advancing EDM through fundamental insight into the process. *CIRP Ann—Manuf Technol* 54(2):64–87

40. Pandit SM, Rajurkar KP (1983) A stochastic approach to thermal modeling applied to electro-discharge machining. *J Heat Transf* 105(3):555–562
41. Yu ZY, Masuzawa T, Fujino M (1998) Micro-EDM for three-dimensional cavities—development of uniform wear method. *CIRP Ann* 47:169–172
42. Narasimhan J, Yu Z, Rajurkar KP (2005) Tool wear compensation and path generation in micro and macro EDM. *J Manuf Process* 7(1):75–82
43. Yu H, Luan JJ, Li JZ, Zhang YS, Yu ZY, Guo DM (2010) A new electrode wear compensation method for improving performance in 3D micro EDM milling. *J Micromech Microeng* 20:055011
44. Zhang L, Du J, Zhuang X, Wang Z, Pei J (2015) Geometric prediction of conic tool in micro-EDM milling with fix-length compensation using simulation. *Int J Mach Tools Manuf* 89:86–94
45. Pei J, Zheng B, He L (2013) Arithmetic and experimental study of fix-length compensation based on conical bottom shape of electrode in micro-EDM. In: *ASME 2013 international mechanical engineering congress and exposition*, vol 2A: Advanced manufacturing, San Diego, California, USA, 15–21 Nov 2013
46. Pei J, Zhuang X, Zhang L, Zhu Y, Liu Y (2018) An improved fix-length compensation method for electrical discharge milling using tubular tools. *Int J Mach Tools Manuf* 124:22–32
47. Karthikeyan G, Sambhav K, Ramkumar J, Dhamodaran S (2011) Simulation and experimental realization of Microchannels using a ED-milling process. *Proc Inst Mech Eng, Part B J Eng Manuf* 225(12):2206–2219
48. Ho C, Tai Y (1998) Micro-electro-mechanical-systems (MEMS) and fluid flow. *Annu Rev Fluid Mech* 30:579–612
49. Liu K, Lauwers B, Reynaerts D (2009) Process capabilities of Micro-EDM and its applications. *Int J Adv Manuf Technol* 47(1–4):11–19
50. Patel D, Jain VK, Ramkumar J (2016) Micro texturing on metallic surfaces: state of the art. *Proc Inst Mech Eng, Part B: J Eng Manuf* 232(6):941–964
51. Ali MY (2009) Fabrication of microfluidic channel using micro end milling and micro electrical discharge milling. *Int J Mech Mater Eng* 4:93–97
52. Hung J, Yang T, Li K (2011) Studies on the fabrication of metallic bipolar plates—Using micro electrical discharge machining milling. *J Power Sources* 196(4):2070–2074

# Chapter 3

## Micro-EDM with Translational Tool Motion: The Concept of Micro-Electro-Discharge-Slotting



Vishal John Mathai and Harshit K. Dave

**Abstract** Application of micro-fabrications is immense in today's life as many products have micro-features on it as a part of aesthetics or functionality. In this chapter, novel technique called Micro-Electro-Discharge-Slotting (MEDS) has been discussed in detail. The process can be used as an alternative in case of issues difficulties in carrying out commonly used micro-EDM process variant like micro-electro-discharge milling. Micro-Electro-Discharge-Slotting, due to its specialty in its tool actuation strategy, can reduce inaccuracies that may incur in the machined feature due to deformation of the micro-tool electrode. Further, a novel micro-electrode fabrication technique, namely foil as tool electrode (FAST) EDM, has also been discussed for cutting and dressing of micro-electrodes. The technique can be used in the absence of sophisticated micro-machining facilities to fabricate micro-electrodes with relative low mechanical distortion. To understand the parameter effects, a case study has also been discussed for both the processes.

**Keywords** Micro-EDM · Tool kinematics · Micro-fabrication · Micro-slot

### 3.1 Feature Generation Using Micro-EDM with Tool Actuation: A Comparative Assessment

Product downscaling is one of the areas that has been identified as the need of the day as the same has immense applications in the various fields like health care and aerospace. Such concepts in reality are implemented by carrying out different types

---

V. J. Mathai

Department of Mechanical Engineering, Amal Jyothi College of Engineering, Kanjirappally, Kerala, India  
e-mail: [vishaljohnmathai@gmail.com](mailto:vishaljohnmathai@gmail.com)

H. K. Dave (✉)

Department of Mechanical Engineering, S. V. National Institute of Technology, Surat, Gujarat, India  
e-mail: [harshitkumar@yahoo.com](mailto:harshitkumar@yahoo.com)

© Springer Nature Singapore Pte Ltd. 2019

G. Kibria et al. (eds.), *Micro-electrical Discharge Machining Processes*, Materials Forming, Machining and Tribology, [https://doi.org/10.1007/978-981-13-3074-2\\_3](https://doi.org/10.1007/978-981-13-3074-2_3)

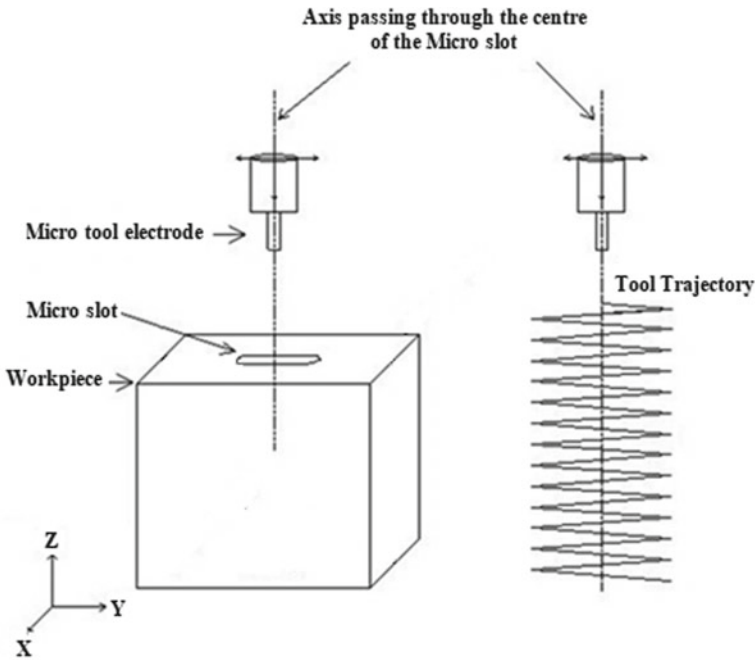
of micro- or nano-level manufacturing techniques. These can either be a material removal or material addition-based techniques, with each having its own unique advantages and limitations. Other than these techniques, surface modification techniques like isostatic pressing and hot isostatic pressing have also been reported to creating such features.

If we observe various types of products around us, one of the most commonly seen category micro-feature is slots or channels of different shapes and size. Such features have wide range of applications in biomedical and micro-electro-mechanical systems (MEMS), etc. [1, 2]. Different types of micro-manufacturing techniques have been reported for fabrication of such features. This has been either traditional or advanced micro-manufacturing techniques. Even though relatively cost-effective, one of the major limitations of traditional as well as mechanical-based micro-manufacturing techniques is the effect of mechanical properties of the substrate material. Thermal and chemical energy-based advanced micro-manufacturing techniques and three process variants are used in this context, and micro-electro-discharge machining is a process that has been widely used in this regard.

Micro-electro-discharge machining (MEDM) process is capable of generating simple to complex geometries of micron size on electrically conductive material using a micro-tool electrode moved in a predefined fashion. The material is removed in the form of micro-craters with the help of precisely controlled and repetitive sparks [3]. However, to reduce the limitations associated with the machining method in terms of tool wear, surface quality, etc., the concept of hybridization has also been reported. However, choice of the mode of hybridization depends on the geometry of the target micro-feature.

In case of fabrication of micro-slots or channels, two modes of application of MEDM are possible; (i) to use a tool electrode having the size and shape of the target slot and carry out conventional die sinking [4] and (ii) to use a tool electrode having the size similar to or smaller than the size of the target slot and carry out machining with additional tool kinematics [5, 6]. Despite a simple strategy, some of the issues that are involved in the first method are the effort needed to fabricate micro-electrode having the shape of the micro-slot, lack of flushing at the inter-electrode gap due to minimum tool motion, etc. These technical difficulties may be countered to a certain extent by second method in which a simple tool is used to fabricate a complex-shaped slot by making it move along a predefined path with or without a rotational or vibrational motion.

One of the most commonly employed MEDM process variant for fabrication of micro-slots or channels is micro-electro-discharge milling (MEDM). Application of this method is not restricted to fabrication of slots but also for generating 3D micro-features with high aspect ratios [7, 8]. Since the technique employs a rotating micro-tool electrode translated along a predefined path, the issues pertaining debris accumulation in the inter-electrode gap also can be avoided. Many research works have been reported on the effect of process parameters on response characteristics like tool wear and surface roughness [9, 10]. The intense wear that usually occurs on the tool electrode during EDM-based processes has been reported to be a critical issue in this process variant as well. However, many end-wear



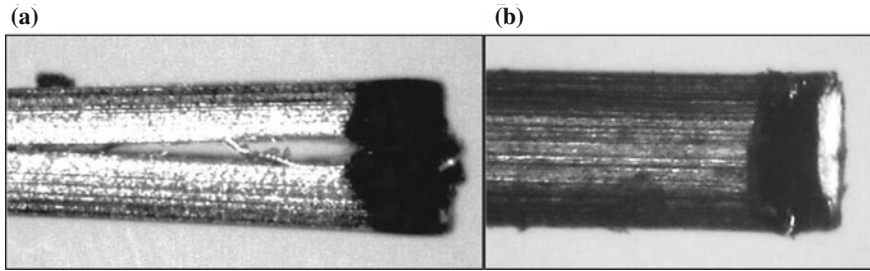
**Fig. 3.1** Concept of Micro-Electro-Discharge-Slotting process for fabrication of linear slots

compensation techniques as well as wear reduction techniques have also been proposed by many researchers [11–13].

Even though the process is widely accepted for micro-manufacturing, the quality of the target features also depends on the quality of micro-tool electrode used for machining. The electrode that will be used for machining micro-features must be free from any sort of distortions and deformations. However, for a researcher, who have relatively low experience or if the machine tool does not have sophisticated micro-fabrication facilities, such issues are bound to happen. If an electrode of poor quality is employed for machining, it will result into generation of low-quality feature. The inaccuracy will further be aggravated if the tool is subjected to additional motion, like rotation in the case of MED milling. Hence, it is important to devise a strategy with which a micro-tool can be fabricated with limited facilities as well as use them with effectiveness closer to that can be achieved through MED milling.

### 3.2 Concept of Micro-Electro-Discharge-Slotting

Micro-Electro-Discharge-Slotting (MEDS) is a variant of MEDM, a tool electrode without rotational motion is made to scan over the workpiece surface. The micron-



**Fig. 3.2** a Micro-electrode with crack and b micro-electrode with pinch effect (magnification: 75 $\times$ )

sized tool electrode is made to move along a trajectory as defined by the operator. The choice of the type of path depends on the shape of the micro-slot. During tool actuation, the axis of the tool electrode will be perpendicular to the workpiece surface. The translational motion is accompanied by feed in the Z direction as well. Figure 3.1 shows the mode of tool actuation in the case of machining of a linear slot. A similar strategy shall be followed to generate any shape of slots by programming the tool path according to the micro slot shape and making the micro tool scan along the same.

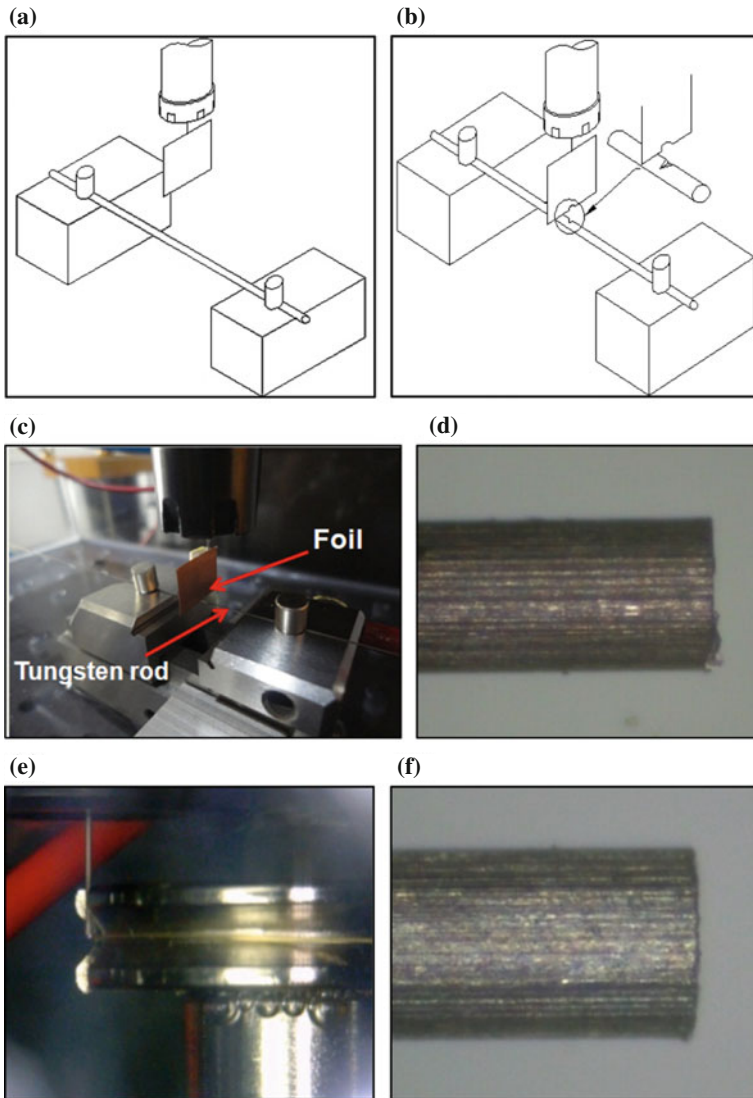
Since the tool is not rotating, any distortion in terms of bending will not affect the dimensional and geometrical accuracy of the feature to a bigger extent. Simultaneously, the translational motion of the tool electrode will facilitate the proper ejection of debris from the machining zone, thereby providing the level of process stability as in the case of MED milling.

### 3.3 Micro-electrode Fabrication: Concept of FAST

Influence of mechanical forces on the micro-tool electrode must be minimized to avoid any type of deformation on the same. If mechanical methods are employed for fabricating micro-electrodes from commercially available electrode raw material, the possibility of getting the electrode bend is very high. Even if extreme care is taken to avoid such deformation, the micro-rod tip may tend to get cracked or pinched as shown in Fig. 3.2.

Hence, a force-free machining technique is always preferable for fabrication of micro-electrodes, and MEDM itself is a good option for the same. Foil as tool electrode (FAST) EDM technique, a process variant of commonly used MEDM process, can be used alongside with micro-wire electro-discharge grinding (MWEDG) for deformation-free micro-electrodes.

In FAST EDM technique, a foil electrode is used to cut small pieces of micro-electrode from the commercially available long micro-rod. The foil electrode is die-sunk on the micro-rod which is held by magnetic pins as shown in Fig. 3.3a, b.

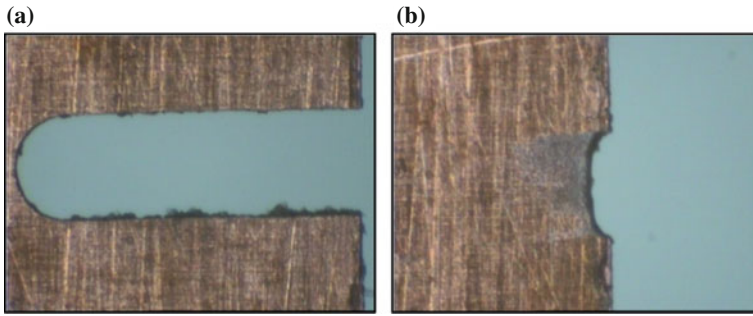


**Fig. 3.3** a–c Concept FAST EDM and d–f post-processing of micro-electrodes fabricated by FAST EDM using MWEDG

Once the foil completely crosses the micro-rod, it can be ensured that the micro-rod is cut and the foil electrode can be lifted to its home position.

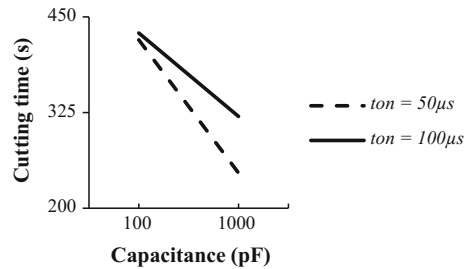
Figure 3.3c shows the original set-up that has been employed for demonstrating FAST EDM technique. The commercially available micro-rod is sliced into small pieces by performing a die-sinking operation using a foil electrode having a thickness of 60  $\mu\text{m}$ . It can be inferred from Fig. 3.3d that the end of micro-electrode cut using





**Fig. 3.4** Wear observed on the foil electrode in FEDM under **a** straight polarity and **b** reverse polarity (magnification: 100 $\times$ )

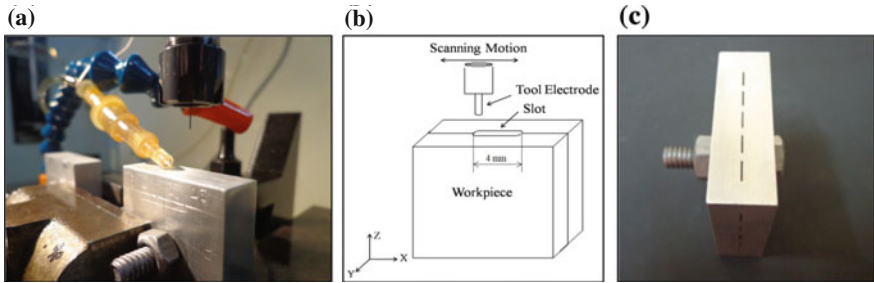
**Fig. 3.5** Effect of variation of capacitance and pulse ON time on cutting time in FEDM



FAST technique is not perfectly flat. Hence to make it flat, the electrode must be subjected to MWEDG. For this, the cut electrodes are mounted on to the spindle using a collet system. The micro-electrode with rotational motion is fed against the moving micro-wire (as shown in Fig. 3.3e) to get the micro-electrode tip ground and hence flat as can be seen in Fig. 3.3f.

Prior to implementation of FEDM for electrode cutting, a set of experiments have been carried out to identify the preferable set of process parameters. Effects of electrode polarity, pulse ON time and capacitance on electrode wear and cutting time have been investigated. Figure 3.4a, b shows the intensity of wear observed on the foil electrode under straight and reverse polarities. Figure 3.5 shows the variation in cutting time with change in capacitance and pulse ON time. In straight polarity condition (foil electrode: negative; tungsten rod: positive), intense wear has been observed on the foil electrode. But on reversing the polarity, the electrode has been cut with lower extent of material loss from the foil electrode. The difference in wear observed on the foil may be attributed to the difference in carbon deposition on the electrodes [14, 15]. Hence, it can be inferred that reverse polarity is preferable for FEDM technique.

Figure 3.5 shows the effect of variation of capacitance and pulse ON time on electrode cutting time using FEDM carried out under reverse polarity condition. It can be inferred from the graph that cutting time is low when electrodes are processed under high capacitance levels. It is also worth noting that even though the effect



**Fig. 3.6** a Experimental set-up, b workpiece and slot configuration and c workpiece with slots along the split line

**Table 3.1** Parameter levels and values

Parameters	Units	L1	L2	L3
Current	A	0.3	1.5	–
Voltage	V	30	40	50
Pulse ON time	μ.s	31	46	61
Pulse OFF time	μ.s	30	46	60
Scanning speed	mm/s	0.07	0.09	0.13
Aspect ratio	–	1	1.5	2

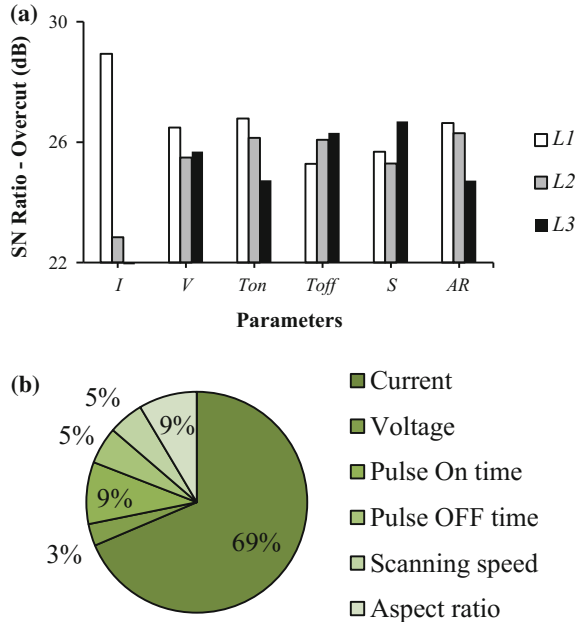
is not that significant at lower levels of capacitance, it can be seen that the cutting time is relatively higher when high pulse ON time condition is employed with high capacitance condition.

### 3.4 Case Study: Generation of Linear Micro-slots with Conventional EDM Tool

To assess the feasibility of the process, Micro-Electro-Discharge-Slotting process has been carried out by using conventional EDM tool. Linear slots have length of 4 mm are made on aluminium blocks in split piece configuration as shown in Fig. 3.6. The micro-slots are made along the split line so that the slots can be opened and studied. Tungsten micro-rods having diameter of 300 μm and length 8 mm are fabricated using FAST EDM technique. The machining has been carried out with drip flushing at the machining zone.

The study has been carried out by varying six parameters, viz. current, voltage, pulse ON time, pulse OFF time, scanning speed and aspect ratio of the feature. The experiments are designed using Taguchi’s L<sub>18</sub> orthogonal array. The parameter levels employed for machining are shown in Table 3.1. Current has been varied at two levels and rest of the parameters at three levels.

**Fig. 3.7 a** Effect of process parameters on overcut, **b** percentage contribution of process parameters on overcut

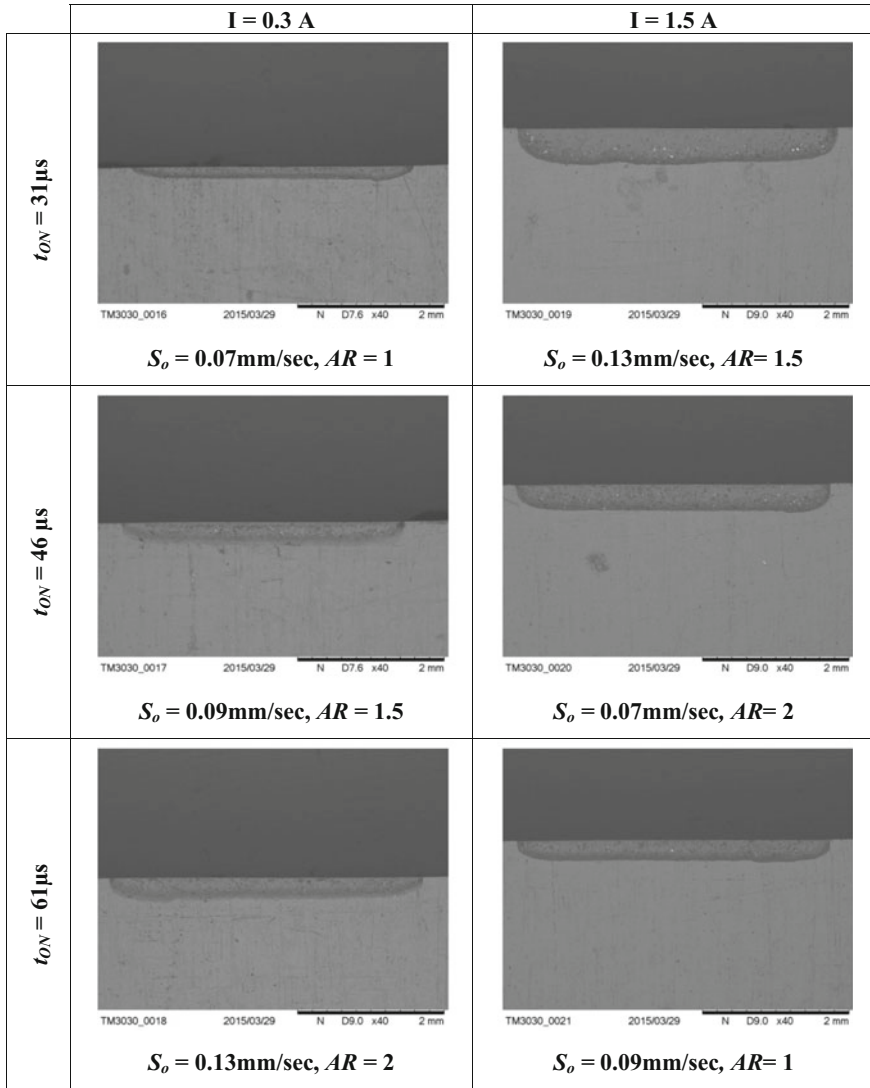


All the parameter values except that for aspect ratio are preset on the machine tool. Aspect ratio has been defined as the ratio of slot depth to tool diameter used, and the same is varied by changing the depth of the slot keeping the electrode diameter constant. The response values have been converted into signal-to-noise ratio.

### 3.4.1 Effect of Process Parameters on Overcut and Slot Quality

Figure 3.7a, b, respectively, shows the effect of various process parameters on overcut in micro-slots generated by micro-ED slotting process and the percentage contribution result obtained through analysis of variance. Figure 3.8 shows the cross-sectional view of the slots obtained under different machining conditions.

It can be inferred from the graphs that current has a significant effect on overcut of micro-slots machined. The result is in line with inference that can be deduced from the ANOVA as well. This may be mainly due to the tendency to lose more material at high discharge or due to the effect of secondary discharges caused by debris particles moving out of the machining zone. Hence, a lower current value is preferable for reducing overcut. Similar inferences can be deduced in the case of variation of pulse ON time.



**Fig. 3.8** Micro-slots machined under different conditions

In the case of gap voltage, the overcut tends to increase initially; however, for higher values the response tends to reduce again. Like in the case of variation of current, an increase in voltage will result in increase in discharge energy and hence amount of material removed per spark. However, being a parameter that is proportional to inter-electrode gap, an increase in the parameter may result in reduction in energy intensity of the sparks, leading to lower amount of material removal. It is also worth noting that the parameter does not have a significant effect on overcut.

It can also be seen that a higher pulse OFF time and scanning speed of the tool electrode are preferable as it resulted in features with relatively lower overcut. Such an inference may be due to the effect of both these parameters on inter-electrode gap flushing.

Further, it can also be inferred from the graphs that aspect ratio of the target feature also contributes to the extent of overcut in it. It can be seen that the overcut increases with increase in aspect ratio. This may be due to the ineffective flushing that tends to happen with increase in depth of the target feature. In the absence of pressurized external flushing, which cannot be employed in the case of MEDM, the situation may further get aggravated, thereby leading to increase in overcut.

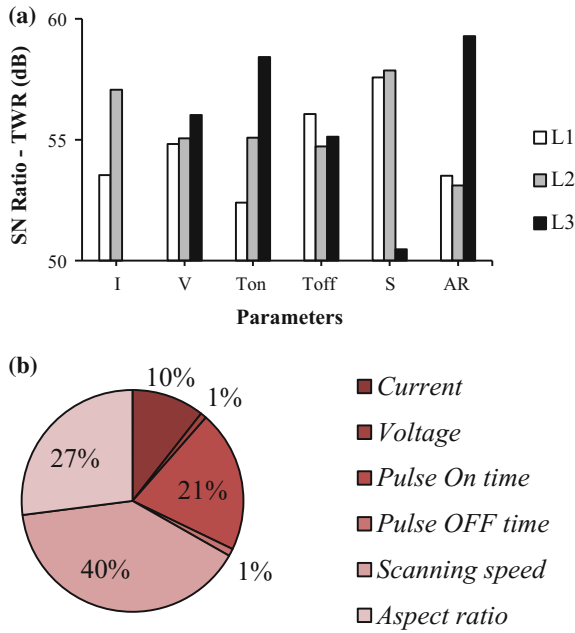
With reference to Fig. 3.8, it can be understood that high current values are preferable for machining features with high aspect ratio. Further, to machine micro-features with better bottom surfaces, higher values of pulse ON time and scanning must be chosen.

### ***3.4.2 Effect of Process Parameters on Tool Wear Conditions***

Wear on the tool electrode has been studied in terms of tool wear rate. Figure 3.9 shows the signal-to-noise ratios obtained for the response characteristic. Further, images of micro-electrodes used under different machining conditions are shown in Fig. 3.10.

From Fig. 3.9a, it can be observed that the wear on the micro-tool electrodes used under 1.5 A condition is lesser than that observed on a tool electrode used at 0.3 A, which contradictory against the reported results. Further, it is also observed that the tip of the electrodes used at 1.5 A condition, which is shown in Fig. 3.10, has a 'bulged tip' condition. This reason for such an observation may either be due to the possibilities of residues getting deposited or due to the influence of anodic polarity of the electrode [14, 16]. The reduction in wear with increase in gap voltage, which can be seen from the graph, may be attributed to the reduction in energy intensity with increase in spark gap. Similar inference can be drawn in the case of variation of pulse ON time. In the case of variation of pulse OFF time, the trend has been found to be contradictory. The tool wear rate has been found to be least when the value of pulse OFF time is smallest.

In the case of variation of non-electrical parameters, viz. scanning speed and aspect ratio of the feature, two distinct trends can be seen. It can be understood that the tool wear rate decreases initially and then increases with higher values of scanning speed. This implies that an intermediate level of scanning speed is preferable. As too motion provides turbulence in the machining zone, the debris removal becomes effective, making the process stable. But when higher scanning speeds are employed, the tool electrode will not get ample time to remove the material from the workpiece surface effectively, thereby resulting in higher process completion time. This will lead to prolonged exposure of the tool electrode to machining condition and hence unanticipated material loss from the same.

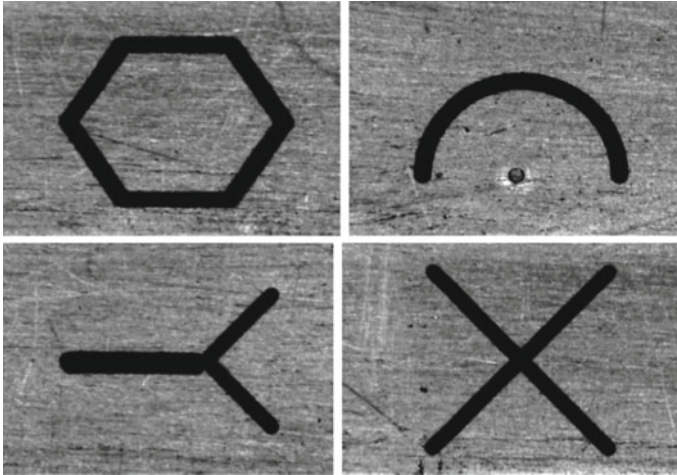


**Fig. 3.9** a Effect of process parameters on tool wear rate, b percentage contribution of process parameters on tool wear rate

	$t_{ON} = 31\mu s$	$t_{ON} = 46\mu s$	$t_{ON} = 61\mu s$
<b>I = 0.3 A</b>			
	$S_o = 0.09\text{ mm/sec}; AR = 1.5$	$S_o = 0.13\text{ mm/sec}; AR = 2.0$	$S_o = 0.07\text{ mm/sec}; AR = 1.0$
<b>I = 1.5 A</b>			
	$S_o = 0.13\text{ mm/sec}; AR = 1$	$S_o = 0.07\text{ mm/sec}; AR = 1.5$	$S_o = 0.09\text{ mm/sec}; AR = 2.0$

**Fig. 3.10** Tip of micro-electrodes used under different parameter combinations

In the case of variation of aspect ratio, it can be seen that as the parameter increases, the tool wear rate increases initially. But on further increase, the tool wear rate is observed to decrease. This decrease in tool wear rate at higher values of aspect ratio may be due to the improper removal of debris from the machining zone under such



**Fig. 3.11** Examples of nonlinear slots that can be generated using MEDS process

conditions, thereby leading to deposition of material on the micro-electrode. This can be clearly seen in the images shown in Fig. 3.10.

The critical inference that can be drawn from ANOVA, which is shown in Fig. 3.9b, is that parameters that influence the flushing conditions, viz. scanning speed of the tool electrode and aspect ratio of the micro-feature, influence the tool wear rate most significantly.

### 3.5 Application of Micro-ED Slotting in Micro-feature Generation

The concept of MEDS can be extended to generations to other complex-shaped features. Figure 3.11 shows some of the features that have been machined using MEDS. It can be understood that the process can very well be employed for generating features in a single or sequential steps. The process can be of good use in fabricating complex channel systems like in biomedical or lab-on-a-chip set-ups in which intersecting slots and curved slots are mostly involved. Further, the process can also be used to create dies and moulds for creating micro-features.

The process can be extended to any type of feature generation in which micro-ED milling is employed. Another highlighting advantage is that unlike in the case of micro-ED milling, sharp-cornered slots can also machined with the help of MEDS technique with the use of a prismatic tool electrode.

### 3.6 Summary

Micro-Electro-Discharge-Slotting is a micro-machining technique that can be used for machining micro-slots or channels on any material that is electrically conductive. The concept of tool actuation in the process negates the effect of any physical distortion of the micro-electrode on feature quality. Unlike in the case of micro-electro-discharge milling, sharp-cornered features can also be generated. Further, the concept of foil as tool electrode EDM has been discussed for micro-electrode cutting. Being a method that is totally free from application of mechanical forces, the process can very well be used to fabricate distortion-free electrodes. Such electrodes can be used for both micro-ED-based slotting and milling operations.

### References

1. Soares RRG, Santos DR, Chu V, Azevedo AM, Aires-Barros MR, Conde JP (2017) A point-of-use micro fluidic device with integrated photodetector array for immunoassay multiplexing: detection of a panel of mycotoxins in multiple samples. *Biosens Bioelectron* 87:823–831
2. Wang T, Wang J, He J, Wu C, Luo W, Shuai Y, Zhang W, Chen X, Zhang J, Lin J (2018) A comprehensive study of a micro channel heat sink using integrated thin-film temperature sensors. *Sensors* 18(1):299–304
3. Ho KH, Newmann ST (2003) State of the art electrical discharge machining. *Int J Mach Tools Manuf* 43:1287–1300
4. Murali M, Yeo SH (2004) A novel spark erosion technique for the fabrication of high aspect ratio micro-grooves. *Microsyst Technol* 10:628–632
5. Lim HS, Wong YS, Rahman M, Edwin Lee MK (2003) A study on the machining of high-aspect ratio micro-structures using microEDM. *J Mater Process Technol* 140:318–325
6. Kuo CL, Huang JD (2004) Fabrication of series-pattern micro-disk electrode and its application in machining micro-slit of less than  $\mu\text{m}$ . *Int J Mach Tools Manuf* 44:545–553
7. Karthikeyan G, Ramkumar J, Dhamodaran S, Aravindan S (2010) Micro electric discharge milling process performance: an experimental investigation. *Int J Mach Tools Manuf* 50:718–727
8. Uhlmann E, Piltz S, Doll U (2005) Machining of micro/minature dies and moulds by electrical discharge machining-recent development. *J Mater Process Technol* 167:488–493
9. Mehruz R, Ali MY (2009) Investigation of machining parameters for the multiple-response optimization of micro electrodischarge milling. *Int J Adv Manuf Technol* 43:264–275
10. Yan J, Kaneko T, Uchida K, Yoshihara N, Kuriyagawa T (2010) Fabricating microgrooves with varied cross-sections by electro discharge machining. *Int J Adv Manuf Technol* 50:991–1002
11. Yan MT, Lin SS (2011) Process planning and electrode wear compensation for 3D micro-EDM. *Int J Adv Manuf Technol* 53:209–219
12. Nguyen VQ, Duong TH, Kim HC (2015) Precision micro based on real-time monitoring and electrode wear compensation. *Int J Adv Manuf Technol* 79(9–12):1828–1838
13. Chiou AH, Tsao CC, Hsu CY (2015) A study of the machining characteristics of micro EDM milling and its improvement by electrode coating. *Int J Adv Manuf Technol* 78:1857–1864
14. Rajurkar KP, Levy G, Malshe A, Sundaram MM, McGeough J, Hu X, Resnick R, DeSilva A (2006) Micro and nano machining by electro-physical and chemical processes. *CIRP Ann—Manuf Technol* 55(2):643–666
15. Natsu W, Kunieda M, Nishiwaki N (2004) Study on influence of inter-electrode atmosphere on carbon adhesion and removal amount. *Int J Electr Mach* 9:43–50
16. Kunieda M, Lauwers B, Rajurkar KP, Schumacher BM (2005) Advancing EDM through fundamental insight into the process. *CIRP Ann—Manuf Technol* 54(2):64–87



# Chapter 4

## Micro-Wire-EDM



Taylor Daniel, Chong Liu, Junyu Mou and Muhammad P. Jahan

**Abstract** Micro-wire-electro-discharge machining (micro-WEDM) is a widely used non-conventional micromachining process to fabricate three-dimensional (3D) complex micro-features in difficult-to-machine materials. This chapter offers a concise overview on the micro-WEDM process. A brief overview on the process mechanism, system components, parameters and variants of micro-WEDM has been provided in the chapter. In addition, some of the innovative applications and advanced research studies on the micro-WEDM have been discussed in brief. Finally, current challenges that limit the wide application of micro-WEDM in industries, as well as opportunities for future research, have been discussed at the end of the chapter.

**Keywords** Micro-wire-EDM · System components · Process mechanism Applications · Advanced research · Recommendation for future research

### 4.1 Introduction

The electrical discharge machining (EDM) process removes electrically conductive materials from the part to create features using thermoelectric energy generated between the electrode and the workpiece submerged in the dielectric fluid. The gap between the workpiece and electrode, called ‘spark gap’, provides a space allowing the pulse discharges to remove material from the workpiece by melting and

---

T. Daniel · C. Liu · J. Mou · M. P. Jahan (✉)  
Department of Mechanical and Manufacturing Engineering,  
Miami University, Oxford, OH 45056, USA  
e-mail: [jahanmp@miamioh.edu](mailto:jahanmp@miamioh.edu)

T. Daniel  
e-mail: [danieltm@miamioh.edu](mailto:danieltm@miamioh.edu)

C. Liu  
e-mail: [liuc12@miamioh.edu](mailto:liuc12@miamioh.edu)

J. Mou  
e-mail: [mouj@miamioh.edu](mailto:mouj@miamioh.edu)

© Springer Nature Singapore Pte Ltd. 2019  
G. Kibria et al. (eds.), *Micro-electrical Discharge Machining Processes*, Materials Forming, Machining and Tribology, [https://doi.org/10.1007/978-981-13-3074-2\\_4](https://doi.org/10.1007/978-981-13-3074-2_4)

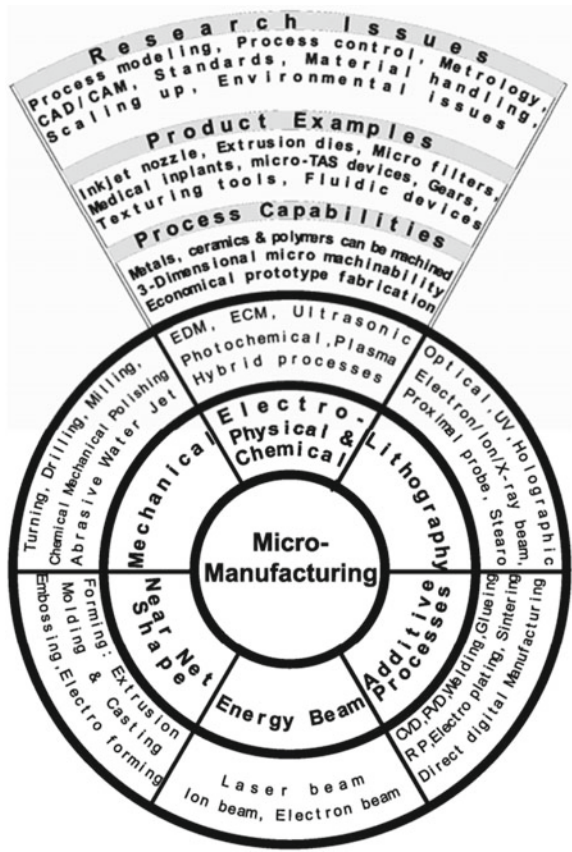
evaporation. Micro-EDM process has become one of the widely used methods for making high-aspect-ratio micro-features due to achievable small process forces and repeatability. There are, currently, four types of micro-EDM technology used in manufacturing to machine complex micro-features [1].

- The micro-wire-EDM process uses wires with 50–250  $\mu\text{m}$  diameters to cut a workpiece made of electrically conductive material.
- The die-sinking micro-EDM process makes mirror image in the part by the electrode with same micro-features on it.
- The micro-EDM drilling process is used to make micro-holes on the workpiece with microelectrodes of diameter as small as 5–10  $\mu\text{m}$ .
- The micro-EDM milling process is used to make 3D micro-cavities by milling with microelectrodes of diameter as small as 5–10  $\mu\text{m}$ .

Although there are many research papers published to announce the improvement of these processes, they are still not very popular in modern manufacturing industries. This is due to the fact that, the availability of the tools to satisfy the micro-EDM machining and the reliability of the product characteristics after the process are still not enough currently [2]. The demand for micromachining has increased rapidly in many sectors, such as microelectronics, optics and biotechnology. Products with micro-features need component dimensions with hundreds of micrometres. Researchers from worldwide academia and industry are trying to improve the existing technologies and find the innovation methods to meet this need. Lithography-based micro-fabrication processes are currently being used extensively to produce features with micrometre or sub-micrometre dimensions for micro-electromechanical systems (MEMS). But the lithography-based processes have limitation, for example, it has limit choice of materials, it has limitation on the geometry of the part, and it needs huge amount of investment. The tool-based micro-parts production technologies may replace lithography-based technologies to produce parts made of different materials to meet the growing demands of MEMS. Micro-EDM is one such process, as it is one of the most widely used and advanced tool-based micromachining processes, currently reported in academia and industries. Figure 4.1 shows the classification of micro-manufacturing processes along with their capabilities and research issues [3].

Electro-physical and chemical micromachining processes, such as micro-EDM and micro-ECM, have significant advantages over conventional mechanical micromachining processes, as the cutting tools do not contact the workpiece surface directly, thus avoiding frequent tool breakage and elastic deformation. They are flexible when machining small quantities of parts. Micro-EDM has further advantages over micro-ECM process in terms of process capability, machining speed and part complexity, as it is capable of fabricating micro-features ranging from simple micro-holes to complex micro-moulds. For minimizing the material removal in each step, the energy for discharge is reduced from  $10^{-6}$  to  $10^{-7}$  J. Table 4.1 shows dimensions that can be achieved by each type of micro-EDM [3]. Although the basic principle of material removal mechanism is same for each variant of micro-EDM, there are differences in the process geometry, system components and applications. This chapter aims to provide a comprehensive overview on the micro-wire-EDM (WEDM).

**Fig. 4.1** Classification of micro-manufacturing processes [3]



**Table 4.1** Micro-EDM capabilities [3]

Micro-EDM variant	Geometric complexity	Minimum feature size	Maximum aspect ratio	Surface quality $R_a$ ( $\mu\text{m}$ )
Drilling	2D	5 $\mu\text{m}$	~25	0.05–0.3
Die-sinking	3D	~20 $\mu\text{m}$	~15	0.05–0.3
Milling	3D	~20 $\mu\text{m}$	~10	0.5–1
WEDM	2 ½ D	~30 $\mu\text{m}$	~100	0.1–0.2
WEDG	Axi-sym.	3 $\mu\text{m}$	30	0.8

## 4.2 Process Mechanism of Macro- and Micro-WEDM

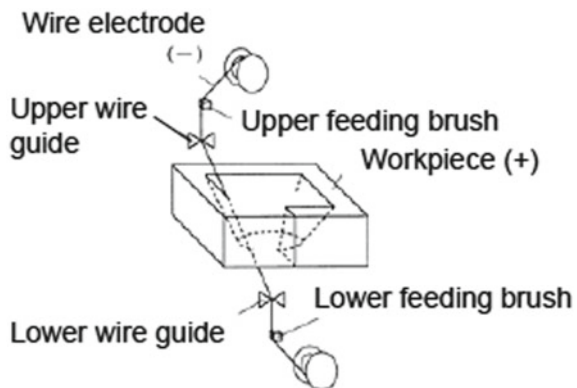
The difference between the macro- and micro-WEDM is basically the difference in the part size that is machined. However, the advanced research indicates differences in the size of the tool used, fabrication method, discharge energy used, movement

resolution of the axis, gap control mechanism and flushing mechanism [4]. Usually, when a macro-part (dimensions higher than 1 mm) is manufactured by the WEDM machine, it is named macro-WEDM. On the contrary, it is named micro-WEDM when a part with dimensions less than 1 mm ( $0\text{--}999\ \mu\text{m}$ ) is made in a wire-EDM machine.

In micro-WEDM, a continuous wire electrode ( $50\text{--}250\ \mu\text{m}$ ) is kept driving through the part by wire running system and without making any contact with the part. Compared to the traditional mechanical micromachining processes, the part is not cut by direct contact between the electrode and workpiece. Instead, it is machined by the pulse (electrical discharge), that is generated between the electrode and part. While the wire electrode is driving through the part, a series of rapid, repetitive and discrete spark discharges are created inside the dielectric fluid between the wire electrode and part by the power system [5]. The spark discharges were also called pulses. And the power system is a DC power supply. When the power system is switched on, the part and wire electrode are connected to positive and negative terminal correspondingly and an increasing voltage is created between the electrode and part. In a very short amount of time, the voltage reaches a certain point (breakdown voltage) where an electric discharge (pulse) happened. For micro-WEDM, the pulse size is usually  $10^{-7}$  to  $10^{-6}$  J. Due to the intense heat created during the pulse discharges, a small amount of materials from both wire electrode and part are vaporized and tiny craters are left both on wire electrode and part. By selecting the polarity of the workpiece and electrode, the material removal from wire electrode and workpiece can be controlled. Due to the facts that both the part and wire electrode are eroded during the cutting and the wire diameter is much smaller compared to the cutting surface, the wire electrode needs to be replaced at a certain speed by the wire running system and controlled under an optimal tension. Figure 4.2 shows the basic schematic representation of the micro-WEDM [6].

Additionally, micro-WEDM has a better surface finish due to the fact that all parameters are significantly smaller than the traditional WEDM, and the amplitude of wire vibration and wire lag is minimized. In order to prevent stray capacitance

**Fig. 4.2** Basic set-up for micro-WEDM [6]



or leakage of charges from the gap, the machine tool configuration is redesigned in micro-WEDM. The arc or other abnormal discharges are avoided by a pulse discrimination system, and the process accuracies are also increased to the maximum by minimizing the wire vibration and wire lag amplitude [7].

### 4.3 Micro-wire-EDM System Components

Micro-WEDM is the application of wire-EDM at micro-scale, and hence, the systems components of a micro-WEDM are similar to that of conventional wire-EDM with extending capabilities to generate much smaller scales of discharge energy. In a micro-WEDM machine, the components include

- Wire running system;
- Computerized numerical control system (CNC system);
- Power system;
- Dielectric flushing system.

In Fig. 4.3, a micro-WEDM machine with all the necessary systems is displayed [5]. A wire running system contains a wire electrode, a feeding spool, a tension clutch, a wire break switch, an upper wire guide, a lower wire guide and a wire cutting and collection pail. A CNC system that controls the  $U$ ,  $V$ ,  $X$  and  $Y$  system works based on the original point that is set on the part. A power system has a positive terminal and negative terminal, as described in the process mechanism section, the positive terminal is connected to the part and the negative terminal is connected to the wire electrode. During the cutting process, any point between the upper flushing valve and lower flushing valve is immersed in the dielectric fluid.

#### 4.3.1 Wire Running System

Due to the fact that in micro-WEDM process, the part and wire electrode were both eroded up, and the wire running system is a crucial system. For micro-WEDM, the electrode wire has much smaller diameter than the macro-scale wire-EDM, so the electrode is much easier to break due to the erosion. For the desired wire running system, the new wire should continuously be delivered to the part to be machined under a constant tension. Once the desired tension was guaranteed, the problems such as machining streaks, taper, vibration marks and wire breaks could be reduced to the minimum level or even prevented. However, the optimal wire tension depends on and also changes with the input discharge energy [8].

A basic wire running system contains a wire electrode supply device, an electromagnetic brake, a wire breakage sensor, two idle rollers, wire electrode, an upper guide, a lower guide a couple of DC motor and a waste bin [9]. The wire electrode

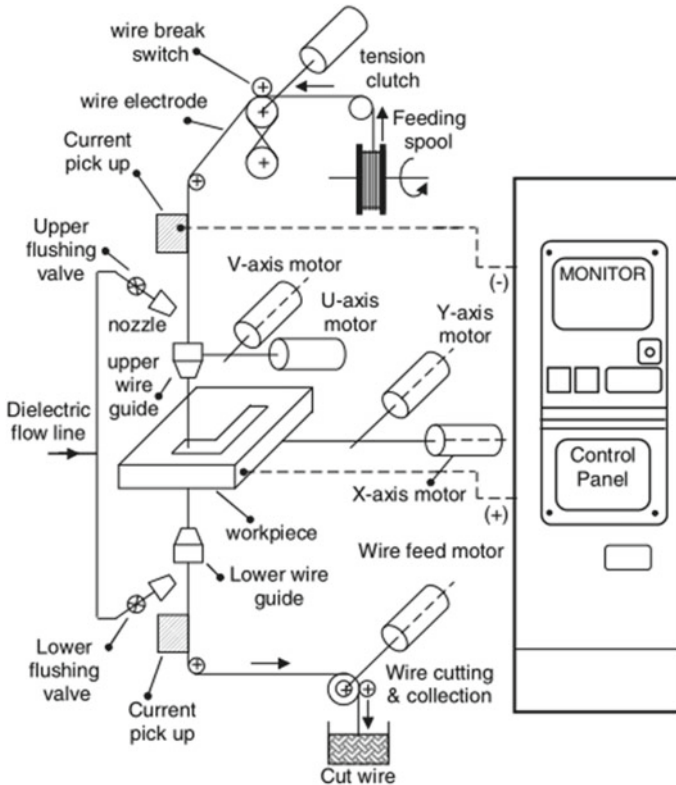


Fig. 4.3 Basic structure of a WEDM machine [5]

goes from wire electrode supply device all the way to the waste bin. The electric discharge pulses occur between the upper guide and the lower guide. The wire breakage sensor will detect the tension of the wire electrode and make sure new wire electrode is always prepared to use. The upper guide and lower guide make sure the wire electrode is in the correct place. The relative motion between the upper guide and the lower guide enable the cutting of the variation of the part possible. The overall driving force of the wire electrode is provided by the DC motor down at the bottom. And all the waste wire electrodes are collected at the waste bin.

### 4.3.2 Computerized Numerical Control System (CNC System)

In order to acquire a desired shape and high accuracy, the wire movement is controlled by a series of computer numerical control (CNC) codes that are typed by the operator. The micro-WEDM machine is designed to have the ability of reading and operating

based on the CNC code. By reading the CNC code, the micro-WEDM machine is able to move the  $U$ -,  $V$ -,  $X$ - and  $Y$ -axis motor. The  $U$ - and  $V$ -axis motor controls the motion of upper wire guide. The  $X$ - and  $Y$ -axis motor controls the motion of part. By combining the motion of  $U$ -,  $V$ -,  $X$ - and  $Y$ -axis, the micro-WEDM machine is able to produce a variety of complicated 3D shapes at micro-scale. Additionally, with the application of the servo control system, the machining accuracy and the surface roughness of the part can be greatly improved, by making it possible to fabricate micro-scale parts with a higher precision [10].

Figure 4.4 demonstrates the basic logic of a micro-WEDM control system [10]. An IBM compatible computer is used to relay the information to driven card. After the driven card received the information, the information is amplified and transferred to piezoelectric ceramics motions, which made the motion in  $X$ - and  $Y$ -axis possible. Combining the motion in  $X$ - and  $Y$ -axis and the electric discharge, the workpiece is able to be cut in any desired shape. Additionally, the system also contains the discharge detector, which is able to convert the real-life discharge difference information into digital signal. Once the digital signal passed through the discharge states statistics analysis, the IBM compatible computer will be able to readjust the motion of  $X$ - and  $Y$ -axis based on the detected discharges.

### 4.3.3 Power System

Currently, there are two types of power systems available: transistor type and resistor–capacitor (RC) type. The transistor type has advantage of fewer adjustments required and easy to operate. And the RC type is better for generating comparatively lower discharge energy and hence found to be more suitable for micro-EDM [4]. Both systems generate electric discharges and pulses, between the part and wire electrode. During the actual operation, the positive terminal of the power system is connected to the workpiece and the negative terminal of the power system is connected to the wire electrode. Due to the different electrical property between the wire electrode and the workpiece, the material removal from workpiece and electrode also differs.

Figure 4.5 shows the basic circuits for RC and transistor-type pulse generator for micro-WEDM [6]. In a basic RC circuit, the capacitor is parallel with the power

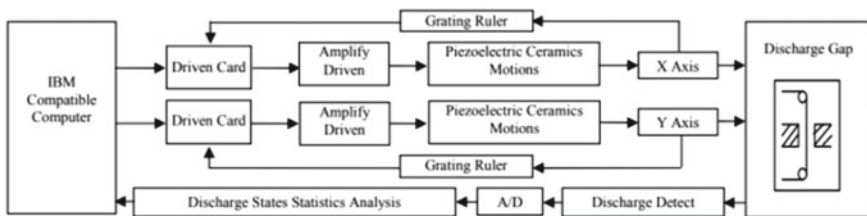
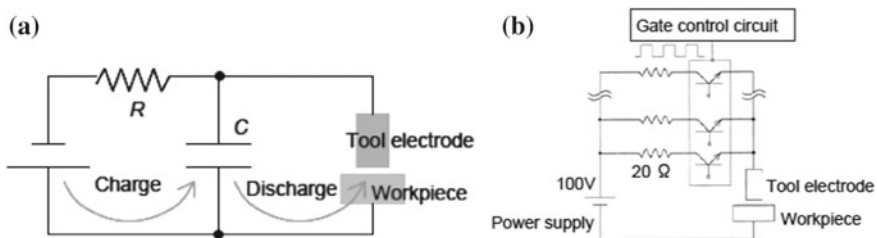


Fig. 4.4 Control system of micro-WEDM [10]

source. The resistor is in series with the power source. And the pulse generated by a basic RC-type power system could be classified as four types: normal discharge, effective arc discharge, transient short circuit and complex pulse. In a basic transistor-type pulse generator, the resistors and transistors are connected in parallel. The discharge current depends on the sum of transistors remaining ON simultaneously, allowing for comparatively higher discharge current during machining. For micro-WEDM, the pulse frequency should be set high in order to achieve the smallest crater sizes that provide the smoothest finished surface. In addition, a higher current-limiting resistance and a higher pulse-control frequency both contribute to a better surface finish during micro-WEDM [11].

#### 4.3.4 Dielectric Flushing System

During the actual operation, the part to be machined and the wire electrode is immersed in the dielectric fluid. In order to make a micro-WEDM machine working properly, a dielectric flushing system needs to meet three crucial requirements. The dielectric fluid needs to block the circuit, cools the part as well as flush away the removed debris which means the dielectric fluid needs a high electric resistance that prevents the electric flow between the workpiece and wire electrode until the breakdown voltage is achieved. In order to make sure the workpiece is able to cool down in a short period of time, the dielectric fluid also needs a high thermal conductivity which allows the heat flux between the workpiece and wire electrode remain high. Additionally, in order to remove the debris from the workpiece in a fast manner, the dielectric fluid needs to have a low viscosity. Based on the requirements, the dielectric fluid could be deionized water or oil under the room temperature condition. In the dry micro-WEDM, the deionized water or oil is replaced by air or gaseous medium. Due to the fluid property of gas, the removed material is flushed away by the high-pressure gas flow or sucked by the vacuum debris removal tube [12].



**Fig. 4.5** a RC or relaxation-type pulse generator and b transistor-type pulse generator for micro-WEDM system [6]



### 4.3.5 Filtering Systems and Deionizing Subsystem

In micro-WEDM, the debris from the workpiece are washed away from the machined zone and flowed with the dielectric fluid. When the content of the debris in the dielectric fluid reaches a certain level, the resistance of dielectric fluid decreases and turns out to conduct the electric flow. In order to meet the goal of recycling the dielectric fluid, the dust, the debris of machined parts and the dissolved ions need to be filtered from the dielectric circuit.

In filtering system, the collected deionized water first goes through disposable paper filters and then goes through a mixed-bed deionizer cartridge, which is used for correcting the water resistivity. After those two steps, special additives or extra polishing operation is added to the water to avoid the rust formation or remove the existed oxides [13].

In case of reducing the conductivity of the water, the water is stored in a clean tank. Once the control system monitors an undesired conductivity of the water, the water is forced into a deionizing resin by a pump. After going through the deionizing resin, all the contaminants from water are removed and the cleaned water with desired level of deionization goes back to the clean tank [13].

## 4.4 Micro-WEDM Parameters and Wire Materials

### 4.4.1 Electrical Parameters

The major electrical parameters for transistor-type pulse generator are gap voltage, peak current, pulse duration, pulse interval and duty ratio. For RC type, the major parameters are voltage and capacitance. In addition to these major parameters, discharge energy, pulse frequency, electrode polarity are also considered as electrical parameters for micro-WEDM. The discharge energy (DE) is a parameter that indicates the combined effect of all the parameters. The DE for transistor and RC type are calculated by the equations listed below [4]:

For transistor-type pulse generator, the discharge energy per single pulse  $q$  is expressed as,

$$q = u_e \times i_e \times t_e \quad (1)$$

where  $u_e$  is discharge voltage,  $i_e$  discharge current and  $t_e$  is pulse duration.

For RC-type pulse generator, the discharge energy per single pulse  $q$  is expressed as,

$$q = (1/2)CV^2 \quad (2)$$

where  $C$  is the capacitance used for machining,  $V$  is the discharging voltage.

The gap voltage, expressed in  $V$ , is the voltage between the workpiece and the wire electrode applied during micro-WEDM. The peak current, expressed in Amp, is the amount of current flowing through the wire electrode and the workpiece during the discharging process. The pulse duration, commonly expressed in  $\mu\text{s}$ , is the duration of a single pulse generated from the pulse generator. The pulse interval, also expressed in  $\mu\text{s}$ , is the time interval between two consecutive pulses. The duty ratio, commonly expressed in %, is the fraction of pulse duration over total cycle time (pulse duration + pulse interval). Pulse frequency, expressed in Hz, is the number of cycles produced in a single second. The discharge energy, commonly expressed in  $\mu\text{J}/\text{pulse}$ , is the energy supplied by a single pulse discharge. The electrode polarity in the micro-WEDM is important to consider, as the amount of material removal is controlled by the selection of electrode polarity. In micro-WEDM, comparatively higher material removal rate from the workpiece is obtained, when the workpiece is anode and wire electrode is used as cathode (negative polarity). The material removal rate (MRR) in micro-WEDM increases with increase of gap voltage, peak current, pulse duration, discharge energy, pulse frequency and duty ratio and decrease of pulse interval. The surface finish improves with the reduction of voltage, current, pulse duration and discharge energy and increase of pulse interval. The tool wear ratio generally increases with increase of discharge energy, voltage, current and pulse duration. However, too low discharge energy and gap voltage also increase the tool wear due to unstable machining conditions.

#### **4.4.2 Non-electrical Parameters**

Wire tension and wire feed rate are the two important non-electrical parameters in micro-WEDM. Control over the tension in the wire in micro-WEDM is essential to efficient and accurate machining. Machining using a wire with too low tension causes a degraded surface finish and a less accurate part. This is due to the wire being allowed to bend as well as the larger vibrations will be induced on the wire due to the low tension. Conversely, too much tension in the wire can cause the wire to break. The parameters must be adjusted to comply with the capabilities of the wire. For example, for fast cutting one must use high energy and low tension. Conversely, for precision cutting, low energy and a high tension are ideal [14].

Wire feed rate is the speed at which the wire travels through the spark gap during machining. Wire feed rate should be optimized. At slow wire feed rate, frequent wire breakage occurs due to wire wear, and at high wire feed rate, the material removal rate decreases slightly due to inadequate spark concentrations.

Micro-wire-EDM can be done with various wire diameters, ranging from around 50 to 250  $\mu\text{m}$ . The desired wire diameter depends on the minimum cut/slit width in the design of the part to be machined. Larger diameter wires can handle a larger discharge current by increasing the rate of material removal. If a design that has both slits and other inner cuts, smaller diameter wire can provide better accuracy [14].

The kerf is the width of the cut made by the wire. This includes the diameter of the wire as well as the spark gap on either side of the wire. This is arguably the most important characteristic in micro-wire-EDM, as it determines the accuracy of the part as well as the machining time. The kerf is greatly affected by the wire tension and feed rate of the wire electrode. The pressure of the dielectric also affects the kerf. In dry micro-WEDM, the pressure of the dielectric gas affects the kerf. As seen in Fig. 4.6, a higher pressure increases the kerf, but also makes its surface finish more uniform [15]. It is also known that kerf is more variable when cutting a thicker part. The kerf increases as workpiece thickness decreases.

### 4.4.3 Wire Materials

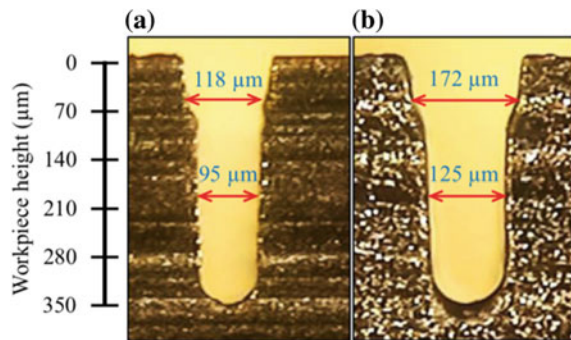
Common wire materials used in micro-WEDM include but are not limited to copper, brass, aluminium brass, tungsten–copper, molybdenum and tungsten. The good electro-thermal properties and potential machinability of these materials make them good candidates for micro-WEDM.

Copper wires are not typically used anymore for micro-WEDM because they have a low melting point and low tensile strength. This makes the copper wire less usable because it is more likely to fail under stress or be altered by the heat of machining [13].

Brass wires are considered the general use wire for micro-WEDM machining. Brass is a combination of copper and zinc (approximately 35%). The addition of zinc to the wire increases its tensile strength. The zinc in the wire can vaporize during machining, which adds another degree of coolant other than what is provided by the dielectric fluid [13].

Molybdenum could be a good wire choice if the wire is required to have a much higher tensile strength than that is needed for general machining. Molybdenum also has a higher melting point than brass, which allows it to withstand more temperature

**Fig. 4.6** Slots cut in dry micro-WEDM at a constant air pressure of **a** 0.1 MPa and **b** 0.2 MPa [15]



without depreciating the characteristics of the wire. However, molybdenum is very expensive and not effective with thick workpiece [13].

Tungsten is a good alternative to molybdenum because it can withstand a high degree of fatigue before failing, making it a good wire choice due to the higher currents it is able to transmit. Tungsten has a higher fatigue strength than brass and a higher melting point. These traits allow tungsten wires to transmit more energy, effectively increasing the cutting speed and decreasing the production time [14].

Brass wires have a low fatigue strength, but are still widely used in micro-WEDM because the brass wire is capable of high MRR. To increase the durability of the brass wire, it is actually cored with steel and only the outer coating of the wire is brass. This preserves the electrical properties of the brass with the added strength of the steel [14]. The wire for micro-WEDM can be coated with another material. For example, electrically conductive boron-doped CVD diamond (B-CBD) and polycrystalline diamond (PCD) are two coatings used to improve the machinability of the wire. This coating improves the wire's ability to maintain its properties under high stress and high temperature. This results in improved surface finish as well as the ability for the wire to withstand higher stresses due to increased machining speed or increased depth of cut without failure of the wire. The improved surface finish comes from a decreased crater diameter caused by the applied wire electrode. A smaller crater diameter results in a better surface finish. B-CBD produces smaller craters than tungsten-copper and PCD-coated wires under the same conditions [16].

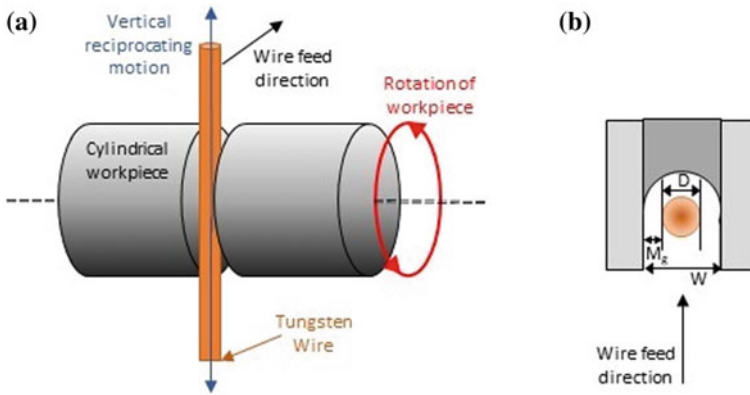
## 4.5 Variants of Micro-wire-EDM

### 4.5.1 Cylindrical Micro-WEDM

Some parts, such as micro-rotating structures, cannot be easily machined by micro-wire-EDM due to their geometry. A variation of micro-wire-EDM has been analysed which uses a rotating wire as the tool to machine the intricate cylindrical parts, known as cylindrical wire-EDM, as shown in Fig. 4.7 [17]. This process is similar to traditional micro-wire-EDM, except that the workpiece is rotating as the wire cuts. This allows for machining cylindrical dimensions that were not available on the traditional micro-wire-EDM machine.

As seen in Fig. 4.7,  $W$  is the kerf width,  $M_g$  is the machining gap, and  $D$  is the diameter of the wire. These dimensions are related by the equation. The rotating groove width ( $W$ ) is being the sum of the diameter of the wire ( $D$ ) and two machining gaps ( $M_g$ ), because there is a gap on either side of the wire. Including the machining gap in dimensions and diameter choice of wire is critical, especially when machining parts on the micro-level [17].

The ideal wire tension is approximately 1.2 N. This ensures enough tension in the wire to keep tight tolerances, constant voltage transmission and good surface finish without too high of a danger of the wire breaking catastrophically. An 80 V open



**Fig. 4.7** **a** 3D diagram of rotating workpiece being machined and **b** 2D diagram from aerial view, as if looking down the wire [17]

voltage, 60 V reference voltage, 1.5 k $\Omega$  discharge resistance and 470 pF discharge capacitance were found to be the ideal electrical parameters for the cylindrical micro-WEDM process. The wire moving into the workpiece at 25  $\mu\text{m}/\text{min}$  is the optimal speed for machining. The optimal revolving speed workpiece is 5000 rpm. These values can change depending on the electrical properties of the material to be machined as well as the choice of wire material.

### 4.5.2 Micro-WEDG

Another variation of the micro-WEDM is the micro-WEDG for microelectrode fabrication. The micro-WEDG allows in situ fabrication of high-aspect-ratio microelectrodes with diameter down to sub-10  $\mu\text{m}$ , as can be seen in Fig. 4.8. A study was reported in recent years with a tungsten workpiece and a copper wire for the electrode. The tungsten wire was rotated and moved towards the electrode, effectively grinding it down without the use of a grinding wheel. This is useful to make parts with a high aspect ratio that must be precisely dimensioned, such as tools to be used for micro-EDM die-sinking or drilling. The surface roughness of the workpiece worsened as the workpiece rotations is increased, because this removes more material. Removing more materials faster causes larger, more sporadic craters to be left in the workpiece. Similarly, a high discharge energy removes more material at a time as well, leaving large craters. Larger craters on the surface result in a rougher surface. The WEDG process may be better understood by the diagram shown in Fig. 4.8 [18].

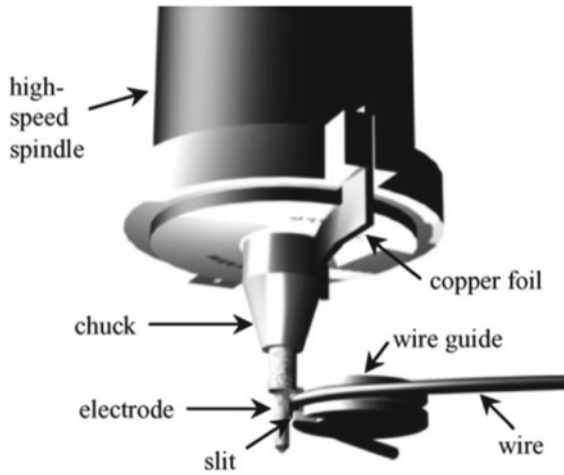


Fig. 4.8 Micro-WEDG to fabricate micro-tool [18]

### 4.5.3 Rotary Disc Micro-EDG and Micro-EDM

The rotary disc micro-electrical discharge grinding (micro-EDG) can be considered as a variation of micro-WEDM, where a continuously travelling wire electrode is replaced with a rotary disc and used for fabricating high-aspect-ratio microelectrodes by the same way micro-WEDG works. In a rotary disc micro-EDG, an electrically conductive disc with thickness of 500  $\mu\text{m}$  or less is used instead of continuously travelling wire electrode. As the rotary disc rotates, the workpiece to be machined is brought close to the disc and feed into the disc with a small depth of cut each time. The polarity of the workpiece and disc electrode can be straight or reverse based on the material removal rate and depth of cut provided. Figure 4.9 explains the differences in the working principle of rotary disc micro-EDG with micro-WEDG [19].

The rotary disc electrode (RDE-micro-EDM) is another variant process of micro-WEDM process where discharges occur between a rotary tool called disc and the workpiece with the presence of dielectric fluid. The disc is commonly made of conductive hard materials like tool steel or carbide and the thickness ranging from several microns to few millimetres. The process is used for cutting of billets and bars with smaller kerf and burr-free surface. Figure 4.10 displays the representation of the working principle of RDE-micro-EDM process [20].

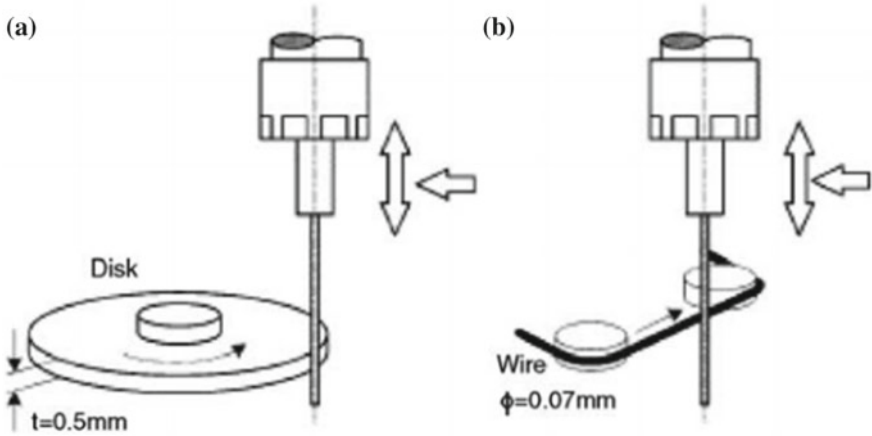


Fig. 4.9 Schematic diagram explaining working principle of **a** rotary disc micro-EDG and **b** micro-WEDG [19]

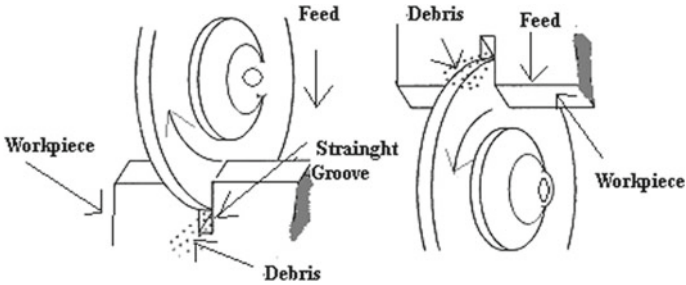
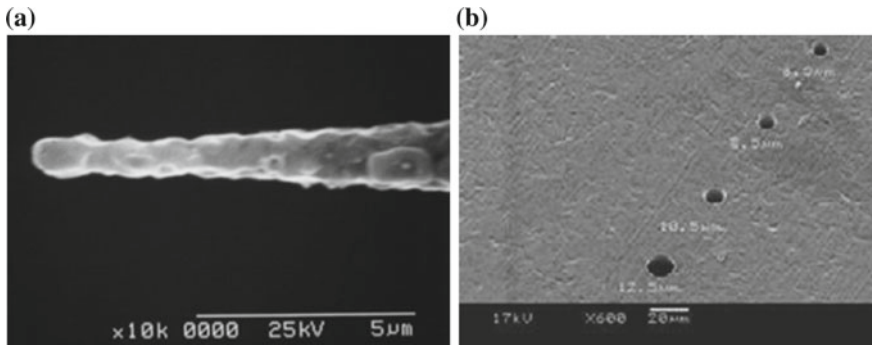


Fig. 4.10 Schematic diagrams showing the working principle of rotary disc electrode micro-electro-discharge machining (RDE-micro-EDM) [20]

## 4.6 Applications of Micro-wire-EDM

### 4.6.1 *In Situ Microelectrode Fabrication for Micro-EDM*

In situ fabrication of microelectrode is essential to machine micro-holes accurately or in dense or preset arrays of micro-holes. In many cases, micro-WEDG is used first to machine high-aspect-ratio microelectrodes as shown in Fig. 4.11a. The continuously travelling wire allows machining down the diameter of the micro-holes to as small as 5–10  $\mu\text{m}$ , which are not obtainable with other processes. The micro-WEDG also minimizes the inaccuracy due to handling of small electrodes as well as position inaccuracy. Then, the micro-holes are machined in a workpiece using the micro-EDM drilling process, as can be seen by Fig. 4.11b.



**Fig. 4.11** **a** High-aspect-ratio microelectrodes fabricated by micro-WEDG [6], **b** micro-holes fabricated by the on-machine fabricated microelectrodes [21]

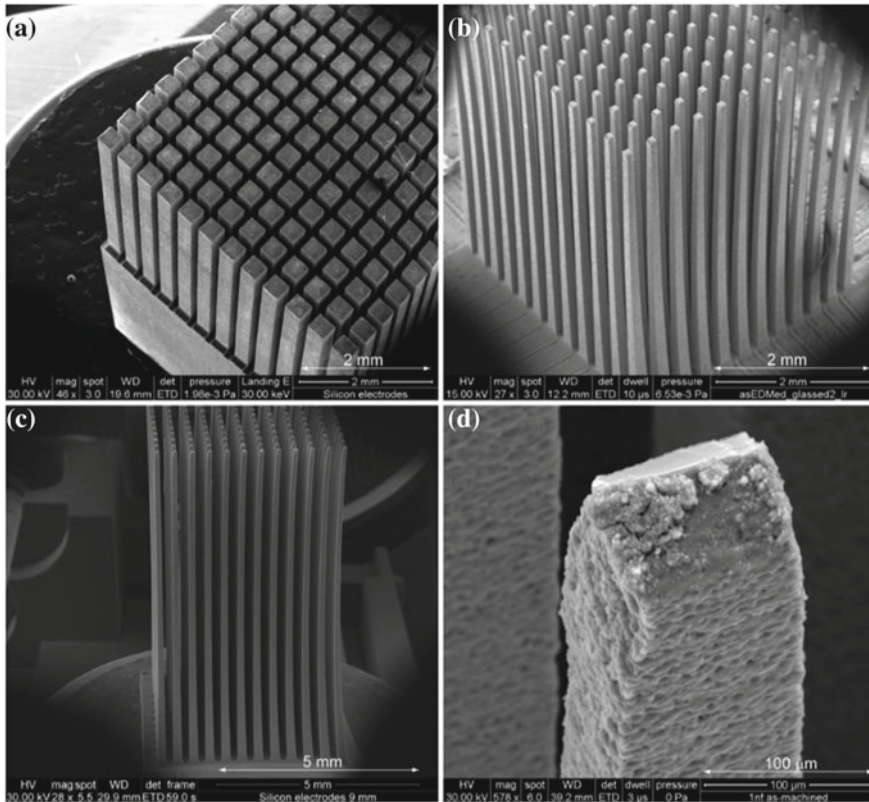
### 4.6.2 *Microelectrode Fabrication for MEMS Application*

Micro-WEDM is being researched in the application of healthcare and MEMS industries. Neuroscientists need extremely thin and precise needles/probes to analyse and perform surgery on the brain. Ideally, they will disrupt as little extraneous tissue as they can in doing this. Micro-WEDM was used in a study to fabricate electrodes from a highly conductive silicon. The needle shape of the probes (necessary for precision and smooth insertion) was achieved by chemical washing a glass coating-off of the silicon at varying rates, but the base of the needle is machined with micro-wire-EDM. Figure 4.12 shows images of the needles during the machining process [22]. Note that each column will be one needle when the process is complete. Using micro-WEDM enables extremely high aspect ratio (1:60) in the silicon needles. This low diameter to high height ratio enables long, extremely thin needles to be produced. This could allow neuroscientists to be able to affect less tissue in the brain while penetrating deeper than previous tools have allowed.

### 4.6.3 *Micro-gear Fabrication*

Micro-wire-EDM is able to fabricate gears that are close to the target dimensions and have good surface finish [23]. At the microscopic level, even a very small machining error can compromise the gear because of its small size. Micro-wire-EDM can be used to machine micro-gears with dimensions less than 100  $\mu\text{m}$ . Micro-fabrication by other methods such as focused ion beam, LIGA is expensive and takes a long time to produce parts. Micro-gears had better surface finish when machined at low discharge energies and high pulse on times, even though this greatly increased the machining time. This in turn maximizes the cost of machining. Still, the process is more economical than other micro-fabrication processes. Figure 4.13 shows the fabricated micro-



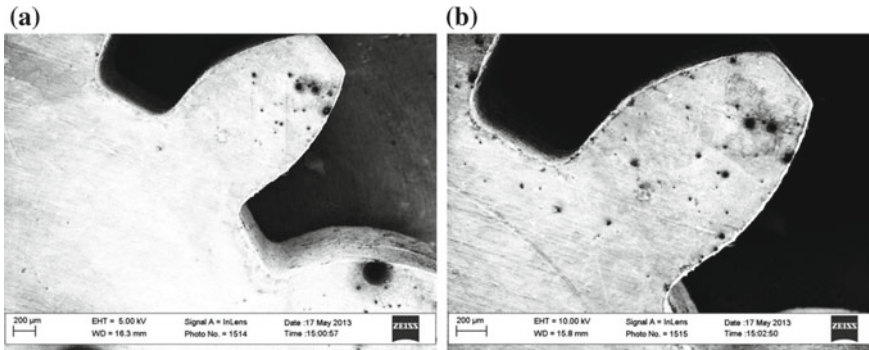


**Fig. 4.12** SEM images of **a** 5-mm-long straight columns, **b** 5-mm-long tapered columns, **c** 9-mm-long tapered columns and **d** a column tip before chemical finishing processes [22]

gear by micro-WEDM [23]. They reported the analysis of optimization of the micro-WEDM process for improving the accuracy and surface finish of the fabricated gear.

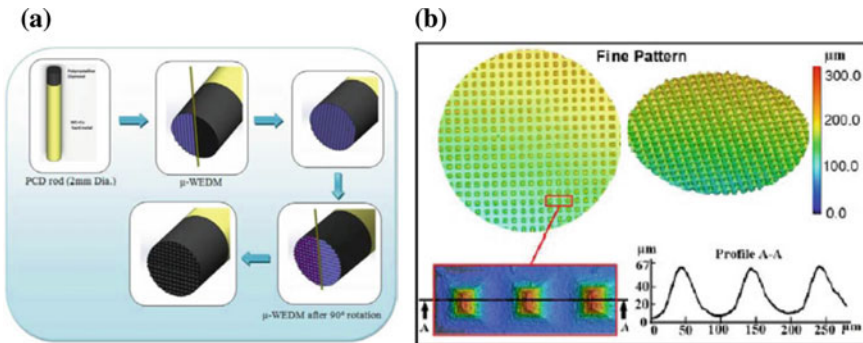
#### **4.6.4 Fabrication of PCD Planarization Tool for Polishing Silicon for Semiconductor Industries**

Silicon is a semiconductor that is useful if it can be machined accurately. It is difficult to machine on the surface of silicon with micro-WEDM because it is difficult to orient the silicon precisely to the fixturing station. Silicon must be pre-machined before the precision machining takes place. This is due to the inaccuracies that arise from fixture of the workpiece. Micro-WEDM is used to machine the PCD that is then used to polish the silicon. It is useful to use micro-wire-EDM to machine the PCD because of the high accuracy, which will ultimately allow the PCD to machine a more precise



**Fig. 4.13** SEM image of a micro-scale spur gear machined by the micro-WEDM, **a** and **b** shows the images of same gear at 40× and 80× magnifications [23]

silicon part. A tungsten wire was used at low discharge energies to machine PCD tool using micro-WEDM. A surface roughness of 0.6 μm was realized in a PCD of 2 μm grain size. As it can be seen in Fig. 4.14 [24], the PCD rod was machined by micro-WEDM to form a cross-hatched pattern on one end of the rod. That end of the rod was then used in conjunction with a chemical to polish the silicon plates. The precision of machining of the PCD rod is essential so that the rod can leave a glassy finish on the silicon plates. Figure 4.15 shows that the micro-WEDM-fabricated PCD tool can be used for obtaining very smooth surface finish in ductile machining of silicon [24].



**Fig. 4.14** **a** Fabrication of PCD planarization tool for micromachining of silicon using micro-WEDM, **b** surface and profile of a fine patterned planarization tool fabricated by micro-WEDM [24]

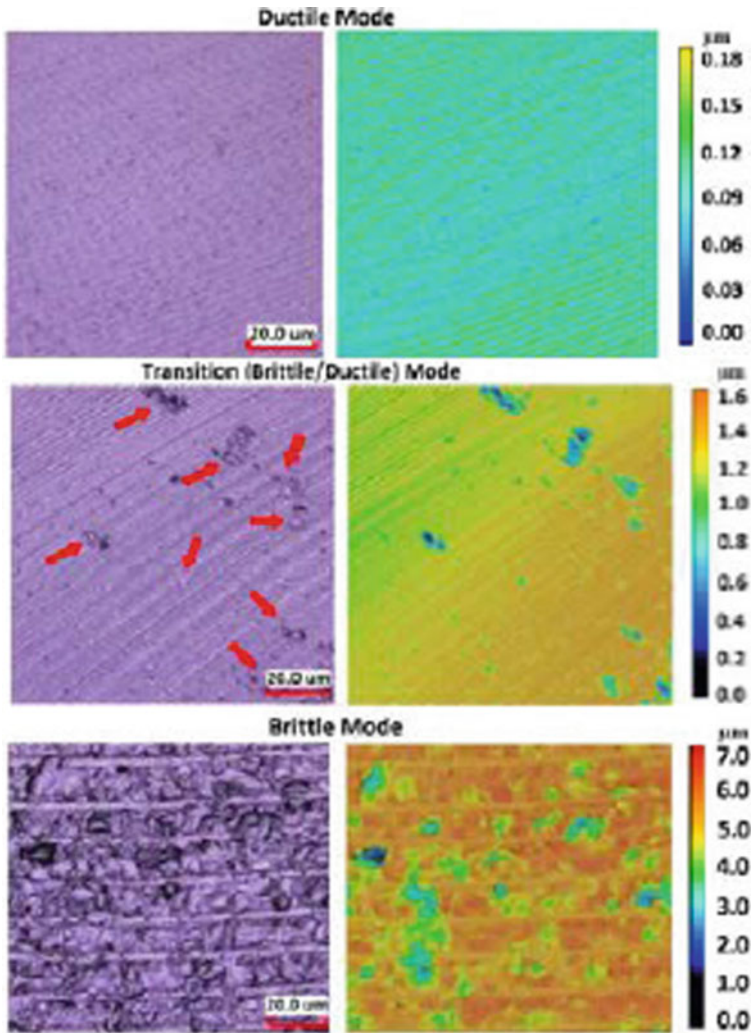


Fig. 4.15 Ductile, ductile-to-brittle transition and brittle mode machining of silicon wafer using micro-WEDM-fabricated PCD tool [24]

### 4.6.5 Microstructuring of Complex 3D Parts

There is an increasing need for micro- and meso-scale complex 3D parts produced in hard-to-machine materials, such as high strength steels, nickel and titanium alloys, tungsten carbide or even ceramics. Titanium and nickel alloys are extremely hard to machine accurately through traditional practices, but it is necessary to have a strong and light material in the aerospace industry. Micro-WEDM provides the capability

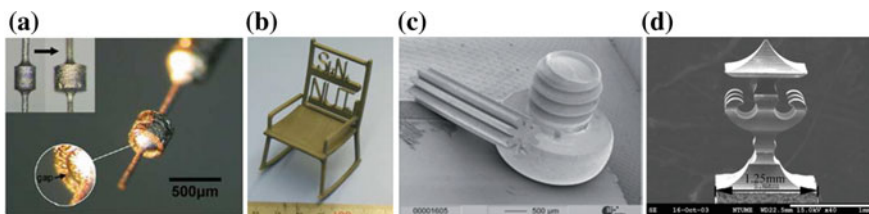
and flexibility of making complex 3D structures in hard materials with high accuracy and repeatability. Figure 4.16 shows the examples of microstructures machined by micro-WEDM process [25–28].

## 4.7 Advanced Research on Micro-wire-EDM

### 4.7.1 Applications of Micro-WEDM in Hybrid Micromachining

One of the areas where micro-WEDM has found its extend capabilities are applying the variants of micro-WEDM and integrate micro-WEDM with other micromachining processes to create sequential and hybrid micromachining processes. In most of the cases, micro-WEDM or micro-WEDG is used as the first process to be applied for fabrication of microelectrodes or parts before applying another process sequentially. Some of the examples are

- Micro-WEDG and micro-EDM-drilling: micro-WEDG is used to fabricate in situ microelectrode with high aspect ratio and small diameter and then uses the fabricated microelectrode to drill micro-holes in the difficult-to-machine material.
- Micro-WEDM and micro-EDM drilling: micro-WEDM is used to fabricate arrays of microelectrodes and then applies the arrays of microelectrodes to machine arrays of micro-holes in a single shot. This process is found to be very useful in mass fabrication of arrays of micro-holes for MEMS applications.
- Micro-WEDM and micro-grinding: micro-WEDM process is used to fabricate PCD tool for planarization and grinding/polishing of silicon and other brittle materials. The fabricated planarization PCD tool is able to machine the silicon substrate in ductile mode.
- Micro-WEDG and micro-milling/micro-grinding: in this process, the micro-WEDG is used to fabricate the cutting tool and then uses the fabricated cutting tool for machining micro-slots in micro-milling and/or micro-grinding applications.



**Fig. 4.16** Examples of 3D microstructures machined by micro-WEDM; **a** micro-ball joint made by micro-WEDM [25], **b** steel gear made by micro-WEDM [26], **c** pagoda machined by micro-WEDM [27], **d** chair machined by  $\text{Si}_3\text{N}_4$  in insulating ceramics by micro-WEDM [28]

### ***4.7.2 Modelling of the Spark Erosion and Process Mechanism***

There have been few research studies on modelling the stochastic nature of the sparking and discharging phenomena in micro-wire-EDM process. Advanced research in this category includes the fundamental study of the process mechanism, and control and sensing of the discharging phenomena to further improve the performance and capabilities of micro-WEDM.

A recent study on predicting the erosion rate in micro-wire-EDM process found that the plasma current and the plasma radius increased with duration of discharge energy [29]. During a spark, the plasma temperature increases slowly with time and it has no relation between the velocity of the wire electrode. The diameter of the wire has direct effect on the temperature around the wire surface. Additionally, the erosion rate of the workpiece is proportionate to the plasma temperature and is independent on the wire feed rate.

A PC-based real-time control system has been found to be effective for monitoring the instability during machining and to improve the accuracy in micro-WEDM [30]. The control system minimizes the unstable discharge ratio, thus enhancing the machining efficiency and performance. In finish micro-WEDM, the roughness of surface was reduced by 10% without decreasing the machining efficiency using the proposed control system. In addition, the application of an active wire feed apparatus and multilayer damped vibration absorber (MDVA) to minimize wire tension vibration can reduce geometric error and kerf width and improve surface finish [31].

It has also been reported that by applying the relaxation circuit with three RC combinations, the micro-WEDM machine was able to produce a high-density, peak and short-pulse-time current train which ended up with finer surface finish. Additionally, the feed rate of micro-WEDM was increased by 1.6 times by applying the 3 RC relaxation circuits compared to the original design in machining both aluminium and copper alloys [32].

### ***4.7.3 Enhancing the Performance of Micro-WEDM by Assistance of Vibration***

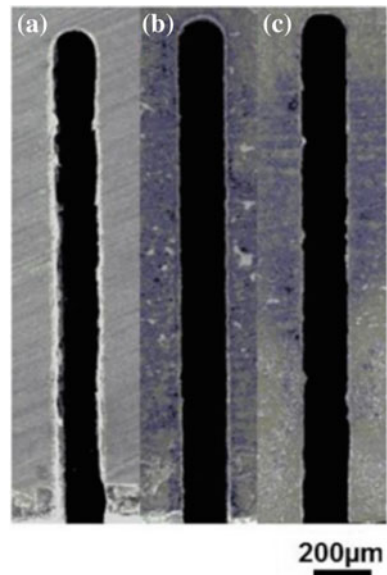
It has been reported by several researchers that application of low frequency or ultrasonic vibration to the workpiece during machining can help improve the performance of micro-WEDM [12, 33]. When a vibration is applied to either the workpiece or the wire electrode, the machining efficiency is both higher than the machining efficiency of the conventional WEDM. Additionally, the material removal rate increases with vibration applied to wire electrode [12]. Applying vibration to the wire electrode may induce inaccuracy to certain profiles to be machined by micro-WEDM [12]. Furthermore, the thicker the workpiece, the greater the influence of vibration on improving machining efficiency. The research also reported that no matter which part

the vibration was applied on the surface roughness was significantly improved. The application of vibration was found to be effective in dry micro-WEDM as well [34]. It was found that the machining time was significantly reduced and the machining efficiency was improved, when vibration was introduced in the dry micro-WEDM [33, 34].

#### 4.7.4 *Enhancing the Performance of Micro-WEDM of Silicon Using Conductive Coating*

Micro-WEDM has been found to be comparatively less efficient in machining semi-conductive silicon (Si) compared to metals with higher electrical conductivity. In order to solve the challenges imposed by machining of silicon, a recent study proposed providing electrically conductive coating on the silicon wafer before machining it with micro-WEDM [35, 36]. A conducting material, such as gold, is coated on the silicon wafer and then is removed after machining. The proposed method increases MRR significantly and found to be very stable. In addition, the process creates comparatively smoother surface finish compared to uncoated silicon wafer. The proposed method of conductive coating may extend the application of micro-WEDM in silicon machining for sensors and MEMS applications. As shown in Fig. 4.17, both the heat-affected zone (HAZ) and surface finish at the rim got improved in the slots in gold-coated silicon compared to the slots in uncoated part [36].

**Fig. 4.17** SEM image of the machined slots by micro-WEDM process, **a** for uncoated Si, **b** Si coated for 5 min and **c** Si coated for 10 min [36]





### **4.7.5 Development of Dry Micro-WEDM**

Recently, dry micro-WEDM is found to be an effective alternative of micro-WEDM due to its capability of providing smooth surface finish in addition to being a greener process [15]. In dry micro-WEDM, the machining is performed in air or gaseous medium, instead of, in liquid dielectrics traditionally used in micro-WEDM. The removed craters are flushed away by the high-pressure gas supplied into the gap. The kerf width and surface roughness depend on the pressure at which gaseous dielectric is injected into the spark gap. In addition, the feed rate and electrical parameters affect the machining performance of dry micro-WEDM.

## **4.8 Challenges in Micro-WEDM and Future Research Opportunities**

Micro-WEDM could be a reliable and effective manufacturing process in industry for providing 3D complex parts with high precision and fine surface finish. However, there are still some challenges until micro-WEDM can become a repeatable and reliable process and be fully used by micro-manufacturing field of industry. There are still some research issues need to be explored about micro-WEDM.

The first challenge is the difficulty and inconvenience in handling of small wire electrodes. The main reason is that the trend used to reduce the wire diameter has problems with handling electrodes and machined parts. Existing micro-wire-EDM machines need long time for machine preparation to take wires with smaller diameters (about 0.03 mm). The wire installation is inconvenient and unreliable with long distance between spool position and threading nozzle, because it was so hard for thin wire to take the dynamic forces. As a result, the wire always breaks, and it requires manual installation. The handling of the micro-parts while manufacturing on the wire-EDM machine is also a problem. Sometimes, a single part needs another process after a separation cut, because there is a possibility for the part to be lost in the tank.

The second issue relates to small holes used for threading the wire through the part. The holes on the part could have tiny diameters with high aspect ratio. For common sense, those tiny holes can be machined by micro-drilling. The positions of holes should be accurate with the measuring point. Threading through those kinds of holes is difficult. Producing electrodes with unachievable geometry would cost lots of money and wasted time. There should be extra devices to prepare the electrode, in order to decrease the operating difficulty and error.

The third challenge is about the micro-WEDM process itself. Because the micro-WEDM is based on very small scale of dimensions, the manufacturing process should be planned carefully, and the features on the part and the tolerances on the surface on the part are really small as well. The result of error might be significant, if the operator does not design the process very well. There are two possible reasons that can cause

the errors: the imperfection of the wire electrode and the stochastic nature of the sparking process. Future research should focus on the modelling and simulations of the sparking phenomena, the sources of inaccuracies and how to minimize the inaccuracies by controlling the sparking and discharge process.

The last but not least problem is about the measurement. It is difficult to measure dimensions of features and surface quality for micro-parts fabricated by micro-WEDM. Surface roughness is an important characteristic for micro-WEDM process; however, for now, there is no standard method to measure it on the machine. The recast layer and heat-affected zone can be analysed using metallography after taking out the parts from the machine. However, there should be some standard equipment to measure those without damaging the parts. On-machine measurement of dimensions is already available in the micro-WEDM machines. Future research should focus on performing more in situ measurement of surface quality and providing instantaneous feedback to the machining process while performing the micro-WEDM.

The above-mentioned challenges limit the performance and application of micro-WEDM. Based on the problems discussed above, the future research on micro-WEDM could be planned. When planning the micro-WEDM process, all aspects of dimensional accuracy and tolerance should be taken into consideration, from microelectrode fabrication to its application. Those activities can cause accumulation of errors. The optimization of parameters needs to be taken into consideration, and the empirical methods or simulations should be considered before carefully carrying out the experiments on the machine. The well-developed algorithms and strategies are required for obtaining competitive micro-WEDM technology.

## References

1. Jahan MP, Rahman M, Wong YS (2011) A review on the conventional and micro-electrodischarge machining of tungsten carbide. *Int J Mach Tools Manuf* 51:837–858
2. Pham DT, Dimov SS, Bigot S, Ivanov A, Popov K (2004) Micro-EDM-recent developments and research issues. *J Mater Process Technol* 149:50–57
3. Rajurkar KP, Levy G, Malshe A, Sundaram MM, McGeough J, Hu X, Resnick R, DeSilva A (2006) Micro and nano machining by electro-physical and chemical processes. *CIRP Ann* 55(2):643–666
4. Jahan MP, Asad ABMA, Rahman M, Wong YS, Masaki T (2011) Micro-Electro Discharge Machining ( $\mu$ EDM). In: Koc M, Ozel T (eds) *Micro-manufacturing: design and manufacturing of micro-products*. Wiley, New York, pp 301–346
5. Puri AB (2017) Advancements in micro wire-cut electrical discharge machining. In: Kibria G, Bhattacharyya B, Davim JP (eds) *Non-traditional micromachining processes-fundamentals and applications*. Springer International Publishing AG, Switzerland, pp 145–178
6. Kunieda M, Lauwers B, Rajurkar KP, Schumacher BM (2005) Advancing EDM through fundamental insight into the process. *CIRP Ann* 54(2):599–622
7. Kibria G, Bhattacharyya B, Davim JP (2017) *Non-traditional micromachining processes-fundamentals and applications*. Springer International Publishing AG, Switzerland



8. Han F, Cheng G, Feng Z, Isago S (2008) Thermo-mechanical analysis and optimal tension control of micro wire electrode. *Int J Mach Tools Manuf* 48:922–931
9. Yan MT, Fang CC (2008) Application of genetic algorithm-based fuzzy logic control in wire transport system of wire-EDM machine. *J Mater Process Technol* 205:128–137
10. Huang RN, Lou YJ, Chi GX (2010) Research on servo feeding system of micro WEDM. In: 2010 international conference on digital manufacturing & automation, Changsha, China, 18–20 Dec 2010
11. Yan MT, Chiang TL (2009) Design and experimental study of a power supply for micro-wire EDM. *Int J Adv Manuf Technol* 40:1111–1117
12. Hoang KT, Yang SH (2013) A study on the effect of different vibration-assisted methods in micro-WEDM. *J Mater Process Technol* 213:1616–1622
13. Ghodsiyeh D, Moradi M (2015) Wire electrical discharge machining. In: Jahan MP (ed) *Electrical discharge machining (EDM): types, technologies and applications*. Nova Science Publishers, Inc. New York
14. Klocke F, Lung D, Lung D, Thomaidis D, Antonoglou G (2004) Using ultra thin electrodes to produce micro-parts with wire-EDM. *J Mater Process Technol* 149:579–584
15. Hoang KT, Yang SH (2015) Kerf analysis and control in dry micro-wire electrical discharge machining. *Int J Adv Manuf Technol* 78:1803–1812
16. Uhlmann E, Roehner M (2008) Investigations on reduction of tool electrode wear in micro-EDM using novel electrode materials. *CIRP J Manuf Sci Technol* 1:92–96
17. Wang Y, Chen X, Wang Z, Li H (2016) Fabrication of micro-rotating structure by micro reciprocated wire-EDM. *J Micromech Microeng* 26(11):115014
18. Chern GL, Wu YJ, Cheng JC, Yao JC (2007) Study on burr formation in micro-machining using micro-tools fabricated by micro-EDM. *Precis Eng* 31:122–129
19. Lim HS, Wong YS, Rahman M, Lee EMK (2003) A study on the machining of high-aspect ratio micro-structures using micro EDM. *J Mater Process Technol* 140:318–325
20. Chow HM, Yan BH, Huang FY (1999) Micro slit machining using electro-discharge machining with a modified rotary disk electrode (RDE). *J Mater Process Technol* 91(1–3):161–166
21. Asad ABMA, Masaki T, Rahman M, Lim HS, Wong YS (2007) Tool-based micromachining. *J Mater Process Technol* 192–193:204–211
22. Tathireddy P, Rakwal D, Bamberg E, Solzbacher F (2009) Fabrication of 3-dimensional silicon microelectrode arrays using micro electro discharge machining for neural applications. In: *Transducers 2009, Denver, CO, USA, 21–25 June, 2009*
23. Gupta K, Jain NK (2014) Analysis and optimization of micro-geometry of miniature spur gears manufactured by wire electric discharge machining. *Precis Eng* 38:728–737
24. Oliaeia SNB, Karpat Y (2016) Fabrication of PCD mechanical planarization tools by using  $\mu$ -wire electrical discharge machining. *Procedia CIRP* 42:311–316
25. Yeo SH, Tan LK (1999) Effects of ultrasonic vibrations in micro electro-discharge machining of microholes. *J Micromech Microeng* 9(4):345–352
26. Schoth A, Forster R, Menz W (2005) Micro wire EDM for high aspect ratio 3D microstructuring of ceramics and metals. *Microsyst Technol* 11(4–5):250–253
27. Liao YS, Chen ST, Lin CS (2005) Development of a high precision tabletop versatile CNC wire-EDM. *J Micromech Microeng* 15(2):245–253
28. Tani T, Fukuzawa Y, Mohri N, Saito N, Okada M (2004) Machining phenomena in WEDM of insulating ceramics. *J Mater Process Technol* 149(1–3):124–128
29. Das S, Joshi SS (2010) Modeling of spark erosion rate in microwire-EDM. *Int J Adv Manuf Technol* 48:581–596
30. Kwon S, Sung Lee SG, Yang MY (2015) Experimental investigation of the real-time micro-control of the WEDM process. *Int J Adv Manuf Technol* 79:1483–1492
31. Wang PW, Yang CS (2013) Analysis and design of wire transport system in micro wire-electro discharge machining. *J Micro Nano-Manuf* 1:021006–3
32. Chen ST, Chen CH (2015) A novel power source for high-precision, highly efficient micro w-EDM. *J Micromech Microeng* 25:075027

33. Unune DR, Mali HS (2017) Experimental investigation on low-frequency vibration assisted micro-WEDM of Inconel 718. *Eng Sci Technol Int J* 20:222–231
34. Hoang KT, Yang SH (2014) Experimental study and process optimization for vibration-assisted dry micro-WEDM. *J Korean Soc Precis Eng* 31(3):215–222
35. Saleh T, Rasheed AN, Muthalif AGA (2015) Experimental study on improving  $\mu$ -WEDM and  $\mu$ -EDM of doped silicon by temporary metallic coating. *Int J Adv Manuf Technol* 78:1651–1663
36. Rasheed AN, Muthalif AGA, Saleh T (2014) Improving  $\mu$ -wire electro-discharge machining operation of polished silicon wafer by conductive coating. In: 9th international conference on micromanufacturing (ICOMM 2014) Paper No. 72, Singapore, 26–28 March 2004

# Chapter 5

## Reverse Micro-EDM



Sachin Adinath Mastud

**Abstract** Micro-EDM is an extensively used micromachining process to fabricate microcavities on metallic surfaces. Material erosion in micro-EDM is realized by imparting controlled sparks between electrodes submerged under the dielectric fluid. Recently, micromanufacturing is in demand and resulted in miniaturization of switches, screws, gears, shafts, and other mechanical components. High aspect ratio arrayed features are used as electrodes in micro-EDM and micro ECM processes, elements of MEMS, interface elements in biomedical devices for capturing neural signals, a source of plasma, etc. Existing micromanufacturing processes have limitations in machining of high aspect ratio arrayed features of different sections on metallic surfaces. Similarly, functional surfaces which can control friction, corrosion, wettability, and hemocompatibility are difficult to fabricate by existing micromachining processes. Reverse micro-EDM (R-MEDM) process has been originated from micro-EDM process. It reverse replicates the microcavities from electrode on work-piece. Intricate machining of features with high aspect ratio can be easily realized via R-MEDM process. Use of electrode vibration enables textured surface fabrication in R-MEDM. Electrode vibration provides pulsating movements to dielectric fluid and increases debris velocity which enhances process stability.

**Keywords** Reverse micro-EDM · Textured surfaces · High aspect ratio structures  
Vibration-assisted R-MEDM

### 5.1 Introduction

Micro-EDM is one of the versatile micromanufacturing processes capable of fabricating 3D components on metals. The basic working principle of micro-EDM can be separated as ignition phase, heating phase, and removal phase. Ignition phase establishes a transfer of electrons between electrodes, heating phase involves plasma

---

S. A. Mastud (✉)

Department of Mechanical Engineering, V.J.T.I., Matunga (East), Mumbai 400019, India  
e-mail: [samastud@me.vjti.ac.in](mailto:samastud@me.vjti.ac.in)

© Springer Nature Singapore Pte Ltd. 2019

G. Kibria et al. (eds.), *Micro-electrical Discharge Machining Processes*, Materials Forming, Machining and Tribology, [https://doi.org/10.1007/978-981-13-3074-2\\_5](https://doi.org/10.1007/978-981-13-3074-2_5)

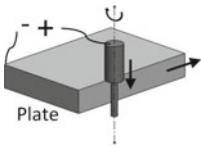
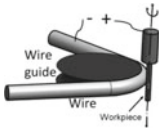
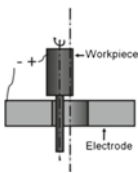
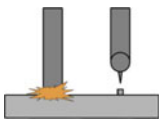

formation, and heating of electrodes. During the material removal phase, voltage and current are switched off, and due to imploding action of the plasma, the molten metal is ejected from the anode surface. The material erosion forms a crater on the workpiece. The eroded metal solidifies in the presence of dielectric and small particles known as debris are formed. The presence of debris particles drastically reduces breakdown strength of dielectric. Accumulation of debris particles leads to formation of arcing and short-circuiting which reduces machining efficiency. Thus, proper debris flushing is extremely important in controlling the stability of micro-EDM and R-MEDM processes. There are numerous applications of micro-EDM to fabricate cavities, slots, and 3D microparts. Applicability of micro-EDM process can be enhanced to fabricate textured functional surfaces and high aspect ratio arrayed features. Reverse micro-EDM which is developed as a variant of micro-EDM can realize fabrication of high aspect ratio arrayed microrods and textured surfaces. Following sections of the chapter summarize applications and manufacturing processes for fabrication of arrayed microrods and textured surfaces.

## 5.2 High Aspect Ratio Arrayed Features: Manufacturing Processes and Applications

The desired function of the microparts drives the cross section and the aspect ratio of microfeatures, e.g., very thin features (high surface-to-volume ratio) are required for heat transfer and cooling applications while triangular-sectioned arrayed features are required for micropunching applications. High aspect ratio arrayed microfeatures of typically 50–100  $\mu\text{m}$  diameter and 800–1000  $\mu\text{m}$  interelectrode spacing are required in applications like electrodes in micromachining techniques, components of MEMS, interface elements in biomedical devices for capturing neural signals, and a source of plasma [1–3]. There are some micromachining processes exist for fabrication of stand-alone/arrayed microfeatures. Sacrificial block and wire electrical discharge grinding, micro-wire EDM, mechanical micromachining, and microdischarge deposition are commonly practiced processes.

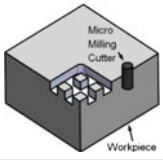
Manufacturing capabilities and limitations of these processes are highlighted in Table 5.1. Stand-alone features are machined by block EDG, micro-wire EDG, micro-EDM self-drilling process, and micro-EDM deposition. Micro-wire EDM and micromilling can produce arrayed features, but the cross-sectional geometries of features and low repeatability are the limitations of these processes. Being a conventional process, it is also associated with a tool breakage and wear issues. Hence, there is a need of developing an alternate micromachining process which can fabricate arrayed microrods of high aspect ratio.

**Table 5.1** Micromachining processes to fabricate single and/or arrayed microfeatures

Operation	Schematic	Typical feature size	Process drawback	Reference
<i>Block electrical discharge grinding (block EDG)</i>				
Material erosion between fixed block electrode and revolving workpiece		Microrods of about 3 μm in diameter with aspect ratio of 10, 0.6–0.8 μm $R_a$ surface roughness	Stand-alone single cylindrical features can be fabricated, spindle rotational errors affects accuracy of machined feature	[4, 5]
<i>Micro WEDG process</i>				
Material erosion between moving wire and revolving workpiece		Microrod of about 5 μm diameter with 50 μm length 0.8–1 μm $R_a$ surface finish	Stand-alone single cylindrical features can be fabricated, spindle rotational errors affects dimensional accuracy	[6, 7]
<i>Micro-EDM self drilling</i>				
Micro-EDM for initial fabrication of holes and with change in polarity machining of arrayed features		Microelectrode with 5 μm diameter and aspect ratio of 25 has been machined successfully	Stand-alone single cylindrical features can be fabricated, low machining accuracy due to tool wear	[6, 7]
<i>Micro-EDM deposition</i>				
Material melting by sparking and layer-by-layer deposition		Microrods of 190 μm in diameter and 7350 μm height have been fabricated	Difference in density of deposited material at core. Low surface finish and surface damage	[8]
<i>Micro-wire EDM</i>				
Material erosion by sparking. Wire feed in cross directions		10 × 10 array of 21 × 21 μm cross section, 700 μm height, 100 aspect ratio	Difficult to fabricate cylindrical cross-sectioned features, limitation of spacing between features	[9]

(continued)

**Table 5.1** (continued)

Operation	Schematic	Typical feature size	Process drawback	Reference
<i>Micromilling</i>				
Mechanical material removal using high-speed micromilling process		Micro tower, height 1 $\mu\text{m}$ , $25 \times 25 \mu\text{m}$ square base and a triangular roof of $14^\circ$	Not suitable if number of features are larger, machining of hard material is difficult	[10]

### 5.3 Textured Surfaces: Manufacturing Processes and Applications

Textured surface is used in applications where the surface geometry plays a critical role in the functional behavior of part. A summary of applications of textured surfaces in fields of self-cleaning surfaces, optics, and manufacturing fluid flow and biomedical is highlighted in Table 5.2. These textured surfaces are broadly called as positive and negative textured surfaces. Positive textured surfaces have micropillars on surfaces whereas negative textured surfaces have microdimples. A host of conventional and unconventional machining techniques can be used to create a texture on metallic as well as nonmetallic surfaces. A summary of typical texture surfaces created, advantages, and limitations of these processes is presented in Table 5.3. It appears that most of the processes are suitable for texturing on macroscale surfaces, and they fail to create a repeatable pattern of features on metallic microparts. Laser beam machining is being used widely to textured surfaces, but this process can create only negative textured surfaces, and there is a thermal damage of workpiece. Since machining forces are absent in micro-EDM process, fabrication of high aspect ratio microfeatures of less than  $40 \mu\text{m}$  is feasible with modifications in process. R-MEDM is a capable process of fabricating high aspect ratio features and textured surfaces of varying cross section. R-MEDM process is not limited to machining of easy-to-erode metals, but it is equally applicable over difficult-to-erode metals such as titanium and tungsten alloys. The working of R-MEDM process is illustrated in the following sections.

### 5.4 Basics of Reverse Micro-Electrical Discharge Machining (R-MEDM)

R-MEDM is derived from micro-EDM process. Fundamentally, no difference exists between the principle of material erosion between micro-EDM and R-MEDM process. Refer Fig. 5.1 for differences in electrode geometries and machined features

**Table 5.2** Application areas of textured surfaces

Application area	Application
<p><b>Energy/heat transfer [11]</b> Increased heat transfer and boiling rate by higher contact area between different phases</p>	<ul style="list-style-type: none"> <li>• Fuel economy: surface texture and geometrical modification can reduce hydrophilic nature of surface used in fuel storage and transportation</li> <li>• Triangular grooves for computer cooling systems, laser-diode arrays, metal quenching, and medical treatments</li> <li>• Textured surface enhances the boiling mechanism</li> </ul>
<p><b>Self-cleaning surfaces [12]</b> For easy-to-clean, dirt-free surfaces</p>	<ul style="list-style-type: none"> <li>• Dirt-free surfaces for improved stone statue cleaning, solar cells, windows, etc.</li> </ul>
<p><b>Optics</b> Creation of self-cleaning effects, transparent/highly reflective hydrophobic surfaces</p>	<ul style="list-style-type: none"> <li>• Self-cleaning effect: enhanced efficiency of heat extraction by self-cleaning nature of panels, lenses, and mirrors</li> </ul>
<p><b>Manufacturing [13]</b> To increase tool life and reduce cutting forces in machining</p>	<ul style="list-style-type: none"> <li>• Machining: Textured tools for reduced chip friction enhanced tool life for difficult to cut superalloys</li> <li>• Reduction in heat generation in grinding and polishing processes</li> <li>• Texture on microend effectors improves gripping of micro-objects</li> </ul>
<p><b>Fluid flow and micro-fluidics [14]</b> Textured surfaces for enhanced fluid flow with reduced turbulence and drag. Key application ranges from biology to energy</p>	<ul style="list-style-type: none"> <li>• Drag reduction: less energy for pumping fuel through pipes, increase in maneuverability and acceleration of ships and submarines</li> <li>• Anti-ice surfaces for high voltage lines and aircrafts</li> <li>• Self-moving droplet and liquids by purely using electrostatic effects</li> </ul>

in these processes. Electrodes of varying cross sections are used to machine replicate microcavities in micro-EDM. In contrast, microcavities are used to fabricate microrods in R-MEDM process. Microcavity pattern is initially machined on a thin metallic foil using micromilling, microdrilling, laser ablation, or any of the other suitable micromachining processes. This thin plate electrode acts as a cathode (tool). The workpiece surface is matched over microcavities on cathode. Sparking takes place wherever there is interface between electrodes. Thus, pattern of microrods fabricated on workpiece is exactly a replica of pattern of microcavities. Microrod is generated from each of the microcavity premachined on a cathode, refer Fig. 5.2, wherein two microrods being fabricated from two microholes present on electrode. The cross section of a fabricated microrod is exactly replica of a cross section of microcavity. The aspect ratio of microrod is controlled by the total feed given to moving electrode. R-MEDM process has shown the advantages over other micro-manufacturing processes used for the fabrication of microrods. These processes

**Table 5.3** Manufacturing processes to create textured surfaces

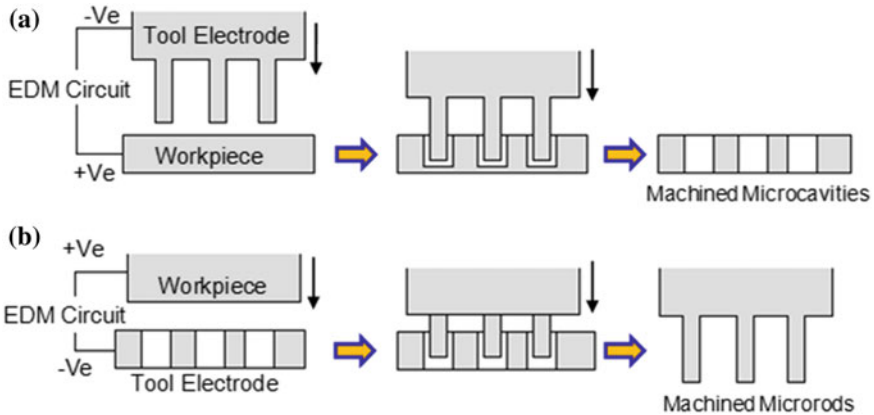
Reference	Work done	Advantages and limitations
<i>Grinding</i>		
Stepien [15]	Surface texturing on HSS single helical grinding wheel	<b>Advantages:</b> simple, productive and inexpensive method, machining over large surface area <b>Limitations:</b> low aspect ratio features, infeasible to free-form texture on
Stepien [16]	Use of grooved grinding wheels for surface texturing, developed model to predict the grinding force during surface texturing	
<i>Laser machining</i>		
Soveja et al. [17]	Texturing of TiA6V alloy using Nd:YAG laser. Surface roughness (3D) of 4–15 μm is obtained during process	<b>Advantages:</b> contactless process, high precision and accuracy, machining of complex forms over larger surfaces is feasible, can machine metals as well as nonmetals with good effectiveness <b>Limitations:</b> resolidified materials, difficult to achieve biocompatible surface textures
Baldacchini et al. [18]	Surface texturing of silicon surface using Femto-second laser contact angle higher than 160° is feasible	
Kannan et al. [19]	Surface pattern of parallel groves is formed on Ti6Al4V using laser. Surface shows a hydrophobicity even for drop impact test	
<i>Rolling</i>		
Franzen et al. [20]	Formation of macroscopic texture on tool surfaces required for deep drawing. Longitudinal, transverse, and zigzag pattern of textures were formed on the surface have 6.5 μm depth and 0.9 mm width.	<b>Advantages:</b> faster process than laser machining, extruded features is not feasible <b>Limitations:</b> unsuitable for non planer surface texturing, texturing on thin foils of metals and microparts is not feasible
<i>Abrasive jet machining</i>		
Wakuda et al. [21]	Microcavities of about 100 μm dimension, 5–20% space density. Reduction in coefficient of friction upto 0.10.	<b>Advantages:</b> most economical, hard and brittle materials can be textured <b>Limitations:</b> poor dimensional control, surface damage, pillared textures are not realizable

(continued)



**Table 5.3** (continued)

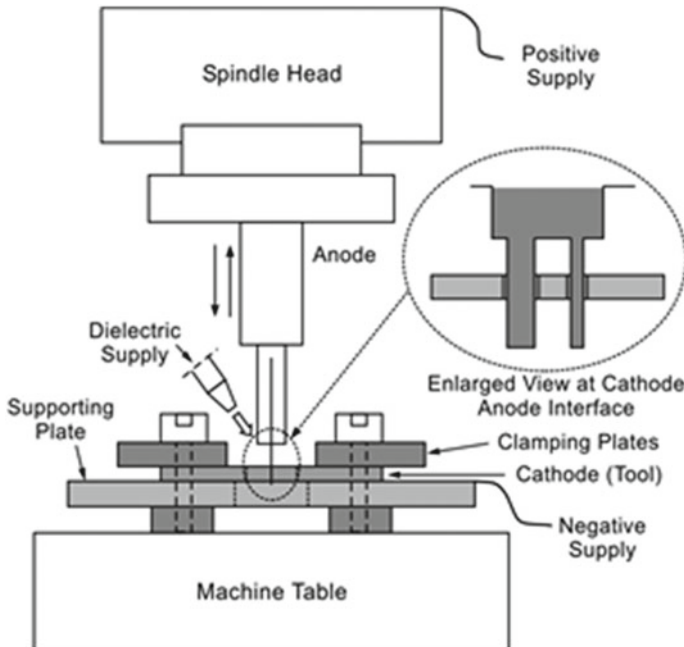
Reference	Work done	Advantages and limitations
<i>Electrical discharge machining</i>		
Koshy et al. [22]	Surface texture obtained by discharges over a tool surface and also by machining parallel grooves (100 $\mu\text{m}$ width and depth) on HSS inserts	<b>Advantages:</b> functional machining of surface with roughness varying 1.0–10 $\mu\text{m}$ , machining on superalloys and hardened metals is feasible, texturing over large surface is achievable, dimpled structures <b>Limitations:</b> white layer formation on surface, repeated pattern on surface is not machinable
Simao et al. [23]	EDM process is used to form a surface used to form a random pattern of crater on surface. Ra value of surface varies between 0.6 $\mu\text{Ra}$ to 6.5 $\mu\text{Ra}$ depending on the process parameters used	
<i>Electrochemical machining</i>		
Costa et al. [24]	Texturing on low carbon steel, depth of 50 $\mu\text{m}$ has been machined using maskless electrochemical process	<b>Advantages:</b> high density; positive and negative texture can be achieved <b>Limitations:</b> poor geometrical and dimensional accuracy of texture



**Fig. 5.1** Working of **a** micro-EDM and **b** R-MEDM

are listed in Table 5.1. Comparatively, R-MEDM process is precise, accurate and imparts lesser surface damage. Also, added advantage of R-MEDM process is the ability to fabricate positive texture on metallic surfaces. Main limitation of the process is difficulties in preparation of microcavities on plate electrode (cathode).

Processing parameters in R-MEDM can be broadly categorized as electrical and nonelectrical parameters. Important processing parameters and their significance are



**Fig. 5.2** Electrode (cathode)-workpiece (anode) arrangement in reverse micro-EDM [25]

listed in Table 5.4. Electrical parameters for the resistance–capacitance ( $RC$ ) circuits typically used in micromachining centers are: voltage, capacitance, and threshold. Voltage primarily controls the discharge energy which controls the plasma properties, erosion rate, and molten metal escapement from workpiece. In case of R-MEDM, erosion rate, dimensional accuracy, and surface roughness of fabricated features are controlled by voltage. The spark energy is directly proportional to the capacitance in  $RC$ -pulsed circuits. The effect of capacitance is identical to the effect of voltage, however, capacitance has less impact on process. Threshold is a parameter specified in terms of percentage of applied of voltage. If the set threshold is small, R-MEDM process will be more sensitive to a drop in voltages due to dynamic changes in inter-electrode gaps. In case of R-MEDM, threshold mainly affects the material removal rate and roughness of machined microrods.

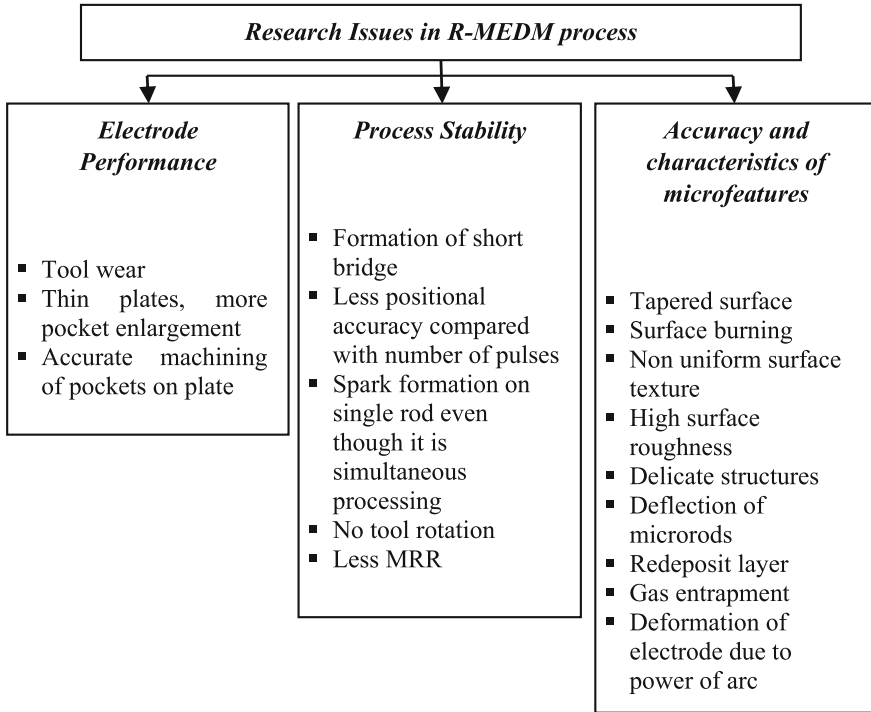
In R-MEDM, nonelectrical parameters include type of dielectric (e.g., kerosene or deionized water), flushing conditions, electrode thickness, and electrode positions. The chemical composition of the dielectric greatly varies the breakdown strength and other physical properties. The type of dielectric fluid used also affects the process responses, such as material removal rate, chemical variation at the surface, and a surface roughness on the machined features. Flushing conditions include the type of jet and dielectric flow rate, the process stability improves with a moving jet flushing at high dielectric velocities. Plate electrode (cathode) thickness mainly affects the

**Table 5.4** Important processing parameters in reverse micro-EDM [26]

Parameter	Definition/Description	Effects on process
Voltage (V)	Open voltage applied between cathode–anode. Typical range of voltage is 80–150 V.	Voltage mainly influences imploding and exploding nature of plasma, erosion rate, machining accuracy, and a surface roughness of machined features
Capacitance (F)	Capacitance controls the maximum energy stored by capacitor before discharge. Capacitance ranges from 10 pF to 1 $\mu$ F capacitance	Number of pulses per unit time and energy of sparking are controlled by capacitance. R-MEDM process is unstable at very low (nF) and very high capacitance levels ( $\mu$ F)
Threshold (% V)	It is specified in terms of % voltage. This parameter controls the sensitivity of a process toward arcing. Threshold values ranges from (20 to 80% V)	Material removal rate and surface roughness of machined feature are affected by threshold. Smaller values of threshold (% V) lead to higher machining time but good surface finish of fabricated features
Dielectric	Fluids with specific breakdown strength. Hydrocarbons with high splash points and varying breakdown strengths	Affects white layer formation on machined surface, material removal rate, and surface roughness
Plate thickness	Thin foils of 100–600 $\mu$ m thickness used as electrodes. Microfeatures are initially machined on plate thickness	Smaller plate thickness is preferred in R-MEDM. Interface areas between plate machined featured and cavity surface on plate electrode is higher for thicker plates. Tool wear and machining accuracy are controlled by plate thickness
Feature size	The cross-sectional area of machined feature. Features of about 40 $\mu$ m can be machined	For smaller feature sizes, debris particles get entrapped in interelectrode gap and lead to short-circuiting. Relatively, it is easier to machine larger features in R-MEDM

overlapping area between electrodes. It is difficult to micromachine through holes on thicker plates as well as to flush debris through interelectrode gaps.

Reverse micro-EDM process requires technological improvements in various areas before this process can be used to fabricate accurate and precise features. As shown in Fig. 5.3, process improvements are required in better erosion resistance of electrode material and better process stability and dimensional accuracy of machined features. Short-circuiting and arcing due to debris entrapment limit the workpiece area over which features can be generated in R-MEDM. Arcing during R-MEDM changes heat distribution pattern and leads to higher tool wear rates. Electrode rotation is commonly used in micro-EDM to enhance debris flushing. However, such electrode rotation is not feasible in R-MEDM while machining arrayed features.

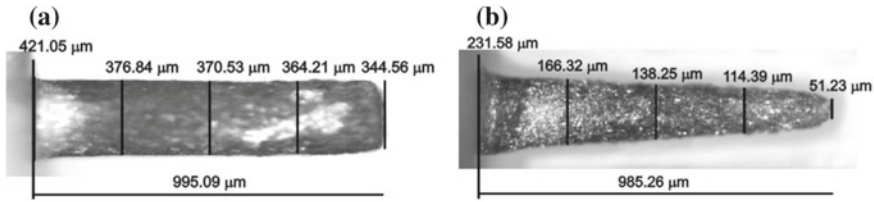


**Fig. 5.3** Improvements required in R-MEDM process

This limits the R-MEDM erosion rate. Also, tool wear during R-MEDM process elongates initially machined microcavity which naturally leads to corresponding dimensional inaccuracies on machined features.

## **5.5 Machining of High Aspect Ratio Features Via R-MEDM**

As mentioned earlier, high aspect ratio arrayed microrods find applications varying from tool electrode to the components of biomedical devices. It may be noted that R-MEDM, unlike most of the existing micromachining processes, is capable of fabricating arrayed features of any desired shape and center-to-center distances. Based on a melting point, electrical conductivity, and thermal conductivity, the workpiece materials may be classified as ‘easy-to-erode’ and ‘difficult-to-erode’ materials, e.g., brass is an ‘easy-to-erode’ material while tungsten carbide is a ‘difficult-to-erode’ material. In R-MEDM, cathode electrode needs to be pre-machined to create required



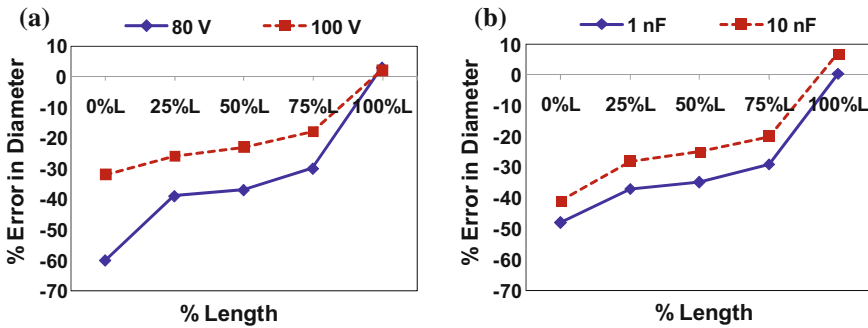
**Fig. 5.4** Dimensional accuracies of brass microrods of **a** 400  $\mu\text{m}$  square and **b** 200  $\mu\text{m}$  cylindrical cross section [26]

microcavities, and it is desirable to use a thin metallic plate of 200–300  $\mu\text{m}$  thickness. Use of thicker plate electrodes imposes difficulties while machining microcavities.

### 5.5.1 Reverse Micro-EDM of Easy-to-Erode (Brass) Material

Copper is being a widely used electrode material due to its high thermal and electrical conductivities which leads to less tool wear rate. A high material removal rates and low surface roughness values are feasible to be obtained in reverse micro-EDM of brass by use of copper as electrode. Typical response parameters measured during experimental works on R-MEDM process are material erosion rate, dimensional accuracy, surface roughness, and surface morphology in the fabricated features.

Accuracy of microrods of 400  $\mu\text{m}$  square and a 200  $\mu\text{m}$  cylindrical cross section machined up to 1 mm length on 2-mm-diameter brass rod is shown in Fig. 5.4a, b. It is expected that R-MEDM should produce microrods of uniform cross section throughout its length. However, it is a taper is observed on the fabricated microrods. Highest inaccuracies in dimension are observed at the tip (0% L) which decreases toward root of fabricated microrods (100% L). Very high-dimensional inaccuracies (60%) are observed at low voltages. At low gap voltage values (e.g., 80 V), the interelectrode gap is minimal at the time of discharge. This small gap obstructs debris dispels from interelectrode gap. Also, at low voltages, discharge energy is not sufficient to provide a plasma explosion/dielectric implosion impact on debris to drive out the debris. Accumulation of debris in interelectrode gap results short-circuiting. Sensing the short-circuiting machine retracts spindle head to relive short-circuit conditions. The tip of machined microrod experiences multiple sparking and subsequently results in higher-dimensional inaccuracies. Under the influence of potential, debris may form a chain and temporary weld to either of the electrode. Chemical analysis of microrods fabricated in R-MEDM has shown significant amount of electrode material deposition on fabricated microrods. Increase in oxygen and carbon percentage with reduction in percentage of base material on workpiece surface indicates oxidation and confined burning. Therefore, systematic improvements and post-processing are essential in R-MEDM process to control the surface damage.



**Fig. 5.5** a % error in dimension at the tip (0% L) and root (100% L) at varying (a) voltage and b capacitance levels [25]

Identical effects of capacitance are observed in R-MEDM. As shown in Fig. 5.5b, increase in capacitance increases discharge energy and leads to better process stability compared to low discharge energies at low capacitance levels. Also, chemical analysis of microrods indicates a higher content of oxygen and carbon at the tip compared to root. SEM image at the tip and root of a microrod fabricated in R-MEDM process is shown in Fig. 5.6. It shows significant difference in the surface morphology along the length of microrod. Surface closer to tip shows larger craters while the surface at the root is comparatively smooth.

### 5.5.2 Reverse Micro-EDM of Difficult-to-Erode (Tungsten Carbide) Material

As discussed in the previous section, the fabricated arrayed microrods in R-MEDM have poor dimensional accuracies if process parameters are not controlled at optimum level. Tungsten carbide is categorized as one of the difficult-to-erode material due to high melting point and electrical resistivity. The high tool wear rate offers additional challenges in controlling the dimensional inaccuracies of fabricated features in R-MEDM process. Since, thin electrode plates are required in R-MEDM process for the ease of drilling/milling microholes, even a small amount of tool wear would completely damage the electrode plates made of conventional tool materials like copper and graphite. Tungsten Copper (70% tungsten, 30% copper) is a superior electrode material due to combined benefits of tungsten (high melting point) and copper (good electrical conductivity). Therefore, WCu is the suggested electrode material for R-MEDM of WC which is difficult-to-erode material (Fig. 5.7).

A taper of  $1.2^{\circ}$ – $1.5^{\circ}$  is observed on the fabricated microrods mainly due to (1) side wear of microhole used as a tool and (2) higher erosion rate along the tip region due to frequent arcing and short-bridge conditions. Although, fabrication of high aspect ratio microrods on WC is more challenging than machining of features on

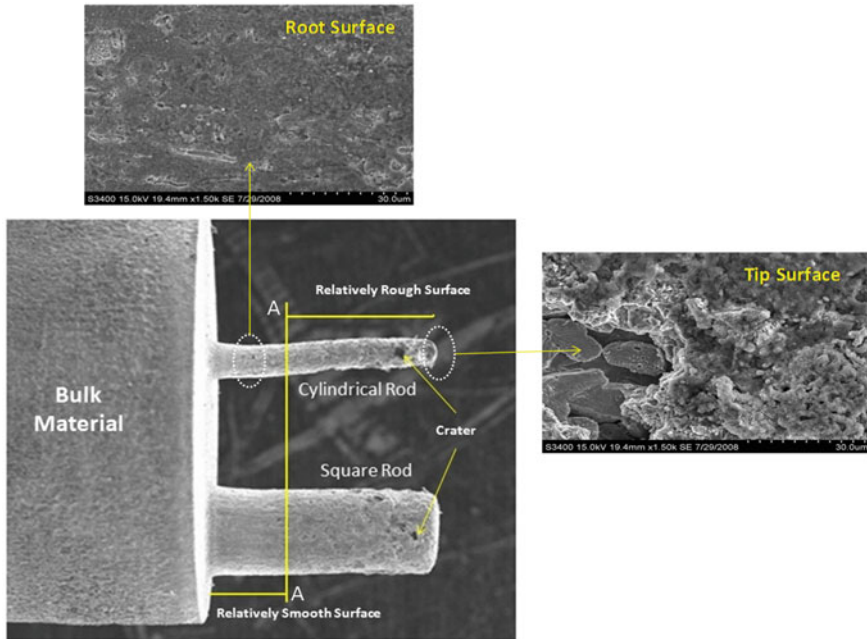


Fig. 5.6 Morphology of fabricated microrods in R-MEDM [25]

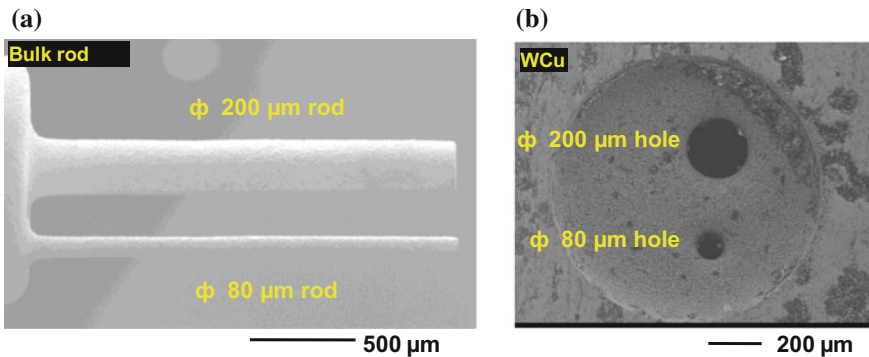
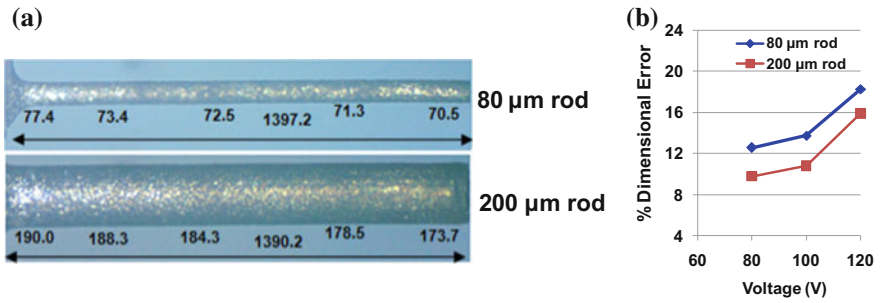
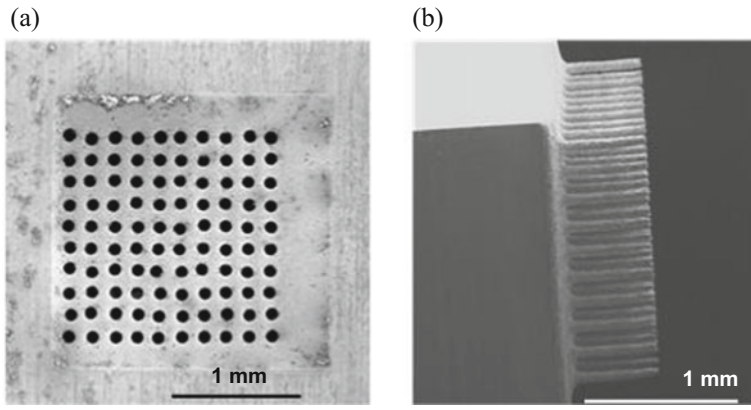


Fig. 5.7 a Fabricated tungsten carbide microrods using b microholes on WCu plate [27]

brass, the dimensional accuracy achieved on WC is much higher than that obtained on brass microrods, refer Fig. 5.8a, b. This is primarily due to the usage of WCu plate electrode which has very less wear rate. Voltage and capacitance control the dimensional accuracy, erosion rate, and tool wear rate. Also, plate thickness controls the dimensional accuracy and a surface roughness of microrods [27, 28]. To reveal the capability of R-MEDM process for generating microfeatures over larger surface area on WC, a 10 × 10 array (100 microrods) with diameter of individual microrod



**Fig. 5.8** a Measured dimensions on  $\phi$  80 and  $\phi$  200  $\mu\text{m}$  rods fabricated using WCu as electrode and b effect of voltage on 80 and 200  $\mu\text{m}$  at different voltage levels [27]



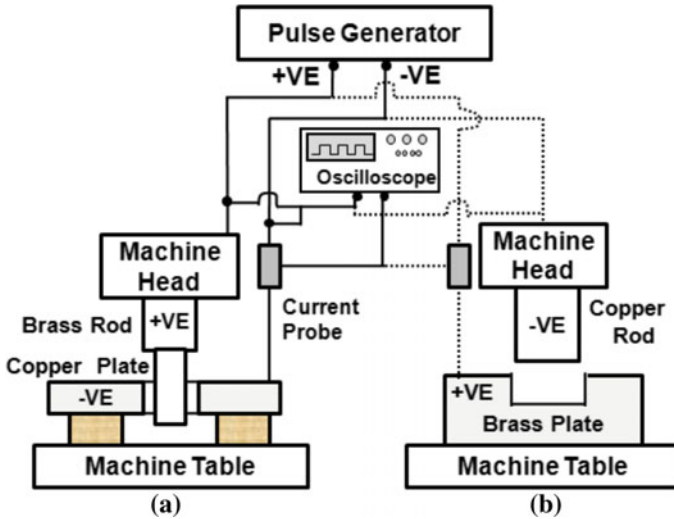
**Fig. 5.9** a WCu electrode having  $10 \times 10$  microhole array used as electrode to R-MEDM b  $10 \times 10$  array on WC [27]

less than 100  $\mu\text{m}$  and length of 500  $\mu\text{m}$  was machined using reverse micro-EDM, see Fig. 5.9. Electrode consists of a  $10 \times 10$  microhole array microdrilled on 300  $\mu\text{m}$  tungsten copper plate. Machining time required for fabrication of such structures is exceptionally high (more than 20 h). Hence, this process needs to be further improved in terms of erosion rate for economical machining of arrayed microrods on larger surface areas.

### 5.6 Process Mechanics Comparison of R-MEDM and Micro-EDM

During electrical erosion process, molten workpiece material is escaped during plasma implosion stage. This molten metal disintegrated in the presence of dielectric



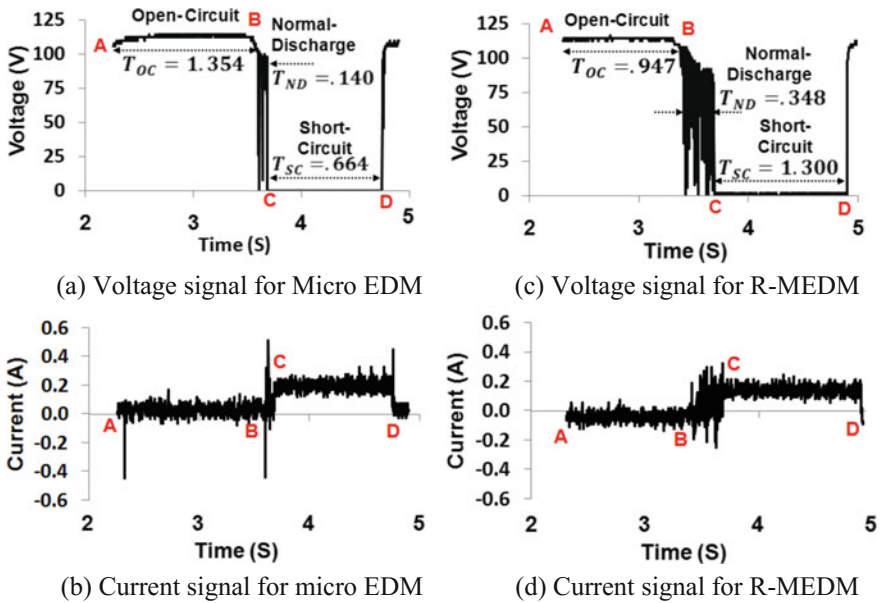


**Fig. 5.10** Setup to capture voltage–current signals in a R-MEDM (fabrication of microrod) and b micro-EDM (machining of microcavity) [28]

and solidifies as a debris particle. In presence of debris particles, breakdown strength of dielectric reduces drastically. Thus, flushing of debris is very critical in R-MEDM for enhancing erosion rate. In case of reverse micro-EDM, simultaneous machining of features alters its process response. The  $V-I$  (voltage/current) signals are commonly analyzed to characterize the process stability. Hence, process mechanics comparison in terms of voltage–current signals between R-MEDM and micro-EDM processes provides in-depth understanding of process behavior.

Although principle of material removal is identical in micro-EDM and R-MEDM processes, differences in the geometries of tool and machined feature vary the machining response of these processes. At identical processing parameters, surface roughness values on the microcavity machined in micro-EDM and microrod in R-MEDM are different. The debris sticking and resolidification on microrod fabricated in R-MEDM point to a different debris flow pattern in these processes. SEM images shows debris sticking on the microrods fabricated via R-MEDM process [27]. With a progress of machining time, impact of debris on process alters. The setup which is used to capture  $V-I$  signals during micro-EDM and reverse micro-EDM is shown in Fig. 5.10. The  $V-I$  signals obtained during the machining cycle points to varying machining conditions. Although all processing parameters will have a different impact on micro-EDM and R-MEDM process, but voltage, capacitance, and the threshold are prime parameters that affect the behavior of process in both micro-EDM and R-MEDM processes.

Signature of  $V-I$  signals varies during the progress of machining in micro-EDM and R-MEDM. Cavities are generated in micro-EDM process whereas microrod is fabricated in R-MEDM. With the increasing aspect ratio of microholes in micro-



**Fig. 5.11** Comparison of voltage and current signals for (a–b) micro-EDM and (c–d) R-MEDM [28]

EDM, flushing of debris becomes more challenging. In converse, debris accumulation is not a severe issue case of R-MEDM while fabricating single microrod. The debris flushing in R-MEDM is more difficult while fabricating microrods over larger workpiece areas, i.e., while creating a textured surface.

Figure 5.11 shows typical profile of the  $V-I$  signals captured during micro-EDM and the R-MEDM process after 5 min from the start of process. Typical  $V-I$  signals show different regions based on the voltage and current values at specific time instances. These specific regions are:

- (1) **Open-circuit (OC) region:** At the start of cycle, there is large interelectrode gap and spindle head start to approach the other electrode. Open-circuit region is characterized by high voltage–no current region (region AB shown in Fig. 5.11a, b). Breakdown strength of dielectric is maintained. Accumulation of debris particles from previous discharges will reduce the open-circuit time.  $T_{OC}$  indicates an open-circuit time in Fig. 5.11a.
- (2) **Normal discharge time (NDT) region:** At, the optimum interelectrode gap there is transfer of electrons from cathode to anode through dielectric. Collision of electrons with ions increases gap temperature which further leads to discharges (sparking). This is a most important region since actual material erosion happens during this period. Most favorable conditions of process for material erosion are registered in this region. Continuous spiking is seen in this region which indicates the passing of discharge current. Region BC shown in Fig. 5.11a

denotes the normal discharge region. NDT is shown as  $T_{ND}$  in Fig. 5.11a. Higher NDT indicates higher material removal and stable processing.

- (3) **Short-circuiting (SC) region:** After, the sparking and debris are generated in the interelectrode gap. The presence of debris drastically reduces the breakdown strength of dielectric and leads to the formation of short-circuiting. Debris particles temporarily get welded to either of the electrode. This condition is called as short-circuiting. Short-circuit duration indicates debris accumulation-related problems. Short-circuiting is characterized by the passage of high current at very low voltages, see Fig. 5.11a–d. Region CD shown in Fig. 5.11 indicates the short-circuiting duration. Shorter short-circuit durations are better to attain higher material erosion rate. Electrode vibrations and magnetic force assistance are used to quickly relieve short-circuit conditions.

$$\text{Normal-discharge time(NDT)\%} = \frac{T_{ND}}{T_{ND} + T_{SC} + T_{OC}}$$

$$\text{Short-circuit time(SCT)\%} = \frac{T_{SC}}{T_{ND} + T_{SC} + T_{OC}}$$

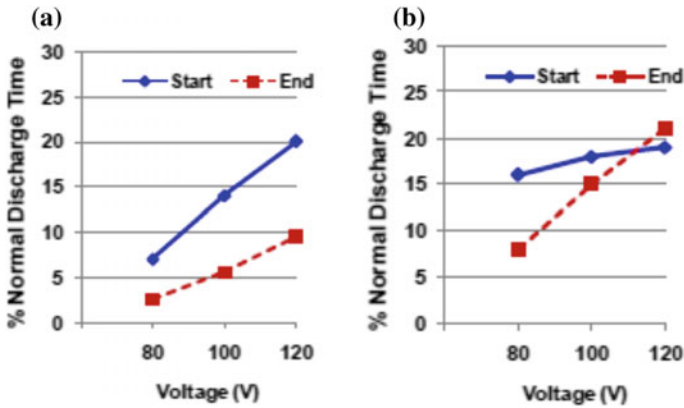
where,

$T_{ND}$  Normal-discharge duration

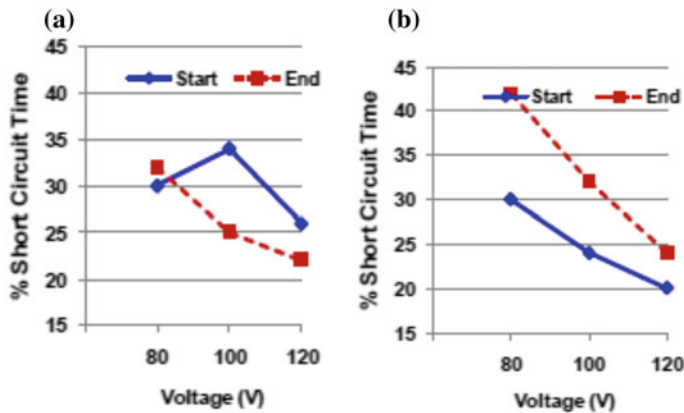
$T_{SC}$  Short-circuit duration

$T_{OC}$  Open-circuit duration

Normal discharge and short-circuit times can be estimated for signal captured during machining using equations Eqs. 5.1 and 5.2, respectively [29]. The V–I signals are captured at the Start (at 5 min after beginning of process) and at the End (at 90 min after beginning of process). In micro-EDM and R-MEDM processes, percentage of normal discharge time increases with an increase in voltage at the Start as well as End of process, refer Fig. 5.12a, b. Discharge energy has a square relation with a voltage. At higher voltage level, there is an increase in discharge energy; higher discharge energies increase material removal rate as well as enhance debris flushing efficiency by better implosion/explosion action of plasma. Enhanced debris flushing and effective material removal are probable reasons for higher percentage of NDT at higher voltage levels such as 120 V. As shown in Fig. 5.12, for any voltage setting, R-MEDM process has higher NDT% than micro-EDM. This difference in %NDT is more pronounced at 120 V in R-MEDM, whereas in case of micro-EDM, there is no significant difference in percentage of NDT. This clearly shows that R-MEDM process can be operated effectively even at high voltage levels.



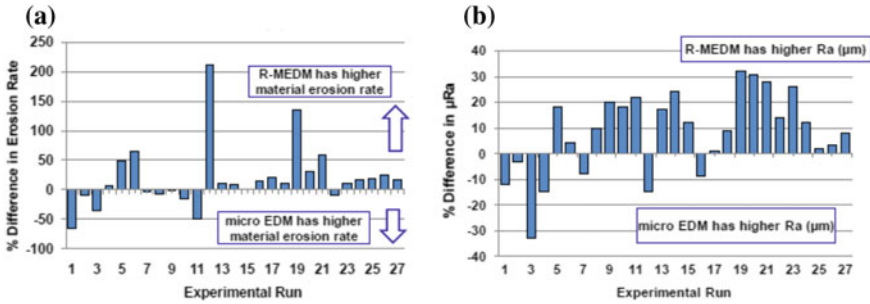
**Fig. 5.12** Variation in % of normal discharge time for **a** micro-EDM and **b** R-MEDM at the Start (5 min after beginning of process) and at the End (90 min after beginning of process)



**Fig. 5.13** Variation in % of short-circuit time for **a** micro-EDM and **b** R-MEDM at the Start (5 min after beginning of process) and at the End (90 min after beginning of process)

Debris entrapment in interelectrode gap is indicated by a short-circuit time (SCT). Larger SCT indicates debris deposition and sticking during the process. Percentage of SCT decreases with an increase in voltage. As discussed earlier, debris flushing and material erosion mechanism improve with increase in voltage. This fact is again validated in Fig. 5.13a, b. As the aspect ratio of microhole and microrod fabricated in micro-EDM and R-MEDM process increases, probability of debris entrapment rises. Reverse micro-EDM process seems to have higher SCT% than micro-EDM mainly at low voltage (80 V). Similar trend of high process instability at low voltage (80 V) is reported in literature [2].

Since NDT% is higher in R-MEDM process compared to micro-EDM, correspondingly, the material erosion rate must also be higher in R-MEDM. The difference



**Fig. 5.14** Percentage difference observed in the **a** material erosion rates and **b** surface roughness between micro-EDM and R-MEDM [29]

in erosion rates between R-MEDM and micro-EDM during different experimental conditions indicates that R-MEDM has higher erosion rate than micro-EDM process, see Fig. 5.14a. With the increase in depth of microcavity formed in micro-EDM, debris flushing is challenging. This limits the aspect ratio which can be obtained in micro-EDM process. However, for R-MEDM process, the fabricated microrod does not pose major obstructions for debris flushing provided fabrication of single microrod is undertaken. At identical processing conditions, surface roughness on fabricated microrod in R-MEDM is higher than surface roughness of microcavity generated in micro-EDM. This trend in surface roughness is possibly due to debris movement and sticking on fabricated microrods. Comparatively, fabrication of smaller microrod in R-MEDM and higher erosion rates mitigate the debris escapement. Ultimately, there are high probabilities that short-bridge conditions will be occurred due to debris entrapment in R-MEDM. Refer Fig. 5.14b for a trend in surface roughness.

Although, R-MEDM process can be used for fabricating high aspect ratio features, the inherent process instability due to debris entrapment in the interelectrode gap limits its applicability for machining arrayed features over relatively larger areas. Note that if the R-MEDM process can be extended to larger areas, it can be used to create engineered/textured surfaces. To accomplish this end, vibration-assisted R-MEDM process needs to be used for the creation of textured surfaces by machining micropillars over a larger surface area.

## 5.7 Vibration-Assisted Reverse Micro-EDM for Texturing Applications

It has been observed that the primary challenges in the R-MEDM process are low erosion rate and instabilities induced due to debris entrapment, specifically, while machining relatively large areas. Consequently, textured surfaces cannot be created on ‘difficult-to-erode’ material using the R-MEDM process unless the above-mentioned issues are addressed. There are several examples in nature which exhibit

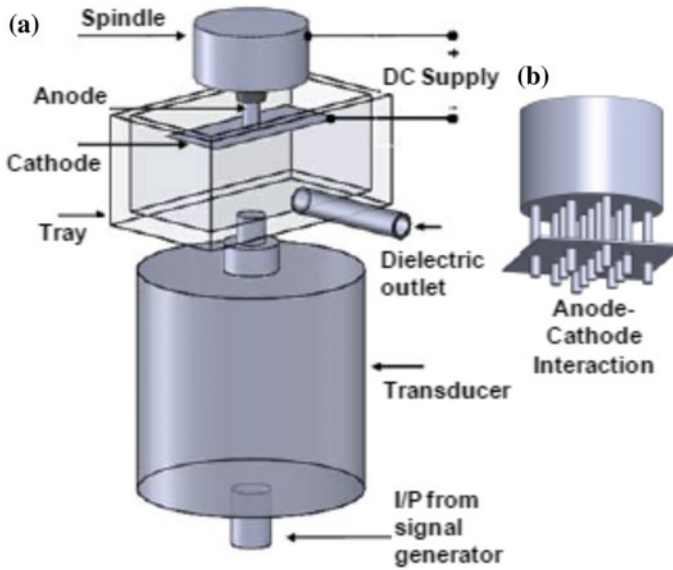
unique functional responses due to the presence of specific texture on their surfaces, e.g., super-hydrophobicity of lotus leaf, frogs which can easily climb wet/dry surface, and aquatic animals like sharks which can accelerate fast through water. Lotus leaf shows super-hydrophobicity due to the presence of hierarchical microfeatures of 15–25  $\mu\text{m}$  covered with natural wax. To extend the application of reverse micro-EDM process for fabrication of textured surfaces, it is required to improve the process via external means to increase the normal discharge duration in the process by dispelling debris effectively. The surface texture is the creation of repeated pattern of microfeatures on a surface. The size, shape, and surface density of features can be controlled to achieve specific functional response of surface.

Numerous methods are available for creating a negative textured surface. Negative textured surface consists of dimples on surface, whereas positive texture consists of pillared microfeatures. Numerous mesoscale manufacturing techniques can be used to create dimpled textures. Laser beam machining, chemical machining, etching, abrasive jet machining, etc. are commonly used processes to create textured surfaces. Majority of these processes fail to create a positive texture without surface damage, and they are probabilistic in controlling feature locations (exceptions being laser machining and chemical machining). R-MEDM process can be used to create positive textured surfaces.

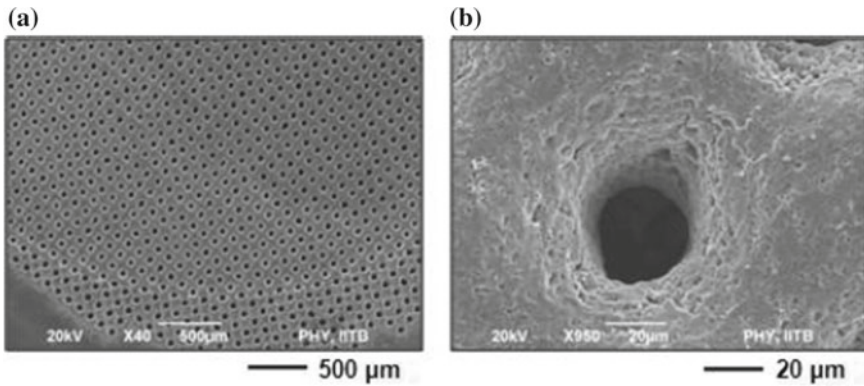
Initial attempts to create texture on larger Ti6Al4V surfaces have failed due the debris entrapment and tool failures. Due to high melting point of this alloy, it is categorized as 'Difficult-to-Erode' material. Also, fabrication of textured surfaces over very large surface areas poses additional challenges of debris escapement in R-MEDM. With the electrode vibration assistance, it is possible to fabricate textured surfaces in R-MEDM. A positive surface texture consisting of 40–50  $\mu\text{m}$  in diameter pillars located at center-to-center distance of 100  $\mu\text{m}$  on a face of Ti6Al4V rod of 4 mm in diameter is created. Along with electrical parameters, frequency and amplitude of electrode vibrations have been identified as processing parameters in R-MEDM. Fabrication of such a textured surface is infeasible for R-MEDM unless vibration-assisted electrode is used. As shown in Fig. 5.15, typical setup of vibration-assisted R-MEDM consists of small tray mounted on piezoelectric transducer. Transducer provides a required sinusoidal vibration to plate electrode.

To fabricate a textured surface in R-MEDM process, it is required to prepare a tool electrode. Thin foils of 75  $\mu\text{m}$  thickness can be used as the cathode, see Fig. 5.16. A copper plate is laser ablated to produce microholes of about 40  $\mu\text{m}$  diameter. The plate electrode was vibrated along the spindle movement direction using a piezoelectric transducer having capability to vibrate tray without damping effects. Although, frequencies as high as 40 kHz were used in micro-EDM, it is found that comparatively low frequencies of 3–6 kHz at 1–2  $\mu\text{m}$  amplitude are sufficient to realize a texture over larger surfaces in R-MEDM.

Other than the voltage and capacitance of circuit, other main operating parameters for vibration-assisted reverse micro-EDM are amplitude and frequency of electrode vibrations. Amount of change in interelectrode gap is controlled by amplitude. At higher amplitude, there would be larger compression of the dielectric which would effectively dispel the debris out of interelectrode gap. The frequency of electrode



**Fig. 5.15** a Setup of vibration-assisted R-MEDM and b workpiece-tool interaction in R-MEDM [30]

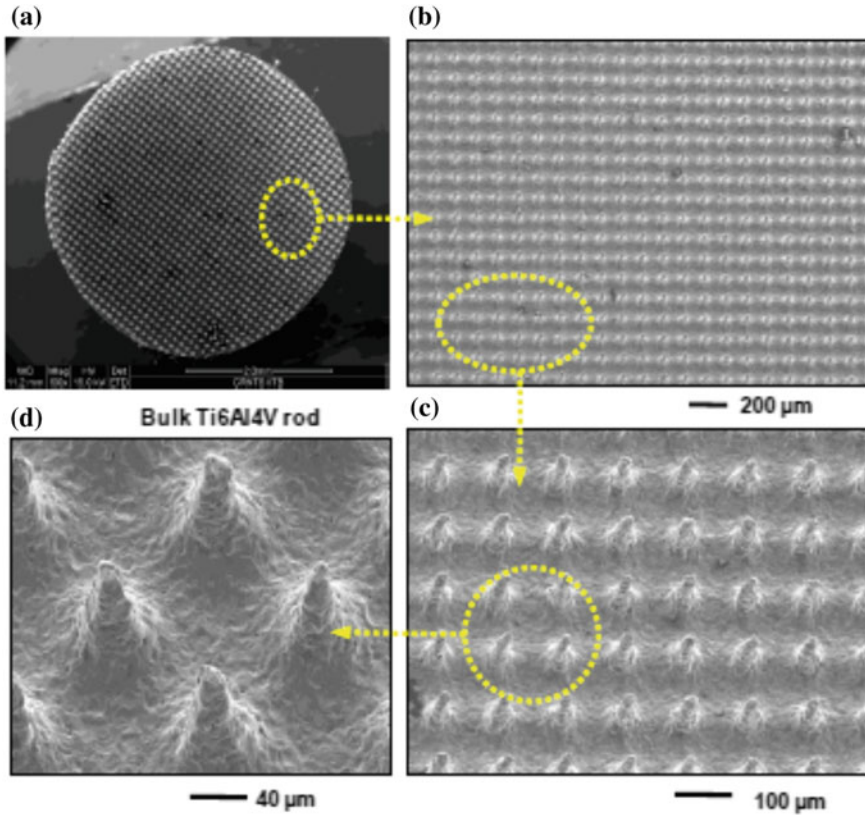


**Fig. 5.16** a SEM images of laser ablated plate electrode, b magnified image of individual microhole on plate electrode [30]

vibrations governs occurrence of change in interelectrode gap. Thus, frequency primarily controls the cycles per time, variation in dielectric pressure at the sparking zone. SEM images of the fabricated texture at different magnifications generated by R-MEDM process are shown in Fig. 5.17.

The electrode vibration in R-MEDM primarily improves the process due to cyclic pressure variation in the particle-laden dielectric in the sparking zone. Dielectric fluid is squeezed out of the interelectrode gap when the vibrating electrode moves





**Fig. 5.17** a–d Images of positive surface texture generated using vibration-assisted R-MEDM [30]

toward other electrode. On the other hand, the dielectric fluid is drawn back into the gap when vibrating electrode moves away from the workpiece. This cyclic pressure variation and flow field reversal in the dielectric fluid impede the localized debris agglomeration, thereby improving the process stability. Due to small electrode gaps (about  $10\ \mu\text{m}$ ), even small electrode vibrations of  $1\text{--}3\ \mu\text{m}$  amplitude are capable of imparting notable improvements in R-MEDM. During R-MEDM for surface texturing, about 30% reduction in time is observed with variation in amplitude from  $0.5$  to  $2.0\ \mu\text{m}$  (refer Fig. 5.18). Impact of frequency is also notable in R-MEDM. Increase in frequency aids in microstreaming and cavitation effects. As shown in Fig. 5.19, 29% reduction in machining time is noticed for variation of frequency from  $3$  to  $6\ \text{kHz}$ . Point that with no electrode vibration, it is not possible to create a texture on Ti6Al4V.



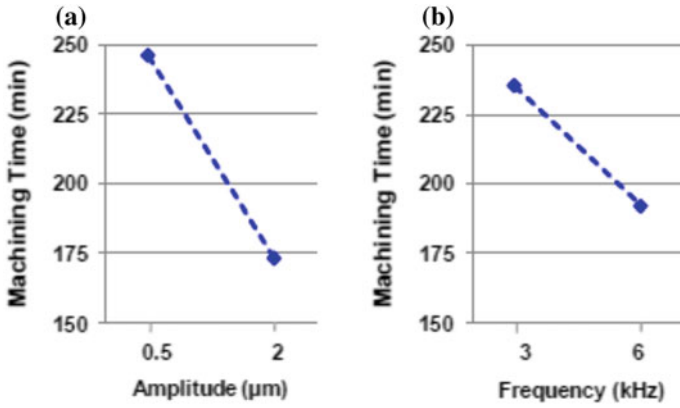


Fig. 5.18 Main effect plot of **a** amplitude and **b** frequency on machining time

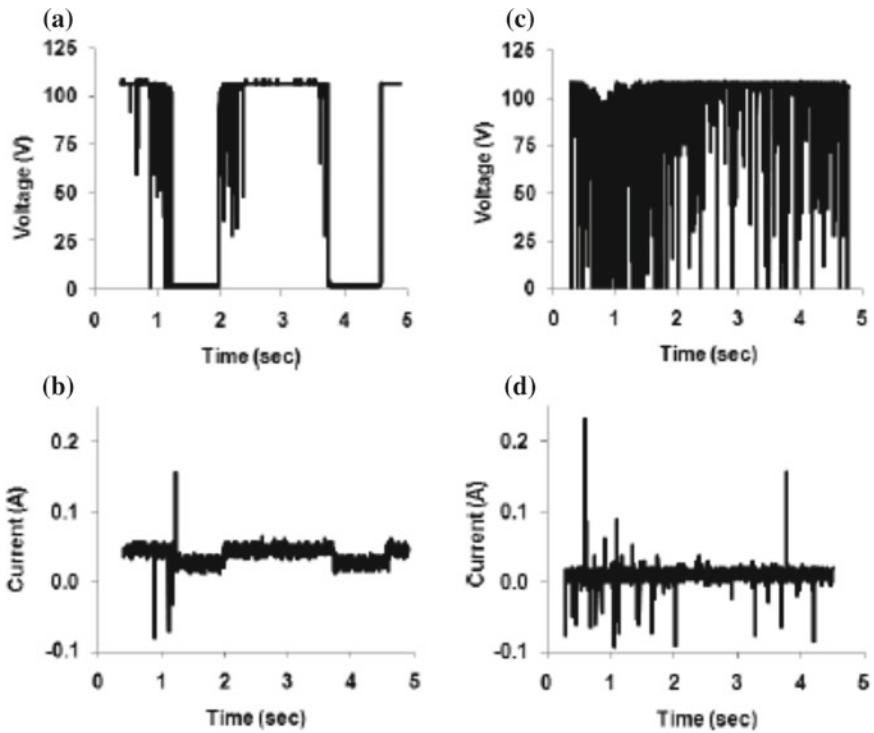
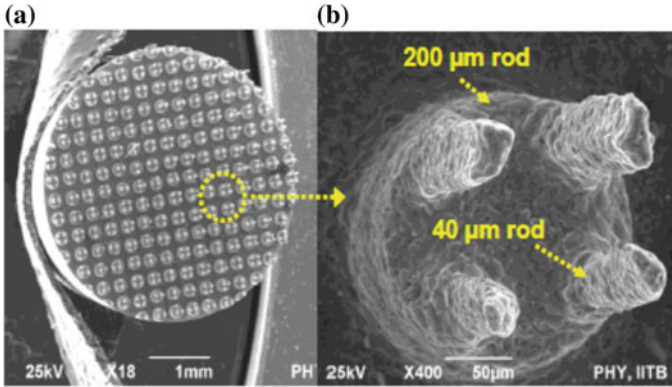


Fig. 5.19 V–I signals for **a** normal R-MEDM and **b** vibration-assisted R-MEDM (at 100 V, 1 nF, 2.0  $\mu\text{m}$  amplitude and 6 kHz frequency)

Voltage–current (V–I) signals captured during machining of textured surfaces with normal R-MEDM and R-MEDM assisted with electrode vibration are shown in



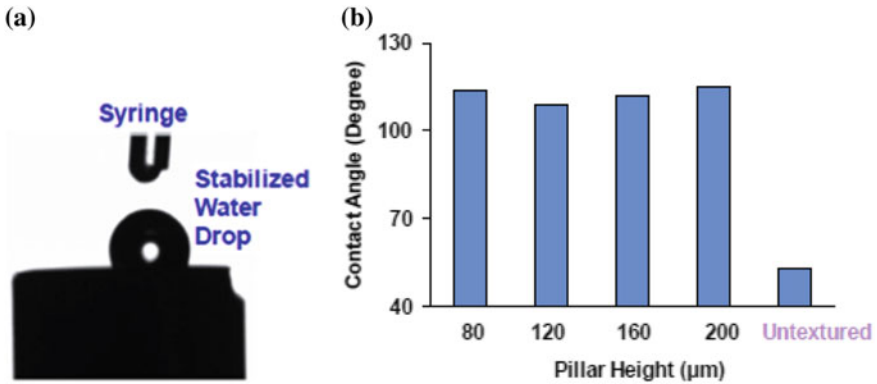
**Fig. 5.20** **a** Hierarchical texture machined on Ti6Al4V and **b** arrayed pillars machined on single pillar

Figs. 5.19a–d. Note the differences in normal discharge, open-circuit and short-circuit regions in R-MEDM and vibration-assisted R-MEDM processes. Clearly, electrode vibrations ( $2.0\ \mu\text{m}$  amplitude and  $6\ \text{kHz}$  frequency) have totally eliminated the open-circuit and short-circuit conditions in vibration-assisted R-MEDM. This is the reason why vibration assistance is essential to create texture in R-MEDM process.

A hierarchical pillared texture contains smaller pillars fabricated on a larger base pillar. Electrode vibration assistance is used in R-MEDM to create hierarchical texture. The base pillars are  $200\ \mu\text{m}$  in diameter and  $400\ \mu\text{m}$  height. Base pillars were machined using a copper foil which contains  $200\ \mu\text{m}$  holes microdrilled. After machining of base pillars, the copper foil is replaced by other copper foil which has laser ablated  $40\ \mu\text{m}$  microholes. The fabricated structures contain  $40\ \mu\text{m}$  pillars located randomly over base pillars, see Figs. 5.20a–b.

To test the texture fabricated by R-MEDM process, contact angle of few samples of varying pillar height is tested using Gonimeter instrument. The higher the contact angle, better is a hydrophobicity of surface. For lotus leaf which is super-hydrophobic in nature, contact angle will be more than  $150^\circ$ . Figure 5.21a shows a single drop rested on a textured surface having  $40\ \mu\text{m}$  diameter pillars of  $200\ \mu\text{m}$  height. Note that the textured surface of varying heights ( $80\text{--}120\ \mu\text{m}$ ) shows contact angle above  $112^\circ$ , whereas untextured (plain) surface has very small contact angle  $53^\circ$ .

It is found that vibration-assisted R-MEDM can create textured surface, which is otherwise infeasible with normal R-MEDM. Electrode vibrations have altered process mechanics of R-MEDM and debris accumulation issues can be countered. The debris flow modeling explained in the next section quantifies the effects of electrode vibrations on the dielectric and debris movement.



**Fig. 5.21** **a** Single water drop rested on textured surface and **b** contact angle measured in untextured and textured surfaces

## 5.8 Debris Modeling in Vibration-Assisted Reverse Micro-EDM

Under the influence of potential, debris particles form chains and affect the discharge transitivity. In high aspect ratio micro-EDM, debris accumulation and uneven short-circuit result a barreling of holes. It is challenging but essential task to flush the debris out of interelectrode gaps of few microns. Electrode vibrations improve the material erosion rate and the stability of R-MEDM process, thereby making surface texturing feasible. Another phenomenon which is governed by debris is short-bridge formation. The passing of current through debris causes it to weld with either of the electrode. Short-bridge condition takes more time to relieve than short-circuiting. Preventing accumulation of debris particles is thus very important in controlling the stability of micro-EDM and its variant processes. Various enhanced dielectric flushing techniques such as rotating electrodes, magnetic force assistance, grooved electrodes, and electrode vibration are used in micro-EDM. However, electrode vibration is the most effective technique of all. Electrode vibration impacts are improved process stability, enhanced process capability, and generation features over larger surface areas. Possibly pulsating flow may be induced in dielectric with an electrode vibration.

Typical setup used for electrode vibration-assisted R-MEDM is shown in Fig. 5.22a, b; the cathode can be vibrated using piezoelectric transducer suitable capacity. Note the changes in the front interelectrode gap with the different electrode positions. Position A is the lower position of electrode vibration. At this position, interelectrode gap is highest, whereas position C is upper position of vibrating electrode. Interelectrode gap is smallest at upper position of vibrating electrode. Position B is a mean position where plate has highest velocity. This variation in electrode gaps is a main cause for forced debris flushing.

There is no exhaustive study which has quantified and related the processing parameters with the size, shape, and number of debris generated. Debris simula-

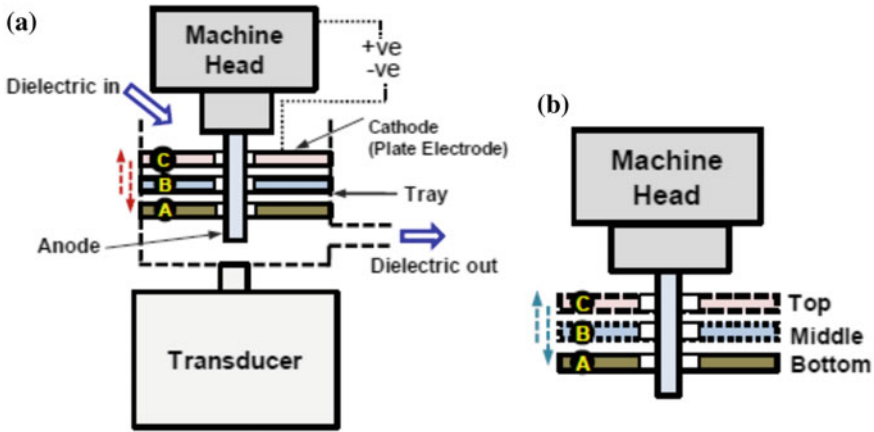


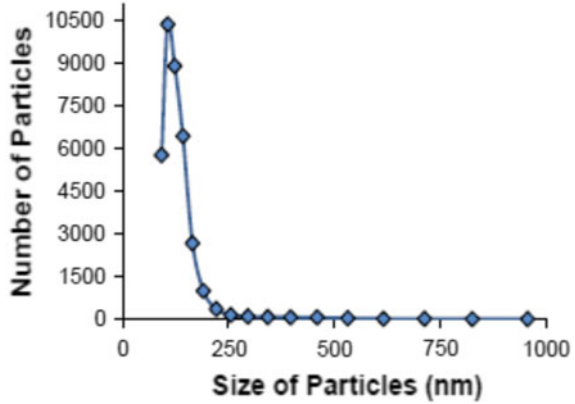
Fig. 5.22 a Vibration-assisted R-MEDM and b top, middle, and bottom positions of vibrating plate

tion studies in micro-EDM and wire EDM also have assumed very few number of debris located initially [31, 32]. As noted earlier, there is no fundamental difference between micro-EDM and R-MEDM in principle of material erosion. Therefore, a mathematical model is established to envisage the number of debris generated in R-MEDM. Further, simulation study is conducted by injecting of debris particles in the interelectrode gap and effects of electrode vibrations on pattern of debris and dielectric movement. A relation is established between number of debris particles and the crater size based on the debris size distribution obtained by Laser Particle Size Analyzer (LPSA). It is assumed that electrode is vibrating at 1, 3, and 6 kHz frequencies and 0.5 and 1  $\mu\text{m}$  amplitude. Effects of frequency and amplitude on the debris flow are analyzed on the basis of time taken to flush the debris out of electrode gap, average debris velocity, and the dielectric velocity profile. Under the influence of electrode vibrations, debris particles, and dielectric fluid gain momentum.

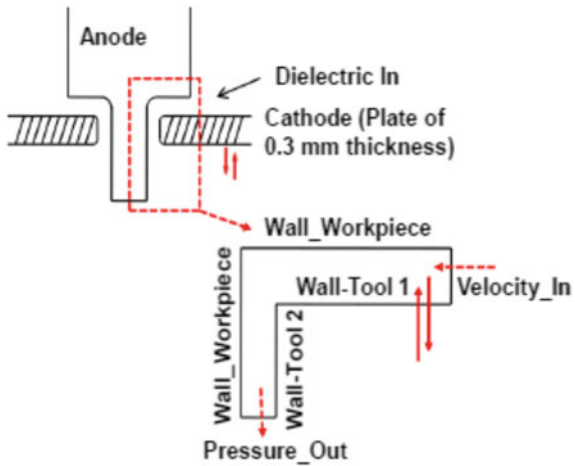
Theoretical number of debris entering in the sparking region per discharge is quantified on the basis of crater size generated per discharge and a debris size distribution. Detailed discussion on the model can be found in one of the published study [29]. It is found that approximately 36,000 debris particles of different sizes are produced per discharge, see Fig. 5.23 for the estimated number of debris particles of different diameters generated per discharge.

The ejection velocity of debris can be represented by Eq. 3. This equation is obtained based on the energy balance of single discharge, details of which are also presented in earlier work [30].  $p$  is discharge energy,  $r'$  is radius of debris particle,  $E_T$  is discharge energy,  $\rho$  is density of work material,  $K$  and  $a$  are constants, and  $\gamma$  is surface tension. It is estimated that debris has ejection velocity close to sonic velocity (328 m/s).

**Fig. 5.23** Number of debris particles of varying sizes per discharge [30]



**Fig. 5.24** Domain and boundary conditions [30]



$$V = \sqrt{\frac{\frac{4}{3}\pi\rho E_T r'^3 - 1.44\pi^2\gamma r'^2 K E_T^a}{\frac{2}{3}\pi\rho K E_T^a r'^3}} \tag{3}$$

Reverse micro-EDM case of fabrication of single microrod fabrication is shown in Fig. 5.24. Axi-symmetric problem is considered with a selected domain is inter-electrode gap. Anode (workpiece) is fixed while cathode (plate electrode) vibrates at sinusoidal frequencies of different frequencies and amplitude. ‘Wall-Tool-1’ and ‘Wall-Tool-2’ boundaries are vibrated vertically at 1, 3, and 6 kHz frequencies and 0.5 and 1 μm amplitude using user-defined function (UDF) in Ansys simulation software.

The domain dimensions are represented in Fig. 5.25. It is assumed that 8 μm is interelectrode distance at the time of discharge. The length of channel is 500 μm, and the channel is divided into different zones. It is thought that there is single discharge

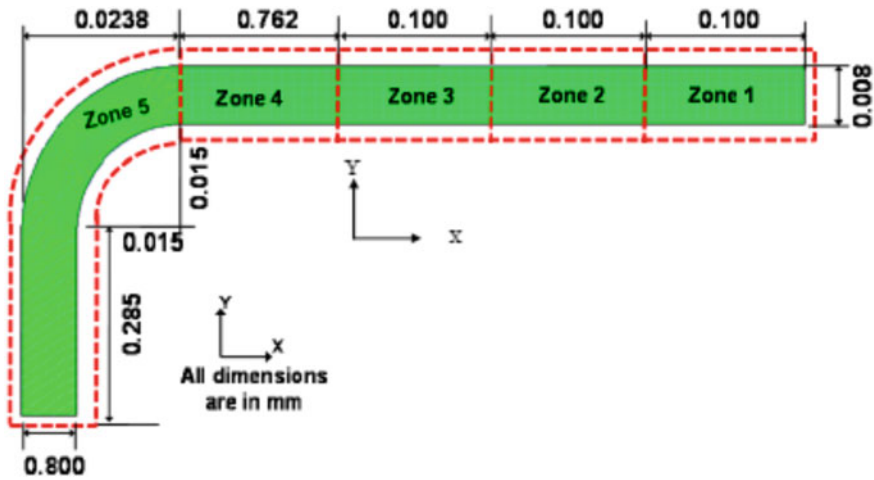


Fig. 5.25 Dimensions of the simulation domain [30]

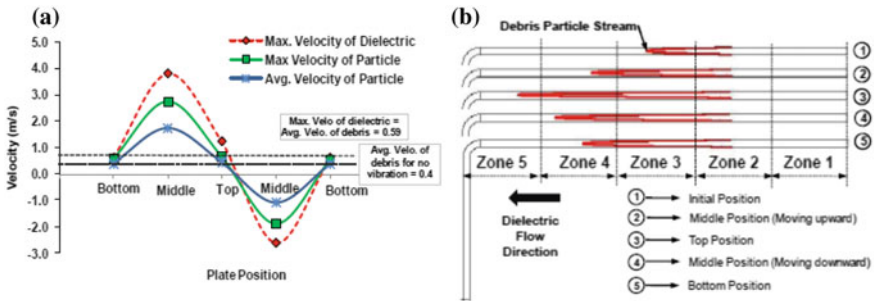
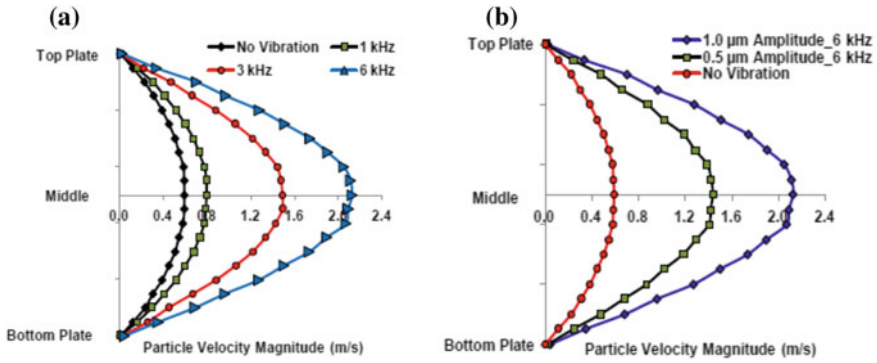


Fig. 5.26 a Influence of electrode plate position on variation in debris and dielectric velocity and b position of the debris front position at different positions of the plate electrode [30]

in Zone 2 and thus 360,000 particles are injected in Zone 2 at the 330 m/s injection velocity. The dielectric inlet is from right side of channel with 0.4 m/s inlet velocity. Boundary vibration alters the volume of horizontal section of the channel. The trend of result obtained in simulation studies are benchmarked with earlier studies on vibration-assisted micro-EDM [33, 34]. In these studies, it is pointed that reversal in dielectric velocity vectors is expected with the forward–backward movement of vibrating electrode.

Flow velocity of dielectric fluid and average velocity of debris particles vary with the vibrating plate position, refer Fig. 5.26a. For stationary electrode condition (normal R-MEDM), maximum velocity of dielectric in the channel is 0.59 m/s while debris has a constant velocity of 0.4 m/s. For the forward movement of plate from bottom to middle position, dielectric velocity increases to 3.8 m/s. This increased velocity of dielectric reduces to 0.64 m/s at the top position of electrode. For further



**Fig. 5.27** Variation in the average velocity of debris particles with **a** frequency and **b** amplitude of vibration [30]

movement of plate electrode from top to bottom position, there is reversal in the dielectric velocity vector. It indicates that for forward movement of plate electrode, dielectric is flushed out of interelectrode gap, whereas during return stroke, dielectric is pulled inside interelectrode gap. This momentum of dielectric is transferred to debris particles. Velocity vectors of debris particles also get reversed with change in direction of motion of plate electrode, refer Fig. 5.26a. The effect of plate vibrations on debris particle stream is shown in Fig. 5.26b. Note that from the initial position to top position of plate electrode, debris particle stream is pushed forward by the dielectric. However, during return motion of plate electrode from top to bottom position, debris stream is pulled inside the channel. Although, there is pulsating motion to dielectric, there is net forward movement of debris toward channel outlet. Due to this pulsating motion of debris particles, there will be less probability of debris accumulation which causes short-circuit. Net result of electrode vibrations is high process stability. Oscillatory motion of debris along the channel length is totally absent in case of normal R-MEDM (no electrode vibrations). Debris particles also take more time to completely flush out of interelectrode gap.

In case of flow through channel, there is zero velocity of fluid at the boundaries and it is maximum at the center of channel. Therefore, it is expected that debris particles will also have a maximum velocity at the center of channel. Figure 5.27a–b show the velocity of debris particles under the influence of varying amplitude and frequencies. Top represents the upper boundary of channel, while bottom plate represents the vibrating plate. Middle represents the center of a channel. It is found that with for the greater values of electrode frequencies, average velocity of debris particles increases. At no electrode vibration condition, maximum velocity of debris particles is 0.58 m/s. This velocity increases to 0.8, 1.5, and 2.1 m/s with increase in frequency of vibration to 1, 3, and 6 kHz, respectively. Pulsating nature of dielectric motion intensifies with increase in frequency of vibrations. Similarly, amplitude of vibration also imparts larger momentum and increases average velocity of debris particles, refer Fig. 5.27b. For normal R-MEDM (without electrode vibrations), maximum velocity of debris

particles is 0.58 m/s. Maximum velocity of debris particles increases from 0.58 to 1.5 and 2.1 m/s as the amplitude is increased to 0.5 and 1  $\mu\text{m}$ , respectively, from no vibration condition. It points that electrode vibrations have a positive impact on R-MEDM process, and it is essential to provide electrode vibrations during creation of textured surfaces.

## 5.9 Summary

Reverse micro-EDM (R-MEDM) has originated for micro-EDM process. R-MEDM process has shown a potential for accurate fabrication of high aspect ratio features as well as textured surfaces. It is important to set optimum electrical parameters on R-MEDM process. At optimum parametric levels, R-MEDM is stable and produces dimensionally accurate features. Process seems to be mainly affected by the capacitance and voltage. The physical properties of plate electrode are very critical in R-MEDM, since thin foils of these materials are used as electrodes. WCu is found to be a suitable material for fabrication of difficult-to-erode material like tungsten carbide. The process mechanics studies indicates that impact of debris on process behaviour is substantially different in micro-EDM and R-MEDM. Material erosion in R-MEDM is higher than micro-EDM at identical parameters. Electrode vibration in R-MEDM process has improved the applicability for surface texturing applications. The debris flow simulations in R-MEDM indicate the pulsating motions of dielectric and debris. Electrode vibrations of higher amplitudes and frequencies impart greater velocities to dielectric and debris particles. Debris accumulation in electrode channel is prevented by pulsating motion of dielectric which drastically enhances R-MEDM process stability.

## References

1. Masuzawa T, Kuo C, Fujino M (1994) A combined electrical machining process for micro-nozzle fabrication. *CIRP Ann Manuf Technol* 43:189–192
2. Kim B, Park J, Chu C (2006) Fabrication of multiple electrodes by reverse EDM and their application in micro ECM. *J Micromech Microeng* 18:843–850
3. Penache C, Gessne C, Braüning-Demian C, Scheffler P, Spielberger L, Hohn O (2002) Microstructured electrode arrays: a source of high pressure non-thermal plasma. In: Ochkin VN (ed) *Spectroscopy of non equilibrium plasma at elevated pressures*. SPIE, Bellingham, Washington, pp 17–25
4. Liao Y, Cheng M, Liao K (2009) An on-line pulse trains analysis system of the wire-EDM process. *J Mater Process Technol* 209:4417–4422
5. Lim H, Wong Y, Rahman M, Lee E (2003) A study on the machining of high-aspect ratio micro-structures using micro EDM. *J Mater Process Technol* 140:318–325
6. Liu K, Wu H, Shaw K, Ng S (2008) Ultra precision machining of micro structure arrays. *SIMTech (Singapore Institute of Manufacturing Technology) Tech Rep* 9(4):205–212
7. Rajurkar K, Lev G, Malshe A, Sundaram M, McGeough J, Hu X, Resnick R, DeSilva A (2006) Micro and nano machining by electro-physical and chemical processes. *CIRP Ann—Manuf Technol* 55:643–666



8. Jin B, Cao G, Wang Z, Zhao W (2007) A micro-deposition method by using EDM. *Key Eng Mater* 339:32–36
9. Chen S (2007) A high-efficiency approach for fabricating mass micro holes by batch micro EDM. *J Micromech Microeng* 17:1961–1970
10. Takeuchi Y, Suzukawa H, Kawai T, Sakaida Y (2006) Creation of ultra-precision microstructures with high-aspect ratios. *CIRP Ann Manuf Technol* 55:107–110
11. Nosonovsky M, Bhushan B (2009) Superhydrophobic surfaces and emerging applications: non-adhesion, energy, green engineering. *Curr Opin Colloid Interf Sci* 14:270–280
12. Genzer J, Efimenko K (2006) Recent developments in superhydrophobic surfaces and their relevance to marine fouling: a review. *Biofouling (J Bioadhes Biofilm Res)* 22:339–360
13. Obikawa T, Kamio A, Takaoka H, Osada A (2011) Micro-texture at the coated tool face for high performance cutting. *Int J Mach Tools Manuf* 51:966–972
14. Malshe A, Rajurkar KP, Samant A, Hansen H, Bapat S, Jiang W (2013) Bio-inspired functional surfaces for advanced applications. *CIRP Ann Manuf Technol* 62:607–628
15. Stepien P (2007) Grinding forces in regular surface texture generation. *Int J Mach Tools Manuf* 47:2098–2110
16. Stepien P (2011) Deterministic and stochastic components of regular surface texture generated by a special grinding process. *Wear* 271(3–4):514–518
17. Soveja A, Cicala E, Grevey D, Jouvard J (2008) Optimisation of TiA6 V alloy surface laser texturing using an experimental design approach. *Opt Lasers Eng* 46(9):671–678
18. Baldacchini T, Carey J, Zhou M, Mazur E (2006) Super-hydrophobic surfaces prepared by micro-structuring of silicon using a femto-second laser. *Langmuir* 22:4917–4919
19. Kannan R, Sivakumar D (2008) Drop impact process on a hydrophobic grooved surface. *Colloids Surf A: Phys-chem Engineer Aspects* 317:694–704
20. Franzen V, Witulski J, Brosius A, Trompeter M, Tekkaya AE (2010) Textured surfaces for deep drawing tools by rolling. *Int J Mach Tools Manuf* 50:969–976
21. Wakuda M, Yamauchi Y, Kanzaki S, Yasuda Y (2003) Effect of surface texturing on friction reduction between ceramic and steel materials under lubricated sliding contact. *Wear* 254:356–363
22. Koshy P, Tovey V (2011) Performance of electrical discharge textured cutting tools. *CIRP Ann—Manuf Technol* 60(1):153–156
23. Simao J, Aspinwall D, Wise M, Subari K (1989) Surface texture transfer in simulated tandem and temper mill rolling using electrical discharge textured roll. *J Mater Process Technol* 5:177–189
24. Costa H, Hutchings IM (2009) Development of a mask-less electrochemical texturing method. *J Mater Process Technol* 209:3869–3878
25. Mujumdar S, Mastud S, Singh R, Joshi SS (2009) Experimental characterization of reverse micro-EDM process for fabrication of high-aspect ratio micro rod arrays. *Proc Inst Mech Engineer, Part B: J Eng Manuf* 225:1–18
26. Mastud S, Garg M, Singh R, Joshi SS (2012) Recent developments in the reverse micro electrical discharge machining in the fabrication of arrayed micro features. *Proc Inst Mech Eng, Part C: J Mech Eng Sci* 226:367–384
27. Mastud S, Singh R, Joshi SS (2012) Analysis of fabrication of arrayed micro-rods on tungsten carbide using reverse micro-EDM. *Int J Manuf Technol Manage* 26(1–4):176–195
28. Mastud S, Singh R, Joshi SS (2010) Reverse micro EDM of tungsten carbide for machining microrod arrays. *International Workshop on Microfactories*, 24–28 Oct 2010, Daegoon, Korea
29. Mastud S, Singh R, Samuel J, Joshi SS (2011) Comparative analysis of the process mechanics in micro Electrical Discharge Machining (EDM) and Reverse micro-EDM. *ASME-International Manufacturing Science and Engineering Conference (MSEC)*, 13–17 June 2011, Corvallis, Oregon, USA
30. Mastud S, Garg M, Singh R, Samuel J, Joshi SS (2012) Experimental characterization of vibration assisted reverse micro Electrical Discharge Machining (EDM) for surface texturing. *ASME-International Manufacturing Science and Engineering Conference (MSEC)*, 4–8 June 2012, University of Notre Dame, South Bend, USA

31. Okada A, Uno Y, Onoda S, Habib S (2009) Computational fluid dynamics analysis of working fluid flow and debris movement in wire EDMed kerf. *CIRP Ann Manuf Technol* 58(1):209–212
32. Cetin S, Okada A, Uno Y (2004) Effect of debris distribution on wall concavity in deep-hole EDM. *JSME Int J, Ser C* 47(2):553–559
33. Mastud S, Kothari N, Singh R, Joshi SS (2014) Modeling debris motion in vibration assisted reverse micro Electrical Discharge Machining process (R-MEDM). *J Microelectromech Syst* 24(3):661–667
34. Rajurkar KP, Pandit S (1996) Formation and Ejection of EDM debris. *Trans ASME, J Eng Ind* 108:22–26

# Chapter 6

## Micro-EDM Performance Using Different Dielectrics



Ved Prakash, Alok Kumar Das and Somnath Chattopadhyay

**Abstract** EDM process became industrially viable after the discovery of the influence of different dielectric on machining performance. Dielectric fluid used by different micro-electrical discharge machining operation has huge impact on the machining performance like MRR and surface finish. Earlier only hydrocarbon oil was used as dielectric that affects health safety and environment. Through this paper, authors present a literature review on the application of dielectrics which are better substitute to hydrocarbon oil and how hydrocarbon oil can also be used more efficiently. Some of the work depicts that water-based dielectrics can also be used in die sink EDM instead of hydrocarbon oil. Apart from liquid dielectric, micro-EDM is also possible in gaseous media such as oxygen, air, helium, and argon. But gas-assisted micro-EDM needs further more research to make it industrially viable.

**Keywords** Micro-EDM · Dielectrics fluids · Powder additives · Deionized water Dry EDM

### 6.1 Introduction

Micro-EDM is an established modern method of manufacturing which has been widely used for the production of dies and molds. It is also a versatile technique for drilling micro-holes and micro-milling of 3D contours. In micro-EDM, material is removed by melting and vaporization through a series electrical sparks nearest

---

V. Prakash

Advance Manufacturing Group, CSIR-Central Mechanical Engineering Research Institute, Durgapur, West Bengal, India  
e-mail: [vedprakash.n@gmail.com](mailto:vedprakash.n@gmail.com)

A. K. Das (✉) · S. Chattopadhyay

Department of Mechanical Engineering, IIT (ISM), Dhanbad, India  
e-mail: [eralok@yahoo.co.in](mailto:eralok@yahoo.co.in)

S. Chattopadhyay

e-mail: [somuismu@gmail.com](mailto:somuismu@gmail.com)

© Springer Nature Singapore Pte Ltd. 2019

G. Kibria et al. (eds.), *Micro-electrical Discharge Machining Processes*, Materials Forming, Machining and Tribology, [https://doi.org/10.1007/978-981-13-3074-2\\_6](https://doi.org/10.1007/978-981-13-3074-2_6)

125

to tool and workpiece. The electrical spark erodes material from workpiece, and small amount of material is also removed from tool. The basis of EDM was first observed by Sir Robert Boyle in 1694, when he reported the occurrence of electrical discharge in a gap. Although, EDM became an established manufacturing process in 1940 by Boris and Natalie I. Lazarenko when they unearthed the deciding role of the dielectric, after which EDM has gained a pronounced growth [1].

Classification of EDM can also be done on the basis of different dielectrics for particular operation to be performed. Hydrocarbon oil is generally used for die sink EDM, while deionized water is suitable for wire-EDM, micro-EDM, and deep hole drilling of high aspect ratio. Hydrocarbon oil like kerosene has an adverse effect on health, and environment, which allowed researchers to use water based dielectric and gases in micro-EDM process.

## 6.2 Role of Dielectric

For a long period of time, the dielectric was thought to be necessary for EDM. The role of dielectric is defined to squeeze the generated bubble at discharge zone, cool the debris, and flush out the debris from the inter-electrode gap. It was traditionally rendered that the majority of the material is removed by the end of spark phenomena as during the course of discharge, the bubble pressure would prevent the expansion of the bubble by the inertia and viscosity of the surrounding dielectric liquid. However, recent research showed that material removal occurs during the discharge process instead of at the end of discharge [2]. This is validated by Hayakawa et al. [3] where a high-speed camera was used to investigate the single discharge for material removal. Yoshida and Kunieda et al. (1998) [4] found no difference in the formation and distribution of debris in liquids and air medium having pulse on time more than 90  $\mu$ s. As the arc column in liquid and air becomes equivalent to each other with increase in diameter of the bubble, which is proportional to the duration of discharge when pulse on time is greater than 90  $\mu$ s. Hence, it can be concluded that material removal can take place without liquid dielectric. Moreover, the liquid dielectric aid to cool and flush the debris particle rather than for material removal.

## 6.3 Water-Based Dielectric

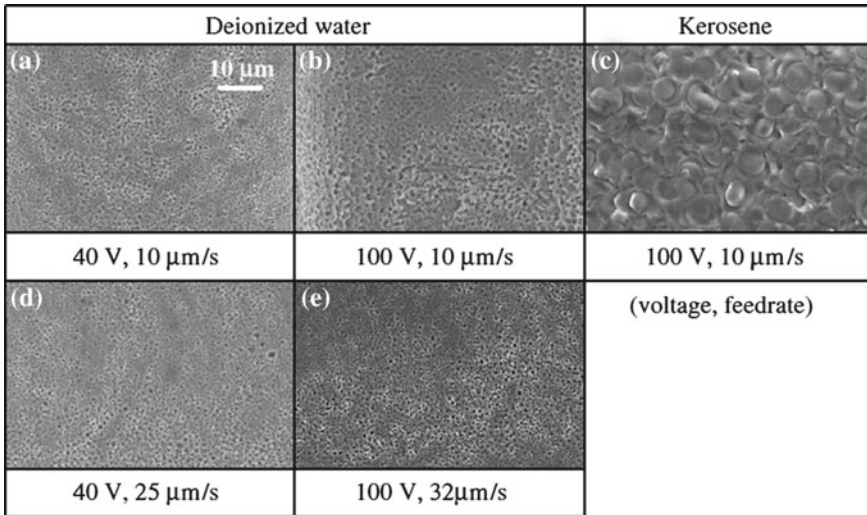
In die sink EDM, the MRR is lower when plain water is applied as dielectric as compared to hydrocarbon oil. However, tool wear is lower when plain water is used. In some specific process parameters such as brass electrode as tool with negative polarity and deionized water or tap water as dielectric, the MRR is higher [5]. The material removal phenomena in water-based dielectric have higher thermal stability, and high power input can also be obtained in some special conditions for higher MRR. The major difference between hydrocarbon-based micro-EDM and water-

based dielectric micro-EDM is attributed to eight times high specific boiling energy of water-based dielectric, and also the boiling occurs at lower temperature [6]. Some researchers also reported that the pulse duration has also a major contribution on surface roughness with different dielectric. Jilani et al. [7] observed that with pulse duration less than 500  $\mu\text{s}$ , the tap water produced better surface finish ranging from 40 to 60  $\mu\text{m}$  as compared to distilled water and hydrocarbon liquid. They also reported that for pulse duration larger than 500  $\mu\text{s}$ , there is large cumulating of gases near tool and workpiece interface which affects the breakdown of dielectric during discharge that causes reduction in MRR. For machining of Ti-6Al-4V in die sink EDM, distilled water is superior to hydrocarbon oil. TiC is formed on workpiece surface when hydrocarbon oil is used. Since, TiC has higher melting point, than Ti alloy which is to machined by electrical discharge process, the instinct force generated by spark with TiC is unstable in discharge zone that results in lower MRR. On the contrary,  $\text{TiO}_2$  is formed in case of distilled water having melting point lesser than TiC; hence, the instinct pressure of spark is found to be more stable than with TiC, and the material removal rate increases. Kibria et al. [8] also found the same result of machining Ti-6Al-4V with deionized water; they also used  $\text{B}_4\text{C}$  with deionized water and kerosene, where  $\text{B}_4\text{C}$  with deionized water shown an excellent increase in material removal rate because  $\text{B}_4\text{C}$ -mixed deionized water leads to uniform discharge over the workpiece which ultimately increases the efficiency of machining.

In case of micro-EDM, microelectrode as tool is used, and the electrode wear ratio when kerosene is used as dielectric is higher which decreases the machining accuracy. Hence, the use of deionized water can reduce the tool wear. In micro-EDM with kerosene as dielectric, the machining gap is smaller at lower voltage and also produces large amount of carbon which results in unstable machining. Same gap can be maintained by deionized water with high resistivity. Since deionized water does not produce carbon, discharge is stable and machining becomes faster. Kim et al. performed micro-EDM of stainless steel (304 SS) with WC electrode using kerosene and deionized water as dielectric fluid. The maximum tool feed rate using kerosene was 10  $\mu\text{m/s}$  without electrical short circuit between tool electrode and workpiece, whereas in case of deionized water, the maximum tool feed rate can go up to three times more than using kerosene as dielectric. The tool wear ratio is also reduced by 96% as compared to hydrocarbon oil. The reason for higher tool feed rate and lower tool wear was attributed to no carbon generation with deionized water and electrochemical dissolution. Figure 6.1 shows the comparison of surface generation by kerosene and deionized water as dielectric at different voltage and feed rate [9].

## 6.4 Micro-EDM with Water-Based Organic Compounds

Performance of deionized water can be further improved by the addition of organic compounds of larger molecular weight. Compounds such as ethylene glycol 400, polyethylene glycol 600, dextrose raise the viscosity of working fluid. These compounds are decomposed by spark, which produces gases and generates higher pres-



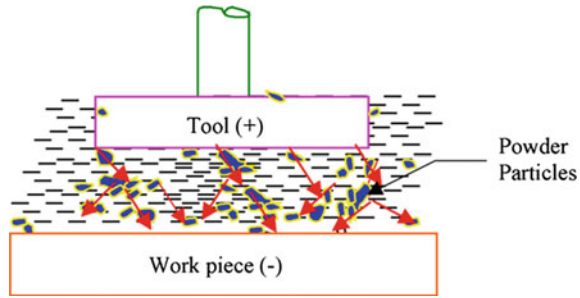
**Fig. 6.1** Comparison of surface generation by kerosene and deionized water [9]

sure than those of produced by disintegration of pure water. Generation of higher pressure by decomposition of organic compounds increases the dislodging of molten metal and debris from craters which subsequently increases the MRR. Based on this concept, Komij et al. used 87% glycerin as dielectric and machined 56 NiCrMoV 7 with graphite electrode which increased the MRR up to 40% and reduces the tool wear by 90% when compared with hydrocarbon oil. An increase in the concentration of glycerin up to 100% can be further used for machining larger parts like forging dies [10].

## 6.5 Powder-Mixed Micro-EDM

Powder-mixed micro-EDM is quite different from conventional micro-EDM. In this process, the dielectric is mixed with powder at nano–micro scale. At suitable voltage with powder particle, the inter-electrode gap is increased and the powder mixed in liquid dielectric energizes and arranges themselves in zigzag manner, as shown in Fig. 6.2. The powder particles get charged in the presence of electric field and accelerated by electric field. The powder particles are arranged under discharge zone and gather in clusters. This zigzag formation of powder particles helps in bridge formation between tool and workpiece which leads to the early explosion. Faster sparking and increased gap cause higher MRR and easy removal of debris from gap between tool and workpiece. Powder-mixed micro-EDM also reduces the tool wear ratio [11].

**Fig. 6.2** Principle of powder-mixed EDM [11]



Researchers around the world are using different conductive, semi-conductive, and non-conductive powders to examine the performance of micro-EDM on MRR, surface finish, and tool wear. Mohri et al. [12] observed finishing operation with dielectric containing silicon powder which provided highly reflective surface over  $500\text{ cm}^2$  area. Rozenek et al. [13] in Japan found positive result of conductive and non-conductive powder-mixed micro-EDM. The wider dispersion of discharge zone and increased gap distance tool and electrode enhance the MRR and flushing of debris. They found the gap distances increases up to three times as that of conventional micro-EDM process. Also at larger gap, the stray capacitance is reduced which affect the surface quality. Chow et al. [14] performed powder-mixed micro-EDM (PMMEDM) with SiC and Al powder using Ti-6Al-4V as workpiece and copper as tool. They reported that Al and SiC powder increased the MRR. Both Al and SiC extended the inter-electrode gap. The added powder disperses the discharge energy to obtain better surface finish. Chow and Yang et al. (2008) [15] proposed that the use of powder like SiC helps in bridging the gap which creates two separate spark pulse from a single pulse duration that also disseminates discharge energy in many folds. Micro-craters are then formed by spark, and also micro-nano size debris are generated, the small size debris are flushed out efficiently and ultimately increases the MRR. The flushing of debris from tool and workpiece gap reduces the adhesion of debris which improves surface roughness. Since in conventional micro-EDM at low peak current and narrow gap, abnormal discharges like arcing and short circuit occur. Additionally, the short distance between tool and workpiece creates stray capacitance which increases the tool and workpiece area and disturbs the discharge phenomena. The capacitive effect results in more deeper and irregular craters that make the appearance of EDMed surface dull. Figures 6.3 and 6.4 shows the influence of SiC powder added over pure water on material removal rate and tool wear.

To obtain mirror-like finish over larger area, Pecas et al. [16] used silicon in dielectric for areas below  $32\text{ cm}^2$ , but for area up to  $64\text{ cm}^2$ , a high reflective surface was also generated. The use of silicon reduces the crater diameter and also reduced the depth of crater. Figure 6.5 shows surface texture obtained with and without silicon powder. The mirror finish surface obtained by powder addition in dielectric is also validated by Yeo et al. [17] where electrical discharge machining was conducted with powder-mixed dielectric and without powder-mixed dielectric at low discharge

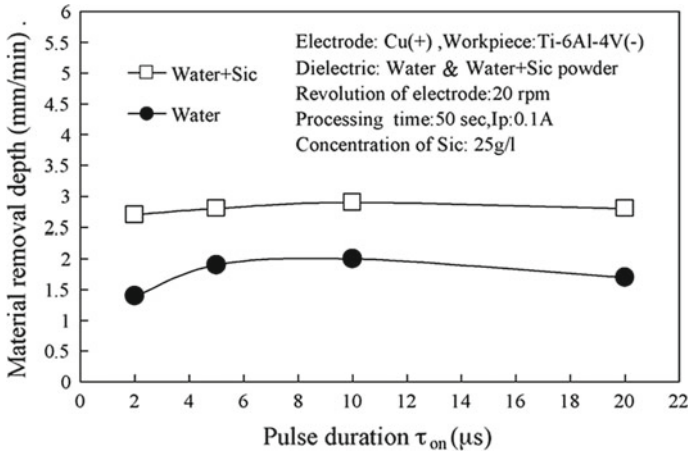


Fig. 6.3 Effect of water and water-added SiC powder on MRR [15]

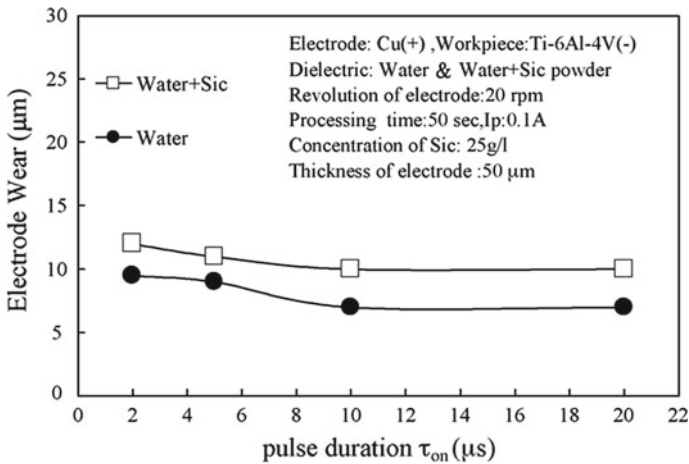
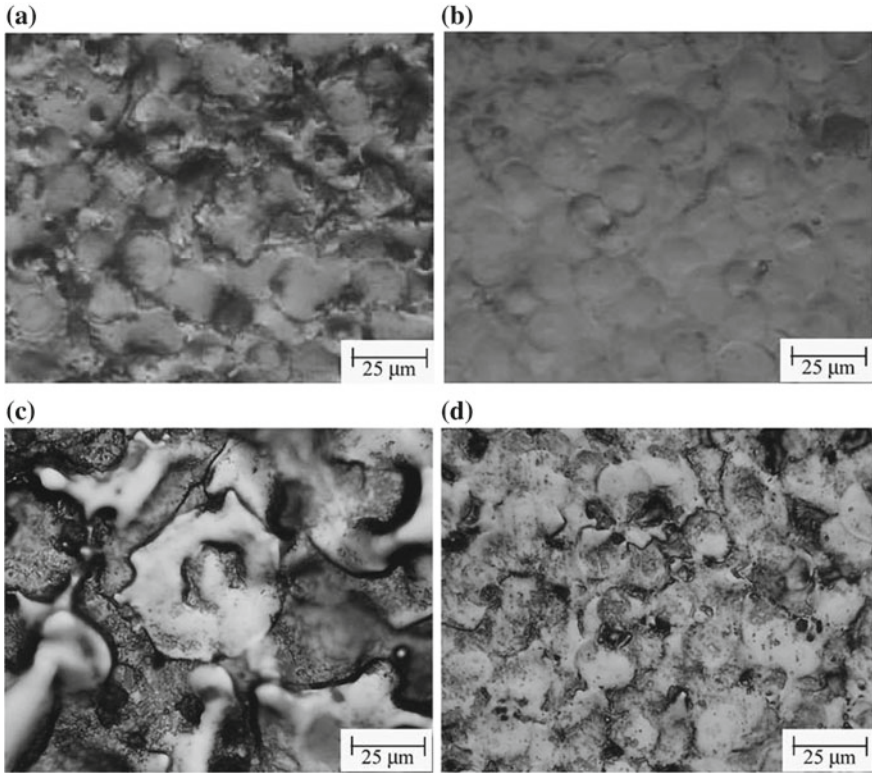


Fig. 6.4 Influence of water and water-added SiC powder on tool wear [15]

energies of 2.5, 5, and 25  $\mu$ J. Craters with smaller diameters and more consistent circular shapes were produced. The presence of powders in dielectrics also lowers the quantity of charge flowing between tool and workpiece and slows down the rate at which these charge flow.

As it is clear from these works that added powder in dielectric increases MRR and improves surface finish. Ultrasonic vibration along with the use of powder in dielectric increases MRR. The ultrasonic vibration provides proper dispersion of powder to the workpiece and prevents the additive from being sedimented at the bottom. Also the ultrasonic vibration of the dielectric minimizes adherence caused by debris that gets attached to the workpiece.





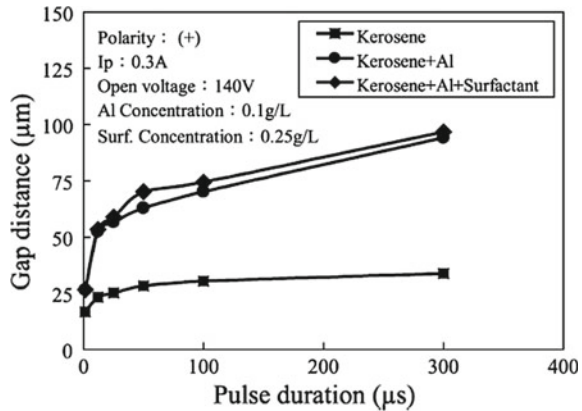
**Fig. 6.5** Microstructures of workpiece area of  $32 \text{ cm}^2$  **a** with liquid dielectric, **b** with liquid dielectric-mixed silicon powder, and for a workpiece area of  $64 \text{ cm}^2$ , **c** with liquid dielectric, **d** with liquid dielectric-mixed silicon powder [16]

Effect of powder and surfactant-added dielectric in micro-EDM is also reported by some researchers, as the electrostatic force among fine conductive powders leads to agglomerate the powders. A surfactant can separate the powders in dielectric and mix it homogeneously. As a result, surface finish obtained can be better than without the surfactant. Wu et al. [18] employed Al powder in Polyoxyethylene-20-sorbitan monooleate surfactant. Figure 6.6 shows Al powder with and without surfactant. Surfactant molecules serve as steric barriers, which separate the agglomerated powder and disseminate them homogeneously in dielectric which improves surface finish.

## 6.6 Gas-Assisted Micro-EDM

The use of gas as dielectric in micro-EDM is unquestioned, as it is known that dielectric performs restriction of discharge to obtain larger energy density for higher

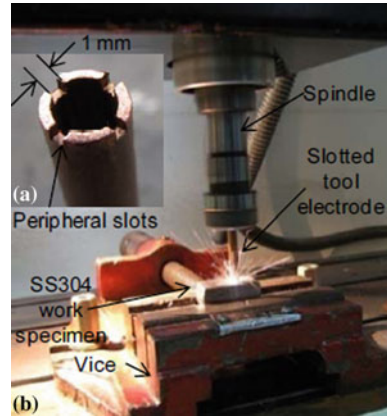
**Fig. 6.6** Effect of different dielectric on surface roughness [18]



MRR and improved surface finish. A paper published by NASA in 1985 reported that EDM process is also possible in dry medium of argon or helium gas. Other gases that can perform dry EDM include air and oxygen. In fact, Kunieda et al. (1997) proposed that performance of EDM with air and oxygen is better than hydrocarbon oil and water-based dielectric in some special conditions. They found that higher material removal rate can be obtained using tubular electrode with straight polarity which has very thin wall, i.e., wall thickness less than 0.3 mm. The major benefit of micro-EDM using gases is very low tool electrode wear (almost zero). The flow of gas at high velocity results in higher MRR due to oxidation [19]. In conventional micro-EDM, kerosene oil causes carbon deposition over the machined surface decomposed from hydrocarbon dielectric. Whereas in case dielectrics which are water based, formation of micro-cracks occurs, also there is electrolysis due to conductivity of water and rusting of tool and workpiece. Dry micro-EDM technique has several advantages over liquid dielectric-based micro-EDM such as formation of very thin recast layer. The low dielectric strength of gases leads to easy formation of plasma. Due to less viscosity of gases and lower heat concentration debris are removed from tool and workpiece gap more efficiently [20]. In order to increase the MRR in dry micro-EDM, many steps are being taken; Kammute et al. applied piezoelectric actuators in dry EDM that increases MRR with spindle servo frequency. Joshi et al. used pulsating magnetic field instead of permanent magnetic field in dry EDM which increased the MRR by 130% [21]. Application of ultrasonic vibrations in gas-assisted micro-EDM also increases the MRR than in air. It was first experimented by Zhang et al. The investigation reported that higher the value of open voltage, pulse on time, amplitude of vibration, the MRR will be more. They also advocated oxygen for higher MRR than atmospheric air [22].

Specially designed electrodes can also improve the performance of micro-EDM in gas medium. Certain modification in geometry of tool would enhance the performance by helping in easy escape of debris that ultimately increases the MRR. Puthumana et al. [23] carried out dry EDM with electrodes which were slotted at the peripheral and found that application of electrode with slotted peripheral helps

**Fig. 6.7** Dry EDM experimental setup using slotted tool [23]



in flushing the debris even much efficiently than without slotting. They used the tool with four peripheral slots which apart from increasing MRR also increased the depth of crater and reduced TWR. This effect is attributed to efficient flushing of debris. They also found that increasing the slots by more than four causes spattering of plasma channel by gas. Figure 6.7 shows dry EDM experimental setup with peripheral slotted tool.

There are also some findings on near-dry EDM where at low discharge energy, the machining stability is quite good and also the surface generated by micro-EDM is better than liquid dielectric micro-EDM at low discharge energy. For better surface finish, near-dry EDM is found to be very beneficial at same energy level than dry EDM and liquid dielectric-based EDM. The hypothesis behind better surface finish is that liquid particles get dispersed in the gas medium in same manner as powder particles in PMD EDM. In this case, the stray capacitance between tool and electrode is also reduced. Tao et al. [24, 25] compared dry EDM and near-dry EDM, where EDM with oxygen gave higher MRR and exothermal oxidation of workpiece. In dry EDM, high discharge current and lower pulse interval were found most significant for higher MRR. In case near-dry EDM fine surface finish was obtained, since the liquid phase in near-dry EDM tends to increase the electric field which ultimately increases the discharge gap and makes the spark stable at low discharge energy. It was demonstrated that electrolysis can be prevented by nitrogen and helium gas and better surface finish is achieved in near-dry EDM. They concluded that by decreasing discharge current, pulse-on time and increasing pulse interval were the key factor for better surface finish.

## 6.7 Micro-EDM with Less Viscous Dielectric Oils

Low viscosity oils which are specially formulated can also be used to improve the performance of micro-EDM. Using high-pressure flushing equipment, the fluid is allowed to flow, and time required to fill the dielectric tank is calculated. The dielectric possessing high viscosity takes more time than dielectric having less viscosity to fill the dielectric tank. This way, the selection of low viscosity dielectric improves micro-EDM efficiency. The electrodes of smaller cross-sectional area require a dielectric of lower kinematic viscosity. Less viscous dielectric provides efficient flushing of debris and also cools the spark area of the electrode. Higher material removal rate can be achieved with low viscosity dielectrics when tools are smaller, fragile, and highly vulnerable hydraulic damage of tools. As the pins used in die sink EDM experience dynamic effect of liquids by vertical-orbital or simply vertical movement in die sink EDM. The tool must displace a considerable amount of dielectric during its movement toward workpiece and should also withstand vacuum pressure during its movement away from workpiece. The less viscous dielectric decreases the hydraulic forces; hence, it applies less outside pressure and effect on the tool features [26].

## 6.8 Summary

It is evident that hydrocarbon liquid dielectrics are better than deionized/distilled in die sink EDM, but application of water-based dielectrics also results in higher MRR in some special situation. Addition of organic compounds to deionized water also gives better results in roughing and finishing operation. It is found that some of the commercial water-based dielectrics provide similar or higher than that of hydrocarbon dielectrics. The use of powder-mixed dielectrics is an another evolution in micro-EDM; powder-mixed dielectric instead of pure dielectric such as hydrocarbon oil and deionized water gives higher MRR and good surface finish. Some results show that pure dielectric can be replaced by powder-mixed dielectric for enhanced performance of micro-EDM. The performance of micro-EDM improves with less viscous dielectrics. The machining cycle time is affected much by less viscous dielectrics than hydrocarbon oils having greater viscosity. Higher material removal rate can also be achieved by gas-assisted micro-EDM in specific machining condition; however, a lot of work is needed to be done to make gas-assisted micro-EDM industrially viable.

## References

1. Leão FN, Pashby IR (2004) A review on the use of environmentally-friendly dielectric fluids in electrical discharge machining. *J Mater Process Technol* 149(1–3):341–346
2. Zhang Y, Liu Y, Shen Y, Ji R, Li Z, Zheng C (2014) Investigation on the influence of the dielectrics on the material removal characteristics of EDM. *J Mater Process Technol* 214(5):1052–1061

3. Hayakawa S, Sasaki Y, Itoigawa F, Nakamura T (2013) Relationship between occurrence of material removal and bubble expansion in electrical discharge machining. In: Proceedings of the 17th CIRP Conference on Electro Physical and Chemical Machining (ISEM), pp 174–179
4. Yoshida M, Kunieda M (1996) Study on the distribution of scattered debris generated by a single pulse discharge in EDM process. *J Jpn Soc Electr Mach Eng* 30(64):27–36
5. Erden AP, Temel D (1982) Investigation on the use of water as a dielectric liquid in EDM. In: Proceedings of the twenty-second international machine tool design and research conference, Palgrave, London, pp 437–440
6. Abbas NM, Solomon DG, Bahari MF (2007) A review on current research trends in electrical discharge machining (EDM). *Int J Mach Tools Manuf* 47(7–8):1214–1228
7. Jilani ST, Pandey PC (1984) Experimental investigations into the performance of water as dielectric in EDM. *Int J Mach Tool Des Res* 24(1):31–43
8. Kibria G, Sarkar BR, Pradhan BB, Bhattacharyya B (2010) Comparative study of different dielectrics for micro-EDM performance during microhole machining of Ti-6Al-4V alloy. *Int J Adv Manuf Technol* 48(5–8):557–570
9. Kim BH, Chu CN (2007) Micro electrical discharge milling using deionised water as a dielectric fluid. *J Micromech Microeng* 17(5):867
10. Koenig W, Joerres L (1987) Aqueous solutions of organic compounds as dielectrics for EDM sinking. *CIRP Ann Manuf Technol* 36(1):105–109
11. Singh S, Bhardwaj A (2011) Review to EDM by using water and powder-mixed dielectric fluid. *J Miner Mater Charact Eng* 10(2):199–230
12. Mohri N, Saito N, Narumiya H, Kawatsu Y, Ootake H, Tsunekawa Y, Takawashi T, Kobayashi K (1987) Finishing on the large area of work surface by EDM. *J Jpn Soc Precis Eng* 53(1):124–130
13. Rozenek M, Kozak J, Dabrowski L (2002) Electrical discharge machining in dielectric-powder media. *Int J Manuf Sci Technol* 4(1):54–60
14. Chow HM, Yan BH, Huang FY, Hung JC (2000) Study of added powder in kerosene for the micro-slit machining of titanium alloy using electro-discharge machining. *J Mater Process Technol* 101(1–3):95–103
15. Chow HM, Yang LD, Lin CT, Chen YF (2008) The use of SiC powder in water as dielectric for micro-slit EDM machining. *J Mater Process Technol* 195(1–3):160–170
16. Pecas P, Henriques E (2003) Influence of silicon powder-mixed dielectric on conventional electrical discharge machining. *Int J Mach Tools Manuf* 43(14):1465–1471
17. Yeo SH, Tan PC, Kurnia W (2007) Effects of powder additives suspended in dielectric on crater characteristics for micro electrical discharge machining. *J Micromech Microeng* 17:N91
18. Wu KL, Yan BH, Huang FY, Chen SC (2005) Improvement of surface finish on SKD steel using electro-discharge machining with aluminum and surfactant added dielectric. *Int J Mach Tools Manuf* 45(10):1195–1201
19. Kunieda M, Yoshida M (1997) Electrical discharge machining in gas. *CIRP Ann* 46(1):143–146
20. Govindan P, Joshi SS (2010) Experimental characterization of material removal in dry electrical discharge drilling. *Int J Mach Tools Manuf* 50(5):431–443
21. Liqing L, Yingjie S (2013) Study of dry EDM with oxygen-mixed and cryogenic cooling approaches. *Procedia CIRP* 6:344–350
22. Zhang QH, Zhang JH, Deng JX, Qin Y, Niu ZW (2002) Ultrasonic vibration electrical discharge machining in gas. *J Mater Process Technol* 129(1–3):135–138
23. Puthumana G, Joshi SS (2011) Investigations into performance of dry EDM using slotted electrodes. *Int J Precis Eng Manuf* 12(6):957–963
24. Tao J, Shih AJ, Ni J (2008) Experimental study of the dry and near-dry electrical discharge milling processes. *J Manuf Sci Eng* 130(1):011002
25. Tao J, Shih AJ, Ni J (2008) Near-dry EDM milling of mirror-like surface finish. *Int J Electr Mach* 13(1):29–33
26. Chakraborty S, Dey V, Ghosh SK (2015) A review on the use of dielectric fluids and their effects in electrical discharge machining characteristics. *Precis Eng* 40:1–6

# Chapter 7

## Powder-Mixed Microelectric Discharge Machining



**Basil Kuriachen**

**Abstract** Microelectric discharge machining ( $\mu$ EDM) is introduced to the manufacturing industry to produce microfeatures and microholes on difficult to machining materials such as titanium- and nickel-based alloys and other heat-resistant electrically conductive metals and alloys. Even though  $\mu$ EDM can be used to machine any electrically conductive materials, there are many problems to be addressed in order to make it as an accurate and reliable process. Some of the problems associated are low material removal rate, tool wear rate, high surface roughness, and poor dimensional accuracy. This chapter presents powder-mixed microelectric discharge machining as one of the viable alternatives to overcome some of the inherent difficulties associated with microelectric discharge machining process. Suspension of electrically conductive and semiconductive powders in the dielectric can strongly influence the process in a desirable manner. Moreover, the added powder particle gets re-solidified along with the tool material on the machined surface and opens a new possibility to modify the machined surface by selecting the appropriate alloying elements in the required proposition. This approach needs to be thoroughly addressed to explore as ‘ $\mu$ EDM alloying’.

**Keywords** Powder-mixed  $\mu$ EDM ·  $\mu$ EDM alloying · Material removal rate  
Surface modification · Surface roughness · Inter-electrode gap · Tool wear rate

### 7.1 Introduction

In the last few decades, materials with unique mechanical and metallurgical properties like titanium, nickel, cobalt, and other heat-resistant superalloys as well as MMCs were developed to meet the extreme applications in aerospace and various other industries. In addition, miniaturization is no more a fashion; rather, it is the

---

B. Kuriachen (✉)

Mechanical Engineering Department, National Institute of Technology Mizoram, Aizawl 796012, Mizoram, India

e-mail: [basilkuriachen@gmail.com](mailto:basilkuriachen@gmail.com)

© Springer Nature Singapore Pte Ltd. 2019

G. Kibria et al. (eds.), *Micro-electrical Discharge Machining Processes*, Materials Forming, Machining and Tribology, [https://doi.org/10.1007/978-981-13-3074-2\\_7](https://doi.org/10.1007/978-981-13-3074-2_7)

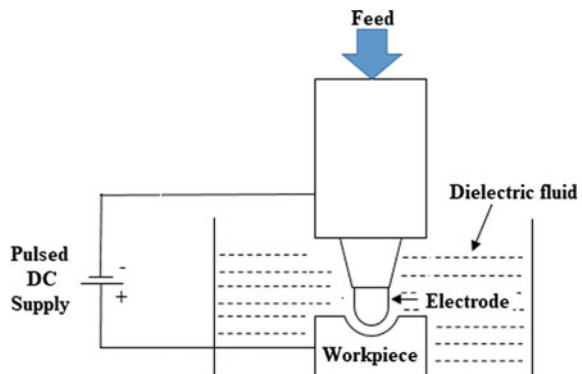
137

need of the hour due to less material and space requirements. Micromachining is a value-adding element for many capacities where size reduction harvests economic and technical aids. In order to keep alongside with sophisticated microparts design on difficult to machine materials, microelectric discharge machining ( $\mu$ EDM) is proved to be an effective and viable alternative to produce complex three-dimensional components. However, the performance of  $\mu$ EDM in terms of machining speed, MRR, and surface finish needs to be improved to meet the productivity challenges. Therefore, researchers have suggested that suspension of micro-/nanoparticles in the dielectric medium during microelectric discharge machining has several advantageous in improving the process capabilities and to produce sound machined surface. This chapter presents the working principle, mechanism of material removal, important electrical and non-electrical parameters, effect of powder on various machining responses as well as on machined surfaces.

## 7.2 Working Principle

The material removal mechanism of electric discharge machining (EDM) and  $\mu$ EDM is similar except in the discharge energy and the size of the features produced. Generally, EDM machining of microfeatures of size in the range of 1–1000  $\mu$ m and discharge energy less than 1000  $\mu$ J is considered as microelectric discharge machining ( $\mu$ EDM). The basic scheme of microelectric discharge machining can be illustrated as shown in Fig. 7.1. The electrodes are connected to a suitable DC electric power and separated by an inter-electrode gap (IEG) based on servo voltage and maintained throughout the machining. The workpiece and the tool are either submerged in dielectric or a forced circulation of dielectric using an external pumping mechanism is used. Generally, deionized water, kerosene, or paraffin oils are used as the dielectric fluid. The continuous circulation of dielectric helps to improve the flushing efficiency of the dielectric fluid. Hence, it is preferred. Once, a suitable electric supply is established, the dielectric breakdown takes place and sparks are generated.

**Fig. 7.1** Basic scheme of electric discharge machining



The heat energy produced as a result of electric sparks liquefy and evaporate a minor percentage of electrodes (both tool and workpiece). Hence, the working principle of  $\mu$ EDM/EDM can be named as localized melting and vaporization.

Explanation of a typical microelectric spark is a difficult task as it exists only for fraction of micro- or nanoseconds as well as size reduction. Moreover, application of hydrodynamics, thermodynamics, and other several theories of science and engineering made the process become more versatile. Hence, it is not an easy task to enlighten the mechanism of electric spark in  $\mu$ EDM. Many theories have been proposed by researchers and available in the literature and divided into electrothermal and electromechnical models. In the first theory, the removal of material takes place due to the localized melting and vaporization as results of heat transfer from the superheated plasma channel established between the tool and workpiece, whereas, in the second model, it is considered yielding as the main mechanism of erosion. It is explained that the workpiece is subjected to an electrostatic force which instigates stress, and localized area higher than the yield strength is dislodged. From the two theories, electrothermal theory is broadly accepted due to the fact that it can explain many of the practical phenomena associated with the EDM/ $\mu$ EDM/PM $\mu$ EDM material removal. Hence, electrothermal theory for material removal is explained in detail. In a typical EDM spark as shown in Fig. 7.2, electrons are ejected from the cathode and gain momentum towards anode under the influence of electric potential. These electrons get bombarded with dielectric molecules, neutral atoms and split the molecules into positively charged ions and negatively charged electrons; thereby, an avalanche of electrons and ions is formed. All the electrons formed in the inter-electrode gap (IEG) get accelerated towards the anode (workpiece), and ions get accelerated to the cathode (tool electrode); thereby, a plasma channel is established between the tool and workpiece. This results in the breakdown of IEG. As a result of the high temperature and pressure developed on the plasma channel, gas bubbles are produced. The pressure within these bubbles is reported as 6–14 bar. It accelerates the superheating. The difference in pressure inside and outside of the bubbles results in cavitation during the breakdown, and molten metal gets expelled. Also, the dielectric surges back into the plasma. Sudden elimination of the plasma and some molten metal remain as re-solidified layer on the workpiece.

The application of powder particle into the dielectric medium is one of the developments to improve the processes capabilities of  $\mu$ EDM. Even though the working principle is similar to  $\mu$ EDM, it has a different mechanism of sparking phenomena. Once the powder particle mixed with the dielectric, the IEG pollution with powder particle in the dielectric takes place. The conductive or semiconductive particle in IEG gets energized during the application of electric potential as shown in Fig. 7.3. It acts as a conductive column between the tool and electrode and workpiece. This improves the dielectric strength of the dielectric fluid. This formation of conductive column of powder promotes the discharge of capacitor before attaining the full charge and the required voltage. This enhances the early discharge and reduces the discharge energy per sparks. Moreover, the energy gets distributed among the workpiece, tool, and dielectric more effectively, thereby produces small diameter crater with more consistency throughout the machined surface. This is not only improving the flushing



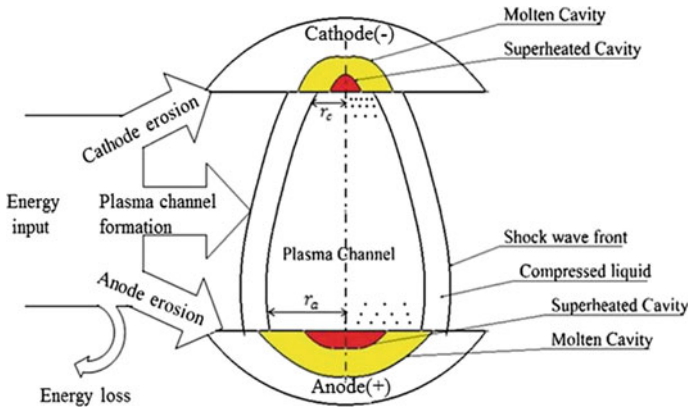
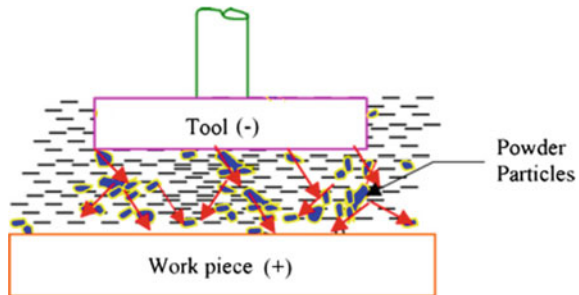


Fig. 7.2 Schematic diagram of EDM spark

Fig. 7.3 Principle of PM $\mu$ EDM [1]



efficiency but also surface finish [1–4]. In addition, the micro-/nanopowder particles in the IEG also get melted along with the tool and workpiece as well as get solidify on the machined surface along with the electrode material. The melting and re-solidification also depend on the discharge energy which mainly depends on the pulse generation used in the circuit.

### 7.3 Pulse Generator

RC circuit as shown in Fig. 7.4 was used in EDM equipment in the early stages of its invention. This was replaced by power transistors as shown in Fig. 7.5 which is generally used in conventional EDM machines due to its capabilities to generate high pulse duration [5]. Even though RC pulse generators are used in  $\mu$ EDM due to the possibilities to obtain significantly short pulse duration with consistent discharge energies [5], Jahan et al. [6] have studied and compared the effects of relaxation-type and transistor-type pulse generators in micro-ED machining of tungsten carbide and concluded that relaxation type is more suitable for micromachining applications

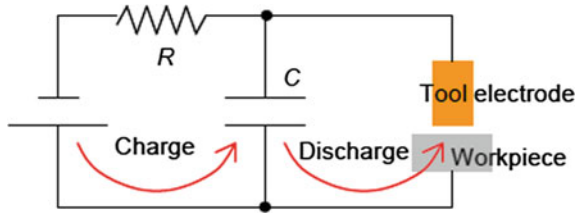


Fig. 7.4 Relaxation-type pulse generator [5]

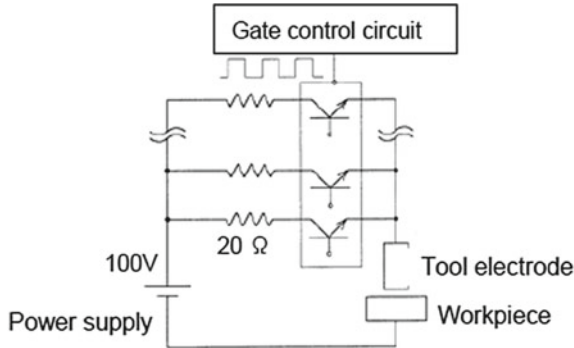


Fig. 7.5 Transistor-type pulse generator [5]

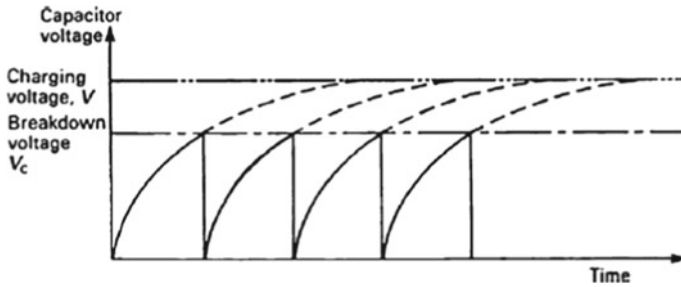


Fig. 7.6 Variation of capacitor voltage with time in RC circuit [7]

because of its capability to reduce the pulse energy per sparks. In RC type at low resistance, a primary release of energy will follow, but if it is large, the capacitor will accomplish an upper charge before the discharge occurs [7]. Figure 7.6 shows the variation of instantaneous voltage in the inter-electrode gap with time in RC circuit. As observed from Fig. 7.4, the capacitor gets charged from the DC source (V) through the resistance (R). The instantaneous voltage across the IEG follows the relation

$$V_i = V \left( 1 - e^{-\frac{t}{RC}} \right) \tag{7.1}$$

where ' $t$ ' is the time at the instant ' $V$ ' is applied.  $R$  and  $C$  are the resistance and capacitance value of the discharge circuit. As shown in Fig. 7.6, the ' $V_i$ ' tries to approach to ' $V$ ' if allowed. However, the inter-electrode gap (through servo control mechanism), tool electrode, and dielectric medium, etc., are adjusted in such a way to discharge the capacitor, while the ' $V_i$ ' reaches the discharge voltage ' $V_c$ '. At this instance, the complete discharge of the capacitor takes place and the energy released into the inter-electrode gap which is equal to

$$E_d = \frac{1}{2} C V_d^2 \quad (7.2)$$

The major portion of the machining time is used to charge the capacitor after each discharge, whereas the discharge time ' $t_d$ ' is approximately (10%) of the charging time ' $t_c$ '. Hence, the heat flux incident on the surface of the workpiece can be calculated as follows

$$Q_i = \frac{E_d}{t_d} \quad (7.3)$$

where  $t_d$  is the discharge time in which the actual spark takes place. The total discharged heat is scattered between the workpiece, tool, and dielectric. Majority of the heat energy is carried away by the dielectric fluid. Hence, only a small portion of heat is available on the workpiece for the removal of material. This is represented by ' $\eta$ '. Therefore, the available heat flux for removal of material can be calculated as follows

$$Q_a = \eta Q \quad (7.4)$$

where  $Q_a$  is the heat flux incident on the anode. The heat flux density can be calculated as

$$q = \frac{Q_a}{\pi r_s^2} \quad (7.5)$$

where  $r_s$  is the spark radius. The heat flux distribution for the removal of material from  $\mu$ EDM can be written by adopting Gaussian distribution of heat flux as follows

$$q_r = 3.157 q e^{-3\left(\frac{r}{r_s}\right)^2} \quad (7.6)$$

The influence of suspended particle in the dielectric can be incorporated in Eq. 7.6 by introducing a new parameter ' $K_n$ '.

$$q_r = K_n 3.157 \frac{\eta Q}{\pi r_s^2} e^{-3\left(\frac{r}{r_s}\right)^2} \quad (7.7)$$

where ‘ $K_n$ ’ depends on the size, type, and % of particles in the dielectric. For graphite powder of 30  $\mu\text{m}$  average diameter, frequency constant ‘ $K_n$ ’ is considered as 2.4. Moreover, the electric discharge mechanism in powder-mixed  $\mu\text{EDM}$  depends on various process parameters, and it can be broadly classified into electrical and non-electrical parameters.

### 7.4 PM $\mu\text{EDM}$ Process Parameters

The independent variables of PM $\mu\text{EDM}$  can be classified into two, i.e. electrical and non-electrical parameters as depicted in Fig. 7.7.

#### 7.4.1 Electrical Parameters

Important variables under this category are voltage, capacitance, current, pulse off time, pulse on time, polarity, and pulse waveform. Discharge voltage is depended on spark gap and breakdown strength of the working fluid. The open gap voltage increases until the discharge (ionization path between electrodes) occurs through the dielectric. Once the current starts to flow through the inter-electrode gap (discharge starts), voltage drops and stabilizes at the working gap. This voltage regulates the IEG between the leading edges of the electrode and workpiece. Therefore, an upper voltage setting increases the inter-electrode gap, which in turn progresses the flushing settings as well as supports to become stable the machining [8, 9]. Increase in open-circuit voltage increases the MRR, electrode wear ratio (RWR) and SR due to the increase in electric field strength. Jahan et al. [10] have been experimentally

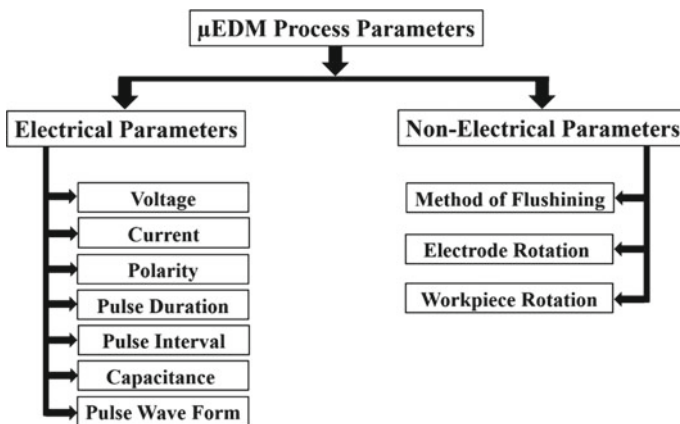


Fig. 7.7  $\mu\text{EDM}$  parameters

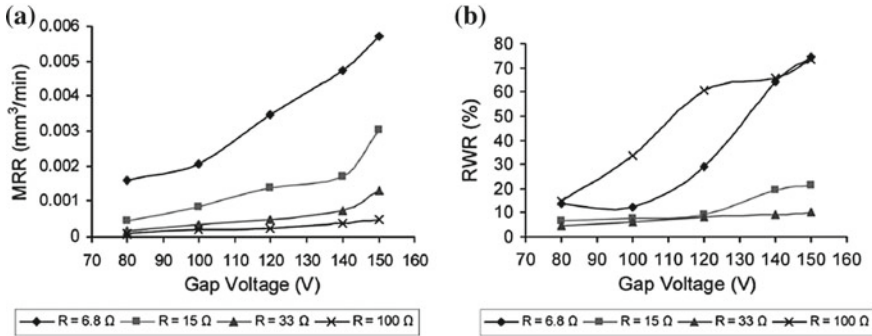


Fig. 7.8 Variation of a MRR, b RWR with respect to voltage [11]

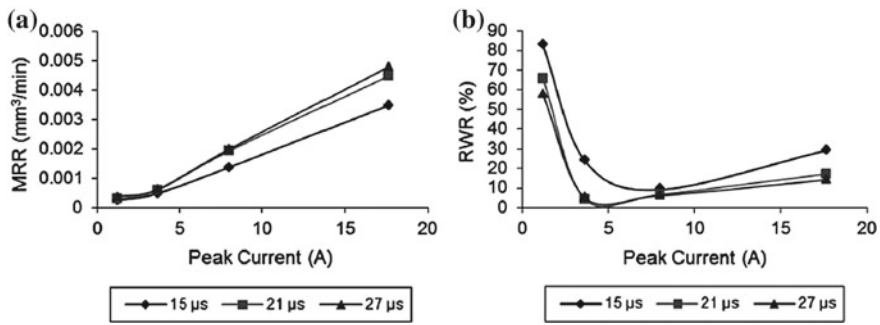
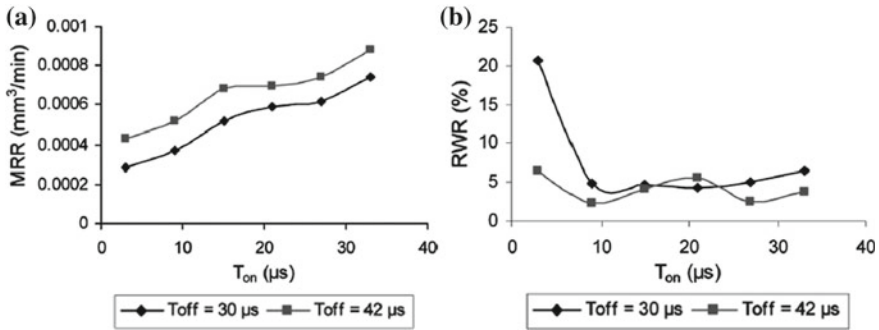


Fig. 7.9 Variation of current on a material removal rate, b RWR during μEDM of tungsten carbide [11]

investigated the influence of gap voltage during the micro-ED drilling of cemented carbides using tungsten electrodes, and effect of voltage on EWR and MRR at various resistance is shown in Fig. 7.8.

Another significant electrical parameter is current in microelectrical discharge machining. It is the quantity of current used during machining and measured in amperage. For each pulse, it surges until it reaches the required level, which is expressed as the peak current. The all-out amount of the current is decided by the surface area of the cut. During roughing operation, upper value of current is used which gives better MRR. The setting of peak current in EDM is important because the machined cavity is exact replica of the tool. Graphite and other improved tool materials can work on higher peak current without much damage [12]. The variation of material removal rate and RWR is depicted in Fig. 7.9.

Pulse duration is also known as pulse on time. It is the time in which the energy is applied and measured in microseconds. The duration of the pulse and the frequency of pulse are important as the actual work is done during the pulse on time. With longer pulse, the energy applied is high; the amount of material gets melted also will be increased. The size of the crater formed is broader and deeper in the short pulse



**Fig. 7.10** Variation of **a** material removal rate, **b** RWR of tungsten carbide with respect to discharge time [11]

on time. This in turn increases the surface roughness, and prolonged sparking time allows more energy to absorb into the electrodes, thereby results in increased recast and HAZ zone [7, 10]. Figure 7.10 illustrates the variation of sparking time with respect to MRR and RWR.

In  $RC$  circuit, the pulse energy is mainly depending on the discharge voltage and capacitance. The maximum energy per pulse is obtained by Eq. 7.2. The effect of voltage is discussed in the previous sections. In  $RC$  circuit, the capacitance decides the pulse on time and its frequency of discharging [6]. Jahan et al. [6] investigated the effect of capacitance on the performance of  $\mu$ EDM and found that with an increase in capacitance, the MRR increased due to the increase in the discharge energy. As the capacitance increase, the discharge current also increases which results in deep crater.

Polarity of the workpiece can be fixed as either positive or negative. The plasma channel created between the workpiece and electrode is composed of both electrons and ions. The momentum of electrons is higher than ions due to light in weight compared to ions. The electrons possess quicker action in the plasma channel and convert the kinetic energy on the anode, and maximum material removal took place, whereas ions move relatively slower than electrons and converts less energy in the cathode; thereby, less material removal takes place in cathode. However, while running longer discharges, the early electron process predominance charges to positron process, resulting in cathode wear. So, polarity of the electrodes is generally determined by experiments and is a matter of tool material, work material, current density, and pulse length combinations [7]. The wrong selection of polarity can have significant implications on speed, wear, and stability of machining [13, 14]. Some of the general polarity guide lines are listed in Table 7.1. Due to the faster-accelerating electron in the plasma channel, the material removal volume in single discharge is higher at the anode compared to the volume at the cathode. This effect is known as polarity effect [14]. Figure 7.11 shows the comparison of electrode wear in boron-doped CVD-diamond (B-CVD) as electrode at positive and negative polarity. B-CVD

**Table 7.1** General polarity guidelines [13]

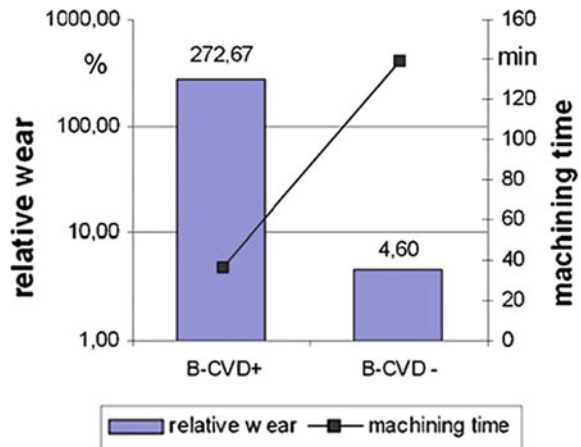
Tool	Workpiece	Remarks
Graphite (+)	Steel (-)	General purpose
Graphite (-)	Steel (+)	High speed and 20% wear
Graphite (-)	Copper (+)	General purpose
Copper tungsten (+)	Steel (-)	General purpose
Copper tungsten (+)	Carbide (-)	General purpose

leads to fifty times higher wear with positive polarity than with negative polarity. The machining time also increased simultaneously by more than 200%.

Pulse interval is also known as the pulse off time. It is the time, in which the machining (or sparks) does not occur. It affects the machining speed, stability, and the machined surface. The melted workpiece (debris) during the pulse on time is ejected and flushed away with the dielectric fluid during pulse off time. The machining operation is faster at shorter interval as shown in Fig. 7.12. But, if the off time is too short, the debris will not have flushed away effectively and increase the chance to occur secondary sparking as well as prolonged machining time and reduce the material removal rate.

The pulse waveform is generally rectangular; however, pulse with various other forms is also used for electric discharges. Generators with trapezoidal pulses can reduce the comparative wear of cathode (generally tool) to small values. The actual profile of a single EDM pulse is as shown in Fig. 7.13.

**Fig. 7.11** Comparison of tool polarity and electrode relative wear [14]



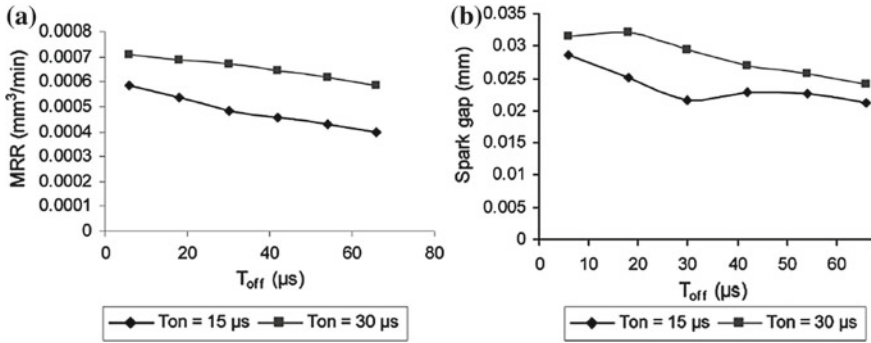


Fig. 7.12 Variation of pulse on and off time on a MRR, b spark gap during micro-EDM of WC-Co [11]

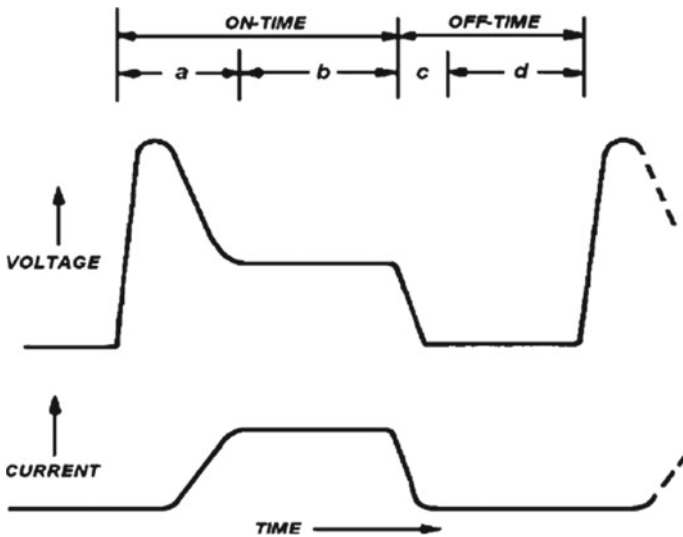


Fig. 7.13 Actual pulse of a single EDM pulse [15]

### 7.4.2 Non-electrical Parameters

Non-electrical parameters have also significant effect on machining and optimizing performance measures like electrical parameters. The main non-electrical parameters include flushing and electrode rotation along with powder concentration.

Dielectric flushing is important in electrical discharge machining. The dielectric fluid should have the basic characteristics such as high dielectric strength and swift recapture after breakdown and flushing capability. MRR, TWR, and recast layer are exaggerated by the dielectric fluid and technique used for flushing [7, 16]. The flushing flow rate plays important role in crack density in the machined surface



which can be minimized by optimum flushing rate [16]. Kerosene, deionized water, and hydrocarbon oils are used as dielectric fluid. Among them, hydrocarbon oils and kerosene decompose during machining and deposit carbon on the machined surface. Deionized water is used where the carbon-free surfaces need to be produced.

Electrode rotation helps to generate favourable centrifugal forces in the fluid and flush away the debris from the inter-electrode gap effectively. Electrode rotation causes two things on the dielectric fluid. Firstly, it creates a centrifugal force on the dielectric fluid and pulls out the unwanted materials. Secondly, it creates some turbulence in the fluid which allows the fresh fluid to enter in the gap and wash away the particles [17]. Hence, improvements in the machining responses have been reported due to effective flushing and electrode rotation [10].

## 7.5 Effect of Powder on IEG

The suspension of powder in the dielectric fluid enlarges the inter-electrode gap. As discussed earlier, the inter-electrode gap is influenced by voltage, flushing methods, dielectric, etc. The studies showed that increase in the powder concentration increases the inter-electrode gap [18]. Figure 7.14 shows the enlargement of hole diameter against the increase in the powder concentration in the dielectric fluid as well as comparison of dielectric fluid mixed with dielectric fluid mixed with silicon, aluminium, and pure dielectric fluid. As evident from Fig. 7.15, the increase in the powder concentration increases the additional gap pollution which leads to the high probability to occur the primary discharge between the tool and powder particles instead of tool and workpiece. This is due to the fact that the conductive or semi-conductive powder particles get energized and reduce the effective discharge gap (distance between the tool and powder particles), thereby reduces the breakdown voltage under the influence of electric field in the IEG. Hence, the early discharge of capacitance (before full charging) takes place, and secondary sparks may exist between the powder particles and workpiece; thereby, the inter-electrode gap gets increases compared to pure dielectric. The magnitude of increase in IEG depends on the variation of material and electrical properties of the powder particles suspended in the dielectric. In case of pure dielectric fluid, there is no additional gap pollution (other than with debris) between the tool and workpiece and the discharge takes place between the tool and workpiece. Hence, the inter-electrode gap is comparatively larger in PM $\mu$ EDM compared to  $\mu$ EDM.

## 7.6 Effect of Powder on MRR

The variation of machining responses is widely depending on the type and material properties of the powder particles. Kuriachen and Mathew [1] have conducted a study on the effect of powder (SiC) suspension in the dielectric on material removal rate

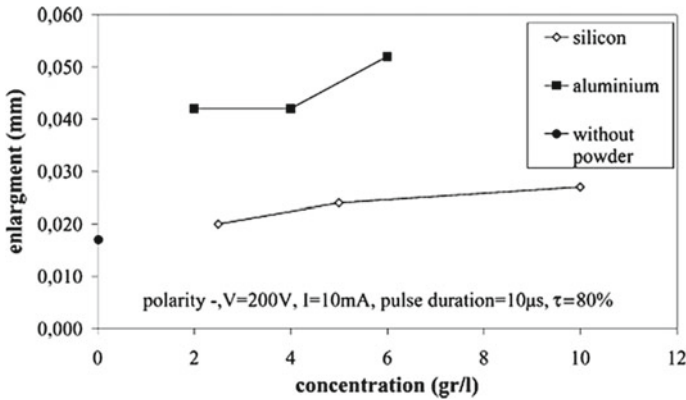


Fig. 7.14 Variation of IEG with powder concentration during PM $\mu$ EDM [18]

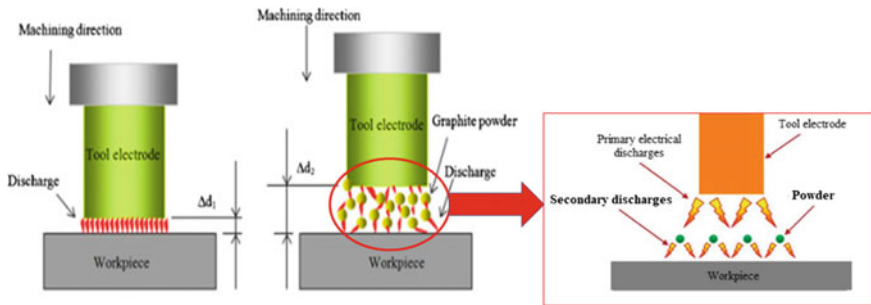
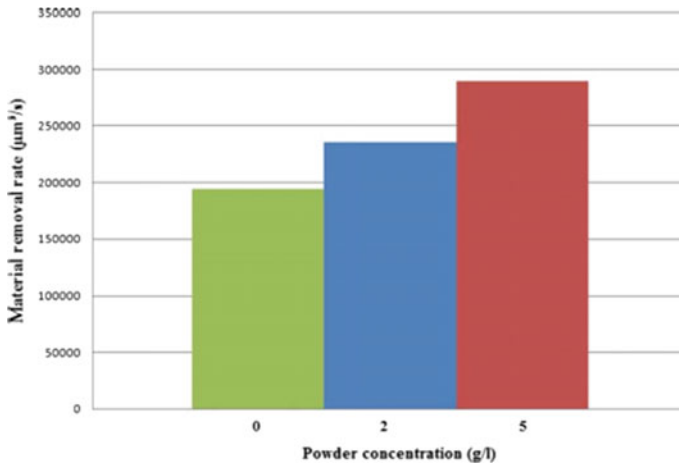


Fig. 7.15 Comparison of sparking phenomena in  $\mu$ EDM and PM $\mu$ EDM [19, 20]

(MRR). From the results reported, the material removal rate found to increase when the semiconductive particle concentration (SiC) varied from 5 to 25 g/L. However, the variation with respect to capacitance and voltage showed a different trend. Initially, i.e. variation of 5–15 g/L of powder concentration increased MRR; thereafter, it found to be decreasing. This is due to the fact that increase in powder concentration increases the IEG pollution with SiC which improves the bridging of the discharge gap between the electrodes. Due to this bridging effect, the insulating strength of the dielectric decreases. Hence, the chance of easy short circuit takes place. It results in early explosion of discharges [9]. Hence, early discharge of the partially charged capacitor takes place; i.e. the capacitor may not get charged fully. It results in the reduction of discharge energy release into the IEG. Therefore, the amount of material removed also reduces proportionally. Secondly, once the short circuit happens, the tool moves backward and searches for new optimum gap to start with new sparks. This results in the increase in machining time to complete the required machining cavity. This in turn reduces the MRR.

On the contrary, Prihandana et al. [21] reported that suspension of micro-MoS<sub>2</sub> powder in the dielectric increases the material removal rate as shown in Fig. 7.16.



**Fig. 7.16** Variation of MRR with respect to powder concentration [21]

It can be clearly understood that high concentration of powder (5%-micro-MoS<sub>2</sub>) particles increases the material removal rate compared to 2 and 0% powder in the dielectric. It is due to the semiconductor property of the powder particles; thereby, the dielectric strength of the fluid is reduced and increased the inter-electrode gap. The increase in IEG along with high powder concentration in IEG reduces the adhesion of the particles to the tool and workpiece, thereby reduces the chances of bridging of IEG. This results in the reduction of short circuiting and reduces the machining time and increases the MRR [21, 22]. Therefore, it can be concluded that the effect of powder on the MRR not only depends on the powder concentration in the dielectric but also depends on the type, material, and electric properties of the tool.

## 7.7 Effect of Powder on Tool Wear Rate

Effect of powder concentration in dielectric on the tool wear shown that increase in powder concentration increases the tool wear. Due to the presence of less powder particle in the IEG at low level of powder concentration (5 g/L), the proportion of energy available at the cathode for removal is less in contrast to anode. Therefore, small amount of material gets removed at low level of powder concentration. At higher level of powder concentration (25 g/L), the existence of redundant amount of powder leads to unstable electric discharge [10]. At the interaction of voltage and powder concentration at higher levels, the maximum amount of material found to be removed from the tool electrode [1, 23].

### 7.8 Effect of Powder on Machining Time

As discussed in the Sect. 7.6, the pure dielectric fluid with relatively low flow rate in the narrow IEG increases the chances of adhesion of debris in the IEG whereby the bridging and short-circuiting take place. Once short circuiting is detected by the servo control mechanism, the tool retracts in the reverse direction and searches for a new optimum IEG as depicted in Fig. 7.17. This results in increased machining time and reduces machining efficiency. Studies reported by Prihandana et al. [19] with the suspension of graphite particles in the dielectric as shown in Fig. 7.18, with increase in powder concentration (graphite) 0–10%, the machining time reduced by 14–20 times faster. This is interpreted as the 10 g/l of graphite powder in the dielectric effectively bridge the IEG thereby frequency of quality discharge increases thus the machining time [19].

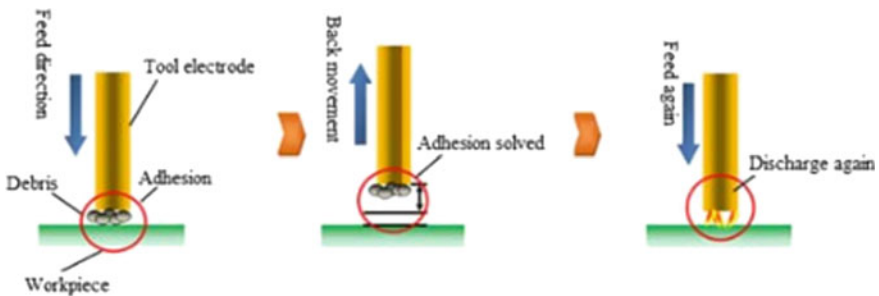


Fig. 7.17 Effect of adhesion on machining stability [19]

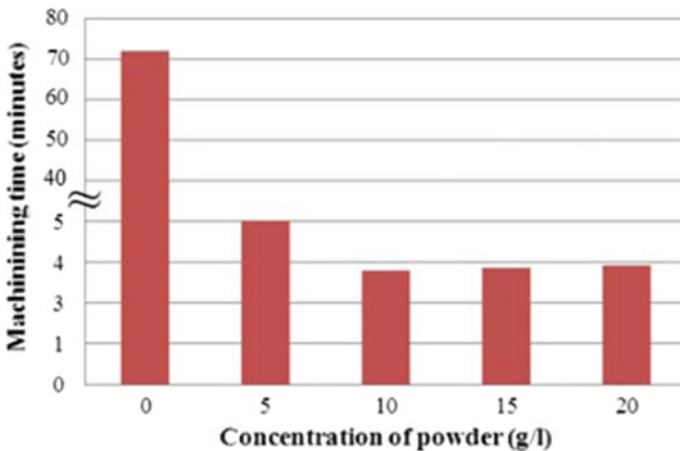


Fig. 7.18 Variation of machining time with respect to graphite powder concentration [19]

### 7.9 Effect of Powder on Surface Roughness

Unlike material removal rate, the increase in powder concentration in the dielectric reduces the surface roughness and improves the surface finish as shown in Fig. 7.19. Beyond the scope of the type and material properties of powders, all the conductive or semiconductive powder in dielectric decreases the surface roughness and improves the surface finish. Researcher’s explained this trend is due to the fact that increase in powder concentration increases the number of powder particles in the IEG. These particles get energized as discussed earlier and produce the spark between the tool and

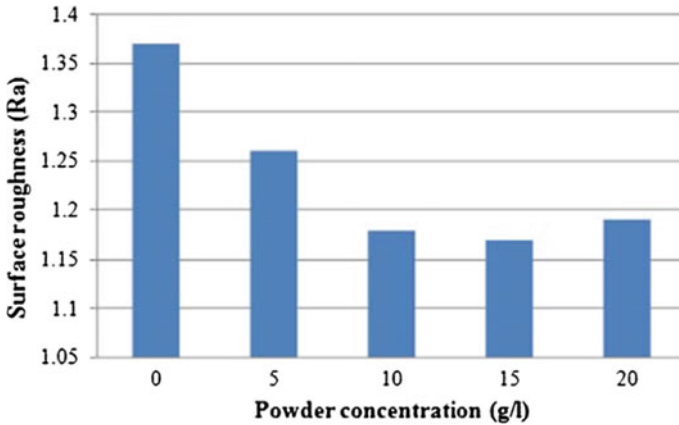


Fig. 7.19 Variation of surface roughness with powder concentration [19]

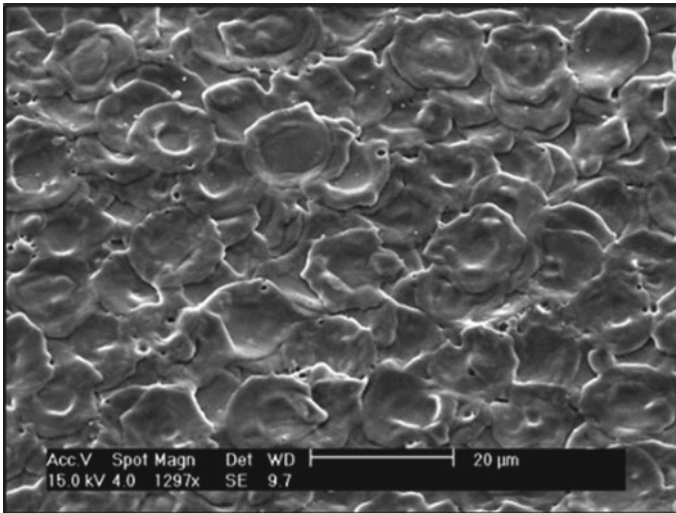
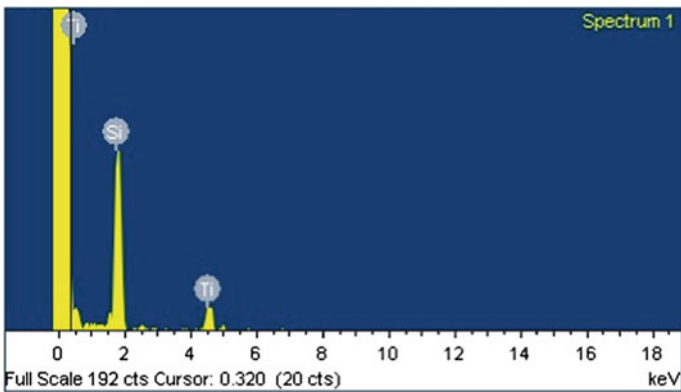


Fig. 7.20 SEM image of the graphite PMμED machined surface [19]

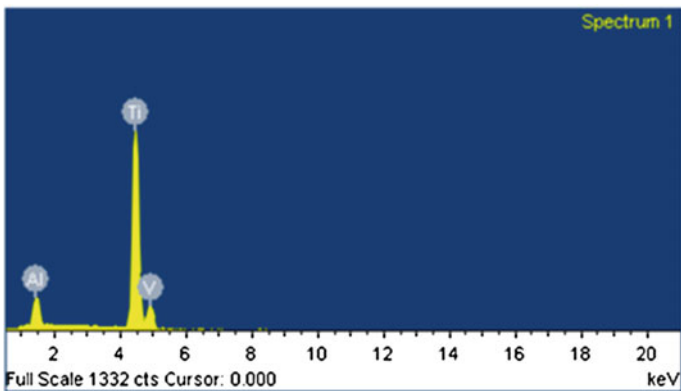
powder particle as well as with the powder and workpiece (secondary sparks). This reduces the intensity of sparks, thereby produces low intensive and more uniform craters on the machined surface instead of high intensive shallow craters for the same discharge energy as shown in Fig. 7.20. This phenomenon results in the reduction of  $R_a$  and  $R_{max}$  (surface roughness) of the produced surface.

### 7.10 Effect of Powder on Machined Surface

Researchers have established and proved that some of the melted material get re-solidify on the machined surface due to the cooling effect of dielectric fluid. This is more relevant in the case of powder PM $\mu$ EDM due to the enhancement of the thermal conductivity of the fluid. Kuriachen [23] have investigated the possibility

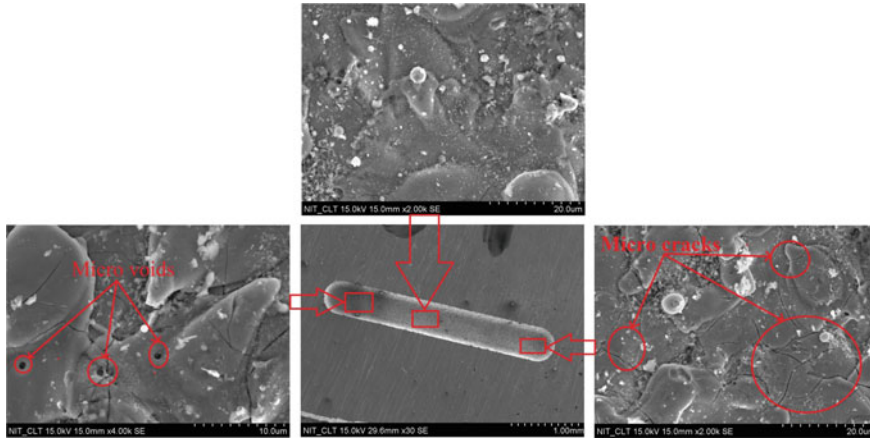


(a) EDS composition analysis of  $\mu$ PAMEDM processed Ti-6Al-4V surface



(b) EDS composition analysis of unprocessed Ti-6Al-4V surface

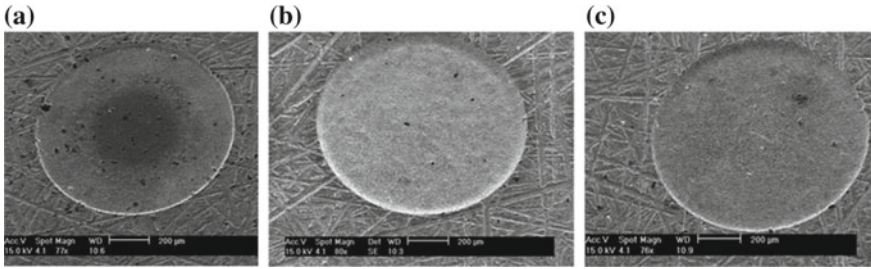
**Fig. 7.21** EDS composition analysis [1]



**Fig. 7.22** SEM images of the microslot at a capacitance of  $0.1 \mu\text{F}$ , voltage of 115 V, and powder concentration of 15 g/L [1]

of developing microelectric discharge alloying by suspending SiC powder in the dielectric. Analysis of the machined surface (Fig. 7.22) of titanium alloy confirms the existence of a thin re-solidified layer. It was also found that microcracks, small pits, residues of recast, etc., are identified towards the end of the microchannel machined. However, only a few microcracks are observed at the centre of the channel. This is reported as the fact that tool remains more time towards the ends of the microchannel. Hence, more thermal residual stress is experienced. Further analysis through EDX revealed (Fig. 7.21) that silicon material gets migrated on to the machined surface, whereas it was not present on the unprocessed surface. In addition to silicon, the residuals of the tool material are also detected on the machined surface. Hence, the material from tool and dielectric is present in the plasma, and a small portion gets solidify on the machined surface. Moreover, the surface properties also get altered due to the frequent heating and cooling cycles. The microhardness of the machined surface gets increased. It was reported that 100% improvement in the micro hardness of the powder EDMed surface [24].

Prihandana et al. [21] studied the effect of  $\text{MoS}_2$  micropowder in the dielectric along with ultrasonic vibration on the mechanical surface. The comparison of pure dielectric mixed with micro- $\text{MoS}_2$  particle revealed that a significant difference in quality of the surface is produced. The machined surface with pure dielectric shown a significant deposition of carbon particles at the centre of the blind microhole produced as shown in Fig. 7.23, whereas only a small amount of carbon deposition is detected during the machining with micro- $\text{MoS}_2$  particle-mixed dielectric. This is due to the decomposition of kerosene and attach to the machined surface. However, suspending  $\text{MoS}_2$  maintains the high degree of dry lubricity since it is a dry lubricant. In addition, due to the increase in IEG, the  $\text{MoS}_2$ -mixed dielectric reduces the chance of arcing and short circuiting and increases the flushing efficiency; this in turn



**Fig. 7.23** a Pure dielectric, b dielectric with 2 g/l MoS<sub>2</sub>, c dielectric with 5 g/l MoS<sub>2</sub> [21]. Study of workpiece vibration

reduces the carbon deposition and surface microcracks. Moreover, the high electrical conductivity of MoS<sub>2</sub>-suspended fluid facilitates the increase in the IEG.

## 7.11 Research on PM $\mu$ EDM

Tan and Yeo [25] have developed a numerical model to predict the surface characteristics of PM $\mu$ EDM and estimated the plasma channel enlargement feature caused by the existence of powder particle in dielectric as 1.07 at 0.02 g/l of powder concentration. The comparison of results shown that PM $\mu$ EDM model is sound. MoS<sub>2</sub> nanopowder (50 nm)-suspended dielectric was used to improve the fine finish of micro-EDM of Inconel 718 surface by Prihandana et al. [26]. The results showed that 5 g/l of powder concentration can achieve the better microholes and maximum material removal rate. Wang et al. [27] established that plasma channel in aluminium powder-mixed kerosene is more stable than pure kerosene and also found that stability increased with increase in current. Tiwary et al. [28] have compared the influence of various dielectrics, namely DEF-92, deionized water, and Cu powder-mixed deionized water during  $\mu$ EDM and shown that Cu powder in dielectric can significantly improve the performance  $\mu$ EDM in terms of MRR, TWR and OC.

Liew et al. [29] studied the effect of carbon nanofibre-suspended dielectric in  $\mu$ EDM on silicon carbide. Two types of EDM test (time controlling method and depth controlling method) were executed with various fibre concentrations. The electrosparking behaviour, MRR, EWR, electrode geometry, IEG, surface topography, and surface destruction were changed with the addition of carbon nanofibre in both tests. Suspension of carbon nanofibre improved the electrosparking rate of recurrence, MRR, and spark gap. Moreover, the form accuracy of microcavity and surface finish improved, and crater size reduced. Carbon nanofibre was moderately stick to the workpiece and prevented the material relocation among the electrode and workpiece.

Feasibility of improving the surface appearances in the PM $\mu$ EDM of tungsten carbide with graphite nanopowder-suspended dielectric was investigated by Jahan et al.



[30]. Study on the enactment of powder-mixed  $\mu$ EDM was carried out, and surface characteristics were analysed in positions of surface features, crater characteristic, surface roughness ( $R_a$ ), and peak to valley roughness ( $R_{max}$ ). Spark gap, electrode wear and MRR were affected by graphite powder concentration. The surface finish and MRR were improved by the occurrence of graphite nanopowder in the dielectric, and EWR is reduced. For PM $\mu$ EDM, the surface is uneven and imperfection-free related with sinking  $\mu$ EDM. But the material removal rate is maximum during the powder suspended sinking  $\mu$ EDM because of large area visible to machining. The average surface roughness and maximum peak to valley distance reduce as the powder concentration to certain limit thereafter increases as a result of powder settling as well as bridging of the IEG. For an optimum concentration of 2 g/L and voltage of 60 V, the lowest value of  $R_a$  and  $R_{max}$  was obtained for milling micro-EDM. The EWR also reduces with increase in powder concentration up to certain level and then increases.

Prihandana et al. [20] suspended nanographite particle in the dielectric with the application of ultrasonic vibration to overcome the powder settling issues and understood that it is an alternative to enhance the surface properties and to achieve faster machining. A technique by calculating the discharge pulse number has overcome the imprecision issues in nanographite PMD micro-EDM process. The suspension of nanopowder in dielectric fluid has abridged machining time by 35%. The upsurge in spark IEG and the increased powder percentage of nanographite in dielectric fluid affected the discharge to be further stable and decrease the requirement of retracting the tool electrode which results in reduced machining time. Moreover, nanopowder improved the machined surface integrity by reducing the chances of microcracks in the machined surface due to the uniform discharge distribution.

Jahan et al. [31] investigated the possibility of enlightening the  $R_a$  value of PM $\mu$ EDM tungsten carbide while graphite, aluminium, and alumina as the nanopowders. The effects of different powder characteristics were investigated analytically and experimentally and identified the existence of conductive or semiconductive powder lowered the dielectric strength of the dielectric, thereby larger IEG. Thus, the surface finish, MRR, EWR were found to be improved. The discharging process becomes more uniform, and thus, the craters become shallow. Semiconductive graphite powder can result in fault-free surface with better surface finish. Conductive aluminium powder gives higher spark gap and MRR. But nonconductive alumina powder did not show any significant effect on process performance.

In another study, Tan et al. [32] evaluated the recast layer thickness and identified the possibility for applying PMD on recast layer decrease and surface alteration. The process responses under various independent variables like particle concentration, nanosized particles, and sub-microsecond pulse on time duration were studied. SiC powder of powder granularity in the nanometre range and powder concentration of 5 g/L were used for the studies. The pulse on time of 606 ns provides longer interaction time and wider expansion of plasma channel. The electrode rotation speed of 1000 rpm generates thicker recast layer than 3000 rpm. The absorption of discharge energy by powder particle generates narrower melt pool, while the ease of

plasma channel expansion reduces plasma over pressure and facilitates molten material retention and overlapping recast layer formation.

The influence of SiC powder concentration in the dielectric and electric discharge energy in micro-EDM of Ti-6Al-4V with WC electrode is presented by Ali et al. [33]. Input variables were identified as SiC concentration, electric discharge energy. Addition of SiC powder reduces surface roughness up to a concentration of 20 g/l. The ANOVA shows that most influential factor on roughness is powder concentration, whereas electric discharge energy influences mostly on MRR and EWR. Cyril et al. [34] experimentally analysed the effect of powder concentration along with voltage, capacitance, feed, and rpm on various machining responses with aluminium, graphite, and silicon carbide-mixed dielectric fluid and found that a significant reduction in MRR and tool wear.

Yeo et al. [35] carried out single RC discharge experiments at different low discharge energies to study the effect of powder additives suspended in dielectric on crater characteristics for micro-EDM. Discharge energies of 2.5, 5, and 25  $\mu\text{J}$  were used. The crater formed is with small diameter and depth and has more consistent circular shape due to the presence of additives.

By studying the process using different dielectric fluids such as kerosene, kerosene with aluminium powder, and kerosene with SiC powder, Chow et al. [36] investigated the machinability of titanium alloy on micro-EDM. Addition of both powders to kerosene improves the material removal depth, discharge gap, and surface roughness. However, it is identified that material removal depth is found to be more for SiC powder while the significant improvement on surface roughness is for Al powder addition. Due to the largest gap obtained between electrode and workpiece, Al powder addition produces largest slit expansion. The EWR is increased due to the addition of powders which disturbs the adherence of carbon nuclides attached to the surface of electrode.

In another study, Chow et al. [37] investigated the microslit EDM process performance for Ti alloy using SiC powder in pure water as working fluid with small discharge energy. Conductivity of pure water increases with the addition of SiC powder, and thus, the discharge gap is increased. Due to the dispersion of discharge energy, surface roughness and MRR improved. Meanwhile, the addition of SiC to pure water increases the slit expansion and electrode wear than pure water.

## 7.12 Summary

Powder-mixed microelectric discharge machining is a growing day by day especially in the advanced micromachining of superalloys. To meet the requirement of miniaturization on the advanced materials and to overcome the processes inabilities of  $\mu\text{EDM}$ , PM $\mu\text{EDM}$  is established as a viable and simple alternative. The improvements on the process capabilities mainly depend on the powder material properties, size, and its concentration in the dielectric. Generally, researchers have used conductive and semiconductive material powders. The presence of these external powders increases

the IEG and can produce better surface finish. This chapter mainly discussed the effect of powder particles in the dielectric on the working principle and its effect on various process responses. The effect of powders on the machined surface opens a new scope for exploring the possible  $\mu$ ED alloying for the biomedical implants as a cheaper alternative where the conventional micromachining is not adequate. The research on various bio-inspired powder particles and its effect on the surface of bio-implants need to be addressed. In addition, a thorough research and development are also required to get the uniform recast layer on the surface to achieve the PM $\mu$ EDM as a possible alloying technique. Hopefully, a few guidelines to achieve this transition were provided.

## References

1. Kuriachen B, Mathew J (2016) Effect of powder mixed dielectric on material removal and surface modification in microelectric discharge machining of Ti-6Al-4V. *Mater Manuf Process* 31(4):439–446
2. Kansal HK, Sehijpal S, Kumar P (2007) Effect of silicon powder mixed EDM on machining rate of AISI D2 die steel. *J Manuf Process* 9:13–22
3. Paulom P, Elsa H (2008) Effect of the powder concentration and dielectric flow in the surface morphology in electrical discharge machining with powder-mixed dielectric (PM $\mu$ -EDM). *Int J Adv Manuf Technol* 37:1120–1132
4. Yeo SH, Tan PC, Kurnia W (2007) Effects of powder additives suspended in dielectric on crater characteristics for micro electrical discharge machining. *J Micromech Microeng* 17:91–98
5. Kunieda M, Lauwers B, Rajurkar KP, Schumacher BM (2005) Advancing EDM through fundamental insight into the process. *CIRP Ann* 54(2):64–87
6. Jahan MP, Wong YS, Rahman M (2009) A study on the quality micro-hole machining of tungsten carbide by micro-EDM process using transistor and RC-type pulse generator. *J Mater Process Technol* 209:1706–1716
7. Kumar S, Singh R, Singh TP, Sethi BL (2009) Surface modification by electrical discharge machining: a review. *J Mater Process Technol* 209:3675–3687
8. Klocke F, Lung D, Antonoglou G, Thomaidis D (2004) The effects of powder suspended dielectrics on the thermal influenced zone by electro-discharge machining with small discharge energies. *J Mater Process Technol* 149:191–197
9. Kansal HK, Sehijpal S, Pradeep K (2007) Technology and research developments in powder mixed electric discharge machining (PMEDM). *J Mater Process Technol* 184(1–3):32–41
10. Garg RK, Singh KK, Sachdeva A (2010) Review of research work in sinking EDM and WEDM on metal matrix composite materials. *Int J Adv Manuf Technol* 50:611–624
11. Jahan MP, Wong YS, Rahman M (2012) Experimental investigations into the influence of major operating parameters during micro-electro discharge drilling of cemented carbide. *Mach Sci Technol* 16:131–156
12. Mishra PK (2011) *Nonconventional Machining*. Narosa Publishing House, India
13. Kern R (2008) Sinker electrode material selection EDM today (July/August 2008 Issue)
14. Uhlmann E, Roehner M (2008) Investigations on reduction of tool electrode wear in micro-EDM using novel electrode materials. *CIRP J Manuf Sci Technol* 1:92–96
15. Fuller JE (1996) Electrical discharge machining. *ASM Mach Handb* 16:557–564
16. Wong YS, Lim LC, Lee LC (1995) Effects of flushing on electro-discharge machined surface. *J Mater Process Technol* 48:299–305
17. Karthikeyan G, Ramkumar J, Dhamodaran S, Aravindan S (2010) Micro electric discharge milling process performance: an experimental investigation. *Int J Mach Tools Manuf* 50(8):718–727

18. Klocke F, Lung D, Antonoglou G, Thomaidis D (2004) The effects of powder suspended dielectrics on the thermal influenced zone by electrodischarge machining with small discharge energies. *J Mater Process Technol* 149(1–3):191–197
19. Prihandana GS, Mahardika M, Hamdi M, Wong YS, Miki N, Mitsui K (2013) Study of work-piece vibration in powder-suspended dielectric fluid in micro-EDM processes. *Int J Precis Eng Manuf* 14(10):1817–1822
20. Prihandana GS, Mahardika M, Hamdi M, Wong YS, Mitsui K (2011) Accuracy improvement in nanographite powder-suspended dielectric fluid for micro-electrical discharge machining processes. *Int J Adv Manuf Technol* 56(1–4):143–149
21. Prihandana GS, Muslim M, Hamdi M, Wong YS, Mitsui K (2009) Effect of micro-powder suspension and ultrasonic vibration of dielectric fluid in micro-EDM processes-Taguchi approach. *Int J Mach Tools Manuf* 49(12–13):1035–1041
22. Wong YS, Lim LC, Rahuman I, Tee WM (1998) Near-mirror-finish phenomenon in EDM using powder-mixed dielectric. *J Mater Process Technol* 79(1–3):30–40
23. Kuriachen B (2015) Numerical modelling, simulation and experimental investigations of the micro electric discharge machining of Ti-6Al-4V, Ph.D. thesis submitted to National Institute of Technology Calicut, Kerala, India
24. Sanjeev K, Batra U (2012) Surface modification of die steel materials by EDM method using tungsten powder-mixed dielectric. *J Manuf Process* 14(1):35–40
25. Tan PC, Yeo SH (2013) Simulation of surface integrity for nanopowder-mixed dielectric in micro electrical discharge machining. *Metall Mater Trans B* 44(3):711–721
26. Prihandana GS, Sriani T, Mahardika M, Hamdi M, Miki N, Wong YS, Mitsui K (2014) Application of powder suspended in dielectric fluid for fine finish micro-EDM of Inconel 718. *Int J Adv Manuf Technol* 75(1–4):599–613
27. Wang X, Liu Y, Zhang Y, Sun Q, Li Z, Shen Y (2016) Characteristics of plasma channel in powder-mixed EDM based on monopulse discharge. *Int J Adv Manuf Technol* 82(5–8):1063–1069
28. Tiwary AP, Pradhan BB, Bhattacharyya B (2018) Investigation on the effect of dielectrics during micro-electro-discharge machining of Ti-6Al-4V. *Int J Adv Manuf Technol* 95(1–4):861–874
29. Liew PJ, Yan J, Kuriyagawa T (2013) Carbon nanofiber assisted micro electro discharge machining of reaction-bonded silicon carbide. *J Mater Process Technol* 213:1076–1087
30. Jahan MP, Rahman M, Wong YS (2011) Study on the nano-powder-mixed sinking and milling micro-EDM of WC-Co. *Int J Adv Manuf Technol* 53:167–180
31. Jahan MP, Rahman M, Wong YS (2010) Modelling and experimental investigation on the effect of nanopowder-mixed dielectric in micro-electrodischarge machining of tungsten carbide. *Proc Inst Mech Eng [B]* 224:1725–1739
32. Tan PC, Yeo SH (2011) Investigation of recast layers generated by a powder-mixed dielectric micro electrical discharge machining process. *Proc Inst Mech Eng [B]* 225(7):1051–1062
33. Ali MY, Atiqah N, Erniyati (2011) Silicon carbide powder mixed micro electro discharge milling of titanium alloy. *Int J Mech Mater Eng* 6(3):338–342
34. Cyril J, Paravasu A, Jerald J, Sumit K, Kanagaraj G (2017) Experimental investigation on performance of additive mixed dielectric during micro-electric discharge drilling on 316L stainless steel. *Mater Manuf Processes* 32(6):638–644
35. Yeo SH, Tan PC, Kurnia W (2007) Effects of powder additives suspended in dielectric on crater characteristics for micro electrical discharge machining. *J Micromech Microeng* 17:N91
36. Chow HM, Yang LD, Lin CT, Chen YF (2008) The use of SiC powder in water as dielectric for micro-slit EDM machining. *J Mater Process Technol* 195:160–170
37. Chow HM, Yan BH, Huang FY, Hung JC (2000) Study of added powder in kerosene for the micro-slit machining of titanium alloy using electro-discharge machining. *J Mater Process Technol* 101(1–3):95–103

# Chapter 8

## Vibration-Assisted Micro-EDM Process



K. Mishra, B. R. Sarkar and B. Bhattacharyya

**Abstract** In the current trend of modern technology, demand for accurate miniaturized machined parts made of newly developed extremely hard and brittle materials is increasing continuously and conventional machining and advanced machining processes are becoming obsolete to meet these requirements. Micro-EDM is capable to fabricate micro-tools and miniaturized machined components, but still the machining speed is pretty low. In the  $\mu$ -EDM process, it is very difficult to remove small debris particles from the vicinity of the narrow machining gap which results in unwanted short circuits and arcing. Especially, due to very small energy of discharge, very low open voltage, and the stray capacitor in the RC type circuits, the machining becomes almost impossible. Thus, to overcome these problems in micro-EDM, vibration can be effectively applied to the tool, workpiece as well as to the machining fluid in order to obtain higher machining speed with high accuracy without significantly increasing the electrode wear.

**Keywords** Micro-EDM · Vibration-assisted · Frequency · Inclined feeding · Self-adaptive control · Performance improvement

### 8.1 Introduction

Miniaturization is a keyword in the current fashion of technology and research. In the last few decades, micro-EDM has been established itself as an essential technique for industrial application. Due to the regular increasing demand of miniaturization, further improvement of the process is required particularly concerning its capability

---

K. Mishra (✉) · B. R. Sarkar · B. Bhattacharyya  
Department of Production Engineering, Jadavpur University, Kolkata, India  
e-mail: [mishra.koushik050@gmail.com](mailto:mishra.koushik050@gmail.com)

B. R. Sarkar  
e-mail: [sarkarbiplab\\_s@rediffmail.com](mailto:sarkarbiplab_s@rediffmail.com)

B. Bhattacharyya  
e-mail: [bb13@rediffmail.com](mailto:bb13@rediffmail.com)

© Springer Nature Singapore Pte Ltd. 2019  
G. Kibria et al. (eds.), *Micro-electrical Discharge Machining Processes*, Materials Forming, Machining and Tribology, [https://doi.org/10.1007/978-981-13-3074-2\\_8](https://doi.org/10.1007/978-981-13-3074-2_8)

to precisely manufacture complex structures with a smaller dimension. Micro-EDM products are used for several purposes in micro-fluidic and micro-machining application, e.g., micro-nozzles for inkjet printer, micro-channels for turbine blades cooling system, injection nozzles for fuel systems, and different drug delivery orifices. Also, it is a common feature in different micro-products used in aerospace, automotive, medical, biomedical, nuclear sector, etc., where materials have to resist wear and bear high temperature and pressure. Micro-EDM is a thermal process that directly employs electrical sparks for the erosion of any non-insulating material; it is basically a non-contact-type machining technique as there is no such physical contact between the tool and the workpiece [1].

In micro-EDM, job electrode and the tool electrode are apart from each other by a narrow gap known as spark gap and also filled with a liquid called dielectric. With the application of high-voltage pulsed power in between workpiece and tool electrode, discharge starts due to the breakdown of the dielectric in the small spark gap. Electrical discharges produce intense heat in the sparking zone which results in melting and evaporation of materials from both the electrodes. As this phenomenon occurs in a dielectric medium, after cooling and resolidification of molten materials are then turn into some tiny spherical debris which are retained in that tiny spark gap. In micro-EDM, spark gap is very less which is in the order of a few microns and removal of debris from that small gap is a great challenge. This debris should be removed from the sparking zone; otherwise, it leads to abnormal discharges as well as unstable machining. During micro-EDM, because of inefficient washout of the tiny particles, regular adhesion in between two electrodes terminates the machining operation. During micro-EDM, to overcome these burdens, vibrations can be introduced to the tool, workpiece as well as to the dielectric. During micro-EDM, with the application of vibration, the stability of the machining performance can be improved by eliminating arcing and short circuit by flushing out of the debris particles from the narrow tool electrode and workpiece gap.

## 8.2 Challenges in Micro-EDM

Beside various advantages, micro-EDM has to face various challenges which limit its applicability to the related industry. Normally, in micro-EDM, spark gap is kept in the order of a few microns and removal of gaseous bubbles and debris from that small gap is a great challenge. However, debris which is produced during machining should be removed from the sparking zone instantly; otherwise, for the time being, the debris concentration will be higher and that leads to abnormal discharges as well as unstable machining. In micro-EDM, because of ineffective washout of the tiny particles, continuous adhesion between two electrodes terminates the machining operation. Thus, even when the machining is possible, an extensive time is required for machining.

### **8.3 Improvement of Machining Performances of $\mu$ -EDM with Aid of Vibration**

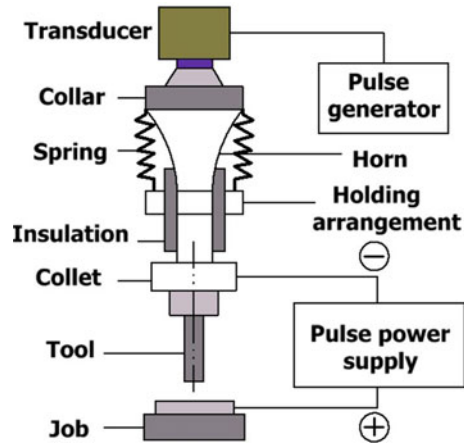
During  $\mu$ -EDM, the above-mentioned challenges can be overcome by applying two most easy and effective ways: One is by giving high-pressure flushing and another is by applying rotation to the tool. But due to the vulnerability and size restrictions, conventional high flushing techniques such as jet flushing and tool rotation cannot be applied in micro-EDM. Therefore, in micro-EDM, it is essential to utilize other alternating techniques to assist the flushing. Thus, the application of vibrations during micro-EDM can be a compatible technological approach to meet these challenges. Vibrations can be useful when it applies to the EDM tool, workpiece, or dielectric [2]. In micro-EDM system, assistance of vibration not only increases the material removal rate but also reduces the chances of arcing and short circuit by flushing out of tiny particles from the narrow space in between two electrodes. Micro-EDM system with aid of vibration using piezoelectric also improves the capability of machining with higher aspect ratio cavities and process stability [3]. With the range of frequency, vibration can be classified into two categories: One is high frequency, and another is low frequency. If the frequency range is above 20 kHz, then it is stated as ultrasonic frequency. Two types of vibration can be used to assist micro-EDM performances depending on their different applications. Generally, high-frequency vibration can be useful when it applies to any of the electrodes as well as to the dielectric, whereas low-frequency vibration is mostly effective when it applies to the workpiece position. In the next subsequent sections, the influence of vibration on various positions as well as performance characteristics of micro-EDM has been discussed.

#### ***8.3.1 Effects of High-Frequency Vibration***

##### **8.3.1.1 Vibration to the Tool**

Vibrations can be useful when it applies to the EDM tool, workpiece, or dielectric. In this section, the influence of vibration when it applies to the tool on various responses of  $\mu$ -EDM has been considered. Tool vibration-assisted micro-EDM setup has two main subunits: One is a high-frequency vibration originator system, and another is a fixture of tool electrode holding arrangement which is compatible with vibration assistance. Generally, the ultrasonic generator is attached to the micro-EDM machine head using a holding fixture and to fit the size of the horn a collar is used. The function of the collar is to support a spring-supported arrangement to transmit the ultrasonic vibrations to the electrode tip. Again, with the help of springs, this total arrangement is attached to the pulse producer unit through a transducer. To prevent electrical hazard, insulation needs to be provided between the end of concentrator and shank of container. The upper portion of the part is prepared to fix the accessory to the collet of the electrode and to maintain the proper conductivity; the attachment of the

**Fig. 8.1** Representation of vibration assembly for tool vibration-assisted micro-EDM



electrode should be made of high conductive material. Figure 8.1 shows a schematic diagram of the vibration assembly with all the subassembly parts [4]. The pulse originator is able to generate high-frequency waves in which maximum power at the output, the frequency, and the amplitude is in the range of 1000–1200 W, 20–40 kHz, and 10–25  $\mu\text{m}$ , respectively.

#### (i) Improvement of machining stability with aid of vibration in micro-EDM

As already stated that in micro-EDM, inappropriate removal of the small debris particles from the tiny spark gap leads to regular contact between two electrodes which results in longer machining time. Machining time is also increased with the increment of workpiece length. The word ‘adhesion’ means making a bridge in between the workpiece and the tool electrode because of melted debris as shown in Fig. 8.2. This adhesion makes a connection in between workpiece and tool electrode which causes an electrical short circuit and leads to unstable machining condition. To prevent these phenomena, an insulation recovery arrangement is included with the  $\mu$ -EDM machine. Normally, a  $\mu$ -EDM machining system utilizes a steady-state feed control mechanism that intends to a feeding system. When this kind of contact occurs, usually the system tries to control to shift the worktable to the opposite direction to maintain the preferred spark distance between two electrodes. Longer workpiece length exhibits a smaller amount of inflexibility when the workpiece length is constant. Again, stiffness of the workpiece decreases with the enlargement of the workpiece due to amplifying of the mandrel. This signifies a larger deflection of the workpiece and require adequate force to rectify this contact. So, after the short circuit, large feeding-back action occurs which results in the increment of machining time and this incident has a straight influence on the stability of discharges. In the next paragraph, it has been elaborated that how this problem can be overcome with the help of vibration.

With aid of vibration, not only debris remaining in the tiny distance between two electrodes can be efficiently removed but also it helps to diminish the chances of



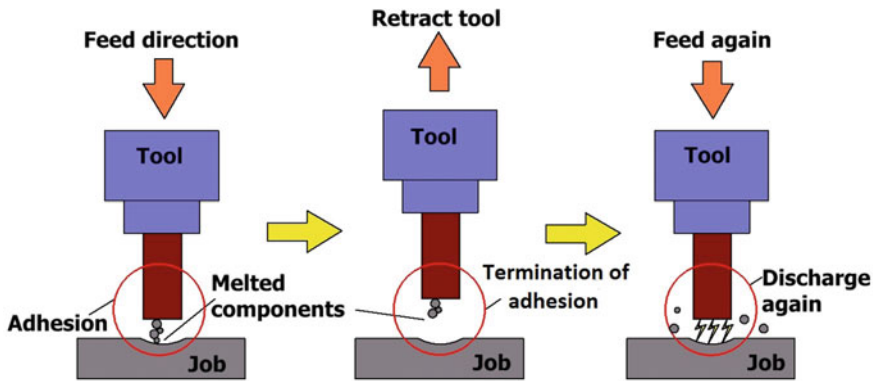


Fig. 8.2 Influence of adhesion on the stability of machining

short circuits by reducing the frequent adhesion with the workpiece electrode. Again, giving vibration to the tool, increment of the discharge pulse frequency is possible which directly reduces the table feeding-back action. This leads to the decrement of the time of machining and improves the stabilization of the spark discharge current.

High-frequency vibration with the constant amplitude of vibration leads to lesser machining time, this implies the flow of small debris particles, and the recovery from the contact is more proficient in the high-speed extension and reduction of the piezoelectric. However, amplitude of the vibration has less influence on the hindrance of contact of two electrodes as well as on the short circuit. As an example, at frequencies of 100 Hz and 1 kHz with 1  $\mu\text{m}$  of amplitude, the machining time is shorter for 1 kHz than 100 Hz. Further decrement of the time taken for machining can be possible with the increment of amplitude of the vibration, i.e., at 1 kHz of frequency and the amplitude of 1.5  $\mu\text{m}$ . Again, with the comparison with the perpendicular and parallel vibration, perpendicular vibration is more responsible for lower machining time than the other [5].

#### (ii) Influence of vibration on the efficiency of machining, electrode wear, and MRR

As the blending phenomena at the vicinity of sparking zone is improved with the higher amplitude which is responsible for good removal of the flushing of small debris particles as well as enhancement of the efficiency of machining. The proficient flushing also helps to decrease irregular sparks, thus reducing the tool wear. Hence, higher amplitude of vibration leads to elevated machining rate with lesser tool wear. Further increase may cause a collision between the electrode and the workpiece, which terminates the machining. At larger amplitude of vibration in the horizontal direction also affect the dimensional accuracy of the machined profiles.

For the vibratory tool, improvement of removal of debris from the spark gap can be possible due to the pressure change at the narrow gap, as a result continuous supply of fresh dielectric into the narrow spark gap. The amount of recast layer deposited on

the machined surface also reduces with the aid of vibration. As a result, a significant amount of enhancement of MRR is possible in case of micro-EDM process with aid of vibration with compare to normal  $\mu$ -EDM process. Again, in micro-EDM process, due to the initial lower discharge energy, resolidification of the molten metal on the workpiece occurs, which is the root cause to decrease in MRR. Vibration to the tool increases the discharge energy within a single discharge which accomplished into the small machining gap and causes the MRR to increase.

### 8.3.1.2 Vibration to the Workpiece

At the time of  $\mu$ -EDM, vibration is useful when it applies to the tool electrode as well as to the job electrode and in both the cases there is a chance for improving the machining condition. The adhesion of solidified molten debris in the tiny spark gap causes arcing which frequently occurs as well. Increment of material removal rate, fabrication of high aspect ratio machine cavities, enhancement of immovability of the process, lessening of short circuit and arcing and influence of frequency and amplitude of the vibration, etc., can be possible with the assistance of vibration when it applies to the workpiece. Improvement of flushing conditions and the better removal of particles from the tiny spark gap are the root cause of those possibilities of improvements. Enhancement of flushing ability of resolidified molten metal from the vicinity of the machining zone and simultaneously changing the pressure in the narrow spark gap lead to more number of effective sparks which results in increment of material removal rate [2].

Figure 8.3 exhibits the control mechanism for  $\mu$ -EDM with aid of workpiece vibration. A sine wave is generated by the signal generator with the specified amplitude and frequency to the piezoelectric power supply which impels the piezoelectric actuator as per the requirement of workpiece vibration. With the help of monitoring module, the online feedback control system for the spark gap is achieved. In servo mechanism of the tool, the feedback signal of the tool is sent into the power unit for the comparison of this with the value of predefined position. The motion of the X-Y bench is recognized by the CNC programming in the CAD/CAM software by interpolation, simulation and planning of pre-identified tool path. To reduce error in machining due to the wear from the sidewall of the tool and the error in positioning of the X-Y bench and the predefined paths are planned with forward and backward motion. Hence, tool electrode and the X-Y worktable can be controlled separately. Predefined milling layer depth depends on the speed at which the tool moves, energy state of the spark as well as state of the spark discharges.

#### (i) Effect of workpiece vibration on MRR, TWR, and taper angle

The influence of ultrasonic power with various gap current values on rate of material removal, tool wear rate, and taperness has been studied by the researchers, and corresponding effect of with and without vibration is noted as shown in Fig. 8.4 [6]. From Fig. 8.4a, it can be seen that rate of material removal decreases a little when gap current is higher with the application of vibration and followed by it increases. It has

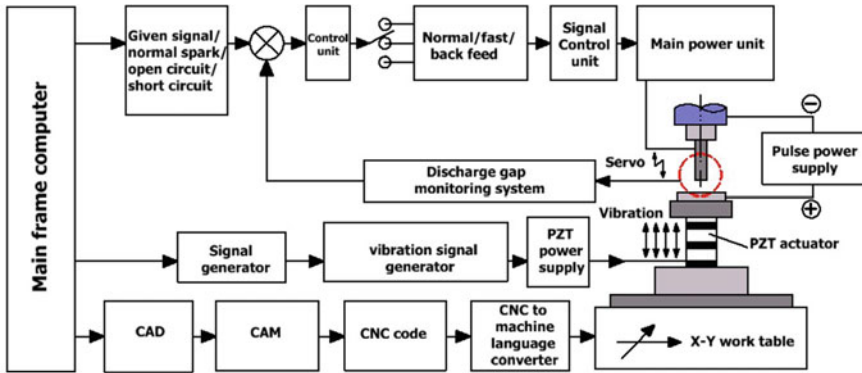
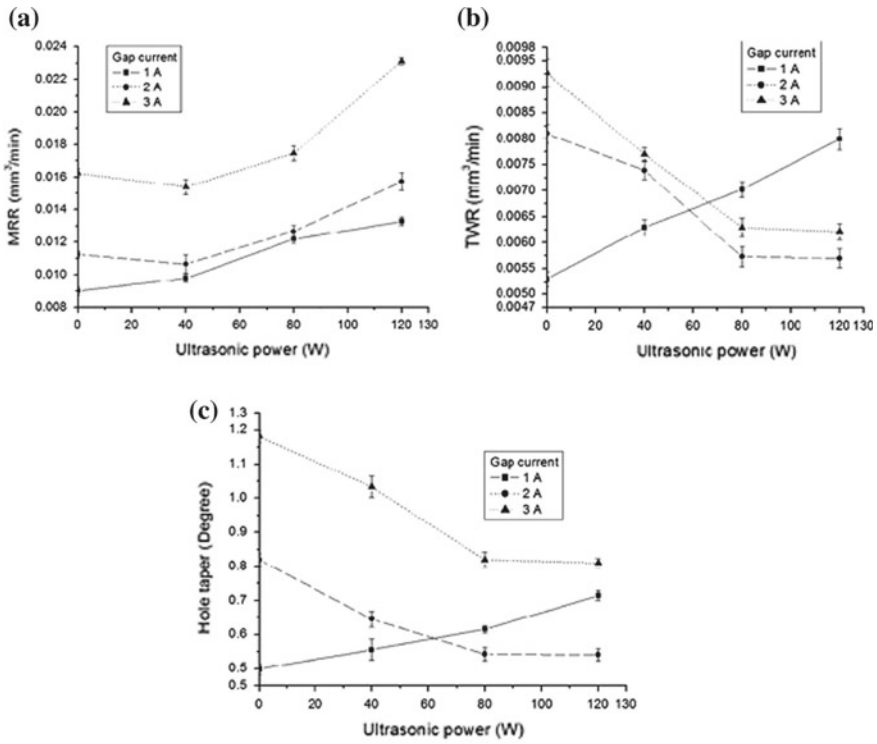


Fig. 8.3 Details of a control mechanism for  $\mu$ -EDM with aid of workpiece vibration

been increased gradually at 1 A of gap current. At 1 A gap current, it has been also seen from the figure that from 0 to 40 W, 40 to 80 W, and 80 to 120 W rate of material removal increases by 8.88, 24.53, and 9.11%, respectively. In the beginning, from 0 to 40 W of ultrasonic power, rate of material removal decreases by 5.31% with gap current of 3 A, followed by it enhances by 13.54% when the ultrasonic power changes from 40 to 80 W and again from 80 to 120 W, and it enhances considerably by 31.43% because of good removal of flushing of debris from the narrow spark gap with the application of high-frequency vibration. From the figure, it can also be seen that up to 40 W of ultrasonic power with large value of gap current, material removal rate is decreased a little and then it increases. The reason behind that at high current, inactive pulses as well as short-circuits increases significantly and flushing with very low amount of ultrasonic power is not sufficient to remove the tiny particles from the narrow spark gap during micro-EDM.

From Fig. 8.4b, it can be observed that a higher value of gap current is responsible for reducing tool wear rate when ultrasonic power increases. At 3 A of gap current, from 0 to 40 W and from 40 to 80 W of ultrasonic power, tool wear rate decreases by 16.92 and 18.27%, respectively, and beyond 80 W of ultrasonic power, a little decrement of tool wear rate has been observed. With the increment of ultrasonic power, amplitude of vibration also increases, which leads to improvement of the dielectric flushing by pumping action to the job and dielectric results in reducing short-circuiting, arcing as well as secondary discharges; thus, tool wear rate condenses at a higher value of gap current. Again, due to low discharge energy at lower value of gap current, short-circuiting and arcing are significantly reduced; thus, tool wear rate is gradually amplified. However, a higher value of ultrasonic power leads to good removal of flushing which results in continuous increment of rate of tool wear.

From Fig. 8.4c, it can also be seen that hole taper reduces with ultrasonic power. It can be seen that from 0 to 40 W of ultrasonic power, the hole taper drastically reduced by 13.39%; however, it decreases by 11.25% with 40–80 W. The amplitude



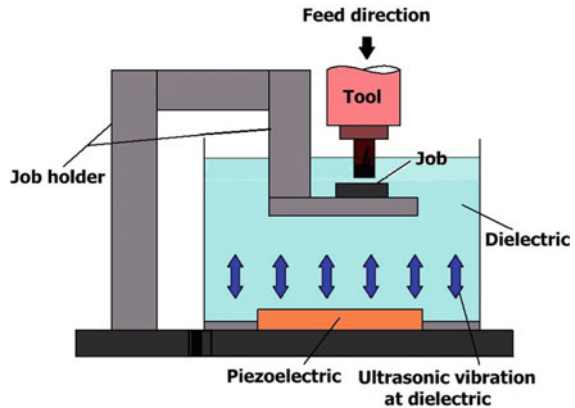
**Fig. 8.4** Influence of ultrasonic power on **a** material removal rate, **b** tool wear rate, and **c** taperness for different values of gap current at  $T_{on} = 6 \mu s$  and  $T_{off} = 20 \mu s$  [6]

of vibration increases with the increment of ultrasonic power leading to improvement of flushing at the vicinity of the narrow machining zone as well as spark gap, and that is the reason behind the decrement in taperness of the micro-hole. However, at gap current of 1 A, taperness of the micro-hole has been increased due to the combined effect of low discharge energy and superior flushing condition with the ultrasonic vibration [6].

### 8.3.1.3 Vibration to the Dielectric

Generally, vibration to the dielectric is given when powder-mixed electrolyte is used during micro-EDM. During  $\mu$ -EDM processes, giving ultrasonic vibration to the dielectric fluid can be a best alternative option instead of using stirrer [7]. Stirrer is used effectively to the dielectric tank to spread the powder throughout the dielectric fluid, and it restricts the deposition of the powder in the underneath of the dielectric tank. However, stirrer has its own limitation that it cannot prevent the powder from agglomeration. It is not suggested to introduce straight or indirect flushing due to

**Fig. 8.5** Schematic of ultrasonic vibration at dielectric fluid



the use of fragile micro-tool and flushing flow; hence, stirrer can also be capable to retain the dimensional accuracy during  $\mu$ -EDM process. The main purpose for introducing high-frequency vibration to the dielectric fluid is not only to overcome the accumulation of micro-powder particles at the underneath of the dielectric tank but also to enhance the kinetic energy of tiny debris particles. For this reason, better removal of debris from the narrow spark gap is possible which results in a least amount of short circuits taking place during spark discharge. Again, another aspect of giving vibration to the dielectric is it is cost-effective than giving vibration at the tool electrode or to the job electrode. The main reason for using ultrasonic bath is to avoid accumulation and deposition of the powder in the underneath of the tank however; principally, any kind of commercial high-frequency bath can also be utilized to vibrate the dielectric fluid as shown in Fig. 8.5. Normally, in ultrasonic bath, frequency range of vibration is kept in the order of 40–45 kHz for increasing the kinetic energy of debris particles and the value of frequency cannot be unaltered during machining.

**(i) Effect of dielectric vibration on MRR, TWR, and average tool feed rate**

Ultrasonic vibration at the dielectric fluid is a major aspect for enhancing the removal rate of the workpiece material. In  $\mu$ -EDM, to prevent the deposition of the powder at the underneath of the dielectric reservoir and for better circulation of powder, it is required to give high-frequency vibration to the dielectric fluid. Generally, high-frequency vibration is introduced to the base of the ultrasonic bath and due to this reason powder does not reconcile at the base of the ultrasonic bath and homogeneously mixed throughout the dielectric. As the flow of powder between the tool and the job supports the debris removal process, it improves the rate of removal of the material. Again, the chance for enhancement of material removal rate is increased as the ultrasonic vibration is giving to the dielectric fluid and decreases the chances of adhesion due to the debris which otherwise sticks to the job. It has been seen by the researchers that, in the same machining condition when assisting high-frequency

vibration to the dielectric fluid, rate of removal of material increases compared to machining without ultrasonic vibration [7].

In case of  $\mu$ -EDM, tool wear is higher than conventional EDM process in addition to other non-conventional processes. In any  $\mu$ -machining processes, tool wear should be taken into account as far as machining accuracy and cost are concerned. In micro-EDM, machining speed is pretty low comparing with other thermal machining processes due to the unwanted short circuit and arcing [2]. These short circuits and abnormal discharges mainly occur due to the difficulty of debris removal from the vicinity of the narrow spark gap. So far, in order to overcome this problem in EDM process, several techniques have been proposed. Researchers have already reported that the influence of ultrasonic vibration to the machining performances when it applies to the tool electrode [3, 4], to the workpiece [5, 8]. or to the dielectric fluid [7]. With the assistance of vibration, it not only helps to circulate the dielectric fluid but also helps to get rid of the tiny debris particles from the narrow spark gap width by reducing abnormal discharges, short circuits, and arcing. So, for achieving higher machining speed with high accuracy, high-frequency vibration to the dielectric fluid in  $\mu$ -EDM can be successfully applied [9].

In addition, vibration to the dielectric fluid produces stirring effect of the dielectric and leads to homogeneous distribution of debris particles in the narrow spark gap which results in lessening the chances of short circuits and irregular spark discharges; therefore, machining speed increases. It has been reported by the researchers that the 90% of machining time is reduced by applying vibration to the dielectric fluid [9].

### ***8.3.2 Effects of Low-Frequency Vibration***

Generally, low-frequency vibration should be in the range of 1–999 Hz or it is less than 1 kHz. Researchers have proved that sometime low-frequency vibration is more helpful than the high-frequency vibration because its low level of discharge energy makes it more appropriate for improving both the process characteristics and accuracy of the micro-hole in micro-EDM. Normally, low-frequency vibration is given to the workpiece instead of given to the tool or dielectric because of its effectiveness and process simplicity.

A simple vibration device with very simple mechanism can be able to create low-frequency vibration in the workpiece. A schematic representation of the whole vibratory system is shown in Fig. 8.6. Here, some rotary vibrators are used as actuator and vibration is produced due to its unbalanced mass. The working principle of the system is plain but efficient and cost-effective. The job holding device is fixed to the vibratory system, and when the power switch is set on, the job holding device vibrates with the same amplitude and frequency of the motors in the vertical direction [10].

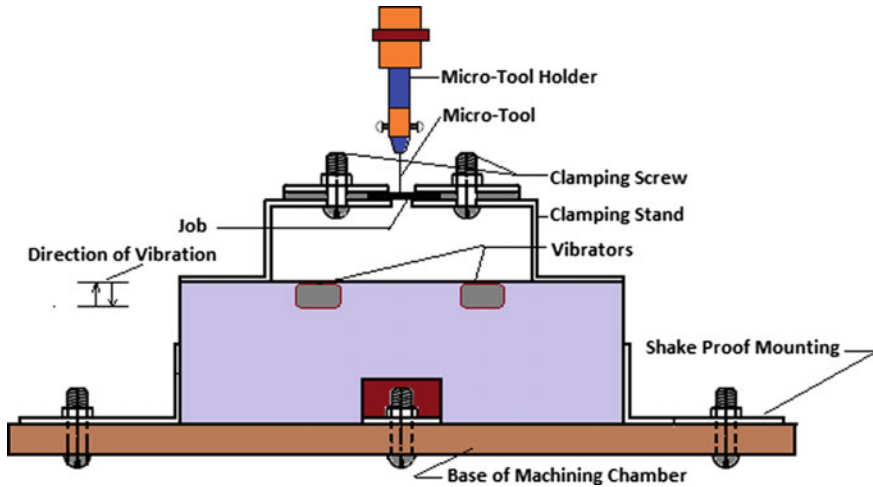


Fig. 8.6 Schematic of the whole vibratory system [10]

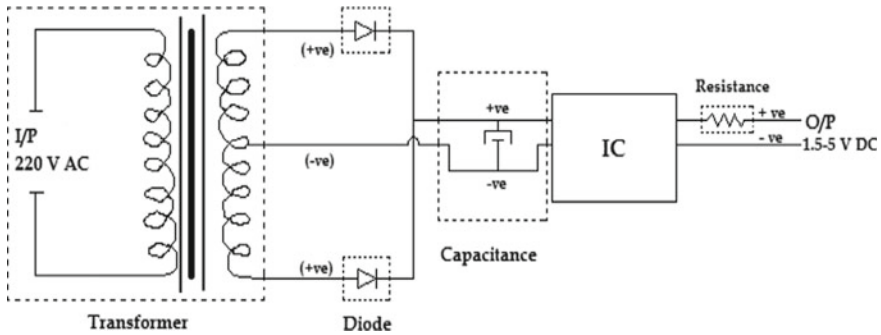
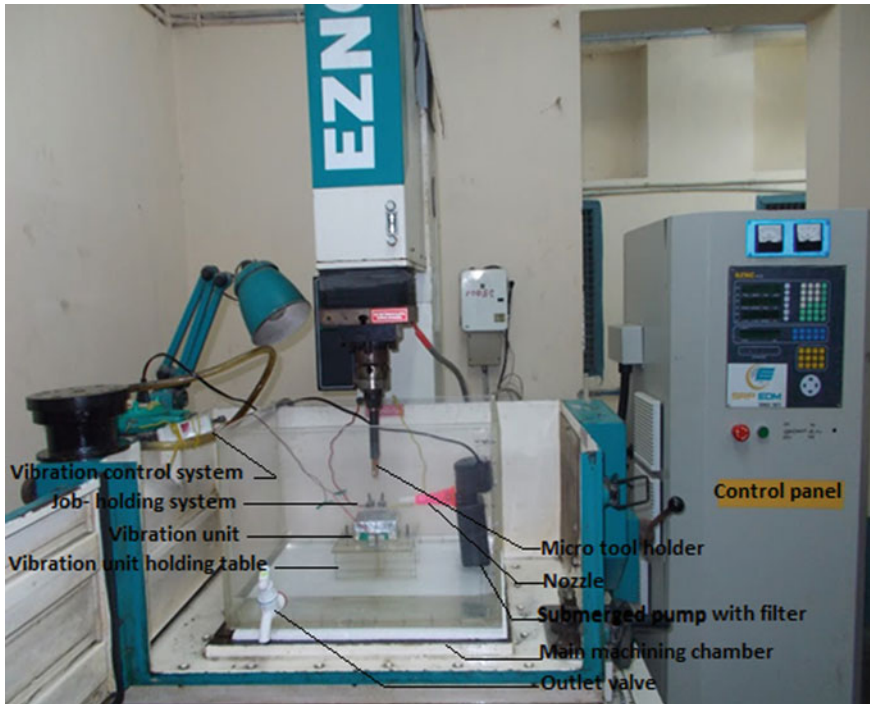


Fig. 8.7 Representation of circuit used in the vibratory unit to regulate output voltage and vibrational characteristics [10]

Those vibrating motors run with 4–6 V DC, so it is best suitable to run with 4 V DC battery. But, during running condition, battery discharges continuously with time and for this reason vibrational amplitude and frequency also diminish with the time. So, in order to fix this issue, an electrical circuit as depicted in Fig. 8.7 should be incorporated into the vibratory system to regulate output voltage and vibrational characteristics as desired. With this circuit, a 220 V AC (input) is converted to 4 V DC (output), and with the variation of output voltage, vibrational amplitude as well as frequency also varies. Here, in this vibratory system, the nature of vibration is sinusoidal. A photographic view of in-house developed micro-EDM setup with aid of low-frequency vibration is depicted into Fig. 8.8 [10].

Another very simple and effective way to induce vibration to the workpiece is when an electromagnet is used as an actuator. With the aid of a power tran-





**Fig. 8.8** Photographic view of micro-EDM system with aid of low-frequency vibration. *Courtesy* Non Traditional Machining Lab-II of Production Engg. Dept., Jadavpur University, Kolkata

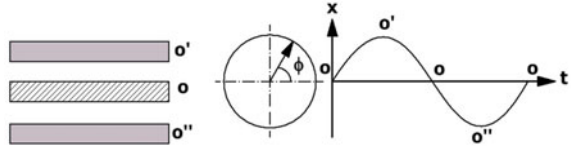
sistor switch, the electric power is supplied to the electromagnet periodically. By a frequency controllable pulse generator, the ON–OFF sequence of the power transistor is controlled. After turning ON the switch, the electromagnet is energized due to receiving power from the circuit which generates a dragging stroke at the vibration pad. The beams which are connected to just beneath the vibration pad are bend at that moment. When the electromagnet is de-energized, flexure beams release and press on the vibration pad to the upward position. With this technique, low-frequency oscillation is induced on the job electrode that is fixed on the top of the vibration unit [11].

#### (i) **Modeling in micro-EDM with vibrating workpiece**

In this section, the modeling in micro-EDM with workpiece vibration has been discussed. From this section, it can be stated that low-frequency vibration is more suitable for removal of debris particles rather than ultrasonic vibration. It can also be understood that the actual reason behind the improved flushing of small debris particles from the narrow spark gap with the assistance of vibration. Improvement of the flushing of dielectrics during micro-EDM, and amplitude and frequency of



**Fig. 8.9** Correlation in between time and displacement of a vibrating workpiece



the vibration and phase angle are the main contributing factors [11]. To postulate the theoretical model, the following are some basic assumptions:

- (i) Vibration always follows a simple and pure harmonic path.
- (ii) The job electrode is kept absolutely in the horizontal position.
- (iii) Direction of the vibration is totally vertical to the job electrode.
- (iv) Debris elements also vibrate with the same amplitude and frequency, velocity and acceleration of the vibration.
- (v) There is no electrical field and sparking force act in the vicinity of the machining zone.

**(a) Mathematical representation of the system**

The correlation in between time and displacement of a vibrating workpiece is shown in Fig. 8.9. The displacement of vibrating workpiece,  $x$  at any instantaneous position of the workpiece, is as follows:

$$x = a \sin \omega t + \varnothing \tag{8.1}$$

where,  $a$  is the amplitude of vibration in  $\mu\text{m}$ ,  $\omega$  is the angular frequency in  $\text{rad/s}$ , and is equal to  $2\pi f$ .  $f$  is the frequency of vibration in  $\text{Hz}$ ,  $t$  is the time in second, and  $\varnothing$  is the phase angle in rad. Then, the velocity and the acceleration of the workpiece at particular point are as follows:

$$\dot{x} = a\omega \cos(\omega t + \varnothing) \tag{8.2}$$

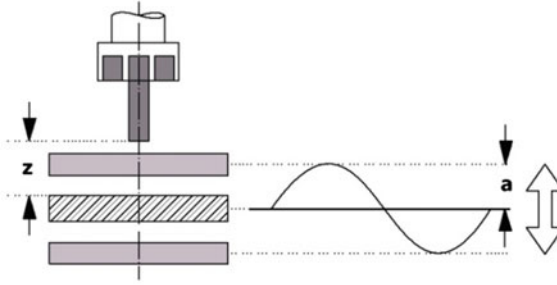
$$\ddot{x} = -a\omega^2 \sin(\omega t + \varnothing) \tag{8.3}$$

Let us consider the utmost acceleration positions of the job electrode are at  $O'$  and  $O''$  positions, and then, utmost acceleration can be written as:

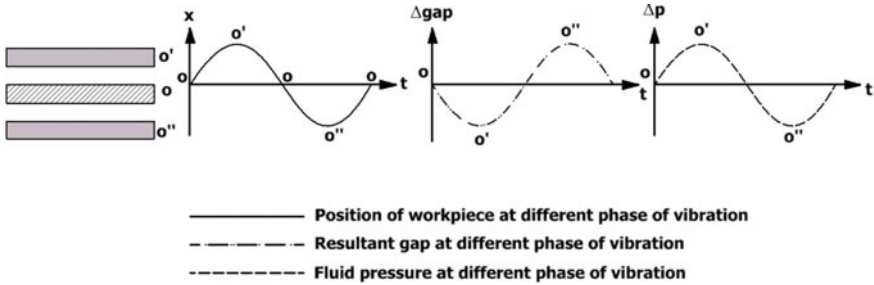
$$\ddot{x}_{\text{max}} = \pm a\omega^2$$

As  $O'$  and  $O''$  the utmost acceleration positions of the job electrode, thus, at that positions,  $\sin(\omega t + \varnothing)$  is equal to 1 and therefore the equation can be expressed as follows:

$$\ddot{x} = \pm a\omega^2 \sin(\omega t + \varnothing) \tag{8.4}$$



**Fig. 8.10** Vibration-assisted micro-EDM process



**Fig. 8.11** Gap distance and fluid pressure within the gap in micro-EDM with aid of vibration

**(b) Gap distance and gap fluid pressure in  $\mu$ -EDM with aid of vibration**

A representation of the workpiece vibration during  $\mu$ -EDM process has been depicted in Fig. 8.10. Figure 8.10 shows the deviation of location of the job electrode, distance, and pressure of fluid in the gap at the time of  $\mu$ -EDM process. Then, the equivalent, highest, and lowest gap distance can be written as follows:

$$\Delta\text{gap} = z \pm a \tag{8.5}$$

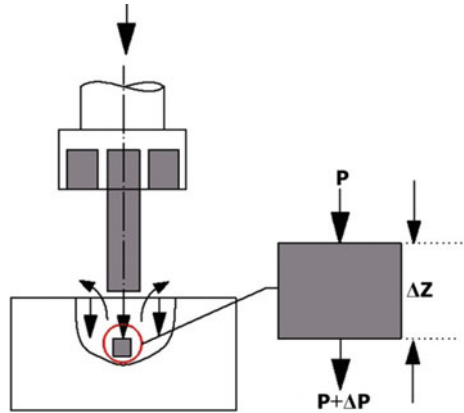
$$\Delta\text{gap}_{\text{max}} = (z + a) \text{ at } O'' \tag{8.6}$$

And,

$$\Delta\text{gap}_{\text{min}} = (z - a) \text{ at } O' \tag{8.7}$$

In Fig. 8.11, it can be seen that at the time of upward movement of the workpiece, i.e., at  $O''$  position, the equivalent gap distance shortens. Due to this, pressure of dielectric fluid increases in the gap, and for this reason, fluid ejects from the sidewall of the tool which directly influences for flushing out the debris particles from the vicinity of the narrow machined zone [11].

**Fig. 8.12** Pressures exerted on the micro-fluid cell



**(c) Modeling of the change in pressure in the gap at the time of vibration**

During  $\mu$ -EDM, micro-fluid cell in the dielectric feels some amount of stress due to the decrement of gap distance as shown in Fig. 8.12. Then, the pressure exerted by the micro-fluidic cell in the vicinity of the narrow gap distance can be expressed as follows:

$$P \cdot S + \Delta G - (P + \Delta P)S = F \tag{8.8}$$

Here,  $\Delta A$  and  $\Delta Z$  are the cross-sectional area and the height of the micro-fluidic cell.  $S$  is the total cross-sectional area,  $\Delta P$  is the change in pressure,  $\Delta G$  is the change of force for gravity  $g$ , and  $F$  is the resultant force exerted on micro-fluid cell. If,  $\Delta G = (\Delta m)g$ ,  $\Delta m = \rho \cdot S \cdot \Delta z$  and  $F = (\Delta m)\ddot{x}$

then, Eq. (8.8) becomes as follows:

$$P \cdot S + (\Delta m)g - P \cdot S - \Delta P \cdot S = (\Delta m)\ddot{x} \tag{8.9}$$

And difference in fluid pressure  $\Delta P$  can be expressed as

$$\Delta P = \rho \cdot \Delta z (g - \ddot{x}) \tag{8.10}$$

As the micro-fluidic particle vibrates at the similar frequency and amplitude of the workpiece, thus the acceleration can be expressed from Eq. (8.4) as follows:

$$\ddot{x} = \pm a\omega^2 \sin(\omega t + \varnothing)$$

Therefore, combining Eqs. (8.4) and (8.10),  $\Delta P$  can be written as:

$$\Delta P = \rho \cdot \Delta z [g \pm a\omega^2 \sin(\omega t + \varnothing)] \tag{8.11}$$

If  $c = a\omega^2 \sin(\omega t + \varnothing)$ , then Eq. (8.11) becomes

$$\Delta P = \rho \cdot \Delta Z(g \pm c) = \rho \cdot \Delta z \cdot g(1 \pm c/g) \quad (8.12)$$

From Eq. (8.12), it can be stated that the value of  $\Delta P$  is always positive when the  $c/g$  value is less than 1; thus, the pressure does not alter from time to time and there is no effect of vibration achieved during machining. On the contrary, if the value of  $c/g$  is greater than 1, then the value of  $\Delta P$  is altered with the movement from the mean position of the workpiece. So, for improvement of the flushing process by periodical suction and discharge in the vicinity of the narrow working gap, the value of  $c/g$  should be always kept more than unity.

### (ii) Effects of low-frequency vibration on various responses of $\mu$ -EDM

In micro-EDM, material is removed not only from the workpiece but also from the tool and size and shape of micro-hole is just a replica of that micro-tool. Therefore, in this section, six  $\mu$ -EDM performance characteristics, i.e., metal removal rate (MRR), tool wear rate (TWR), over cut (OC), taperness, roundness, and machining gap (MG), have been considered. The method of calculating and the effects of low-frequency vibration on these performance criteria are described as follows:

#### (a) Influence of vibration on MRR and TWR

Rate of metal removal in  $\mu$ -EDM is defined as the amount of metal removed from the workpiece per unit time and usually expressed as given below in  $\mu\text{g}/\text{min}$ . It has been calculated by the weight loss of the workpiece per unit time.

$$\text{MRR} = \frac{W_{\text{bw}} - W_{\text{aw}}}{t} \text{ (mg/min)}. \quad (8.13)$$

where

$W_{\text{bw}}$  is weight of the workpiece before machining (mg),  
 $W_{\text{aw}}$  is weight of the workpiece after machining (mg), and  
 $t$  time taken for machining

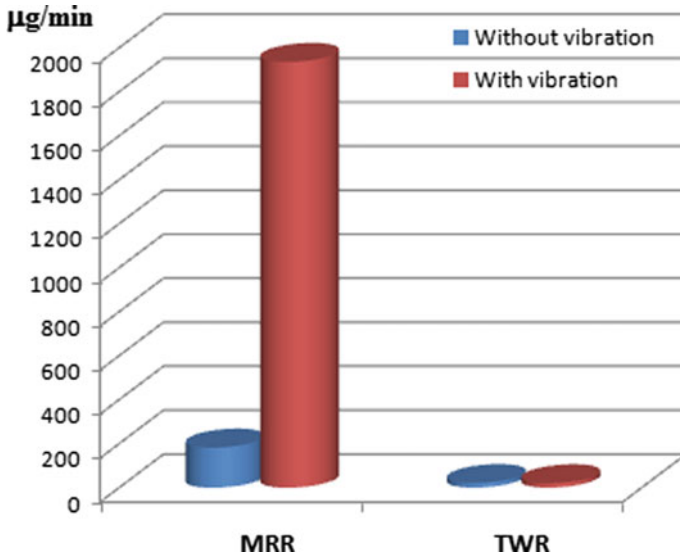
Tool wear rate in  $\mu$ -EDM is defined as the amount of metal eroded from the tool per unit time, and it is usually expressed as given below in  $\text{mg}/\text{min}$ .

$$\text{TWR} = \frac{W_{\text{bt}} - W_{\text{at}}}{t} \text{ (mg/min)}. \quad (8.14)$$

where

$W_{\text{bt}}$  is mass of the tool before machining (mg),  
 $W_{\text{at}}$  is mass of the tool after machining (mg), and  
 $t$  time taken for the operation

A comparative study has been shown in Fig. 8.13, and the experiment conducted at the multi-objective optimized machining condition is deduced from gray Taguchi analysis, i.e., with  $-ve$  polarity, 2 A current, vertical direction of flushing, and 3  $\mu\text{s}$



**Fig. 8.13** Effect of vibration on MRR and TWR at  $t = ve'/2A/V/3 \mu s$

of pulse on time. From Fig. 8.13, it can be observed that with the aid of low-frequency vibration to the workpiece, there is a significant improvement of material removal rate compared to tool wear rate. It may be stated that after applying vibration, machining stability can be enhanced by the reduction in abnormal discharges, short circuits, and arcing. Whereas a higher value of amplitude of vibration leads to more frequent contact in between two electrodes, thus short circuiting and arcing increase. It has been seen that for machining micro-holes, the normal spark discharges enhance with the aid of workpiece vibration during  $\mu$ -EDM and this phenomenon plays a crucial role for increasing metal removal rate by reducing machining time and also reduces tool wear rate. Again, it has been seen that discharge ratio also improves due to the application of vibration for the enhancement of flushing process which again plays a vital role for increasing MRR.

**(b) Influence of vibration on OC and MG**

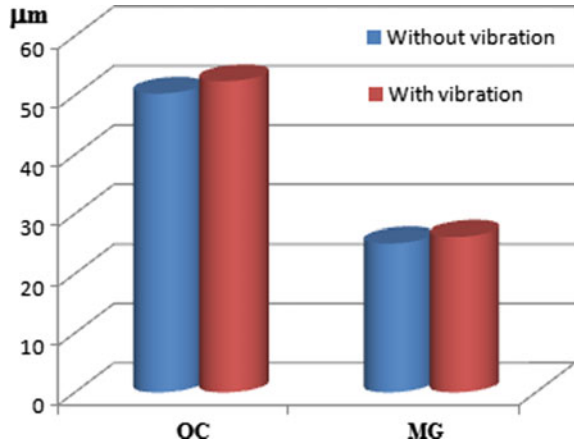
Overcut is the additional amount of material removed by the tool during micro-EDM drilling operation. It is the diametrical deviation in between the micro-EDM machined hole and the tool. The overcut is calculated as follows:

$$OC = \frac{\sum D}{N} - d_T \tag{8.15}$$

where

- $D_i$  micro-hole diameter at  $i$ th section ( $\mu m$ ),
- $d_T$  tool diameter ( $\mu m$ ), and

**Fig. 8.14** Effect of vibration on OC and MG at  $'-ve'/2A/V/3 \mu s$



$N$  number of measurements

In  $\mu$ -EDM drilling, the machining gap is the differences in space from the wall of micro-hole to the surface of tool. This space distance is mainly comprised of critical space distance and the discharge space distance. Critical space distance is the distance from the dielectric fluid at which dielectric starts to break down and sparks begin. Discharge space distance is nothing but the machining depth of the drilled micro-hole. Hence, machining gap (MG) has been calculated by the equation as follows:

$$MG = \frac{1}{2} \left[ \frac{D + d}{2} - d_T \right] \quad (8.16)$$

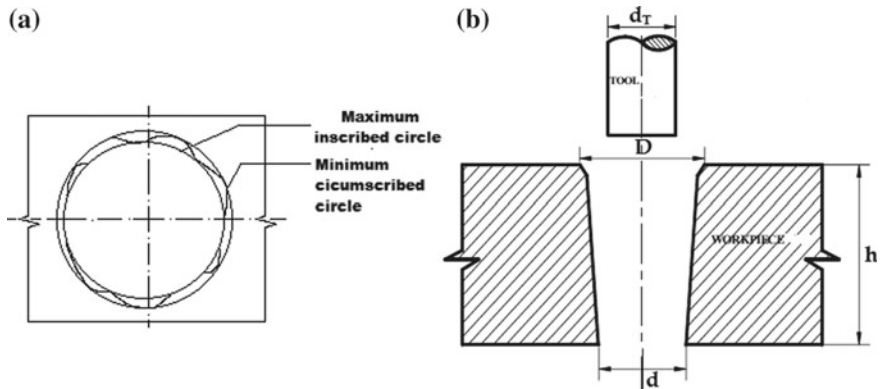
where

$D$  is the diameter of micro-hole at entry ( $\mu m$ ),  
 $d$  is the diameter of micro-hole at exit ( $\mu m$ ), and  
 $d_T$  is the diameter of the tool ( $\mu m$ )

From Fig. 8.14, it has been observed that there is a slight increment of OC and MG with the effects of vibration. So, vibration has a slightly negative impact on overcut and machining gap. It is due to the combined effect of vertical flushing and longitudinal vibration. Debris particles are not get removed from the micro holes which creates a secondary sparking (arcing) and that arcing increases the hole size of drilled micro-holes.

### (c) Influence of vibration on taperness and roundness

Generally, for drilled micro-holes, taper angle has been calculated by Eq. (8.17) and Fig. 8.15.



**Fig. 8.15** Schematic view of micro-drilled hole: **a** top view of drilled micro-hole and **b** cross-sectional view of drilled micro-hole

$$\text{Taperness} = \frac{(D - d)}{2h} \times \frac{180}{\pi} \text{ (Degree)} \quad (8.17)$$

where

$D$  is micro-hole diameter at entry side ( $\mu\text{m}$ ),

$d$  is average micro-hole diameter at exit side ( $\mu\text{m}$ ), and

$h$  is the width of the plate

In the  $\mu$ -EDM drilling for entrance and exit hole, roundness is defined by the maximum inscribed circle diameter to the minimum circumscribed circle diameter. The value of roundness should be always in between 0 and 1. The value of roundness closer to one indicates that the hole is also closer to a true circle. For an exact circular hole, the roundness value should be always one. So, the value of roundness is calculated by the ratio of maximum inscribed circle of the hole at entry/exit side to minimum circumscribed circle diameter of the hole at entry/exit side as depicted in Fig. 8.15.

From Fig. 8.16 it is seen that taperness has been slightly deteriorated but the roundness has been improved significantly for the effects of vibration. The reason behind this is the surface achieved by  $\mu$ -EDM with aid of vibration at the said parameters combination is comparatively finer and free of burrs.

### 8.3.3 *Effects of Inclined Feeding with Low-Frequency Vibration*

In micro-EDM drilling with inclined feeding and low-frequency vibration, both the tool and job are kept inclined with some definite angle. Machining can be possible by giving feed to the electrode by keeping either inclined downstairs or else inclined

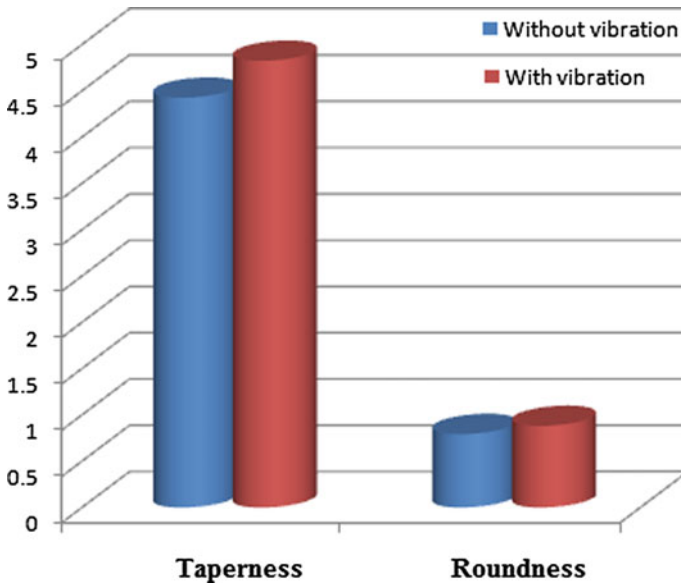


Fig. 8.16 Effect of vibration on taperness and roundness at  $-ve' / 2A/V/3 \mu.s$

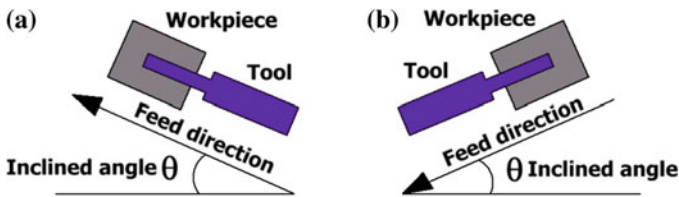


Fig. 8.17 Schematic of inclined feeding mechanism a upward and b downward

upstairs as shown in Fig. 8.17. Generally, while feed is giving to the downward inclined position, it assists stream of the dielectric fluid into the spark area, but it cannot help for removal of debris. However, it is anticipated that the debris should be ejected from the machined zone without any difficulty. In case of downward inclined feeding, debris can be ejected from the machining gap with the help of bubbles evacuation and due to the buoyancy force. Due to the pressure difference in upward inclined feeding, the spark gap can be void which leads to flow of dielectric into the machining gap. Due to the accumulation of bubbles at the underneath of the machined zone, the movement of the debris and dielectric can be delayed and sometimes can be more complex. For simplicity of understanding, the angle for upward inclined feeding is indicated as positive and the angle for downward inclined feeding is indicated as negative as shown in Fig. 8.17a, b, respectively.



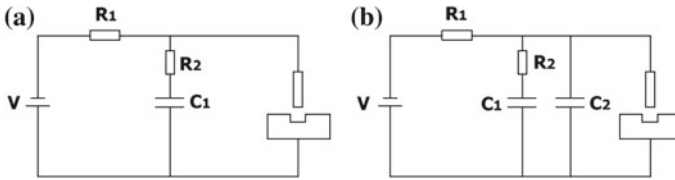
When vibration is useful at same parameter settings, the inefficient pulses decreased considerably in addition to it surface become very fine with comparatively lesser craters produced.

A traditional three-axis  $\mu$ -EDM machine is tailored in order to intend the inclined feeding in the micro-EDM drilling system. On the Z-axis of the stage, the drilling head with a preferred inclined angle is attached. The job electrode should also be kept inclined with the same angle so that the surface of the job electrode is vertical to the tool electrode axis. The inclined feeding motion can be achieved by appropriate controlling of the relative motions in between X- and Z-axis stages. A PZT actuator is attached at the end of the spindle head for putting together vibration to the tool electrode. A function generator is allied with the actuator through the controller, thus, the system can supply axial vibration with any waveform with the higher frequency and amplitude [12].

### 8.3.4 Self-adaptive Control in Micro-EDM

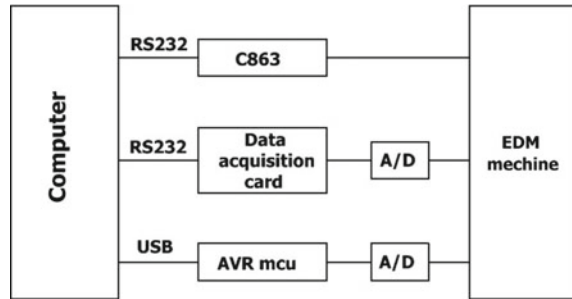
Although  $\mu$ -EDM is originated from traditional EDM, there are several similarities and dissimilarities. Alike to conventional EDM, micro-EDM has no cut force and for this reason, the apparatus is uncomplicated and its control mechanism is also very easy. In the machining method of EDM, spark between electrode and workpiece is responsible for removing materials from the workpiece in the form of tiny particles. However, in micro-EDM, burdens like very low operating voltage, small discharge gap and the very narrow pulse width still exist. EDM process is not so stable due to the difficulty to eliminate tiny particles from the narrow spark gap which leads to arc discharging as well as short circuit at the time of micro-EDM operation. So, to resolve these burdens, vibration can be incorporated into the workpiece, tool as well as dielectric during EDM operation. With the assistance of vibration, electrical erosion in the form of tiny particles can easily be removed; however, it may also lead to frequent arcing and short circuit which results in difficulty for controlling of micro-EDM process. Thus, quality of the machined profile as well as machining efficiency cannot be ensured. So, to resolve these issues, a new type of micro-EDM technique is introduced [13]. This new system is unlike to the conventional  $\mu$ -EDM where, sensing the discharge conditions, it can recognize the self-regulation. Accordingly, the stability of spark discharges, electrode wear ratio, and the effectiveness of  $\mu$ -EDM machining is improved to a large extent compared to the conventional  $\mu$ -EDM. An equivalent circuit for self-adaptive  $\mu$ -EDM is depicted in Fig. 8.18a. As in this circuit, actuator cannot allow a high current so, a series of resistance are incorporated. These act as a shield and protects from damage due to large current and thus this actuator acting an crucial role in the circuit by acting as a capacitance. In Fig. 8.18b, an improved circuit is shown and the capacity of this actuator is fixed.

The self-adaptive control in  $\mu$ -EDM system comprises of several subsystems, e.g., servo control system, spindle, two electrodes, working table, piezoelectric, the base of the machine, data acquisition system, and a mainframe computer. The servo



**Fig. 8.18** Equivalent circuit

**Fig. 8.19** Control system for the self-adaptive  $\mu$ -EDM



system is based on PI-based nano-position system with C863 microcontroller which not only controls the movement of the three axes but also senses the velocity and position of the axis followed by sending them to the mainframe computer. The control system for self-adaptive micro-EDM is shown in Fig. 8.19. During micro-EDM, the servo system impels the working table and tool to the accurate place. If any inconveniences occur, it sends back the error signal to computer. To sense the voltage in between the tool and the job and also to realize the insight into the machine, a simple analog-to-digital circuit is used. The function of the microcontroller is to examine that analog-to-digital circuit, and it sends a signal to stop the axis when the voltage tends to zero. The data acquisition card is used to detect the discharge status during micro-EDM. The advantages of incorporation of self-adaptive control in the micro-EDM system are as follows:

(i) **Reduce short circuit by the system**

In self-adaptive control in  $\mu$ -EDM, the piezoelectric is normally kept paralleled with the tool electrode and the job electrode. At the time of short circuits, the voltage between the tool and the job electrodes is reduced and gradually reduces to zero which is also the consequent voltage of piezoelectric. As the voltage of the piezoelectric actuator is reduced to zero, it shrinks and make the workpiece down by increasing the distance between the job and the tool electrode and it continues until the short circuit is terminated.

(ii) **Improvement of stability of the process**

With the self-adaptive control in  $\mu$ -EDM, processing stability can be improved. With the help of self-adaptive principle by piezoelectric, constant sparks with no or

a few short circuits can be attained. A continuous waveform, uniform sparks, and the large distinction between two spark waveforms are achieved by the application of piezoelectric for self-adaptive control in  $\mu$ -EDM.

### (iii) **Improving process efficiency**

In traditional  $\mu$ -EDM, the servo feed control mechanism simply impels the tool in the feed direction when there is no spark and retracts the tool backward at the time of short circuit or arcing. With the help of self-adaptive control in  $\mu$ -EDM, feedback time can be reduced by sending commands to the system; thus, machining can be done even at a very low voltage. So, with the help of self-adaptive control, adjusting the discharge gap and eliminating the short circuit can also be possible by the system itself.

### (iv) **Reducing the tool wear**

An unavoidable circumstance in  $\mu$ -EDM is tool electrode wear, and the most influencing factors are electrode material, different process parameters, the dielectrics, etc. In EDM, abnormal tool wear rate increases at the short circuit or arcing condition. In self-adaptive micro-EDM, when the piezoelectric actuator contracts, the gap in between the tool and the job electrodes turns into larger which can accelerate the flow of working dielectric. Acceleration of the flow of dielectric leads to reduce the abnormal discharges and thus short circuit can be avoided as well as the decrement of abnormal electrode wear is possible.

## **8.4 Summary**

Vibration-assisted micro-EDM is established to be efficient in modern machining practices not only for enhancing the stability of the process and merit of the products but also for increasing machining stability by reducing machining time. The inflexibility of the job electrode influences the machining time, and it has been already revealed that the inflexibility of the job electrode should be concerned in favor of micro-EDM for deep-hole drilling. Micro-EDM process with aid of vibration is also useful to all the high precision machining procedures, and it can achieve machining of any complex shapes at the high speed, which is not easily obtained in conventional machining. In micro-EDM process with aid of vibration, increment of the discharge pulse frequency as well as reduction of feeding-back action of the table is possible. Low-frequency vibration also can be taken into account for improvement of various responses of micro-EDM. With the help of adaptive control in micro-EDM technique, not only short circuit but also processing stability can be eliminated by itself, and processing efficiency is improved. Moreover, a significant reduction in electrode wear could be observed. Proper mechanism of machining process employing vibration for the up-gradation of machining needs to be developed and further augmentation of the processes are yet to be studied in depth.

## References

1. Sundaram MM, Pavalarajan GB, Rajurkar KP (2008) A study on process parameters of ultrasonic assisted micro EDM based on Taguchi method. *J Mater Eng Perform* 17(2):210–215
2. Garna R, Schubert A, Zeidler H (2011) Analysis of the effect of vibrations on the micro-EDM process at the workpiece surface. *Precision Eng* 35(2):364–368
3. Abbas NM, Solomon DG, Bahari MdF (2007) A review on current research trends in electrical discharge machining (EDM). *Int J Mach Tools Manuf* 47(7–8):1214–1228
4. Srivastava V, Pandey PM (2012) Effect of process parameters on the performance of EDM process with ultrasonic assisted cryogenically cooled electrode. *J Manufact Process* 14(3):393–402
5. Endo T, Tsujimoto T, Mitsui K (2008) Study of vibration-assisted micro-EDM—the effect of vibration on machining time and stability of discharge. *Precis Eng* 32(4):269–277
6. Singh P, Yadava V, Narayan A (2018) Parametric study of ultrasonic-assisted hole sinking micro-EDM of titanium alloy. *Int J Adv Manuf Technol* 94(5–8):2551–2562
7. Prihandana GS, Mahardika M, Hamdi M, Wong YS, Mitsui K (2009) Effect of micro-powder suspension and ultrasonic vibration of dielectric fluid in micro-EDM processes-Taguchi approach. *Int J Mach Tools Manuf* 49(12–13):1035–1041
8. Huang H, Zhang H, Zhou L, Zheng HY (2003) Ultrasonic vibration assisted electro-discharge machining of microholes in Nitinol. *J Micromech Microeng* 13:693
9. Ichikawa T, Natsu W (2013) Realization of micro-EDM under ultra-small discharge energy by applying ultrasonic vibration to machining fluid. *Procedia CIRP* 6:326–331
10. Mishra K (2015) Investigation on the influence of vibration during micro-drilling of aluminium by electro-discharge machining process, PG dissertation, Jadavpur University, Kolkata, India
11. Jahan MP, Wong YS, Rahman M (2012) Evaluation of the effectiveness of low frequency work piece vibration in deep-hole micro-EDM drilling of tungsten carbide. *J Manuf Process* 14(3):343–359
12. Liao YS, Liang HW (2016) Study of vibration assisted inclined feed micro-EDM drilling. *Procedia CIRP* 42:552–556
13. Fu XZ, Zhang Y, Zhang QH, Zhang JH (2013) Research on piezoelectric self-adaptive Micro-EDM. *Procedia CIRP* 6:303–308

# Chapter 9

## Tool Wear Compensation in Micro-EDM



Rahul Nadda, Chandrakant Kumar Nirala and Probir Saha

**Abstract** This chapter accentuates the inherently persistent tool wear issue and its consequences in variants of micro-electro-discharge machining ( $\mu$ -EDM). The consequences can be seen in the terms of deterioration of precision of the micro-holes and productivity. Although, the tool wear is well explored in  $\mu$ -EDM and its variant processes, but a very limited efforts have been made to resolve this issue other side. A pulse discrimination system based-real-time tool wear compensation strategy in  $\mu$ -EDM is anticipated to be a possible technique to get rid of the tool wear issue in  $\mu$ -EDM drilling. In this regard, an approach which is basically a modification in the existing approach has been discovered and implemented to achieve the desired depth of the micro-hole(s). The proposed approach has been applied to two different work-tool material combinations and input parameters. The potentiality of the approach has been proven results by comparing it with that other trusted techniques like ‘uniform wear method’ (UWM).

**Keywords**  $\mu$ -EDM drilling · Micro-holes · Pulse discrimination system  
Real-time · Uniform wear method

---

R. Nadda · C. K. Nirala (✉)  
Department of Mechanical Engineering, Indian Institute  
of Technology, Ropar 140001, Punjab, India  
e-mail: [nirala@iitrpr.ac.in](mailto:nirala@iitrpr.ac.in)

R. Nadda  
e-mail: [rahulnadda74@gmail.com](mailto:rahulnadda74@gmail.com)

P. Saha  
Department of Mechanical Engineering, Indian Institute  
of Technology, Patna 801103, Bihar, India  
e-mail: [psaha@iitp.ac.in](mailto:psaha@iitp.ac.in)

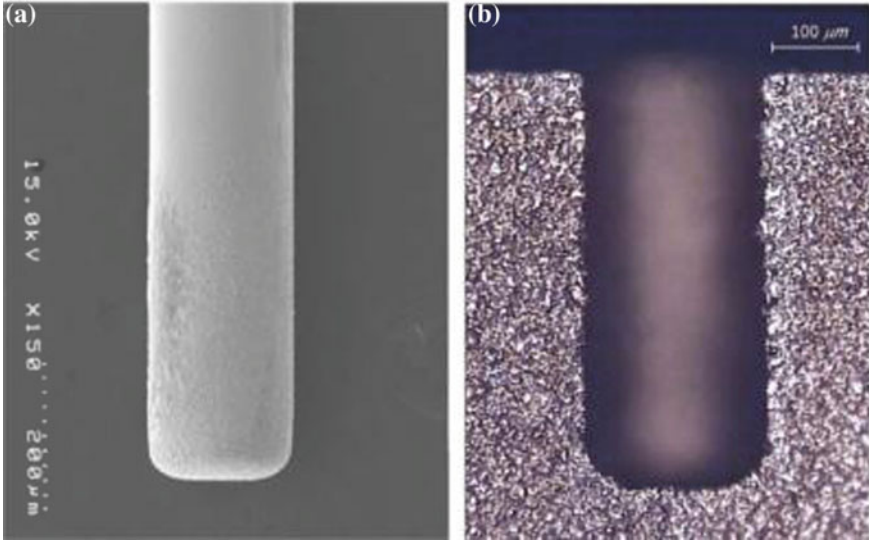
© Springer Nature Singapore Pte Ltd. 2019  
G. Kibria et al. (eds.), *Micro-electrical Discharge Machining Processes*, Materials  
Forming, Machining and Tribology, [https://doi.org/10.1007/978-981-13-3074-2\\_9](https://doi.org/10.1007/978-981-13-3074-2_9)

## 9.1 Introduction

Micro-electro-discharge machining ( $\mu$ -EDM) is widely used non-conventional fabrication technology specifically when removal of vibration, mechanical stresses, and chatter is required [1]. The study of  $\mu$ -EDM has fetched a lot of advancements due to capability of fabrication in micron level with very high accuracy irrespective of the workpiece hardness.  $\mu$ -EDM has been extensively adopted for fabrication of micro-mechanical parts, optical devices, injection nozzles, and micro-tools [2–4]. The technology has demonstrated its ability of machining a wide array of microstructures like 60  $\mu\text{m}$  diameter micro-rods [5] and three-dimensional  $\mu$ -holes [6]. Such features are fabricated by adopting variant types of  $\mu$ -EDM alternatives which are principally distinguished based upon the electrode movement (i.e.,  $\mu$ -EDM milling,  $\mu$ -EDM drilling) and electrode or workpiece polarity. However, in manufacturing tool design is a very complicated and time-consuming method due to the complex geometry, rough machining, electrode wear, and discharge gap [7]. The micro-machining is well defined as the ability to fabricate features with the dimensional arrays from 1 to 999  $\mu\text{m}$ . The rapid recurring spark discharge from the pulse generator is used to remove electrically conductive material among the workpiece or tool electrode in the existence of liquid dielectric. Some of the variants methods such as  $\mu$ -EDM drilling,  $\mu$ -EDM milling, and reverse  $\mu$ -EDM ( $R\mu$ -EDM) which are used for the fabrication of micro-features are discussed separately. Associated tool wear issues are also discussed in the respective sections.

### 9.1.1 $\mu$ -EDM Drilling

The  $\mu$ -EDM drilling employs a continuously rotating solid or hollow tool. The hollow tool is advantageous over the solid one as it facilitates propelling and sucking the dielectric liquid through an inner conduit in the tool [8]. In 1986, Kurafuji and Masuzawa [9] first performed a study on EDM in micron level and proposed about the structural errors in the fabricated parts because of the tool wear. After that Mohri et al. [10] examined the tool wear during EDM process and they found that the layer of carbon which accumulated on anode and cathode has highest impact on the TWR (tool wear ratio) and MRR. To demonstrate profiles of the tool and drilled cavities, Jeong and Min [11] performed a numerical simulation for  $\mu$ -EDM drilling process with round tool. They found that the profile determination outcomes are similar to experimental one with an inaccuracy of 13%. The real scanned electron microscopic view of electrode and fabricated electrode-workpiece with drilled distance is depicted in Fig. 9.1.

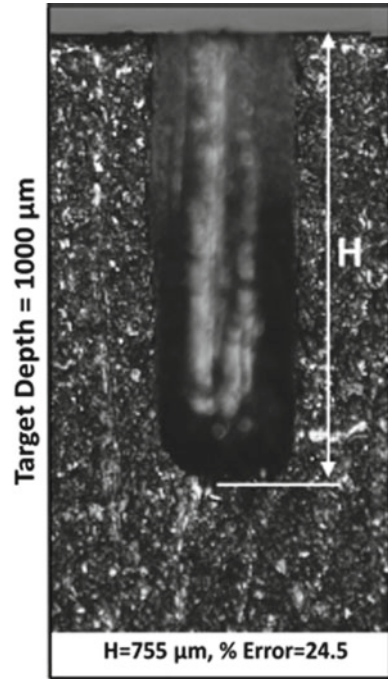


**Fig. 9.1** Real scanned electron microscopic view of fabricated electrode and workpiece with drilled distance 580 μm [11]

**9.1.1.1 Tool Wear in μ-EDM Drilling**

In μ-EDM drilling with a suitable electrode, the thermal resistance across the pivot of electrode is high. The electrode is, therefore, eroded rapidly as the temperature of electrode preserved at a higher array. Since a micro tool of cylindrical shaped is employed for drilling, the profile of the tip of the tool quickly deteriorate while machining. The tool wear arises at both the tip and the side surface of tool. The wear of tip is responsible for the errors in tool span approximation. The side surface erosion of tool influences the profile of holes formed during fabrication and may not be avoided in maximum circumstances. Figure 9.2 shows the tool wear which took place during μ-EDM drilling of brass specimen with copper electrode of 200 μm [12]. μ-EDM drilling has not attained extensive recognition in micro-manufacturing productions due to the tool wear which tends to dimensional error in fabricated products as seen. μ-EDM drilling is capable to drill elevated aspect ratios of micro- and macro-cavities in different aerospace alloys which are above the abilities of traditional twist drilling method [13]. In such situations, error in depth even in some proportion affected by electrode wear may eliminate the component. With the optimization of progression factors in μ-EDM drilling, this inaccuracy can be reduced, but it needs implementation of huge test runs and additionally, this optimized setting is effective only for a fixed work electrode material combination [14]. The tool wear in μ-EDM drilling not only affects accuracy of μ-holes but also reduces the machining efficiency. If the span of μ-holes is smaller than 5 μm, the dimensional error produced by the tool wear in μ-holes cannot be abandoned [3].

**Fig. 9.2** A cross section of  $\mu$ -EDM drilled hole representing the longitudinal tool wear [12]

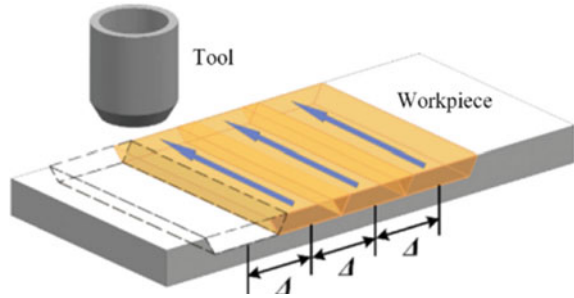


### 9.1.2 $\mu$ -EDM Milling

$\mu$ -EDM milling utilizes simple profile tool in the three-dimensional displacement to manufacture complex shapes.  $\mu$ -EDM milling accumulates the cost and time on fabricating the complex tools. In such arrangement, material is separated layer by layer with a layer width range up to 0.1  $\mu\text{m}$ . The schematic diagram of flat milling process by employing tubular tools is depicted in Fig. 9.3. However, the volumetric TWR in  $\mu$ -EDM milling is greater as compared to die-sinking  $\mu$ -EDM. The wear in tool during machining makes it smaller. Especially, in micro-ranges sometimes, it is incredible to machine the workpiece with tool for die-sinking  $\mu$ -EDM. So  $\mu$ -EDM milling is attaining abundant attention in micro-machining. The major issue in  $\mu$ -EDM milling is the huge TWR which is effect of a regular error and reduction in precision [15]. To overcome this problem, a modern process has been established to compensate TWR and sustain the fabrication precision [16, 17]. A well-known uniform wear method (UWM) associates the longitudinal electrode wear compensation and a superior tool path algorithm, which significantly enhance the  $\mu$ -EDM milling accuracy [18]. UWM adopts the counter machining with extremely low tool feed for every layer, and only the base of tool is employed for fabrication. The bottom of the tool is constantly smooth after the fabrication of each layer due to the to and fro scanning path of tool. Pie et al. [19] used a tubular tool and proposed a flat milling process which depends upon the constant length compensation process.



**Fig. 9.3** Schematic diagram of plane milling process by using tubular electrodes [19]

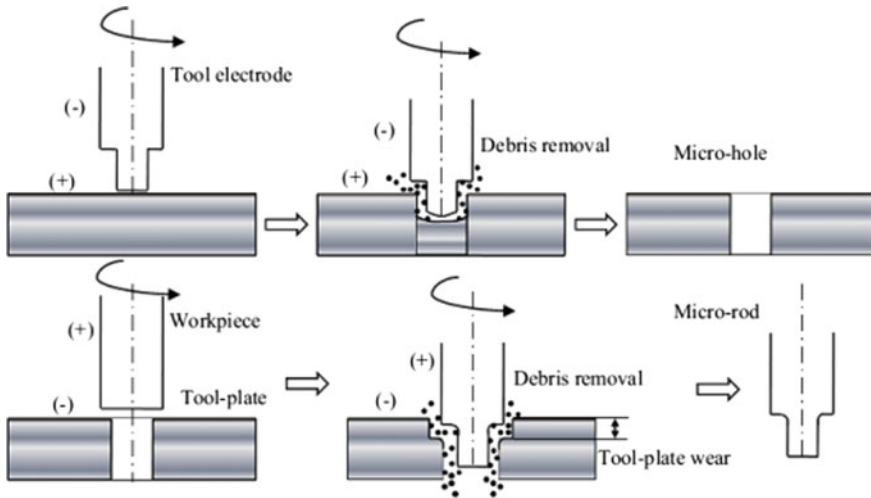


### 9.1.2.1 Tool Wear in $\mu$ -EDM Milling

In  $\mu$ -EDM milling during the fabrication with a cylindrical tool, the constant downward traverse of tool causes the quick stabilization of tool profile and coupled with arising electrode wear. This study overcomes the drawbacks of previously studied constant tool length compensation processes. The determination of tool wear is depending upon the volume of specimen extracted for that part and providing the approximation of comparative volumetric wear. After the fabrication of every layer, the electrode span is checked by using reference probe.

### 9.1.3 Reverse $\mu$ -EDM Method

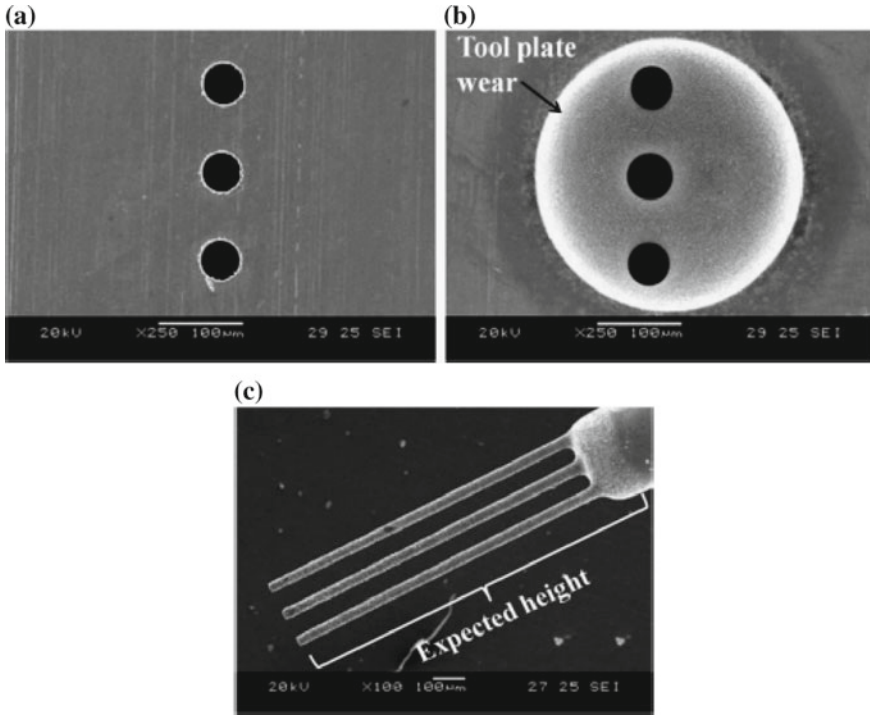
A developing  $R\mu$ -EDM method has already depicted its optimal ability for fabrication of micro-electrodes on metallic surface irrespective of their toughness [20–22]. This micro-electrode range may again be employed to fabricate variety of  $\mu$ -holes by  $\mu$ -EDM drilling and therefore minimizing the machining time. In  $R\mu$ -EDM, an array of  $\mu$ -holes on a metallic surface is used as an cathode whereas a huge dimension of specimen which acts as an anode is adjusted over the cathode. A cylindrical rod (anode) of comparatively large diameter which is placed above the holes is traversed at a measured feed. The removal of material from the surface of cylindrical rod occurs where a material to material boundary exists. This causes the replication of shape of holes from tool surface to cylindrical rod surface. The cross-sectional area of machined features on cylindrical rod appears like the cross-sectional area of holes already fabricated on tool. The  $R\mu$ -EDM process is performed in two stages. In the first stage, holes are manufactured on the plate tool with the assistance of micro-machining method. In second stage, plate tool is supported on the  $\mu$ -EDM machine to generate a reverse copy of those holes on the specimen. Figure 9.4 depicts the  $R\mu$ -EDM method obtained through reversing the polarity of  $\mu$ -EDM drilling.



**Fig. 9.4** Schematic of Rμ-EDM process and pictorial vision of tool plate before and after machining [21]

### 9.1.3.1 Tool Wear in Reverse μ-EDM Method

The tool wear is determined to investigate the duration for which different electrodes can be fabricated by a workpiece electrode of specified thickness. As the longitudinal wear is more effective in comparison with lateral wear in Rμ-EDM, the TWR is calculated from the longitudinal wear. This method is steady and no short circuit is recorded except the duration in which the cylindrical rod penetrates the tool plate. Figure 9.5 depicts the range of μ-holes before the machining which is employed during fabrication. The diameter of all the μ-holes was 45 μm before the machining. Figure depicts the range of μ-holes after fabrication. The dimension of μ-holes was changed from 45 to 55 μm during fabrication due to the rapid spark discharge. The thermal properties of tool plate changes at high temperature and tool wear will occur which causes the manufacturing error in electrode [22]. Nirala et al. [21] adopted the actual volume removal in real-time ( $V_{RT}$ ) method and productively applied to Rμ-EDM approach to form the necessary summit of micro-rods. They used an equivalent type of method which is applied in μ-EDM drilling for manufacturing accurate μ-holes. Hence, further some attempts are required to enhance structural precision of micro-rods fabricated via μ-EDM milling method. The compensation of electrode wear is, therefore, essential to attain significant correctness of the manufactured products.



**Fig. 9.5** Tool plate with array of micro-holes **a** before machining **b** after machining and **c** fabricated array micro-rods [22]

## 9.2 Tool Wear Compensation Methodologies

Since 1980s, compensation of electrode wear is mostly obtained through the determination of electrode length regularly during fabrication. In view of this, several tool wear measuring methods like machine vision, laser array sensors, and electrical circuit were established [23]. However, these methods are still being employed for variant functions in fabrication but have not demonstrated to be innovative in electrode wear compensation. Therefore, Bleys et al. [24] proposed electrode wear compensation method for  $\mu$ -EDM milling in real time by counting the type and amount of normal discharge. The compensation of tool wear in real-time method can disable the limitation of offline tool wear compensation method and tends to the entire removal of dimensional error caused because of the electrode wear.

### ***9.2.1 Offline Tool Wear Compensation***

The offline tool wear compensation process determined the electrode wear mainly in the form of tool wear or calculated at a regular interval of time during the machining. These methodologies are employed for variant features in fabrication but till now these methodologies are not established as a trendsetter in tool wear compensation. The reason behind this is the periodical analysis disruption of fabrication which results in larger machining duration. The electrode wear problem in  $\mu$ -EDM was primarily attempted using offline compensation and one compensation method generally known as UWM is discussed in the next section as below.

#### **9.2.1.1 Uniform Wear Method**

In UWM, the whole machining procedure is performed by milling several thin layers one by one. To maintain the machining depth, the electrode is compensated for a length every time before the equivalent layer is machined. In 1998, Yu et al. [18] introduced the UWM which is very familiar machining approach to compensate longitudinal electrode wear in  $\mu$ -EDM milling. This approach is capable to recover the electrode profile to its actual shape after machining one layer. Moreover, the UWM is already incorporated with CAD/CAM to fabricate random three-dimensional  $\mu$ -holes [25]. Kruth et al. [26] introduced a predictable wear compensation approach where the electrode wear for each section of the electrode is measured by offline prediction. This compensation process is further depending upon the offline determination of volumetric relative wear and does not influence much the online wear compensation. The tool wear was used widely in various offline electrode wear compensation approaches; however, several problems exist in measuring tool wear. Initially, the tool wear is highly affected by both the materials and methods which must be modified by experiments for an appropriate geometry and need a high setup time [15]. Secondly as the dimension of electrode is extremely small and removal of material from electrode is considerably less as compared to the specimen, the determination of TWR is influenced by high inaccuracy [27]. These issues in offline tool wear compensation motivated researchers to think for some online techniques which can compensate the tool wear in real time.

### ***9.2.2 Online Tool Wear Compensation***

This method principally depends upon the volume removal per discharge (VRD) from the tool or the specimen. The compensation of tool wear was obtained mostly by counting the discharge pulses and multiplying it by a constant value of VRD to get the volume removal from the tool or specimen in real time ( $V_{RT}$ ). Counting the discharge pulses literally assumes the pulses have an identical thermal energy which later

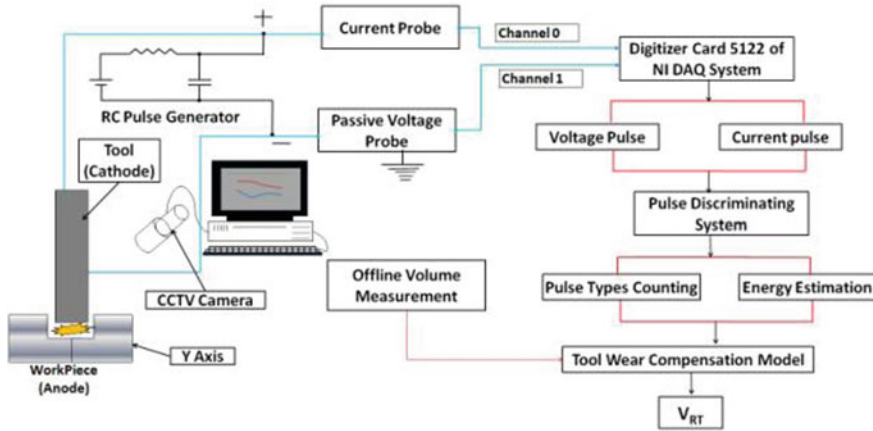


Fig. 9.6 Schematic diagram of improved VRD method [12]

proved to be not isoenergetic [12]. Additionally, assumptions like the constant VRD is also proved to be wrong as the VRD varies with machining depth, especially in case of  $\mu$ -EDM drilling. Hence, assuming the discharge pulses as isoenergetic and the VRD as constant will definitely result in the under or over estimation of  $V_{RT}$  which will consequently tend to an inaccuracy in monitoring of tool wear. Therefore, groups of researchers worked to improve the existing VRD approach of tool wear compensation and termed the new approach as modified or improved VRD methods. The improved VRD method which is basically an attempt to address the non-isoenergetic nature of discharge pulses and varying VRD with machining progress is discussed separately.

### 9.2.2.1 Improved VRD Method

The improved VRD method involves two features, one is the variation of VRD with the depth of machining and the other is role of non-isoenergetic pulses in material removal. The above-mentioned features approximate the VRD more precisely. VRD is determined at several depths of fabrication by recognizing genuine amount of contributing pulses ( $N_p$ ) and finally a significant relation among VRD and  $N_p$  is achieved. To determine this  $N_p$ , a pulse discrimination system which has potential to discriminating among the contributing, less contributing and non-contributing pulses is needed to determine the actual contributing pulses in the next section. Figure 9.6 shows schematic of investigational flowchart for evolving pulse discrimination approach for improved VRD method. The flowchart of tool wear compensation based upon the improved wear method used for the compensation of electrode wear during fabrication is depicted in Fig. 9.7.

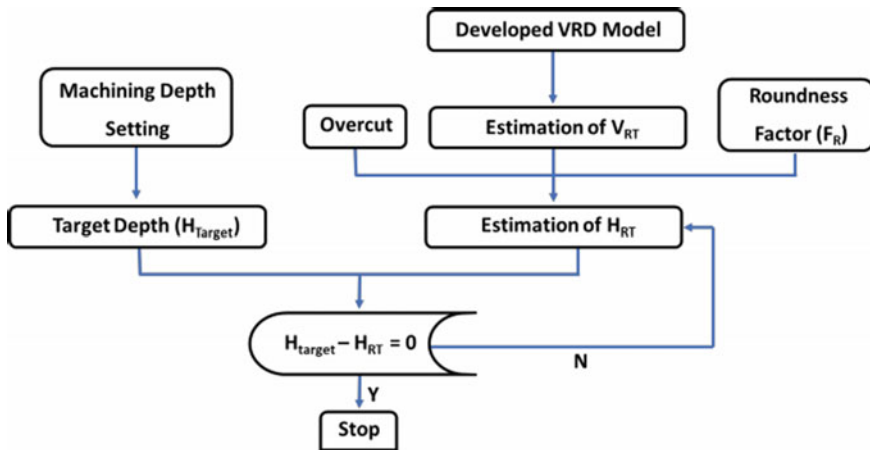


Fig. 9.7 Flowchart for tool wear compensation [21]

### 9.2.2.2 Development of Pulse Discriminating Method

In the beginning stage, spark discharge situations are recognized with the help of the signals received through the current and voltage probe. The pulses are classified into four different sets, i.e., normal pulse, effective pulse, arcing pulse, and short circuit pulse depending upon the following conditions. In terms of normal pulse, rapid drop in voltage takes place from  $U_o$  to 72% of  $U_o$ . These pulses are generally responsible for the removal of material. The  $\mu$ -EDM mainly consists of resistor-capacitor type pulse generator where the discharge occurs when capacitor is completely electrically charged to  $U_o$ . However, some discharges may occur as the capacitor is not fully charged to  $U_o$ . The effective spark erosion pulse is described as a pulse where the discharge voltage ranges between 65 and 72% of  $U_o$ . These effective pulses are like that of normal pulses with variation in the magnitude of charging and discharging voltage. Arcing is recognized during the process when charging voltage does not come back to 65% of  $U_o$  and significant discharge takes place. This shows that due to the incomplete deionization of the dielectric liquid the repetitive discharges take place. Short circuit pulses have no contribution in the removal of material. These pulses are defined as a pulse having charging velocity less than 55% of  $U_o$  or appear as smooth line on a respectable level. The flowchart of pulse discriminating system and the distinctive current and voltage pulses development in  $\mu$ -EDM drilling at the starting point of machining process are depicted in Figs. 9.8 and 9.9, respectively.

It is well recognized that the high range of pulse in a resistance-capacitor circuit integrated with  $\mu$ -EDM machine is based upon its voltage and capacitance. This can be provided by an expression as shown in Eq. (9.1):

$$E_p = \frac{1}{2} \times C \times (U_o)^2 \quad (9.1)$$

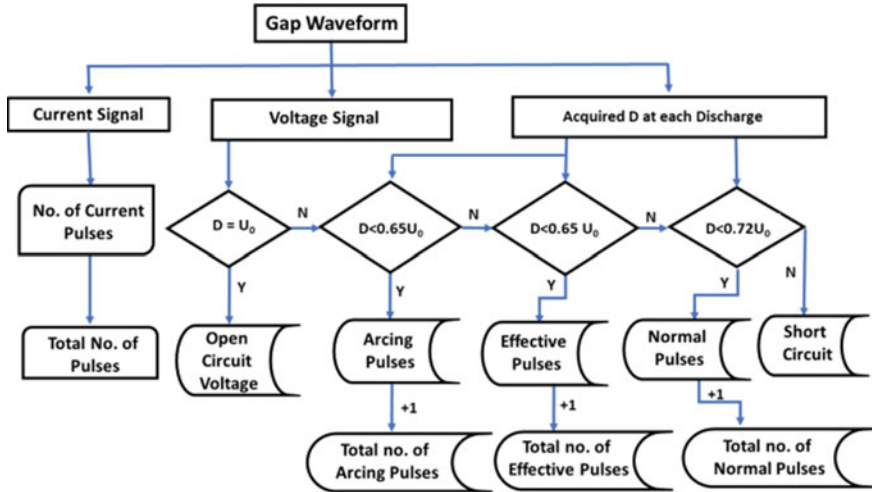


Fig. 9.8 Flowchart of pulse discrimination method [28]

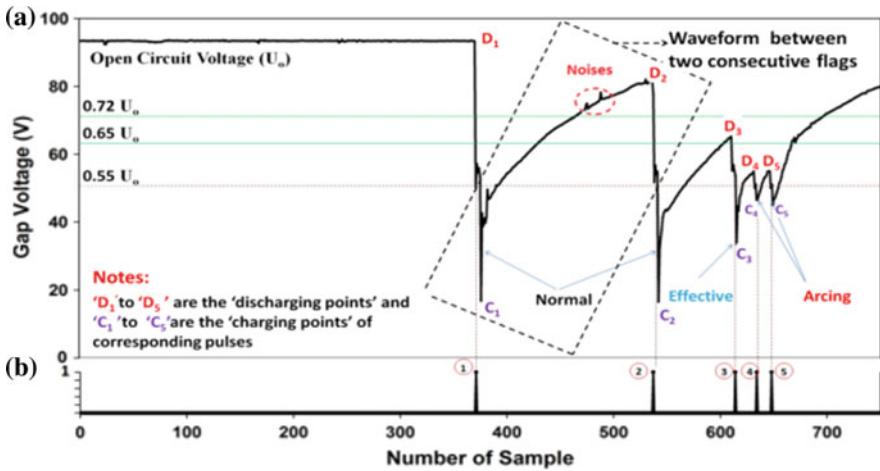


Fig. 9.9 Schematic of different types of pulses in  $\mu$ -EDM [21]

Here,

$E_p$  is the maximum provided energy of a pulse.

$U_0$  is the operator defined voltage which is termed here as open circuit voltage between electrode and specimen.

$C$  is the capacitance

However, only half of the overall effective pulses ( $\eta_{eff}$ ) have been recognized in real time to produce an influence similar to the normal pulses. By using this relation,

$N_p$ , which is number of actual contributing pulses, can be provided as follow in Eq. (9.2):

$$N_p = \frac{1}{2} \eta_{\text{eff}} + n_n \quad (9.2)$$

It is already observed that due to the increase of machining depth, the frequency, shape and size of pulses are altered even without any change in parametric conditions. In other words, as shown in Fig. 9.10 the enhanced pulse frequency at deeper depth tends to the partially charging of the capacitor which causes the fluctuation of energy in each pulse. Though, it becomes necessary to check the influence of such alteration in the nature of different pulses on average energy, as the average energy provides a better signal for process stability. The greater the average energy deviation the smaller will be the process stability. This could be referred to the circumstances that the captured current and voltage signals are normally overlaid with a huge amount of beeps in the machine. When processing such beeps, a number of real signals fraction is also rejected which tends to smoothening and successively reduction of pulse size. The number of contributing pulses on starting, middle and near to the finish of  $\mu$ -EDM drilling method was employed to understand the influence of alteration in energy content for contributing pulses on average energy.

### 9.2.2.3 Development of Relationship Between VRD and $N_p$

#### *Empirical analysis of VRD*

This section represents the research done by Nirala et al. to establish an improved VRD method of tool wear compensation in  $\mu$ -EDM [12]. For the empirical analysis of VRD, the  $\mu$ -EDM experiments have been performed using hybrid  $\mu$ -EDM machine tool (make: MIKROTOOL; model: DT-110) as depicted in Fig. 9.11. The determination of VRD needs information on the removal of volume from the specimen and time taken in particular machining operation. Cross sections of drilled  $\mu$ -holes are calibrated by employing a method termed here as ‘information from picture’. The 3D microscope generally known as ‘synchronous transport module’ is employed to take sectional pictorial view step by step as presented in Fig. 9.12. The leftward and rightward regions of specimen are examined for equivalence and after the examination a minor error of 0.025% has been obtained.

The VRD is calculated by dividing measured actual volume removed ( $V_{\text{actual}}$ ) with  $N_p$ . For finding the VRD, an array of  $\mu$ -EDM drilling experiments have been performed by selecting two electrodes and work material combinations and two input parametric criteria which provide two different discharge energies for fabrication. The experimental condition including the material and parameter combination is detailed in Table 9.1. In the tool wear compensation, the  $\mu$ -EDM drilling testing has been performed at different depths which resembles the variant  $N_p$  as shown in Fig. 9.13. Functional relationship between the VRD with respect to the  $N_p$  can be seen in the research paper originally published by Nirala et al. [12] Sample images



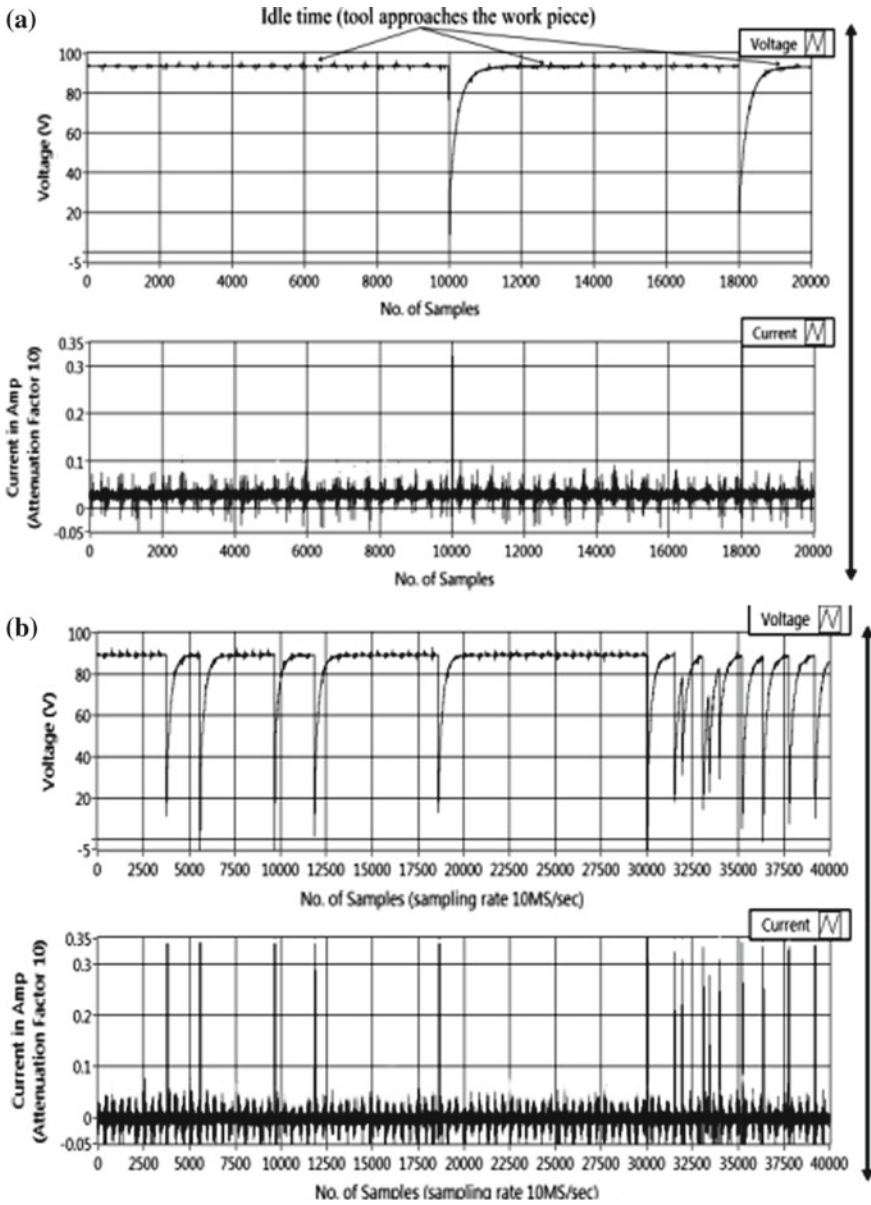


Fig. 9.10 Different voltage and current pulses at a starting, b middle, c near to the finish of  $\mu$ -EDM drilling method [28]

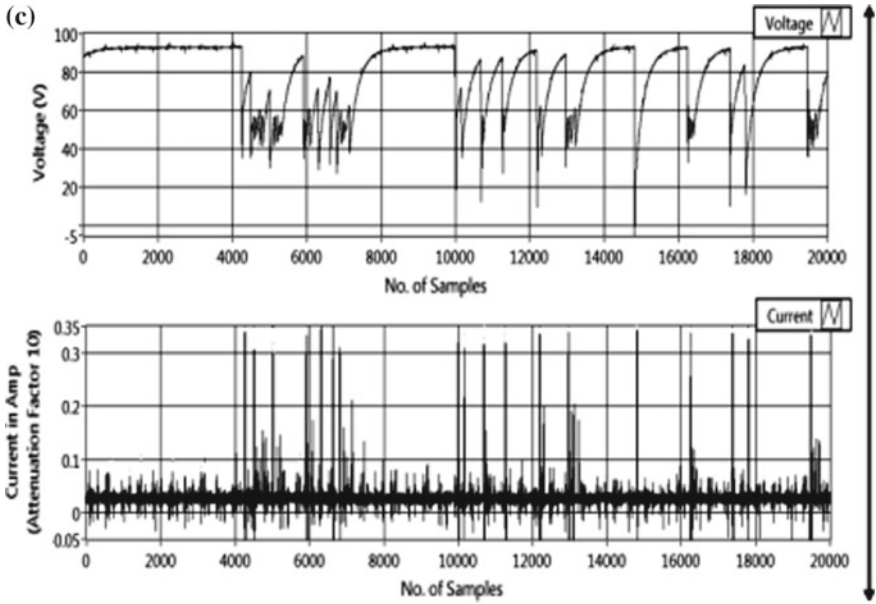


Fig. 9.10 (continued)

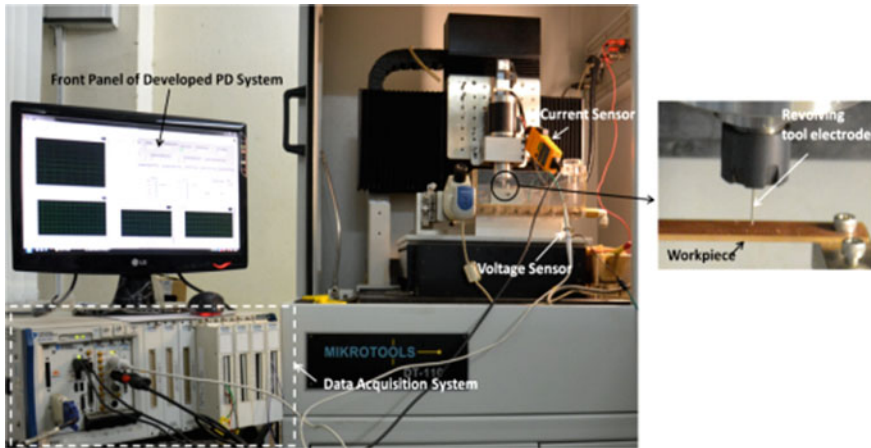
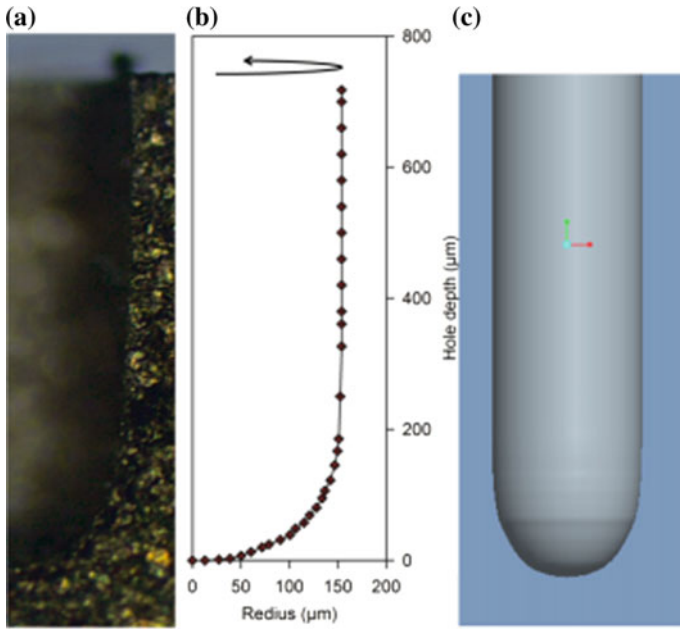


Fig. 9.11 Photographic view of experimental setup [28]



**Fig. 9.12** Stages of volume determination **a** μ-EDM drilled hole **b** the boundary and data points of hole, **c** μ-hole CAD design [12]

of the μ-holes drilled according to the machining condition given in Table 9.1 are shown in Fig. 9.13a, b.

**9.2.2.4 Estimating  $V_{RT}$  and  $H_{RT}$  Using Developed Pulse Discrimination System**

The amount of  $V_{RT}$  is measured by using the following relation given in Eq. (9.3):

$$V_{RT} = VRD \times N_P \tag{9.3}$$

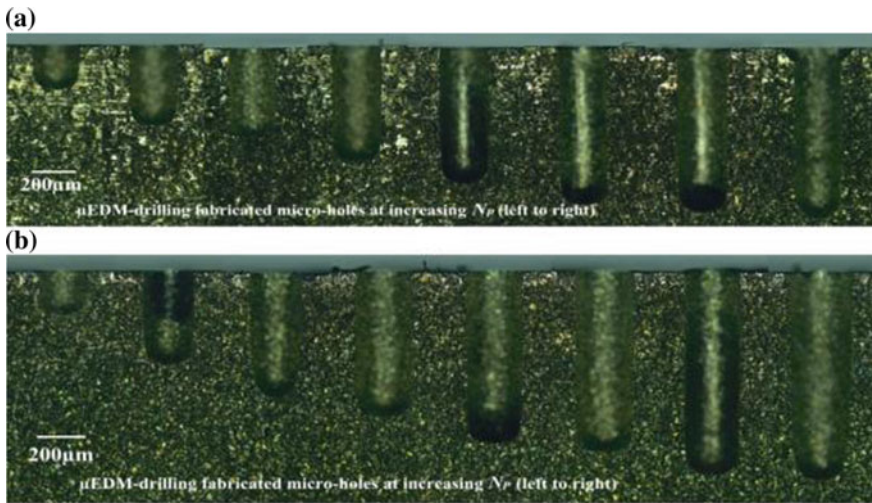
Once  $V_{RT}$  is measured, it is employed to determine the height of machined μ-holes ( $H_{RT}$ ) in real time by integrating roundness and taper of μ-holes. The roundness at edge or taper at side of μ-holes surface depicted above in Fig. 9.14 are combined by presenting a parameter known as roundness factor ( $F_R$ ). The measurement of  $H_{RT}$  from  $V_{RT}$  requires equivalent data on length of μ-holes. For this determination inlet span of μ-holes are measured.

**Overcut estimation**

The gap for discharge in μ-EDM drilling process tends to a higher span as compared to span of electrode and such increase in span is known as overcut. The μ-holes

**Table 9.1** Experimental condition for establishment of functional relation of VRD [12]

1st material combination	<b>Workpiece (anode)</b>	<b>Tool (cathode)</b>
	1.5 mm thick Brass plate	Copper electrode of diameter 200 $\mu\text{m}$
2nd material combination	Workpiece (anode)	Tool (cathode)
	1.5 mm thick Brass plate	Brass electrode of diameter 300 $\mu\text{m}$
Spindle speed	2000 RPM (fixed for all experiments)	
Feed rate	0.2 mm/min (fixed for all experiments)	
No. of experiments	Total 64 experiments from the two parametric settings (8 at each setting and at each material combinations repeated twice)	
1st material combination	<b>Parametric Criteria 1</b>	<b>Parametric Criteria 2</b>
	Capacitance: 10 nF Voltage: 90 V	Capacitance: 40 nF Voltage: 90 V
2nd material combination	<b>Parametric Criteria 1</b>	<b>Parametric Criteria 2</b>
	Capacitance: 10 nF Voltage: 90 V	Capacitance: 40 nF Voltage: 90 V



**Fig. 9.13**  $\mu$ -EDM machined holes for 1st material arrangement at **a** criterion setting 1 and **b** criterion setting 2 [12]

with overcut are depicted in Fig. 9.14a. Here ‘ $D$ ’ is the diameter at arrival.  $D_1$  which is equivalent to electrode diameter shows a simulated diameter of  $\mu$ -holes having no overcut. At different alternatives setting a complex overcut is achieved for the arrangement of variant materials. This is because of the enhancement in capacitance which tends to higher average spark energy.

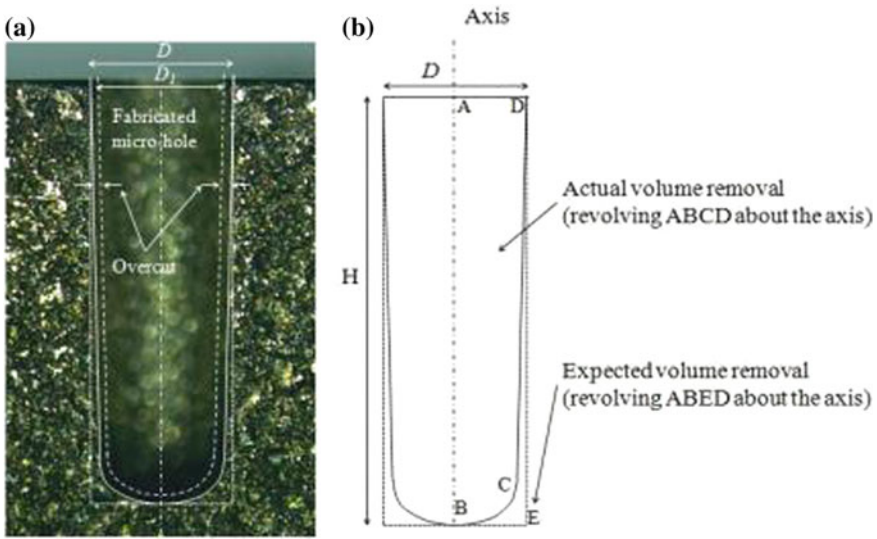


Fig. 9.14 a Typically formed  $\mu$ -hole, b determination of roundness factor [12]

**Roundness factor ( $F_R$ ) determination**

The roundness of edge of the  $\mu$ -hole is an intrinsic drawback of EDM method. A distinctive illustration of such roundness which is named as BC is depicted in Fig. 9.14b. To integrate this taper and roundness in the measurement of  $H_{RT}$  of the  $\mu$ -holes  $F_R$  has been presented. The  $F_R$  is termed as a ratio of predicted to actual amount of volume removal. The predicted volume removal will be consistently higher as compared to the actual volume removal due to the development of taper and roundness. To analyze such volumes, depth ( $H$ ) of  $\mu$ -holes was formed to be accessible. The  $F_R$  has been determined by employing Eq. (9.4) as shown below:

$$F_R = \frac{\text{Predicted volume removal}}{\text{Actual volume removal}} \tag{9.4}$$

An experimental design has been developed to calculate its variation with  $N_p$ . From these calculations, it has been obtained that  $F_R$  begins with a data which is larger than 1 and after that progressively reaches at unity. Generally, on fabrication of  $\mu$ -holes the roundness rises incredibly, and this influences the  $F_R$  up to a large extent. Once a semi-spherical profile is obtained on the electrode tip, and it is noticed that tool electrode roundness does not alter more. Therefore, the expected removal value and actual removal value enhanced about the equivalent amount with the enhancement of the depth. However, Pham et al. [25] proposed that strength of electric field exists greater at corner of electrode tip and forming a normal erosion of corner. This normal

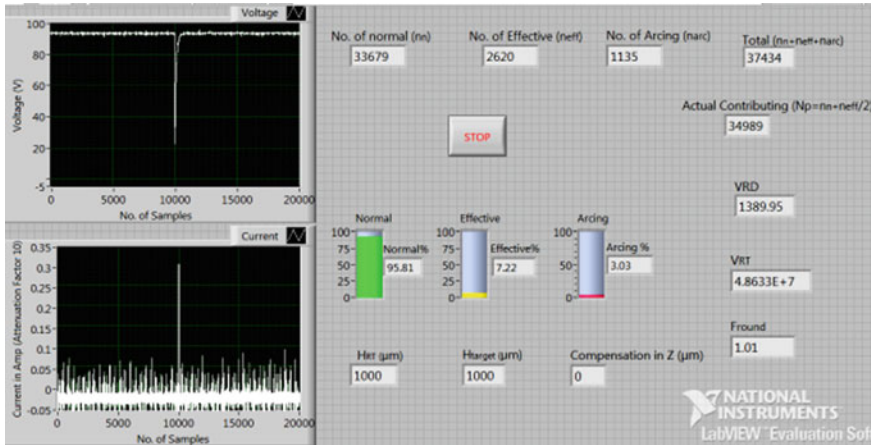


Fig. 9.15 LABVIEW front panel for tool wear compensation method [21]

tool erosion remains continue till the tool electrode tip converts to circular shape or the corner vanishes. The  $F_R$  is formed while combining with the established PD method and  $H_{RT}$ .

### 9.2.2.5 Determination of Real-Time Depth of the $\mu$ -Hole ( $H_{RT}$ )

When  $V_{RT}$  is determined, it relates to  $F_R$  in order to determine the  $H_{RT}$ . The relation for  $H_{RT}$  is presented in Eq. (9.5):

$$H_{RT} = \frac{V_{RT} \times F_R}{\left[\frac{\pi}{4} D^2\right]} \tag{9.5}$$

After the determination of  $H_{RT}$ , the fabrication is continued until  $H_{RT}$  relates with required compensation across the tool wear. The front panel for established electrode wear compensation is depicted in Fig. 9.15 due to which the significant  $H_{RT}$  is formed.

## 9.3 Authentication of Proposed Method

### 9.3.1 Proposed Process

The designed method to compensate the tool wear is employed for small or large machine aspect ratio  $\mu$ -holes. The significance of designed method is analyzed adjacent to the manufacturing of both shorter and deep  $\mu$ -holes. The target depth for

small and deeper  $\mu$ -holes of first electrode and workpiece combinations are selected as 500 and 1000  $\mu\text{m}$ , respectively. Similarly, the equivalent target depth for second material combination has been selected as 400 and 700  $\mu\text{m}$ . The fabrication has been sustained until the target height matches with  $H_{RT}$  and the variation becomes zero. These tool wear compensated results are then evaluated using uniform wear method (UWM), a widely used and well accepted offline tool wear compensation method, and regular process with no tool wear compensation.

### 9.3.2 Uniform Wear Method

The UWM is much-admired method to compensate electrode wear. This approach improves assumptions of already calculated tool wear. The UWM is thus used for calculating the tool wear experimentally. The essential tool wear has been calculated by accepting the variation between the deepness of  $\mu$ -holes to be machined and programmed Z-axis. The volume of eroded electrode can be determined by using Eq. (9.6) as follow:

$$\text{Volumetric removed tool} = (Z - H) \times \frac{\pi}{4} D_1^2 \quad (9.6)$$

where  $D_1$  is equal to the diameter of the electrode. Considering that the diameter of machined  $\mu$ -hole is equivalent to diameter of electrode, the worn-out size of the specimen is then determined by employing  $D_1$  and depth of the  $\mu$ -holes. The relation for determining the worn-out volume from the workpiece is depicted in Eq. (9.7)

$$\text{Volume worn out from the workpiece} = H \times \frac{\pi}{4} D_1^2 \quad (9.7)$$

After merging Eqs. (9.6) and (9.7), the relation obtained for the tool wear is provided by using the formulation as follow:

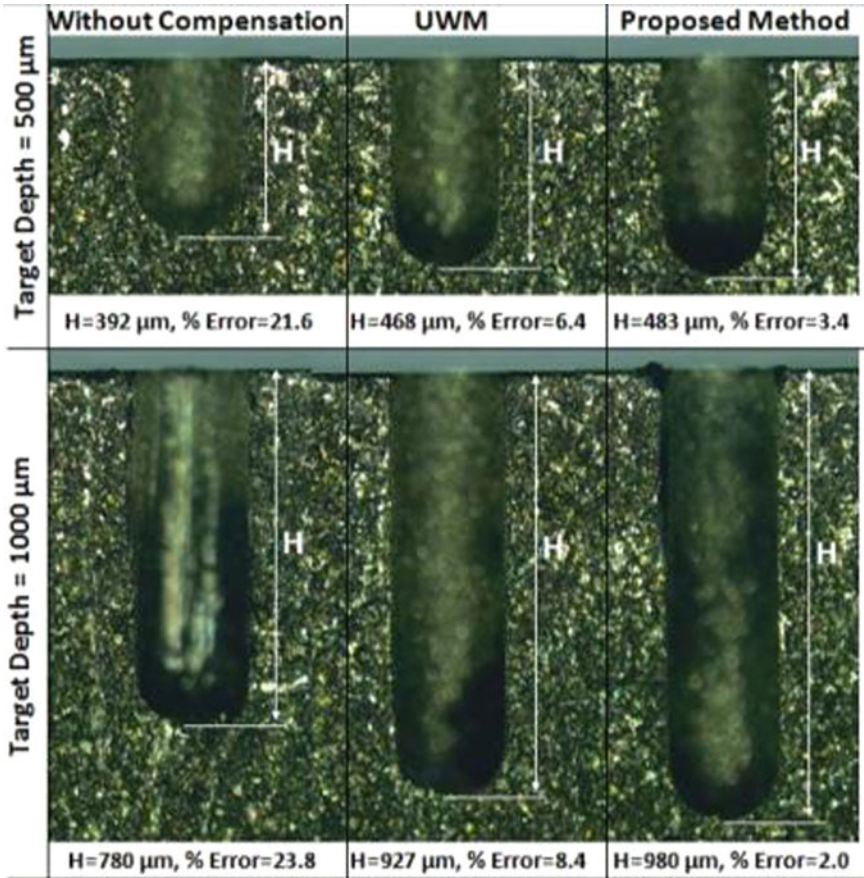
$$\text{TWR} = \frac{(Z - H)}{H} = \frac{\text{Volumetric erosion of electrode}}{\text{volume worn out from workpiece}} \quad (9.8)$$

Z-axis compensation as mentioned above is similar to electrode wear in  $\mu$ -EDM drilling and is provided by using the expression as mentioned in Eq. (9.9)

$$Z = H + \text{TWR} \times H = H \times (1 + \text{TWR}) \quad (9.9)$$

After the calculation as mentioned above, a virtual study of proposed tool wear compensation method among normal and UWM method is reported. The comparison has been performed by using variant target heights (500, 1000  $\mu\text{m}$  and 400, 700  $\mu\text{m}$ ) with different material combinations. Such a broad array of target height would ascertain to effectiveness of proposed approach for the production of deep and small





**Fig. 9.16** Evaluation of the proposed process with actual process for  $V = 90\text{ V}$  and  $C = 10\text{ nF}$  and 1st material combination [12]

$\mu$ -holes. The virtual responses of such suggested approach with UWM and without compensation method has been depicted in Figs. 9.16 and 9.17, respectively.

### 9.4 Results and Discussion

The response depicts stability of the proposed technique of tool wear compensation above different alternative techniques in terms of manufacturing the variant  $\mu$ -holes more precisely. By using first material combination, the proposed method recovers the error by 18.2 and 21.8% beside the target depth of 500 and 1000  $\mu\text{m}$  correspondingly as compared to normal method. Similarly, by using the second material



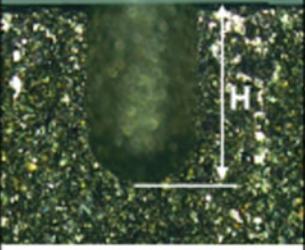
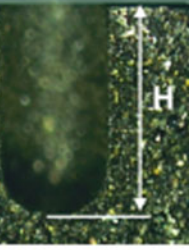

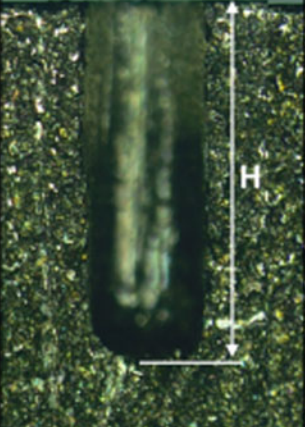
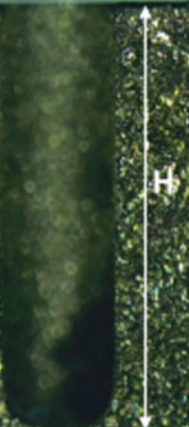

	Without Compensation	UWM	Proposed Method
Target Depth = 500 $\mu\text{m}$			
	H=381 $\mu\text{m}$ , % Error=23.8	H=458 $\mu\text{m}$ , % Error=8.4	H=481 $\mu\text{m}$ , % Error=3.8
Target Depth = 1000 $\mu\text{m}$			
	H=755 $\mu\text{m}$ , % Error=24.5	H=891 $\mu\text{m}$ , % Error=10.9	H=964 $\mu\text{m}$ , % Error=3.6

Fig. 9.17 Evaluation of the proposed process with actual process for  $V = 90\text{ V}$  and  $C = 40\text{ nF}$  and 1st material combination [12]

combination, the 20 and 20.9% enhancement has been obtained for equivalent target distances. When evaluating with UWM, the suggested technique provides depth error improvement up to 3.0 and 6.4% at 1st alternative setting and 4.6 and 7.3% at 2nd alternative setting, respectively. The results obtained for both the material combination are depicted in Figs. 9.18 and 9.19. The above responses show that the suggested technique is capable to employ for manufacturing deeper as well as shallow  $\mu$ -holes with depth error of nearly 4% even for an electrode material which removes quickly. The 0% error in compensation of electrode wear is not possible due to the human and model errors.

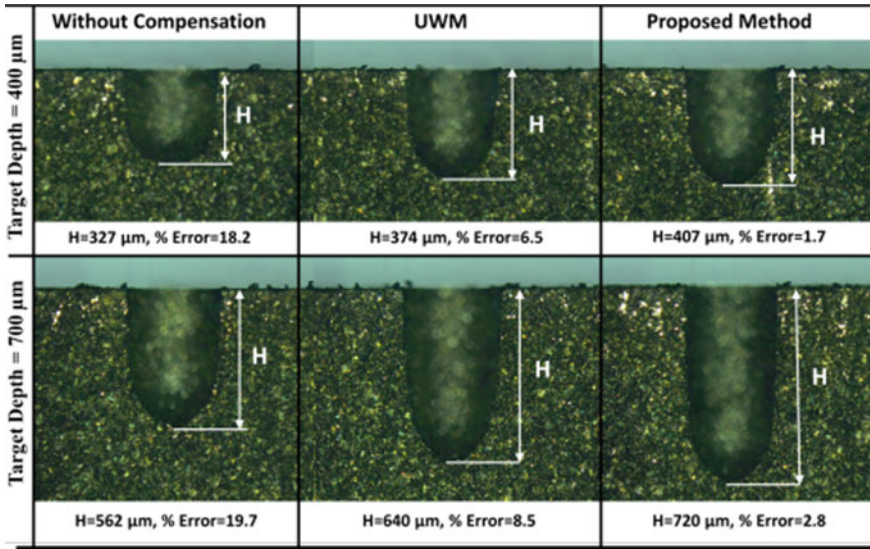


Fig. 9.18 Evaluation of the proposed process with actual process for  $V = 90\text{ V}$  and  $C = 10\text{ nF}$  and 2nd material combination [12]

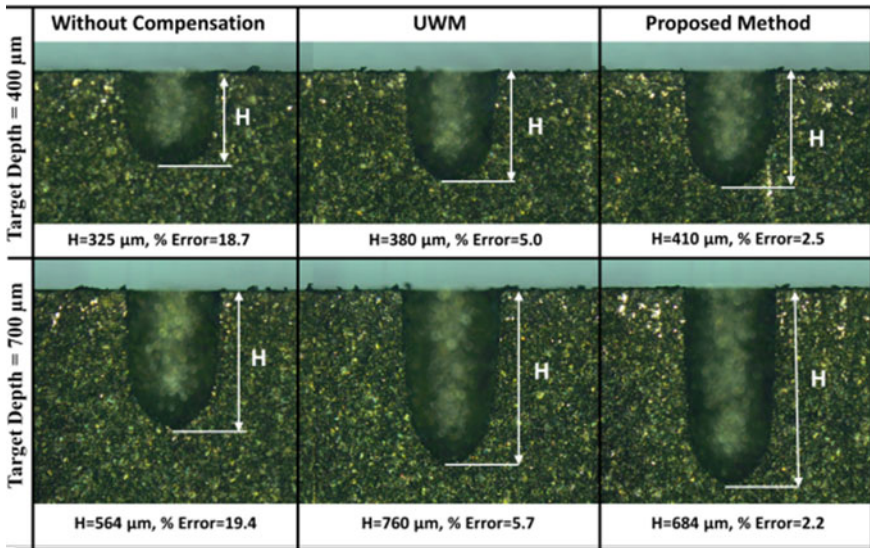


Fig. 9.19 Evaluation of the proposed process with actual process for  $V = 90\text{ V}$  and  $C = 40\text{ nF}$  and 2nd material combination [12]

## 9.5 Summary

The following conclusions can be drawn:

1. A real-time tool wear compensation for  $\mu$ -EDM drilling process is proposed based on in-house developed pulse discriminating system.
2. The discovered method utilizes the proposed 'improved volume removal per discharge (VRD) approach' to compensate the tool against the electrode wear in the process.
3. The method follows the sequence of estimation 'real-time material removal volume' ( $V_{RT}$ ) from the workpiece and then finally the 'real-time depth' ( $H_{RT}$ ) of the micro-hole(s).
4. For the correct estimation of  $H_{RT}$ , the roundness at the tool time is taken care by introducing 'roundness factor' ( $F_R$ ). The overcut has also been taken care in real time to estimate a precise  $V_{RT}$ .
5. The potentiality of the discovered method is verified by successful fabrication of micro-holes of the required target depth at two different parametric settings and material combinations with a nominal error of less than 4%.
6. The method is also compared with the other existing techniques at the end and found having a significant improvement.

## References

1. Jiang Y, Wansheng Z, Xuecheng X, Lin G, Xiaoming K (2012) Detecting discharge status of small-hole EDM based on wavelet transform. *Int J Adv Manuf Technol* 50:171–183
2. Rajurkar KP, Levy G, Malshe A, Sundaram MM, McGeough J, Hu X, Resnick R, DeSilva A (2006) Micro and nano machining by electro-physical and chemical processes. *CIRP Ann Manuf Technol* 55:643–666
3. Masuzawa T, Tonshoff HK (1997) Three dimensional micro machining by machine tools. *CIRP Ann Manuf Technol* 46(2):621–628
4. Kuneida M, Lauwers B (2005) Advancing EDM through fundamental insight into the process. *CIRP Ann Manuf Technol* 54:64–87
5. Brousseau EB, Dimov SS, Pham DT (2010) Some recent advances un multi material micro and nano manufacturing. *Int J Adv Manuf Technol* 47:161–180
6. Rajurkar KP, Yu ZY (2000) Three dimensional micro EDM using CAD/CAM. *CIRP Ann* 49(1):127–130
7. Ding XM, Fuh JYH, Lee KS (2002) Computer aided EDM electrode design. *Comput Ind Eng* 42:259–269
8. Yilmaz O, Okka MA (2010) Effect of single and multi-channel electrodes applications on EDM fast hole drilling performance. *Int J Adv Manuf Technol* 51:185–194
9. Kurafuji H, Masuzawa T (1968) Micro EDM of cemented carbide alloys. *J Japan Soc Electrical Mach Eng* 2(3):1–16
10. Mohri N, Suzuki M, Furuya M, Saito N, Kobayashi A (1995) Electrode wear process in electrical discharge machining. *CIRP Ann Manuf Technol* 44:165–168
11. Jeong YH, Min BK (2007) Geometry prediction of EDM drilled holes and tool electrode shapes of micro EDM process using simulation. *Int J Mach Tools Manuf* 47:1817–1826

12. Nirala CK, Saha P (2017) Precise  $\mu$ EDM-drilling using real-time indirect tool wear compensation. *J Mater Process Technol* 240:176–189
13. Kuppan P, Rajadurai A, Narayanan S (2008) Influence of EDM process parameters in deep hole drilling of Inconel 718. *Int J Adv Manuf Technol* 38:74–84
14. Nirala CK, Reddy B, Saha P (2013) Optimization of process parameters in micro electro discharge drilling: a Taguchi approach. *Adv Mater Res* 622–623:30–34
15. Narasimhan J, Yu Z, Rajurkar KP (2005) Tool wear compensation and path generation in micro and macro EDM. *J Manuf Processes* 7:75–82
16. Bleys P, Kruth J, Lauwers B, Zryd A (2002) Real-time tool wear compensation in milling EDM. *CIRP Ann* 51:157–160
17. Richard J, Demellayer R (2013) Micro EDM milling development of new machining technology for micro machining. *Procedia CIRP* 6:292–296
18. Yu ZY, Masuzawa T, Fujino M (1998) Micro EDM for the three dimensional cavities development of uniform wear method. *CIRP Ann* 47:169–172
19. Pei J, Zhuang X, Zhang L, Zhu Y, Liu Y (2018) An improved fix-length compensation method for electrical discharge milling using tubular tools. *Int J Mach Tools Manuf* 124:22–32
20. Kim BH, Park BJ, Chu CN (2006) Fabrication of multiple electrodes by reverse EDM and their application in micro ECM. *J Micromech Microeng* 16:843
21. Nirala CK, Saha P (2016) A new approach of tool wear monitoring and compensation in R $\mu$ EDM process. *Mater Manuf Processes* 31:483–494
22. Mastud S, Garg M, Singh R, Joshi SS (2012) Recent developments in the reverse micro electrical discharge machining in the fabrication of arrayed micro features. *Proc Inst Mech Eng J Mech Eng Sci* 226:367–384
23. Yan MT, Huang KY, Lo CY (2009) A study on electrode wear sensing and compensation in micro EDM using machine vision system. *Int J Adv Manuf Technol* 42:1065–1073
24. Bleys P, Kruth JP, Lauwers B (2004) Sensing and compensation of tool wear in milling EDM. *J Mater Process Technol* 149:139–146
25. Pham DT, Ivanov A, Bigot S, Popov K, Dimov S (2007) An investigation of tube and rod electrode wear in micro EDM drilling. *Int J Adv Manuf Technol* 33:103–109
26. Kruth JP, Bleys P (2000) Measuring residual stress caused by wire EDM of tool steel. *Int J Electrical Mach* 5:23–28
27. Puranik MS, Joshi SS (2008) Analysis of accuracy of high-aspect-ratio holes generated using micro-electric discharge machining drilling. *Proc Inst Mech Eng J Eng Manuf* 222:1453–1464
28. Nirala CK, Saha P (2015) Evaluation of  $\mu$ EDM-drilling and  $\mu$ EDM-dressing performances based on online monitoring of discharge gap conditions. *Int J Adv Manuf Technol* 85:1995–2012

# Chapter 10

## Sequential Micro-EDM



MD. Rashef Mahbub, Asma Perveen and Muhammad P. Jahan

**Abstract** In this chapter, different sequential conventional and non-conventional micromachining processes with micro-EDM have been discussed elaborately with their applications in modern-day research and industrial fields. The necessity and advantages of sequential micromachining processes and their difference from hybrid micromachining have been carefully identified. Micro-EDM combined with micro-grinding, micro-milling, micro-turning, micro-ECM, micro-drilling, laser micromachining, LIGA have been discussed with their advantages over respective single processes. The common issues that generally stand in the way of pulling out sequential processes successfully or hamper their accuracy have also been addressed. The chapter also suggests some initiatives to solve those issues. While wrapping up, the chapter emphasizes on the fact that how sequential micromachining, if properly implied, can solve a lot of problems that currently available single processes are dealing with and widen the vast possibility of micromachining of 3D complex structure with high level of accuracy.

**Keywords** Micro-EDM · Sequential machining · Micromachining  
Combined machining · Micro-level accuracy · Micro-tools

---

MD. Rashef Mahbub · M. P. Jahan (✉)  
Department of Mechanical and Manufacturing Engineering, Miami University, Oxford, OH  
45056, USA  
e-mail: [jahanmp@miamioh.edu](mailto:jahanmp@miamioh.edu)

MD. Rashef Mahbub  
e-mail: [mahbubm@miamioh.edu](mailto:mahbubm@miamioh.edu)

A. Perveen  
Department of Mechanical Engineering, Nazarbayev University, Astana, Kazakhstan  
e-mail: [asma.perveen@nu.edu.kz](mailto:asma.perveen@nu.edu.kz)

© Springer Nature Singapore Pte Ltd. 2019  
G. Kibria et al. (eds.), *Micro-electrical Discharge Machining Processes*, Materials  
Forming, Machining and Tribology, [https://doi.org/10.1007/978-981-13-3074-2\\_10](https://doi.org/10.1007/978-981-13-3074-2_10)

## 10.1 Introduction

With the advancement of technology in each of the scientific and research area, tools and devices are getting small to smaller and complex to even more complex every day [1]. Now in manufacturing field, it is possible to deliver micro-, or even nano-level accuracy, surface roughness, and desired microstructure which were unimaginable even couple of decades earlier. These newly introduced micromachining technologies and newly fabricated micro-components have very wide application in biomedical fields, information science, aerospace engineering, optical industries and so on.

In biomedical fields, especially while designing implants for hip, knee, and dental purposes, the level of precision and accuracy have to be pinpoint as any small defect in designing and manufacturing might lead to very severe consequences for the person who is carrying it. You have to look into account every detail of the materials you are working on, do research on the medium and bone micro-morphology and then you have to design and deliver the desired product with infinitesimal accuracy [2]. In optical fields, devices like optical waveguides, fiber-optic connectors, micro-lens arrays also need micro-level accuracy and precision [1]. Different kind of surface micromachining and smoothing technologies have advanced the research in microfluidics section and increased their application in Bio-MEMS area [3]. The invention of micro- and nano-materials and their massive usage in information science are also touching a new horizon every day. All these applications that are mentioned and the vast majority that cannot be mentioned on the small scope of this chapter imply how important micromachining and micro-components are in today's scientific research and industrial application.

Quite a few numbers of fabrication procedures have been invented and are being used on a daily basis for machining micro-components. Micro-electric discharge machining (micro-EDM), micro-electrochemical machining, laser micromachining, micro-grinding, micro-turning, micro-milling, micro-drilling, and Lithographie, Galvanoformung, Abformung, i.e., Lithography, Electroplating, and Molding (LIGA) are some of the most popular methods to produce micro-level manufacturing products. Some of these machining techniques are conventional, and some are non-conventional. Each of them has certain advantages and disadvantages, and none of them are suitable for all kind of materials and design procedures. Some techniques are speedy than others, some are better in surface finishing, some consume less machining time, some require less power supply, some methods are less costly than others and so on and so forth. So choosing a single definite method for creating a specific micro-accurate product is very difficult sometimes.

That is where comes the necessity and application of sequential micromachining techniques. As said earlier, each of these processes has their own pros and cons, so combining themselves with a proper technique sometimes come really handy; in that way, we can use advantages of a certain machining process, and where it is not perfect or become clumsy, we can use another machining process there. There are a lot of examples and applications of such kind of micromachining processes. The scope of this book chapter mainly deals with sequential micromachining with micro-

EDM process. Micro-EDM has been combined with micro-ECM, micro-grinding, micro-turning, micro-milling, LIGA, micro-drilling, laser micromachining and so on. Sometimes micro-EDM has been used for shaping the metal, sometimes for finishing, sometimes for making electrode, or some other micro-component for using it on some other machining process later on. In this book chapter, all these sequential and combined micromachining process have been discussed elaborately with their experimental setup, parameters optimization, and applications.

Before jumping into that, things to keep in mind that there are certain differences between hybrid micromachining and sequential micromachining. In hybrid micromachining, two or more processes are involved at the same time to remove material or do the machining task. While in sequential machining, the machining processes are one after another, that means, sequentially. The machining processes might be carried out on the same experimental setup that does not necessarily make it hybrid as long as they are both not employed to do the machining simultaneously. This book chapter completely deals with sequential micro-EDM, so hybrid micro-EDM processes like vibration-assisted micro-EDM, laser-assisted micro-EDM, magnetic-assisted micro-EDM, powder-mixed micro-EDM are not in the scope of this book chapter.

## 10.2 Advantages and Properties of Sequential Micro-EDM

Sequentially combining conventional and non-conventional micromachining processes has certain advantages as mentioned earlier. Some of them are listed below:

- There exists a lot of processes which are not perfect for machining certain materials that can be machined by micro-EDM, but they are better at finishing. Combining those processes can deliver better outcome than using micro-EDM or that process alone.
- Tool wear of the electrode is one of the main concerns while using micro-EDM which can be eliminated by sequential machining.
- In so many cases, combining another micromachining process with micro-EDM speeds up the whole process and results in higher productivity.
- Micro-EDM often makes machine components for other machining processes, like electrode or other machine parts for drilling, milling, grinding.
- The cumulative process force can be minimized by sequential micromachining.
- Some complex shape of machined part cannot be achieved by a certain machining technique. Micro-EDM combined with other micromachining can solve this issue.



### 10.3 Prerequisites of Sequential Micromachining

Sequential micromachining has a lot of advantages as discussed above, but the task of pulling out such a combined micromachining process is not a very easy one. The machine tools demand certain requirement for this kind of sequential system. Accurate measurement of machine tool is also necessary which is often not provided. Also, the preciseness required in this kind of combined machining process is really tough to deliver, which conventional CNC machine often fails to do. In conventional machining processes, thermal deformation, mechanical failure, tool wear, chatter, and vibration are very common phenomena that obstructs machining super precise, micro-components, and machine parts. Making this kind of ultra-precise machine parts also requires extraordinary and complex setup which is very expensive and mostly avoided if not pre-planned. So, the primary requirements of developing such kind of sequential, integrated, and combined machining system are to create multi-purpose machine tools and setup from the very beginning keeping in mind that it can be integrated sometimes for specific application.

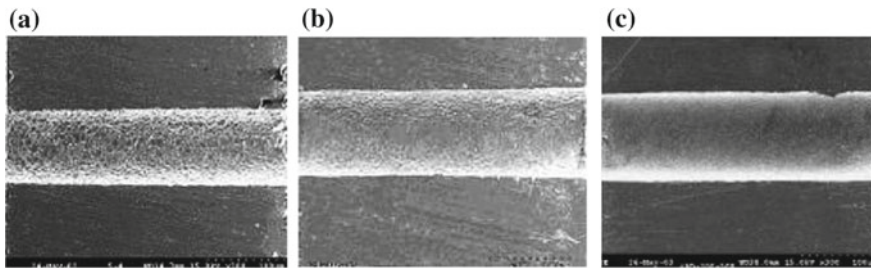
### 10.4 Sequential Micro-EDM and Its Applications

#### 10.4.1 *Sequential Micro-EDM and Micro-grinding*

Micro-EDM has been very popular in manufacturing industries and research fields because of its low setup cost, better precision and accuracy, and wide design freedom [4]. Mechanical stress, chatter, and vibration problems are not an issue here because it is a no-contact process and no cutting force is applied during machining. There have been a lot of research to study sequential and hybrid machining based on micro-EDM. It has been integrated with micro-ECM, laser micromachining, electropolishing, micro-milling, micro-grinding and so many other similar processes [5]. Most of this sequential and hybrid machining approaches are applied because of the fact that micro-EDM, with its numerous advantages, has some disadvantages too. It delivers poor surface quality because of the recast layer formed on the machine surface. That region machined by micro-EDM is generally populated with discharged craters and micro-cracks [6]. This issue deteriorates the diametrical and geometrical shape accuracy of machine holes. On the other hand, conventional grinding often finds it difficult to extend its preciseness and accuracy level in micro-level. Micro-EDM with high-frequency dither grinding (HFDG) combined has been studied to overcome the problem stated above.

A pulse generator, a power amplifier, and a dither mechanism consist of a basic HFDG system. The workpiece kept fixed at the center of dither mechanism. The frequency matching with the resonance frequency of the carrier creates dither resonance. The core and the workpiece both are driven in radial back and forth gyrate motion while operating. This motion coupling with the micro-EDM spindle performs





**Fig. 10.1** SEM images of micro-holes throughout the process, **a** after micro-EDM, before grinding, **b** after grinding with circular tool, and **c** after grinding with stepped circular tool [7]

**Table 10.1** Machining parameters for HFDG [7]

Machining parameters of HFDG	
Diameter of tool	100 $\mu\text{m}$
Dither voltage	50 V
Dither frequency	3 kHz
Grinding duration	15 min

the polishing operation of micro-hole. This relative motion between the workpiece and tool electrode performs the grinding by alumina particles and helps in improving the surface roughness of micro-hole [6].

A high nickel alloy was used in this study as machining material. The micro-EDM study tries to optimize electrode gap voltage in terms of different peak current as this gap voltage has an impact on material removal rate, diameter variation in entrance and exits, electrode wear rate, and expansion of micro-holes. Same parameter sets were then used for HFDG machining.

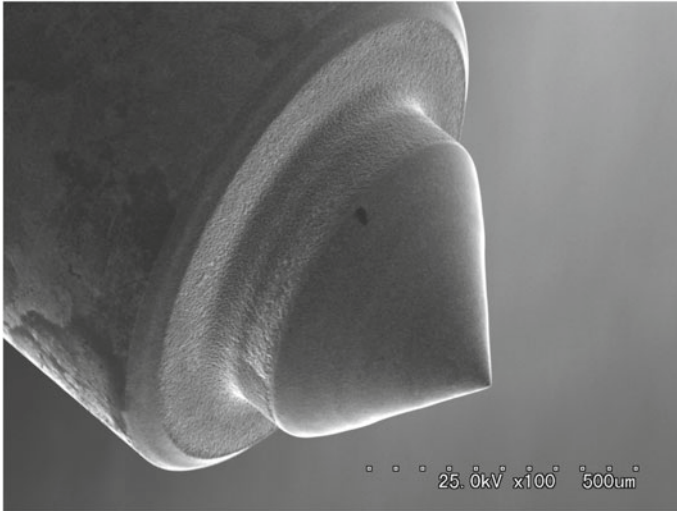
Circular and stepped circular electrodes were used for performing grinding, and the SEM images of cross sections of micro-holes illustrate the results. It is obvious that both the electrodes improve the surface roughness but the stepped circular one performs better, as can be seen from Fig. 10.1. The machining parameters for HFDG process is listed in Table 10.1.

In another study, a combination of micro-EDM and grinding method has been tried sequentially where a polycrystalline diamond (PCD) tool was trued by micro-EDM and then it was used in grinding. High-precision microstructures like V-grooves can be processed in this combined method [1].

The particle size of the PCD tool that was shaped by micro-EDM was 0.5  $\mu\text{m}$ . Both processes, micro-EDM and grinding, used the same bearing system to ensure the tool rotation accuracy. A three-axis machine platform was used to conduct the grinding experiment where changing electric discharge energy conditions can control surface roughness of the tool. A DC motor of 3000 rpm was used to drive the tool [1]. The electric discharge condition for shaping the tools and the resulting surface roughness are presented in Table 10.2. The SEM image in Fig. 10.2 shows a grinding PCD tool sharpened by micro-EDM process.

**Table 10.2** Electric discharge condition and resulting surface roughness [1]

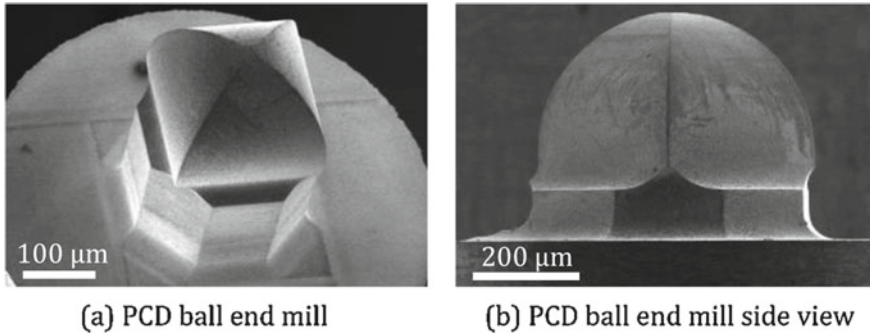
Tool no.		1	2
Discharge conditions	Capacitance of capacitor	10 pF	3300 pF
	Processing voltage	70 V	110 V
Tool's surface roughness (Ra)		0.20 $\mu\text{m}$	0.78 $\mu\text{m}$

**Fig. 10.2** Micro-EDM sharpened tool [1]

#### 10.4.2 Sequential Micro-EDM and Micro-milling

Fabrication of complex three-dimensional microstructure has been an urgent call in modern-day manufacturing industries. While doing so with hard molds, generally grinding is chosen where they use micro-diamond wheels. But the newly emerged glass products are too sophisticated to be machined by grinding wheels. They are also axis asymmetric. These complex 3D shapes can be processed with micro-milling technology, which is one of the most important features in mechanical micromachining processes [8–10]. For micromachining hard and brittle material, it is required to achieve the micromachining in ductile phase, and the geometrical configuration and accuracy of micro-end mills promote these requirements [11].

Often times polycrystalline diamond (PCD) and cubic boron nitride (CBN) are used as micro- and nano-level milling cutter material as they are super hard which ensures longer tool life. Traditional grinding wheels have specific limitations for size and deliver comparatively less material removal rate. Wire electric discharge machining (WEDM) is very popular to fabricate this type of micromachining tools as most of the metals are either conductive or the binders used in these materials



**Fig. 10.3** PCL ball end mill manufacture by WEDM to later use in micro-milling [12]

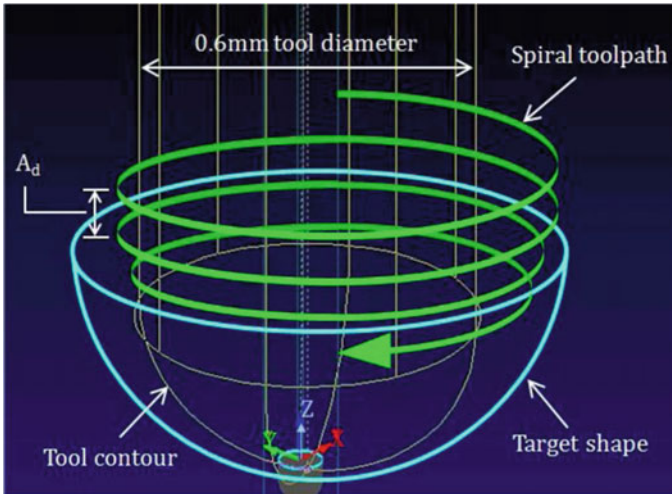
make them conductive [11]. So, fabricating the milling tools in micro-EDM and then using it sequentially in micro-milling have been quite a common feature.

A precise small-scale wine-glass gyroscope has been manufactured by micro-milling process, and productivity, quality and geometrical accuracy have been investigated all through the process. The main aim was fabricating the silicon cavity to use it later as a mold for thin wall diamond hemisphere as this is the primary part of the wine-glass gyroscope.

The advantage of using mechanical micro-milling is that it does not need any post-processing. The PCD ball end mill, which has a 0.3 mm four-flute, was made using a six-axis WEDM. Figure 10.3 shows the PCD ball end mill manufactured by WEDM. The negative rake angle confirms the ductile mold machining [12]. As the shape of the machined feature was quite complicated and tough to comprehend, Fig. 10.4 is provided to get a better understanding of tool geometry.

The experiment was conducted with seven trials, on each of which spindle speed and feed rate were kept constant. The approach type and depth of cut were varied mainly to investigate maximum possible material removal rate that can be achieved without producing crack. In Table 10.3, parameters and subsequent results for top and bottom edge are listed, and cycle times are also mentioned. A green color in the table denotes almost flawless result, and yellow indicates poor while the red one signifies occurrence of chipping from moderate to severe level [12].

It was found from this experiment that this sequential process of making the PCD tool with EDM and then micro-milling with that can deliver excellent geometrical accuracy in the expense of productivity. WEDM has been also used on analyzing accuracy of fabrication of micro-milling tools. The process was modelled taking two typical micro-ball end mills. It was found that fabrication accuracy is proportional to designed micro tool geometry [11].



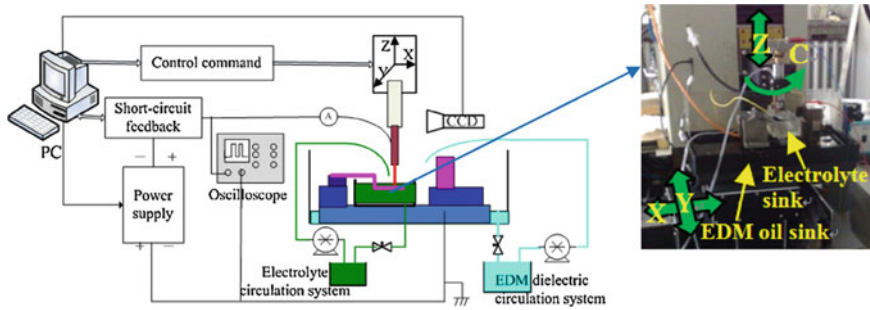
**Fig. 10.4** Schematic of tool shape, tool path, and target feature [12]

**Table 10.3** Parameters and results of micro-milling experiment [12]

	1	2	3	4	5	6	7
Approach type	Vertical	Vertical	Vertical	Vertical	Spiral	Spiral	Spiral
Feed rate (mm/min)	492	492	492	492	492	492	492
Ad (μm)	0.1	0.2	0.5	1	0.1	0.2	0.5
Top edge							
Bottom							
Cycle time	21	11	5	3	22	12	6

### 10.4.3 Sequential Micro-EDM and Micro-ECM

As said earlier, being a non-contact and almost no cutting force process, micro-electro-discharge machining is one of the most popular methods of machining miniature parts and 3D microstructures. It can machine material of a wide range and is also capable of producing complex 3D objects. Width and depth of electric discharge erosion pits determine the surface quality, electrode wear, and tool servo stability, which replicates the machining accuracy in micro-EDM. But being a thermal process, micro-EDM sometimes generates recast layer and micro-crack which harms the machined surface. Also, it requires the use of multiple electrodes because of electrode wear, which also lowers the efficiency. Whereas micro-ECM does not have these issues of electrode wear and preparing multiple electrodes. It also does not generate heat damaged layer or micro-crack on the machine surface, so surface roughness is improved by this method. Having all these advantages, micro-ECM is



**Fig. 10.5** Combined machine setup of micro-EDM and micro-ECM [13]

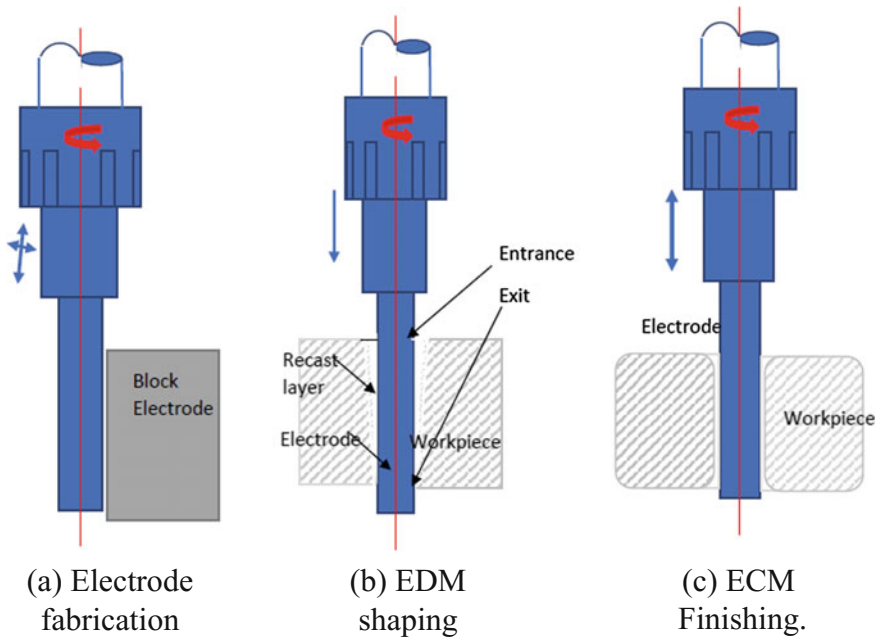
not suitable for parts machining of metallic materials because of the stray corrosion during the process that results in hampering shape accuracy. That is why the study has been progressed combining this two methods, where shaping has been done by micro-EDM and the finishing has been conducted by micro-ECM.

Same machine tool and tungsten electrode were used for both process, but oil was used in EDM and electrolyte was used in ECM. The power system was independent in both cases. The machine system had three axes where  $X$ - and  $Y$ -axes were driven by AC servo motor and a linear motor drove the  $Z$  axis. The rotational speed of the electrode could be varied between 0 and 4000 rpm. Figure 10.5 shows the combined micro-EDM and micro-ECM machine tool [13]. The electrode that was used in both process was fabricated in situ by an anti-copying block. The workpiece and EDM oil bath kept fixed on the workbench while the ECM electrolysis bath was added after the micro-EDM process to avoid clamping error of electrode and workpiece.

To investigate this sequential machining process, various machining conditions have been tried. The tungsten electrode had a diameter of 0.1 mm, and a 304 stainless steel with a thickness of 0.4 mm was used as a workpiece. The parameters that were varied were machining voltage, tool feed rate, and initial machining gap.

This process has three main steps as shown in Fig. 10.6. Using Block Electro Discharge Grinding (Block EDG) method, a tungsten rod of 0.5 mm was grinded into 0.1 mm for using in micro-EDM and micro-ECM process. The electrode was fed about 1.5 mm in  $Z$ -direction. The bottom of the electrode always stays under the hole exit [14]. On later two parts with that fabricated electrode, first micro-EDM shaping and then micro-ECM finishing were done.

The system delivers its optimum performance at machine voltage 10 V, initial machining gap 10  $\mu\text{m}$ , and tool feed rate 10 mm/s. The ECM finishing was able to lower down the micro-EDM-machined surface roughness from 0.707 to 0.143  $\mu\text{m Ra}$ . It was also able to improve the surface quality by eliminating burrs, micropores, recast layer, and craters completely. It was found that faster electrode feed rate smoothens the surface and improves workpiece shape as well. This combined method overall has proven to be very useful in machining complex 3D metallic microstructure [13].



**Fig. 10.6** Sequential machining process of EDM and ECM [14]

Micro-EDM also has been sequentially used with electrochemical etching process. A combination of micro-EDM and electrochemical etching has been used to produce an array of microelectrodes. Using wire EDM, rectangular columns of size  $0.2 \text{ mm} \times 0.2 \text{ mm}$  were machined and then to turn them into cylindrical columns, electrochemical etching was used. A wide dimensional range of micrometers can be processed in this sequential method [15].

For the microelectrode material, tungsten was used. The workpiece was mounted in the EDM tank perpendicular to the EDM wire, and the initial cut was performed through one tungsten plane. Once the square microelectrodes are done producing, they kept immersing on electrolyte while current flows between anode and cathode. The electrolysis happens over there to turn the square microelectrode to cylindrical shape. The square electrodes machined by WEDM are presented in Fig. 10.7. The dimension of the fabricated electrodes was  $1.5 \times 0.2 \times 0.2 \text{ mm}$  each, and there was  $800 \mu\text{m}$  spacing between each neighboring electrode.

The recessed holder that carries array of microelectrodes is immersed in KOH solution of 2 M/L at about 1.5 mm depth. As cathode, two stainless steel plates were used. It is kept parallel to the array electrode and DC power is applied. The side view of the cylindrical electrodes that were used later on for producing micro-holes is presented in Fig. 10.8. Those electrodes have diameter between  $39.340.6 \mu\text{m}$  and the tolerance kept controlled within 3.25% [15].



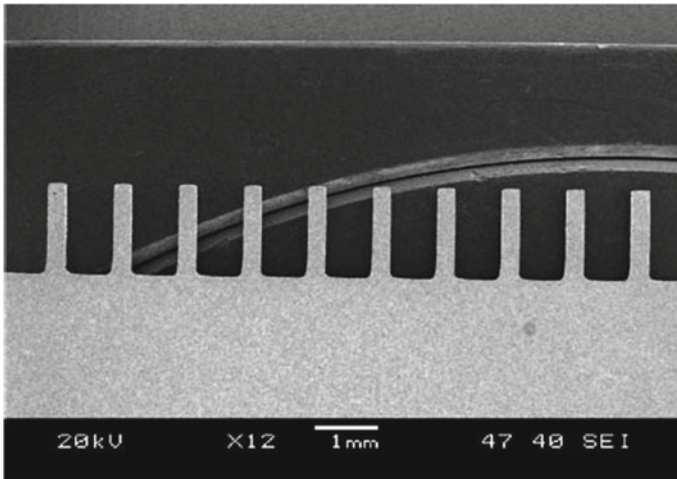


Fig. 10.7 SEM image of micro-EDM-fabricated square electrode [15]

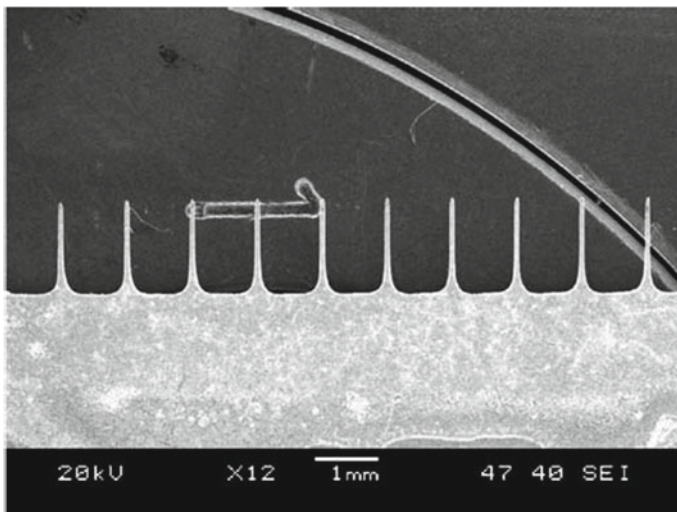


Fig. 10.8 Cylindrical microelectrode processed by electrochemical etching [15]

#### 10.4.4 Sequential Micro-EDM and Laser Micromachining

Combining two of the most popular methods of micromachining, micro-EDM and laser micromachining, is gaining more popularity, and it has a wide range of application, especially in fuel injection nozzles and assembling micro-parts. Often times, these two processes are sequentially applied after mechanical micro-drilling, which makes it a combination of three sequential micromachining processes.

For reducing the pollutant emission to the environment and achieving a higher energy efficiency, it is a prerequisite in diesel fuel injection nozzle to have hole size less than 145  $\mu\text{m}$ . Micro-EDM drilling is one of the most popular methods available there for this purpose, but it faces challenges as constantly decreasing hole size demands higher tooling cost because of frequent breakage of electrode [16]. Material removal rate is also less in this process [16, 17]. Researchers have been trying using nanosecond pulse laser beam for this purpose, but it cannot deliver industrial standard hole quality because of producing larger recast and heat-affected zone [18]. Pico-second and femtosecond lasers have the potential to deliver better quality micro-hole [19], but the drilling time is generally too long.

First in 1-mm-flat plates of nickel-chromium alloy, laser holes were drilled to evaluate the optimum parameters of hole drilling for a fuel injection nozzle. Then real holes with those parameters were drilled from 10 to 120  $\mu\text{m}$ , in steps of 10  $\mu\text{m}$ . The final target was to achieve 140  $\mu\text{m}$  hole size. Different types of holes, namely positive, negative, blind, parallel, were drilled to investigate which one delivers the most perfect EDM cycle time. Zeiss optical microscopy was used to measure the laser holes, and HAZ at entry and exit diameter was also taken in considerations to evaluate [20].

For the accurate alignment of EDM electrode and laser-drilled holes, accurate fixturing was used. Deionized water and solid tungsten carbide electrode were used in the EDM process of drilling micro-holes. A new on-line cutting method was applied for dressing the EDM electrode in the gap of each hole drilling. This saves more time compared to standard EDM electrode dressing. For electrode wear investigation, electrode shape was investigated after each drill, and image analysis was done to avoid misalignment. Morphology and microstructure of drilled holes were evaluated through SEM images [20].

The main target of this study was to drill a 140  $\mu\text{m}$  hole with a 110- $\mu\text{m}$ -electrode in the shortest time. It was found that for fastest EDM cycle time, the optimum one was an 80  $\mu\text{m}$  parallel laser hole. Considering dressing time, the production time was reduced by 70% using micro-EDM application. Hole quality was also much more improved while doing sequential laser and micro-EDM drilling. Figure 10.9 shows the comparison of the surface quality with laser micromachining and combined laser and micro-EDM process. The first one implies SEM image of an 80  $\mu\text{m}$  diameter laser hole where processing time was around 1 s. The later one is the cross section of a laser-EDM hole of 140  $\mu\text{m}$  diameter where processing time was 9 s [20].

Another major application of sequential laser with micro-EDM is in assembling process. Producing 3D complex microstructures and then micro-assembling are quite complicated processes to deal with. There are a number of things to consider and worry about while doing so. Positional uncertainty is an important factor to consider in any kind of assembly equipment. It can occur from a number of reasons like manufacturing errors, thermal effects, control errors. Cumulative tolerance is also another thing to take into consideration. The tolerance gets accumulated while assembling two small parts that reduces the assembled accuracy. Also, when we are talking about micro-components, we are dealing with very small dimensions, and the part may fail or behave in an uncontrolled manner because of the force acting



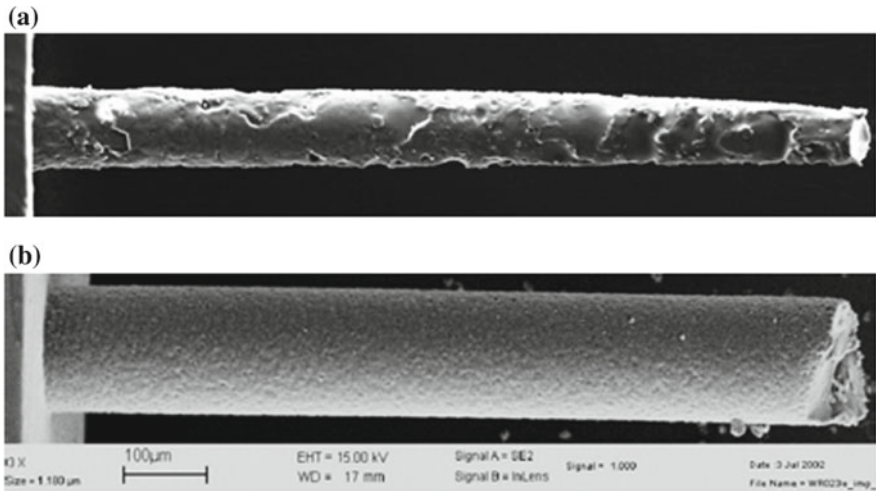


Fig. 10.9 Cross-sectional image of a laser and laser-EDM hole after EDM drilling [20]

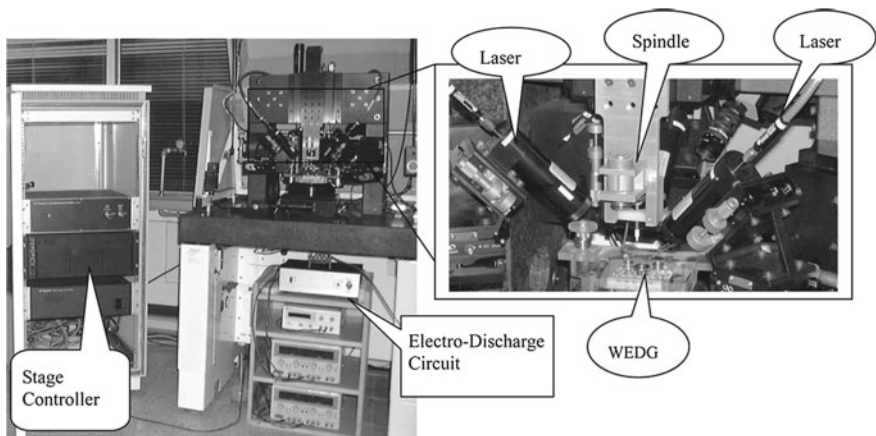
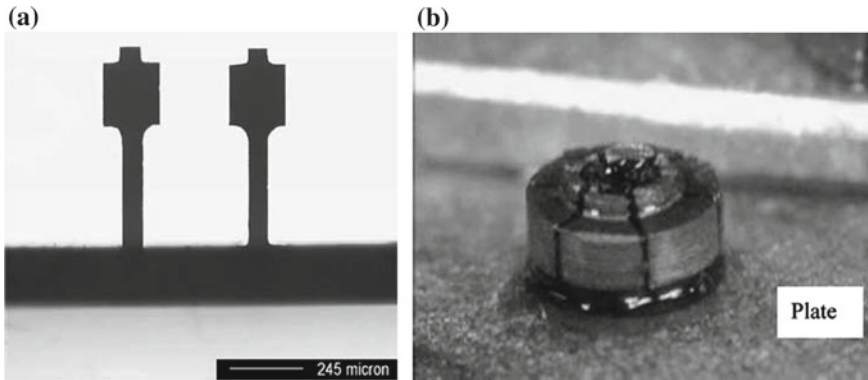


Fig. 10.10 Sequential micro-EDM and laser setup [21]

on the surface. This problem is not very rare while handling small component and joining surfaces at assembly [21].

To overcome those problems stated above, the study has been progressed using a laser welding system integrated with a micro-EDM process. In this integration system, the micro-EDM handles the job of fabricating micro-components that have to be assembled, and later on the laser does the micro-joining for the assembly. This combined system is capable of eliminating or at least reducing the positional and dimensional inaccuracy that we talked about earlier. Figure 10.10 shows the machining setup for this combined system.



**Fig. 10.11** a Multi-pin-plate mold with square patterned top b pin-plate microstructure with a hollow construction [21]

While assembling micro-pins, further machining can be done according to necessity with micro-EDM process. CAD/CAM can also be used for making a more diversifying pattern on top [21]. Figures 10.11a–b show an example of such a multiple plate mold where the top has been further machined to give it a square pattern and a pin-plate microstructure where on top a hollow construction was made later on.

#### 10.4.5 Sequential Micro-EDM and LIGA

Micro-components have become very essential part of modern-day manufacturing industries. The fabrication technology which can fabricate high-aspect ratio microstructures in a wide range of materials are of prime interests to the new researchers. The LIGA process can be applied for mass producing high-aspect ratio microstructures. It can deliver very fine pattern and smooth sidewall surfaces [22]. But one of the main disadvantages is practically it is limited to a very few metals. Whereas micro-EDM is capable of producing three-dimensional microstructure [23], and with the help of electrochemical etching, fine surfaces on the structure can also be achieved [24]. Generally, the electrode that is used for producing pattern is made by wire electro-discharge grinding (WEDG), and it takes a long time to produce one. The electrode needs regular replacing due to wear, and shaping and changing the tool are also time-consuming. These things affect EDM's shape accuracy. To solve these issues, a new method of combining LIGA and micro-EDM has been proposed which can process different kinds of bulk materials to deliver microstructure of high aspect ratio with ultra-fine pattern. These microstructures can be used as micro-components in MEMS device as well as micro-tools in different machining processes [25].

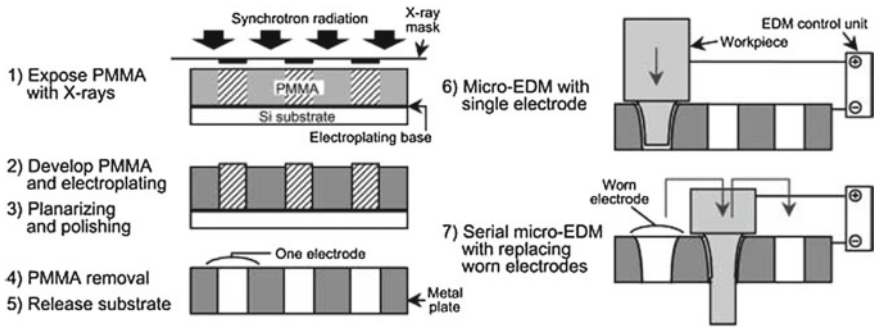


Fig. 10.12 Sequential LIGA and micro-EDM process flow [25]

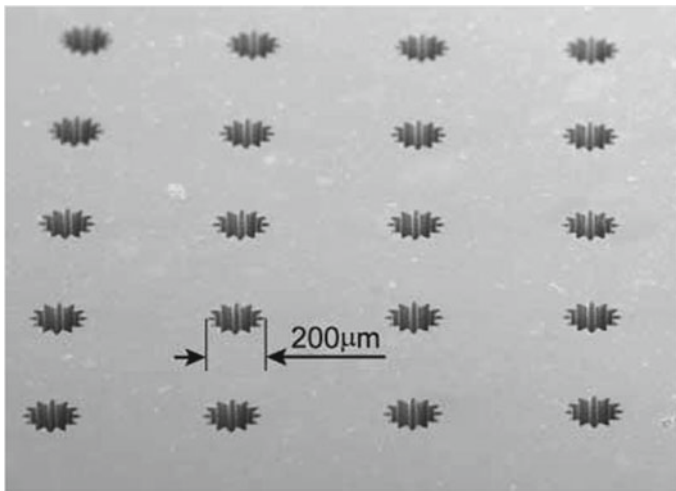


Fig. 10.13 LIGA fabricated negative-type nickel electrode array [25]

Figure 10.12 shows the flow of combined LIGA and micro-EDM process. In this flow, steps 1–5 consists of LIGA process used to fabricate electroplated electrodes for the micro-EDM process, and steps 6 and 7 were the application of fabricated electrodes in micro-EDM process. Electrodes with negative-type microstructures and ultra-fine patterns are fabricated using this sequential process. Accurate control of the electrode location in the metal plate was ensured by photolithographic technique of electrode fabrication. Figure 10.13 shows an array of negative-type nickel electrodes produced by the LIGA method.

This combined micromachining of LIGA and micro-EDM has other uses too, for example, in nozzle plates fabrication. Usually electroplating or laser machining are used for manufacturing nozzle plates of ink jet printer heads, but with electroplating, it is really tough to achieve a nozzle diameter less than 50  $\mu\text{m}$ . The disadvantage of laser machining is that the equipment is very expensive. Combining LIGA and

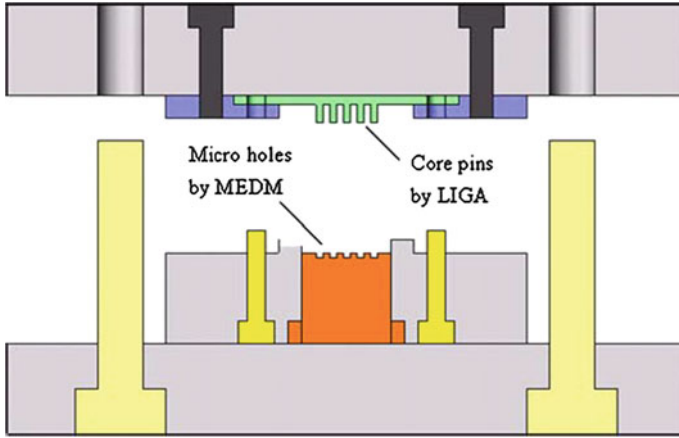


Fig. 10.14 Process setup for core pins by LIGA and micro-hole by micro-EDM [26]

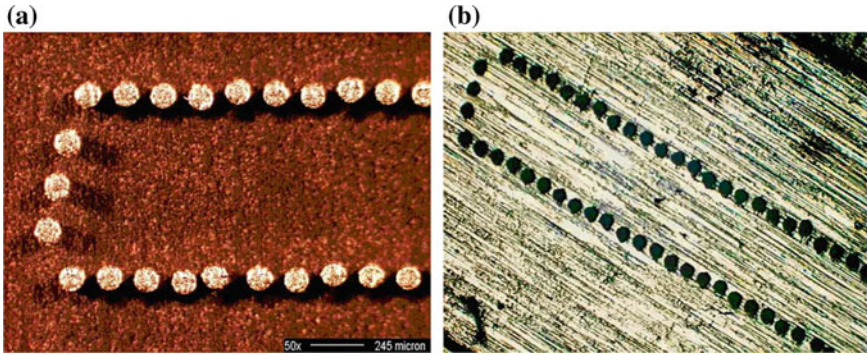


Fig. 10.15 a Micro-core pins produced by LIGA, b micro-holes generated by micro-EDM [26]

micro-EDM technology, a new microinjection molding method was introduced for manufacturing nozzle plates. This new technique can ensure improved positioning and alignment accuracy of the nozzles [26]. Each nozzle plates were 7 mm × 4 mm with a thickness of 0.05 mm. Each nozzle diameter was 0.1 mm, and the plate had 60 micro-through holes [26].

LIGA is popular for positional accuracy and accurate pitch distance. So, LIGA was used to fabricate 60 micro-core pins. The fabricated micro-core pins were later used as electrode for machining micro-holes. This method improves the assembly accuracy of two cavities. Micro-EDM was used for manufacturing 60 micro-holes in this method [26]. The process setup for fabricating core pins by LIGA and micro-hole by micro-EDM is shown in Fig. 10.14. The microscopic image of 60 micro-core pins by LIGA method and 60 micro-holes by micro-EDM are illustrated in Fig. 10.15.

### 10.4.6 Sequential Micro-EDM and Micro-turning

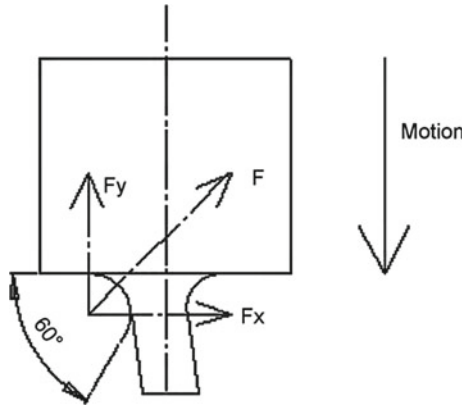
To deliver high-precision and dimensional accuracy while fabricating microstructure, it has been pretty common to sequentially use two or even more manufacturing processes. Most of the time, this combination combines traditional (micro-grinding, turning, milling, etc.) and non-traditional methods, among which micro-EDM is the most common one.

As we all know, micro-EDM is a non-contact process that uses very little to no force as it uses the electric discharge between electrode and workpiece to machine any conductive ductile, brittle, or super hardened materials. For this reason, micro-EDM is a very popular method in micromachining of materials, but it has certain disadvantages as well, primarily to be mentioned high electrode wear ratio and low material removal rate. Changing electrode once in a while can be a getaway card from electrode wear, but it harms the accuracy because of changing the setup or re-clamping of the microelectrode [1]. Another approach might be to create a long enough electrode at the very beginning and to fabricate the electrode in situ for further machining.

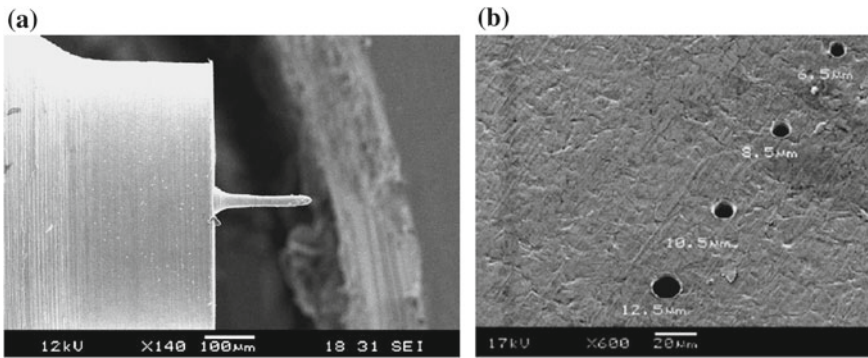
There have been a number of approaches for fabricating tool electrode by using sacrificial electrodes. Block Electro Discharge Grinding, wire electro-discharge grinding, etc., are some of them. But all these sacrificial electrodes using methods have some disadvantages in common. These processes are error prone and difficult for automation. It needs regular operation checking and needs manual compensation of the error while demanding quite a few hours of machining time as well [27]. So, preparing the microelectrode with micro-turning process and then using it for micro-EDM has been tried and become quite successful.

Deflection of the shaft during machining might be a crucial issue while fabricating thin electrode by turning. The workpiece deflects both in normal and tangential directions and also in the top surface of the cutting tool. It is extremely difficult achieving a straight shaft, and the tool either breaks or starts wobbling because of excessive radial cutting force [27].

PCD inserts conventionally have 100  $\mu\text{m}$  tool nose radius which divide the shaft cutting force into two components of  $F_x$  and  $F_y$ . As shown in Fig. 10.16,  $F_x$  component contributes to the deflection of the shaft and  $F_y$  component does the actual cutting. So, this  $F_x$  component needs to be reduced to get a straight shaft with small diameter, and the commercial PCD needs to be modified for this purpose. Therefore, the PCD tool is modified by minimizing/eliminating the  $F_y$  component using block micro-EDG process. Micro-electric discharge grinding (micro-EDG) was performed with the help of a sacrificial electrode to achieve a tool with very sharp edge. The micro-shafts that were produced were 2 mm long with a diameter less than 20  $\mu\text{m}$ . Less than 10 min was required to perform this fabrication process. Figure 10.17a shows a micro-shaft machined by conventional micro-turning process. Despite brass having large wear, the electrode produced was capable of machining around 40 holes on a SUS plate whose thickness is 50  $\mu\text{m}$ . Figure 10.17b shows



**Fig. 10.16** Motion and force component shown for a commercial tool [27]



**Fig. 10.17** **a** The 22- $\mu\text{m}$ -electrode fabricated by micro-turning process after machining ten micro-holes on 100  $\mu\text{m}$  thick stainless steel plate, showing some wear, **b** different diameter holes with very high aspect ratio on a 50- $\mu\text{m}$ -plate of stainless steel [27]

SEM image of different diameter holes with very high aspect ratio on a 50- $\mu\text{m}$ -plate of stainless steel machined by fabricated microelectrode.

### 10.4.7 Sequential Micro-EDM, Micro-drilling and Electropolishing

Electropolishing method was first invented in 1935 and is quite popular in manufacturing industries to improve the surface quality of machined materials. In this process, a passive film is developed by anode surface through selective dissolution. As thin film has lower elective resistivity it impels the anode current to be concentrated more at peak. This results in brightened and passivated workpiece surface which promotes



better corrosion resistance as well [28]. Because of craters, micro-cracks and recast layer formation, micro-EDM, with all its advantages yet deliver poor surface quality. To eliminate those detrimental effects of micro-EDM, some studies have been progressed by using electropolishing as a post-processing mechanism for better surface finish [29, 30].

Sequential micro-EDM with electropolishing has been tried to improve the surface quality of machined micro-holes. This process is actually a combination of three sequential machining processes. First, micro-WEDG was used to fabricate the microelectrode for machining micro-holes. Then these electrodes were used for drilling micro-holes by micro-EDM drilling, and later on electropolishing was used for the improvement of surface roughness of machined micro-holes. Nickel alloy was used as workpiece material because of its excellent inherent properties which shield against magnetic disturbance. To avoid insoluble reaction products, acid solution was used for electrochemical machining [31].

Different electrolytic voltages (1, 2, 3, and 5 V) have been applied in the electropolishing to investigate various performance characteristics of micro-holes. Also, parameters as machining time and electrode rotational speed have also been varied to see their effects on different performance phenomena. It is obvious that electropolishing can improve the surface quality of micro-EDM drilled micro-holes by quite a big margin and delivers a smoother and burr-free surface. Even this method is capable of finishing the burrs on the hole entrance of very complex shaped micro-holes. Stagnant electrolyte with a concentration ratio of 1:10 and motionless electrode were found to deliver best performance for this study. In terms of voltage and machining time, electrolytic voltage of 2 V and electrolysis time of 5 min promoted best result in this case.

## 10.5 Summary

At present, a significant number of hard alloys, ceramics, and composites are used in research and industrial field of manufacturing, which are very difficult to machine using commonly available conventional machining processes. Even non-conventional machining processes, i.e., EDM, ECM, Laser, are also not capable enough to process everything as modern-day manufacturing demands machining of 3D complex intricate shapes with ultra-precision accuracy and amazing surface finish. These emerging set of demands are too much to handle by a single machining process, hence there rises the necessity of sequential micromachining process. Micro-EDM sequentially with other micromachining processes can solve a lot of those issues that were unsolvable before.

In this book chapter, different micromachining processes used sequentially with micro-EDM has been discussed elaborately. The chapter discusses advantages of such kind of machining process over a single process and also distinguishes its differences from hybrid micromachining. Hybrid micromachining processes such as vibration-assisted micro-EDM, laser-assisted micro-EDM, magnetic-assisted micro-EDM, and

powder-mixed micro-EDM were outside of the scope of this chapter. Rather this chapter focuses on sequential micro-grinding, micro-turning, micro-drilling, micro-EDM, micro-ECM, laser micromachining with micro-EDM.

The applications of these sequential processes have been discussed thoroughly. The chapter also tries to address the common issues that stand in the way of applying this kind of sequential micromachining processes and suggests possible initiatives to solve those problems. Illustrating all about sequential micro-EDM processes, the chapter wraps it up with a hope that proper application of sequential micro-EDM will widen the possibility of modern-day micromachining of 3D complex shapes with ultra-precision accuracy and high-quality surface finish.

## References

1. Wada T, Masaki T, Davis D (2002) Development of micro grinding process using micro EDM trued diamond tools. In: ASPE proceeding, annual meeting, pp 16–19
2. Akça K, Chang T, Tekdemir İ, Fanuscu MI (2006) Biomechanical aspects of initial intraosseous stability and implant design: a quantitative micro-morphometric analysis. *Clin Oral Implant Res* 17(4):465–472
3. Okandan M, Galambos P, Mani SS, Jakubczak JF (2001) Development of surface micromachining technologies for microfluidics and bioMEMS. *SPIE Proc* 4560:133–139
4. Lim HS, Wong YS, Rahman M, Edwin Lee MK (2003) A study on the machining of high-aspect ratio micro-structures using micro-EDM. *J Mater Process Technol* 140(1–3):318–325
5. Ho KH, Newman ST (2003) State of the art electrical discharge machining (EDM). *Int J Mach Tools Manuf* 43(13):1287–1300
6. Liu HS, Yan BH, Chen CL, Huang FY (2006) Application of micro-EDM combined with high-frequency dither grinding to micro-hole machining. *Int J Mach Tools Manuf* 46(1):80–87
7. Liu HS, Yan BH, Chen CL, Huang FY (2006) Application of micro-EDM combined with high-frequency dither grinding to micro-hole machining. *Int J Mach Tools Manuf* 46(1):80–87
8. Wissmiller DL, Pfefferkorn FE (2009) Micro end mill tool temperature measurement and prediction. *J Manuf Processes* 11(1):45–53
9. Cheng X, Wang Z, Nakamoto K, Yamazaki K (2010) Design and development of PCD micro straight edge end mills for micro/nano machining of hard and brittle materials. *J Mech Sci Technol* 24(11):2261–2268
10. Kang IS, Kim JS, Seo YW (2008) Cutting force model considering tool edge geometry for micro end milling process. *J Mech Sci Technol* 22(2):293–299
11. Cheng X, Yang X, Zheng G, Huang Y, Li L (2014) Fabrication accuracy analysis of micromilling tools with complicated geometries by wire EDM. *J Mech Sci Technol* 28(6):2329–2335
12. Fonda P, Nakamoto K, Heidari A, Yang HA, Horsley DA, Lin L, Yamazaki K (2013) A study on the optimal fabrication method for micro-scale gyroscopes using a hybrid process consisting of electric discharge machining, chemical etching or micro-mechanical milling. *CIRP Ann* 62(1):183–186
13. Zeng Z, Wang Y, Wang Z, Shan D, He X (2012) A study of micro-EDM and micro-ECM combined milling for 3D metallic micro-structures. *Precis Eng* 36(3):500–509
14. He XL, Wang YK, Wang ZL, Zeng ZQ (2013) Micro-hole drilled by EDM-ECM combined processing. *Key Eng Mater* 562–565:52–56
15. Wang MH, Zhu D (2009) Fabrication of multiple electrodes and their application for micro-holes array in ECM. *Int J Adv Manuf Technol* 41(1–2):42–47
16. Pham DT, Dimov SS, Bigot S, Ivanov A, Popov K (2004) Micro-EDM—recent developments and research issues. *J Mater Process Technol* 149(1–3):50–57



17. Weng FT, Her MG (2002) Study of the batch production of micro parts using the EDM process. *Int J Adv Manuf Technol* 19(4):266–270
18. Dausinger F (2000) Precise drilling with short-pulsed lasers. High-power lasers in manufacturing. SPIE proceedings, vol 3888, pp 180–188
19. Meijer J, Du K, Gillner A, Hoffmann D, Kovalenko VS, Masuzawa T, Ostendorf A, Poprawe R, Schulz W (2002) Laser machining by short and ultrashort pulses, state of the art and new opportunities in the age of the photons. *CIRP Ann* 51(2):531–550
20. Li L, Diver C, Atkinson J, Giedl-Wagner R, Helml HJ (2006) Sequential laser and EDM micro-drilling for next generation fuel injection nozzle manufacture. *CIRP Ann Manuf Technol* 55(1):179–182
21. Kuo CL, Huang JD, Liang HY (2003) Fabrication of 3D metal microstructures using a hybrid process of micro-EDM and laser assembly. *Int J Adv Manuf Technol* 21(10–11):796–800
22. Guckel H, Skrobis KJ, Christenson TR, Klein J (1994) Micromechanics for actuators via deep X-ray lithography. Electron-beam, X-ray, and ion-beam submicrometer lithographies for manufacturing IV. SPIE Proc 2194:2–11
23. Masaki T, Kawata K, Masuzawa T (1990) Micro electro-discharge machining and its applications. In: IEEE proceedings on micro electro mechanical systems, an investigation of micro structures, sensors, actuators, machines and robots, pp 21–26
24. Takahata K, Aoki S, Sato T (1997) Fine surface finishing method for 3-dimensional micro structures. In: Proceedings of ninth international workshop on micro electromechanical systems, pp 291–296
25. Takahata K, Shibaike N, Guckel H (2000) High-aspect-ratio WC-Co microstructure produced by the combination of LIGA and micro-EDM. *Microsyst Technol* 6(5):175–178
26. Tseng SC, Chen YC, Kuo CL, Shew BY (2005) A study of integration of LIGA and M-EDM technology on the microinjection molding of ink-jet printers' nozzle plates. *Microsyst Technol* 12(1–2):116–119
27. Asad ABMA, Masaki T, Rahman M, Lim HS, Wong YS (2007) Tool-based micro-machining. *J Mater Process Technol* 192–193:204–211
28. Hung JC, Yan BH, Liu HS, Chow HM (2006) Micro-hole machining using micro-EDM combined with electropolishing. *J Micromech Microeng* 16(8):1480–1486
29. Ramasawmy H, Blunt L (2002) 3D surface characterisation of electropolished EDMed surface and quantitative assessment of process variables using Taguchi Methodology. *Int J Mach Tools Manuf* 42(10):1129–1133
30. Hocheng H, Pa PS (1999) Electropolishing and electrobrightening of holes using different feeding electrodes. *J Mater Process Technol* 89:440–446
31. Sato T (1994) Nontraditional machining. Yokendo, Tokyo

# Chapter 11

## Near Net Shape Machining by Micro-EDM and Micro-WEDM



Tanveer Saleh and Rubina Bahar

**Abstract** Near net shape is a concept that is widely used in the recent years to address the issues of sustainability and resource optimization in the manufacturing sector. Near net shape (NNS) processes are the processes that require least or no post-processing to manufacture a product. Electro-discharge machining (EDM) is a non-conventional machining process that uses spark erosion principle for machining conductive material. If the tool in the EDM is a flexible metallic wire, then the process is termed as wire EDM. Further to this, when the discharge energy, tool and wire diameter, and the machined features are in micron domain, the machining technique is termed  $\mu$ EDM or  $\mu$ WEDM. In  $\mu$ EDM/ $\mu$ WEDM, the resultant structure does not require any post-processing to attain the final dimensional accuracy and surface finish; therefore, these processes can be considered as NNS processes. In this chapter, different applications of  $\mu$ EDM and  $\mu$ WEDM have been discussed as NNS process.

**Keywords** Micro-EDM · Micro-WEDM · Near net shape processing

### 11.1 Introduction

The manufacturing industry has continuously gone through the evolution process to meet various market and social demands. Previously, for many years lower manufacturing cost and higher production rate were the main goals for the manufacturing researchers. However, the increasing demand for lowering the adverse effect on the environment and society has also been influencing manufacturing research

---

T. Saleh (✉)

Department of Mechatronics Engineering, International Islamic University Malaysia, Selangor, Malaysia

e-mail: [tanveers@iium.edu.my](mailto:tanveers@iium.edu.my)

R. Bahar

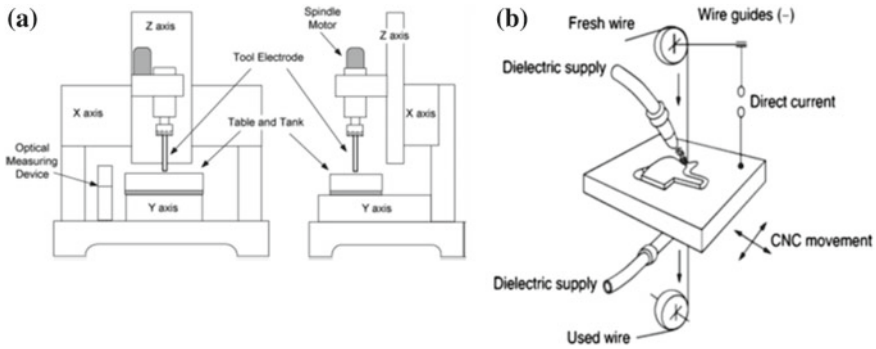
Department of Mechanical and Materials Engineering, Lee Kong Chian Faculty of Engineering and Science, University Tunku Abdul Rahman (UTAR), Selangor, Malaysia

e-mail: [rubina@utar.edu.my](mailto:rubina@utar.edu.my)

© Springer Nature Singapore Pte Ltd. 2019

G. Kibria et al. (eds.), *Micro-electrical Discharge Machining Processes*, Materials Forming, Machining and Tribology, [https://doi.org/10.1007/978-981-13-3074-2\\_11](https://doi.org/10.1007/978-981-13-3074-2_11)

231



**Fig. 11.1** a A typical  $\mu$ EDM setup [3]. b A typical  $\mu$ WEDM setup [4]

recently to achieve a sustainable and more environmentally friendly solution [1]. As a result, manufacturing researches have been evolved to propose new processes that can achieve the final shape of the product by eliminating if not minimizing the finishing steps. The standard term used for such manufacturing processes is called near net shape (NNS) process which aims to minimize finishing operations (e.g., grinding, polishing). As a result, reduction of the wastage of raw material (e.g., swarf, flashing) and energy can be easily achieved by these NNS methods [2].  $\mu$ Electro-discharge machining ( $\mu$ EDM) is considered as an NNS process for fabricating components in meso- and micro-scale. EDM is a non-conventional machining process where mechanical interaction between the tool and the workpiece is not present. In the EDM process, the material is removed by the action of electrical discharge between the tool and the workpiece. The basic principle of the machining is a process when the material of the workpiece is removed through high-frequency sparks between the tool (electrode) and the workpiece immersed into the dielectric fluid like oil, deionized water. As the discharge energy (in  $\mu$ -joule range) becomes very low to create these sparks, the process is then referred as  $\mu$ EDM. This  $\mu$ EDM is a promising machining technology to produce features in micron domain for different engineering applications. The main difference between conventional EDM and  $\mu$ EDM lies in the level of discharge energy and the size of the tool used during the operation. In  $\mu$ EDM, very low discharge energy with high frequency is used ( $\sim\mu$ -joule). Further, typical tool and feature size in  $\mu$ EDM are in order of less than or equal to  $100\ \mu\text{m}$ .  $\mu$ -Wire electro-discharge machining ( $\mu$ WEDM) is a variant  $\mu$ EDM where the flexible metallic wire is used as a tool instead of a rigid micro-shaft. Figure 11.1 describes the working principle of  $\mu$ EDM and  $\mu$ WEDM operation. In both the cases, an RC or a transistor-based pulse generator is used to create continuous electrical discharges between the tool and the workpiece. This operation is usually carried out on three-to-five-degree-of-freedom machines to fabricate miniature parts with notable complex shapes and features. In the next sections, we will discuss how these two micro-fabrication technologies ( $\mu$ EDM and  $\mu$ WEDM) contribute in the field of near net shape (NNS) manufacturing.

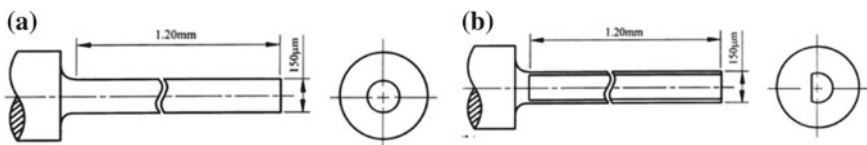
## 11.2 $\mu$ EDM as a Near Net Shape (NNS) Process

$\mu$ EDM has been evolved significantly to achieve high precision and low surface roughness on the finished product. These are the two major requirements for the manufacturing process to be considered as an NNS process. This is why  $\mu$ EDM has been drawing considerable attention from the researchers and engineers as potential near net shape machining process.  $\mu$ EDM can be performed mostly in two ways. In the first method, the tool moves toward the workpiece in one direction which is called die-sinking  $\mu$ EDM. This method is applicable mostly to produce fine micro-holes for various applications such as nozzles for automobiles, aerospace jet cooling holes. However, in order to fabricate 3D parts, the tool of the  $\mu$ EDM is programmed to move in three dimensions in the second method. This method is known to be scanning/milling  $\mu$ EDM. In the next few sections, various aspects of  $\mu$ EDM and  $\mu$ EDM milling will be discussed.

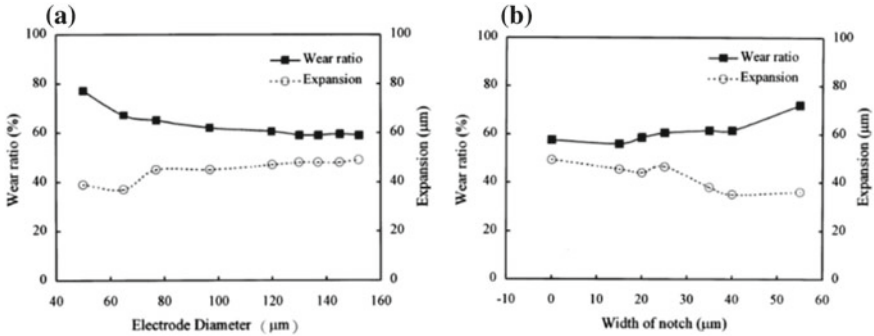
### 11.2.1 $\mu$ EDM for Fabricating Micro-holes and Micro-hole Array

The most common application of  $\mu$ EDM as an NNS process is to drilling a micro-hole and micro-hole array. Yan et al. [5] studied micro-hole machining on difficult-to-cut material such as carbide. The tool material was copper. They studied different aspects in their research such as polarity of the machining, the rotational speed of the tool, and electrode shape in order to identify the effect of each parameter on the tool wear rate and accuracy of the machined holes. Figure 11.2a, b shows the two types of electrode used in their research [5].

Figure 11.3a shows the effect of tool diameter on the wear ratio (WR) and the expansion of the hole (due to debris accumulation and secondary discharges). Figure 11.3b on the other hand demonstrates how WR and the expansion of the hole are affected by the notch width. It can be inferred from Fig. 11.3a that the increase in the diameter of the tool decreases the WR, and at higher diameter, the expansion of the holes' diameter is independent of the tool diameter. However, interestingly it was observed that higher notch radius decreases the expansion of the hole diameter significantly primarily because of the better debris flushing. However, the wear ratio also increases as the notch width increases.

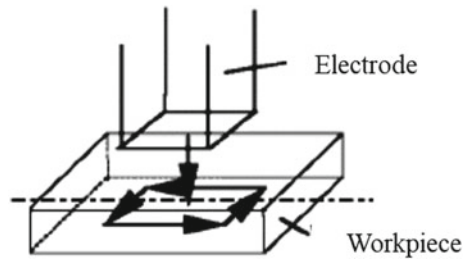


**Fig. 11.2** a Conventional circular electrode [5]. b An electrode with a notch [5]



**Fig. 11.3** a Wear ratio and hole’s expansion varied with electrode diameter for conventional electrode [5]. b Wear ratio and hole’s expansion varied with electrode diameter for an electrode with notch [5]

**Fig. 11.4** Planetary movement of the electrode for effective debris removal [6]



The authors also found that reverse polarity is beneficial for EDMing of carbide with the copper tool instead of the normal polarity. Higher rotational speed was also found to be advantageous for proper debris flushing which led to the lower spark gap.

Yu et al. [6] proposed a technique that used the planetary movement of the electrode during the EDM drilling process. Therefore, better flushing of the debris can be achieved. The method resulted in high-aspect ratio blind hole machining with complex electrode shape. Figure 11.4 [6] describes the concept of the  $\mu$ EDM drilling with planetary movement. The planetary motion provided to the tool helps to flush the debris more effectively. By using this method, an aspect ratio (of the machined hole) of 18 was achievable which is  $1.8\times$  higher when the planetary movement of the electrode was not used.

The researchers also observed that use of deionized water as the dielectric medium significantly improves the EDM performance regarding machining rate as compared to conventional mineral oil-based dielectric. Figure 11.5 [6] shows the graph of the machining time for the two cases. By using the  $\mu$ EDM with planetary movement, the authors [6] successfully machined complex shaped, high-aspect ratio blind holes as shown in Fig. 11.6 [6].

Jahan et al. [7] studied the effects of different tool materials on the fine finishing of tungsten carbide by  $\mu$ EDM operation. The experimented three different tool

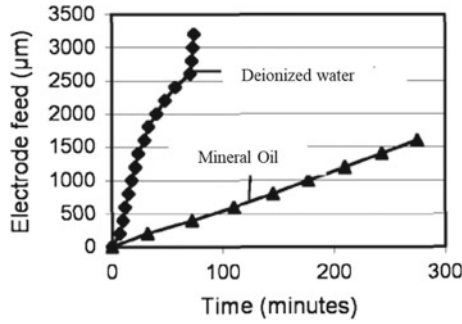


Fig. 11.5 Effect of the dielectric medium on the machining time during the  $\mu$ EDM operation [6]

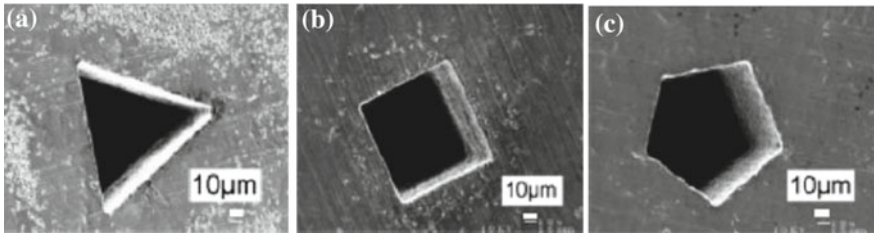


Fig. 11.6 Complex shaped blind hole machined by  $\mu$ EDM [6] a triangular b square c pentagon

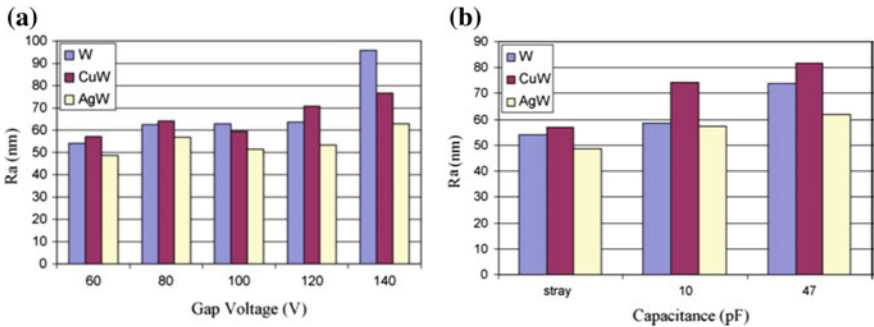
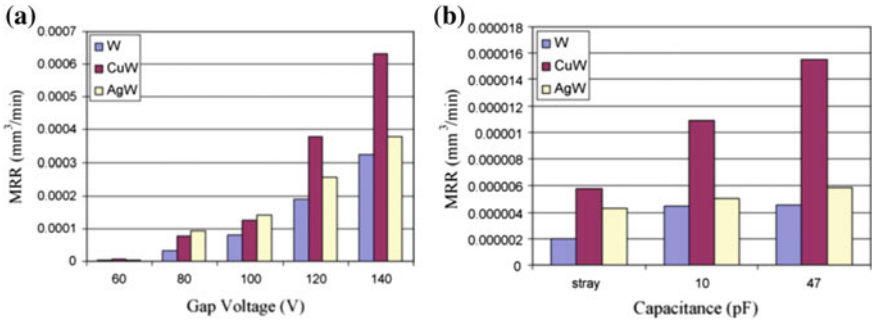


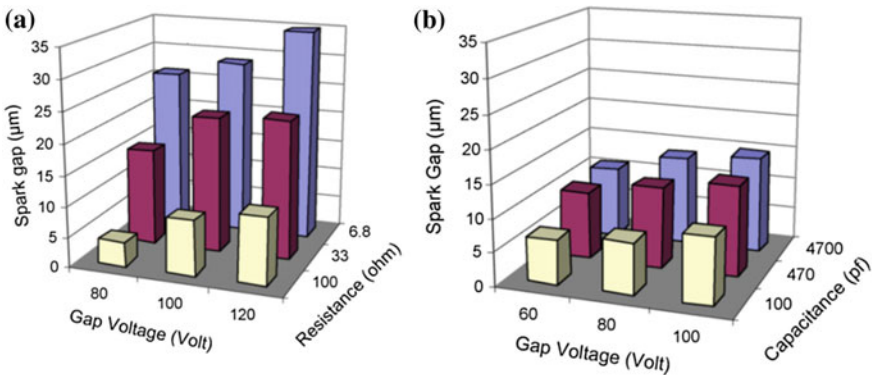
Fig. 11.7 Effect of electrode material on the machined surface’s roughness at various discharge parameters a variation of the voltage; b variation of the capacitance [7]

materials, namely tungsten (W), copper tungsten (CuW), and silver tungsten (AgW). It was observed that AgW provides better surface roughness in most of the discharge condition as compared to the other two tool materials. Figure 11.7 shows the average surface roughness of the machined hole using three different tool materials at different discharge voltages and capacitances. It can be seen AgW helps to generate smoother machined surface at different discharge voltages and capacitances.

In terms of material removal rate (MRR), AgW was also found to perform better than other electrode material, i.e., MRR was higher for AgW electrode. However,



**Fig. 11.8** Effect of electrode material on the material removal rate (MRR) at various discharge parameters **a** variation of the voltage; **b** variation of the capacitance [7]

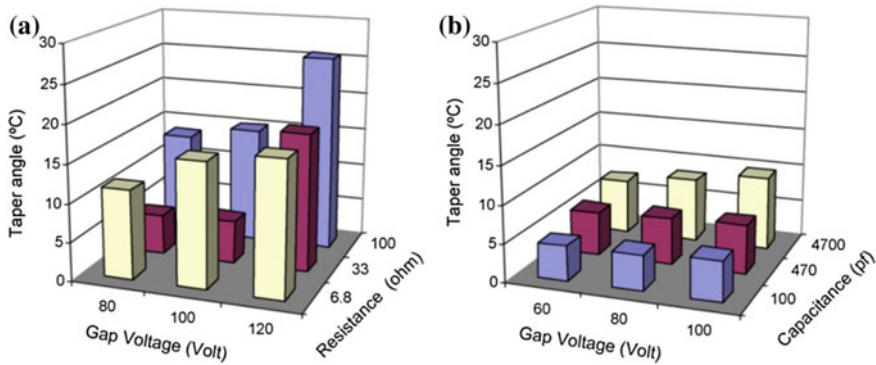


**Fig. 11.9** Effect of the EDM power supply type on the spark gap; **a** transistor-based power supply **b** RC circuit-based power supply [8]

the electrode wear was found to be high for AgW electrode. Figure 11.8 shows the MRR variation for different discharge parameters for three different electrodes.

Jahan et al. [8] also studied and compared the effect of RC-based and transistor-based EDM power supply for the micro-machining of tungsten carbide. The main objective of their study was to achieve quality micro-holes with less dimensional distortion, better surface finish, and less spark gap. In order to achieve low discharge energy into the gap between the electrode and the workpiece, RC generator was observed to perform better as compared to the transistor-based power supply. As a result, the spark gap was found to be smaller for the RC-based power supply. Figure 11.9 shows the study of the spark gap at various discharge energy levels. Further to this, dimensional distortion was observed to be less for the case of the RC-based power supply.

Figure 11.10 shows the effect of the two power supplies on the taper angle of the machined holes. It is clear from Fig. 11.10 that RC-based pulse generator helps to create micro-holes by µEDM with better dimensional accuracy (i.e., less tapered).



**Fig. 11.10** Effect of the EDM power supply type on the taper angle of the machined holes; **a** transistor-based power supply **b** RC circuit-based power supply [8]

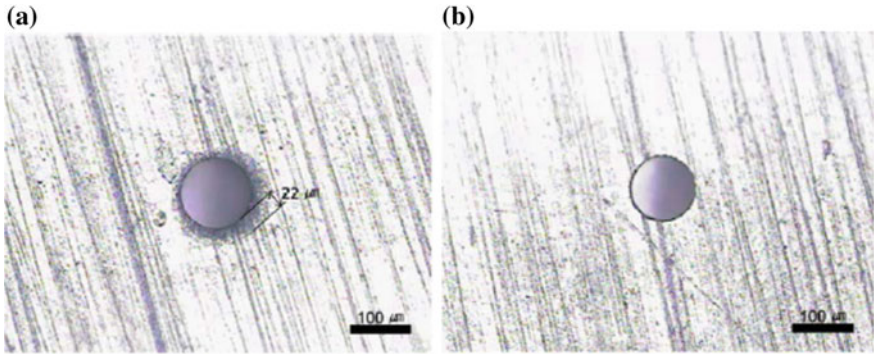
Finally, the morphological study confirmed that micro-holes machined using the RC-based  $\mu$ EDM power supply were free from burr and resolidified molten metal.

The authors concluded from their study that for  $\mu$ EDM operation RC pulse generator performs better than the transistor-based pulse generator in terms of the quality of the final machined product.

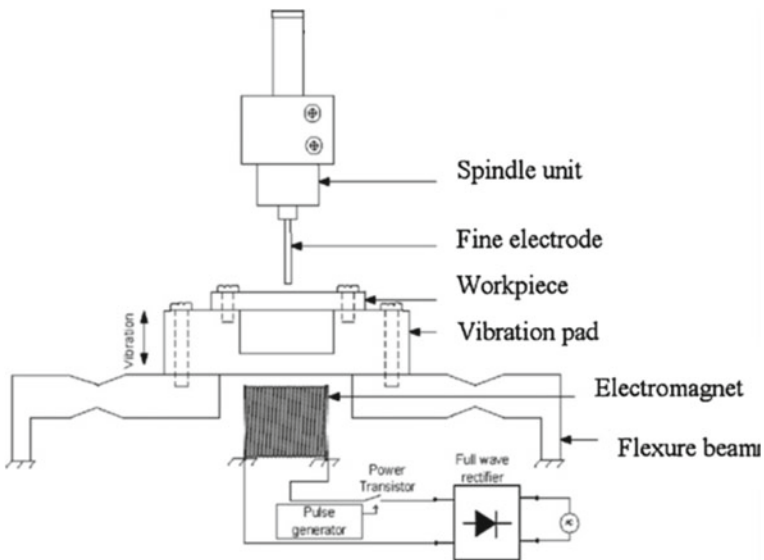
Song et al. [9] investigated the use of deionized water as the dielectric on drilling tungsten carbide by  $\mu$ EDM. They observed that the ionization of the dielectric corroded the machined surface when deionized water was used. In order to tackle this problem, researchers [9] proposed to use the bipolar power supply and triangular-shaped tool electrode. A bipolar pulse power source alternates the polarity of the workpiece and the tool periodically. Hence, the time of the workpiece being positively charged was reduced which helped to minimize the corrosion of the workpiece. Further, since the electrolytic corrosion reaction occurs between the side of the electrode and the surface of the workpiece, the small side area of the triangular electrode also helped to reduce these reactions as compared to the conventional cylindrical electrodes. Finally, the authors succeeded to achieve a corrosion-free machined hole using a triangular electrode and a bipolar EDM power supply. Figure 11.11 confirms this result.

Jahan et al. [10–12] later investigated the use of low-frequency vibration device for removing the debris effectively to achieve high-aspect ratio micro-holes by  $\mu$ EDM. Hence by doing that improving the  $\mu$ EDM drilling to achieve high-aspect ratio micro-holes. Figure 11.12 shows the experimental setup for the vibration-assisted  $\mu$ EDM process. As shown in the Fig. 11.12 [10–12], the workpiece was mounted on a fixture (ferromagnetic) that was arranged like a simply supported beam. An electromagnet was placed underneath the beam and was actuated by a pulsed power supply that caused electromagnet to be magnetized and demagnetized periodically. Thus, the fixture together with the workpiece was vibrating vertically with a low amplitude and subsonic frequency. This low-frequency vibration helped to remove the debris more effectively from the machining zone and helped to achieve a deeper hole as





**Fig. 11.11** Quality of the micro-hole machined by  $\mu$ EDM [9]; **a** corroded hole when machined by cylindrical electrode and conventional EDM power supply with deionized water as the dielectric medium **b** corrosion-free hole when machined by triangular electrode and bipolar EDM power supply with deionized water as the dielectric medium



**Fig. 11.12** Low-frequency vibration-assisted  $\mu$ EDM setup used by [10–12]

compared to the conventional  $\mu$ EDM (without vibration). Figure 11.13 [11] shows that machining time was reduced significantly as the vibration-assisted  $\mu$ EDM was conducted.

Another profound observation that can be derived from Fig. 11.13 [11] is that vibration plays a more dominant role in reducing the machining time at lower discharge energy, which suggests vibration will be helpful more for fine finishing operation using the  $\mu$ EDM process.

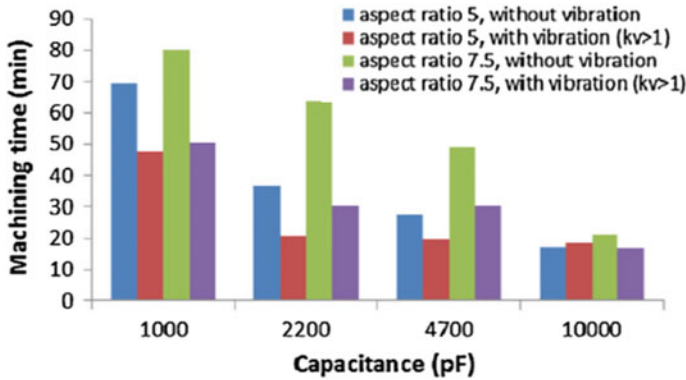


Fig. 11.13 Effect of low-frequency vibration on the machining time [11]

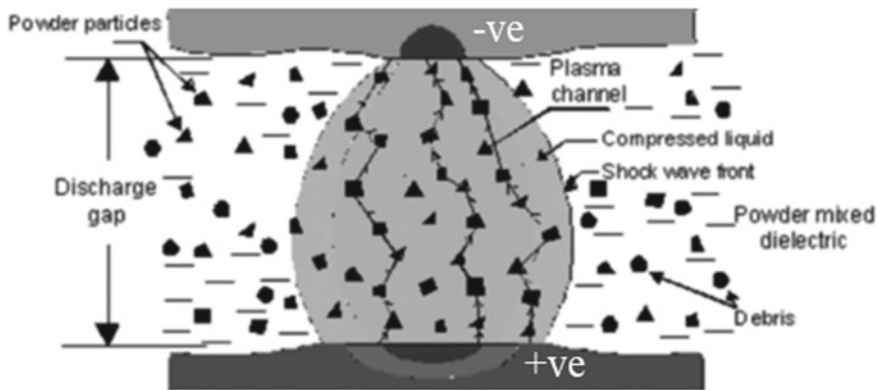
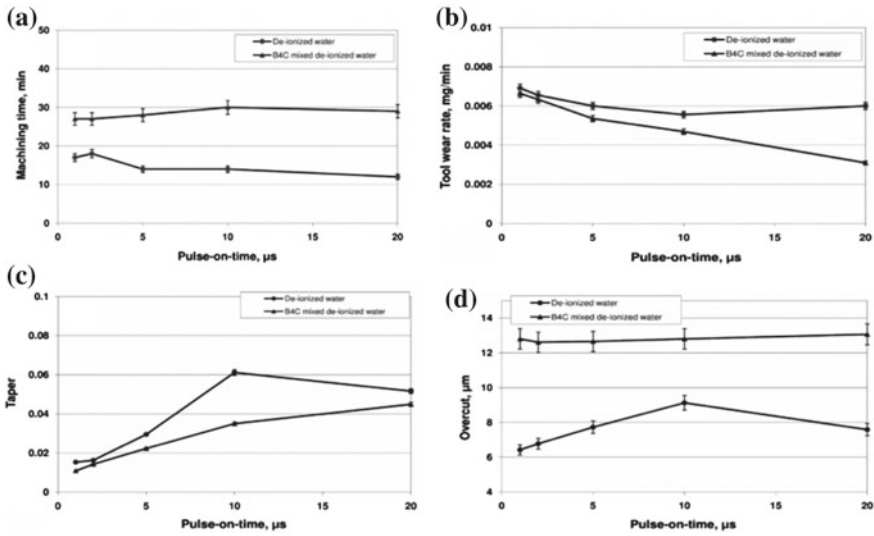


Fig. 11.14 Principle of powder-assisted  $\mu$ EDM [13]

Kibria [13] investigated the effect of powder-mixed dielectric over conventional dielectric during the  $\mu$ EDM machining of the titanium alloy. In the  $\mu$ EDM, the machining zone fills with pure dielectric fluid. However, as the additive particles (conductive) are mixed with the working fluid, it helps to reduce the dielectric strength of the fluid by forming conductive chain-like structure as described in Fig. 11.14 [13]. As the dielectric strength of the fluid gets weaker, the electric discharge between the electrode and the workpiece occurs easily. Figure 11.15a–c [13] confirms that in the major aspects (machining time, tool wear, and taperness) powder-mixed  $\mu$ EDM performs better in contrast to conventional  $\mu$ EDM. However, as the powder reduces the dielectric strength of the fluid, spark created during the machining was large which resulted in larger overcut as shown in Fig. 11.15d. Although, this problem can be overcome by reducing the discharge energy level during the  $\mu$ EDM process.

Hourmand et al. [14] described various methods of achieving high-aspect ratio micro-holes using different types of electrodes. Figure 11.16 [14] describes a method



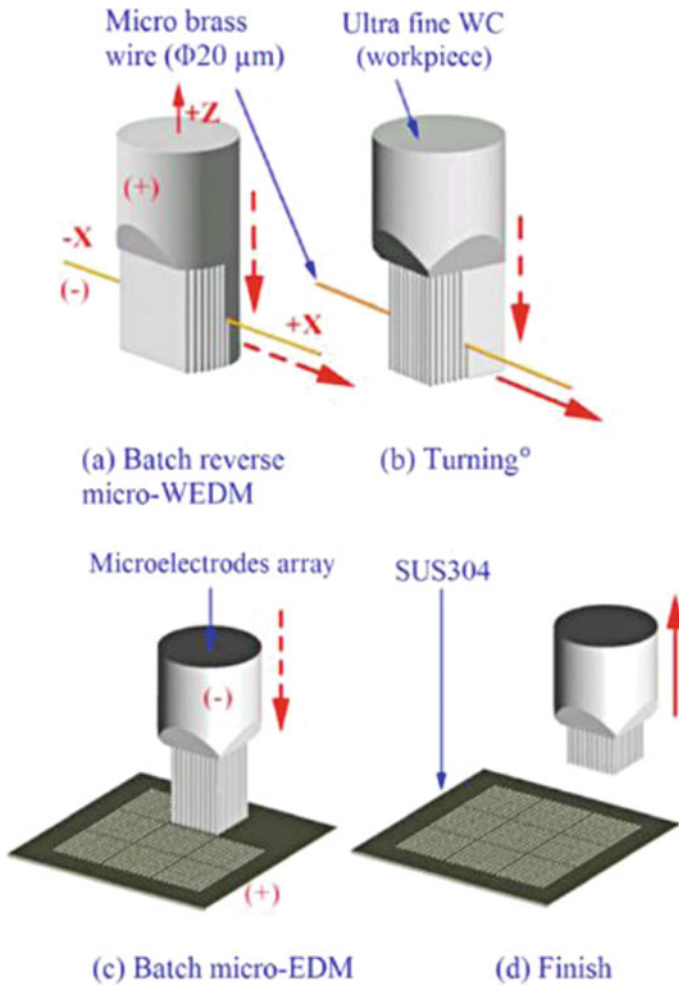
**Fig. 11.15** Effect of powder-mixed dielectric on the  $\mu$ EDM performance; **a** machining time **b** tool wear rate; **c** taperness; **d** overcut [13]

of high-throughput fabrication of arrays of electrodes and micro-holes. At the first step, a wire electrode cuts several micro-slits on a rigid micro-shaft as described in Fig. 11.16a.

Once finished, the shaft is rotated 90° and the same operation is repeated as shown in Fig. 11.16b. The completion of the two operations described in Fig. 11.16a, b creates multiple electrode arrays. This electrode array is then used to drill micro-holes in batch mode as shown in Fig. 11.16c. Figure 11.16d shows the expected product after the completion of the step shown in Fig. 11.16c. Figure 11.17 [14] shows micro-hole array fabricated using the process demonstrated in Fig. 11.16 [14].

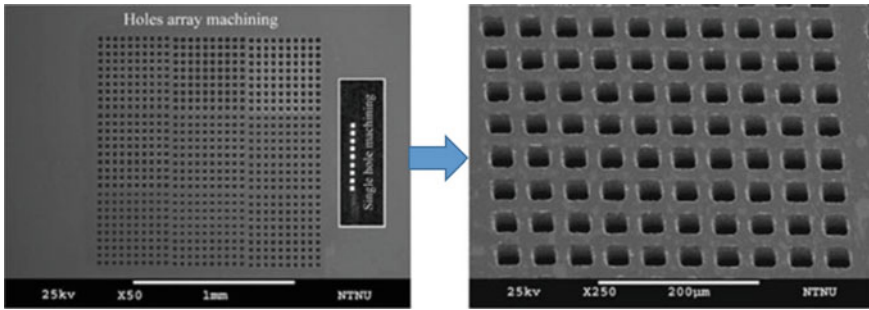
### 11.2.2 Batch Mode Fabrication by $\mu$ EDM

Takahata et al. [15, 16] discovered a new method of producing electrode array using the LIGA method and then used that electrode array to carry out  $\mu$ EDM in batch mode. Figure 11.18 [15] describes the complete process from electrode fabrication to the  $\mu$ EDM operation. In the first step, the Si substrate was covered with the electroplating base. Next, a 300- $\mu$ m PMMA sheet was attached to the substrate. After exposing the PMMA through a mask electroplating of the copper (Cu) was carried out, and finally, remaining PMMA was removed. The electroplated Cu was used as the electrode to conduct the electro-discharge machining. Figure 11.19 [15] shows

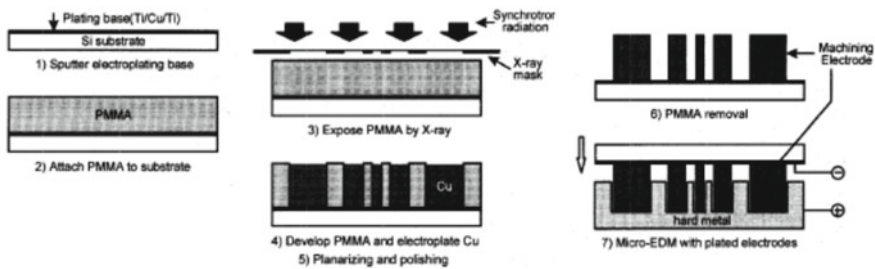


**Fig. 11.16** Steps of an array of micro-hole fabrication; **a, b** tool fabrication **c, d** micro-hole machining [14]

the scanning electron microscopic (SEM) image of the fabricated gear like Cu electrode array. The mask machined (by  $\mu$ EDM) using these electrode has another very interesting application to fabricate very high-aspect ratio microstructure as explained in Fig. 11.20 [15]. In Fig. 11.20, the base mask can be created using the electrodes manufactured by the process explained by Takahata et al. [15]. A solid rod was taken as the workpiece, and the mask was used as the tool to carry out the  $\mu$ EDM operation. As there will be some electrode erosion because of the  $\mu$ EDM operation, single mask cannot be used to fabricate high-aspect ratio structure. Therefore, the



**Fig. 11.17** Machined square hole by the process described in [14]; right-hand side figure demonstrates high magnification image [14]



**Fig. 11.18** LIGA process to fabricate  $\mu$ EDM electrode array for batch mode operation [15]

researchers used sequentially different unused masks to fabricate the final shape. Figure 11.21 [15, 16] shows one such fabricated structure with high aspect ratio.

Recently, Sarwar et al. [17] used the similar technique of LIGA- $\mu$ EDM-based hybrid method for the batch mode patterning of carbon nanotube (CNT) forest. The experimental setup is described in Fig. 11.22 [17]. The array of the electrodes was fabricated using the LIGA process. Once the electrodes were fabricated, it was mounted on the Z-axis of the EDM setup and connected to the EDM power supply through a conductive tape. Figure 11.23 [17] shows the fabricated Cu electrode array and machined CNT forest. Sarwar et al. [17] observed that when multiple electrode arrays was used to pattern the CNT forest, the discharge energy could go to as low as 8 nJ. The average surface roughness of the patterned forest was found to be  $\sim 230$  nm without any contamination from the electrode material (confirmed by the EDX analysis).

Takahata et al. [18–20] further improved the multi-electrode array system for carrying out the batch mode  $\mu$ EDM operation by implementing partitioned electrode arrays with lithographically patterned interconnect. The concept is described in Fig. 11.24a [20], and the corresponding electrical connection is shown in Fig. 11.24b [20]. It is clear from Fig. 11.24 [20] that each electrode was connected separately with the discharge circuit. The separate connection of the individual electrode with the circuit helps to improve the machining rate significantly as shown in Fig. 11.25 [20].

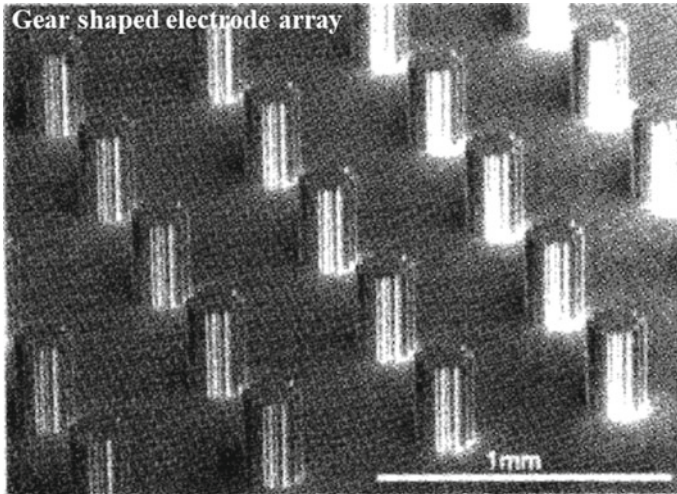


Fig. 11.19  $\mu$ EDM electrode array fabricated by the LIGA process [15]

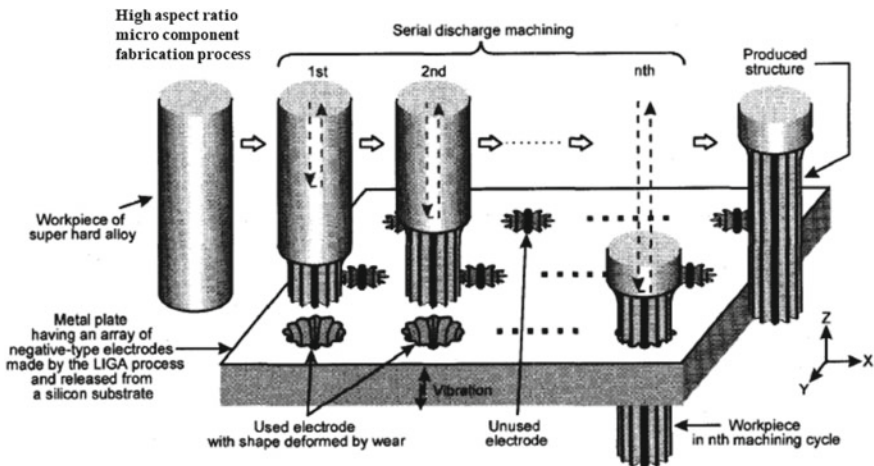
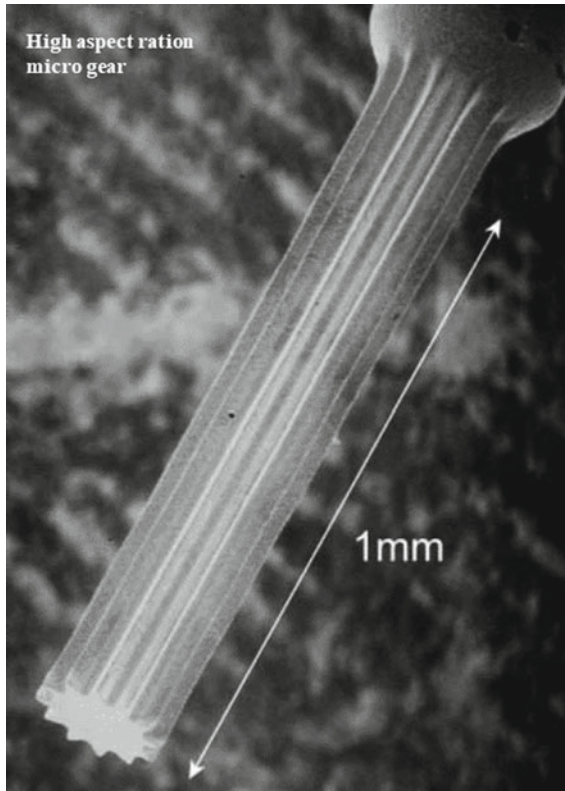


Fig. 11.20 Method of manufacturing high-aspect ratio micro-components using the  $\mu$ EDM process [15]

The experiment was conducted with eight Cu electrodes with  $100\ \mu\text{m} \times 100\ \mu\text{m}$  square cross section, and individual leads were connected to varying numbers of RC circuits for different groups. It is clear that the machining time was lengthened linearly with electrode area per circuit. As eight RC pairs were used, the machining rate was found to be  $>2\times$  higher than a single RC pair.





**Fig. 11.21** High-aspect ratio micro-structure fabricated by a process described by [15, 16]

### 11.2.3 3D Fabrication by Scanning/Milling $\mu$ EDM

In the case of scanning or milling  $\mu$ EDM, the tool electrode has the freedom to move not only in the vertical (die-sinking) direction ( $Z$ ) but also in the horizontal  $X/Y$  plane. In 1997, Yu et al. [21] conducted early research on 3D  $\mu$ EDM using square-shaped electrode. In order to maintain a uniform electrode wear to achieve precision machining, a zigzag-patterned tool motion was proposed by the researchers as described in [21]. Researchers successfully machined different types of the cavity such as square, rectangular, and inclined using square electrode and zigzag tool path as explained in [21].

Later, Reynaerts et al. [22] proposed micro-structuring silicon (Si) by using  $\mu$ EDM technology to complement conventional etching, depositions, and other photolithographic techniques. They [22] successfully managed to fabricate Si-based micro-gear, resonant beam structure, and micro-die.

Mohri et al. [23] proposed a method of scanning  $\mu$ EDM to produce high-aspect ratio micro-pin for precession engineering application. Figure 11.26a, b [23] shows

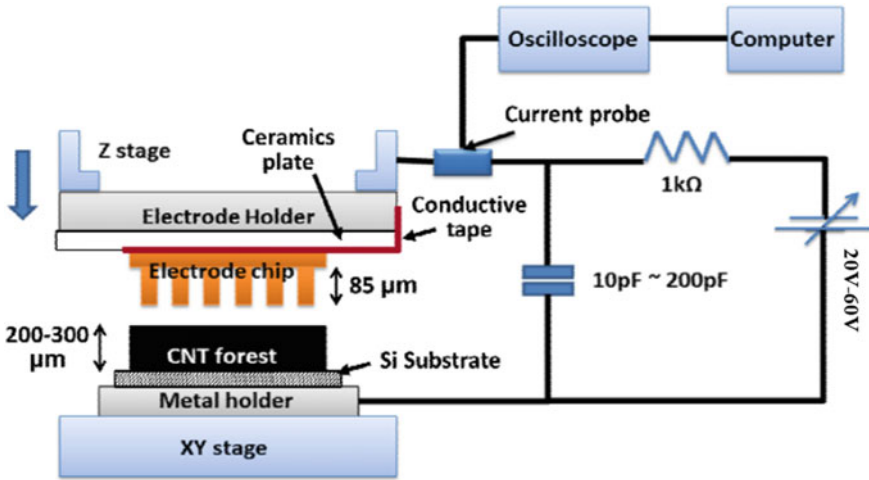


Fig. 11.22 LIGA-μEDM-based hybrid process to machine (batch mode) CNT forest [17]

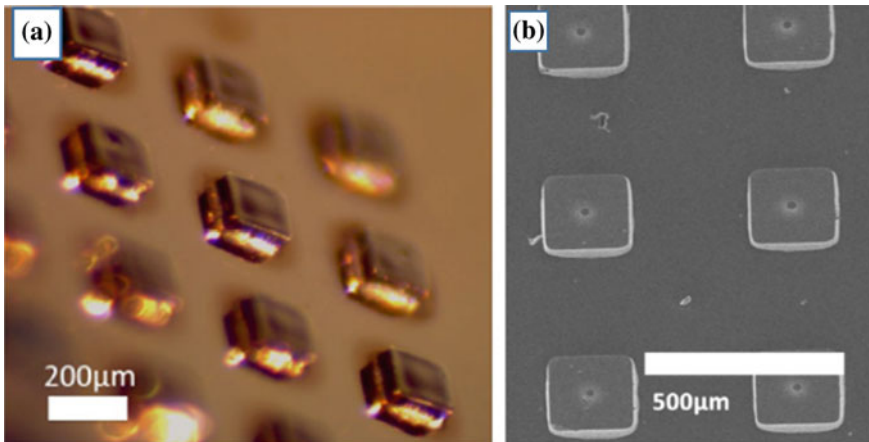
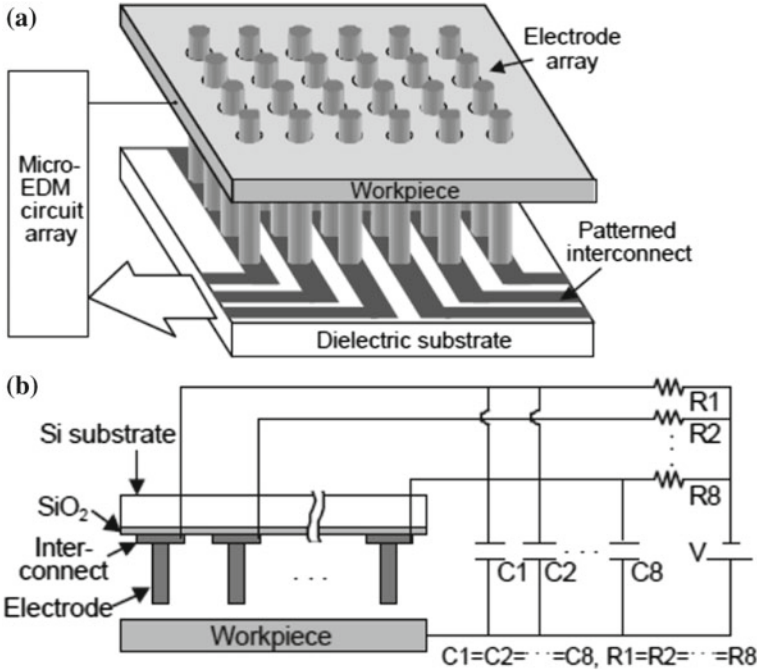


Fig. 11.23 a Fabricated electrode array and b machined CNT forest as described in [17]

the process and the fabricated tool, respectively. In this method, a predesigned slit is used as the negative electrode, and the positive tool passes thru it. The diameter of the tool is reduced because of the controlled pulses occurred between the V-shaped die and the cylindrical tool. The authors successfully produced a micro-tool of diameter 20 μm.

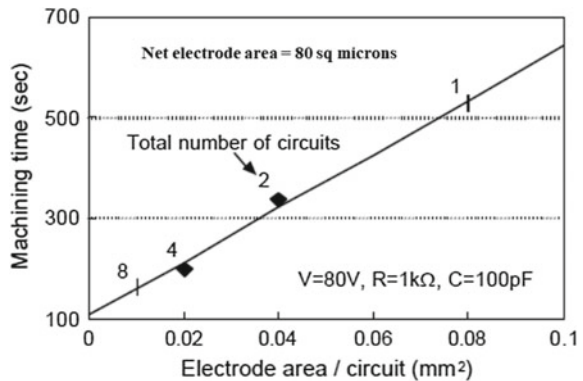
Figure 11.27 [23] demonstrates the transformation of the micro-tool with the progress of the machining time. The fabrication time is reasonable as it took 20 min of machining to form the tool from its original diameter of 500 μm to the final diameter of 20 μm.



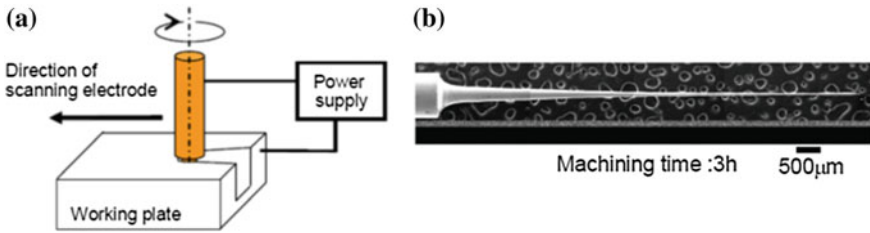


**Fig. 11.24** a Concept of partitioned electrode array b corresponding electrical connection arrangement [20]

**Fig. 11.25** Improvement of the machining time when partitioned electrode arrays are used [20]

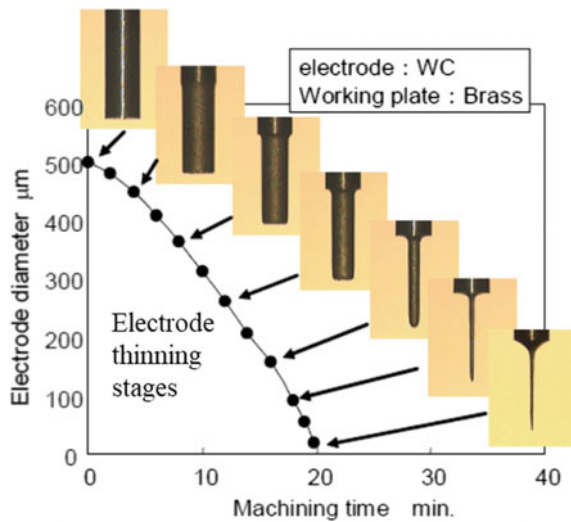


Electrode wear is a serious problem for scanning/milling  $\mu$ EDM as this hinders the product accuracy if not compensated accordingly. There are many approaches to confront this issue. Hao et al. [24] studied a vibration-assisted scanning  $\mu$ EDM system to compensate the tool wear in real time. The tool wear was compensated by monitoring the discharge condition in real time and vibration of the tool aided the system further. Researchers [24] also described the concept of vibration-assisted



**Fig. 11.26** a Method micro-tool fabrication using scanning  $\mu$ EDM. b SEM image of the fabricated micro-tool of 20  $\mu$ m of diameter [23]

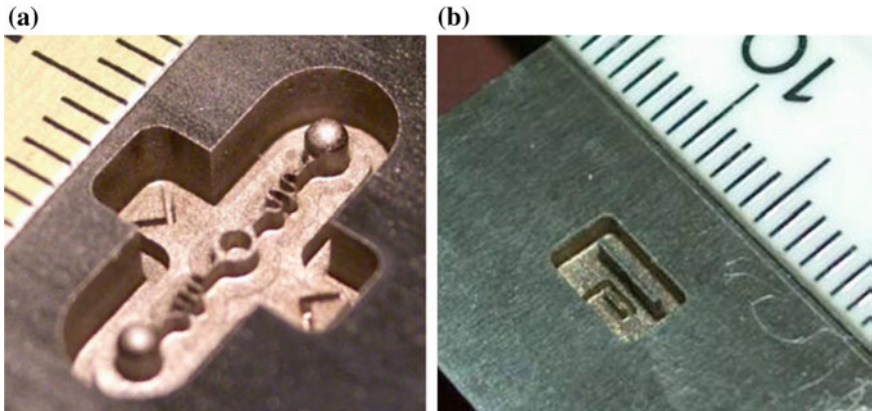
**Fig. 11.27** Transformation of the tool with the machining time fabricated by scanning  $\mu$ EDM [23]



scanning  $\mu$ EDM. As stated earlier, the servo control of the tool was carried out by monitoring the discharge condition. Researchers [24] also demonstrated that the vibration frequency plays a dominant role in achieving higher machining depth. Researchers successfully machined various 3D structures using the method described in [24].

Bissacco et al. [25] investigated the electrode wear and the material removal rate in relation to single discharge thoroughly. They found that the workpiece (steel) material removal was as low as  $1 \mu\text{m}^3$  per unit discharge at low pulse energy. They also observed that material removal per discharge pulse is fairly consistent at constant discharge energy. However, this is not the case for electrode material removal for the single discharge. Therefore, they concluded that electrode wear measurement might not be an effective solution for tool wear compensation during milling  $\mu$ EDM.

Richard et al. [26] investigated the possibility of  $\mu$ EDM as a potential micro-machining technique for fabricating micro-components. Researchers [26] were able to achieve successfully the high-aspect ratio complicated microstructure to prove



**Fig. 11.28** High-aspect ratio microstructures machined by  $\mu$ EDM [26]

the feasibility of  $\mu$ EDM. Figure 11.28 shows some of the machined structures by  $\mu$ EDM milling.

Li [27] implemented a new tool wear compensation method which was based on a scanned area (BSA) for the 3D  $\mu$ EDM milling operation. The proposed method was integrated with the CAD/CAM system and was implemented for each layer of machining. Micro-machining experiments were conducted using the BSA method, and the results confirmed that BSA method performs better in terms of material removal rate and tool wear ratio as compared to that of other tool compensation methods such as uniform wear method (UWM) and a combination of linear compensation with UWM. The reason for the lower tool wear ratio as noted by the researchers was a reduced number of abnormal discharges due to even distribution tool wear along the whole surface of the machined layer.

Chiou et al. [28] investigated the effect of coating of the tool material on the performance of the  $\mu$ EDM milling of high-speed steel alloy (SKH59). They used three different electrodes in their study, namely tungsten carbide (WC), silver-coated tungsten carbide (WC-coated Ag), and copper-coated tungsten carbide (WC-coated Cu). It was observed different electrode materials influence different performance parameters of  $\mu$ EDM. In regard to machined surface roughness, WC-coated Ag yielded the lowest surface roughness as compared to the other two electrodes. Similarly, WC-coated Cu electrode enhanced the material removal rate, and pure WC demonstrated the highest wear resistance. The authors [28] concluded from the research findings that coating technique improved the  $\mu$ EDM milling process in various ways.

Nguyen et al. [29] proposed a new tool wear compensation method combining uniform wear method (UWM) and a number of normal discharge (NoN) count. The authors used NNU as the acronym of the proposed method. The proposed algorithm can be understood from Fig. 11.29 [29]. In this method, the useful discharges were counted for machining a certain standard geometry. In the next step, the tool wear (in the length direction) was calculated to find the tool wear/unit discharge ( $\Delta N/\Delta T_e$ ).

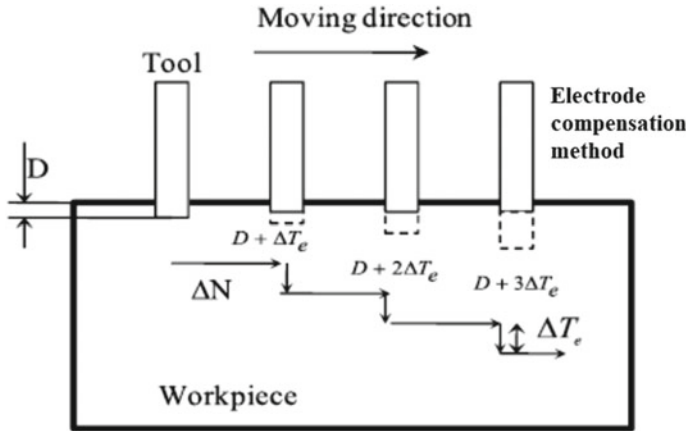
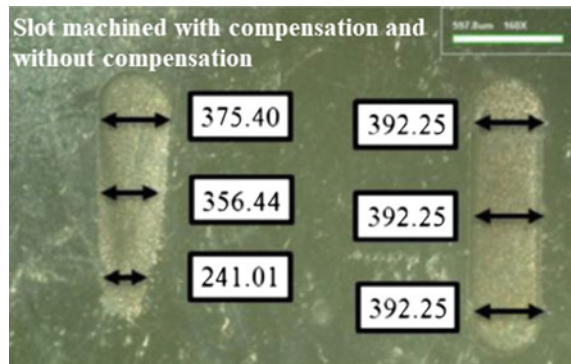


Fig. 11.29 Proposed NNU-based tool wear compensation method [29]

Fig. 11.30 Machined slot by  $\mu$ EDM milling; **a** without tool wear compensation and **b** with tool wear compensation using the NNU method [29]



During actual machining for every  $\Delta N$  count in real time,  $\Delta T_e$  was compensated in the Z-direction as shown in Fig. 11.29 [29]. The implementation of the algorithm significantly improves the accuracy of the machined slot. Figure 11.30 [29] shows two slots machined on nickel—a slot on the left-hand side was machined without the tool wear compensation, whereas the slot on the right-hand side was machined using the newly proposed NNU compensation algorithm. It is obvious from Fig. 11.30 [29] that the slot machined after implementing the NNU algorithm shows no dimensional deviation (in width) throughout the length of the slot as compared to the slot machined by the conventional milling  $\mu$ EDM. From the research, authors concluded that NNU method is very suitable for machining slots, whereas for 3D structure machining, some marginal dimensional deviation was evident in the range of  $\sim 0.2$  to  $\sim 0.3\%$ .

Tong et al. [30] extended his research of servo scanning 3D (SS-3D)  $\mu$ EDM [24] by introducing a rough and fine machining strategy. In SS-3D  $\mu$ EDMing operation, the tooltip that is used for the machining is significantly small which retards the processing efficiency. Therefore, the introduction of the rough machining helped

to overcome the problem of low processing efficiency. In the rough machining, the author used a larger tool area and high discharge energy with faster scanning speed to remove bulk material from the cavity at a shorter time. However, during the finishing process, total material removal was much smaller, and that is why researchers were able to use smaller tooltip with finer discharge settings to achieve higher dimensional accuracy, smoother surface roughness, and sharper edge and corner. The implementation of the rough-finish machining strategy helped to achieve  $2.4\times$  faster machining rate with a high dimensional accuracy of  $<5\ \mu\text{m}$  and low surface roughness of  $S_a=0.38\ \mu\text{m}$ .

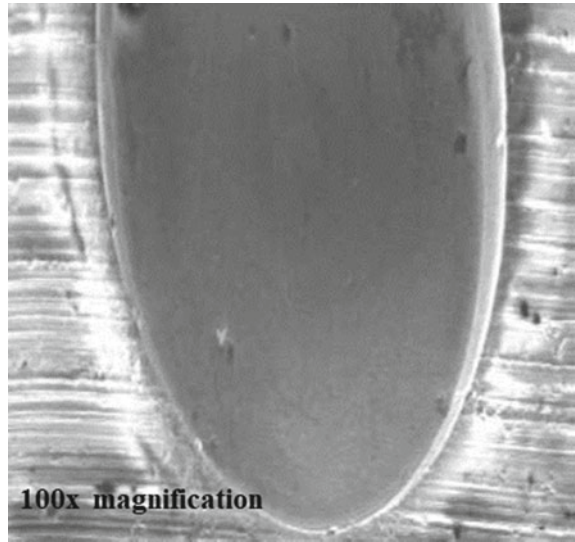
Tong et al. [31] recently introduced batch mode machining of 3D micro-cavity array using servo scanning 3D (SS-3D)  $\mu\text{EDM}$  method. In this research [31], the authors used an array of nine electrodes with a diameter of  $80\ \mu\text{m}$  and a length of  $600\ \mu\text{m}$  of each of them. After proper optimization of the machining parameters, the authors successfully machined an array of nine hexagonal cavities, with a depth of  $112$  or  $120\ \mu\text{m}$ . It is to note that authors [31] fabricated the array of the electrode on the machine to avoid errors occurred for off-machine produced electrodes during mounting.

$\mu\text{EDM}$  milling has also been used for fabricating micro-channels for various engineering applications such as micro-heat exchanger, micro-fluidic applications. Ali [32] investigated  $\mu\text{EDM}$  milling on beryllium copper (BeCu) to fabricate micro-channels for micro-fluidic applications. Sabur et al. [33] also investigated machining micro-channels on non-conductive ceramic  $\text{ZrO}_2$ . To initiate the sparking process, researchers attached a thin conductive tape on top of the  $\text{ZrO}_2$ . As the machining progressed, the conductive tape eroded completely. However, the spark erosion continued because of the presence of the pyrolytic carbon at the machining zone (produced as the by-product of the initial sparks). Authors [33] were successful in achieving effective machining of non-conductive ceramic  $\text{ZrO}_2$  by  $\mu\text{EDM}$  milling. They achieved an MRR of  $1.29 \times 10^{-5}\ \text{mm}^3/\text{s}$ , whereas the average surface roughness of the channel was found to be  $0.25\ \mu\text{m}$  at a discharge setting of  $80\ \text{V}$  and  $0.1\ \text{nF}$ . Figure 11.31 [33] shows the SEM image of the machined slot on  $\text{ZrO}_2$ . In another work, Mohite et al. [34] developed a leaf-like micro-channel heat sink on aluminum as demonstrated in Fig. 11.32 [34]. However, in this research, they [34] used die-sinking EDM instead of EDM milling.

### 11.3 $\mu\text{WEDM}$ as a Near Net Shape (NNS) Process

Wire electro-discharge machining (wire EDM or WEDM) is another technique that surfaced up in the late 60s to cut metals at a relatively slower rate. Similar to EDM, it also employs sparks (either discrete or continuous) to remove materials. Over the time, the process has made significant progress and cutting time has been shortened by 20 times compared to the early machines. Modern wire EDM machines incorporate CNC controls and sensors, and it has been reported that some machines can cut up

**Fig. 11.31** Machined slot on  $ZrO_2$  by mEDM milling [33]



**Fig. 11.32** Micro-channel heat sink on aluminum [34]



to the accuracies  $\pm 0.0001''$  (0.0025 mm), producing surface finishes to 12 rms [35]. This capability makes the process a viable one for near net shape machining.

Wire EDM can be defined as a type of EDM where the spark is generated between the wire electrode and workpiece in the presence of a dielectric medium, mostly deionized water. The water's cleanliness and correct conductivity are one of the controlling factors in getting the desired output.

As described earlier, in the wire EDM process, the generated spark supplies enough thermal energy to erode the workpiece caused by the electric discharges. Wire diameters can start from as low as 0.076 and can go up to 0.30 mm or higher, depending on the required kerf width. During the material removing process, the wire is supplied from a supply spool and wound up to a take-up spool. This process ensures a constant diameter fresh electrode always in action and a consistent kerf width. Brass, copper, tungsten, and molybdenum are mainly used as the material for the wire [36]. As there is a need for spark generation, the workpiece usually is electrically conductive, but the toughness or hardness does not influence the process

to a greater extent because it is all about the spark strength that is considered as the primary energy source of machining [37].

Wire EDM process can be understood through Fig. 11.1b. A moving wire electrode travels across the workpiece during wire EDM process. The wire motion is controlled by a CNC system. The cutting or material removal process in wire EDM takes place by means of spark erosion rather than direct contact between the tool and workpiece material. Therefore, it is a requirement for the work material to be conductive. However, it has been reported to use wire EDM process on machining semiconductors [38] or cemented carbides [39] as well.

The rapid DC pulses between the wire electrode and the workpiece are the reason behind the creation of the spark. A dielectric is applied as a shield between the wire and the workpiece. Most of the cases, deionized water is used for this purpose. The dielectric fluid can be applied within a certain conductivity range, and therefore, using regular tap water is not recommended since they contain different categories of minerals. The water conductivity is controlled by passing through a resin tank to eliminate most of its conductive elements. As during machining, the conductivity rises, an in-process control is maintained throughout the process to maintain the water conductivity.

With all these process parameters, when sufficient voltage is applied, the fluid ionizes, and a precisely controlled spark is generated to erode a small section of the workpiece. The erosion takes place by melting and then vaporization of the workpiece. The electrical pulses can have a very high frequency, up to thousands of times per second.

The near net shape machining aligns mainly toward the finishing processes with high surface quality. Wire EDM can cut very small pieces, and therefore, it is often a better choice for the production of micro- and highly detailed items that would normally be too delicate for other machining options. Apart from the micro-machining of various shapes, wire EDM has been widely used in machining different types of metal matrix composites (MMC), semiconductors, and also 3D printed metal composites. We will examine and present the state-of-the-art research works conducted to apply and improve the wire EDM process to obtain near net shape machining.

### ***11.3.1 Wire EDM Parameters and Their Effect on Surface Roughness***

It is very common for a wire EDMed surface to have carters created by electric sparks. The surface quality is adversely affected by the electrical discharge. The parameter controlling to obtain a better surface has been in practice for decades, and the relevant research revealed that the roughness of WEDMed surfaces increased with increased discharge energy [40] as a result of the formation of larger craters [41]. Besides the discharge energy, other researchers have tried optimization of other machining parameters like the quality of the machined surface depends on the types of material



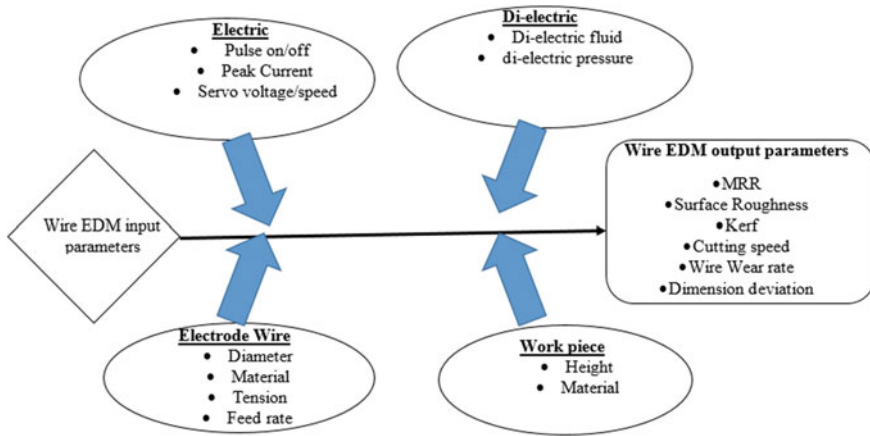


Fig. 11.33 Wire EDM process parameters influencing the surface finish and machining speed [42]

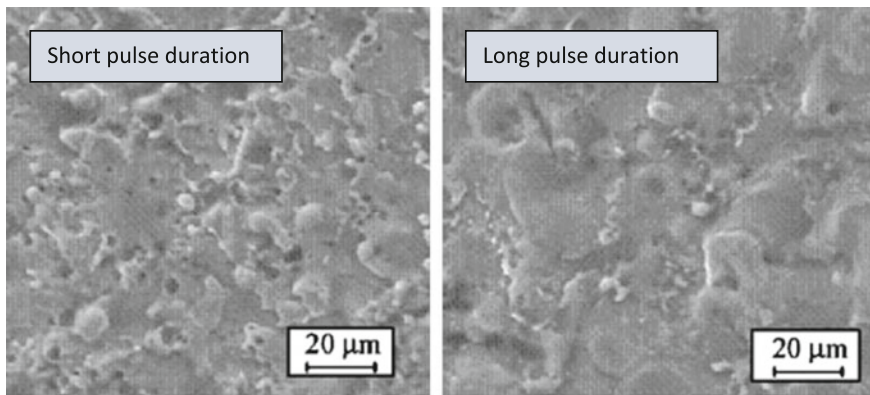


Fig. 11.34 SEM images for short and long pulse duration during wire EDM of alloy steel (Cr12) by a brass wire of 0.2 mm diameter [43]

used for the wire and workpiece, pulse on/off time, dielectric, wire diameter. The summary of parameters affecting the surface quality of wire EDM can be summarized in Fig. 11.33 as found in the review done by [42].

Han et al. [43] conducted an experimental study to understand the effect of machining parameters on the quality of the surface in terms of surface roughness. The major two parameters that had a strong influence on the quality of machined surface were (i) pulse duration and (ii) discharge current. Surface quality in terms of surface roughness got better with decreasing the value of these two parameters. The surface roughness is seen in Fig. 11.34, showing the SEM image for two types of pulse durations—short and long.

In this comprehensive study, the suggested dielectric conductivity was ranged between 10 and 20  $\mu\text{s}/\text{cm}$ . The surface roughness was affected by workpiece mate-



rials' rigidity as well. Aluminum was found to have the lowest surface quality with a surface roughness value nearly  $1\ \mu\text{m}$ , while cemented carbide alloy had the lowest surface roughness of  $0.4\ \mu\text{m}$ . Liao et al. [44] tried with the power circuit control to maintain the finishing process capable of producing high-quality surface. They upgraded a wire EDM machine capable of producing minimum surface roughness of  $0.7\ \mu\text{m}$  by modifying the existing power circuit to have an ignition induced by lower power. With the application of Taguchi design, ANOVA and  $F$  test combined with properly tuned voltage, resistance, capacitance, and type of pulse-generating circuit, the machine was able to produce a surface roughness of  $0.22\ \mu\text{m}$ .

An optimization problem with multiple objectives was formed and solved to select the best possible control settings for a wire EDM setup by Scott et al. [45] in 1991, while [46] tried the optimization through a feedforward neural network to construct the wire EDM process model and found that the neural network could come up with developing a relationship between the cutting parameters and cutting performance. The effect of pulse on/off time, current, and capacitor settings were observed for two output variables: surface roughness and machining speed. Their results revealed that the use of the approach can systematically search the cutting parameters for obtaining an optimum production rate in wire EDM. Besides neural network, [47] performed the optimization through Taguchi method. Over the last three decades, numerous research studies have been accomplished to establish the relationship between the parameters and the performance of wire EDM in terms of surface quality and material removal rate (MRR).

The research on process parameters started to move more toward specific wire EDM processes conducted on specific materials with the progress of the process. Nowadays, wire EDM is a process capable of machining hard metals with intricate shape required. In the next section, we will move deeper into the application of wire EDM for machining different types of materials and the impact on surface quality for near net shape machining.

### ***11.3.2 Application of Wire EDM for Different Metal Composites for Near Net Shape Machining***

The beauty of wire EDM lies in its capability to machine different types of materials including alloy steels, metal–matrix composites, ceramics with conductive properties. Even aerospace parts can be machined by wire EDM although those are hard to machine otherwise due to their high hardness and toughness [44]. It has been observed that for finish machining, ignition at low power and machining at high power is not a good combination. In the recent times, researchers are coming up with ideas to improve the surface for the specific materials. For example, [48] applied wire EDM for machining high-carbon high-chromium steel (wt% 2.01 C and wt% 11.25 of Cr). The wire used was made of brass with 0.25 mm diameter, and their final analysis with Taguchi single response optimization technique showed that wire

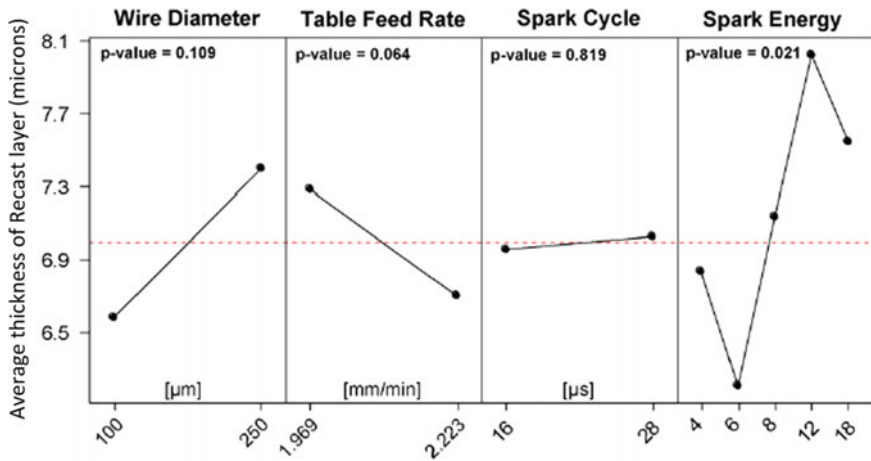


Fig. 11.35 Effect of different machining parameters on the average recast layer thickness [50]

tension was one of the significant controlling parameters to obtain minimum surface roughness along with pulse on/off time and peak current.

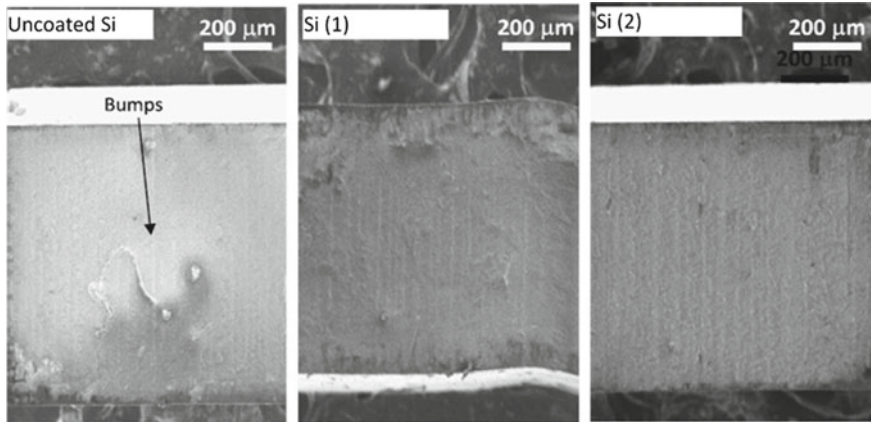
Wire EDM was practiced for machining hybrid metal materials produced by indirect selective laser sintering (ISLS) process [49]. This additive manufactured hybrid metal was capable of near net machining by wire EDM process using 0.25-mm brass wire. An iron/copper/tin (FeCuSn) hybrid alloy was prepared by ISLS, and a 5-mm thick piece was machined using the brass wire. Newton et al. [50] conducted a study on recast layer formation after wire EDM of nickel-based superalloy Inconel 718 which is equally strong across both high and low temperatures. Wire EDM is one of the most suitable processes to machine this material. However, it is necessary to investigate the impact of the recast layer. A recast layer is created as a result of rapid solidification of the molten metal on the surface, thus covering the heat-affected zone (HAZ). Although wire EDM provides thinner recast layer compared to die-sink EDM, a proper investigation is necessary to find the effect of different parameters in wire EDM on recast layer. It was seen from the study that energy per spark along with peak discharge current and current pulse duration contributed in increased recast layer thickness. Although the recast layer was maintained to be between a thickness of 5 and 9 μm on an average, it was observed that the nature was variable. The experimental study involved two different diameter electrodes made of hard brass, with 100 μm and 250 μm, and the dielectric used was deionized water. The annealed Inconel 718 sheet has a thickness of 3.962 mm. Besides wire diameter, other parameters considered were table feed rate, spark cycle, and spark energy. Figure 11.35 shows the overall finding. It is seen from the figure that the surface roughness increased the most with increased energy per spark. Increased wire diameter also affected the surface roughness adversely; the larger diameter wire demonstrated a higher roughness overall.

This work has been supported by a more recent investigation by Sharma et al. [51] where the effect of wire diameter on WEDM performance characteristics including the cutting speed, surface quality, and topography, recast layer, micro-hardness, microstructural and metallurgical changes have been observed for Inconel 718. It was found that machining with smaller diameter wire significantly contributed to improving the overall productivity and also the quality of the machined surface with the same settings of machining variables. Thinner recast layer was observed with smaller diameter with minimum alteration in hardness and quicker manufacturing time.

Al6061 hybrid nanocomposites were wire cut, and the experimental investigations are presented by [52]. The effect of wire EDM parameters for machining on this hybrid composite (with 0.5% SiC and 0.5% B4C composition) was investigated, and it was attempted to achieve a better surface roughness ( $R_a$ ) by adjusting these parameters. The cutting wire was a 0.25-mm-diameter wire made of brass coated with zinc. Wire EDM parameters considered for the study can be categorized into two divisions. The first category was the time parameters that include on ( $T_{on}$ ) time and the off ( $T_{off}$ ) time. The second category was the discharge parameters [i.e., voltage (SV) and the peak current ( $I_p$ )]. All these parameters were tested in four stages. These parameters were considered as inputs to explore their influence on the surface roughness ( $R_a$ ) using Taguchi's DOE. It was found that the surface roughness  $R_a$  value increased with pulse on time,  $T_{on}$  value.  $R_a$  was found to be minimum for lower settings of  $T_{on}$  and  $T_{off}$ . The  $R_a$  value increased with the rise in  $T_{on}$ , particularly at higher  $I_p$ .  $T_{on}$  and  $I_p$  both had a combined effect of increased spark energy that was responsible for making deeper craters. The composite's temperature dropped when longer pulse off time was applied; as a result, smaller crater sizes were achieved. The surface roughness varied within the range of 2.43–3.48  $\mu\text{m}$ . No significant deviation of  $R_a$  with respect to the voltage difference was observed. It could be summarized that  $T_{on}$  had a direct relationship, while  $T_{off}$  was negatively affecting the  $R_a$  for the conducted experiments.

A model of slicing of the thin silicon wafer by wire EDM was developed by [53] earlier in 2014, and later in 2017, wire EDM was used to slice ultra-thin silicon wafer by [54]. The wafer had a size of 140.5  $\mu\text{m}$ , and the slicing rate was 0.96 mm/min. SEM images of the wafers fabricated showed a crack-free surface resulted from a complex material removal phenomena.

The major parameters controlling the process of wire EDM on silicon wafers were found from some preliminary experiments. Two different diameters wires were used, which are 250  $\mu\text{m}$  and 100  $\mu\text{m}$  for the experiments. The dielectric used was deionized water. The anode or workpiece used was a *P*-type polycrystalline Si ingot with a resistivity of 0.5  $\Omega\text{-cm}$ . The workpiece was maintained at a complete submerged condition under the dielectric, and the wire (a cathode for slicing) for the wire EDM was made of brass and had a diameter of 100  $\mu\text{m}$ . The experimental result revealed that it was possible to obtain a minimum wafer thickness of 140.5  $\mu\text{m}$  with kerf loss of 130  $\mu\text{m}$  when the slicing rate was 0.96 mm/min. With the application of a higher slicing rate (1.05 mm/min), it was possible to obtain a wafer thickness of 150  $\mu\text{m}$ , which was within a reasonable range. The minimum kerf loss was 121  $\mu\text{m}$  for this



**Fig. 11.36** SEM image of the cut surface of the machined slots by  $\mu$ -WEDM process with machining condition of 95 V and 1 nF for uncoated Si, Si (with 160-nm coating), and Si (with 320-nm coating) [55]

case. The SEM of wafer surfaces revealed that the wafers were crack-free. However, other features like dents, drops, and holes were still present which indicated the existence of complex material removal phenomena.

Aous et al. [55] studied to improve the  $\mu$ -wire electro-discharge machining and  $\mu$ -electro-discharge machining of silicon by applying a temporary conductive coat (in this case gold). In the case of  $\mu$ -WEDM, the gold coating acted as a shunt conductor and improved the ease of machining. However, for the  $\mu$ -EDM operation gold coating helped to reduce the contact resistance and improved the overall machining performance. In their research, Aous et al. [55] used polished Si sample which was *P*-type with a resistivity of 1–50  $\Omega$  cm and a thickness of 650  $\mu$ m. Three types of samples were arranged with the first set of samples to be silicon (Si) without any temporary conductive layer; the second and third batches were Si layered with gold for 5 min (Si(1)) and 10 min (Si(2)) correspondingly. Si(1) samples had an approximate gold layer thickness of 160 nm, and Si(2) samples' gold layer thickness was 320 nm. Samples were coated using an ion sputtering machine. The method actually aimed for application in rapid prototyping of silicon-based MEMS devices by replacing expensive and complex lithography-based process, which are intended principally for mass fabrication. The silicon wafer was coated with gold as a highly conductive metal to produce electrically conductive Au–Si–Au composite. By using this method, the machined surface quality significantly improved compared to the non-coated surface. Figure 11.36 shows the results below.

In another recent study on wire EDM of silicon coated with gold [56], a novel type of micro-WEDM process has been applied for machining of Si. A combination of gold-coated Si with nanopowder-mixed dielectric has been applied, and the performance has been studied. A temporary coating of gold layer was applied on the

silicon surface, and then, the dielectric mixed with nanopowder was applied during the machining.

The material removal rate and spark gap were studied under the effect of gold coating and different concentrations of nanopowder mixed in the dielectric fluid. The wire used was zinc-coated brass wire with a diameter of 70  $\mu\text{m}$ . The micro-wire EDM was performed with dielectric EDM oil only, and three other concentrations of graphite nanopowder added to it. The preliminary experimental investigation revealed that MRR increased with different carbon concentrations, up to 33% as compared to the bare dielectric medium. The spark gap also increased up to 159% compared to the bare dielectric.

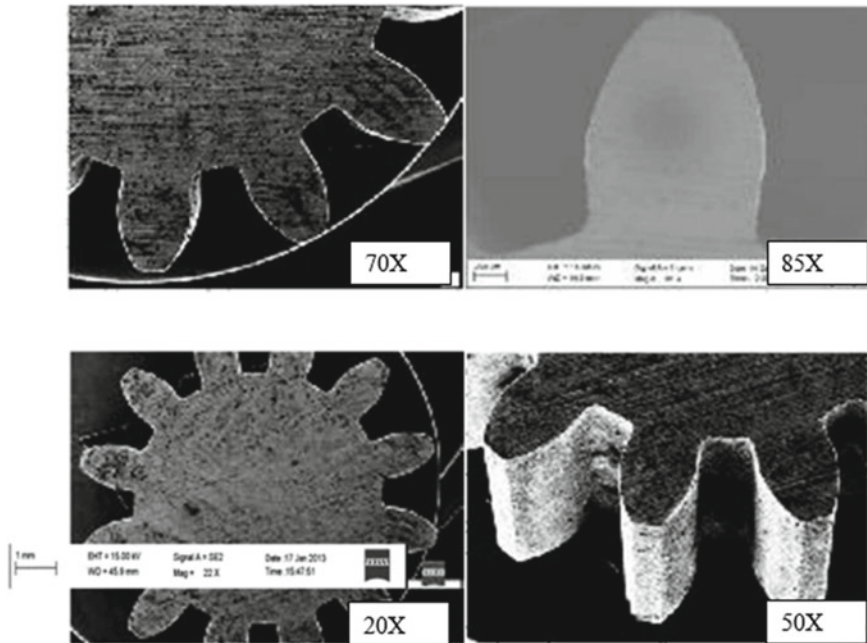
### ***11.3.3 Wire EDM for Special Geometry Design in Near Net Shape Machining***

In this section, mostly special micro-shapes generated by wire EDM will be discussed. Wire EDM has the advantage over other micro-machining processes in terms of machining time for creating special microstructures.

In the recent times with the rapid development of biomedical applications, fabrication of micro-electrodes has drawn significant attention in the micro-manufacturing industry.

Wire EDM has been tried to fabricate micro-electrodes by several researchers; although most of the micro-electrode fabrication is carried out by micro-EDM, some works have been reported using micro-wire EDM as well. Back in 2008, [57] combined two exactly similar or twin electro-wires together with two discharge circuits that caused rapid fabrication of micro-electrode tools. The wire electro-discharge grinding (WEDG) technology, which is most commonly used to fabricate micro-electrodes, a twin-wire EDM system saves up more time because it allowed both roughing and finishing together under one process and resulted in efficient fabrication of micro-electrodes. Reference [58] applied micro-WEDM to fabricate ultra-high-aspect ratio silicon-based micro-electrode array, and [59] later carried out further improvement with arrays including 144 electrodes that had 400  $\mu\text{m}$  pitch. The electrodes were machined on 6- and 10-mm-thick silicon wafers (*P*-type) with a length of 5 and 9 mm, respectively. In this study, attainment of the uniform electrode, as well as the maximum machining rate, was simultaneously attempted by varying the voltage and capacitance for different wire types. Electrode shapes with reduced lateral rigidity were investigated using finite element analysis. To obtain such shapes, the machining was done by micro-wire EDM followed by a two-stage chemical etching that helped to remove the recast layer and reduce the electrode's cross section.

Several meso- and micro-scale gear fabrications have been reported using wire EDM as well. [60] reported the fabrication of high-quality meso-gears made of brass by the wire electric discharge machining (WEDM) process as seen in Fig. 11.37.



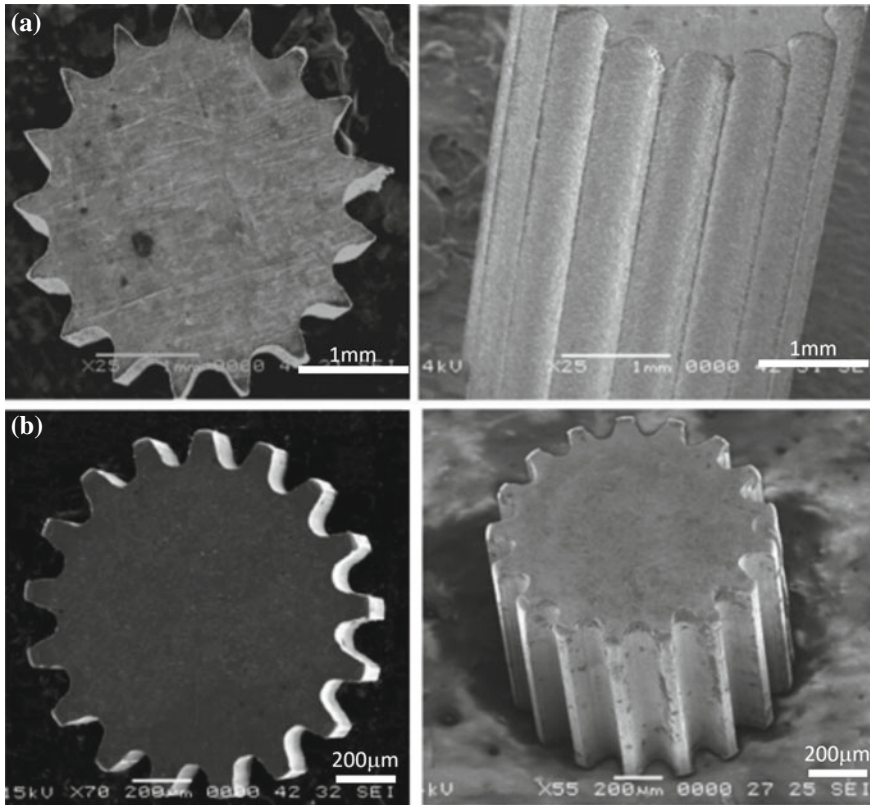
**Fig. 11.37** High-quality meso-gears produced by wire EDM with different magnifications [60]

It has been found that with the controlled process parameters, WEDM can produce high-quality surface with burr-free uniform teeth profile.

A comparative study for producing micro-gears by hobbing and wire EDM has been presented by [61]. It has been reported that in terms of standard and surface integrity, wire EDM is more capable of producing micro-gears compared to hobbing. Ali et al. [62] fabricated a 17-tooth micro-spur gear by conventional wire EDM and micro-wire EDM process. Micro-sized beryllium copper spur gears with 3.5 and 1.2 mm outside diameter were fabricated by conventional and micro-wire EDM. The surface quality and dimensional accuracy were looked into as a measure of performance. An average surface roughness of 50 nm was achieved with a dimensional accuracy of 0.1–1  $\mu\text{m}$  when micro-wire EDM was used for fabrication, while for the conventional wire EDM process, the surface roughness achieved was 1.8  $\mu\text{m}$  with a dimensional accuracy of 2–3  $\mu\text{m}$ . Figure 11.38a, b shows the gear fabricated by conventional wire EDM and by micro-wire EDM, respectively.

When fabricating micro-gears using conventional wire EDM, it can be seen that it is possible to produce such micro-components; however, there are some compromises in terms of surface quality (surface finish), accuracy, and overall dimensions. A micro-gear mold was attempted by Chen et al. [63]. They presented a hybrid process combining micro-reciprocated wire EDM. A 50- $\mu\text{m}$  wire electrode was used in this case; combined with the precision forging, it was possible to fabricate a 10-tooth micro-gear mold with a module of 0.1 mm. This method resulted in a highly efficient

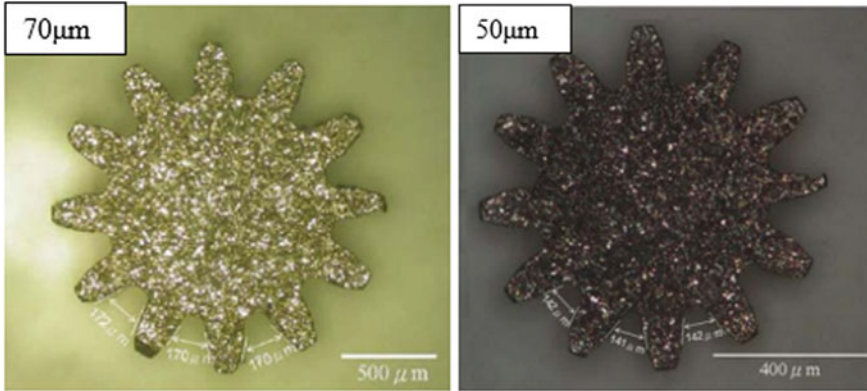




**Fig. 11.38** **a** Miniature spur gear produced by conventional wire EDM [62] and **b** miniature spur gear produced by micro-wire EDM [62]

product that is economical and sustainable. The average tip diameter was  $1169.7 \mu\text{m}$ , and the root diameter was  $719.8 \mu\text{m}$ . The fabrication of micro-gear was conducted in two steps. First, the micro-gear mold was produced from SKD11 using micro-reciprocated wire EDM. Afterward, the precision forging of micro-gears was carried out by the produced micro-gear mold on highly pure copper with ultra-fine grains. It was possible to achieve 3.7 times higher production compared with that of a single process.

A micro-gear was fabricated by pulse control technology applied for wire EDM [64]. The power supply was controlled by a transistor with a low energy discharge circuit. In addition, an iso-frequency pulse control circuit was prepared to maintain high-frequency and lower-energy pulse control. This circuit was used for fabrication of a micro-gear from tool steel SKD11. Two wire diameters were used to manufacture these gears. Each gear had 12 teeth as shown in Fig. 11.39. They also tried the developed power supply process for producing micro-racks as and slots.



**Fig. 11.39** Micro-gears machined with 70 and 50- $\mu\text{m}$  wires [64]

## 11.4 Summary

This chapter focuses on various aspects of  $\mu\text{EDM}$  and  $\mu\text{WEDM}$  about their application as one of the potentials near net shape machining processes. The demand for  $\mu\text{EDM}$  and  $\mu\text{WEDM}$  is growing as the demand for product miniaturization increases. Both these processes have the full capability to meet these new market requirements. Some of the salient points that can be concluded from this chapter are that  $\mu\text{EDM}$  can be used in die-sinking mode or scanning mode. Die-sinking  $\mu\text{EDM}$  is mostly used for micro-hole fabrication, whereas milling/scanning  $\mu\text{EDM}$  is used to fabricate three-dimensional parts. In  $\mu\text{EDM}$ , RC pulse generator performs better as compared to the transistor-based power supply. Finally,  $\mu\text{WEDM}$  is used to cut micro-components with complicated geometry. Both the processes are well capable of achieving high dimensional accuracy with very low surface roughness on the finished product.

## References

1. Marini D, Cunningham D, Corney JR (2018) Near net shape manufacturing of metal: a review of approaches and their evolutions. *Proc Inst Mech Eng Part B J Eng Manuf* 232(4):650–669
2. Marini D, Corney JR (2017) A methodology for near net shape process feasibility assessment. *Prod Manuf Res* 5(1):390–409
3. Son S, Lim H, Kumar AS, Rahman M (2007) Influences of pulsed power condition on the machining properties in micro EDM. *J Mater Process Technol* 190(1–3):73–76
4. Goswami A, Kumar J (2014) Investigation of surface integrity, material removal rate and wire wear ratio for WEDM of Nimonic 80A alloy using GRA and Taguchi method. *Eng Sci Technol Int J* 17(4):173–184
5. Yan BH, Huang FY, Chow HM, Tsai JY (1999) Micro-hole machining of carbide by electric discharge machining. *J Mater Process Technol* 87(1–3):139–145



6. Yu ZY, Rajurkar KP, Shen H (2002) High aspect ratio and complex shaped blind micro holes by micro EDM. *CIRP Ann* 51(1):359–362
7. Jahan MP, Wong YS, Rahman M (2009) A study on the fine-finish die-sinking micro-EDM of tungsten carbide using different electrode materials. *J Mater Process Technol* 209(8):3956–3967
8. Jahan MP, Wong YS, Rahman M (2009) A study on the quality micro-hole machining of tungsten carbide by micro-EDM process using transistor and RC-type pulse generator. *J Mater Process Technol* 209(4):1706–1716
9. Song KY, Chung DK, Park MS, Chu CN (2009) Micro electrical discharge drilling of tungsten carbide using deionized water. *J Micromech Microeng* 19:045006
10. Jahan MP, Saleh T, Rahman M, Wong YS (2011) Study of micro-EDM of tungsten carbide with workpiece vibration. *Adv Mater Res* 264–265:1056–1061
11. Jahan MP, Wong YS, Rahman M (2012) Evaluation of the effectiveness of low frequency workpiece vibration in deep-hole micro-EDM drilling of tungsten carbide. *J Manuf Process* 14(3):343–359
12. Jahan MP, Rahman M, Wong YS, Fuhua L (2010) On-machine fabrication of high-aspect-ratio micro-electrodes and application in vibration-assisted micro-electrodischarge drilling of tungsten carbide. *Proc Inst Mech Eng Part B J Eng Manuf* 224(5):795–814
13. Kibria G, Pradhan BB, Bhattacharyya B (2014) Experimentation and analysis into micro-hole machining of Ti-6Al-4V by micro-EDM using boron carbide powder mixed de-ionized water. *Int J Mater Manuf Des* 1(1):17–35
14. Hourmand M, Sarhan AAD, Noordin MY, Sayuti M (2017) 1.10 micro-EDM drilling of tungsten carbide using microelectrode with high aspect ratio to improve MRR, EWR, and hole quality. In: *Comprehensive materials finishing*. Elsevier, pp 267–321
15. Takahata K, Shibaike N, Guckel H (1999) A novel micro electro-discharge machining method using electrodes fabricated by the LIGA process. Technical digest. In: *IEEE international MEMS 99 conference*. Twelfth IEEE international conference on micro electro mechanical systems, pp 238–243
16. Takahata K, Shibaike N, Guckel H (2000) High-aspect-ratio WC-Co microstructure produced by the combination of LIGA and micro-EDM. *Microsyst Technol* 6(5):175–178
17. Sarwar MSU, Dahmardeh M, Nojeh A, Takahata K (2014) Batch-mode micropatterning of carbon nanotube forests using UV-LIGA assisted micro-electro-discharge machining. *J Mater Process Technol* 214(11):2537–2544
18. Takahata K, Gianchandani YB (2002) Batch mode micro-electro-discharge machining. *J Microelectromech Syst* 11(2):102–110
19. Takahata K, Gianchandani YB (2001) Batch mode micro-EDM for high-density and high-throughput micromachining. Technical digest. In: *MEMS 2001*. 14th IEEE international conference on micro electro mechanical systems, pp 72–75
20. Takahata K, Gianchandani YB (2001) Parallel discharge with partitioned electrode arrays for accelerated batch mode micro-EDM. In: Obermeier E (ed) *Transducers'01 Eurosensors XV*. Springer, Berlin, Heidelberg, pp 1598–1601
21. Yu Z, Masuzawa T, Fujino M (1998) 3D micro-EDM with simple shape electrode part I. *Int J Electr Mach* 3:7–12
22. Reynaerts D, Meeusen W, Brussel HV (1998) Machining of three-dimensional microstructures in silicon by electro-discharge machining. *Sens Actuators, A* 67(1–3):159–165
23. Mohri N, Tani T (2006) Micro-pin electrodes formation by micro-scanning EDM process. *CIRP Ann* 55(1):175–178
24. Hao T, Wang W, Yong L (2008) Vibration-assisted servo scanning 3D micro EDM. *J Micromech Microeng* 18:025011
25. Bissacco G, Valentincic J, Hansen HN, Wiwe BD (2010) Towards the effective tool wear control in micro-EDM milling. *Int J Adv Manuf Technol* 47(1–4):3–9
26. Richard J, Demellayer R (2013) Micro-EDM-milling development of new machining technology for micro-machining. *Procedia CIRP* 6:292–296

27. Li JZ, Xiao L, Wang H, Yu HL, Yu ZY (2013) Tool wear compensation in 3D micro EDM based on the scanned area. *Precis Eng* 37(3):753–757
28. Chiou AH, Tsao CC, Hsu CY (2015) A study of the machining characteristics of micro EDM milling and its improvement by electrode coating. *Int J Adv Manuf Technol* 78(9–12):1857–1864
29. Nguyen VQ, Duong TH, Kim HC (2015) Precision micro EDM based on real-time monitoring and electrode wear compensation. *Int J Adv Manuf Technol* 79(9–12):1829–1838
30. Tong H, Li Y, Zhang L (2016) On-machine process of rough-and-finishing servo scanning EDM for 3D micro cavities. *Int J Adv Manuf Technol* 82(5–8):1007–1015
31. Tong H, Li Y, Zhang L (2018) Servo scanning 3D micro EDM for array micro cavities using on-machine fabricated tool electrodes. *J Micromech Microeng* 28:025013
32. Ali MY (2009) Fabrication of microfluidic channel using micro end milling and micro electrical discharge milling. *Int J Mech Mater Eng* 4(1):93–97
33. Sabur A, Ali MY, Maleque MA, Moudood MA (2014) Micro-EDM for micro-channel fabrication on nonconductive ZrO<sub>2</sub> ceramic. *Int J Automot Mech Eng* 10(1):1841–1851
34. Mohite MB, Gaikwad PVP (2016) Development of EDM Tool for fabrication of microchannel Heat Sink and optimization of single response parameter of EDM by Taguchi Method. *Int J Innovative Res Sci Technol* 2(9):63–70
35. Sommer C (2005) Complete EDM handbook
36. Groover MP (2013) Fundamentals of modern manufacturing
37. Yan MT, Huang PH (2004) Accuracy improvement of wire-EDM by real-time wire tension control. *Int J Mach Tools Manuf* 44(7–8):807–814
38. Luo YF, Chen CG, Tong ZF (1992) Investigation of silicon wafering by wire EDM. *J Mater Sci* 27(21):5805–5810
39. Juhr H, Schulze HP, Wollenberg G, Künanz K (2004) Improved cemented carbide properties after wire-EDM by pulse shaping. *J Mater Process Technol* 149(1–3):178–183
40. Haşçalık A, Çaydas U (2004) Experimental study of wire electrical discharge machining of AISI D5 tool steel. *J Mater Process Technol* 148(3):362–367
41. Rebelo J, Dias AM, Kremer D, Lebrun JL (1998) Influence of EDM pulse energy on the surface integrity of martensitic steels. *J Mater Process Technol* 84(1–3):90–96
42. Patel JD, Maniya KD (2018) A review on: wire cut electrical discharge machining process for metal matrix composite. *Procedia Manuf* 20:253–258
43. Han F, Jiang J, Yu D (2007) Influence of machining parameters on surface roughness in finish cut of WEDM. *Int J Adv Manuf Technol* 34(5–6):538–546
44. Liao YS, Huang JT, Chen YH (2004) A study to achieve a fine surface finish in wire-EDM. *J Mater Process Technol* 149(1–3):165–171
45. Scott D, Boyina S, Rajurkar KP (1991) Analysis and optimization of parameter combination in wire electrical discharge machining. *Int J Prod Res* 29(11):2189–2207
46. Tarng YS, Ma SC, Chung LK (1995) Determination of optimal cutting parameters in wire electrical discharge machining. *Int J Mach Tools Manuf* 35(12):1693–1701
47. Mahapatra SS, Patnaik A (2006) Parametric optimization of wire electrical discharge machining (WEDM) process using Taguchi Method. *J Br Soc Mech Sci Eng* 28(4):52–58
48. Bhatia A, Kumar S, Kumar P (2014) A study to achieve minimum surface roughness in wire EDM. *Procedia Mater Sci* 5:2560–2566
49. Zakaria K, Ismail Z, Redzuan N, Dalgarno KW (2015) Effect of wire EDM cutting parameters for evaluating of additive manufacturing hybrid metal material. *Procedia Manuf* 2:532–537
50. Newton TR, Melkote SN, Watkins TR, Trejo RM, Reister L (2009) Investigation of the effect of process parameters on the formation and characteristics of recast layer in wire-EDM of Inconel 718. *Mater Sci Eng, A* 513–514:208–215
51. Sharma P, Chakradhar D, Narendranath S (2016) Effect of wire diameter on surface integrity of wire electrical discharge machined Inconel 706 for gas turbine application. *J Manuf Process* 24:170–178
52. Das S, Vaiphei SKL, Chandrasekaran M, Samanta S (2018) Wire cut EDM of Al6061 hybrid nano composites: experimental investigations and RSM modeling of surface roughness. *Mater Today Proc* 5(2):8206–8215

53. Joshi K, Sharma G, Dongre G, Joshi SS (2014) Modeling of wire EDM slicing process for silicon. In: 5th International and 26th all India manufacturing technology, design and research conference, AIMTDR 2014, IIT Guwahati, Assam, India
54. Joshi K, Ananya A, Bhandarkar U, Joshi SS (2017) Ultra thin silicon wafer slicing using wire-EDM for solar cell application. *Mater Des* 124:158–170
55. Saleh T, Rasheed AN, Muthalif AGA (2015) Experimental study on improving  $\mu$ -WEDM and  $\mu$ -EDM of doped silicon by temporary metallic coating. *Int J Adv Manuf Technol* 78(9–12):1651–1663
56. Jarin S, Saleh T, Rana M, Muthalif AGA, Ali MY (2017) An experimental investigation on the effect of nanopowder for micro-wire electro discharge machining of gold coated silicon. *Procedia Eng* 184:171–177
57. Sheu DY (2008) High-speed micro electrode tool fabrication by a twin-wire EDM system. *J Micromech Microeng* 18:105014
58. Tathireddy P, Rakwal D, Bamberg E, Solzbacher F (2009) Fabrication of 3-dimensional silicon microelectrode arrays using micro electro discharge machining for neural applications. In: *TRANSDUCERS 2009–2009 international solid-state sensors, actuators and microsystems conference*, pp 1206–1209
59. Rakwal D, Heamawatanachai S, Tathireddy P, Solzbacher F, Bamberg E (2009) Fabrication of compliant high aspect ratio silicon microelectrode arrays using micro-wire electrical discharge machining. *Microsyst Technol* 15(5):789–797
60. Gupta K, Chaube SK, Jain NK (2014) Exploring wire-EDM for manufacturing the high quality meso-gears. *Procedia Mater Sci* 5:1755–1760
61. Gupta K, Jain NK (2014) Comparative study of wire-EDM and hobbing for manufacturing high-quality miniature gears. *Mater Manuf Process* 29(11–12):1470–1476
62. Ali MY, Mustafizul Karim AN, Adesta EYT, Ismail AF, Abdullah AA, Idris MN (2010) Comparative study of conventional and micro WEDM based on machining of meso/micro sized spur gear. *Int J Precis Eng Manuf* 11(5):779–784
63. Chen X, Wang Z, Xu J, Wang Y, Li J, Liu H (2018) Sustainable production of micro gears combining micro reciprocated wire electrical discharge machining and precision forging. *J Clean Prod* 188:1–11
64. Yan MT, Chiang TL (2008) Design and experimental study of a power supply for micro-wire EDM. *Int J Adv Manuf Technol* 40(11–12):1111–1117

# Chapter 12

## Micro-electrochemical Discharge Machining



Ravindra Nath Yadav and Ajay Suryavanshi

**Abstract** Micro-Electrochemical Discharge Machining ( $\mu$ -ECDM) is non-contact type hybrid/combined machining process which comprises two dissimilar energies as thermal and electrochemical. In simple, it is developed by comprising of two non-contact based Unconventional Machining Processes (UMPs) as Electro-Discharge Machining (EDM) and Electrochemical Machining (ECM) positively. It is broadly accepted process that applied in different areas of micro-machining and micro-fabrication related to ceramics especially glass, quartz, and Pyrex. However, it shows potential in shaping of difficult-to-shape electrically conductive materials (heat-treated alloys, titanium alloys, superalloys, Inconel, and composites) also. It is utilized for manufacturing of micro-profiles like through/blind  $\mu$ -holes,  $\mu$ -chutes,  $\mu$ -channels,  $\mu$ -slots,  $\mu$ -grooves, and complex 3D  $\mu$ -profiles. The basic functions of the  $\mu$ -ECDM process are as to eradicate the drawback of EDM and ECM to need of electrical conductivity for machining and also to create micro-/nano-profiles on surface of ceramics. Here, the material can be removed by chemical etching, melting, and vaporization. The present chapter covers various factors related to the  $\mu$ -ECDM as machining mechanism, machining system, configurations, parameters (control and performance), and process capabilities that make easier to understand the basic concept of  $\mu$ -ECDM process.

**Keywords** ECM · EDM · ECSM · Hybrid · Machining · Plasma · Glass

---

R. N. Yadav (✉)

Department of Mechanical Engineering, BBD National Institute of Technology and Management, Lucknow 226028, India

e-mail: [mechrny@gmail.com](mailto:mechrny@gmail.com)

A. Suryavanshi

Department of Mechanical Engineering, Bundelkhand Institute of Engineering and Technology, Jhansi 284128, India

e-mail: [ajay.surya2005@gmail.com](mailto:ajay.surya2005@gmail.com)

© Springer Nature Singapore Pte Ltd. 2019

G. Kibria et al. (eds.), *Micro-electrical Discharge Machining Processes*, Materials Forming, Machining and Tribology, [https://doi.org/10.1007/978-981-13-3074-2\\_12](https://doi.org/10.1007/978-981-13-3074-2_12)

265

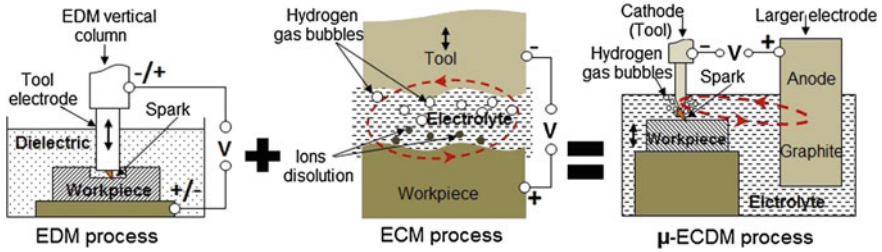
## 12.1 Introduction

The tremendous demand of miniatures in form of micro/nano components/features becomes a fundamental necessity for advanced industries especially in field of automobiles, robotics, aerospace, electronics, computers, and medicals due to suitability to perform different functions within limited space. The shaping of such components becomes difficult for existing traditional and non-traditional manufacturing systems economically. It becomes highly challenging, if miniatures need to be made from ceramics as well as difficult-to-machine materials like heat-treated alloy, tool steel, die steel, titanium alloys, superalloys, and composites. Such materials create many difficulties when Conventional Machining Processes (CMPs) like turning, drilling, milling, shaper, planner are employed due to limitation of tool hardness (tool hardness  $\geq 1.35$ – $1.5$  of workpiece hardness) [1, 2]. Instead of this, higher tool wears, larger cutting forces, poor surface quality (SQ), higher specific energy, and high vibrations limit the wide applicabilities of such advanced materials. Despite this, the advanced industries are looking toward UMPs as a substitute of CMPs for shaping of such difficult-to-machine materials at micro/nano levels. Generally, the UMPs are utilized at various forms of energies (mechanical, chemical, electrochemical, and thermal) for shaping of such materials. The main advantage of the UMPs is no need of tool harder than workpiece. On the other hand, the process capabilities of UMPs are unaffected by workpiece hardness. In general, almost all known materials as hard, brittle, or fragile can be shaped easily with selection of suitable UMP based shaping process.

In various UMPs, the thermal and electrochemical energies based EDM and ECM processes are found more suitable in micro-manufacturing for difficult-to-machine materials, but these processes are limited to conductive (electrically) materials only [1, 3]. Instead of this, EDM suffers with low productivity and recast layers formation while ECM is hazardous process and requires higher specific energy. Therefore, researchers focus on developing a unique shaping process with combination of EDM and ECM that is capable of creating micro/nano profiles on broad ranges of materials either conductive (electrically) or not in nature. Hence, a novel process of shaping comes into the existence which is referred as Micro-Electrochemical Discharge Machining ( $\mu$ -ECDM).

## 12.2 Micro-electrochemical Discharge Machining

Micro-Electrochemical Discharge Machining ( $\mu$ -ECDM) is a combined/hybrid machining process that comprises two most acceptable machining methods (EDM and ECM) as shown in the Fig. 12.1. It utilizes two varieties of energies as thermal and electrochemical for generating  $\mu$ -profiles. In general, it is developed to eliminate the needs of electrical conductivity properties of constituent processes and to enhance the productivity for creation of  $\mu$ -profiles and  $\mu$ -components on surface of



**Fig. 12.1** Combination of EDM and ECM as  $\mu$ -ECDM process

ceramics. In term of performances, it performs much better than constituent processes and gives higher amount (about 5 times and 50 times) of material removal rate (MRR) than the ECM and EDM, respectively [4]. Firstly, it was proposed for drilling of  $\mu$ -holes into glass by Kurafuji and Suda [5]. They were named as Electrochemical Discharge Drilling (ECDD) for glass. Several others names were coined by researchers as Electrochemical Arc Machining (ECAM), Electro-Erosion Dissolution Machining (EEDM), Spark-Assisted Etching (SAE), Spark-Assisted Chemical Engraving (SACE), etc., which are summarized by Yadav [6].

Generally, it is developed to make  $\mu$ -contours on surface of ceramics, especially alumina ( $\text{Al}_2\text{O}_3$ ) glass, quartz, and ceramics. The reasons for this are wide applicability of these materials in various fields as electrical, thermal, and chemical industries for making insulating items like  $\mu$ -pumps,  $\mu$ -actuators, and  $\mu$ -devices for drug delivery systems. However, no any shaping process is found appropriate for machining of these materials effectively at low cost. As results, the wide applicabilities of such materials are limited. The birth of  $\mu$ -ECDM process makes machining of these materials easier in economical ways at micro/nano level. Instead of this, it is effectively utilized in shaping of conductive materials like heat-treated materials, superalloys, dies and tools alloys, titanium, carbides, and metal matrix composites (MMCs) also. In other way, it shows their potential for micro/nano manufacturing of difficult-to-machine objects with complex profiles and with a high geometrical accuracy.

### 12.3 Machining System and Equipments for $\mu$ -ECDM

However, the  $\mu$ -ECDM process covers a long journey in the field of micro-machining for shaping of non-conductive materials but the industrial applications are not in actual practice for micro-machining. Despite this, huge research publications are published and easily available on such process. The majority of research works were carried on the indigenous setup fabricated by particular researchers. Such developed setup has been equipped with the following main components (Fig. 12.2).

- Machining chamber;
- Power supply system;

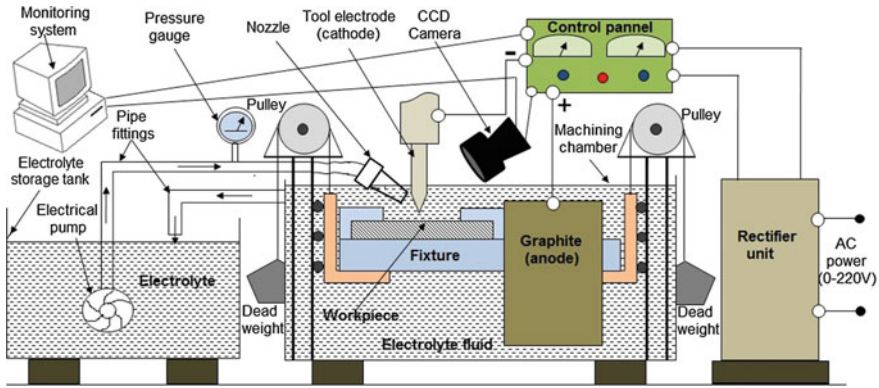


Fig. 12.2 Machining system for  $\mu$ -ECDM process

- Electrolyte feeding system;
- Gap control unit;
- Vision (monitoring) system;
- Exhaust system.

### 12.3.1 Machining Chamber

Machining chamber is described as a domain where  $\mu$ -ECDM phenomenon occurs. Generally, the  $\mu$ -ECDM phenomenon occurs in the existence of electrolyte, which is a corrosive and chemically reactive material. Therefore, machining chamber is fabricated with chemically non-reactive materials, especially glass and looks like a hollow rectangular box with a provision of X, Y, and Z movements. The major components of machining chamber are as given.

- Transparent box;
- Electrolyte;
- Electrodes (anode and cathode);
- Workpiece holding device;
- Workpiece.

Generally, transparent box refers as machining chamber and looks like a box structure. It is made of transparent glass and full of electrolyte at desired level to continue the electrochemical reactions resulting formation of gaseous zone and spark discharges. Electrolyte is expressed as fluid (electrically conductive) that consists of ions and decomposed by electrolysis process. Generally, the electrolytes are either acidic or alkaline based solutions such as HCl, H<sub>2</sub>SO<sub>4</sub>, NaOH, KOH, or NaCl. In majority of cases, the researchers preferred NaOH, KOH, or NaCl solutions as electrolyte fluid as they are comparatively less hazardous and easily available than

acid based electrolyte solutions. In machining chamber, the two electrodes (larger and smaller in size) are kept in such a way that distance of 25–30 mm (approx) is maintained between them [6]. The bigger electrode is prepared from graphite and referred as anode while smaller electrode is known as cathode which is made of conductive materials like copper, brass, nickel, stainless steel, or tungsten. The tool is made as needle-shaped (pointed shape) and kept in a specific manner that it is only dipped 2–3 mm within the electrolyte fluid. The workpiece is kept below the tool in a well specified way that  $\mu$ -gap is maintained between them and also with a provision of workpiece surface just underneath 2–3 mm (approximately) from top surface of electrolyte [6–9]. The workpiece holding device is employed to hold the object at appropriate place and fabricated with chemically non-reactive materials like Perspex, glass, or plastics.

### ***12.3.2 Power Supply System***

Power supply system is important component of machining system for the  $\mu$ -ECDM process. Generally, the DC power (pulse/continuous) with various ratings (voltage = 20–30 V and current = 1 A) is utilized in the  $\mu$ -ECDM process [8]. The power supply system consists of the following main parts/components.

- Transformer (step down);
- Rectifier (silicon controlled);
- Pulse generator;
- Control devices and control panels.

Mainly, the AC current of 220 A can be converted into low voltage DC current through step down transformer and rectifier unit (silicon controlled). A pulse generator mechanism is utilized to generate a pulse current due to better machining responses (higher MRR and better SQ) than the continuous DC current. It also increases the flushing tendency of electrolyte which decreases in recast layers along with stable spark discharge phenomenon. The electrical panels/devices are employed to connect and supply electricity to the different components of machining unit.

### ***12.3.3 Electrolyte Feeding System***

Electrolyte feeding system is a device that used for continuous feeding and subtraction of the electrolyte from machining chamber. Furthermore, it is utilized to sustain the constant height of electrolyte within machining chamber. The main components of electrolyte feeding system are listed below.

- Electrical pump;
- Electrolyte (settling) tank;



- Pressure gauge;
- Control valves;
- Filter and networks of pipes;
- Flushing device.

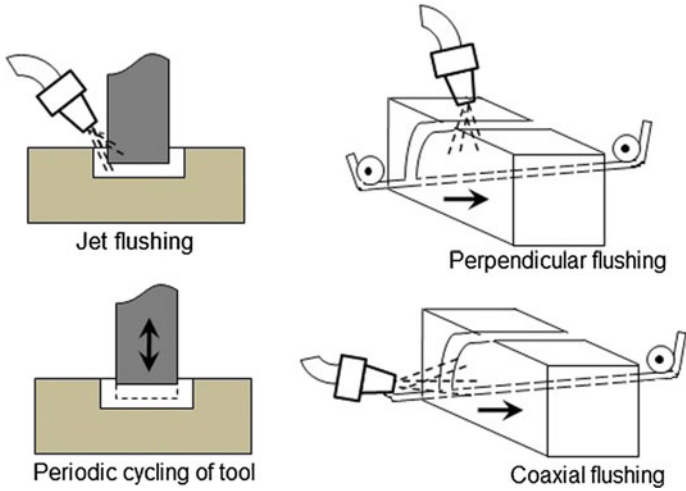
Generally, low velocity electrical pump (centrifugal) is utilized to supply the electrolyte inside the machining chamber because higher velocity of electrolyte leads to unstable discharges resulting responses are declined. The pressure gauge is hereby attached to know the flow pressure of electrolyte while control valves control the amount of flow of electrolyte inside the machining chamber. The extra/undesired electrolyte send back to settling tank through pipes fittings and filtered to eliminate the unwanted or contaminated items through appropriate filter. Furthermore, the cleaned/fresh electrolyte is uniformly fed within machining chamber to sustain a constant level of electrolyte through the electrical pump (centrifugal type), control devices, and pipe networks.

Generally, the flushing device is employed for feeding of electrolyte near the spark zone or tool tip and referred as flushing. The purposes of flushing are to eliminate the by-product from Inter Electrode Gap (IEG) between tool and workpiece, resulting enhancement in the MRR and SQ. The nozzle/jet flushing is mostly beneficial for sinking  $\mu$ -ECDM process. In drilling or any other rotating  $\mu$ -ECDM process, the nozzle/jet flushing is not beneficial because peripheral speed of tool enhances the flushing capability of electrolyte fluid. The various flushing methods related to  $\mu$ -ECDM process are shown in the Fig. 12.3. The jet flushing is more common method for flushing while periodic cycling becomes a good method for flushing during sinking and drilling  $\mu$ -ECDM processes for deep holes machining. The other two methods of flushing device as perpendicular to wire and coaxial to wire are found better for the TW  $\mu$ -ECDM process [4].

#### ***12.3.4 Gap Control Unit***

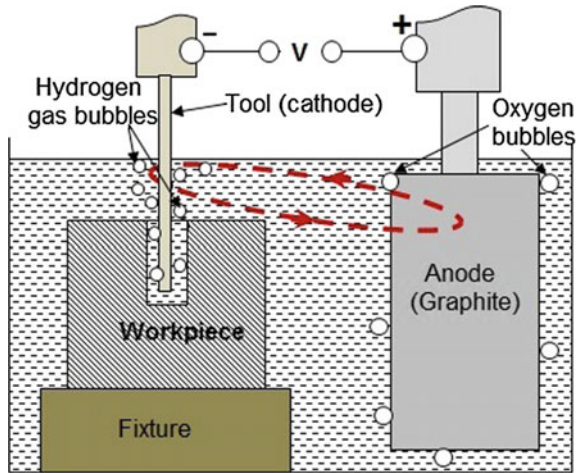
Gap control unit is employed for sustaining a constant gap among workpiece and tool in range of few micrometers. In  $\mu$ -ECDM process, if feed is given to tool toward the workpiece then sparks/discharges are generated initially but no spark condition is achieved after sometimes because the workpiece surface deepened more than 2–3 mm into the electrolyte from the top surface of electrolyte. In this condition, electrochemical reactions and dissolution phenomena occur due to flow of current among cathode and anode in the presence of electrolyte as shown in Fig. 12.4. Therefore, feed given to workpiece toward tool has been found more favorable to avoid such situation. In majority of the cases, the feed mechanisms as gravity control are used by researchers which consist of the following main parts.

- Fixture or workpiece holding device;
- Sliding/vertical column;



**Fig. 12.3** Different methods for flushing

**Fig. 12.4** No spark formation with deeply immersed tool



- Pulleys and rollers;
- Dead weight.

Generally, the gravity control or dead weight feed mechanism is the most common workpiece-feeding gadget that used in the  $\mu$ -ECDM due to easy installation at low cost. Instead of this, several other gap control devices are reported in literatures. These feed devices are screw based mechanism, constant speed mechanism, spring based feed mechanism, and stick-slip actuator as shown in the Fig. 12.5.

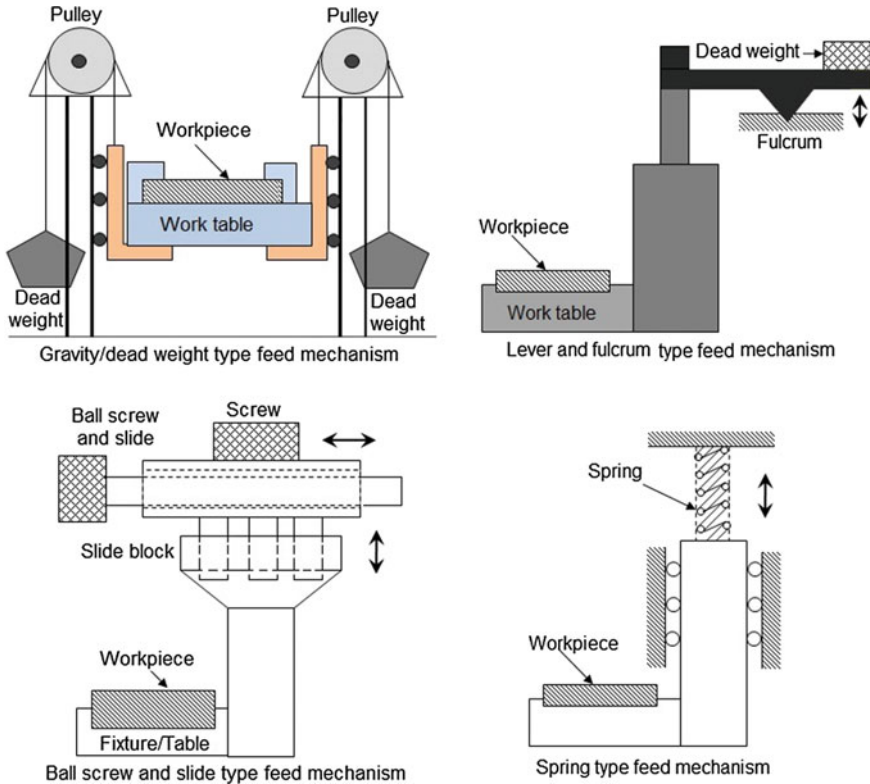
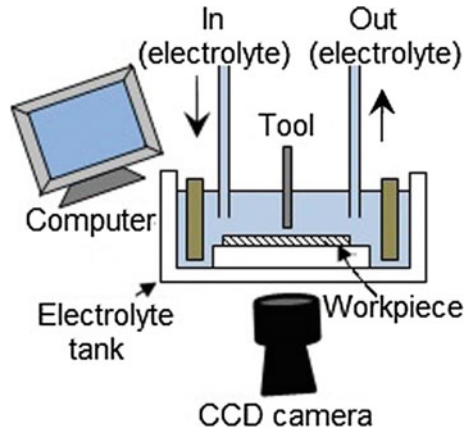


Fig. 12.5 Various feed mechanisms

### 12.3.5 Vision (Monitoring) System

The vision or monitoring system is crucial part for machining unit of the  $\mu$ -ECDM process. The necessities of this are as to precise control, positioning, and monitoring for tool–workpiece interface zone within machining chamber where spark formation phenomenon occurs among tool and gaseous layer. Generally, the vision system consists of a computer device with well-equipped highly sophisticated high speed camera like Charge Coupled Device (CCD) camera or highly precise optical devices. In  $\mu$ -ECDM process, the vision device or camera is kept near to tool–workpiece interface zone for capturing the images and precise control of gap. The vision devices are well associated to monitor system (desktop) as shown in Fig. 12.6. The other vision system as user interface mechanism is found more appropriate to precise on-line gap control. In this device, electrical motor (DC type) and ball screws (two numbers) are employed for conversion of rotating motion of electrical motor into linear motion of tool while linear encoder and servo amplifier (resolution = 1 mm) are employed for precise (micro) control of gap between workpiece and tool.

**Fig. 12.6** Vision/monitoring system



### 12.3.6 Exhaust System

The exhaust system is needed to eliminate the fume gases from the workplace which are produced during machining because of electrical sparks/discharges. Such gases are hot, toxic, and hazardous in nature. It disturbs the vision system of machining unit and also hazardous for respiratory system of the operator. Therefore, a well planned exhaust mechanism becomes necessary which is kept near machining unit that easily exhausts the fume gases from the workplace. Generally, exhaust unit consists of the following main components.

- Duct or pipe networks;
- Chimney;
- Electrical exhaust fan.

Generally, the suction type exhaust device is found much appropriate for the  $\mu$ -ECDM process than the forces type exhaust system due to easy installation at low cost. The electrical fan of exhaust mechanism is switched "ON" before starting the actual machining operation and switched "OFF" after sometime later the completion for complete removal of the fume gases from workplace. In several cases, jet exhaust system shows their potential to release the fume gases from workplace and finds a better device for  $\mu$ -ECDM process to exhaust the fume gases from machining areas.

## 12.4 Electrochemical Discharge Phenomenon

The electrochemical discharge phenomenon of  $\mu$ -ECDM process is complex incident which comprises electrochemical reactions, gas formation, and electrical discharges/sparks in the existence of electrolyte and electrical current. The various

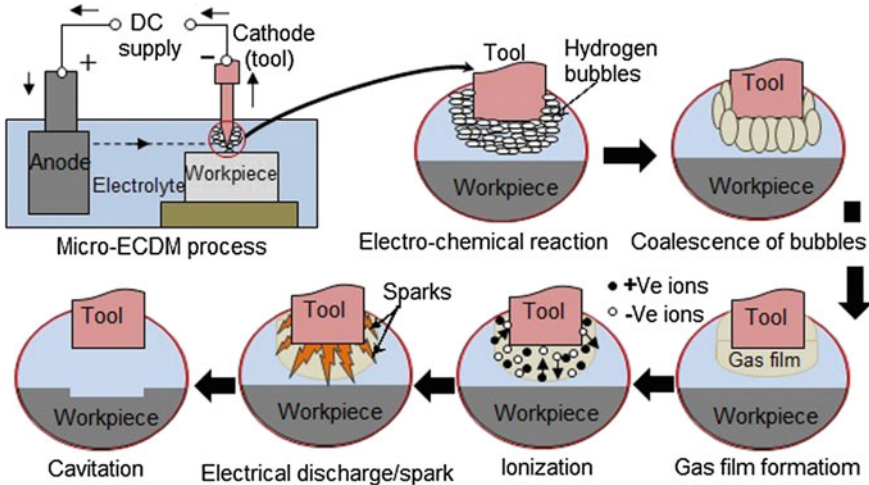


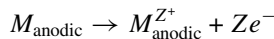
Fig. 12.7 Various phases of  $\mu$ -ECDM process

phases responsible for discharge phenomena related to  $\mu$ -ECDM process are shown in Fig. 12.7 and listed here.

- Electrochemical reactions;
- Coalescence of bubbles;
- Ionization;
- Electrical discharge/spark formation;
- Cavitation.

### 12.4.1 Electrochemical Reactions

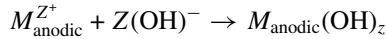
The  $\mu$ -ECDM process occurs in the existence of electrolyte when suitable discharge voltage is employed through anode (graphite electrode) and cathode (tool electrode). In this process, either acidic or alkaline based electrolytes are utilized for electrochemical reactions. In  $\mu$ -ECDM process, the chemical reactions take place when suitable potential difference (20–40 V) is employed between electrodes and electrodes are immersed into electrolyte fluid. The electrolysis begins where metal separates as molecule by molecule from anode surface. Such phenomenon is referred as anodic dissolution, and electrochemical reactions occur as:



where  $M_{\text{anodic}}$  = anode material and  $Z$ =number of ions.

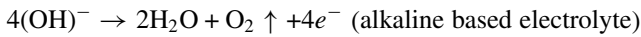
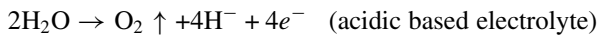
The metallic (positive) ions (+ve) are produced due to anodic dissolution which comprises hydroxide (OH), resulting in formation of metallic hydroxide (MOH).

These metallic hydroxides are insoluble within the water and look as solid precipitates which have no significant affect in the electrochemical reactions. The electrochemical reaction for the metallic hydroxide can be followed as:

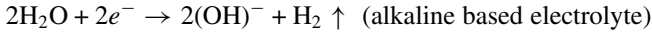
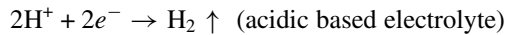


Generally, acidic or alkaline based electrolyte is utilized in the  $\mu$ -ECDM process. Therefore, the electrochemical reaction occurs at anode–electrolyte interface surface and generates the oxygen ( $\text{O}_2$ ) gas while the electrochemical reaction at cathode (tool)–electrolyte interface surface produces the hydrogen ( $\text{H}_2$ ) gas. The electrochemical reactions follow as [6]:

Anode–electrolyte interface surface



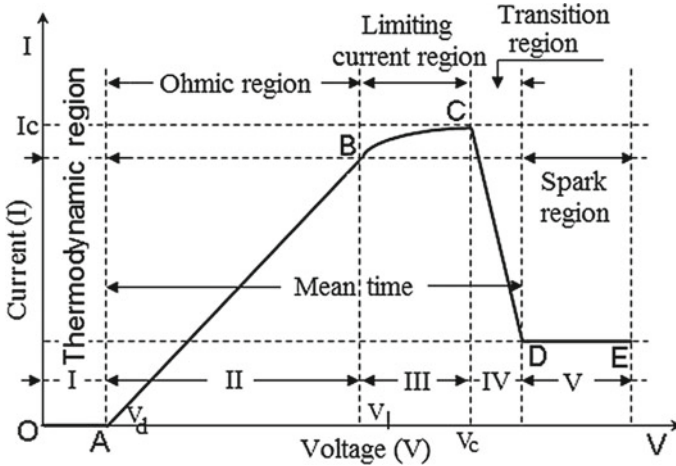
Cathode (tool)–electrolyte interface surface



Due to electrochemical reactions, the  $\text{O}_2$  and  $\text{H}_2$  gases are generated at anode and cathode (tool) surfaces. The  $\text{H}_2$  gases generated surrounding cathode surfaces are responsible for spark discharge phenomenon. Initially, the  $\text{H}_2$  gases generated on surface of cathode are formed as bubbles which are finally converted into gaseous layer and lead to electrical discharges. Of course, the key elements of  $\mu$ -ECDM process are  $\text{H}_2$  gas bubbles and gaseous zone. The creation of bubbles depends upon density of current and discharge voltage. On other hand, the various phases of electrical discharge can be expressed as characteristics of current–voltage (I–V) when mean DC voltages gradually increase into electrolyte cell as expressed in Fig. 12.8.

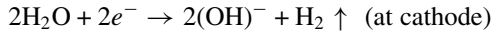
The characteristics of I–V for  $\mu$ -ECDM can be covered in five different zones (Fig. 12.8). The various zones are discussed as follows:

1. **Thermodynamic region:** In this region, current flow is zero or in other hand no flow of current occurs. Therefore, no electrolysis operation occurs until the voltage achieves decomposition (breakdown) voltage ( $V_d$ ). The line OA represents the thermodynamic region on the I–V graph.
2. **Ohmic reason:** In Ohmic region (AB), the I–V graph is almost linear (where  $V_d < V < V_1$ ) and the typical voltage range is of 2–10 V. In this reason, the  $\text{H}_2$  bubbles are formed due to electrolysis of water. It is fact that water particles of



**Fig. 12.8** Current–voltage (I–V) characteristics

electrolyte gain electrons from cathode which are separated as free ions ( $H_2$  and  $OH$ ), and the electrochemical reaction follows as:



3. **Limiting current region:** In limiting current zone BC, the I–V graph is nonlinear (where  $V_1 < V < V_c$ ). In this region, the bubbles are grown and coalescence of bubbles starts to create gas film surrounding the tool surface while current reaches the limiting value as limiting/critical current ( $I_c$ ). The limiting/critical current depends upon tool geometry and electrolyte fluid.
4. **Transition region:** Generally, transition region (CD) is referred as instability zone because such zone may be either similar status of limiting current or spark reasons. In this region, (where  $V_c < V < 1.2V_c$ ) a gaseous layer forms surrounding the tool surface. The thickness of gas layer depends upon tool geometry and electrolyte concentration.
5. **Spark region:** The spark range (DE) refers to the full presence of gaseous layer surrounding tool electrode. The gaseous region works as dielectric material and electrical sparks/discharges occur when critical voltage ( $V > 1.2V_c$ ) is applied through it. Such region has been found appropriate for the machining.

### 12.4.2 Coalescence of $H_2$ Bubbles

In this phase, the  $H_2$  bubbles generated during electrochemical reactions are bonded together and form a gaseous film surrounding the tool. Initially, very small sizes

(25–55  $\mu\text{m}$ ) of bubbles are generated when DC supply voltage (30–60 V) is applied with much low resistance ( $<10\ \Omega$ ) of electrolyte [6]. The mean diameters and density of bubbles depend upon supply voltage. As increase in voltage means increase in mean diameter and density of  $\text{H}_2$  bubbles as which the bubbles are bonded with each other and finally increases in the mean diameter of bubbles. This phenomenon continues till formation of gaseous film surrounding tool surface. The thickness related to gaseous film is as 50–100  $\mu\text{m}$  with cylindrical electrode (dia. = 1 mm) [9]. The gas film works like dielectric and protects the tool with direct effect of electrolyte. The gaseous film is responsible for spark generation and becomes as conductive medium when suitable voltage is employed through it.

### 12.4.3 Ionization

In this phase, the  $\text{H}_2$  gas is ionized into liberated ions as positive (+ve) and negative (–ve) ions when high-density current is applied between electrodes. Due to this, a high electrical field as  $10^6$ – $10^8$  V/m has been build up into gas film [10]. The high-intensity electrical field leads ionization of  $\text{H}_2$  gas into the ions (+ve and –ve). These ions attract toward the dissimilar electrodes (cathode/anode) with a very high velocity. Due to movement of ions, clouds of ions like a cylindrical channel are formed among tool and electrolyte surface within the gaseous zone. Such phenomenon is referred as ionization, and cylindrical column is referred as ionized or plasma column as shown in Fig. 12.9.

### 12.4.4 Electrical Discharge/Spark Formation

The electrical discharge or spark formation in the  $\mu$ -ECDM process is considered as arc creation into the gas. Generally, spark is generated among tool, gas layer, and electrolyte surface when higher current density than critical value (1 A approx.) has been

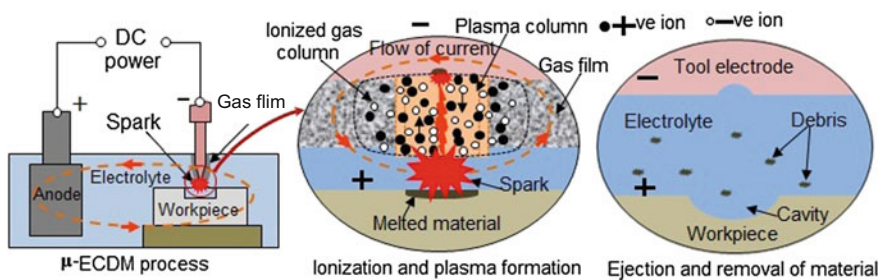


Fig. 12.9 Plasma formation and machining mechanism  $\mu$ -ECDM process



set up. In this situation, supply voltage is more than critical voltage as 25–30 V. The basic reasons for spark formation are bombardment of ions on respective surfaces as shown in Fig. 12.9. In ionized column, the positive (+ve) and negative (–ve) ions are moving with high velocity toward opposite electrodes. Finally (end of journey), the ions strike at respective electrode surfaces (cathode/anode) positively. Consequently, the ions are losing their kinetic energy that are converted into heat energy and seen as plasma column.

Generally, plasma can be described as collection of high temperature and pressure ionized gases. The range of temperature related to plasma is as 800–20,000 °K [10–12]. This high temperature is adequate to eliminate any material (conductive/non-conductive) that is kept near to the plasma. The plasma formation and their temperature depend upon various parameters such as current intensity, electrolyte materials and their properties (thermal and conductivity), concentration, and tool geometry.

### 12.4.5 Cavitation

In  $\mu$ -ECDM process, high temperature up to 20,000 °K has been generated because of electrical sparks. At this temperature, any non-conductive material is kept close to sparking region and maintained a suitable gap between them, then the material has been melted and vaporized resulting material removal takes place. Generally, IEG is much small and in range of few micrometers as 20  $\mu\text{m}$  or  $>25 \mu\text{m}$  [6, 13]. It is maintained constant during machining with suitable gap control mechanism. The various gap control devices are explained in Sect. 12.3.4 and graphically shown in Fig. 12.5. To maintain gap during machining, a well-equipped and precise vision system has been in practice.

## 12.5 Mechanism of Machining

In general, melting and vaporization are basic reasons for removal of material in the  $\mu$ -ECDM process and referred as mechanism of machining. However, the thermal machining and Chemical Machining (ChM) are also responsible for machining. In thermal machining, localized high temperature is raised due to heating by fraction of spark energy, resulting in the melting of material in addition to vaporization also. In other hand, high energy is required for complete vaporization of molten material. Therefore, additional flushing devices are used throughout machining to flush out molten material and avoid growth of recast layers. The majority of machining occurs due to thermal machining but higher energy leads to develop the thermal stresses and cracks inside the machined parts.

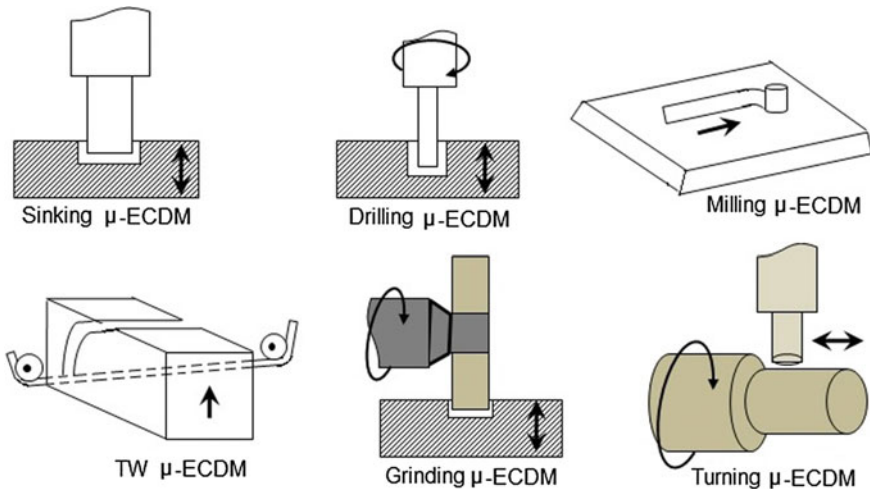
In  $\mu$ -ECDM process, the ChM or chemical etching also leads to material removal because of the chemically reactive nature of electrolyte. Generally, the ChM process is in dominated phase during machining and also a slow process. However, the

capabilities of ChM depend upon type of electrolyte and their concentration, current intensity and duration, material of workpiece and their chemical properties. If material is chemically non-reactive, then the etching operation performed between anode and cathode. However, several researches show that chemical etching plays important roles in removal of material [14]. Therefore, the overall material removal is sum of the material removed by the thermal machining and ChM processes during  $\mu$ -ECDM process.

## 12.6 Configurations of $\mu$ -ECDM Process

The  $\mu$ -ECDM process comes into existence for machining of ceramic materials and to create the features at micro/nano scales. However, it is effectively applied for shaping of difficult-to-shape conductive (electrically) objects too. Due to influence of such process, the researchers developed different configurations of the  $\mu$ -ECDM process as listed below and graphically shown in the Fig. 12.10.

- Sinking  $\mu$ -ECDM process;
- Drilling  $\mu$ -ECDM process;
- Milling  $\mu$ -ECDM process;
- Traveling wire (TW)  $\mu$ -ECDM process;
- Grinding  $\mu$ -ECDM process;
- Turning  $\mu$ -ECDM process.



**Fig. 12.10** Configurations of  $\mu$ -ECDM process

### ***12.6.1 Sinking $\mu$ -ECDM***

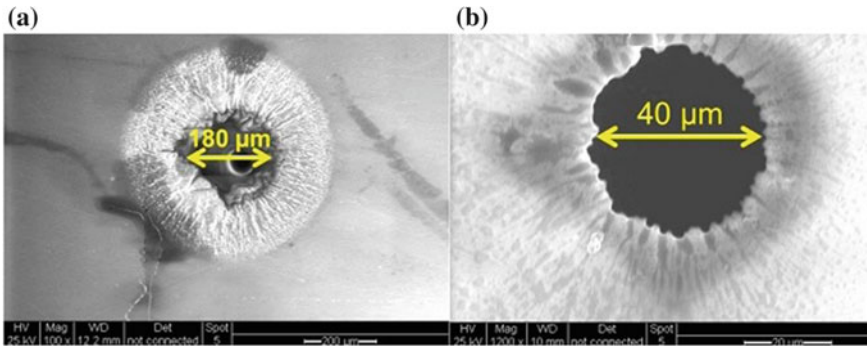
Sinking configuration of  $\mu$ -ECDM is applied to generate micro-holes (through and blind) with stationary tool while feed is given to workpiece. In general, sinking is expressed as holes making operation for low aspect ratio (length: diameter  $<1$ ). It is a better method to create ultra-precision and micro-holes in the orifices, nozzles, mold, and dies, especially fabricated with non-conductive (electrically) materials. It becomes a unique technique for removing the damaged/broken items like drill bits, taps, or bolts into the highly sophisticated parts. The sinking  $\mu$ -ECDM process shows better machining capability than constituent processes as higher MRR while the SQ is closed to the EDMed parts and slightly inferior to the ECMed objects. In this process, an appropriate flushing device must be necessary otherwise debris particles are accumulated into the IEG. Such phenomenon leads to the poor and unstable sparks formation which leads to declination in the process capabilities as lower MRR with poor quality of the finished surface.

### ***12.6.2 Drilling $\mu$ -ECDM***

Drilling configuration of  $\mu$ -ECDM process is also applied for creation of  $\mu$ -holes (through or blind) in non-conductive materials. In this mode, stationary tool of the sinking  $\mu$ -ECDM has been replaced with rotating tool. For this, a rotating gadget with variac (speed control device) is attached with tool-holding mechanism to rotate the tool. Generally, lower speed ( $<25$  r/min) of tool is preferred as higher speed disturbs the gas layer, resulting in poor, weak, and unstable spark formations [15]. The basic purposes of such configuration are improvement in productivity and to achieve better SQ near to polished categories. It is employed for creations of  $\mu$ -devices manufactured from fused silica and crack-free surface with larger aspect ratio as 11:1 [16]. Such type of drilled holes has been shown in Fig. 12.11. In this process, the circularities of holes are better due to reduction in stray corrosion. Instead of this, the peripheral speed of rotating tool effectively improves the flushing capability as which improves the MRR and SQ. Thus, no additional flushing method is needed in such configuration. It is significantly creating the various profiles related to micro/nano holes in non-conductive materials as through holes, blind, or counter holes.

### ***12.6.3 Milling $\mu$ -ECDM***

Milling configuration of  $\mu$ -ECDM is powerful method to create three-dimensional (3D) micro-profiles like  $\mu$ -channels,  $\mu$ -slots,  $\mu$ -chutes,  $\mu$ -grooves, or  $\mu$ -cavities. It proves their capability to produce  $\mu$ -pillars and  $\mu$ -pyramids like complicated



**Fig. 12.11** High aspect ratio holes (1200  $\mu\text{m}$  thick) drilled by  $\mu\text{-ECDM}$  process [16]. **a** Hole diameter at entrance and **b** hole diameter at exit

structures also. In this method, the tool (stationary) of sinking  $\mu\text{-ECDM}$  is replaced in a specific manner as tool electrode gains the linear movement. Such linear motion of tool is adopted as a well defined movement of tool like milling process. The  $X$ ,  $Y$ , and  $Z$  movements of machining chamber facilitate in creation of 3D profiles. Due to linear motion of tool, the sparks also follow the same path as tool electrode, resulting in uniform MRR throughout the machining process. The another method for milling  $\mu\text{-ECDM}$  can be possible with orbital movement of tool which gives better responses than the linear movement of tool during micro-machining for sophisticated 3D profiles. In milling  $\mu\text{-ECDM}$  process, the flushing is needed when tool moves with linear movement but no need of flushing with orbital movement of tool because the flushing is enhanced by circumferential speed of tool electrode. It is beneficial to produce the  $\mu\text{-profiles}$  smaller than 100  $\mu\text{m}$  on the surface of ceramic materials especially glass [17].

#### 12.6.4 TW $\mu\text{-ECDM}$

Traveling wire (TW)  $\mu\text{-ECDM}$  is referred as moving wire  $\mu\text{-ECDM}$  process. In this arrangement, the tool (stationary/rotating) is replaced with traveling wire whose diameter is in micrometer and lesser than 1 mm while moving speed is also very low as few centimeter/min. In this configuration, sparks are created between traveling wire and electrolyte in the presence of gaseous layer while feed is given to the work-piece. The methods of flushing are as parallel to wire direction or perpendicular to wire travel direction (Fig. 12.3). Generally, the moving wires are made from copper, brass, or tungsten. The tungsten wire proves their suitability in micro-machining because copper/brass wires are frequently broken during machining. The process capability in term of MRR is as 5 times and 50 times higher than EDM and ECM, respectively [4]. It demonstrates their strength for micro-cutting on the external and

internal surfaces. It is suitable to generate  $\mu$ -gears on internal/external surfaces,  $\mu$ -cam profiles,  $\mu$ -channels, and highly complex comb-like profiles on the surface of ceramic materials like glass, Pyrex, or quartz.

### ***12.6.5 Grinding $\mu$ -ECDM***

Grinding configuration of  $\mu$ -ECDM is implementation of conventional grinding for shaping of micro-profiles as  $\mu$ -channels,  $\mu$ -slots, or  $\mu$ -grooves. In this configuration, a metallic wheel is utilized to produce electrical discharges/sparks in between wheel and electrolyte surface. The wheel used in the  $\mu$ -ECDM process is either metallic (without abrasives) or metallic (with abrasives). In abrasive based wheels, the abrasives ( $\text{Al}_2\text{O}_3$ , SiC, CBN, diamond, etc.) are bonded with metallic materials (copper, brass, bronze, or mild steel). The metallic parts of wheel are responsible for sparks creations. The abrasive based wheel performs better (higher MRR and superior SQ) than metallic (without abrasives) wheel. In this approach, the direct flushing is avoided because it enhances with peripheral speed of wheel. However, the much higher velocity is always avoided because it damages the  $\text{H}_2$  bubbles and sparks formation, resulting in lower MRR and poor SQ.

Grinding  $\mu$ -ECDM is expanded in various configurations such as face grinding  $\mu$ -ECDM, surface grinding  $\mu$ -ECDM, and cut-off grinding  $\mu$ -ECDM. Circumferential surface of wheel is utilized in surface and cut-off grinding configurations for shaping while face end of wheel has been employed for face grinding  $\mu$ -ECDM process. The face grinding configuration is employed for shaping of end/face surface of bar, shaft, or cylindrical profiles where wheel diameter is always greater than diameter of workpiece. The cut-off mode is appropriate for shaping of grooves, slots, or parting-off workpieces. In the other hand, the surface grinding configuration is suitable for  $\mu$ -grinding of slots, channels, key ways, or surface machining. In majority of the cases, the metallic diamond wheel is preferred because of its ability in cutting of ceramics with low tool wear capabilities.

### ***12.6.6 Turning $\mu$ -ECDM***

Turning  $\mu$ -ECDM is employed for shaping of circular rotating objects like shafts or bars made of ceramics. It is development of turn machining into the  $\mu$ -ECDM process. In this method, the workpiece is in rotating nature while feed is given to the tool in axial direction. Due to rotating of workpiece, the direct flushing is avoided because rotational velocity of workpiece assists to entry of fresh electrolyte within gap and also in removal of debris particles. The uninterrupted feeding of fresh electrolyte becomes beneficial as higher MRR, superior SQ, and declination in the  $\mu$ -cracks on the machined surfaces. In turning  $\mu$ -ECDM process, the heat of sparks speed up the electrochemical reactions resulting a bit of material has been detached

from workpiece as which higher MRR. In this mode, the workpiece is always in horizontal position through machining and tool travels in axial direction. Therefore, no need of feed mechanism as which the process becomes smoother and economical. It is implemented in the different  $\mu$ -turning modes like plane turning, face turning, step turning, taper turning, and micro-thread cutting.

### 12.7 Process Variables and Responses

The  $\mu$ -ECDM is a really complicated process because it comprises the two energy (thermal and electrochemical) based machining processes and their features. Therefore, all parameters related to EDM and ECM are affected by the machining capabilities of  $\mu$ -ECDM process. The process variables with responses are shown in Fig. 12.12. The process variables/parameters are categorized as electrical parameters, tool parameters, electrolyte parameters, and flushing parameters while the MRR, tool wear rate (TWR), and SQ are mainly acceptable process responses or performance measures related to  $\mu$ -ECDM process.

#### 12.7.1 Electrical Parameters

The common electrical parameters those are influencing the machinability of  $\mu$ -ECDM are voltage, current intensity, polarity, pulse on-time, and pulse off-time. Generally, discharge voltage is a key factor that concerns with IEG. The larger amount of discharge voltage means more gap distance resulting in easy ejection of debris from IEG but simultaneously leads to higher tool wear. The most desirable voltage ranges for  $\mu$ -ECDM are as 30–40 V positively. The other control parameter

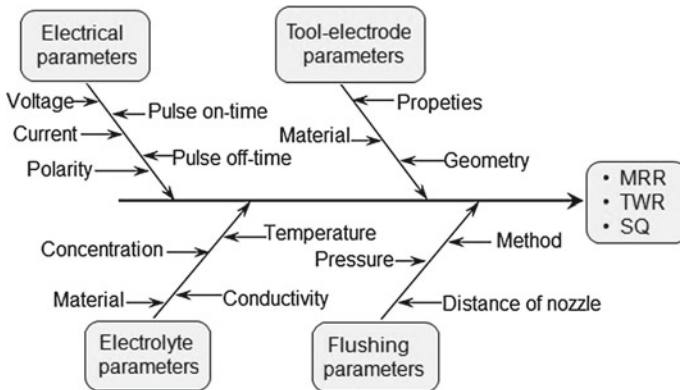


Fig. 12.12 Process variables and responses

as current is not much considerably influencing the responses because very low intensity of current (1 A) is utilized in the machining. However, either continuous or pulse type current is applied for machining and results of pulse type current are much better than the continuous type current.

The polarity is a significant parameter that influences the responses related to  $\mu$ -ECDM. It is utilized to signify the connectivity of electrodes with electrical supply system. In general, two forms of polarities as direct and reverse are utilized to connect the tool (cathode) and graphite electrode (anode). In direct polarity, the tool (cathode) is associated to negative (–ve) terminal and graphite electrode (anode) is connected to positive (+ve) terminal while the reversed connectivity of terminals with electrodes refers to reverse polarity [18]. Generally, reverse polarity provides higher MRR and poor SQ than direct polarity. However, direct polarity shows better potential for creation of micro/nano components by  $\mu$ -ECDM process.

The pulse duration or pulse on-time and pulse interval or pulse off-time are also highly influencing parameters. The various spark formation phenomena (ionization, plasma, melting, and vaporization) depend upon pulse on-time. The longer on-time means same heat goes within workpiece for longer time as which melting of more amounts of materials along with their vaporization. However, much longer on-time leads to creation of recast layers and deep cavity formation which requires further machining. The pulse off-time involves in removal of molted material during flushing and longer off-time means more removal of molted material. Such phenomenon is responsible for higher MRR, better SQ, and declination in recast layers. The longer off-time is not forever advantageous, and much longer off-time leads to reduction in the on-time as which declination in machinability.

### ***12.7.2 Tool Parameters***

The common tool parameters that extensively influence the responses are tool materials, their properties, and tool geometry. Generally, materials having several specific properties such as highly conductive (electrically and thermally), chemically non-reactive, and non-corrosive in nature are preferred as tool materials. Some common tool materials are copper, brass, nickel, stainless steel (SS), platinum, and tungsten [9]. However, carbide-based tool like tungsten carbide shows superior performances than SS and tungsten tools which shows slightly higher tool wears. Tool geometry as spherical shape gives better responses than cylindrical shaped tool. This is because that the spherical shaped tool assists the flushing which means enhancement in MRR with superior SQ. In other hand, tube tool proves their strength in higher machinability in term of higher MRR and declination in taper of holes while their manufacturing is much difficult at micro-level.

### ***12.7.3 Electrolyte Parameters***

The electrolyte fluid is a significant valuable material of the  $\mu$ -ECDM process because it leads to electrochemical reaction and sparks formation. Therefore, the electrolyte material, their concentration, working temperature, and conductivity are common factors that affect the responses. Normally, alkaline based electrolyte fluids such as NaOH, KOH, NaCl, NaNO<sub>3</sub> or acidic based electrolytes such as HCl, H<sub>2</sub>SO<sub>4</sub>, and HNO<sub>3</sub> are used as electrolyte materials [9]. The functions of electrolyte fluid are to generate H<sub>2</sub> gas during electrochemical reactions and flush out the debris during ejection from IEG. Therefore, higher concentration leads in production of huge amount of H<sub>2</sub> bubbles. The concentration for electrolyte as 30% at temperature in between 40 to 50 °C is found better for  $\mu$ -ECDM process [19].

### ***12.7.4 Flushing Parameters***

Flushing of electrolyte into IEG is an efficient technique to eliminate debris from gap. The effective flushing means higher MRR along with superior SQ due to generation of strong and stable sparks. The various flushing parameters are flushing pressure, flushing method, and distance of nozzle tip from spark zone. The higher flushing pressure leads in higher and rapid expulsion of melted material from workpiece surface but simultaneously disturbs the spark stability and damages the gas bubbles. Therefore, moderate flushing pressure is always preferred in the  $\mu$ -ECDM process. In same way, the much closer distance of nozzle from spark zone also disturbs the spark phenomenon. The ways of application for electrolyte in machining zone are much critical issues. The various techniques used in electrolyte supply in different processes are shown in Fig. 12.3.

### ***12.7.5 Process Responses***

The various responses are utilized to find the capability of various shaping processes but most common parameters used to find the ability related to  $\mu$ -ECDM process are MRR, TWR, and SQ. In general, MRR and TWR are determined as ratio of mass loss to machining time and expressed in mm<sup>3</sup>/min. The other control parameter SQ covers the wide ranges of parameters and reflects the worth of machined surface. These parameters are as surface roughness, taper in machined holes, circularity of holes, radial over cuts (ROCs), thermal stresses, heat-affected regions, and recast layers. The various research articles show that surface finish is most common response parameter that can be measured with help of surface roughness tester. The other responses as taper, ROCs, and circularity are related to geometry of holes and concentration of electrolyte. These responses increase during machining of holes to get longer aspect



ratio and also with electrolyte concentration. The higher concentration of electrolyte means larger in holes taper, ROCs, and circularity. Thus, low intensity of electrolyte is preferred during  $\mu$ -drilling for higher aspect ratio of holes.

## 12.8 Process Capabilities

The  $\mu$ -ECDM process is developed to generate micro-profiles at surface of non-conductive (electrically) materials like ceramics, glass, alumina, and Pyrex. However, it proves their strength for shaping of conductive (electrically) materials in micro and or nano level also. Therefore, the capabilities of  $\mu$ -ECDM process are covered in various sections as merits, demerits, and applications as explained briefly.

### 12.8.1 Merits

- It is suitable to significantly machine the ceramic and metallic materials.
- It provides higher MRR than constituent (EDM and ECM) processes.
- It effectively creates the micro and/or nano profiles on surface of difficult-to-machine objects and shows their suitability to machine materials either conductive (electrically) or not.
- It is an appropriate process to create very small profiles as micro/nano features on/within the surfaces of tools, molds, dies, or fixtures.
- The performances of process are unaffected by material's properties like hardness, conductivity (electrical and thermal) or toughness.
- Hard, brittle, and fragile objects can be smoothly machined by this method.
- It is suitable to create prototype objects related to medical and aircrafts applications.
- It is highly flexible because it can be developed in various configurations as sinking, drilling, milling, grinding, and turning to create specific profiles on the workpiece surface.

### 12.8.2 Demerits

- The sparks phenomena depend upon gaseous layer but the formation and controlling of the  $H_2$  gas bubbles are still not possible.
- Only fraction of spark energy is utilized for machining while most part of heat is either wasted or gone into electrolyte fluid.
- The stability and dynamics of gaseous layer ( $H_2$  gas) formed around tool surface are much difficult.

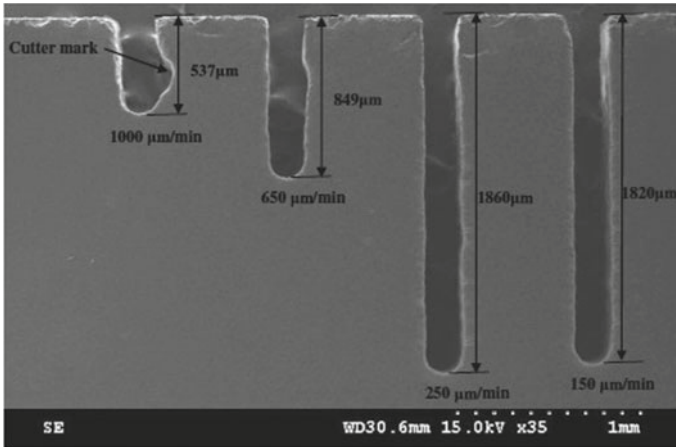
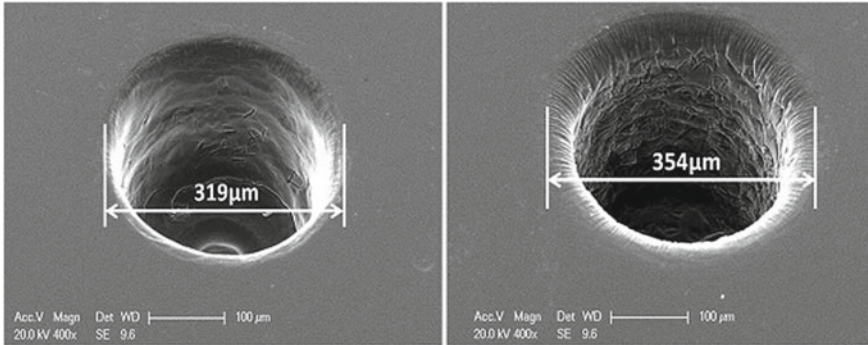


Fig. 12.13 Micro-slits made by TW  $\mu$ -ECDM process [20]

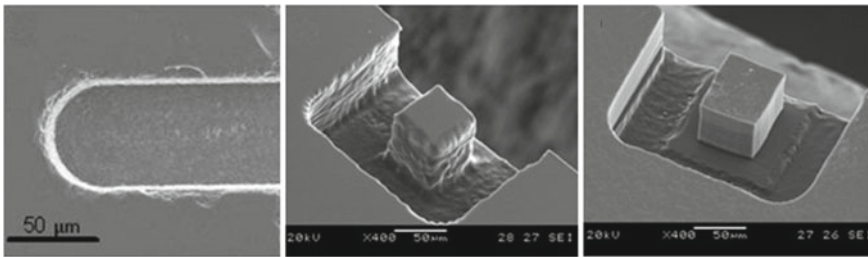
- Machining/drilling of holes for longer aspect ratio is facing difficulties in the supply of electrolyte fluid.
- It is chemically hazardous and reactive in nature.

### 12.8.3 Applications

- It is utilized in fabrication/manufacturing of  $\mu$ -components such as  $\mu$ -accelerometers,  $\mu$ -reactors,  $\mu$ -flow sensors, and  $\mu$ -pumps.
- It is applicable in dies and molds, tools, and fixtures making industries to generate the  $\mu$ -patterns or  $\mu$ -profiles on surface of objects.
- It is applicable to eliminate the broken items like taps, drills, or bolts from the highly sophisticated equipments.
- It is significantly applicable to machine the artificial items used in the medical applications and made of ceramics like artificial knees or bones.
- It is employed to create 3D  $\mu$ -profiles like  $\mu$ -channels,  $\mu$ -grooves,  $\mu$ -chutes,  $\mu$ -pillars,  $\mu$ -pyramids, and  $\mu$ -gears. Some  $\mu$ -profiles created by the different configurations of the  $\mu$ -ECDM process are shown in Figs. 12.13, 12.14, 12.15, 12.16 and 12.17 [17, 20–23].
- The aerospace, nuclear, electronics, electrical, and automobiles are some demanding fields for the  $\mu$ -ECDM process.



**Fig. 12.14** Micro-holes made by drilling  $\mu$ -ECDM process [21]



**Fig. 12.15** Micro-channel and columns/pillars made by grinding  $\mu$ -ECDM process [22]

### 12.9 Micro-ECDM at a Glance

In this section, the various characteristics of the  $\mu$ -ECDM process are summarized that makes easier to understand the different aspects related to it and beneficial for quick review of various characteristics of  $\mu$ -ECDM process. The characteristics of  $\mu$ -ECDM process are as follows:

- $\mu$ -ECDM Hybrid machining process
- Constituent processes EDM and ECM
- Mechanism of machining Melting and vaporization
- IEG In few  $\mu$ m as 20  $\mu$ m or <25  $\mu$ m or slightly more
- Size of gas bubbles 25–55  $\mu$ m
- Thickness of gas layer 50–100  $\mu$ m
- Discharge voltage 30–60 V
- Electrolyte resistance <10  $\Omega$
- Critical voltage 25–30 V
- Critical current 1 A
- Electrical field  $10^6$ – $10^8$  V/m
- Plasma temperature 800–20,000  $^\circ$ K
- Electrolytes NaOH, KOH, NaCl, NaNO<sub>3</sub>, HCl, H<sub>2</sub>SO<sub>4</sub>, and HNO<sub>3</sub>

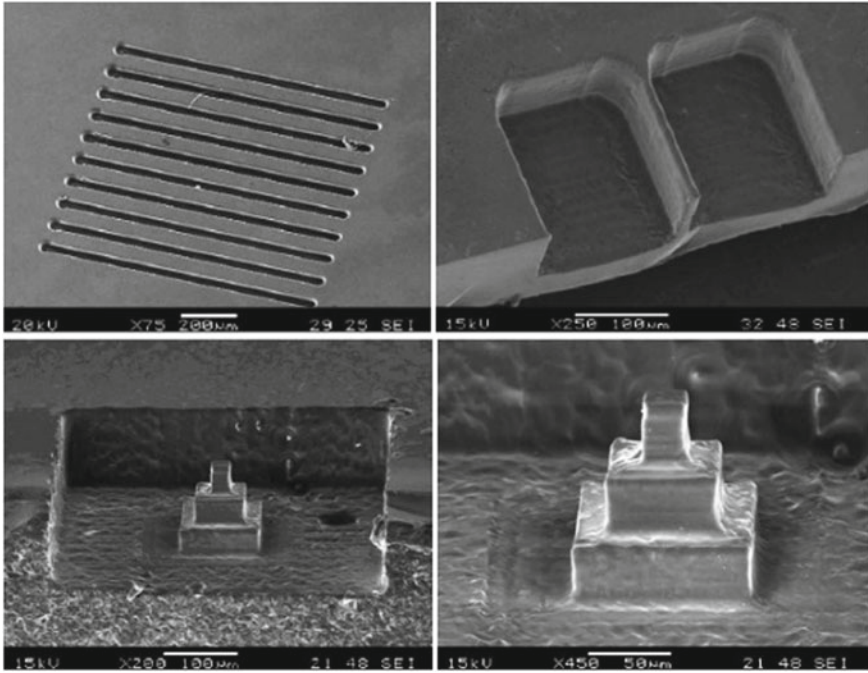


Fig. 12.16 Matrix of  $\mu$ -chutes/grooves,  $\mu$ -wall, and  $\mu$ -pyramids made by  $\mu$ -ECDM [17]

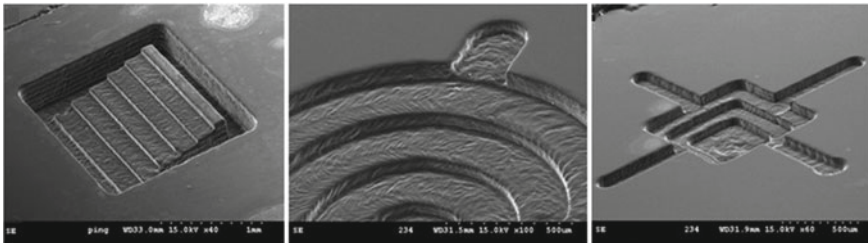


Fig. 12.17 3D complex profiles made by milling  $\mu$ -ECDM process [23]

- Electrolyte temperature 40–50 °C
- Configurations Sinking, drilling, milling, traveling wire, grinding, and turning configurations
- Applicabilities Machining of ceramics and metallic materials, creation of micro/nano profiles
- Advantages Higher MRR than EDM and ECM, suitable for ceramics, metallic (ferrous and non-ferrous) materials, suitable for micro/nano manufacturing, hard, brittle, and fragile objects can be shaped/machined

- Disadvantages Chemically hazardous, uncontrolling of gas bubbles and their formations, drilling of holes of high aspect ratio are difficult in machining
- Applications Micro-manufacturing as dies, molds, tools, fixtures, accelerometers, reactors, flow sensors, and pumps. Removal of damaged drill bits, taps, or bolts from highly complicated items. Shaping of the artificial bones or knees. It is also used to create 3D  $\mu$ -profiles as channels, grooves, pillars, pyramids and  $\mu$ -gears
- Limitations Uncontrolled and undefined generation of bubbles and plasma temperature. Only fraction of temperature utilized in machining. Hazardous in nature
- Demanding industries Aerospace, nuclear, electronics, automobiles, ceramics, tools, mold and dies industries

## 12.10 Summary

The  $\mu$ -ECDM is hybrid/combined shaping method that consists of characteristics of EDM and ECM processes. It shows better capabilities than constituent (EDM and ECM) processes. It is found as a suitable method for shaping of non-conductive objects to create micro-features. Instead of this, it is also appropriate to shape conductive (electrically) materials at micro/nano scales. In the present chapter, different features such as machining systems, mechanism of machining, configurations, control and response variables with process capabilities related to the  $\mu$ -ECDM process are discussed and highlighted. At end of the chapter, the characteristics of process are illustrated in a specific section as  $\mu$ -ECDM at a glance becomes beneficial for readers to recognize the various aspects of process and a quick review of process.

**Acknowledgements** The authors gratefully acknowledge the Elsevier and Springer Nature for their kind permission regarding reprint/reuse of figures from the published papers and also for the Copyright Clearance Centre for their support during getting the reprint/reuse permission from different resources and locations.

## References

1. Ghosh A, Malik AK (1999) Manufacturing science. East-West Press, New Delhi, India
2. Yadav RN (2017) Development and experimental investigation of duplex turning process. *Adv Manuf* 5(2):149–157
3. Jain VK (2004) Advanced machining processes. Allied Publisher Limited, New Delhi, India
4. McGeough JA, Hofy HE (1988) Evaluation of an apparatus for electrochemical arc wire-machining. *J Eng Ind* 110(2):119–123
5. Kurafuji H, Suda K (1968) Electrical discharge drilling of glass. *CIRP Ann* 16:415–419

6. Yadav RN (2018) Electro-chemical spark machining-based hybrid machining processes: research trends and opportunities. *Proc Inst Mech Eng Part B J Eng Manuf.* <https://doi.org/10.1177/0954405418755825>
7. Jain VK, Rao PS, Choudhury SK, Rajurkar KP (1991) Experimental investigations into traveling wire electrochemical spark machining (TW-ECSM) of composites. *J Eng Ind* 113(1):75–84
8. Gupta PK, Divedi A, Kumar P (2015) Developments on electrochemical discharge machining: a review of experimental investigations on tool electrode process parameters. *Proc Inst Mech Eng Part B J Eng Manuf* 229(6):910–920
9. Wuthrich R, Fascio V (2005) Machining of non-conducting materials using electrochemical discharge phenomenon—an overview. *Int J Mach Tools Manuf* 45(9):1095–1108
10. Yerokhin A, Nie X, Leyland A, Matthews A, Dowey SJ (1999) Plasma electrolysis for surface engineering. *Surf Coat Technol* 122(2–3):73–93
11. Natsu W, Ojima S, Kobayashi T, Kunieda M (2004) Temperature distribution measurement in EDM arc plasma using spectroscopy. *JSME Int J, Ser C* 47(1):384–390
12. Kojima A, Natsu W, Kunieda M (2008) Spectroscopic measurement of arc plasma diameter in EDM. *CIRP Ann* 57(1):203–207
13. Fascio V, Wuthrich R, Viquerat D, Langen H (1999) 3D micro structuring of glass using electrochemical discharge machining (ECDM). In: *Proceedings of 1999 international symposium on micromechatronics and human science (P MHS'99)*, Nagoya, Japan, November 23–26, pp 179–183
14. Yang CT, Ho SS, Yan BM (2001) Micro hole machining of borosilicate glass through electrochemical discharge machining (ECDM). *Key Eng Mater* 196:149–166
15. Gautam N, Jain VK (1998) Experimental investigations into ECSD process using various tool kinematics. *Int J Mach Tools Manuf* 38(1–2):15–27
16. Jui SK, Kamaraj AK, Sundaram MM (2013) High aspect ratio micromachining of glass by electrochemical discharge machining (ECDM). *J Manuf Process* 15(4):460–466
17. Cao XD, Kim BH, Chua CN (2009) Micro-structuring of glass with features less than 100 μm by electrochemical discharge machining. *Precis Eng* 33(3):459–465
18. Jain VK, Adhikary S (2008) On the mechanism of material removal in electrochemical spark machining of quartz under different polarity conditions. *J Mater Process Technol* 200(1–3):460–470
19. Bhuyan BK, Yadava V (2014) Experimental study of traveling wire electrochemical spark machining of borosilicate glass. *Mater Manuf Process* 29(3):298–304
20. Kuo KY, Wu KL, Yang CK, Yan BH (2013) Wire electrochemical discharge machining (WECDM) of quartz glass with titrated electrolyte flow. *Int J Mach Tools Manuf* 72:50–57
21. Zhang Z, Huang L, Jiang Y, Liu G, Nie X, Lu H, Zhuang H (2016) A study to explore the properties of electrochemical discharge effect based on pulse power supply. *Int J Adv Manuf Technol* 85(9–12):2107–2114
22. Cao XD, Kim BH, Chu CN (2013) Hybrid micromachining of glass using ECDM and micro grinding. *Int J Precision Eng Manuf* 14(1):5–10
23. Zheng ZP, Wu KL, Hsu YS et al (2007) Feasibility of 3D surface machining on Pyrex glass by electrochemical discharge machining (ECDM). In: *Proceedings of AEMS07*, Nagoya, Japan, 28–30 November 2007, pp 98–103

# Chapter 13

## Multi-response Optimization of Micro-EDM Processes: A State-of-the-Art Review



Soumava Boral, Sarabjeet Singh Sidhu, Prasenjit Chatterjee, Shankar Chakraborty and Agam Gugaliya

**Abstract** The demand of micro-machining with a diameter ranging from microns to some hundred is rising gradually in the field of aerospace, biomaterials, electronics, and automobiles, due to its noteworthy applications and benefits in miniaturized merchandises and gadgets.  $\mu$ -EDM is the well-known non-traditional method used for making micro-metallic holes with assorted benefits like its distinguishing non-contact feature and thermoelectric energy between the workpiece to be machined and the electrode to be used.  $\mu$ -EDM is a modification of the traditional EDM, rendering an imperative function in the generation of micro-features on hard-to-machine materials. In recent years, both processes, i.e., EDM and  $\mu$ -EDM, are used extensively for production of dies, mold making, cavities, and complex 3D structures. The micro-components are typically finished by hard-to-machine materials and hold multifaceted shaped micro-structures that required accuracy in the level of sub-micron machining. This chapter provides an overview and the theoretical study of the latest 10-year researches from 2009 to 2018 that used decision-making and nature-inspired techniques in optimizing machining parameters of  $\mu$ -EDM and  $\mu$ -WEDM processes.

---

S. Boral · A. Gugaliya

Subir Chowdhury School of Quality and Reliability, IIT Kharagpur, Kharagpur 721302, India  
e-mail: [soumava.boral@iitkgp.ac.in](mailto:soumava.boral@iitkgp.ac.in)

A. Gugaliya

e-mail: [agam@iitkgp.ac.in](mailto:agam@iitkgp.ac.in)

S. S. Sidhu

Department of Mechanical Engineering, Beant College of Engineering and Technology, Gurdaspur, Punjab, India  
e-mail: [sarabjeetsidhu@yahoo.com](mailto:sarabjeetsidhu@yahoo.com)

P. Chatterjee (✉)

Department of Mechanical Engineering, MCKV Institute of Engineering Howrah, Howrah 711204, India  
e-mail: [prasenjit2007@gmail.com](mailto:prasenjit2007@gmail.com)

S. Chakraborty

Department of Production Engineering, Jadavpur University Kolkata, Kolkata 700032, India  
e-mail: [s\\_chakraborty00@yahoo.co.in](mailto:s_chakraborty00@yahoo.co.in)

© Springer Nature Singapore Pte Ltd. 2019

G. Kibria et al. (eds.), *Micro-electrical Discharge Machining Processes*, Materials Forming, Machining and Tribology, [https://doi.org/10.1007/978-981-13-3074-2\\_13](https://doi.org/10.1007/978-981-13-3074-2_13)

**Keywords**  $\mu$ -EDM · Multi-response optimization modeling techniques · MCDM

### 13.1 Introduction

In modern manufacturing era, the demand of micro-components has been increasing very rapidly in a variety of domains including electronics, biomedical, optical, energy, and aerospace industries. Materials having unique metallurgical properties, i.e., such as composites of tungsten carbide, nickel alloys, stainless steels, titanium alloys along with many other types of superalloys, are generally machined using  $\mu$ -EDM to fulfill the demands of extreme applications which require high precision tolerances and good surface integrity.  $\mu$ -EDM is a significant process for the production of such features when compared to conventional EDM machining. So far, components with several micrometers length can be machined using  $\mu$ -EDM. However, with the budding requirements of miniature components and machining at micro-levels are ever more entailed in diverse industrial applications, whereas such hard- and tough-to-machine materials are less sensitive to heat, more fatigue and corrosion resistant, and are even more intricate to machine [1–3]. Although due to their very useful mechanical properties, machining of such materials raises an imperative concern in the meadow of manufacturing. EDM is a well-known and cost-efficient non-traditional machining technique for extremely brittle materials [4, 5]. EDM removes materials by the result of fast recurring spark discharges from an electrical pulse generator with the dielectric flowing between the electrode and workpiece material. During the process, no mechanical cutting forces subsist between the workpiece and electrode.  $\mu$ -EDM is the application of electric discharge machine in micro-field.  $\mu$ -EDM has comparable attributes as of EDM except for that discharge energy, axis movement resolutions, and tool size used in micron level, and whenever using EDM process in  $\mu$ -field, the low range of energy is fetching imperative [6, 7]. As the forces between the electrode tool and the workpiece used are insignificant, the inaccuracy caused by the deformation of tool is nearly nil [8]. Therefore,  $\mu$ -EDM is an extensively used system in the present industry for elevated precision machining in almost all conductive materials.

The current  $\mu$ -EDM technology used for machining micro-holes can be grouped into the following types:

- $\mu$ -wire electrical discharge machining (WEDM), where cutting is done through the conductive material using a wire diameter of around 0.02 mm.
- Die-sinker  $\mu$ -EDM, where mirror image is produced on the workpiece using an electrode with micro-features.
- $\mu$ -drilling EDM, where micro-electrodes having diameter range of 5–10  $\mu$ m are employed to drill micro-holes in the workpiece.
- $\mu$ -milling EDM, where micro-electrodes having diameter 5–10  $\mu$ m are utilized to generate 3D cavity by implementing a movement approach analogous to that in traditional milling.



With the introduction of newer materials and ever-increasing requirement of better quality products with superior features along with precision, surface finish and elevated dimensional accuracy have uncovered the use of different  $\mu$ -EDM processes. Each of these  $\mu$ -EDM processes has numerous parameters (controllable), which principally control the outputs. Selection of the suitable input parameters and their values with levels to get the desired output or responses can be achieved if the decision maker (DM) has enough technical familiarity about these parameters and their potential impact upon the performance of the underlying process. As a consequence, assessment of the best possible combination of such parameters for any  $\mu$ -EDM process is an imperative job for achieving shorter machining time. However, the task of selecting the optimal parameter combination turns into complicated attributable to the existence of some complex thermal and chemical observations in the machining region.

For a specified work material and shape feature arrangement, the aspired setting of the parameters may not be always straightforwardly obtained from the user manual or manufacturers' handbook. Also, very frequently, these process parameters are very restricted in nature and remote from the most favorable values, which ultimately hold back the complete exploitation of the process competencies. Thus, it is unquestionably a confront to make certain that the chosen process parameters upshot in most favorable or in the vicinity of best possible machining performance eventually lead to the application of a range of optimization models in this territory. Thus, the objective of this chapter is to summarize the significant contributions of different techniques used for parametric optimization of  $\mu$ -EDM processes with the intention of comprehending the performance of each process parameter and strength, weakness, and future prospects of the optimization techniques.

## 13.2 Overview of $\mu$ -EDM Process

### 13.2.1 Principle of $\mu$ -EDM

$\mu$ -EDM process is relatively analogous with the working principle of the conventional EDM which is basically used to eliminate metal by means of applying a short duration electrical discharge and high current density between the tool and workpiece. In this process, with the increase in potential difference across the electrodes, the non-conductive dielectric fluid splints down and turns into conductive. Throughout this period, thermal energy is released due to the spark generated and material removal occurs by melting and evaporation. Using  $\mu$ -EDM, it is promising to machine precise micro-features like micro-holes, micro-slot by controlling the amount of energy released [9, 10]. As the tool and the workpiece never come into direct contact which results in a smaller amount of generated force and adjustment in the electrical parameters like current, voltage, duty cycle, frequency, it is feasible to manage the spark energy in  $\mu$ -EDM application. The important feature for which

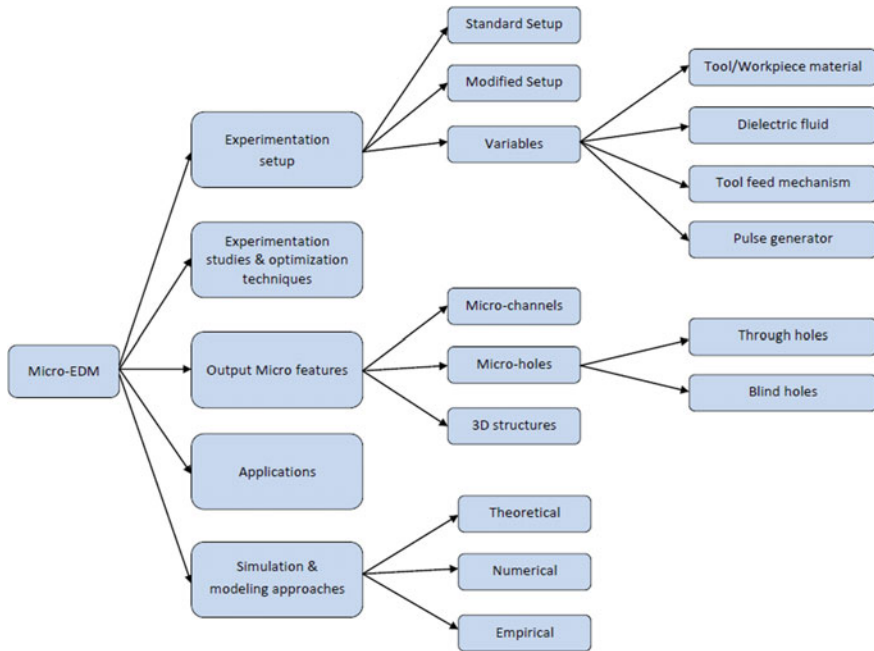
$\mu$ -EDM is considered as an absolute essential in the micro-machining domain is its superior machining capability on several types of conductive and semi-conductive materials with high surface finish irrespective of their hardness. In  $\mu$ -EDM, usually, a cylindrical electrode or workpiece rotates using a spindle system. A constant flow of debris along with dielectric medium assists the immovability of the machining process. An array of metal alloys including copper [11], titanium alloy Ti-6Al-4V [12–15], high carbon tool steel [16–18], grade 304 stainless steel [19, 20], high nickel alloys [21–23], tungsten carbide (TiC) [24, 25], ceramics [26, 27] can be easily machined using  $\mu$ -EDM setup.

### ***13.2.2 A Short Review of Experimental Investigation on $\mu$ -EDM Process***

Majority of the precedent investigators have mainly spotlighted on the applications, working technology, workable materials, material removal rate (MRR), machining parameters and their impact of machining performance and component quality, tool electrode wear, and so on. Benefits and limitations of the process have also been reported in many instances [28]. Figure 13.1 presents the various thrust areas of  $\mu$ -EDM research.

Masuzawa [29] introduced wire electrical discharge grinding (WEDG) in  $\mu$ -EDM to fabricate miniature electrodes and micro-components. Wang et al. [30] combined  $\mu$ -EDM and  $\mu$ -ultrasonic vibration lapping (MUVL) and proposed a technique to produce high precision micro-holes with high aspect ratios. The scanning electron microscope (SEM) photographs revealed that the surface roughness (SR) visibly improved, and the micro-hole cross-section became cylindrical when the MUVL was employed along with  $\mu$ -EDM. Carrying forward, vibration-assisted worktable was designed by Chern et al. [31] in order to punch micro-holes on grade 304 stainless steel and brass strip of diameter 200  $\mu$ m. Higher feed and improved surface finish can be attained using ultrasonic vibrations. With the purpose to eradicate the debris from the tool electrode–workpiece interface, Endo et al. [32] pioneered a vibration-assisted machining process to  $\mu$ -EDM using piezoelectric and found improved machining stability along with the reduction in machining time.

Furthermore, Prihandana et al. [33] investigated a novel approach using ultrasonic vibration-assisted  $\mu$ -EDM with micro-molybdenum disulfide ( $\text{MoS}_2$ ) powder suspended in the dielectric fluid for providing a flat surface, set freed from black carbon spots during machining, and found noteworthy improvement in MRR and surface quality. Another researcher, Liew et al. [34], also applied ultrasonic vibrations to the dielectric medium using the probe-type vibrator to assist  $\mu$ -EDM of deep micro-holes in ceramic materials to examine the geometry of the hole, surface integrity, and steadiness of machining. Results showed that ultrasonic vibrations were more helpful along with nanocarbon fibers in eliminating debris and avoiding the deposition of tool material on machined surface. Yeo et al. [35] studied the crater characteristic



**Fig. 13.1** Classification of research areas in  $\mu$ -EDM

with low discharge energies using silicon carbide particles suspended in dielectric by  $\mu$ -EDM process. They found crater development with small diameter and depth having regular circular form than those constructed in the dielectric with no additive particles.

An area of sub-micron and nanoscale machining was opened when Egashira et al. [36] reported micro-hole of diameter  $0.5 \mu\text{m}$  with silicon electrode using micro-electrical discharge machining with ultrasonic vibrations. Similarly, Han et al. [37] also attempted sub-micrometer-order size machining when they achieved minimum diameter about  $2.8 \mu\text{m}$  using  $\mu$ -EDM and found that reversed polarity possesses smoother surface as contrasted to straight polarity. Abbas et al. [38] explored the influence of frequency by increased discharge current in  $\mu$ -EDM using electrostatic induction feeding as the pulse generator and found better MRR at higher discharge energy. Zou et al. [39] examined that there was high tool wear during machining in the liquid dielectric medium, while  $\mu$ -EDM in gas dielectric exposes nearly no tool wear. Abnormal discharge was there due to low dynamic viscosity, small discharge energy, and low debris concentration of  $\mu$ -EDM in gas generates narrow discharge gap. To overcome this issue and increase the discharge gap, nitrogen plasma jet (NPJ) was used as dielectric during  $\mu$ -EDM in gas. They observed significant improvement in machining performance with an increase in MRR and surface quality using NPJ.

To check the effects of  $\mu$ -EDM on holes' properties of ink jet nozzles for the printer, thin foils of diverse grades of stainless steel were used by the researchers

Allen and Lecheheb [40]. From the results, they concluded that low input energy and grades of stainless steel having low carbon which does not have porous oxide layers were obligatory for better quality nozzle fabrication. Son et al. [41] studied the impact of pulse condition on  $\mu$ -EDM properties. The investigational outcomes showed that the voltage and pulse current impact resolutely on the machining and short EDM pulse is competent to make parts with higher accuracy and superior MRR value. Wang et al. [42] performed experimentation for achieving precise fabrication of intact tool profile in micro-gear by using  $\mu$ -WEDM. The behavior of aluminum oxide- and zirconium dioxide-based electrically conductive ceramic composites was investigated by Ferraris et al. [43] by varying the speed from a spacious range. Another work was performed by Huang and Yan [44] for investigating the changes of micro-structures in the workpiece material by using the hybrid tool of sintered polycrystalline diamond (PCD). This hybrid process bestows with a technique to produce three-dimensional micro-features along with advanced surface superiority and proficient elimination of crystallization layers verified by the surface morphology as a result of using grinding after  $\mu$ -EDM. Liu et al. [45] presented a novel process using  $\mu$ -EDM mingled with high-frequency dither grinding (HFDG) to enhance SR of the micro-holes in high nickel alloy. From SEM, they observed reduced SR with eliminated micro-cracks. Yeo et al. [46] employed various tool materials and input energies to observe the consequences of machining conditions on tool wear, SR, and burr width during machining of zirconium-based bulk metallic glass. It was perceived that lower input energy reduced the SR by approximately 51% and burr width by 63%. Tube electrodes were further encouraging over the rod electrodes in terms of electrode wear ratio. Jahan et al. [47] investigated the surface finish using  $\mu$ -EDM of WC with tungsten (W), copper tungsten (CuW), and silver tungsten (AgW) electrodes. It was established that AgW electrode produces downy and imperfection-free nanosurface with the lowest SR values among the considered electrodes. CuW electrodes achieved the maximum MRR. Silver tungsten appeared best suited for producing smooth, shiny, and high surface finish with a negligible amount of defect on the surface during the  $\mu$ -EDM of tungsten carbide. Similarly, to advance the surface excellence of micro-holes machined on beryllium copper (BeCu) alloys used for micro-liquid-floated gyroscope, Dong et al. [48] investigated different dielectrics and electrodes of multi-diameter. The results illustrated that there was an improvement in the surface topology due to the synchronized application of the multi-diameter electrode and deionized water as well as kerosene as the dielectric medium.

Bamberg and Heamawatanachai [49] presented a novel machining method for  $\mu$ -EDM that triggers the EDM tool on an orbital trajectory. Hole diameter was proportionally increased to the orbital radius with the orbital motion of the tool, promoting increased flushing due to the construction of a larger gap amid the tool electrode and the workpiece. They also investigated that the increased flushing greatly reduced tool wear, significantly improved the machining rate, and yields high surface finish for the holes produced with large depth to diameter ratio (greater than three times). Again in this area, a technique of complex rotary structures machining using  $\mu$ -WEDM was presented by Yukui et al. [50] with the installation of a self-designed high-speed rotating spindle to  $\mu$ -WEDM with two axes to facilitate the processing of multifaceted

rotary structures. Its viability was investigated by producing micro-ball-ended probe of diameters 97.6 and 0.7  $\mu\text{m}$  in  $R_a$ .

Similarly, a deposited layer on the tool electrode was investigated by Murray et al. [51] and found that it offered a protective effect against wear, potentially increasing the life span of the electrode. From the results of SEM and EDS, a rich layer of the workpiece element was observed on the electrode toward its non-operational region. Piezoelectric self-adaptive  $\mu$ -electrical discharge machining was proposed by Fu et al. [52] which can apprehend self-regulation based on various discharge conditions. Improved discharge stability was then compared to traditional  $\mu$ -EDM, along with higher machining performance and effective machining efficiency for micro-structural parts and micro-holes. Trych [53] presented carbon fiber's electrodes in  $\mu$ -EDM and investigated the tool wear behavior under EDM condition.

Additionally, Plaza et al. [54] initiated a novel method of using helically shaped electrode with the helix angle of  $45^\circ$  to overcome insufficient removal of the debris when making a deep hole on Ti-6Al-4V and found 37% decrease in machining time for hole diameter 800  $\mu\text{m}$ . They used graphite and CuW electrodes for machining and concluded that CuW electrodes are best suited for making holes of high aspect ratio. Another work was reported by Maradia et al. [55] by machining graphite electrode of micro-scale with small projection area using the implementation of die-sinking EDM. Results showed low electrode wear when increasing pulse duration at low current. Koyano et al. [56] looked into the effects of electrodes with elevated electric resistance on stainless steel to decrease the MRR during  $\mu$ -EDM because it determines the minimum size of the machinable micro-hole. From the experimental results, they finished off with the conclusion that with augmented value of electrode resistance, the peak value of discharge current decreased and pulse duration increased. With the increase in the resistivity of silicon electrode, the diameter micro-hole produced using  $\mu$ -EDM decreased. A brief study of using tungsten electrode on the aluminum was presented by Mlynarczyk et al. [57] for micro-electro-discharge alloying (EDA). Surface layer subjected to the deposition process contained chemical components of the electrode with recast layer thickness about 20  $\mu\text{m}$ . Resistance-capacitance (RC)-type generator with an alternating current flow in  $\mu$ -EDM through electrical circuit simulation was used by Qian et al. [58] to investigate the output results. Experimental results revealed that using negative electrode polarity with low energy had efficiently supplemented to the MRR. Pellicer et al. [59] observed the influence of inputs and electrode geometry on the accuracy of micro-hole in a tool steel material. Different-shaped copper electrodes were used to investigate H13 hot work tool steel by varying the current, gap voltage ( $V_g$ ), pulse on time ( $T_{on}$ ), and pulse off time ( $T_{off}$ ) during machining.

### 13.3 Applications of Multi-Criteria Decision-Making (MCDM) Methods for Multi-Response Optimization of $\mu$ -EDM Processes

From the general literature survey, it has been well explicit that in most  $\mu$ -EDM case studies, experimentations are conducted using experimental design which successfully identifies the optimal process parameters for a single response characteristic. This single set of process parameter is perhaps most favorable for one quality characteristic, but it may also offer sub-favorable results for other quality traits. The suggested optimal setting has its own characteristic, application, advantages, and limitations. Hence, it is necessary to go for global/multiple optimizations of responses such that a single set of parameters that are most favorable for all the quality traits might be apprehended. The decision for optimization often exhibits the presence of several contradictory criteria for assessing the alternatives. Thus, there is a requirement for making compromise or substitutions concerning the alternative outcomes. MCDM is rapidly evolving for the analysis of such type of multifarious problems due to its inherent competence of evaluating alternatives on the basis of several criteria. MCDM problems can be generally classified as “selection problem” or “mathematical programming problems.” The focus of multi-criteria selection problems is on choosing the most favored alternative(s) from a predetermined set of alternatives. On the other hand, multi-criteria mathematical programming methods intend to select the optimal solution from an unlimited number of realistic alternatives by developing an objective function subjected to some constraints and assumptions.

In this section, the authors address the applications of MCDM methods in the field of the  $\mu$ -EDM process. Natarajan and Arunachalam [60] explored the performance of different responses in a  $\mu$ -EDMed surface using Taguchi’s and grey relational analysis (GRA). Ay et al. [61] applied GRA on  $\mu$ -EDM drilling operation of Inconel superalloy. Tiwary et al. [62] applied technique for the order of preference by similarity to ideal solution (TOPSIS) method to identify the optimal parameters for  $\mu$ -EDM machining of Ti-6Al-4 V alloy. Manivannan and Kumar [63] also applied TOPSIS method to identify the overall performance of the micro-machining of AISI 304 stainless steel. Bhosle and Sharma [64] applied GRA method to find an exclusive parameter setting in machining of Inconel 600 alloy and considered different powerful process parameters like voltage, capacitance ( $C$ ), EDM feed rate (FR),  $T_{on}$ , and  $T_{off}$  in a TiC tool.

Manivannan and Kumar [65] also presented a TOPSIS-based approach for cryogenically cooled  $\mu$ -EDM drilling process on AISI 304 stainless steel and considered many factors including current ( $I_p$ ),  $T_{on}$ ,  $T_{off}$ , and  $V_g$  as the input parameters to optimize geometrical characterizations including taper angle (TA), OC, circularity at the entry and exit ( $C_{ent}$  and  $C_{exit}$ ), while MRR, tool wear rate (TWR), and average roughness ( $R_a$ ) were among the considered performance quantifiers. Sapkal and Jagtap [66] used desirability function approach for locating most desired operating conditions in micro-drilling of titanium alloy with the rotary electrode.

### 13.4 Methods for Optimization of Performance Characteristic of $\mu$ -EDM Processes

Recent trends in the optimization of performance characteristics of machining process involve the applications of various nature-inspired or evolutionary or meta-heuristic techniques. Following this trend, Pradhan and Bhattacharyya [67] proposed the applicability of response surface methodology (RSM) coupled with backpropagation-based artificial neural network (ANN) for the optimization of machining characteristics of  $\mu$ -EDM. Somashekhar et al. [68] presented a work where they tried to find the best combination of the parameters of  $\mu$ -WEDM process by taking into consideration the concurrent effects of  $V_g$ ,  $C$ , and FR. Authors planned the experiments by design of experiment (DoE). Subsequently, ANOVA was applied to find out the effect of each input parameter on the output variable. Machining operation was performed on aluminum workpiece. For optimization purpose, genetic algorithm (GA) was proposed to find the best possible inputs. Zhang et al. [69] elucidated the idea to combine support vector machine and non-dominated sorting GA for establishing a process model of  $\mu$ -EDM and optimize the process parameter values for desired outputs. Somashekhar et al. [70] conducted an experiment on  $\mu$ -WEDM setup to estimate the most favorable value of input parameters for preferred output characteristics. They considered  $V_g$ ,  $C$ , and FR as the input variable, whereas output responses were SR and OC. They optimized the value of input variables by using GA. Somashekhar et al. [71] developed an approach by combining the principle of GRA with Taguchi method for optimizing  $\mu$ -WEDM process parameters. In the said experiment, MRR, OC, and SR were considered as the output variables by varying the values of input parameters, namely  $V_g$ ,  $C$ , and FR. ANOVA was utilized to determine the inference of different parameters on grey relational grade (GRG). The obtained GRG values were then utilized to parametric optimization. The proposed method was validated by comparing the results with real-time experiment. Somashekhar et al. [72] studied the effects of  $V_g$ , FR, and  $C$  on the output variables like MRR, OC, and SR. They subsequently showed the applicability of simulated annealing (SA) approach for finding the best combinations of output variables. It is obvious that for the said process, MRR would be maximized, whereas OC and SR were minimized for the desired input variables. Nirala et al. [73] recommended a Taguchi-based approach for optimizing the values of input process parameters in a  $\mu$ -EDM process. In this method, workpiece material was copper, whereas TiC was utilized as tool electrode. Orthogonal array (OA) and signal-to-noise (S/N) ratio concepts were in use for the optimization. Sivaprakasam et al. [74] tried to optimize  $\mu$ -WEDM machining of aluminum matrix composite by RSM. Zinc-coated copper wear was considered as the tool material for the said experimentation. In the said experimentation, various inputs and outputs such as  $V_g$ ,  $C$ , FR, MRR, Kerf width (KW), and SR were considered. The second-order mathematical modeling and ANOVA were performed for the optimization. Jithin et al. [75] optimized the input variables during the machining of Ti-6Al-4V by  $\mu$ -ED milling using the principle of GA. Considered input variables were  $V_g$ ,  $C$ , electrode rotational speed, and FR,



whereas output responses were MRR and TWR. The input parameters were designed through RSM. The developed GA was aimed to minimize the TWR and maximize the MRR. Suganthi et al. [76] presented a hybrid experimentation, where  $\mu$ -WEDM and  $\mu$ -EDM were combined to minimize inaccuracies. The adaptive neuro-fuzzy inference system (ANFIS) and backpropagation neural network were developed for predicting the multi-quality responses generated in  $\mu$ -EDM process. The considered input variables were FR,  $C$ , and  $V_g$ , whereas MRR, SR, and TWR were the outputs. The predicted responses from the developed model were found suitable with practical experimentation. Maity and Mishra [77] carried out experimentation on Inconel 718 superalloy using  $\mu$ -EDM process. ANN model was applied to predict the MRR, OC, and recast layer thickness values. Furthermore, optimization of input parameters was carried out by different heuristics techniques, such as elitist teaching–learning-based optimization (ETLBO), multi-objective differential evolution (MODE), and artificial bee colony (ABC) algorithms. A comparative study was also performed to improve the accuracy of the proposed model based on Pareto-front solutions. Meena et al. [78] employed Taguchi-based GRA model for optimizing input parameters of  $\mu$ -EDM process. In the experimentation, pure titanium was machined. The input variables were current, frequency, and pulse width, whereas output parameters were MRR, electrode WR, and OC of the drilled hole. Through the experimentation, it was found out that current was the most influential parameter for machining pure titanium. Upadhyay et al. [79] employed ANN for predicting the MRR of a  $\mu$ -EDM process. Different input variables, such as voltage,  $C$ , and additives, were considered during the design of the experiment. It was also highlighted that minimal error was present between the real-time experimentation value of MRR and predicted value of ANN. Abidi et al. [80] highlighted the applicability of multi-objective GA-II (MOGA-II) for optimizing  $\mu$ -EDM machining of nickel–titanium-based shape memory alloy. The input variables considered were  $C$ , discharge voltage, and electrode material, whereas output variables were MRR and SR. In their optimization problem, MRR was tried to be maximized while SR was minimized. Other output responses were also highlighted in the work, such as OC, TA, and circularity of the machined hole. Effects of each input variable and their combinations were highlighted with respect to output responses. Tables 13.1 and 13.2 present the summary of different techniques as applied in optimizing machining process parameters, respectively, for  $\mu$ -EDM and  $\mu$ -WEDM processes.

### 13.5 Summary and Future Scopes

$\mu$ -EDM is a well-known machining system having wide applications in various areas such as biomedical, aerospace, manufacturing industry for drilling micro-holes, micro-features, etc. In this chapter, authors have reviewed research papers from 2009 to 2018 on process optimization of  $\mu$ -EDM using MCDM and nature-inspired algorithms and recognized that great research possibilities exist in this area of micro-machining using  $\mu$ -EDM. From the extensive review as presented above, it



**Table 13.1** Tabular review of models used in optimization of process parameters for  $\mu$ -EDM

Reference	Methods applied	Input parameters	Output parameters	Workpiece material (WPM) and tool material (TM) used
Pradhan and Bhattacharyya [67]	<ul style="list-style-type: none"> <li>- RSM</li> <li>- ANN</li> </ul>	<ul style="list-style-type: none"> <li>- <math>I_p</math></li> <li>- <math>T_{on}</math></li> <li>- Flushing pressure</li> </ul>	<ul style="list-style-type: none"> <li>- MRR</li> <li>- TWR</li> <li>- OC</li> </ul>	<ul style="list-style-type: none"> <li>- WPM: Ti-6Al-4V</li> <li>- TM: Tungsten</li> </ul>
Zhang et al. [69]	<ul style="list-style-type: none"> <li>- SVM</li> <li>- Non-sorted GA</li> </ul>	<ul style="list-style-type: none"> <li>- Discharge peak current</li> <li>- <math>T_{on}</math></li> <li>- <math>T_{off}</math></li> <li>- <math>C</math> (<math>\mu</math>F)</li> <li>- Electrode rotating speed</li> <li>- Servo reference speed</li> </ul>	<ul style="list-style-type: none"> <li>- Processing time, electrode wear</li> </ul>	<ul style="list-style-type: none"> <li>- WPM: Aluminum</li> <li>- TM: Brass</li> </ul>
Somashekhar et al. [70]	<ul style="list-style-type: none"> <li>- ANN</li> <li>- GA</li> </ul>	<ul style="list-style-type: none"> <li>- GV</li> <li>- <math>C</math></li> <li>- FR (<math>\mu</math>m/s)</li> <li>- Speed (S)</li> </ul>	<ul style="list-style-type: none"> <li>- MRR</li> </ul>	<ul style="list-style-type: none"> <li>- WPM: aluminum</li> <li>- TM: Tungsten carbide</li> </ul>
Nirala et al. [73]	<ul style="list-style-type: none"> <li>- Taguchi-ANOVA</li> </ul>	<ul style="list-style-type: none"> <li>- GV</li> <li>- <math>C</math></li> <li>- FR</li> <li>- S</li> </ul>	<ul style="list-style-type: none"> <li>- MRR</li> <li>- OC</li> <li>- TWR</li> <li>- Error in depth of hole</li> </ul>	<ul style="list-style-type: none"> <li>- WPM: Copper</li> <li>- TM: Tungsten carbide</li> </ul>
Jithin et al. [75]	<ul style="list-style-type: none"> <li>- RSM</li> <li>- GA</li> </ul>	<ul style="list-style-type: none"> <li>- GV</li> <li>- <math>C</math></li> <li>- Electrode rotational speed</li> <li>- FR</li> </ul>	<ul style="list-style-type: none"> <li>- MRR</li> <li>- TWR</li> </ul>	<ul style="list-style-type: none"> <li>- WPM: Ti-6Al-4V</li> <li>- TM: Tungsten carbide</li> </ul>
Maity and Mishra [77]	<ul style="list-style-type: none"> <li>- ANN</li> <li>- ETLBO</li> <li>- MODE</li> <li>- ABC</li> </ul>	<ul style="list-style-type: none"> <li>- V</li> <li>- <math>I_p</math></li> <li>- <math>T_{on}</math></li> <li>- <math>T_{off}</math></li> </ul>	<ul style="list-style-type: none"> <li>- MRR</li> <li>- OC</li> <li>- Recast layer thickness</li> </ul>	<ul style="list-style-type: none"> <li>- WPM—Inconel 718 superalloy</li> </ul>
Meena et al. [78]	<ul style="list-style-type: none"> <li>- Taguchi-based GRA</li> </ul>	<ul style="list-style-type: none"> <li>- Current</li> <li>- Frequency</li> <li>- <math>T_{on}</math></li> </ul>	<ul style="list-style-type: none"> <li>- MRR, electrode wear</li> <li>- OC</li> </ul>	<ul style="list-style-type: none"> <li>- WPM: Pure titanium</li> <li>- TM: Tungsten carbide</li> </ul>

(continued)

**Table 13.1** (continued)

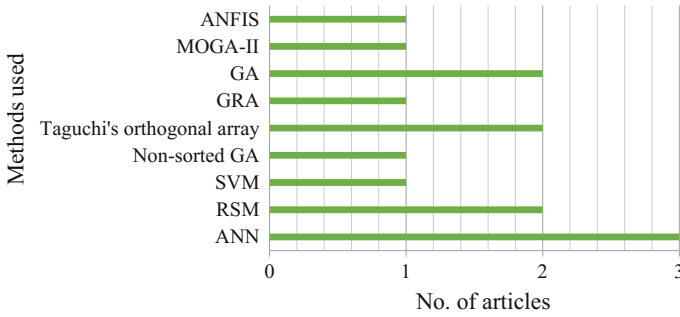
Reference	Methods applied	Input parameters	Output parameters	Workpiece material (WPM) and tool material (TM) used
Upadhyay et al. [79]	– ANN	– V – C – Additive (either Al powder or SiC powder)	– MRR	– WPM: Brass – TM: Brass
Abidi et al. [80]	– MOGA-II	– V – C	– SR – TWR – MRR – OC – Taper angle, circularity	– WPM: Nickel–titanium-based shape memory alloy – TM: Brass and tungsten

has been examined that TOPSIS, GRA, ANN, and GA models are widely used in both  $\mu$ -EDM and  $\mu$ -WEDM processes as depicted in Figs. 13.2 and 13.3 and presented in Tables 13.1 and 13.2, respectively. TOPSIS method is founded on the perception that the most preferred alternative is supposed to have minimum distance from the positive ideal solution (PIS) and maximum distance from the negative ideal solution (NIS). PIS is an imaginary solution for which all the criteria values correspond to the best values, while the NIS is also an imaginary solution for which all the criteria values correspond to the worst values. On the other hand, GRA which is a part of grey system theory is appropriate to deal problems with uncertain information. In this method, experimental data is first made dimensionless using normalization technique to determine grey relational coefficient which represents the relationship between the desired and real data. Then, overall grey relational grade is determined which indicates the overall performance quality of the various responses. Among the vastly used bio-inspired algorithms, ANN, also known as connectionist network, basically mimics the concept of human brain and its mechanism. It is based on a group of coupled nodes called artificial neurons that slackly model the neurons in a biological brain. Every connection, such as synapses in a biological brain, is able to transfer a signal from one neuron to another. It is used to predict the output value, which in turn is dependent on a set of input variables. For efficient prediction of the output variables, at first the ANN is trained with a set of input cases. As the number of training cases increases, the efficiency of the ANN is also increased. But over-training or under-training of the ANN is a major drawback which needs to be properly addressed, whereas in many cases, real-world optimization problems can be constraint as well as unconstrained in nature. To solve such problems, GA is one of the simplest and effective random-based evolutionary algorithms. It is based on natural selection process and modifies an individual solution repeatedly, until the solution is achieved. The term random is used here to describe the random changes

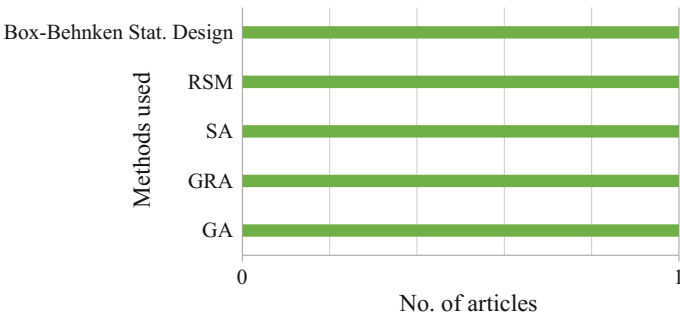
**Table 13.2** Tabular review of optimization of  $\mu$ -WEDM process parameters using different methods

References	Methods applied	Input parameters	Output parameters	WPM and TM
Somashekhar et al. [68]	– GA	– GV – C – FR	– SR – OC	– WPM: Aluminum – TM: Zinc-coated brass wire
Somashekhar et al. [71]	– GRA – ANOVA	– GV – C – FR	– MRR – OC – SR	– WPM: Aluminum – TM: Zinc-coated brass wire
Somashekhar et al. [72]	Simulated annealing (SA)	– GV – C – FR	– MRR – OC – SR	– WPM: Aluminum – TM: Zinc-coated brass wire
Sivaprakasam et al. [74]	RSM	– V – C – FR	– MRR – KW – SR	– WPM: Aluminum metal matrix composite (A413–9% B <sub>4</sub> C) – TM: Zinc-coated copper wire
Suganthi et al. [76]	ANFIS	– FR – C – V <sub>g</sub>	– MRR – SR – TWR	– WPM: Tungsten – TM: Brass

applied to solutions of the current problem to generate another one. GA has become common in use wherever there is the requirement to achieve optimization of the problem. The basic requirement to start with formulating a problem in GA is a genetic representation and fitness function. The result of this review also puts forward future research aspects in various areas such as the development of hybrid  $\mu$ -EDM machining process; manufactured micro-components for further examination; development of modeling and simulation approaches and exploration of novel techniques for process optimization using evidential reasoning, rule-based reasoning, case-based reasoning, development of expert system, and other new MCDM methods.



**Fig. 13.2** Numbers of research articles in optimization of  $\mu$ -EDM process parameters using various techniques (2009–2018)



**Fig. 13.3** Numbers of research articles in optimization of  $\mu$ -WEDM process parameters using various techniques (2009–2018)

## References

1. Jahan M, Rahman M, Wong Y (2011) A review on the conventional and micro-electrodischarge machining of tungsten carbide. *Int J Mach Tools Manuf* 51(12):837–858
2. Ho K, Newman S, Rahimifard S, Allen R (2004) State of the art in wire electrical discharge machining (WEDM). *Int J Mach Tools Manuf* 44(12–13):1247–1259
3. Wong Y, Rahman M, Lim H, Han H, Ravi N (2003) Investigation of micro-EDM material removal characteristics using single RC-pulse discharges. *J Mater Process Technol* 140(1–3):303–307
4. Guitrau EB (1997) *The EDM handbook*. Hanser Gardner Publications Cincinnati
5. Ho K, Newman S (2003) State of the art electrical discharge machining (EDM). *Int J Mach Tools Manuf* 43(13):1287–1300
6. Gao C, Liu Z (2003) A study of ultrasonically aided micro-electrical-discharge machining by the application of workpiece vibration. *J Mater Process Technol* 139(1–3):226–228
7. Nakaoku H, Masuzawa T, Fujino M (2007) Micro-EDM of sintered diamond. *J Mater Process Technol* 187:274–278
8. Tsai YY, Masuzawa T (2004) An index to evaluate the wear resistance of the electrode in micro-EDM. *J Mater Process Technol* 149(1–3):304–309
9. Tan PC, Yeo SH, Tan YV (2008) Effects of nanopowder additives in micro-electrical discharge machining. *Int J Precision Eng Manuf* 9(3):22–26

10. Chen SL, Lin MH, Huang GX, Wang CC (2014) Research of the recast layer on implant surface modified by micro-current electrical discharge machining using deionized water mixed with titanium powder as dielectric solvent. *Appl Surf Sci* 311:47–53
11. Raju L, Sanghvi VS, Somashekhar SH, Singaperumal M (2014) Effect of process parameters on quality of micro holes machined on copper plate using developed  $\mu$ -EDM setup. *Appl Mech Mater* 592–594:229–233
12. Sivaprakasam P, Hariharan P, Gowri S (2014) Modeling and analysis of micro-WEDM process of titanium alloy (Ti-6Al-4V) using response surface approach. *Eng Sci Technol Int J* 17(4):227–235
13. Kibria G, Sarkar B, Pradhan B, Bhattacharyya B (2010) Comparative study of different dielectrics for micro-EDM performance during microhole machining of Ti-6Al-4 V alloy. *Int J Adv Manuf Technol* 48(5–8):557–570
14. Pradhan B, Masanta M, Sarkar B, Bhattacharyya B (2009) Investigation of electro-discharge micro-machining of titanium super alloy. *Int J Adv Manuf Technol* 41(11–12):1094–1106
15. Meena VK, Azad MS (2012) Grey relational analysis of micro-EDM machining of Ti-6Al-4V alloy. *Mater Manuf Processes* 27(9):973–977
16. Saleh T, Dahmardeh M, Nojeh A, Takahata K (2013) Dry micro-electro-discharge machining of carbon-nanotube forests using sulphur-hexafluoride. *Carbon* 52:288–295
17. Liew PJ, Yan J, Kuriyagawa T (2013) Carbon nanofiber assisted micro electro discharge machining of reaction-bonded silicon carbide. *J Mater Process Technol* 213(7):1076–1087
18. Natarajan N, Suresh P (2015) Experimental investigations on the microhole machining of 304 stainless steel by micro-EDM process using RC-type pulse generator. *Int J Adv Manuf Technol* 77(9–12):1741–1750
19. Pandey AK, Tiwari K, Dubey AK (2014) Optimization of the process parameters in micro-electric discharge machining using response surface methodology and genetic algorithm. *Int J Sci Res Publi* 4(9):1–5
20. Jeong YH, Han Yoo B, Lee HU, Min BK, Cho D-W, Lee SJ (2009) Deburring microfeatures using micro-EDM. *J Mater Process Technol* 209(14):5399–5406
21. Yeo S, Murali M, Cheah H (2004) Magnetic field assisted micro electro-discharge machining. *J Micromech Microeng* 14(11):1526–1529
22. Zhang L, Tong H, Li Y (2015) Precision machining of micro tool electrodes in micro EDM for drilling array micro holes. *Precision Eng* 39:100–106
23. Jahan M, Wong Y, Rahman M (2012) Evaluation of the effectiveness of low frequency work-piece vibration in deep-hole micro-EDM drilling of tungsten carbide. *J Manuf Processes* 14(3):343–359
24. Li MS, Chi GX, Wang ZL, Wang YK, Li D (2009) Micro electrical discharge machining of small hole in TC4 alloy. *Trans Nonferrous Met Soc China* 19:s434–s439
25. Saxena KK, Agarwal S, Khare SK (2016) Surface characterization, material removal mechanism and material migration study of micro EDM process on conductive SiC. *Procedia CIRP* 42:179–184
26. Fu Y, Miyamoto T, Natsu W, Zhao W, Yu Z (2016) Study on influence of electrode material on hole drilling in micro-EDM. *Procedia CIRP* 42:516–520
27. Peng Z, Wang Z, Dong Y, Chen H (2010) Development of a reversible machining method for fabrication of microstructures by using micro-EDM. *J Mater Process Technol* 210(1):129–136
28. Kunieda M, Lauwers B, Rajurkar K, Schumacher B (2005) Advancing EDM through fundamental insight into the process. *CIRP Ann* 54(2):64–87
29. Masuzawa T (2000) State of the art of micromachining. *CIRP Ann* 49(2):473–488
30. Wang AC, Yan BH, Li XT, Huang FY (2002) Use of micro ultrasonic vibration lapping to enhance the precision of microholes drilled by micro electro-discharge machining. *Int J Mach Tools Manuf* 42(8):915–923
31. Chern GL, Chuang Y (2006) Study on vibration-EDM and mass punching of micro-holes. *J Mater Process Technol* 180(1–3):151–160
32. Endo T, Tsujimoto T, Mitsui K (2008) Study of vibration-assisted micro-EDM-the effect of vibration on machining time and stability of discharge. *Precision Eng* 32(4):269–277

33. Prihandana GS, Mahardika M, Hamdi M, Wong Y, Mitsui K (2009) Effect of micro-powder suspension and ultrasonic vibration of dielectric fluid in micro-EDM processes-Taguchi approach. *Int J Mach Tools Manuf* 49(12–13):1035–1041
34. Liew PJ, Yan J, Kuriyagawa T (2014) Fabrication of deep micro-holes in reaction-bonded SiC by ultrasonic cavitation assisted micro-EDM. *Int J Mach Tools Manuf* 76:13–20
35. Yeo S, Tan P, Kurnia W (2007) Effects of powder additives suspended in dielectric on crater characteristics for micro electrical discharge machining. *J Micromech Microeng* 17(11):N91–N98
36. Egashira K, Morita Y, Hattori Y (2010) Electrical discharge machining of submicron holes using ultrasmall-diameter electrodes. *Precision Eng* 34(1):139–144
37. Han F, Yamada Y, Kawakami T, Kunieda M (2006) Experimental attempts of sub-micrometer order size machining using micro-EDM. *Precision Eng* 30(2):123–131
38. Abbas NM, Solomon DG, Bahari MF (2007) A review on current research trends in electrical discharge machining (EDM). *Int J Mach Tools Manuf* 47(7–8):1214–1228
39. Zou R, Yu Z, Yan C, Li J, Liu X, Xu W (2018) Micro electrical discharge machining in nitrogen plasma jet. *Precision Eng* 51:198–207
40. Allen D, Lecheheb A (1996) Micro electro-discharge machining of ink jet nozzles: optimum selection of material and machining parameters. *J Mater Process Technol* 58(1):53–66
41. Son S, Lim H, Kumar A, Rahman M (2007) Influences of pulsed power condition on the machining properties in micro EDM. *J Mater Process Technol* 190(1–3):73–76
42. Wang Y, Chen X, Wang Z, Dong S (2018) Fabrication of micro gear with intact tooth profile by micro wire electrical discharge machining. *J Mater Process Technol* 252:137–147
43. Ferraris E, Reynaerts D, Lauwers B (2011) Micro-EDM process investigation and comparison performance of Al<sub>3</sub>O<sub>2</sub> and ZrO<sub>2</sub> based ceramic composites. *CIRP Ann* 60(1):235–238
44. Huang H, Yan J (2016) Microstructural changes of Zr-based metallic glass during micro-electrical discharge machining and grinding by a sintered diamond tool. *J Alloy Compd* 688:14–21
45. Liu HS, Yan BH, Chen CL, Huang FY (2006) Application of micro-EDM combined with high-frequency dither grinding to micro-hole machining. *Int J Mach Tools Manuf* 46(1):80–87
46. Yeo SH, Tan PC, Aligiri E, Tor SB, Loh NH (2009) Processing of zirconium-based bulk metallic glass (BMG) using micro electrical discharge machining (micro-EDM). *Mater Manuf Processes* 24(12):1242–1248
47. Jahan M, Wong Y, Rahman M (2009) A study on the fine-finish die-sinking micro-EDM of tungsten carbide using different electrode materials. *J Mater Process Technol* 209(8):3956–3967
48. Dong S, Wang Z, Wang Y, Liu H (2016) An experimental investigation of enhancement surface quality of micro-holes for Be–Cu alloys using micro-EDM with multi-diameter electrode and different dielectrics. *Procedia CIRP* 42:257–262
49. Bamberg E, Heamawatanachai S (2009) Orbital electrode actuation to improve efficiency of drilling micro-holes by micro-EDM. *J Mater Process Technol* 209(4):1826–1834
50. Yukui W, Xiang C, Weimin G, Zhenlong W, Cheng G (2016) Complex rotary structures machined by micro-WEDM. *Procedia CIRP* 42:743–747
51. Murray J, Zdebski D, Clare A (2012) Workpiece debris deposition on tool electrodes and secondary discharge phenomena in micro-EDM. *J Mater Process Technol* 212(7):1537–1547
52. Fu X, Zhang Y, Zhang Q, Zhang J (2013) Research on piezoelectric self-adaptive micro-EDM. *Procedia CIRP* 6:303–308
53. Trych A (2013) Further study of carbon fibres electrodes in micro electrical discharge machining. *Procedia CIRP* 6:309–313
54. Plaza S, Sanchez JA, Perez E, Gil R, Izquierdo B, Ortega N, Pombo I (2014) Experimental study on micro EDM-drilling of Ti6Al4V using helical electrode. *Precision Eng* 38(4):821–827
55. Maradia U, Knaak R, Dal Busco W, Boccadoro M, Wegener K (2015) A strategy for low electrode wear in meso–micro-EDM. *Precision Eng* 42:302–310
56. Koyano T, Sugata Y, Hosokawa A, Furumoto T (2017) Micro electrical discharge machining using high electric resistance electrodes. *Precision Eng* 47:480–486

57. Mlynarczyk P, Krajcarz D, Bańkowski D (2017) The selected properties of the micro electrical discharge alloying process using tungsten electrode on aluminium. *Procedia Eng* 192:603–608
58. Qian J, Yang F, Wang J, Lauwers B, Reynaerts D (2015) Material removal mechanism in low-energy micro-EDM process. *CIRP Ann* 64(1):225–228
59. Pellicer N, Ciurana J, Ozel T (2009) Influence of process parameters and electrode geometry on feature micro-accuracy in electro discharge machining of tool steel. *Mater Manuf Processes* 24(12):1282–1289
60. Natarajan N, Arunachalam R (2011) Optimization of micro-EDM with multiple performance characteristics using Taguchi method and Grey relational analysis. *J Sci Ind Res* 70(7):500–505
61. Ay M, Çaydaş U, Haşçalık A (2013) Optimization of micro-EDM drilling of Inconel 718 superalloy. *Int J Adv Manuf Technol* 66(5–8):1015–1023
62. Tiwary A, Pradhan B, Bhattacharyya B (2014) Application of multi-criteria decision making methods for selection of micro-EDM process parameters. *Adv Manuf* 2(3):251–258
63. Manivannan R, Kumar MP (2016) Multi-response optimization of micro-EDM process parameters on AISI304 steel using TOPSIS. *J Mech Sci Technol* 30(1):137–144
64. Bhosle RB, Sharma S (2017) Multi-performance optimization of micro-EDM drilling process of Inconel 600 alloy. *Mater Today Proc* 4(2):1988–1997
65. Manivannan R, Kumar MP (2017) Multi-attribute decision-making of cryogenically cooled micro-EDM drilling process parameters using TOPSIS method. *Mater Manuf Processes* 32(2):209–215
66. Sapkal SU, Jagtap PS (2018) Optimization of micro EDM drilling process parameters for Titanium Alloy by rotating electrode. *Procedia Manuf* 20:119–126
67. Pradhan B, Bhattacharyya B (2009) Modelling of micro-electrodischarge machining during machining of titanium alloy Ti-6Al-4V using response surface methodology and artificial neural network algorithm. *Proc Inst Mech Eng, Part B: J Eng Manuf* 223(6):683–693
68. Somashekhar K, Ramachandran N, Mathew J (2009) Modeling and optimization of process parameters in micro Wire EDM by Genetic Algorithm. *Adv Mater Res* 76–78:566–570
69. Zhang L, Jia Z, Wang F, Liu W (2010) A hybrid model using supporting vector machine and multi-objective genetic algorithm for processing parameters optimization in micro-EDM. *Int J Adv Manuf Technol* 51(5–8):575–586
70. Somashekhar K, Ramachandran N, Mathew J (2010) Optimization of material removal rate in micro-EDM using artificial neural network and genetic algorithms. *Mater Manuf Processes* 25(6):467–475
71. Somashekhar K, Mathew J, Ramachandran N (2011) Multi-objective optimization of micro wire electric discharge machining parameters using grey relational analysis with Taguchi method. *Proc Inst Mech Eng, Part C: J Mech Eng Sci* 225(7):1742–1753
72. Somashekhar K, Mathew J, Ramachandran N (2012) A feasibility approach by simulated annealing on optimization of micro-wire electric discharge machining parameters. *Int J Adv Manuf Technol* 61(9–12):1209–1213
73. Nirala C, Reddy B, Saha P (2013) Optimization of process parameters in micro electro-discharge drilling [micro EDM-drilling]: a Taguchi approach. *Adv Mater Res* 622–623:30–34
74. Sivaprakasam P, Hariharan P, Gowri S (2013) Optimization of micro-WEDM process of aluminum matrix composite (A413-B4C): a response surface approach. *Mater Manuf Processes* 28(12):1340–1347
75. Jithin S, Kuriachen B, Mathew J (2013) Multi-objective optimization of micro ED milling of Ti-6Al-4V using genetic algorithm (GA). In: *International conference on precision, meso, micro and nano engineering (COPEN 2013)*, India, pp 157–163, 13–15 Dec 2013
76. Suganthi XH, Natarajan U, Sathiyamurthy S, Chidambaram K (2013) Prediction of quality responses in micro-EDM process using an adaptive neuro-fuzzy inference system (ANFIS) model. *Int J Adv Manuf Technol* 68:339–347
77. Maity K, Mishra H (2016) ANN modelling and Elitist teaching learning approach for multi-objective optimization of  $\mu$ -EDM. *J Intell Manuf* <https://doi.org/10.1007/s10845-016-1193-2>

78. Meena VK, Azad MS, Singh S, Singh N (2017) Micro-EDM multiple parameter optimization for Cp titanium. *Int J Adv Manuf Technol* 89(1–4):897–904
79. Upadhyay A, Prakash V, Sharma V (2018) Optimizing material removal rate using artificial neural network for micro-EDM. In: *Design and optimization of mechanical engineering products*, IGI Global, pp 209–233
80. Abidi MH, Al-Ahmari AM, Umer U, Rasheed MS (2018) Multi-objective optimization of micro-electrical discharge machining of nickel-titanium-based shape memory alloy using MOGA-II. *Measurement* 125:336–349



# Index

## A

Abnormal discharges, 8, 11, 71, 162, 170, 177, 183, 248  
Accumulation of bubbles, 180  
ANOVA, 10, 60, 64, 157, 254, 301, 303, 305  
Arrayed micro-features, 94  
Artificial Bee Colony (ABC) algorithms, 302

## B

Batch micro hole, 11  
Block-EDG, 36, 217  
Bulged tip, 62

## C

Carbon nanofibre, 155  
Carbon nuclides, 157  
Cavitation effects, 114  
Circularity, 6, 9, 13, 285, 286, 300, 302, 304  
Compensation of electrode wear, 190, 191, 193, 205  
Compensation technique, 44, 49  
Complex 3D cavities, 43  
Complex shaped slot, 54  
Conductive boron doped CVD diamond (B-CBD), 78  
Contact angle, 98, 116, 117  
Continuous wire electrode, 70  
Correction factor method, 32, 41, 46

Cubic Boron Nitride (CBN), 214, 282  
Cumulative tolerance, 220  
Cylindrical electrode, 10, 238, 277, 296

## D

Debris evacuation, 6, 40  
Deionized water, 7, 16, 75, 100, 138, 148, 220, 234, 237, 238, 256, 298  
Deionizing resin, 75  
Deionizing Subsystem, 75  
Design of Experiment (DoE), 301  
Dielectric fluid, 3, 7, 8, 32–34, 38, 39, 49, 67, 70, 71, 74, 75, 77, 80, 93, 100, 113, 114, 118, 120, 125, 127, 138, 139, 142, 146–148, 151, 153, 156, 157, 168–170, 174, 178, 180, 232, 239, 252, 258, 295, 296  
Dielectric flushing system, 71, 74  
Difficult-to-erode, 96, 102, 104, 111, 112  
Discharge detector, 73  
Discharge energy, 2, 5, 11, 13, 15, 18, 19, 31, 33, 38, 41, 61, 69, 71, 73, 75, 76, 79, 87, 100, 103, 104, 109, 118, 129, 133, 138–140, 145, 149, 153, 156, 157, 166–168, 170, 213, 231, 232, 236, 238, 239, 242, 247, 250, 252, 294, 297  
3D microfeatures, 27, 40, 44, 47, 48, 54, 67–69, 94, 216, 290, 293, 294

Dry EDM, 11, 39, 132, 133

Dry lubricity, 154

Dry micro-WEDM, 74, 77, 88, 89

## E

Easy-to-erode, 102, 103

$\mu$ -ECDM process, 265, 268–270, 272–274, 277–289

ED-Die sinking, 25, 26, 33, 39, 41

ED-Milling, 23, 26–34, 36–42, 45–49

EDX spectroscopy, 39

Effective arc discharge, 74

Electrochemical dissolution, 127

Electrochemical reactions, 268, 270, 273–276, 282, 285

Electrode polarity, 6, 37, 41, 58, 75, 76, 299

Electrode wear, 6–8, 16, 17, 34, 44, 45, 58, 127, 132, 143, 145, 156, 157, 161, 165, 181, 183, 186–189, 191, 192, 202, 203, 207, 213, 216, 220, 225, 236, 244, 246, 247, 296, 298, 299, 303

Electrode wear rate, 303

Electrolyte feeding system, 268, 269

## F

FAST EDM, 53, 56, 57, 59, 220

Feeding spool, 71

Femto-second lasers, 220

Filtering Systems, 75

Flushing efficiency, 32, 109, 138, 140, 154

Foil as Tool electrode (FAST), 53, 56–59

Foil electrode, 56–58

Frequency of discharging, 145

## G

Gonimeter instrument, 116

Grey Relational Analysis (GRA), 300–305

Grinding  $\mu$ -ECDM, 279, 282, 288

## H

Heat affected zone, 13, 16, 34, 88, 220, 255

Heat flux density, 142

Hierarchical texture, 116

High aspect ratio, 5, 6, 8, 13, 40, 47, 62, 79, 81, 82, 93, 94, 96, 102, 117, 122, 126, 166, 226, 234, 237, 239, 241–244, 247, 248, 258, 281, 299

High Frequency Dither Grinding (HFDG), 212, 213, 298

Hole taperness, 7

Hollow tool, 186

Hydrocarbon oil, 38, 125–128, 132, 134

## I

IEG pollution, 139, 149

Inconel 600, 15, 300

Inconel 718, 7, 13, 155, 255, 256, 303

Indirect Selective Laser Sintering (ISLS), 255

In situ fabrication, 36, 48, 79, 81

Inter-Electrode Gap (IEG), 24, 31, 32, 40, 138–141, 143, 148–152, 154–156, 158, 270, 278, 280, 283, 285, 288

## L

Laser Particle Size Analyzer (LPSA), 118

Linear Compensation Method (LCM), 42, 43

Linear slots, 55, 59, 64

Lithographie, Galvanoformung, Abformung (LIGA), 24, 47, 82, 209–211, 222–224, 240, 242, 243, 245

Longitudinal wear, 24, 28, 41, 42, 44, 45, 49, 190

## M

Machining Gap (MG), 176–178

Mass removal rate, 34

Micro cavity, 107, 111, 155

Micro diamond wheels, 214

Micro dimples, 96

Micro-EDM drilling, 1–5, 7–9, 11–14, 16–19, 68, 81, 86, 177, 179, 181, 220, 227

Microelectrodes, 5, 79, 80, 82, 86, 258

Micro Electro Discharge Slotting (MEDS), 53, 55, 59, 64, 65

Micro-Electro-Mechanical System (MEMS), 13, 31, 47, 54, 68, 82, 86, 88, 93, 94, 222, 257

Microfabrication, 23, 31, 34, 35, 48, 232, 265

Micro fluidic cell, 175

Micro gear, 244, 259, 260

Micro-gear fabrication, 82

Micro-holes array, 233, 240

Micromachining, 25, 33, 35, 37, 67, 68, 70, 84, 86, 93–95, 97, 102, 138, 157, 158, 189, 209, 210, 212, 214, 219, 220, 223, 225, 227, 228, 236, 247, 248, 252, 258, 265, 267, 281, 302

Micropillars, 111

Micro-pillar shaped electrode, 11

Microscale features, 2

Micro-structuring Silicon (Si), 40, 88, 240, 244, 256, 257

Microrods, 94, 95, 97, 100, 102–106, 108, 111

Micro-wire-EDM, 68, 71, 78, 81–83, 86, 87, 89

Milling  $\mu$ -ECDM , 279–281, 289  
 MoS2 micro powder, 154  
 Multi-Criteria Decision-Making (MCDM),  
 300, 302, 305  
 Multilayer Damped Vibration Absorber  
 (MDVA), 87  
 Multi-Objective Differential Evolution  
 (MODE), 302, 303  
 Multi-objective GA-II (MOGA-II), 302, 304

## N

Nano-EDM, 19  
 Nano-fabrication, 35  
 Nano position system, 182  
 Near-dry EDM, 133  
 Near Net Shape (NNS), 231–233, 250  
 Negative textured surfaces, 96, 112  
 NNU algorithm, 249  
 Normal-Discharge Time (NDT), 108–110

## O

Offline tool wear compensation, 191, 192, 203  
 Overall effective pulses, 195

## P

Parylene C, 8  
 PCD planarization tool, 83, 84, 86  
 Piezoelectric actuator, 166, 182, 183  
 Piezoelectric transducer, 112, 117  
 Planetary movement, 12, 234  
 Plasma channel, 3, 4, 31, 39, 41, 133, 139, 145,  
 155–157  
 Plasma column, 3, 277, 278  
 Plate electrode, 40, 97, 99–101, 105, 112, 113,  
 119–122  
 Polycrystalline Diamond (PCD), 78, 83–86,  
 213–215, 225, 298  
 Positive textured surfaces, 96, 112  
 Powder concentration, 147–152, 154–157  
 Powder mixed dielectric, 39, 40, 49, 129, 134,  
 239, 240, 257  
 Power transistor switch, 172

## R

RC type generators, 4  
 Residual stresses, 34, 35

Resistance-Capacitance (RC) circuits, 31, 100,  
 299  
 Re-solidified layer, 139, 154  
 Reverse MEDM, 93, 94, 96, 97, 99–118,  
 120–122  
 Rotary disc electrode, 80, 81  
 Roundness factor, 199, 201, 207

## S

Sacrificial electrode, 36, 225  
 Scanning/milling, 14, 59, 62, 64, 188, 233,  
 241, 244, 246, 247, 249, 250, 261, 296  
 Secondary discharges, 6, 45, 60, 167, 233  
 Secondary sparks, 6, 8, 148, 153  
 Self adaptive control, 181–183  
 Semiconductor property, 150  
 Sequential micro-EDM, 211, 212, 214, 216,  
 219, 221, 222, 225–228  
 Short bridge formation, 117  
 Short Circuit Time (SCT), 110  
 Short circuiting, 8, 101, 103, 109, 117, 150,  
 151, 154, 177  
 Silicon needles, 82  
 Silver Tungsten (AgW), 235, 236, 298  
 Sinusoidal vibrations, 112  
 Slit expansion, 157  
 Spark gap, 17, 32, 39, 40, 62, 67, 76, 77, 89,  
 143, 147, 155, 156, 162, 164–170, 172,  
 180, 181, 234, 236, 258  
 Spark radius, 142  
 Specific boiling energy, 127  
 Spindle servo frequency, 132  
 Square shaped electrode, 244  
 Stagnancy electrolyte, 227  
 Stirrer, 168, 169  
 Straight polarity, 36, 39, 41, 58, 132, 297  
 Stray capacitance, 5, 31, 70, 129, 133  
 Super-hydrophobicity, 112  
 Surfactant, 131  
 SUS 316 stainless steel, 16  
 Synchronous transport module, 196

## T

Thickness of recast layer, 34  
 Ti6Al4V alloy, 16  
 Tool path algorithm, 188

- Tool wear ratio, 76, 127, 128, 186, 248
- Tool wear/unit discharge, 2, 6, 11, 13, 16, 18, 23, 27, 34–36, 39–43, 45, 46, 48, 49, 54, 62–64, 76, 95, 101–105, 126–130, 137, 150, 157, 165–168, 170, 176, 177, 183, 185–194, 196, 202–204, 207, 211, 212, 233, 239, 240, 246–249, 283, 297–300
- TOPSIS, 300, 304
- Transient short circuit, 74
- Translational motion, 56
- Triangular shaped tool electrode, 237
- Tubular electrode, 10, 132
- Turning  $\mu$ -ECDM, 279, 282
- TW  $\mu$ -ECDM process, 270, 287
  
- U**
- Ultra-fine patterns, 223
- Ultrasonic induced vibrations, 8
- Ultrasonic power, 166–168
  
- Uniform Wear Method (UWM), 28, 41–43, 185, 188, 192, 203–205, 248
  
- V**
- Vibration assisted micro-EDM, 12, 16, 18, 163, 164, 183, 211, 227
- Volume Removal per Discharge (VRD), 192, 193, 196, 200, 207
- Volumetric relative wear, 192
  
- W**
- Wire breakage sensor, 71, 72
- Wire electro-discharge grinding, 5, 258
- Wire feed rate, 76, 87
- Wire running system, 70, 71
- Wire vibration, 70, 71
  
- Z**
- Z-axis compensation, 203